Discrete Dynamics in Nature and Society

Nonlinear Dynamics in Financial Systems: Advances and Perspectives

Guest Editors: Chuangxia Huang, Fenghua Wen, Jianping Li, Taishan Yi, and Xiaodong Lin

Nonlinear Dynamics in Financial Systems: Advances and Perspectives

Discrete Dynamics in Nature and Society

Nonlinear Dynamics in Financial Systems: Advances and Perspectives

Guest Editors: Chuangxia Huang, Fenghua Wen, Jianping Li, Taishan Yi, and Xiaodong Lin

Editorial Board

Contents

Nonlinear Dynamics in Financial Systems: Advances and Perspectives, Chuangxia Huang, Fenghua Wen, Jianping Li, Taishan Yi, and Xiaodong Lin
Volume 2014, Article ID 275750, 2 pages

Heterogeneous Fundamentalists in a Continuous Time Model with Delays, Luca Gori, Luca Guerrini, and Mauro Sodini
Volume 2014, Article ID 959514, 6 pages

Fractional Order Stochastic Differential Equation with Application in European Option Pricing, Qing Li, Yanli Zhou, Xinquan Zhao, and Xiangyu Ge
Volume 2014, Article ID 621895, 12 pages

Dynamic CGE Model and Simulation Analysis on the Impact of Citizenization of Rural Migrant Workers on the Labor and Capital Markets in China, Qi Wu and Hao Xiao
Volume 2014, Article ID 351947, 8 pages

Linear Control of Fractional-Order Financial Chaotic Systems with Input Saturation, Junhai Luo, Guanjun Li, and Heng Liu
Volume 2014, Article ID 802429, 8 pages

Analysis on the Impact of the Fluctuation of the International Gold Prices on the Chinese Gold Stocks, Jiankang Jin, Chen Jie, and Quanda Zhang
Volume 2014, Article ID 308626, 6 pages

Estimation of the Treatment Effects of Ownership on the Indirect Financing of Small- and Medium-Sized Enterprises, Xiuzhen Wang, Yi Hu, Xiaohua Xia, and Ying Deng
Volume 2014, Article ID 453458, 6 pages

An Extended SISa Model for Sentiment Contagion, Zhifeng Liu, Tingting Zhang, and Qiujun Lan
Volume 2014, Article ID 262384, 7 pages

Dynamics of Third-Order Nonlinear Neutral Equations, Hua Wang, Li Liu, and Yanxiang Tan
Volume 2014, Article ID 917913, 4 pages

Forecasting Return Volatility of the CSI 300 Index Using the Stochastic Volatility Model with Continuous Volatility and Jumps, Xu Gong, Zhifang He, Pu Li, and Ning Zhu
Volume 2014, Article ID 964654, 10 pages

Incorporating Overconfidence into Real Option Decision-Making Model of Metal Mineral Resources Mining Project, Jian-bai Huang, Na Tan, and Mei-rui Zhong
Volume 2014, Article ID 232516, 11 pages

Model for Dynamic Multiple of CPPI Strategy, Guangyuan Xing, Yong Xue, Zongxian Feng, and Xiaokang Wu
Volume 2014, Article ID 260484, 7 pages

Valuing Convertible Bonds Based on LSRQM Method, Jian Liu, Lizhao Yan, and Chaoqun Ma
Volume 2014, Article ID 301282, 9 pages

The Relations between QFII Holdings and Company Performance: Evidence from China's A-Share Listed Companies, Xiong Wang, Shuanghong Zhou, and Wenqian Fang
Volume 2014, Article ID 821463, 9 pages

Realized Jump Risk and Equity Return in China, Guojin Chen, Xiaoqun Liu, Peilin Hsieh, and Xiangqin Zhao
Volume 2014, Article ID 721635, 13 pages

Project Capital Allocation Combination Equilibrium Decision Model Based on Behavioral Option Game, Meirui Zhong, Anqi Zeng, Jianbai Huang, and Kairong Hong
Volume 2014, Article ID 803073, 11 pages

Pricing Scheme of Ocean Carrier for Inbound Container Storage for Assistance of Container Supply Chain Finance, Mingzhu Yu, Xin Tian, and Lean Yu
Volume 2014, Article ID 216057, 11 pages

Credit Risk Evaluation with a Least Squares Fuzzy Support Vector Machines Classifier, Lean Yu
Volume 2014, Article ID 564213, 9 pages

Measuring Contagion of Subprime Crisis Based on MVMQ-CAViaR Method, Wuyi Ye, Kebing Luo, and Shaofu Du
Volume 2014, Article ID 386875, 12 pages

Pricing Chinese Convertible Bonds with Dynamic Credit Risk, Ping Li and Jing Song
Volume 2014, Article ID 492134, 5 pages

Structural Analysis and Total Coal Demand Forecast in China, Qing Zhu, Zhongyu Zhang, Rongyao Li, Kin Keung Lai, Shouyang Wang, and Jian Chai
Volume 2014, Article ID 612064, 10 pages

Dynamic Pricing Based on Strategic Consumers and Substitutes in a Duopoly Setting, Gongbing Bi, Lechi Li, Feng Yang, and Liang Liang
Volume 2014, Article ID 694568, 9 pages

Pricing Decision under Dual-Channel Structure considering Fairness and Free-Riding Behavior, Yongmei Liu, Chunjie Ding, Chen Fan, and Xiaohong Chen
Volume 2014, Article ID 536576, 10 pages

How Investor Structure Influences the Yield, Information Dissemination Efficiency, and Liquidity, Hongli Che, Xiong Xiong, Juntian Yang, Wei Zhang, and Yongjie Zhang
Volume 2014, Article ID 742182, 8 pages

Risk Measurement for Portfolio Credit Risk Based on a Mixed Poisson Model, Rongda Chen and Huanhuan Yu
Volume 2014, Article ID 597814, 9 pages

A Stochastic Dynamic Programming Approach Based on Bounded Rationality and Application to Dynamic Portfolio Choice, Wenjie Bi, Liuqing Tian, Haiying Liu, and Xiaohong Chen
Volume 2014, Article ID 840725, 11 pages

Carbon Market Regulation Mechanism Research Based on Carbon Accumulation Model with Jump Diffusion, Dongmei Guo, Yi Hu, and Bingjie Zhang
Volume 2014, Article ID 135818, 7 pages

The Changes of Carbon Emission in China's Industrial Sectors from 2002 to 2010: A Structural Decomposition Analysis and Input-Output Subsystem, Guoxing Zhang and Mingxing Liu
Volume 2014, Article ID 798576, 9 pages

An Empirical Study on Listed Company's Value of Cash Holdings: An Information Asymmetry Perspective, Chuangxia Huang, Xin Ma, and Qiujun Lan
Volume 2014, Article ID 897278, 12 pages

Pricing American Options Using a Nonparametric Entropy Approach, Xisheng Yu and Li Yang
Volume 2014, Article ID 369795, 16 pages

Dynamics of Foreign Exchange Networks: A Time-Varying Copula Approach, Gang-Jin Wang, Chi Xie, Peng Zhang, Feng Han, and Shou Chen
Volume 2014, Article ID 170921, 11 pages

Lattice Methods for Pricing American Strangles with Two-Dimensional Stochastic Volatility Models, Xuemei Gao, Dongya Deng, and Yue Shan
Volume 2014, Article ID 165259, 6 pages

Higher Order Mean Squared Error of Generalized Method of Moments Estimators for Nonlinear Models, Yi Hu, Xiaohua Xia, Ying Deng, and Dongmei Guo
Volume 2014, Article ID 324904, 8 pages

Investors' Risk Preference Characteristics Based on Different Reference Point, Fenghua Wen, Zhifang He, Xu Gong, and Aiming Liu
Volume 2014, Article ID 158386, 9 pages

A Nonparametric Operational Risk Modeling Approach Based on Cornish-Fisher Expansion, Xiaoqian Zhu, Jianping Li, Jianming Chen, Yingqi YangHuo, Lijun Gao, Jichuang Feng, Dengsheng Wu, and Yongjia Xie
Volume 2014, Article ID 839731, 8 pages

Study on the Technical Efficiency of Creative Human Capital in China by Three-Stage Data Envelopment Analysis Model, Jian Ma, Yueru Ma, Yong Bai, and Bing Xia
Volume 2014, Article ID 964275, 12 pages

Hindawi Publishing Corporation
Discrete Dynamics in Nature and Society
Volume 2014, Article ID 275750, 2 pages
http://dx.doi.org/10.1155/2014/275750

Editorial

Nonlinear Dynamics in Financial Systems: Advances and Perspectives

Chuangxia Huang,[1] Fenghua Wen,[2] Jianping Li,[3] Taishan Yi,[4] and Xiaodong Lin[5]

[1] *College of Mathematics and Computing Science, Changsha University of Science and Technology, Changsha 410114, China*
[2] *Business School, Central South University, Changsha 410012, China*
[3] *Institute of Policy and Management, Chinese Academy of Science (CAS), Beijing 100190, China*
[4] *Department of Applied Mathematics, University of Western Ontario, London, ON, Canada N6A 5B7*
[5] *Rutgers Business School, Rutgers University, Piscataway, NJ 08854, USA*

Correspondence should be addressed to Chuangxia Huang; cxiahuang@126.com

Received 18 December 2014; Accepted 18 December 2014; Published 31 December 2014

In the recent years, nonlinear dynamics have attracted rapidly growing attention in the fields of finance, economy, mathematical biology, and many other disciplines. In spite of the amount of published results recently focused on financial systems, there remain many challenging open questions. It is important to develop new theories and methods, as well as to modify and refine the well-known techniques for the analysis of new classes of problems.

The aim of this special issue is to gather recent research efforts on the development and applications of nonlinear dynamics. This special issue contains thirty-five research articles. The original papers explored in this special issue include a wide variety of topics such as the following.

Behavioral Finance Modeling. Z. Liu et al. proposed a new model of sentiment contagion, named the SOSa-SPSa model, and found that both numbers of optimism and pessimism will increase with the probability of spontaneity or contagion. X. Gong et al. divided the logarithmic realized volatility into the logarithmic continuous sample path variation and the logarithmic discontinuous jump variation on the basis of the SV-RV model.

J. Jin et al. analysed the impact of the fluctuation of the international gold prices on the Chinese gold stocks. X. Wang et al. investigated the relations between Qualified Foreign Institutional Investors (QFII) holdings and the performance of the A-share listed companies. W. Ye et al. investigated measuring contagion of subprime crisis based on MVMQ-CAViaR method. C. Huang et al. constructed a new proxy for information asymmetry based on the principal component analysis.

Risk Assessment and Credit Analysis. P. Li and J. Song investigated the pricing Chinese convertible bonds with dynamic credit risk. G. Xing et al. proposed a dynamic multiple setting model for gap risk management. G. Chen et al. utilized the realized jump components to explore a new jump (including nonsystematic jump and systematic jump) risk factor model.

R. Chen and H. Yu developed a mixed Poisson model assuming that default probabilities of obligors depend on a set of common economic factors to construct the dependence structure of obligors. L. Yu proposed a least squares fuzzy support vector machine (LS-FSVM) model for the purpose of credit risk evaluation. F. Wen et al. showed that investors' risk preference is time varying and is influenced by previous outcomes.

Portfolio Selection and Optimization. J. Huang et al. showed that incorporating overconfidence into real option decision-making model of metal mineral resources development is a crucial extension of project evaluation theory. W. Bi et al. studied the dynamic portfolio choice problem with multiple variables of stochastic volatility and agents' limited attention. M. Zhong et al. investigated project capital allocation combination equilibrium decision model based on behavioral option game.

Asset Pricing and Arbitrage Techniques. G. Bi et al. constructed a dynamic game to build a two-period dynamic pricing model for two brands of substitutes which are sold by duopoly. J. Liu et al. showed that the proposed LSRQM model fits well the market prices of convertible bonds in China's market and the LSRQM method is effective. Y. Liu et al. rebuilt the linear demand function considering free-riding behavior and modified the pricing model based on channel fairness.

Dynamical Analysis of Stability, Chaos, and Bifurcation on Financial Systems. L. Gori et al. showed that nonlinear dynamic phenomena, such as coexistence of attractors and local and global bifurcations, occur due to the existence of a time gap in the process of adjustment of market prices. J. Luo et al. investigated linear control of fractional-order financial chaotic systems with input saturation. H. Wang et al. investigated the dynamics of third order nonlinear neutral equations.

Numerical Computation and Simulations. Q. Wu and H. Xiao proposed a dynamic CGE model and the simulation results show that changes in supply will affect the labor market structure, the relative factor price, and the investment in and the output of industries. G.-J. Wang et al. proposed a time-varying correlation network-based approach to investigate dynamics of foreign exchange (FX) networks.

Financial Diagnosis and Control. X. Wang et al. adopted propensity score matching (PSM) method to conduct empirical analysis about the treatment effects of indirect financing level of SMEs under different systems.

The response to this special issue was beyond our expectation. We received 61 papers in the interdisciplinary research fields. This special issue includes thirty-five high-quality peer-reviewed articles. These articles contain several new, novel, and innovative techniques and ideas that may stimulate further research in every branch of pure and applied sciences.

Acknowledgments

We would like to express our deepest gratitude to the reviewers, whose professional comments and valuable suggestions guaranteed the high quality of these selected papers. We would like to express our gratitude to the authors for their interesting and novel contributions. We would also like to thank the editorial board's members of this journal, for their support and help throughout the preparation of this special issue. The interested readers are advised to explore these interesting and fascinating fields further. We hope that problems discussed and investigated in this issue may be inspiration and motivation to discover new, innovative, and novel applications in all areas of nonlinear financial dynamics. Chuangxia Huang would like to express the gratitude to the support of the National Natural Science Foundation of China (no. 11101053 and no. 71471020), the Key Project of the Chinese Ministry of Education (no. 211118), and the China Postdoctoral Science Foundation (no. 20140550097).

Chuangxia Huang
Fenghua Wen
Jianping Li
Taishan Yi
Xiaodong Lin

Hindawi Publishing Corporation
Discrete Dynamics in Nature and Society
Volume 2014, Article ID 959514, 6 pages
http://dx.doi.org/10.1155/2014/959514

Research Article

Heterogeneous Fundamentalists in a Continuous Time Model with Delays

Luca Gori,[1] Luca Guerrini,[2] and Mauro Sodini[3]

[1] *Department of Law, University of Genoa, Via Balbi 30/19, 16126 Genoa, Italy*
[2] *Department of Management, Polytechnic University of Marche, Piazza Martelli 8, 60121 Ancona, Italy*
[3] *Department of Economics and Management, University of Pisa, Via Cosimo Ridol 10, 56124 Pisa, Italy*

Correspondence should be addressed to Luca Guerrini; luca.guerrini@univpm.it

Received 14 March 2014; Accepted 17 July 2014; Published 20 August 2014

Academic Editor: Jianping Li

We develop a continuous time model with heterogeneous fundamentalists, imitators, and discrete time delays. We show that nonlinear dynamic phenomena, such as coexistence of attractors and local and global bifurcations, occur due to the existence of a time gap in the process of adjustment of market prices.

1. Introduction

Starting from the seminal paper by Brock and Hommes [1], attention has been placed in building on models that try to mimic the behaviours of financial markets also in the absence of stochastic shocks. A mechanism that has proved to be fruitful in this direction has been the introduction of heterogeneous expectations of financial markets operators [2]. This literature has essentially been developed through the study of discrete time models [3]. For instance, Chiarella et al. [4] deepen the mathematical properties of a two-dimensional dynamic model with fundamentalists and chartists, while Tramontana et al. [5] develop a three-dimensional nonlinear dynamic model of internationally connected financial markets.

By pursuing the line of research of He et al. [6], He and Zheng [7], and He and Li [8], the aim of this paper is to inquire whether complex dynamic phenomena obtained in discrete time models also hold in continuous time models with *discrete* time delays. To this purpose, we use a model similar to that adopted by He and Westerhoff [9] and Naimzada and Ricchiuti [10]. We assume two experts that have different beliefs on the fundamental of an asset and choose their allocations by using the mean-variance criterion in every moment in time [2]. Financial operators are imitators and select allocations established by the two experts depending on performances obtained.

We show that this can generate nonlinear dynamics also in a continuous time framework with time delays. In particular, coexistence of attractors as well as local and global bifurcations can occur.

The rest of the paper is organised as follows. Section 2 sets up the model. Section 3 characterises local stability properties and local bifurcations of equilibria. Section 4 provides some numerical experiments to validate the theoretical results established in Section 3, while also showing the emergence of global bifurcations. Section 5 outlines the conclusions.

2. The Model

We consider a continuous time version of the model developed by Naimzada and Ricchiuti [10] augmented with *discrete* time delays. Specifically, we set up a model with a risk-free asset, characterised by a perfectly elastic supply and an instantaneous rate of return $r > 0$, and a risky asset, with a price per share $x(t)$ and a (stochastic) dividend process $y(t)$. There are two types of market operators (fundamentalists and imitators) and a market maker that behaves as a Walrasian auctioneer. We assume there exist two types (Type 1 and Type 2) of fundamentalists with different beliefs on the fundamental of the traded assets. They are myopic and behave on the basis of the mean-variance criterion at each moment in time. By considering (1) in Naimzada and Ricchiuti [10, page 173], we get the following continuous time version of wealth dynamics of the Type $i = 1, 2$ fundamentalist:

$$\dot{w}_i(t) = rw_i(t) + [\dot{x}(t) + \dot{y}(t) + y(t) - rx(t)]\, q_i(t), \quad (1)$$

where $w_i(t)$, $\dot{w}_i(t)$, and $q_i(t)$ are the wealth, its time derivative, and the share of risky asset of fundamentalist i at time t, respectively.

The objective of Type i fundamentalist is therefore the following:

$$\max_{\{q_i(t)\}} E_i[\dot{w}_i(t) + w(t)] - \frac{a}{2} V_i[\dot{w}_i(t) + w(t)], \quad (2)$$

where $a > 0$ is a parameter that measures the degree of risk aversion of both agents. By assuming that the variance is constant and is given by σ^2, the maximisation programme (2) gives the following market demands of the risky asset:

$$q_i(t) = \frac{E_i[\dot{x}(t) + \dot{y}(t) + y(t) - rx(t)]}{a\sigma^2}. \quad (3)$$

Similarly with Naimzada and Ricchiuti [10], we assume that both fundamentalists have the same correct expectations on dividend dynamics, that is, $E_i[\dot{y}(t)] = \dot{y}(t)$, but heterogeneous expectations on price per share dynamics, that is, $E_i[\dot{x}(t)+x(t)] = F_i > 0$. This means that every fundamentalist expects that the value of the risky asset tends to a level believed as being its fundamental. From (3), it follows that the share of risky asset of fundamentalist i is given by

$$q_i(t) = \alpha[F_i - P(t)], \quad (4)$$

where $P(t) = (r+1)x(t) - \dot{y}(t) - y(t)$ and $\alpha = 1/(a\sigma^2)$. In addition, we set $F_1 < F_2$ without loss of generality.

In this model, fundamentalists play the role of experts in the market and other agents follow fundamentalists' choices depending on a mechanism that rewards the portfolio allocations based on the fundamental closer to the realised market price. Specifically, we assume the following adjustment rule:

$$\dot{L}(t) = \left[1 - \frac{(F_1 - P(t))^2}{(F_1 - P(t))^2 + (F_2 - P(t))^2}\right] - L(t), \quad (5)$$

where $L(t)$ is the share of agents that follow Type 1 fundamentalist, $\dot{L}(t)$ is the time derivative of $L(t)$, and $(F_i - P(t))^2$ is the squared error related to expert i. Then, this rule stimulates agents to adopt portfolio choices of the fundamentalist whose fundamental value deviates less from the price actually realised on the market.

In addition, we assume the existence of a Walrasian auctioneer that fixes the price of the risky asset according to the following mechanism:

$$\begin{aligned}\dot{P}(t) = \beta\{&[L(t-\tau) + \dot{L}(t-\tau)]\, q_1(t-\tau)\\ &+ [1 - L(t-\tau) - \dot{L}(t-\tau)]\, q_2(t-\tau)\},\end{aligned} \quad (6)$$

where $\beta > 0$ is the speed of adjustment of prices over time. The dynamics of price defined in (6) determines the variation of the market price of the risky asset depending on the price and allocation choices of imitators (followers) made at $t - \tau$. This is a quite realistic assumption with regard to the adjustment rule of prices, given that the time gap τ can be referred to small time intervals (e.g., minutes or hours) as those observed in actual financial markets.

In order to simplify notation, in what follows we omit the time dependence for variables and derivatives referred at time t and use v_d to indicate the state of a generic variable v at time $t - \tau$. Now, by using (4) and (5) to substitute into (6) to eliminate $q_{i,d}$ and $L_d + \dot{L}_d$, respectively, we get

$$\dot{P} = \gamma\left[\frac{(F_1 - P_d)(F_2 - P_d)^2 + (F_2 - P_d)(F_1 - P_d)^2}{(F_1 - P_d)^2 + (F_2 - P_d)^2}\right], \quad (7)$$

where $\gamma := \alpha\beta > 0$.

3. Existence of Equilibria and Local Bifurcations

In this section we perform the analysis of the delay differential equation defined in (7) (see, e.g., [11]).

Equilibria of (7) are obtained by setting $\dot{P} = 0$ and $P_d = P = P_*$ for all t. By doing this, one finds that the nontrivial equilibria P_* of (7) must satisfy the following equation:

$$(F_1 - P_*)(F_2 - P_*)(F_1 + F_2 - 2P_*) = 0. \quad (8)$$

Consequently, (7) has three positive equilibria: $P_* = F_1$, $P_* = F_2$, and $P_* = (F_1 + F_2)/2$.

Let $h = P - P_*$. Then (7) can be transformed into

$$\begin{aligned}\dot{h} = \gamma\Big\{&\big([F_1 - (h + P_*)][F_2 - (h_d + P_*)]^2\\ &+ [F_2 - (h + P_*)][F_1 - (h_d + P_*)]^2\big)\\ &\times \big([F_1 - (h_d + P_*)]^2 + [F_2 - (h_d + P_*)]^2\big)^{-1}\Big\}.\end{aligned} \quad (9)$$

The characteristic equation of the linear part of (9) is given by

$$P(\lambda, \tau) = \lambda - Me^{-\lambda\tau} = 0, \quad (10)$$

where

$$M = \begin{cases} -\gamma, & \text{if } P_* = F_1 \text{ or } P_* = F_2, \\ \gamma, & \text{if } P_* = \dfrac{F_1 + F_2}{2}. \end{cases} \quad (11)$$

When there is no delay, that is, $\tau = 0$ in (9), the characteristic equation becomes $P(\lambda, 0) = \lambda - M = 0$. Then, $P_* = F_1$ and $P_* = F_2$ are locally asymptotically stable ($\lambda = -\gamma < 0$), while $P_* = (F_1 + F_2)/2$ is unstable ($\lambda = \gamma > 0$).

Now, assume that $\tau > 0$ in (9). We will investigate the location of the roots of the transcendental equation. First, it is immediate that (10) has no zero root. Next, we examine when this equation has pure imaginary roots.

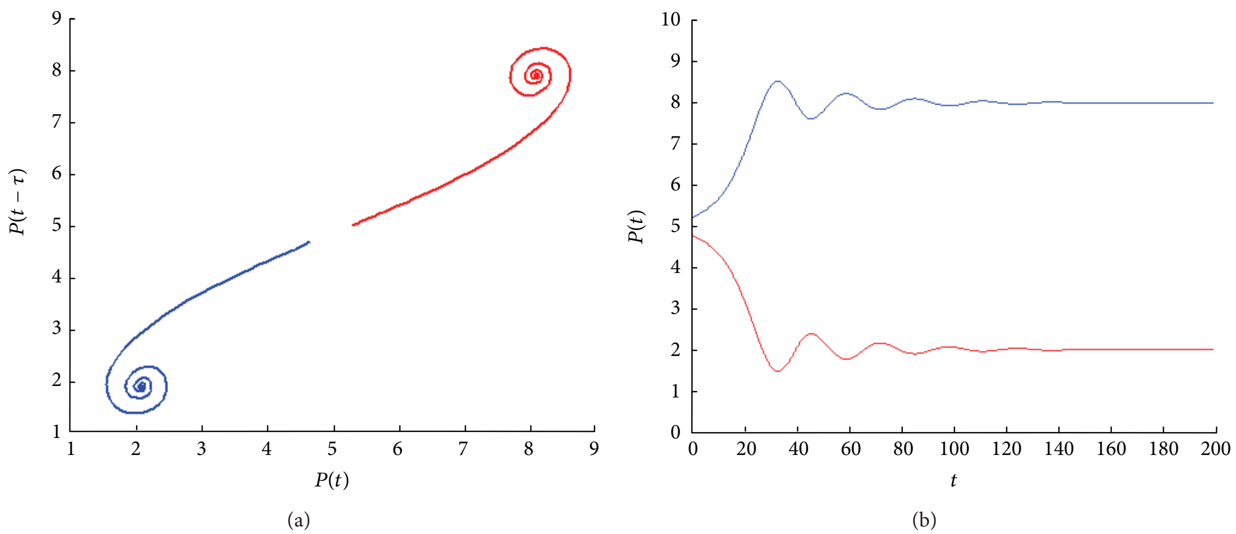

Figure 1: $\tau = 6$. (a) Two trajectories (depicted in blue and red) generated by two different initial conditions $P(t) = 4.8$ (blue line) and $P(t) = 5.2$ (red line), $t \in (-6, 0)$. (b) Corresponding time series.

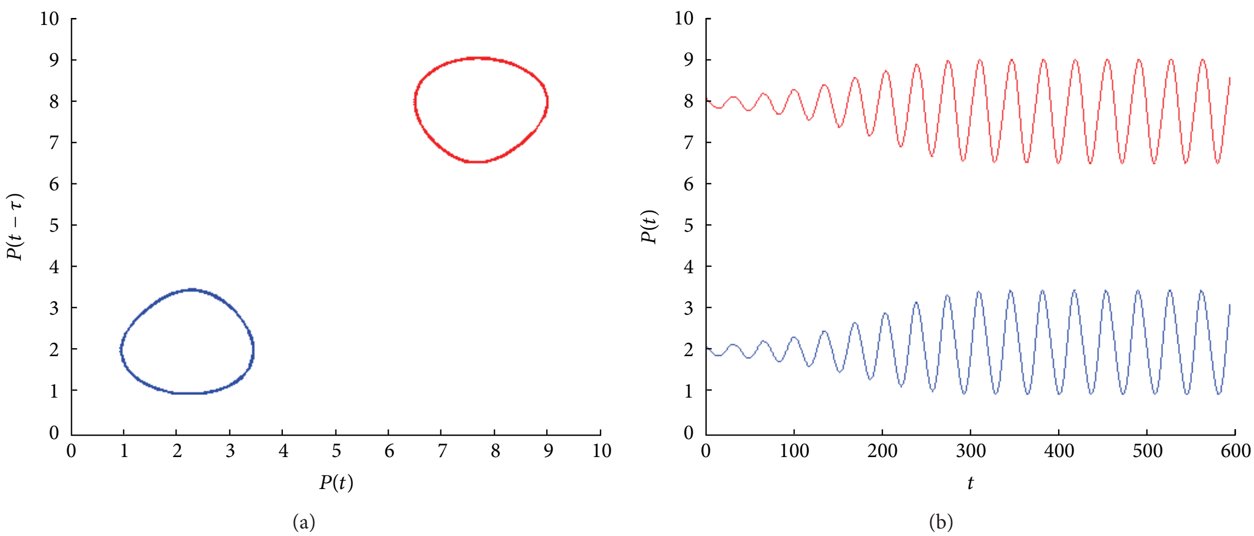

Figure 2: $\tau = 9$. (a) Two attracting closed invariant curves. (b) Corresponding time series with unique maximum and minimum.

Proposition 1. *Characteristic equation* (10) *has a pair of purely imaginary conjugate roots* $\lambda = \pm i\omega_0$ *when* $\tau = \tau_j$ $(j = 0, 1, 2, \ldots)$, *where*

$$\omega_0 = \gamma,$$
$$\tau_j = \begin{cases} \dfrac{1}{\gamma}\left(\dfrac{\pi}{2} + 2\pi j\right), & \text{if } P_* = F_1 \text{ or } P_* = F_2, \\ \dfrac{1}{\gamma}\left(\dfrac{3\pi}{2} + 2\pi j\right), & \text{if } P_* = \dfrac{F_1 + F_2}{2}. \end{cases} \quad (12)$$

Proof. For $\omega > 0$, $\lambda = i\omega$ is a root of (10) if and only if

$$i\omega - Me^{-i\omega\tau} = 0. \quad (13)$$

Separating the real and imaginary parts, we obtain

$$\omega = -M\sin\omega\tau, \qquad 0 = M\cos\omega\tau. \quad (14)$$

If $P_* = F_1$ or $P_* = F_2$, then (14) yield $\omega\tau = \pi/2$ and $\omega = \gamma$; on the other hand, if $P_* = (F_1 + F_2)/2$, then $\omega\tau = 3\pi/2$ and $\omega = \gamma$. The conclusion is immediate. □

From (12), we note that there exists an inverse relationship between the value of γ (and thus of the speed of adjustment of prices over time β) and the bifurcation value of τ. This implies that the speed of adjustment of prices over time β plays a destabilising role in the model (i.e., for a high value of β the Hopf bifurcations occur for a low value of τ), while the variance σ^2 and the degree of risk aversion a play a stabilising role (i.e., for high values of σ^2 and a the Hopf bifurcations occur for a high value of τ).

Lemma 2. $\lambda = i\omega_0$ *is a simple purely imaginary root of* (10), *and all other roots* $\lambda \neq i\omega_0$ *satisfy* $\lambda \neq in\omega_0$ *for any integer* n.

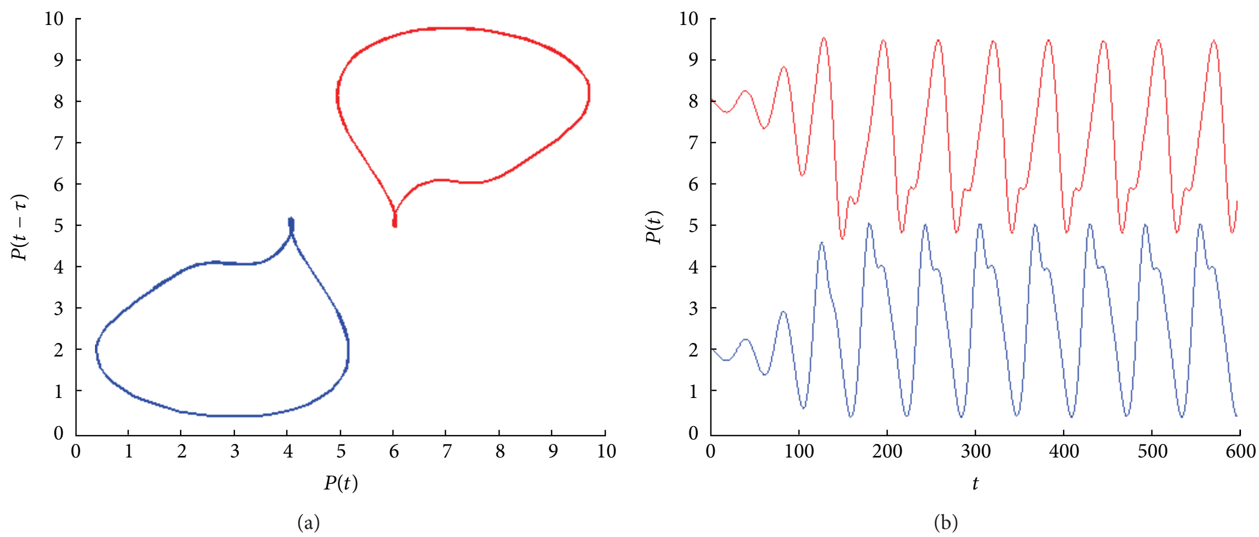

FIGURE 3: $\tau = 12$. (a) Two attracting closed invariant curves. (b) Corresponding time series with two local maxima and minima.

Proof. If $\lambda = i\omega_0$ is not simple, that is, $P(i\omega_0, \tau_j) = P'(i\omega_0, \tau_j) = 0$, then one has $1 + i\omega_0\tau_j = 0$, which is a contradiction. Let us assume that there exists a root λ_n such that $P(\lambda_n, \tau_0) = 0$ and $\lambda_n = in\omega_0$ for some $n \neq 0, \pm 1$. From (14), we get $n^2 = M^2/\omega_0^2 = 1$. Therefore, the statement follows immediately. □

Let $\lambda_j = \nu_j(\tau) + i\omega_j(\tau)$ be the roots of (10) close to $\tau = \tau_j$ that satisfy $\nu_j(\tau_j) = 0$ and $\omega_j(\tau_j) = \omega_0$, where ω_0 and τ_j are defined by (12). The next result indicates that each crossing of the real part of characteristic roots at τ_j must be from left to right; that is, stability is lost at the smallest stability switch and it cannot be regarded later.

Lemma 3. *The following transversality condition $\nu_j'(\tau_j) > 0$ holds.*

Proof. Differentiating both sides of (10) with respect to τ gives

$$\frac{d\lambda}{d\tau} = -\frac{\lambda^2}{1 + \lambda\tau}. \tag{15}$$

Then, we have

$$\left.\frac{d\lambda}{d\tau}\right|_{\tau=\tau_j} = \frac{\omega_0^2}{1 + i\omega_0\tau_j}, \tag{16}$$

which implies

$$\nu_j'(\tau_j) = \frac{\omega_0^2}{1 + \omega_0^2\tau_j^2}, \tag{17}$$

concluding the proof. □

Lemma 4. *Let $P_* = F_1$ or $P_* = F_2$. If $\tau \in [0, \tau_0)$, then all roots of (10) have negative real parts; if $\tau = \tau_0$, then all roots of (10) except $\lambda = \pm i\omega_0$ have negative real parts; if $\tau \in (\tau_j, \tau_{j+1})$ for $j = 1, 2, \ldots$, then (10) has $2(j+1)$ roots with positive real parts.*

Proof. The first part follows noting that the equilibrium P_* is locally asymptotically stable when $\tau = 0$ and so its stability can only be lost if eigenvalues cross the imaginary axis from left to right. Let $\lambda(\tau_0) = \nu + i\omega$ be a root of (10) with $\nu > 0$. Then $\nu = -\gamma e^{-\nu\tau_0}\cos\omega\tau_0$, $\omega = \gamma e^{-\nu\tau_0}\sin\omega\tau_0$, and thus, we derive $(1/\omega)\tan^{-1}(-\omega/\nu) = \tau_0 > 0$, which is a contradiction the left-hand side term of this equation being a negative number. Since the rate of change of the real part of an eigenvalue with respect to τ when $\tau = \tau_j$ is positive, then the number of roots with positive real parts is increasing. Due to the fact above, the number of roots of the characteristic equation with positive real part will be constant for $0 \le \tau < \tau_0$ and equal to the number of eigenvalues with positive real parts when $\tau = 0$ (i.e., zero being P_* stable). For each subsequent interval $\tau_j < \tau < \tau_{j+1}$, the number can be determined from the number in the previous interval $\tau_{j-1} < \tau < \tau_j$ and the number of roots with zero real part at τ_j. □

Spectral properties in the previous lemma immediately lead to stability properties of the zero solution of (9) and, equivalently, of the positive equilibrium P_* of (7).

Theorem 5. *Let τ_j be defined as in (12).*

(1) *The positive equilibrium $P_* = (F_1 + F_2)/2$ is unstable for all $\tau \ge 0$.*

(2) *The positive equilibria $P_* = F_1$ and $P_* = F_2$ are locally asymptotically stable for $\tau \in [0, \tau_0)$ and unstable for $\tau > \tau_0$. Furthermore, (7) undergoes a Hopf bifurcation at P_* when $\tau = \tau_j$ $(j = 0, 1, 2, \ldots)$.*

Remark 6. Since when $\tau = 0$ (7) collapses into a one-dimensional autonomous differential equation, then in the continuous time version of the model by Naimzada and Ricchiuti [10] no persistent oscillations can occur, and the dynamics are therefore monotonic and convergent towards one of the equilibria. This result stresses the importance of

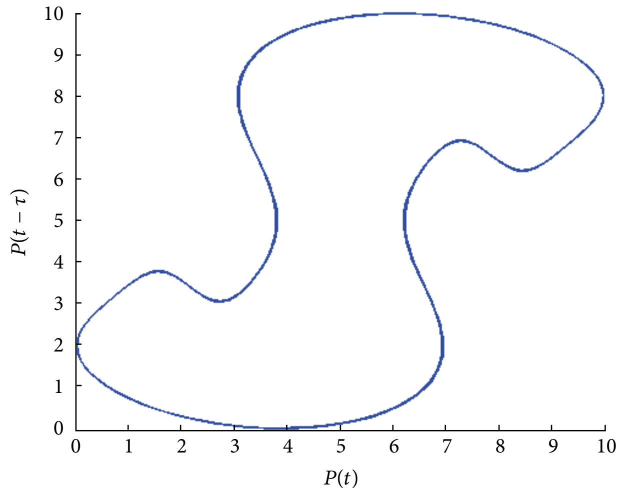

(a)

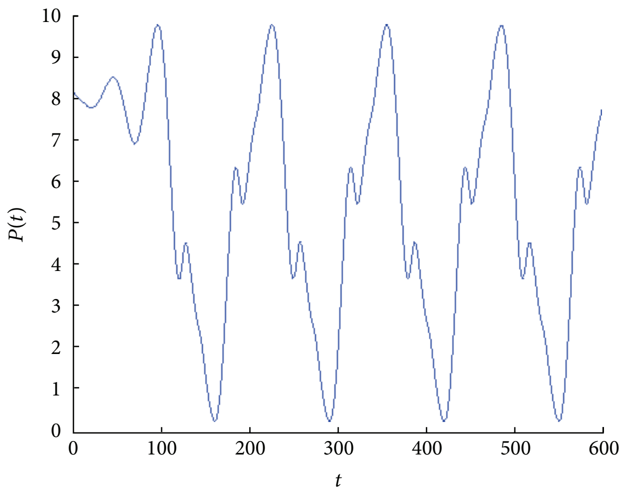

(b)

FIGURE 4: $\tau = 14.3$. (a) A unique attractor generated by the global bifurcation. (b) Corresponding time series with large oscillations.

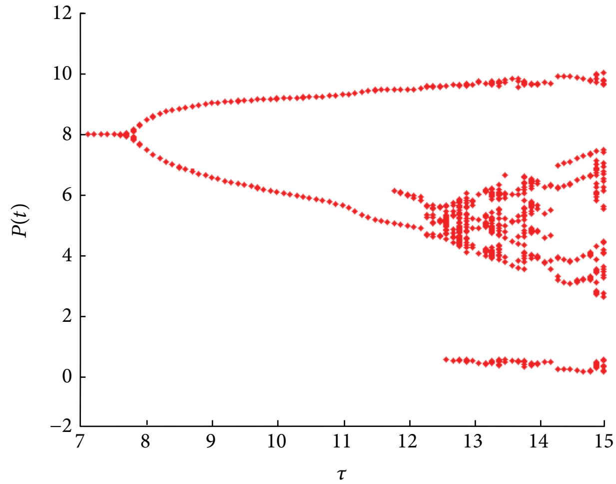

FIGURE 5: Bifurcation diagram for τ showing local maxima and minima of $P(t)$ for a given value of τ. Given the initial condition, for $\tau < \tau_0$ the dynamics converges to the equilibrium $F_2 = 8$. For $\tau = \tau_0$, the equilibrium undergoes a Hopf bifurcation and the dynamics are characterised by oscillations with a maximum and a minimum for $\tau \in (\tau_0, \tau_1)$, with $\tau_1 \simeq 11.6$. Just after τ_1 it is possible to observe the birth of another local extremum. For $\tau = \tau_2$, a global bifurcation occurs and the dynamics lies in a larger portion of the phase plane. We note that for $\tau > \tau_2$ there are several windows in which many maxima and minima coexist, so that fluctuations become more complicated.

time delays in generating endogenous fluctuations in this kind of models.

4. Numerical Simulations

In this section we provide some numerical simulations to validate the theoretical results on local bifurcations stated in Section 3, and we show the occurrence of global bifurcations as well. For this purpose, we fix the following parameter set, $\gamma = 0.2$, $F_1 = 2$, and $F_2 = 8$, and let τ vary. For this parameter values the Hopf bifurcation occurs at $\tau_0 \simeq 7.854$. For $\tau < \tau_0$ (but sufficiently high), the dynamics of the model are oscillatory and convergent towards one of the equilibria depending on the initial conditions (as shown in Figure 1). Just after the Hopf bifurcation value there exist two attracting closed invariant curves (each of which with its basin of attraction), and then the dynamics of prices (and also the shares of imitators of Type 1 and Type 2 fundamentalists) show persistent oscillations (see Figures 2(a) and 2(b)) characterised by unique maximum and minimum points.

By increasing the value of τ, other phenomena are possible. In particular, we observe an increase in the number of local maxima and minima that resembles the sequence of period-doubling bifurcations shown by Naimzada and Ricchiuti [10] in a discrete time model (see Figures 3(a) and 3(b)). When τ increases further, a global bifurcation occurs and the two attractors merge each other. Then, a unique attractor is born (as shown in Figures 4(a) and 4(b)). At this stage, the dynamics of prices are characterised by large oscillations and possibly a high degree of unpredictability as suggested by the bifurcation diagram shown in Figure 5.

5. Conclusion

The debate on whether it is better to adopt continuous time models or discrete time models to describe the behaviours of financial markets operators is still open, as pointed out by He and Li [8, page 974]: “The [discrete time] set up facilitates economic understanding of the role of heterogeneous expectations and mathematical analysis, it, however, faces a limitation when dealing with expectations formed from the lagged prices over different time horizons and a challenge to characterise the adaptive behaviour in a continuous-time.” Generally speaking, in the absence of stochastic shocks the continuous time framework tends to generate regular dynamics. Nevertheless, when one assumes that some economic processes (e.g., the adjustment of prices) react to changes occurred at a certain time gap, the dynamics generated by continuous time models tend to mimic those generated by discrete time models. This paper has confirmed the existence of nonlinear asset price dynamics in a continuous time version (with *discrete* time delays) of the model proposed by Naimzada and Ricchiuti [10], characterised by the existence of fundamentalists with heterogeneous expectations on the value of a risky asset.

Conflict of Interests

The authors declare that there is no conflict of interests regarding the publishing of this paper.

References

[1] W. A. Brock and C. H. Hommes, "A rational route to randomness," *Econometrica*, vol. 65, no. 5, pp. 1059–1095, 1997.

[2] W. A. Brock and C. H. Hommes, "Heterogeneous beliefs and routes to chaos in a simple asset pricing model," *Journal of Economic Dynamics and Control*, vol. 22, no. 8-9, pp. 1235–1274, 1998.

[3] C. Chiarella, R. Dieci, and X. He, "Heterogeneity, market mechanisms, and asset price dynamics," in *Handbook of Financial Markets: Dynamics and Evolution*, T. Hens and K. R. Schenk-Hoppé, Eds., pp. 277–344, North-Holland, Amsterdam, The Netherlands, 2009.

[4] C. Chairella, R. Dieci, and L. Gardini, "Asset price dynamics in a financial market with fundamentalists and chartists," *Discrete Dynamics in Nature and Society*, vol. 6, no. 2, pp. 69–99, 2001.

[5] F. Tramontana, L. Gardini, R. Dieci, and F. Westerhoff, "The emergence of "bull and bear" dynamics in a nonlinear model of interacting markets," *Discrete Dynamics in Nature and Society*, vol. 2009, Article ID 310471, 30 pages, 2009.

[6] X. He, K. Li, J. Wei, and M. Zheng, "Market stability switches in a continuous-time financial market with heterogeneous beliefs," *Economic Modelling*, vol. 26, no. 6, pp. 1432–1442, 2009.

[7] X. He and M. Zheng, "Dynamics of moving average rules in a continuous-time financial market model," *Journal of Economic Behavior and Organization*, vol. 76, no. 3, pp. 615–634, 2010.

[8] X. He and K. Li, "Heterogeneous beliefs and adaptive behaviour in a continuous-time asset price model," *Journal of Economic Dynamics & Control*, vol. 36, no. 7, pp. 973–987, 2012.

[9] X. He and F. H. Westerhoff, "Commodity markets, price limiters and speculative price dynamics," *Journal of Economic Dynamics and Control*, vol. 29, no. 9, pp. 1577–1596, 2005.

[10] A. K. Naimzada and G. Ricchiuti, "Heterogeneous fundamentalists and imitative processes," *Applied Mathematics and Computation*, vol. 199, no. 1, pp. 171–180, 2008.

[11] J. Hale, *Theory of Functional Differential Equations*, Springer, New York, NY, USA, 3rd edition, 1977.

Hindawi Publishing Corporation
Discrete Dynamics in Nature and Society
Volume 2014, Article ID 621895, 12 pages
http://dx.doi.org/10.1155/2014/621895

Research Article

Fractional Order Stochastic Differential Equation with Application in European Option Pricing

Qing Li,[1] Yanli Zhou,[2,3] Xinquan Zhao,[1] and Xiangyu Ge[1]

[1] *School of Statistics and Mathematics, Zhongnan University of Economics and Law, Wuhan 430073, China*
[2] *School of Finance, Zhongnan University of Economics and Law, Wuhan 430073, China*
[3] *Department of Mathematics and Statistics, Curtin University, Perth, WA 6845, Australia*

Correspondence should be addressed to Yanli Zhou; ylzhou8507@gmail.com and Xiangyu Ge; xiangyu_ge@163.com

Received 20 January 2014; Revised 3 July 2014; Accepted 17 July 2014; Published 13 August 2014

Academic Editor: Jianping Li

Memory effect is an important phenomenon in financial systems, and a number of research works have been carried out to study the long memory in the financial markets. In recent years, fractional order ordinary differential equation is used as an effective instrument for describing the memory effect in complex systems. In this paper, we establish a fractional order stochastic differential equation (FSDE) model to describe the effect of trend memory in financial pricing. We, then, derive a European option pricing formula based on the FSDE model and prove the existence of the trend memory (i.e., the mean value function) in the option pricing formula when the Hurst index is between 0.5 and 1. In addition, we make a comparison analysis between our proposed model, the classic Black-Scholes model, and the stochastic model with fractional Brownian motion. Numerical results suggest that our model leads to more accurate and lower standard deviation in the empirical study.

1. Introduction

Time series incorporating memory structure has been widely used in biological, chemical, and physical system. Memory effects also exist in financial systems. For example, the decision will be effected spontaneously by the past experience of decision makers. Plenty of financial variables with long memory effects have been found [1–4], such as the gross domestic product (GDP), interest rate, foreign exchange rates, stock price, and futures price. Garzareli et al. have proved the existence of memory effects in the stock price series by the conditional probability approach and measured the extent of long memory (autocorrelation) [5].

Memory effect is often measured by the autocorrelation function, and, recently, the Hurst index as an effective tool was introduced to measure the memory effect [6]. The Hurst index is often denoted by H $(0 < H < 1)$. In the case of $0 < H < 0.5$, time series has negative correlation and antipersistent behavior, which is called short-dependence memory. When $H = 0.5$, the time series has no dependence. However, in the case of $0.5 < H < 1$, time series has positive correlation and persistent behavior, which is long-dependence memory. The persistent behavior was also called "Joseph Effect" by Mandelbrot and Wallis [7]. Cajueiro and Tabak [8, 9] have also found that memory effect exists in financial markets.

A number of researchers used fractional Brownian motion to depict the characteristic of memory. Mandelbrot and Van Ness first found that long memory effects exist in stock returns and gave the definition of fractional Brownian motion [10]. Since then, describing the memory by the fractional Brownian motion in financial market becomes more and more popular. For instance, Bęben and Orłowski [11], Huang and Yang [12], Evertsz [13], Lo [14], and Wen et al. [15, 16] have shown that the returns are of long-term (or short-term) dependence in the markets. After Black and Scholes [17] developed the option pricing theory based on the classical stochastic differential equation, a large number of literatures studied the option price based on the fractional Brownian motion. For example, Necula [18], Rostek [19], and Hu and Øksendal [20] obtained the Black-Scholes option pricing formula under fractional Brownian motion. Ren et al. [21] have considered the option pricing model for $0.5 < H < 1$.

In the case of $0 < H < 0.5$, the option pricing formula was studied by Wang et al. [22]. Chen et al. [23] established the mixed fractional-fractional version of Black-Scholes model with $0 < H < 1$ and gave the Ito's formula correspondingly.

However, the memory effects contain not only the noise memory effect but also the trend memory effect. Stochastic differential equation with fractional Brownian motion only describes the noise memory but cannot be used to study the trend memory effect of stock price. So we will describe the trend memory process by using the fractional derivative, which is another effective instrument to describe the memory effect. In particular, fractional calculus has been successfully applied in biology, physics, chemistry, and hydrology. Recently, the concept of fractal has been extended in financial mathematics [24]. This is due to the fact that fractional integral and derivatives can depict the memory and inherent process [25]. It has been realized that fractional derivative provides an excellent mathematical instrument for the description of complex process, irregular increment, memory properties, and intermediate process [25–28].

The fractional derivative is given as below:

$$d^{\alpha}x = \mu(x,t)\,dt^{\alpha}, \tag{1}$$

where α is a fraction. This fractional differential equation is an appropriate mathematical approach to depict memory process of the increment. However, the fractional order derivative above only denotes the memory effect of a fixed process. Since the process in financial market has stochastic effect, we add stochastic process into fractional order ordinary differential equation. In this work, we propose a new model constructed by stochastic differential equation with fractional order. We denote the stochastic process of the asset price by fractional order stochastic differential equation as follows:

$$d^{\alpha}x = \mu(x,t)\,dt^{\alpha} + \sigma(x,t)\,dB(t), \quad \alpha = 2H. \tag{2}$$

In (2), H is the Hurst index, which is an exponent describing the memory of the time series, and can be calculated by the R/SD analysis approach [6]. In the special case of $\alpha = 1$ (i.e., $H = 0.5$), the equation is reduced to the classic stochastic differential equation. Jumarie gave the Taylor's series of fractional order, expressed dx in terms of fractional differential $d^{\alpha}x$ by using Taylor's series of fractional order, and, hence, obtained the expression of $x(t)$, which involves the so-called Mittag-Leffler function [29, 30]. Momani and Odibat presented the numerical approach of differential equation of fractional order [31]. Odibat proposed algorithms to compute the functions of fractional derivative [32].

The rest of this paper is organized as follows. Section 2 gives some basic concepts and theories on the fractional order ordinary differential equations and Hurst index and then establishes the fractional order stochastic differential equation in the financial market. In Section 3, based on the proposed stochastic differential equation with fractional order derivative, we give the corresponding Ito formula under the FSDE and then derive the fractional European option pricing formula. In Section 4, we conduct the empirical analysis of fractional order formula of stock price process by using the Monte Carlo simulation method, and we also make comparison analysis of option pricing formula under FSDE with the classic option pricing formula and option pricing formula based on fractional Brownian motion. The conclusions drawn from this study are presented in Section 5.

2. Fractional Order Stochastic Differential Equation

In this section, we first give some preliminaries about the fractional order ordinary differential equation and then expand them to the field of the stochastic differential equations. Thus, based on these previous research results, we can construct the generalized fractional order stochastic differential equation.

2.1. Fractional Order Ordinary Differential Equations (FODE). Now we introduce the definitions of fractional order integration and fractional order derivative. There exist several definitions of fractional derivatives, which are related to different applications. In our paper, we consider these two definitions, which are Riemann-Liouville integral and Caputo derivative [30].

Definition 1. $f(x)$ is a continuous function. Its Riemann-Liouville fractional integral of order α of function $f(x)$ is defined as follows:

$$I^{\alpha}f(x) = \frac{1}{\Gamma(\alpha)}\int_0^x (x-t)^{\alpha-1}f(t)\,dt \quad \alpha > 0,\ x > 0, \tag{3}$$

where α is a fraction and $\Gamma(\alpha)$ is the Gamma function with $\Gamma(\alpha) = \int_0^{\infty} x^{\alpha-1}\exp(-x)dx$.

Definition 2. Consider the function of Definition 1, and Caputo fractional derivative of order α of function $f(x)$ is defined as

$$\begin{aligned}\frac{d^{\alpha}f}{dx^{\alpha}} &= D^{\alpha}f(x) = I^{m-\alpha}D^{m}f(x)\\ &= \frac{1}{\Gamma(m-\alpha)}\int_0^x (x-t)^{m-\alpha-1}f^{(m)}(t)\,dt,\end{aligned} \tag{4}$$

where α is a fraction, m is an integer and $m = [\alpha]$ is the value of α rounded up to the nearest integer, and $f^{(m)}$ is the ordinary derivative of f.

Based on the definitions above, the following equality holds [33, 34]:

$$f^{(\alpha)}(x) = \lim_{h\to 0}\frac{\Delta^{\alpha}f(x)}{h^{\alpha}}. \tag{5}$$

In order to get the relations between the fractional derivative and ordinary derivative, we introduce the Taylor expansion of fractional order.

Proposition 3. *Assume that the continuous function $f(x)$ has fractional derivative of fractional order $k\alpha$, for any positive integer k at any α, $0<\alpha<1$; then the following equality holds:*

$$f(x+h)=\sum_{k=0}^{\infty}\frac{h^{k\alpha}f^{(k\alpha)}(x)}{\Gamma(1+k\alpha)},\quad 0<\alpha\leq 1, \tag{6}$$

where $f^{(k\alpha)}$ is the derivative of order αk of $f(x)$, which can be denoted by $D^{k\alpha}f$.

Lemma 4. *Assume that $m<\alpha<m+1$, $m\in N$; then,*

$$f^{(m)}(x+h)=\sum_{k=0}^{\infty}\frac{h^{k(\alpha-m)}D^{k(\alpha-m)}f^{(m)}(x)}{\Gamma[1+k(\alpha-m)]},\quad m<\alpha<m+1. \tag{7}$$

Let m be equal to 1 in (7), and take integration with respect to h; we then have the following result:

$$f(x+h)=f(x)+hf'(x)+\sum_{k=1}^{\infty}\frac{h^{1+k(\alpha-1)}}{\Gamma[2+k(\alpha-1)]}f^{(1+k(\alpha-1))}(x). \tag{8}$$

The proof of the lemma above can be found in [29].

By employing the fractional order Taylor formula and (5), we get the applications below. Given that m is an integer with $m\geq 1$, the following results hold:

$$f^{(\alpha)}(x)=\lim_{h\to 0}\frac{\Delta^{\alpha}f(x)}{h^{\alpha}}=\Gamma(1+\alpha)\lim_{h\to 0}\frac{\Delta f(x)}{h^{\alpha}},\quad 0<\alpha\leq 1, \tag{9}$$

$$f^{(\alpha)}(x)=\Gamma(1+(\alpha-m)]\lim_{h\to 0}\frac{\Delta f^{(m)}(x)}{h^{\alpha-m}},\quad m<\alpha<m+1\quad(1\leq m). \tag{10}$$

We then compare the two equations, (8) and (9), when $1<\alpha<2$; thus, the relationship between fractional difference and finite difference is obtained as follows:

(1) Discrete form:

$$\Delta^{\alpha}f=\Gamma(1+\alpha)\Delta f,\quad 0<\alpha\leq 1$$

Continuous form:

$$d^{\alpha}f=\Gamma(1+\alpha)df,\quad 0<\alpha\leq 1$$

(2) Discrete form:

$$\Delta^{\alpha}f=\Gamma(1+\alpha)\left[\Delta f-f'(x)\Delta x\right],\quad 1<\alpha<2$$

Continuous form:

$$d^{\alpha}f=\Gamma(1+\alpha)\left[df-f'(x)dx\right],\quad 1<\alpha<2. \tag{11}$$

For the purpose of constructing the fractional order stochastic differential equations in this section, now we give some results of the integral with respect to dt^{α} in Lemma 5 presented below. Its detailed proof can be obtained in [29, 30].

Lemma 5. *Let $f(t)$ denote a continuous function; then its integral with respect to dt^{α} is defined by the following equalities:*

$$\text{(1)}\quad \int_0^t f(\tau)(d\tau)^{\alpha}=\alpha\int_0^t(t-\tau)^{\alpha-1}f(\tau)\,d\tau\quad 0<\alpha<1,$$
$$\text{(2)}\quad \int_0^t f(\tau)(d\tau)^{\alpha}=\alpha(\alpha-1)\int_0^t(t-\tau)^{\alpha-2}F(\tau)\,d\tau\quad 1<\alpha<2, \tag{12}$$

where $F(t)=\int_0^t f(\tau)d\tau$; on making $f(t)=1$, we can have the result: $\int_0^t f(\tau)(d\tau)^{\alpha}=t^{\alpha}$.

2.2. Memory Effect and the Hurst Index. Time series $X_t=\{X_1,X_2,\ldots,X_N\}$ is a stochastic process with X_t recorded at the discrete times $t=0,1,2,\ldots,N$. A time series has the memory structure, if the lag period information affects the future changes. Time series displays long memory when the correlation between current and lag observations does not weaken to zero quickly over time.

Let X_t be a stationary stochastic process with autocorrelation function $\rho(\tau)$, $\tau=1,2,\ldots,m$, where τ denotes the time lag. If $\sum_{\tau=1}^{m}|\rho(\tau)|=\infty$, X_t is called a long memory process; if $\sum_{\tau=1}^{m}|\rho(\tau)|<\infty$, X_t is called a short memory process, and, otherwise, if $\rho(\tau)=0$, for $\tau\neq 0$, X_t has no memory effect. The classical approach to measure the stochastic memory process is the autocorrelation function. Now, the Hurst index is widely used as an effective substitute of the autocorrelation function to determine long-range or short-range dependence.

The memory effect can be described by the memory parameter, namely, the Hurst index. Hurst index measures the smoothness of time series based on the asymptotic behavior of the rescale of the stochastic process. A key property of memory process is self-similarity, which is denoted by the Hurst index.

Definition 6. Stochastic process $X=\{X_t,\ t=1,2,\ldots,N\}$ is self-similar with Hurst index H for any $a>0$ and at any time t; then we denote it by $X_{at}\overset{d}{=}a^{H}X_t$, where Hurst index describes the self-similarity of stochastic process, and $\overset{d}{=}$ represents equality of the distribution.

In the following lemma, some basic properties are given and the corresponding proofs can be obtained in [6, 8].

Lemma 7. *Suppose a time series $\{X_t,\ t=1,2,\ldots,N\}$ is self-similar with strictly stationary increment; then this time series has the following properties.*

(1) *The expectation of X_t is $E[X_t]=0$ and, thus, $E[X_t^2]=\sigma^2$ for all $t=1,2,\ldots,N$.*

(2) *The covariance function $\gamma(s,t)=E\{[X_s-E(X_s)][X_t-E(X_t)]\}=E[X_sX_t]$, which has the following result:*

$$\gamma(s,t)=\frac{\sigma^2}{2}\left[|s|^{2H}-|s-t|^{2H}+|t|^{2H}\right]. \tag{13}$$

(3) *The autocovariance function of* X_t *is given by* $\gamma(\tau)$, $\tau = 1, 2, \ldots n$, *where* τ *is the lag period:*

$$\gamma(\tau) = E[X_t X_{t+\tau}] = \frac{\sigma^2}{2}\left[|\tau+1|^{2H} - 2|\tau|^{2H} + |\tau-1|^{2H}\right]. \tag{14}$$

(4) *If* $\tau \neq 0$, *then we get the relationship between autocovariance function and Hurst index:*

$$\begin{gathered} \gamma(\tau) = 0, \quad H = 0.5, \\ \gamma(\tau) < 0, \quad 0 < H < 0.5, \\ \gamma(\tau) > 0, \quad 0.5 < H < 1 \end{gathered} \tag{15}$$

which means $\gamma(\tau) > 0$ *in the case of* $0.5 < H < 1$; *similarly, in the case* $0 < H < 0.5$, $\gamma(\tau) < 0$, *and in the case* $H = 0.5$, $\gamma(\tau) = 0$. *According to the autocovariance function, we have that, in the case of* $0 < H < 0.5$, *the times series exhibit short-range dependence; in the case of* $H = 0.5$, *the times series has no dependence, which is a perfect random walk; and in the case of* $0.5 < H < 1$, *time series has long-range dependence.*

The Hurst indexis usually estimated by the R/S statistic approach. Given a stochastic process $\{X_t, t = 1, 2, \ldots, N\}$ of length N, we divide the time interval N into M contiguous subintervals of length n such that $M \times n = N$. For each subinterval, the average value is $X_n = E[X_t] = (1/n)\sum_{t=1}^{n} X_t$.

The running sum of the accumulated deviations from the mean is given as

$$X_{t,n} = \sum_{t=1}^{k}(X_t - E[X_t]), \quad k = 1, 2, \ldots, n. \tag{16}$$

The range over the time period n is

$$R(n) = \max X_{k,n} - \min X_{k,n}, \quad k = 1, 2, \ldots, n. \tag{17}$$

The standard deviation of X_t, $t = 1, 2, \ldots, n$ is

$$\mathrm{SD}(n) = \sqrt{\frac{1}{n-1}\sum_{t=1}^{n}(X_t - E[X_t])^2}. \tag{18}$$

The rescaled range is $(R/\mathrm{SD})(n) = R(n)/\mathrm{SD}(n)$, and the relationship between R/SD statistic and n is

$$\left(\frac{R}{\mathrm{SD}}\right)(n) = \frac{R(n)}{\mathrm{SD}(n)} = \frac{1}{n}\sum_{i=1}^{n}\frac{R(i)}{\mathrm{SD}(i)}. \tag{19}$$

Thus, we can get the result:

$$E\left[\frac{R(n)}{\mathrm{SD}(n)}\right] = \alpha n^H, \quad n \longrightarrow \infty, \tag{20}$$

where α is a constant and H is the Hurst index.

As a consequence, we can get the Hurst index of the observed time by linear regression:

$$\log E\left(\frac{R}{\mathrm{SD}}\right)(n) = H\log n + \log\alpha. \tag{21}$$

2.3. Fractional Order Stochastic Differential Equation (FSDE). Here, we generalize the classic stochastic differential equation to establish the fractional order stochastic differential equation based on the results presented before and then apply it to the option pricing in the next section.

Definition 8. Assuming that a financial asset price is S, according to the fractional ordinary differential equation, and considering the stochastic process, we can get the FSDE as follows:

$$d^\alpha S = \mu(S,t)(dt)^\alpha + \sigma(S,t)\,dB(t), \quad \alpha = 2H, \tag{22}$$

where $\mu(S,t)$ is the drift parameter, $\sigma(S,t)$ is the diffusion parameter, $dB(t)$ is the Wiener process, $dB(t) = \varepsilon\sqrt{dt}$, $\varepsilon \sim N(0,1)$ (normal distribution), and dt and $dB(t)$ are uncorrelated, $dtdt = 0$, $dtdB(t) = 0$, $dB(t)dB(t) = dt$.

In a special case, suppose $\mu(S,t) = \mu S$, $\sigma(S,t) = \sigma S$, and then we have the linear stochastic differential equation:

$$d^\alpha S = \mu S(dt)^\alpha + \sigma S\,dB(t), \quad \alpha = 2H. \tag{23}$$

By using the results of (11), we can rewrite (22) into the following form of dS with respect to dt^α:

$$\begin{aligned} dS &= \frac{\mu(S,t)}{\Gamma(1+\alpha)}(dt)^\alpha + \frac{\sigma(S,t)}{\Gamma(1+\alpha)}dB(t), \\ &\qquad 0 < \alpha \le 1, \quad 0 < H \le 0.5, \\ dS &= \frac{\mu(S,t)}{\Gamma(1+\alpha)}(dt)^\alpha + \frac{\sigma(S,t)}{\Gamma(1+\alpha)}dB(t) + S'(t)\,dt, \\ &\qquad 1 < \alpha < 2, \quad 0.5 < H < 1, \end{aligned} \tag{24}$$

where $S'(t)$ is the first order derivative of S about time t.

3. European Call Option Pricing Based on FOSDE

In this section, the corresponding Ito's formula and European call option pricing formula are derived based on the fractional order stochastic differential equation.

3.1. Ito's Lemma Based on FSDE

Lemma 9. *Assume that the stock price S follows the fractional order stochastic differential equation as below:*

$$d^\alpha S = \mu S(dt)^\alpha + \sigma S\,dB(t), \quad \alpha = 2H; \tag{25}$$

then, the function $f = f(S_t, t)$ *is still an Ito stochastic process, and the following expressions hold.*

When $0.25 < H \le 0.5$

$$\begin{aligned} df = {} & \left[\frac{\partial f}{\partial t} + \frac{\sigma^2 S^2}{2\Gamma^2(1+\alpha)}\frac{\partial^2 f}{\partial S^2}\right]dt + \frac{\mu S}{\Gamma(1+\alpha)}\frac{\partial f}{\partial S}(dt)^{2H} \\ & + \frac{\sigma S}{\Gamma(1+\alpha)}\frac{\partial f}{\partial S}dB(t). \end{aligned} \tag{26}$$

When $0.5 < H < 1$

$$df = \left[\frac{\partial f}{\partial t} + \frac{\sigma^2 S^2}{2\Gamma^2(1+\alpha)}\frac{\partial^2 f}{\partial S^2} + S'(t)\frac{\partial f}{\partial S}\right]dt + \frac{\mu S}{\Gamma(1+\alpha)}\frac{\partial f}{\partial S}(dt)^{2H} + \frac{\sigma S}{\Gamma(1+\alpha)}\frac{\partial f}{\partial S}dB(t). \tag{27}$$

Proof. According to the Ito formula, we notice that

$$\Delta f = \frac{\partial f}{\partial t}\Delta t + \frac{\partial f}{\partial S}\Delta S + \frac{1}{2}\frac{\partial^2 f}{\partial S^2}(\Delta S)^2 + \frac{\partial^2 f}{\partial S\partial t}(\Delta S\Delta t) + \frac{1}{2}\frac{\partial^2 f}{\partial t^2}(\Delta t)^2 \tag{28}$$

and the discrete form of $d^\alpha S = \mu S(dt)^\alpha + \sigma S dB(t)$ is $\Delta^\alpha S = \mu S(\Delta t)^\alpha + \sigma S\Delta B(t)$. □

In this paper, we only consider the case that $0.25 < H < 1$. There are two reasons for this consideration: first, the Hurst index H is much larger than 0 generally; second, when $0.25 < H < 1$, $\alpha = 2H > 0.5$, $(\Delta t)^{2\alpha}$ and $(\Delta t)^{\alpha+0.5}$ are infinitesimal. Hence, we do not need to consider the case of $0 < H \le 0.25$.

(1) In the case of $0.25 < H \le 0.5$, since $E(\varepsilon) = 0$, $E(\varepsilon^2) = 1$, we have

$$\begin{gathered}\Delta S = \frac{\mu S}{\Gamma(1+\alpha)}(\Delta t)^\alpha + \frac{\sigma S}{\Gamma(1+\alpha)}\varepsilon(\Delta t)^{1/2},\\ \Delta S\Delta t = \frac{\mu S}{\Gamma(1+\alpha)}(\Delta t)^{\alpha+1} + \frac{\sigma S}{\Gamma(1+\alpha)}\varepsilon(\Delta t)^{1.5} \longrightarrow 0,\\ 0 < H \le 0.5.\end{gathered} \tag{29}$$

$$(\Delta S)^2 = \frac{\mu^2 S^2}{\Gamma^2(1+\alpha)}(\Delta t)^{2\alpha} + \frac{\sigma^2 S^2}{\Gamma^2(1+\alpha)}\varepsilon^2(\Delta t) + \frac{2\mu\sigma S^2}{\Gamma^2(1+\alpha)}\varepsilon(\Delta t)^{\alpha+0.5} \longrightarrow \frac{\sigma^2 S^2}{\Gamma^2(1+\alpha)}(\Delta t).$$

According to the Ito formula presented above, we can get

$$\begin{aligned}\Delta f &= \frac{\partial f}{\partial t}\Delta t + \frac{\partial f}{\partial S}\Delta S + \frac{1}{2}\frac{\partial^2 f}{\partial S^2}(\Delta S)^2 + \frac{\partial^2 f}{\partial S\partial t}(\Delta S\Delta t) + \frac{1}{2}\frac{\partial^2 f}{\partial t^2}(\Delta t)^2\\ &= \frac{\partial f}{\partial t}\Delta t + \frac{\partial f}{\partial S}\Delta S + \frac{1}{2}\frac{\partial^2 f}{\partial S^2}(\Delta S)^2\\ &= \frac{\partial f}{\partial t}\Delta t + \frac{\partial f}{\partial S}\left[\frac{\mu S}{\Gamma(1+\alpha)}(\Delta t)^\alpha + \frac{\sigma S}{\Gamma(1+\alpha)}\varepsilon(\Delta t)^{0.5}\right] + \frac{\sigma^2 S^2}{2\Gamma^2(1+\alpha)}\frac{\partial^2 f}{\partial S^2}(\Delta t)\\ &= \left[\frac{\partial f}{\partial t} + \frac{\sigma^2 S^2}{2\Gamma^2(1+\alpha)}\frac{\partial^2 f}{\partial S^2}\right]\Delta t + \frac{\mu S}{\Gamma(1+\alpha)}\frac{\partial f}{\partial S}(\Delta t)^{2H} + \frac{\sigma S}{\Gamma(1+\alpha)}\frac{\partial f}{\partial S}\varepsilon(\Delta t)^{0.5}.\end{aligned} \tag{30}$$

Thus, the differential form is given below:

$$df = \left[\frac{\partial f}{\partial t} + \frac{\sigma^2 S^2}{2\Gamma^2(1+\alpha)}\frac{\partial^2 f}{\partial S^2}\right]dt + \frac{\mu S}{\Gamma(1+\alpha)}\frac{\partial f}{\partial S}(dt)^{2H} + \frac{\sigma S}{\Gamma(1+\alpha)}dB(t). \tag{31}$$

(2) In the case of $0.5 < H < 1$

$$\begin{aligned}\Delta S &= \frac{\mu S}{\Gamma(1+\alpha)}(\Delta t)^\alpha + \frac{\sigma S}{\Gamma(1+\alpha)}\varepsilon(\Delta t)^{0.5} + S'(t)\Delta t,\\ \Delta S\Delta t &= \frac{\mu S}{\Gamma(1+\alpha)}(\Delta t)^{\alpha+1} + \frac{\sigma S}{\Gamma(1+\alpha)}\varepsilon(\Delta t)^{1.5} + S'(t)(\Delta t)^2 \longrightarrow 0,\\ (\Delta S)^2 &= \frac{\mu^2 S^2}{\Gamma^2(1+\alpha)}(\Delta t)^{2\alpha} + \frac{\sigma^2 S^2}{\Gamma^2(1+\alpha)}\varepsilon^2\Delta t + \left[S'(t)\right]^2(\Delta t)^2 + \frac{2\mu\sigma S^2}{\Gamma^2(1+\alpha)}\varepsilon(\Delta t)^{\alpha+0.5} + \frac{2\mu SS'(t)}{\Gamma(1+\alpha)}(\Delta t)^{\alpha+1}\\ &\quad + \frac{2\sigma SS'(t)}{\Gamma(1+\alpha)}\varepsilon(\Delta t)^{1.5} \longrightarrow \frac{\sigma^2 S^2}{\Gamma^2(1+\alpha)}\Delta t,\\ \Delta f &= \frac{\partial f}{\partial t}\Delta t + \frac{\partial f}{\partial S}\Delta S + \frac{1}{2}\frac{\partial^2 f}{\partial S^2}(\Delta S)^2\\ &= \frac{\partial f}{\partial t}\Delta t + \frac{\partial f}{\partial S}\left[\frac{\mu S}{\Gamma(1+\alpha)}(\Delta t)^\alpha + \frac{\sigma S}{\Gamma(1+\alpha)}\varepsilon(\Delta t)^{0.5} + S'(t)\Delta t\right] + \frac{\sigma^2 S^2}{2\Gamma^2(1+\alpha)}\frac{\partial^2 f}{\partial S^2}\Delta t\\ &= \left[\frac{\partial f}{\partial t} + \frac{\sigma^2 S^2}{2\Gamma^2(1+\alpha)}\frac{\partial^2 f}{\partial S^2} + S'(t)\frac{\partial f}{\partial S}\right]\Delta t + \frac{\mu S}{\Gamma(1+\alpha)}\frac{\partial f}{\partial S}(\Delta t)^{2H} + \frac{\sigma S}{\Gamma(1+\alpha)}\frac{\partial f}{\partial S}\varepsilon(\Delta t)^{0.5}.\end{aligned} \tag{32}$$

Similarly, we obtain the differential form as follows:

$$df = \left[\frac{\partial f}{\partial t} + \frac{\sigma^2 S^2}{2\Gamma^2(1+\alpha)}\frac{\partial^2 f}{\partial S^2} + S'(t)\frac{\partial f}{\partial S}\right]dt + \frac{\mu S}{\Gamma(1+\alpha)}\frac{\partial f}{\partial S}(dt)^{2H} + \frac{\sigma S}{\Gamma(1+\alpha)}\frac{\partial f}{\partial S}dB(t). \tag{33}$$

To price a European option, we first introduce Lemma 10, which connects the fractional order stochastic differential equations to the partial differential equations.

Lemma 10. *$f(S(t), t)$ is the solution of the partial differential equations:*

$$\frac{\partial f}{\partial t} + rS\frac{\partial f}{\partial S} + \frac{\sigma^2 S^2}{2\Gamma^2(1+\alpha)}\frac{\partial^2 f}{\partial S^2} - rf = 0, \quad 0.25 < H \le 0.5,$$
$$f(S(T), T) = f(S(T)),$$
$$\frac{\partial f}{\partial t} + \left[S'(t) + rS\right]\frac{\partial f}{\partial S} + \frac{\sigma^2 S^2}{2\Gamma^2(1+\alpha)}\frac{\partial^2 f}{\partial S^2} - rf = 0,$$
$$0.5 < H < 1,$$
$$f(S(T), T) = f(S(T)). \tag{34}$$

Proof. First, make portfolios $\Pi = \Delta S - f$ and $d\Pi = \Delta dS - df$.

(1) In the case of $0.25 < H \le 0.5$,

$$\begin{aligned} d\Pi &= \Delta dS - df \\ &= \Delta\left[\frac{\mu S}{\Gamma(1+\alpha)}dt^{\alpha} + \frac{\sigma S}{\Gamma(1+\alpha)}dB(t)\right] \\ &\quad - \left[\left[\frac{\partial f}{\partial t} + \frac{\sigma^2 S^2}{2\Gamma^2(1+\alpha)}\frac{\partial^2 f}{\partial S}\right]dt \right.\\ &\qquad \left. + \left[\frac{\mu S}{\Gamma(1+\alpha)}\frac{\partial f}{\partial S}\right](dt)^{2H} + \frac{\sigma S}{\Gamma(1+\alpha)}\frac{\partial f}{\partial S}dB(t)\right] \\ &= -\left[\frac{\partial f}{\partial t} + \frac{\sigma^2 S^2}{2\Gamma^2(1+\alpha)}\frac{\partial^2 f}{\partial S}\right]dt \\ &\quad + \frac{\mu S}{\Gamma(1+\alpha)}\left(\Delta - \frac{\partial f}{\partial S}\right)(dt)^{2H} \\ &\quad + \frac{\sigma S}{\Gamma(1+\alpha)}\left(\Delta - \frac{\partial f}{\partial S}\right)dB(t). \end{aligned} \tag{35}$$

When $\Delta = \partial f/\partial S$, we can get the riskless asset portfolio

$$d\Pi = \Delta dS - df = -\left[\frac{\partial f}{\partial t} + \frac{\sigma^2 S^2}{2\Gamma^2(1+\alpha)}\frac{\partial^2 f}{\partial S^2}\right]dt. \tag{36}$$

And because the portfolio Π is riskless, according to the Bellman Equation, we have $d\Pi = r\Pi dt$, where r is the riskless rate. Thus, we get the equation $d\Pi = r\Pi dt = -[(\partial f/\partial t) + (\sigma^2 S^2/2\Gamma^2(1+\alpha))(\partial^2 f/\partial S^2)]dt$. Consequently, we obtain the first partial differential equation

$$\frac{\partial f}{\partial t} + rS\frac{\partial f}{\partial S} + \frac{\sigma^2 S^2}{2\Gamma^2(1+\alpha)}\frac{\partial^2 f}{\partial S^2} - rf = 0. \tag{37}$$

(2) In the case of $0.5 < H < 1$,

$$\begin{aligned} \Delta\Pi &= \Delta dS - df \\ &= \Delta\left[\frac{\mu S}{\Gamma(1+\alpha)}(dt)^{\alpha} + \frac{\sigma S}{\Gamma(1+\alpha)}dB(t) + S'(t)\,dt\right] \\ &\quad - \left\{\left[\frac{\partial f}{\partial t} + \frac{\sigma^2}{2\Gamma^2(1+\alpha)}\frac{\partial^2 f}{\partial S^2} + x'(t)\frac{\partial f}{\partial S}\right]dt \right.\\ &\qquad \left. + \frac{\mu}{\Gamma(1+\alpha)}\frac{\partial f}{\partial S}(dt)^{2H} + \frac{\sigma}{\Gamma(1+\alpha)}\frac{\partial f}{\partial S}dB(t)\right\} \\ &= -\left[\frac{\partial f}{\partial t} + \frac{\sigma^2}{2\Gamma^2(1+\alpha)}\frac{\partial^2 f}{\partial S^2} + S'(t)\frac{\partial f}{\partial S}\right]dt \\ &\quad + \frac{\mu S}{\Gamma(1+\alpha)}\left(\Delta - \frac{\partial f}{\partial S}\right)(dt)^{2H} \\ &\quad + \frac{\sigma S}{\Gamma(1+\alpha)}\left(\Delta - \frac{\partial f}{\partial S}\right)dB(t). \end{aligned} \tag{38}$$

When $\Delta = \partial f/\partial S$, we can also get the riskless asset portfolio

$$d\Pi = \Delta dS - df = -\left[\frac{\partial f}{\partial t} + \frac{\sigma^2}{2\Gamma^2(1+\alpha)}\frac{\partial^2 f}{\partial S^2} + S'(t)\frac{\partial f}{\partial S}\right]dt. \tag{39}$$

And again because Π is riskless, we can get the equation

$$d\Pi = r\Pi dt = -\left[\frac{\partial f}{\partial t} + \frac{\sigma^2}{2\Gamma^2(1+\alpha)}\frac{\partial^2 f}{\partial S^2} + S'(t)\frac{\partial f}{\partial S}\right]dt. \tag{40}$$

Similarly, the second partial differential equation can be obtained as below:

$$\frac{\partial f}{\partial t} + \left[S'(t) + rS\right]\frac{\partial f}{\partial S} + \frac{\sigma^2 S^2}{2\Gamma^2(1+\alpha)}\frac{\partial^2 f}{\partial S^2} - rf = 0. \tag{41}$$

□

3.2. European Call Option Based on FSDE. Before we proceed to price the European call option, we make the assumptions as below:

(1) r is the riskless rate and is a constant;

(2) the exchange of the stock is continuous and the stock can be divided;

(3) the tax of the stock exchange is free;

(4) the bonus of the stock cannot be paid within the duration of derivatives;

(5) no arbitrage exists in the market;

(6) the price of stock follows a fractional order stochastic differential equation

$$\frac{d^{\alpha}S}{S} = r(dt)^{\alpha} + \sigma dB(t), \quad \alpha = 2H; \tag{42}$$

(7) the strike price is K;

(8) the maturity is T,

where S is the price of the stock and r is the riskless interest rate; σ is the volatility of the price of stock; H is Hurst parameter of the stock.

In the following work, we will derive the fractional option pricing formula based on the risk-neutral assumption. If the price of underlying asset is subject to the geometric Brownian motion and the return μ is equal to the riskless interest rate r (i.e., $\mu = r$), we have

$$\frac{d^{\alpha}S}{S} = r(dt)^{\alpha} + \sigma dB(t), \quad \alpha = 2H. \tag{43}$$

(1) In the case of $0.25 < H \leq 0.5$, according to Ito's Lemma 9, we can get the price of the stock as

$$\begin{aligned} d(\ln S) = {} & \frac{r}{\Gamma(1+\alpha)}(dt)^{2H} - \frac{\sigma^2}{2\Gamma^2(1+\alpha)}dt \\ & + \frac{\sigma}{\Gamma(1+\alpha)}dB(t), \quad 0.25 < H \leq 0.5. \end{aligned} \tag{44}$$

Integrate (44) and use Lemma 5; then, we can get the solution of S:

$$\begin{aligned} S_T = S\exp\Bigg(& \frac{r}{\Gamma(1+\alpha)}\left(T^{2H} - t^{2H}\right) - \frac{\sigma^2}{2\Gamma^2(1+\alpha)}(T-t) \\ & + \frac{\sigma}{\Gamma(1+\alpha)}(B(T) - B(t))\Bigg). \end{aligned} \tag{45}$$

Therefore, the European call option pricing formula follows:

$$c = Se^{(r/\Gamma(1+\alpha))(T^{2H}-t^{2H})-r(T-t)}N(d_1) - Ke^{-r(T-t)}N(d_2), \tag{46}$$

where

$$\begin{aligned} d_1 = {} & \Bigg(\Gamma(1+\alpha)\ln\frac{S}{K} + r\left(T^{2H} - t^{2H}\right) \\ & + \frac{\sigma^2}{2\Gamma(1+\alpha)}(T-t)\Bigg)\left(\sigma\sqrt{T-t}\right)^{-1} \\ d_2 = {} & \Bigg(\Gamma(1+\alpha)\ln\frac{S}{K} + r\left(T^{2H} - t^{2H}\right) \\ & - \frac{\sigma^2}{2\Gamma(1+\alpha)}(T-t)\Bigg)\left(\sigma\sqrt{T-t}\right)^{-1}. \end{aligned} \tag{47}$$

Proof. The price of the European option is given by $c = e^{-r(T-t)}E[\max(S_T - K), 0]$, where $E(\cdot)$ is the expectation of the option price based on risk-neutral, and the price of the asset S_T obeys the lognormal distribution:

$$\begin{aligned} & \ln S_T - \ln S \\ & \sim N\Bigg(\frac{r}{\Gamma(1+\alpha)}\left(T^{2H} - t^{2H}\right) \\ & \qquad - \frac{\sigma^2}{2\Gamma^2(1+\alpha)}(T-t), \frac{\sigma^2}{\Gamma^2(1+\alpha)}(T-t)\Bigg). \end{aligned} \tag{48}$$

Let $W = (\ln S_T - m)/s$; obviously, $W \sim N(0,1)$, and the probability density function $h(W) = (1/\sqrt{2\pi})e^{-W^2/2}$, where $m = E(\ln S_T) = \ln S + (r/\Gamma(1+\alpha))(T^{2H} - t^{2H}) - (\sigma^2/2\Gamma^2(1+\alpha))(T-t)$, and $s = \sigma\sqrt{T-t}/\Gamma(1+\alpha)$. Hence,

$$\begin{aligned} & E[\max(S_T - K, 0)] \\ & = \int_{-\infty}^{+\infty} \max(S_T - K, 0)\, h(S_T)\, dS(T) \\ & = \int_{K}^{+\infty} (S_T - K)\, h(S_T)\, dS_T + \int_{-\infty}^{K} 0h(S_T)\, dS_T \\ & = \int_{\ln K}^{+\infty} \left(e^{S_T} - K\right) h(\ln S_T)\, d(\ln S_T) \\ & = \int_{(\ln K - m)/s}^{+\infty} \left(e^{S_T} - K\right) h\left(\frac{\ln S_T - m}{s}\right) d\left(\frac{\ln S_T - m}{s}\right) \\ & = \int_{(\ln K - m)/s}^{+\infty} \left(e^{S_T} - K\right) h(\ln S_T)\, d(\ln S_T) \\ & = \int_{(\ln K - m)/s}^{+\infty} \left(e^{sW+m} - K\right) h(W)\, dW \\ & = \int_{(\ln K - m)/s}^{+\infty} e^{(s^2/2)+m}\frac{1}{\sqrt{2\pi}}e^{-(W-s)^2/2}dW \\ & \quad - KN\left(\frac{m - \ln K}{s}\right) \\ & = Se^{(r/\Gamma(1+\alpha))(T^{2H}-t^{2H})}N(d_1) - KN(d_2), \end{aligned} \tag{49}$$

where

$$\begin{aligned} d_1 = {} & \Bigg(\Gamma(1+\alpha)\ln\frac{S}{K} + r\left(T^{2H} - t^{2H}\right) \\ & + \frac{\sigma^2}{2\Gamma(1+\alpha)}(T-t)\Bigg)\left(\sigma\sqrt{T-t}\right)^{-1}, \\ d_2 = {} & \Bigg(\Gamma(1+\alpha)\ln\frac{S}{K} + r\left(T^{2H} - t^{2H}\right) \\ & - \frac{\sigma^2}{2\Gamma(1+\alpha)}(T-t)\Bigg)\left(\sigma\sqrt{T-t}\right)^{-1}. \end{aligned} \tag{50}$$

So we get the European option pricing formula as follows:

$$\begin{aligned} c &= e^{-r(T-t)} E\left[\max\left(S_T - K, 0\right)\right] \\ &= e^{-r(T-t)} \left[S e^{(r/\Gamma(1+\alpha))(T^{2H}-t^{2H})} N\left(d_1\right) - KN\left(d_2\right)\right] \\ &= S e^{(r/\Gamma(1+\alpha))(T^{2H}-t^{2H})-r(T-t)} N\left(d_1\right) \\ &\quad - K e^{-r(T-t)} N\left(d_2\right). \end{aligned} \tag{51}$$

□

(2) In the case of $0.5 < H < 1$, in a similar way, according to Ito's Lemma 9, the price of the stock is

$$\begin{aligned} d\left(\ln S\right) = {} & \frac{r}{\Gamma\left(1+\alpha\right)} (dt)^{2H} + \left(\frac{S'}{S} - \frac{\sigma^2}{2\Gamma^2\left(1+\alpha\right)}\right) dt \\ & + \frac{\sigma}{\Gamma\left(1+\alpha\right)} dB\left(t\right). \end{aligned} \tag{52}$$

Notice that $(S'/S)dt = d(\ln S) = \ln S_{t+1} - \ln S_t = m(t)$, $m(t)$ represents the daily logarithm returns of stock S, and $m(t) = \mu(t)dt$, $\mu(t)$ is the returns of one year; thus, $S'/S = \mu(t)$, and (52) can be written as below:

$$\begin{aligned} d\left(\ln S\right) = {} & \frac{r}{\Gamma\left(1+\alpha\right)} (dt)^{2H} + \left(\mu\left(t\right) - \frac{\sigma^2}{2\Gamma^2\left(1+\alpha\right)}\right) dt \\ & + \frac{\sigma}{\Gamma\left(1+\alpha\right)} dB\left(t\right). \end{aligned} \tag{53}$$

By integrating (52) and employing Lemma 5, we get the solution of S:

$$\begin{aligned} S_T = S \exp\Bigg[& \frac{r}{\Gamma\left(1+\alpha\right)} \left(T^{2H} - t^{2H}\right) + \int_t^T \mu\left(s\right) ds \\ & - \frac{\sigma^2}{2\Gamma^2\left(1+\alpha\right)} \left(T-t\right) + \frac{\sigma}{\Gamma\left(1+\alpha\right)} \left(B\left(T\right) - B\left(t\right)\right)\Bigg]. \end{aligned} \tag{54}$$

Consequently, the European call option pricing formula is obtained:

$$\begin{aligned} c = {} & S e^{(r/\Gamma(1+\alpha))(T^{2H}-t^{2H}) + \int_t^T \mu(s)ds - r(T-t)} N\left(d_1\right) \\ & - K e^{-r(T-t)} N\left(d_2\right), \end{aligned} \tag{55}$$

where

$$\begin{aligned} d_1 = {} & \left(\Gamma\left(1+\alpha\right) \ln\frac{S}{K} + \int_t^T \mu\left(s\right) ds \right. \\ & \left. + r\left(T^{2H} - t^{2H}\right) + \frac{\sigma^2}{2\Gamma\left(1+\alpha\right)} \left(T-t\right)\right) \left(\sigma\sqrt{T-t}\right)^{-1}, \\ d_2 = {} & \left(\Gamma\left(1+\alpha\right) \ln\frac{S}{K} + \int_t^T \mu\left(s\right) ds + r\left(T^{2H} - t^{2H}\right) \right. \\ & \left. - \frac{\sigma^2}{2\Gamma\left(1+\alpha\right)} \left(T-t\right)\right) \left(\sigma\sqrt{T-t}\right)^{-1}. \end{aligned} \tag{56}$$

Proof. Let $W = (\ln S_T - m)/s$, and it is obvious that $W \sim N(0,1)$, so the probability density function $h(W) = (1/\sqrt{2\pi})e^{-W^2/2}$, where

$$\begin{aligned} m &= \widehat{E}\left(\ln S_T\right) \\ &= \ln S + \int_t^T \mu\left(s\right) ds - \frac{\sigma^2}{2\Gamma^2\left(1+\alpha\right)} \left(T-t\right) \\ &\quad + \frac{r}{\Gamma\left(1+\alpha\right)} \left(T^{2H} - t^{2H}\right), \quad s = \frac{\sigma(T-t)^{0.5}}{\Gamma\left(1+\alpha\right)}. \end{aligned} \tag{57}$$

Hence,

$$\begin{aligned} & E\left[\max\left(S_T - K, 0\right)\right] \\ &= \int_{-\infty}^{+\infty} \max\left(S_T - K, 0\right) h\left(S_T\right) dS_T \\ &= \int_K^{+\infty} \left(S_T - K\right) h\left(S_T\right) dS_T \\ &= \int_{(\ln K - m)/s}^{+\infty} \left(e^{sW+m} - K\right) h\left(W\right) dW \\ &= \int_{(\ln K - m)/s}^{+\infty} e^{(s^2/2)+m} \frac{1}{\sqrt{2\pi}} e^{-(W-s)^2/2} dW \\ &\quad - KN\left(\frac{m - \ln K}{s}\right) \\ &= S e^{\int_t^T \mu(s)ds + (r/\Gamma(1+\alpha))(T^{2H}-t^{2H})} N\left(d_1\right) - KN\left(d_2\right), \end{aligned} \tag{58}$$

where

$$\begin{aligned} d_1 = {} & \left(\Gamma\left(1+\alpha\right) \ln\frac{S}{K} + \int_t^T \mu\left(s\right) ds + r\left(T^{2H} - t^{2H}\right) \right. \\ & \left. + \frac{\sigma^2}{2\Gamma\left(1+\alpha\right)} \left(T-t\right)\right) \left(\sigma\sqrt{T-t}\right)^{-1}, \\ d_2 = {} & \left(\Gamma\left(1+\alpha\right) \ln\frac{S}{K} + \int_t^T \mu\left(s\right) ds + r\left(T^{2H} - t^{2H}\right) \right. \\ & \left. - \frac{\sigma^2}{2\Gamma\left(1+\alpha\right)} \left(T-t\right)\right) \left(\sigma\sqrt{T-t}\right)^{-1}. \end{aligned} \tag{59}$$

Finally, the European option pricing formula is given as below:

$$\begin{aligned} c &= e^{-r(T-t)} E\left[\max\left(S_T - K, 0\right)\right] \\ &= e^{-r(T-t)} \left[S e^{\int_t^T \mu(s)ds + (r/\Gamma(1+\alpha))(T-t)^{2H}} N\left(d_1\right) - KN\left(d_2\right)\right] \\ &= S e^{(r/\Gamma(1+\alpha))(T^{2H}-t^{2H}) + \int_t^T \mu(s)ds - r(T-t)} N\left(d_1\right) \\ &\quad - K e^{-r(T-t)} N\left(d_2\right). \end{aligned} \tag{60}$$

From the result we derived, the option price formula contains mean value function $\int_t^T \mu(s)ds$ of the logarithmic returns of stock price, which is the effect of trend memory. Therefore, we proved that trend memory exists in the financial systems.

Now, we give the European call option pricing formula under the risk-neutral measure. Let the mean returns of stock be equal to the riskless rate r; by taking the expectation of the returns in case $0.5 < H < 1$, we have $E[\mu(t)] = \mu = r$, where r is the riskless returns. Then, we simplify the mean value function $\int_t^T \mu(s)ds = \int_t^T \mu\, ds = \mu(T-t) = r(T-t)$ and have $\mu - r = 0$; thus, we get the option pricing formula

$$c = Se^{(r/\Gamma(1+\alpha))(T^{2H}-t^{2H})} N(d_1) - Ke^{-r(T-t)} N(d_2), \tag{61}$$

where

$$\begin{aligned} d_{41} &= \left(\Gamma(1+\alpha)\ln\frac{S}{K} + r\left(T^{2H}-t^{2H}\right) \right. \\ &\quad \left. + \left(r + \frac{\sigma^2}{2\Gamma(1+\alpha)}\right)(T-t)\right)\left(\sigma\sqrt{T-t}\right)^{-1}, \\ d_{42} &= \left(\Gamma(1+\alpha)\ln\frac{S}{K} + r\left(T^{2H}-t^{2H}\right) \right. \\ &\quad \left. + \left(r - \frac{\sigma^2}{2\Gamma(1+\alpha)}\right)(T-t)\right)\left(\sigma\sqrt{T-t}\right)^{-1}. \end{aligned} \tag{62}$$

□

4. Results and Discussion

To explain the memory effects in financial market, we make some comparisons in this section between our proposed European option pricing model and its underlying stock price equation and the well-known classic models, such as the Black-Scholes model (Black and Scholes (1973) [17]) and Black-Scholes model under fractional Brownian motion (Necula (2002) [18], Hu and Øksendal (2003) [20]).

4.1. Comparing European Pricing Formula with Other Models. (1) Classical Black-Scholes model: $dS = rSdt + \sigma SdB(t)$ [17].

The European option pricing formula is $c = SN(d_{11}) - Ke^{-r(T-t)}N(d_{12})$, where

$$\begin{aligned} d_{11} &= \frac{\ln(S/K) + \left(r + \sigma^2/2\right)(T-t)}{\sigma\sqrt{T-t}}, \\ d_{12} &= \frac{\ln(S/K) + \left(r - \sigma^2/2\right)(T-t)}{\sigma\sqrt{T-t}}. \end{aligned} \tag{63}$$

The classical Black-Scholes model was established under the assumption that the price process is Markov process and that the price process is independent and has no memory effect; however, the memory effects exist in price process.

(2) SDE with fractional Brownian motion: $dS = rSdt + \sigma SdB_H(t)$ [18, 20].

The European option pricing formula is $c = SN(d_{21}) - Ke^{-r(T-t)}N(d_{22})$, where

$$\begin{aligned} d_{21} &= \frac{\ln(S/K) + r(T-t) + \left(\sigma^2/2\right)\left(T^{2H}-t^{2H}\right)}{\sigma\left(T^H - t^H\right)}, \\ d_{22} &= \frac{\ln(S/K) + r(T-t) - \left(\sigma^2/2\right)\left(T^{2H}-t^{2H}\right)}{\sigma\left(T^H - t^H\right)}. \end{aligned} \tag{64}$$

The fractional Brownian motion model has improved the Black-Scholes model by considering the memory effect of the asset price but only considered the memory effect of the noise.

(3) Fractional order SDE (FSDE model): $d^\alpha S = rS(dt)^\alpha + \sigma SdB(t)$, $\alpha = 2H$.

In the case of $0.25 < H \le 0.5$, the European call option pricing formula is

$$c = Se^{(r/\Gamma(1+\alpha))(T-t)^{2H} - r(T-t)} N(d_{31}) - Ke^{-r(T-t)} N(d_{32}), \tag{65}$$

where

$$\begin{aligned} d_{31} &= \left(\Gamma(1+\alpha)\ln\frac{S}{K} + r\left(T^{2H}-t^{2H}\right) \right. \\ &\quad \left. + \frac{\sigma^2}{2\Gamma(1+\alpha)}(T-t)\right)\left(\sigma\sqrt{T-t}\right)^{-1}, \\ d_{32} &= \left(\Gamma(1+\alpha)\ln\frac{S}{K} + r\left(T^{2H}-t^{2H}\right) \right. \\ &\quad \left. - \frac{\sigma^2}{2\Gamma(1+\alpha)}(T-t)\right)\left(\sigma\sqrt{T-t}\right)^{-1}. \end{aligned} \tag{66}$$

When $H = 0.5$, the option formula is reduced to the classic option formula.

In the case of $0.5 < H < 1$, the European call option pricing formula is

$$c = Se^{(r/\Gamma(1+\alpha))(T^{2H}-t^{2H})} N(d_{41}) - Ke^{-r(T-t)} N(d_{42}), \tag{67}$$

where

$$\begin{aligned} d_{41} &= \left(\Gamma(1+\alpha)\ln\frac{S}{K} + r\left(T^{2H}-t^{2H}\right) \right. \\ &\quad \left. + \left(r + \frac{\sigma^2}{2\Gamma(1+\alpha)}\right)(T-t)\right)\left(\sigma\sqrt{T-t}\right)^{-1}, \\ d_{42} &= \left(\Gamma(1+\alpha)\ln\frac{S}{K} + r\left(T^{2H}-t^{2H}\right) \right. \\ &\quad \left. + \left(r - \frac{\sigma^2}{2\Gamma(1+\alpha)}\right)(T-t)\right)\left(\sigma\sqrt{T-t}\right)^{-1}. \end{aligned} \tag{68}$$

In the paper, our model takes a new memory effect into consideration, which is called the trend memory effect of the asset price.

Table 1: Simulation results of SDE model.

Simulation times	Real value	Mean value	Standard deviation	Error rate	Confidence interval
100	2445	2351.9	198.6958	3.81%	[2313, 2390.8]
1000	2445	2358.7	195.7074	3.53%	[2346.5, 2370.8]
10000	2445	2357	200.5667	3.60%	[2353.1, 2360.9]
100000	2445	2360	202.2802	3.48%	[2358.7, 2361.2]

Table 2: Simulation results of SDE with FBM.

Simulation times	Real value	Mean value	Standard deviation	Error rate	Confidence interval
100	2445	2358.2	77.4242	3.55%	[2343.0, 2373.3]
1000	2445	2360.8	76.3254	3.44%	[2356.1, 2365.6]
10000	2445	2360	78.0423	3.48%	[2358.6, 2361.6]
100000	2445	2361.2	78.5882	3.43%	[2360.8, 2361.7]

Table 3: Simulation results of FSDE.

Simulation times	Real value	Mean value	Standard deviation	Error rate	Confidence interval
100	2445	2362.7	19.0566	3.37%	[2359.1, 2366.5]
1000	2445	2368.4	21.1279	3.13%	[2367.2, 2369.8]
10000	2445	2367.0	19.7396	3.19%	[2366.7, 2367.5]
100000	2445	2369.5	20.4312	3.09%	[2369.5, 2369.7]

4.2. Comparing the Asset Price Equation with Other Models. The underlying asset price equations to be used to make comparison are given as follows:

(1) the SDE model: $dS = rSdt + \sigma S dB(t)$ [17].

The stock price equation is $S_T = S\exp[(r-\sigma^2/2)(T-t)+\sigma\Delta B(t)]$;

(2) the SDE model with fractional Brownian motion: $dS = rSdt + \sigma S dB_H(t)$ [18, 20].

The stock price equation is $S_T = S\exp[r(T-t)-\sigma^2(T-t)^{2H}+\sigma\Delta B_H(t)]$;

(3) the fractional order SDE model: $d^\alpha S = rS(dt)^\alpha + \sigma S dB(t)$, $\alpha = 2H$;

when $0.25 < H \le 0.5$, the stock price equation is

$$S_t = S_{t-1}\exp\left[\frac{r}{\Gamma(1+\alpha)}\Delta t^{2H} - \frac{\sigma^2}{2\Gamma^2(1+\alpha)}\Delta t + \frac{\sigma}{\Gamma(1+\alpha)}\varepsilon\Delta B(t)\right]. \tag{69}$$

However, when $0.5 < H < 1$, the stock price equation is

$$S_t = S_{t-1}\exp\left[\frac{r}{\Gamma(1+\alpha)}\Delta t^{2H} + \left(r - \frac{\sigma^2}{2\Gamma^2(1+\alpha)}\right)\Delta t + \frac{\sigma}{\Gamma(1+\alpha)}\varepsilon\Delta B(t)\right]. \tag{70}$$

To illustrate the proposed FSDE model, we simulate the three types of stochastic differential equations presented above by using the Monte Carlo simulation method and then make comparison of these three different models. The data used in the empirical analysis is the daily closing price index series of CSI300 index of China. The time range is from January 4, 2012, to October 27, 2012, with the initial value $S_0 = 2299$ (the price index on January 4, 2012) and the final value $S_T = 2445$. We choose the one-year bonds interest rate $r = 2.65\%$ in China as the riskless rate and the mean yield $\mu = 0.0266$. The Hurst parameter is $H = 0.6614$, which is estimated by R/S analysis approach. Given a 95 percent confidence interval, the simulation results are shown in Tables 1, 2, and 3.

From the results in Tables 1–3, by using Monte Carlo simulation, we conclude that the error of our proposed FSDE model is smaller than the conventional SDE model and SDE with FBM model. If we take the simulating process 100000 times, which is large enough for the error analysis, we obtain that the error rate of SDE model is 3.48%, the SDE driven by fractional Brownian motion model is 3.43%, and the FSDE model is 3.09%, respectively.

In addition, the standard derivation of simulation is also much lower than the SDE model and SDE with FBM model, and the confidence interval is smaller than those two classic models. In the same way, when we simulate 100000 times, the standard deviation of SDE model is 202.2802, the SDE driven by fractional Brownian motion model is 78.5882, and FSDE model is 20.4312. Thus, we get the conclusion that the FSDE has about 10 times lower standard derivation than the SDE model and about 2.5 times lower standard derivation than the SDE driven by fractional Brownian motion model.

5. Conclusions and Future Research

Because the fractional order ordinary differential equations can capture the memory effect in the financial system, we established the fractional order stochastic differential equation by adding the stochastic process into the fractional ordinary differential equation. Based on this stochastic differential equation with fractional order, we apply the fractional order stochastic differential equation to the financial market. We constructed the stock price $d^{\alpha}S = \mu(S,t)dt^{\alpha} + \sigma(S,t)dB(t)$, where $\alpha = 2H$, H is Hurst index, and derived the stock price process in the cases of $0.25 < H \leq 0.5$ and $0.5 < H < 1$, respectively, and the European call option pricing formula under the fractional order stochastic differential equation. From the European option pricing formula, we find the trend memory in stock price process when Hurst index is between 0.5 and 1.

In addition, we made some comparisons in terms of the pricing option formula and its underlying stock price process between our proposed approach and the other two classical models. We find that the new approach leads to a better result than the classic approach and fractional Brownian motion approach when we simulate the stock prices by Monte Carlo simulation.

It would be an interesting work if we improve our model by connecting fractional ordinary differential equation with fractional Brownian motion, which can describe both the trend memory and the noise memory.

Conflict of Interests

The authors declare that there is no conflict of interests regarding the publication of this paper.

Acknowledgments

The first author acknowledges the scholarship funds for the funds for fostering one hundred best Ph.D. degree papers (2013YB1901) provided by Zhongnan University of Economics and Law and also acknowledges the support of the School of Mathematics Science in Monash University for International Joint Training for Ph.D. This research was supported by the Chinese National Social Science Foundation (10BJY104).

References

[1] E. Panas, "Long memory and chaotic models of prices on the London metal exchange," *Resources Policy*, vol. 27, no. 4, pp. 485–490, 2001.

[2] B. J. West and S. Picozzi, "Fractional Langevin model of memory in financial time series," *Physical Review E—Statistical, Nonlinear, and Soft Matter Physics*, vol. 65, no. 3, Article ID 037106, 2002.

[3] F. Wen and Z. Liu, "A copula-based correlation measure and its application in chinese stock market," *International Journal of Information Technology and Decision Making*, vol. 8, no. 4, pp. 787–801, 2009.

[4] F. Wen, X. Gong, Y. Chao, and X. Chen, "The effects of prior outcomes on risky choice: evidence from the stock market," *Mathematical Problems in Engineering*, vol. 2014, Article ID 272518, 8 pages, 2014.

[5] F. Garzareli, M. Cristelli, A. Zaccaria, and L. Pietronero, "Memory effects in stock price dynamics: evidence of technical trading," *Scientific Reports*, vol. 4, article 4487, 2014.

[6] H. E. Hurst, "Long-term storage capacity of reservoirs," *Transactions of the American Society of Civil Engineers*, vol. 116, pp. 770–799, 1951.

[7] B. B. Mandelbrot and J. R. Wallis, "Noah, Joseph and operational hydrology," *Water Resources Research*, vol. 4, no. 5, pp. 909–918, 1968.

[8] D. O. Cajueiro and B. M. Tabak, "The Hurst exponent over time: testing the assertion that emerging markets are becoming more efficient," *Physica A: Statistical Mechanics and its Applications*, vol. 336, no. 3-4, pp. 521–537, 2004.

[9] D. O. Cajueiro and B. M. Tabak, "Ranking efficiency for emerging markets," *Chaos, Solitons and Fractals*, vol. 22, no. 2, pp. 349–352, 2004.

[10] B. B. Mandelbrot and J. W. Van Ness, "Fractional brownian motions, fractional noises and applications," *Society for Industrial and Applied Mathematics*, vol. 10, no. 4, pp. 422–437, 1968.

[11] M. Bęben and A. Orłowski, "Correlations in financial time series: established versus emerging markets," *The European Physical Journal B*, vol. 20, no. 4, pp. 527–530, 2001.

[12] B. Huang and C. W. Yang, "The fractional structure in multinational stock returns," *Applied Economics Letters*, vol. 2, pp. 67–71, 1995.

[13] C. J. G. Evertsz, "Fractional geometry of financial time series," *Fractals*, vol. 3, pp. 609–616, 1995.

[14] A. W. Lo, "Long term memory in stock market prices," *Econometrica*, vol. 59, pp. 1279–1313, 1991.

[15] F. Wen and X. Yang, "Skewness of return distribution and coefficient of risk premium," *Journal of Systems Science and Complexity*, vol. 22, no. 3, pp. 360–371, 2009.

[16] F. Wen, Z. He, and X. Chen, "Investors' risk preference characteristics and conditional skewness," *Mathematical Problems in Engineering*, vol. 2014, Article ID 814965, 14 pages, 2014.

[17] F. Black and M. Scholes, "The pricing of option and corporate liabilities," *Journal of Political Economy*, vol. 81, pp. 637–659, 1973.

[18] C. Necula, "Option pricing in a fractional Brownian motion environment," *Social Science Research Network*, 2002.

[19] S. Rostek, *Option Pricing in Fractional Brownian Markets*, vol. 622 of *Lecture Notes in Economics and Mathematical Systems*, Academic Press, Springer, Berlin, Germany, 2009.

[20] Y. Hu and B. Øksendal, "Fractional white noise calculus and applications to finance," *Infinite Dimensional Analysis, Quantum Probability and Related Topics*, vol. 6, no. 1, pp. 1–32, 2003.

[21] F. Ren, X. Wang, and J. Liang, "A proof for French's empirical formula on option pricing," *Chaos, Solitons and Fractals*, vol. 12, no. 13, pp. 2441–2453, 2001.

[22] X. Wang, W. Qiu, and F. Ren, "Option pricing of fractional version of the Black-Scholes model with Hurst exponent H being in (1/3, 1/2)," *Chaos, Solitons and Fractals*, vol. 12, no. 3, pp. 599–608, 2001.

[23] J. Chen, F. Ren, and W. Qiu, "Option pricing of a mixed fractional-fractional version of the Black-Scholes model," *Chaos, Solitons and Fractals*, vol. 21, no. 5, pp. 1163–1174, 2004.

[24] W. Chen, "Nonlinear dynamics and chaos in a fractional-order financial system," *Chaos, Solitons and Fractals*, vol. 36, no. 5, pp. 1305–1314, 2008.

[25] I. Pollubny, *Fractional Differential Equations*, Academic Press, San Diego, Calif, USA, 1999.

[26] S. Das, *Functional Fractional Calculus for System Identification and Controls*, Springer, Berlin, Germany, 2008.

[27] R. Caponetto, G. Dongola, L. Fortuna, and I. Petras, *Fractional Order Systems: Modeling and Control Applications*, World Scientific, River Edge, NJ, USA, 2010.

[28] C. A. Monje, Y. Chen, B. Vinagre, D. Xue, and V. Feliu, *Fractional-Order Systems and Controls: Fundamentals and Applications*, Springer, London, UK, 2010.

[29] G. Jumarie, "On the representation of fractional Brownian motion as an integral with respect to $(dt)^a$," *Applied Mathematics Letters*, vol. 18, no. 7, pp. 739–748, 2005.

[30] G. Jumarie, "On the solution of the stochastic differential equation of exponential growth driven by fractional Brownian motion," *Applied Mathematics Letters: An International Journal of Rapid Publication*, vol. 18, no. 7, pp. 817–826, 2005.

[31] S. Momani and Z. Odibat, "Numerical comparison of methods for solving linear differential equations of fractional order," *Chaos, Solitons and Fractals*, vol. 31, no. 5, pp. 1248–1255, 2007.

[32] Z. M. Odibat, "Computational algorithms for computing the fractional derivatives of functions," *Mathematics and Computers in Simulation*, vol. 79, no. 7, pp. 2013–2020, 2009.

[33] G. Jumarie, "Stochastic differential equations with fractional Brownian motion input," *International Journal of Systems Science: Principles and Applications of Systems and Integration*, vol. 24, no. 6, pp. 1113–1131, 1993.

[34] G. Jumarie, "Fractional Brownian motions via random walk in the complex plane and via fractional derivative. Comparison and further results on their Fokker-Planck equations," *Chaos, Solitons and Fractals*, vol. 22, no. 4, pp. 907–925, 2004.

Hindawi Publishing Corporation
Discrete Dynamics in Nature and Society
Volume 2014, Article ID 351947, 8 pages
http://dx.doi.org/10.1155/2014/351947

Research Article

Dynamic CGE Model and Simulation Analysis on the Impact of Citizenization of Rural Migrant Workers on the Labor and Capital Markets in China

Qi Wu[1,2] and Hao Xiao[1,2,3]

[1] *School of Economics and Trade, Hunan University, Changsha, Hunan 410079, China*
[2] *China-Australian Economic Policy Research Center, Hunan University, Changsha, Hunan 410079, China*
[3] *Academy of Mathematics and Systems Science, Chinese Academy of Sciences, Beijing 100190, China*

Correspondence should be addressed to Qi Wu; bluesky_sea8587@126.com

Received 18 April 2014; Revised 8 July 2014; Accepted 10 July 2014; Published 11 August 2014

Academic Editor: Chuangxia Huang

This paper investigates the effect of the policy of citizenization of rural migrant workers on the factor market in a dynamic CGE model, which contains multiple dimensions of labor heterogeneity, a labor-lagged adjustment mechanism, and a dynamic investment mechanism. The simulation results show that changes in supply in the labor market will affect the labor market structure, the relative factor price, and the investment in and the output of industries.

1. Introduction

There have been large-scale migrations of surplus rural labor to cities in China. Benefiting from the demographic dividend of rural labor transfer, China's economy has maintained a rapid growth rate of 9-10% per year. With the widening urban-rural income gap [1–3] and aging population [4, 5], China is in a critical period of economic reform and transition. Urbanization that aims to balance urban and rural development is considered the pointcut in further deep reform. The policy of citizenization of rural migrant workers is the essential measure in promoting this urbanization because it can promote rural surplus-labor transfer, break urban and rural employment market segmentation, and solve the periurbanization phenomenon [6, 7]. In addition, it can speed up the process of urbanization, expand domestic demand, and boost economic growth [8–10].

Previous relevant research has mainly applied qualitative research techniques to define the concept of citizenization of rural migrant workers [11, 12] and to study the obstacles in the process of citizenization of rural migrant workers [13]. Only a few of these studies used quantitative methods to calculate the effect of the policy of citizenization of rural migrant workers, and most focused on the partial equilibrium analysis in analyzing one aspect of the economic effects [14, 15]. However, the citizenization of rural migrant workers is a systematically evolutionary project relating to economic and social aspects. It can affect factor markets through adjusting relative prices and demand in the factor market. To quantify the direct and indirect links between structural change in the labor factor and capital factor, we apply a dynamic computable general equilibrium (CGE) model with detailed sectors and intersectoral linkage information. It is important to analyze the general equilibrium effects of labor-market programs [16, 17]. Studies on the dynamic CGE model date back to Dixon's MONASH Model [18, 19]. Following that, Mai et al. [20] built a MONASH-style dynamic Computable General Equilibrium model of China (CHINAGEM) to estimate and explain its economic policies. Tran et al. [21] developed a dynamic multiregional computable general equilibrium model of Australia (DIAC-TERM) with special emphasis on the labor market. Meagher et al. [22] analyzed and forecasted the performance of a labor market built around the MONASH general equilibrium model of the Australian economy. Dixon and Jorgenson [23] reviewed options for labor market modeling and discussed the wage-forming mechanism and involuntary unemployment in CGE models. Mai [24] developed the Monash-Multi-Country (MMC) model, which is an advanced dynamic CGE model with explicit bilateral investment flows between countries/regions explicitly modeled at an industry level. Xiao [25] built a financial applied general equilibrium (FAGE) model for China. Horridge [26] created the enormous regional model (TERM), which treats each region of a single country as a separate economy. By far, the CGE model framework including labor market, capital market, and regions has been the most systematically established.

A great deal of relevant research has applied the above models to simulate the impact of labor-market and capital-market reform, such as structural changes, employment changes, and economic growth [27–30]. However, only a few studies explicitly analyzed the effect of the policy of citizenization of rural migrant workers on the factor market. In this paper, we use the CHINAGEM model to explore and simulate the effects of the policy of citizenization of rural migrant workers in China on economic growth and structural changes in the labor and capital factor markets over a period of ten years from 2010 to 2020.

2. Overview of the Model

2.1. CGE Model Description. It is appropriate to use CHINAGEM to simulate the segmented labor market and dynamic investment in China. In this section, we will briefly cover modeling and simulation techniques. According to Mai et al. [20], the production factors include labor force, capital, and land. Under the cost-minimization and profit-maximization assumptions, the production activity of the CGE model is set up as nested CES functions. The top nest is expressed as (1), where $i = 1, \ldots, n+2$ are intermediate goods input (n) and primary and other costs, X_{ij} is the effective input, Z_j is industry $j's$ activity level, and A_j and A_{ij} are technological coefficients.

For each industry j, we assume that

$$\begin{aligned} &\underset{i=1,\ldots,n+2}{\text{Leontief}}\left\{\frac{X_{ij}}{A_{ij}}\right\} = A_j Z_j, \quad j's = 1,\ldots,h, \\ &\underset{i=1,\ldots,m}{\text{Leontief}}\{f_i\} = \text{minimum}\left\{f_1, f_2, \ldots, f_m\right\}. \end{aligned} \tag{1}$$

Given the units of input, different sources of intermediate goods are combined to provide effective input according to the Armington nest, which is expressed as (2), where $X_{(is)j}$ is the input of i from sources (domestic and imported) to current production in industry j, ρ, and b are parameters, ρ is greater than −1 and not equal to zero, and b is nonnegative.

Consider

$$\begin{aligned} X_{ij} &= \underset{s=\text{dom,imp}}{\text{CES}}\left\{\frac{X_{(is)j}}{A_{(is)j}}; \rho_{ij}, b_{(is)j}\right\}, \\ &\qquad i = 1,\ldots,n; \ j = 1,\ldots,m, \\ \underset{s=\text{dom,imp}}{\text{CES}}&\left\{\frac{X_{(is)j}}{A_{(is)j}}; \rho, b_s\right\} = \left(\sum_s \frac{X_{(is)j}}{A_{(is)j}}^{-\rho} b_s\right)^{-(1/\rho)}. \end{aligned} \tag{2}$$

In the primary nest, labor, capital, and land are combined to form effective input according to (3), in which $X_{(n+1,s)j}$ is the input of primary factor of type s to production industry j; h_s, Q_s, and κ are parameters; h_s is less than 1 and not equal to zero; Q_s is positive; and $\sum_s Q_s = 1$. The skill nest in the labor factor is the same CES nest.

Consider

$$\begin{aligned} &X_{n+1,j} \\ &= \underset{S=\text{labour,capital,land}}{\text{CRESH}}\left\{\frac{X_{(n+1,s)j}}{A_{(n+1,s)j}}; h_{(n+1,s)j}, Q_{(n+1,s)j}, K_{(n+1,s)j}\right\}, \\ &\sum_s \left(\frac{X_{(n+1,s)j}/A_{(n+1,s)j}}{X_{n+1,j}}\right)^{h_s} \frac{Q_s}{h_s} = \kappa. \end{aligned} \tag{3}$$

2.2. Dynamic Flow of the Multivariate Supply of the Labor Submodule in the Segmented Labor Market. To specify labor demand categories, the CGE model updates the multivariate supply of the labor submodule to quantify the multiple dimensions of labor heterogeneity. The multivariate supply of the labor submodule divides the production sectors into agricultural and nonagricultural sectors and sets up the multiple labor transfer matrix on the basis of different household registration, occupation, and skill. The labor categories are then subdivided into five further types: AG, RNAG, RUE, UUSE, and USE. (Agriculture employment (AG), rural non-agriculture employment (RNAG), rural-urban employment (RUE), urban unskilled employment (UUSE), and urban skilled employment (USE).) In consideration of the entrants into the labor market, the submodule subdivides the labor categories into newly added and non-newly added labor force.

The model assumes labor supply from labor category o does not want to be unemployed and prefers to supply to the same industry which they were employed in the previous year. Different categories of labor supply are subject to the Hukou constraint, which indicates that (1) the rural categories (AG, RNAG, RUE, RAGU, and RUU) can only offer rural activities of employment (AG, RNAG, and RUE), (2) the urban categories (UUSE, USE, UU, and NURB) can only make offers of urban activities (UUSE and USE), and (3) the rural new entrants (NRUR) can offer rural as well as urban activities.

Consider

$$\begin{aligned} L^{s^t}_{jo,\text{nnl}} &= L^{s^{t-1}}_{jo,\text{nnl}} * S^{t-1}_{jo,\text{nnl}}, \\ L^{s^t}_{jo,\text{nl}} &= \delta. \end{aligned} \tag{4}$$

$L^{s^t}_{jo,\text{nnl}}$ is the number of the o type of nonnew labor force in year t, $L^{s^t}_{jo,\text{nl}}$ is the number of the o type of new labor force in year t, $L^{s^{t-1}}_{jo,\text{nnl}}$ is the number of the o type of nonnew labor force in year $t-1$, $S^{t-1}_{jo,\text{nnl}}$ is the proportion of the o type of nonnew labor force in year $t-1$ flow to the j industry in the year t, $S^{t-1}_{jo,\text{nnl}} = 0.99$, and δ is the exogenous parameter.

The dynamic mechanism in the labor market is adjusted dynamically by means of the change in real wages. The lagged adjustment of the labor market is built into the hypothetical conditions: in the short run, wage rigidity and employment elasticity are changeable, and, in the long run, the wage is changeable and the employment rate remains relatively stable. Equation (5) is the dynamic adjustment of labor employment levels. In the first year of the policy, the labor market deviates from full employment. The degree of deviation that is decided by the variable ∂_1 has been decreasing over time. Equation (6) is the dynamic adjustment of real wages. The degree of real-wage deviation increases every year. Therefore, in the initial state of the labor market, there is full employment and the ratio of real wages to expected wages is equal to 1. Assuming a policy to promote the demand for labor, real wages and employment levels will be higher than expected. The labor-supply curve is a vertical shift until real wages grow and the labor market goes back to the level of full employment.

Consider

$$\frac{L^t_{\text{TOT}}}{L^t_{\text{TOT}_f}} - 1 = \partial_1 * \left[\frac{L^{t-1}_{\text{TOT}}}{L^{t-1}_{\text{TOT}_f}} - 1\right] + F(t), \tag{5}$$

$$\frac{\text{atw}^t}{\text{atw}^t_f} - 1 = \left[\frac{\text{atw}^{t-1}}{\text{atw}^{t-1}_f} - 1\right] + \partial_2 * \left[\frac{L^t_{\text{TOT}}}{L^t_{\text{TOT}_f}} - H\left(\frac{\text{atw}^{t-1}}{\text{atw}^{t-1}_f}\right)\right] + F\_\text{atw}^t. \tag{6}$$

In (5) and (6), atw is the rate of real wage, L_{TOT} is employment, H is the long-term labor supply function and is set to equal 1, f is the simulation value without policy impact, ∂_1 and ∂_2 are the employment adjustment and wage adjustment parameters, and F is the policy shock function, which is given an exogenous value in the year t and set to zero in subsequent years.

In order to achieve dynamic equilibrium in the labor market, it is assumed that wages are variable and there is full employment. After the policy shock, on the basis of exogenous labor supply, the multiple equilibria of the labor market are adjusted by changes in the rate of real wages in the various departments.

Consider

$$\begin{aligned}
\text{EL}^s_{j,ub} &= \text{EF}^{s_0}_{j,wl} + \theta_{\text{alsl}} \sum_{\text{a}} \text{tmig}_{a,b,j,l}, \\
\text{EL}^s_{j,\text{ru}} &= \text{EF}^{s_0}_{j,wl} - \theta_{\text{alal}} \sum_{\text{a}} \sum_{sl} \sum_{i \in ub} \text{tmig}_{a,b,j,sl}, \\
\text{TNL}^s_{j,lo} &= \frac{\text{TNL}^{s_0}_{j,lo}}{\text{EL}^{s_0}_{j,lo}} \text{EL}^s_{j,lo}, \\
D^d_{i,lo} &= \text{TNL}^s_{i,lo}.
\end{aligned} \tag{7}$$

$\text{EL}^s_{j,ub}$ is the effective labor supply for the non-farm sector in the city, $\text{EL}^s_{j,ru}$ is the effective labor supply for the non-farm sector in the rural agricultural sector, $\text{EF}^{s_0}_{j,wl}$ is the initial total effective labor supply for various industries, θ_{alsl} and θ_{alal} are the respective coefficients of effective labor and actual labor, tmig is the total labor force transfer, $\text{TNL}^s_{j,lo}$ is the standardized total labor supply of the o type in department j, and $D^d_{i,lo}$ is the total labor demand of the o type in department j.

2.3. The Dynamic Mechanism of Investment. The rate of return is introduced to depict the relationship between capital stock and investment. The model distinguishes various kinds of investment behavior. Equation (8) represents the process of capital accumulation. It reflects that the current capital stock is equal to the previous capital stock plus the current investment and minus the depreciation. Equation (9) is the investment-supply function, where the equilibrium expected rate of return is an inverse logistic function of the proportionate growth of capital stock. Equation (10) defines the actual rates of return under static expectations. It implies that the rate of return decreases as the investment rises. These two equations reveal the relationship between the expected rate of return and investment.

Consider

$$K_{j,t+1} = K_{j,t} + I_{j,t} - D_j * K_{j,t}, \tag{8}$$

$$\begin{aligned}
\text{EROR}_j &= \text{DIS}_j + \left\{\text{RORN}_j + F_\text{EROR}_J_i + F_\text{EROR}\right\} \\
&\quad + \left(\frac{1}{C_j}\right) * \left[\text{Ln}\left(K_\text{GR}_j - K_\text{GR_MIN}_j\right) \right. \\
&\quad - \text{Ln}\left(K_\text{GR_MAX}_j - K_\text{GR}_j\right) \\
&\quad - \text{Ln}\left(\text{TREND}_K_j - K_\text{GR_MIN}_j\right) \\
&\quad \left. - \text{Ln}\left(K_\text{GR_MAX}_j - \text{TREND}_K_j\right)\right],
\end{aligned} \tag{9}$$

$$\text{EROR\_ST}_{j,t} = -1 + \frac{\left[\left(1 - T_{t+1}\right) * Q_{j,t+1}/\Pi_{j,t} + \left(1 - D_j\right)\right]}{\left(1 + \text{R\_INT\_PT\_SE}_t\right)}. \tag{10}$$

K and I represent capital and investment, respectively, D represents depreciation rate, DIS_j is a measure of the difference between the expected rate of return and the equilibrium expected rate of return in industry j, EROR and EROR_ST represent an expected rate of return and an expected rate of return under static expectations, RORN is the historically normal rate of return, F_EROR_J and F_EROR allow for vertical shifts in the capital supply curves, K_GR is the expected growth of capital stock (equal to the ratio of investment to capital stock), TREND_K is the historically normal capital growth rate, T is the tax rate applying to capital income, Q is the rental rate on capital, Π is the cost of an extra unit of capital, R_INT_PT_SE is the static expectation of the real post-tax interest rate, and C is a positive parameter.

3. Simulation Scene Design

According to China's 12th Five-Year Plan and data from the All-China Federation of Trade Unions (ACFTU) [31], this paper sets up the simulation scene of citizenization of rural migrant workers in phases and dynamically simulates and analyzes the effect of citizenization of rural migrant workers on China's economic growth in the post-international economic crisis era from 2010–2020 (Table 1). China's 12th Five-Year Plan clearly points out that the urbanization rate should grow from 47.5% to 51.5% in the years 2011–2015. To achieve this goal, Han [32] predicted that if the agricultural labor force transfer speed is maintained at 2% per year from 2006 to 2030, the level of urbanization will increase 0.7-0.8 percentage points annually and the level of urbanization will reach 61% in the year 2030. An ACFTU (2011) research report suggested that if citizenization of rural migrant workers continues at around 3% (approximately 300 million people) per year, the urbanization target of China's 12th Five-Year Plan will be achieved. According to the CHINAGEM base period database and ACFTU's data, the paper broke down the policy-shock value of the rural labor force to an average annual decrease of 0.65% and the urban unskilled labor supply to an average annual increase of 1.2%. The simulation of the policy of citizenization of rural migrant workers is implemented in five-year periods starting in 2010.

4. Simulation Results and Analysis

According to the CHINAGEM model simulation results, citizenization of rural migrant workers has a significant influence on employment and investment structure. Based on the shock to the labor supply, the labor market adjusts by the mechanism of the labor transition matrix and wages. The change in the labor market affects the rate of return in the capital market and is the primary factor input in the industry. The output and the macroeconomics tend to change as a whole. The transmission mechanism of the simulation shock is provided in Figure 1, the exogenous variables are set outside the model, and the endogenous variables are determined by the model.

4.1. The Labor Employment Effect. From the perspective of total employment (Table 2) in the labor market, it can be seen that the citizenization of rural migrant workers can effectively improve labor force employment in the whole society. From 2011–2015, total employment of the labor force grows rapidly, increasing from 0.11% to 0.54%. From 2016–2020, the growth rate of labor force employment declines, but maintains growth momentum. Total labor employment in the whole society increases by 0.05% in 2020.

With regard to changes of employment ratios in various industries, it can be seen that primary-industry employment obviously decreases, while employment increases in the secondary and tertiary industries. Growth in the tertiary industry is particularly evident.

On one hand, in terms of labor employment rates in the urban-rural labor market, changes in urban labor force employment are slower than in the rural labor force. In 2020, urban labor force employment increases by 5.88%, while rural labor force employment falls by 6.47%. On the other hand, from the perspective of various types of employment, the supply of and demand form skilled labor and skilled labor increases in urban areas while decreasing in rural areas. In 2020, UUSE employment sees a greater increase than USE at approximately 3.02% and 2.81%, respectively. RUE, RNAG, and AG employment rates decrease by approximately 2.66%, 2.50%, and 1.60%, respectively (Figure 2).

4.2. The Effect of Factor Market Structure Adjustment. Affected by the changes in labor force employment, the prices of the labor factor change correspondingly. As the relative price of this factor changes, the capital accumulation effect promotes growth in the capital and labor markets. In terms of urban and rural labor-factor prices, the wage gap between urban and rural labor narrows. Real wages for the rural labor force continue to rise while real wages for urban labor decrease significantly. In 2020, real wages for AG workers rise by 10.49%, for RANG workers by 9.23%, and for RUE workers by 9.15%, but real wages decrease for UUSE workers by 7.03% and for USE workers by 7.68% (Table 3).

Return on capital increases relative to the baseline before it reaches its deviation level in 2017 and decreases in the following years, specifically, by 0.27% in 2011, by 0.40% in 2017, and by 0.53% in 2020. As a result, the amount of capital stock enlarges during the seven-year period during which the policy is implemented and, subsequently, narrows during the last three years. Taking the capital accumulation effect into consideration, the influence of the generalized citizenization process is more obvious.

4.3. The Industry Output Effect. Primary-industry output decreased slightly, especially in animal husbandry and in fishery. The changes in the labor and capital factor markets lead to an increase in output by the secondary and tertiary industries, in which migrant-worker employment is relatively high. In secondary industries, the output of manufacturing increases more obviously because the excess supply of migrant workers is reflected in the decrease in their wage rates. In tertiary industries, the output of construction, education, health, information transmission, storage, postal services, and real estate increases strongly, by 0.32%, 0.21%, 0.20%, 0.19%, and 0.17%, respectively, mainly because

Table 1: Simulation scene design.

Type of scene	The simulation scene
Baseline	(1) The total population and the growth of the total workforce are exogenous; (2) the tax rate remains unchanged on the basis of differences in wage levels and the agricultural labor force can continue to transfer to nonagricultural sectors; and (3) technology and capital depreciation rates are exogenous variables.
Citizenization of rural migrant workers	(1) Relative to the base period, 300 million migrant workers are citizenized annually from 2011 to 2015; (2) according to the CHINAGEM base period database and ACFTU's data, the paper breaks down the policy-shock value of the rural labor force to an average annual decrease of 0.65% and the urban unskilled labor supply to an average annual increase 1.2%; and (3) other exogenous variables are set to the same levels as in the baseline scenario.

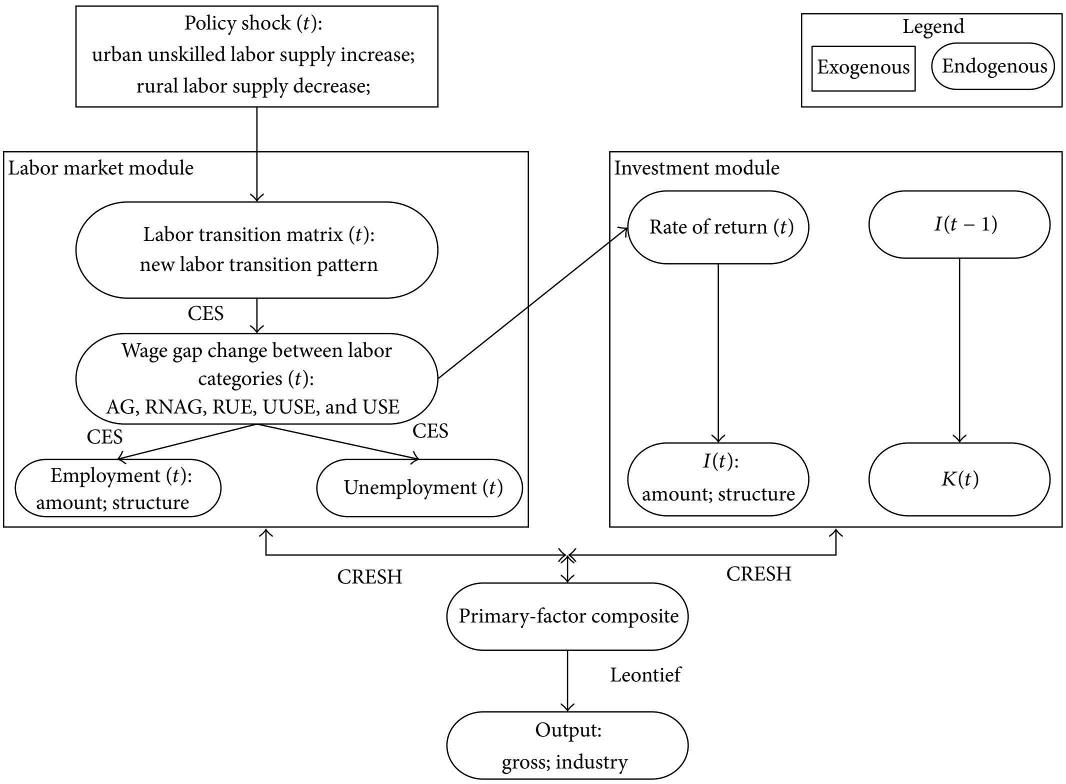

Figure 1: The transmission mechanism of the simulation shock.

of investment growth, especially in governmental public-services spending (Table 4).

5. Conclusion

In this paper, we used a dynamic computable general equilibrium model of China to estimate the effect of the policy of citizenization of rural migrant workers. We designed the policy scenarios based on data calculated by the development goals of China's 12th Five-Year Plan. Normally, under the dynamic mechanisms of the labor market and investment, the citizenization of rural migrant workers can expand employment and the scale of investment, accelerate structural adjustment, and boost economic growth in China. The simulation results show that (1) supply changes in the labor market will affect employment rates in the urban-rural labor market and will optimize the urban-rural labor market employment structure, (2) structural changes in the labor factor market will increase the real wages of rural migrant workers and cause a relative rise in capital factor prices, which causes the labor market and capital factor market to achieve a new equilibrium at a higher employment level, and (3) the quantity of the production factor used in each industry will change with the factor-price effect. The output of second and tertiary industries will increase.

There is still much space for improving the model, which requires a more detailed database. It will be worthwhile to classify labor by different education levels and occupation types, to relax the static expectation assumption and to estimate the elasticity of substitution of factors in each industry.

Table 2: The total employment (% change deviation from baseline).

	2011	2012	2013	2014	2015	2016	2017	2018	2019	2020
Total employment	**0.10**	**0.25**	**0.38**	**0.47**	**0.54**	**0.45**	**0.31**	**0.18**	**0.09**	**0.05**
Primary industry	**0.01**	**−0.01**	**−0.11**	**−0.26**	**−0.46**	**−0.72**	**−0.95**	**−1.11**	**−1.20**	**−1.23**
Secondary industry[1]	**0.19**	**0.51**	**0.87**	**1.21**	**1.53**	**1.61**	**1.54**	**1.43**	**1.34**	**1.26**
MotorVhc	0.35	0.81	1.22	1.57	1.86	1.78	1.57	1.39	1.28	1.21
ElecCommsEqp	0.30	0.77	1.30	1.83	2.34	2.49	2.43	2.30	2.17	2.05
Meters	0.21	0.62	1.16	1.76	2.38	2.73	2.84	2.83	2.76	2.67
ToysSportEqp	0.20	0.60	1.13	1.71	2.33	2.68	2.81	2.82	2.77	2.70
NFerrOre	0.16	0.47	0.86	1.26	1.63	1.76	1.69	1.55	1.39	1.25
ClothesShoes	0.16	0.45	0.82	1.23	1.63	1.83	1.87	1.84	1.79	1.75
Tertiary industry	**0.24**	**0.62**	**1.01**	**1.39**	**1.75**	**1.83**	**1.76**	**1.68**	**1.63**	**1.58**
Real estate	0.45	1.16	1.94	2.73	3.51	3.79	3.77	3.67	3.57	3.46
Construction	0.43	0.95	1.36	1.65	1.84	1.57	1.20	0.94	0.80	0.74
Insurance	0.29	0.79	1.37	1.97	2.57	2.83	2.86	2.82	2.77	2.71
Tourism	0.29	0.74	1.26	1.77	2.25	2.40	2.35	2.22	2.09	1.97
Health	0.27	0.71	1.22	1.75	2.27	2.49	2.52	2.50	2.46	2.43
Education	0.23	0.63	1.10	1.58	2.07	2.30	2.35	2.33	2.31	2.27

[1] MotorVhc represents automobile manufacturing; ElecCommsEqp represents communications equipment manufacturing; Meters represents instrumentation industry; ToysSportEqp represents toys, sports, and entertainment goods industry; NFerrOre represents non-ferrous metal mining; ClothesShoes represents textile and garment, shoes, and hat manufacturing industry.

Table 3: The changes of the factor price in 2010–2020 (% change deviation from baseline).

		2011	2012	2013	2014	2015	2016	2017	2018	2019	2020
Real wage	AG	0.58	1.71	3.24	5.05	7.07	8.60	9.58	10.13	10.40	10.49
	RNAG	0.54	1.47	2.70	4.17	5.80	6.99	7.87	8.50	8.94	9.23
	RUE	0.53	1.45	2.67	4.12	5.73	6.90	7.78	8.41	8.85	9.15
	UUSE	−0.64	−1.67	−2.89	−4.23	−5.61	−6.34	−6.71	−6.89	−6.99	−7.03
	USE	−0.39	−1.28	−2.46	−3.82	−5.28	−6.40	−7.03	−7.38	−7.58	−7.68
Rate of return		0.27	0.55	0.72	0.78	0.75	0.40	0.00	−0.29	−0.45	−0.53
Capital stock		−0.001	0.034	0.114	0.226	0.354	0.487	0.582	0.629	0.642	0.637

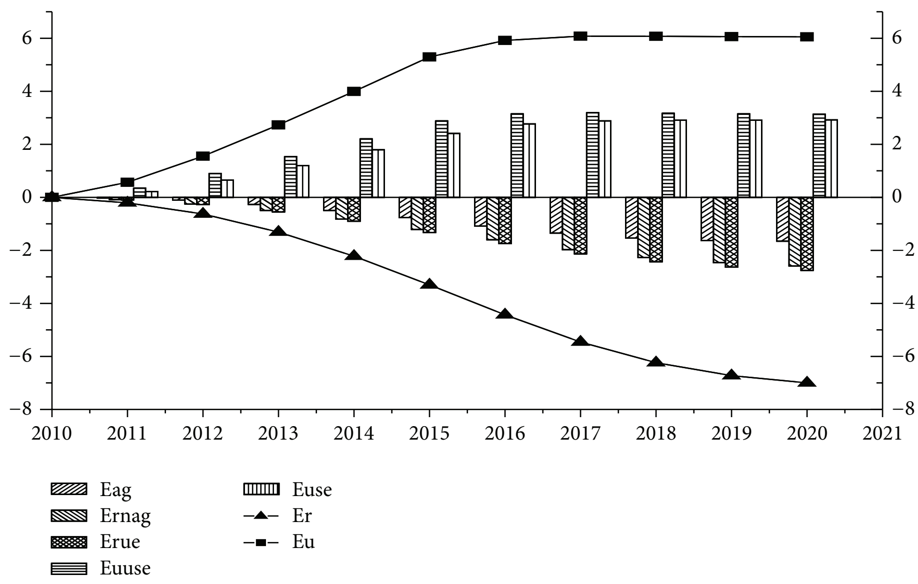

Figure 2: The changes of the labor market structure in 2010–2020 (% change deviation from baseline, *E* is the employment amount).

Table 4: The output of industry in 2011–2020 (% change deviation from baseline).

	2011	2012	2013	2014	2015	2016	2017	2018	2019	2020
Primary industry	**0.01**	**−0.01**	**−0.08**	**−0.20**	**−0.36**	**−0.57**	**−0.77**	**−0.90**	**−0.98**	**−1.01**
Farming	0.02	0.02	−0.01	−0.08	−0.18	−0.34	−0.50	−0.61	−0.68	−0.71
Forestry	0.13	0.27	0.36	0.36	0.30	0.04	−0.25	−0.48	−0.65	−0.75
Animal husbandry	−0.03	−0.13	−0.30	−0.55	−0.83	−1.14	−1.39	−1.55	−1.64	−1.67
Fishery	−0.03	−0.10	−0.23	−0.41	−0.63	−0.86	−1.05	−1.18	−1.24	−1.26
Other agricultural	0.06	0.17	0.29	0.40	0.52	0.54	0.51	0.48	0.47	0.48
Secondary industry[2]	**0.12**	**0.34**	**0.60**	**0.87**	**1.14**	**1.26**	**1.25**	**1.21**	**1.16**	**1.11**
NonmetalProd	0.21	0.53	0.84	1.12	1.36	1.34	1.20	1.06	0.96	0.90
FerrMetals	0.20	0.52	0.87	1.22	1.54	1.61	1.55	1.46	1.39	1.33
SpecialMac	0.20	0.52	0.88	1.25	1.60	1.71	1.68	1.61	1.54	1.49
GenpurMac	0.19	0.50	0.83	1.15	1.45	1.51	1.44	1.33	1.24	1.17
TransEquip	0.16	0.42	0.70	0.97	1.22	1.26	1.19	1.10	1.02	0.96
Tertiary industry	**0.17**	**0.44**	**0.75**	**1.07**	**1.37**	**1.47**	**1.45**	**1.40**	**1.36**	**1.34**
Construction	0.32	0.74	1.10	1.37	1.56	1.38	1.08	0.85	0.72	0.65
Health	0.22	0.58	1.00	1.44	1.89	2.09	2.13	2.12	2.10	2.08
Education	0.20	0.56	0.98	1.43	1.87	2.09	2.14	2.13	2.11	2.08
ITCompt[3]	0.19	0.49	0.82	1.14	1.46	1.54	1.50	1.44	1.39	1.35
Real estate	0.17	0.49	0.91	1.37	1.85	2.13	2.25	2.28	2.28	2.26

[2]NonmetalProd represents Non-metallic mineral manufacturing; FerrMetals represents ferrous metal smelting and rolling processing industry; SpecialMac represents special equipment manufacturing; GenpurMac represents general equipment manufacturing; TransEquip represents transportation equipment manufacturing.
[3]ITCompt represents information transmission, computer service, and software industry.

Conflict of Interests

The authors declare that there is no conflict of interests regarding the publication of this paper.

Acknowledgments

Research is supported by National Natural Science Foundation of China (no. 70873039, no. 71203062, and no. 70925006) and Doctoral Fund of Ministry of Education of China (no. 10YJC790295).

References

[1] J. Y. Lin, G. Wang, and Y. H. Zhao, "Regional inequality and labor transfer in China," *Economic Development and Cultural Change*, vol. 52, no. 3, pp. 587–603, 2004.

[2] S. Li and X. M. Yue, "The income gap between urban and rural areas in China is the world's highest," *Theoretical Reference*, vol. 4, pp. 50–52, 2005.

[3] F. Cai and M. Y. Wang, "Why didn't labor mobility to narrow the income gap between urban and rural areas," *Economic Perspectives*, vol. 8, pp. 4–10, 2009.

[4] J. Banister, D. E. Bloom, and L. Rosenberg, "Population aging and economic growth in china," PGDAWorking Paper 53, 2010, http://www.hsph.harvard.edu/pgda/WorkingPapers/2010/PGDA_WP_53.pdf.

[5] F. Modigliani and S. L. Cao, "The Chinese saving puzzsle and the life-cycle hypothesis," *Journal of Economic Literature*, vol. 42, no. 1, pp. 145–170, 2004.

[6] A. Watson, "Citizenization of rural migrant workers: the path of solving China's economic imbalances," *Chinese Urban Economy*, vol. 4, pp. 50–51, 2009.

[7] S. Li, "China's market-oriented reform and income distribution," *Journal of Shanghai Finance University*, vol. 98, pp. 5–9, 2010.

[8] F. Cai and D. W. Wang, "Sustainability of China's economic growth and labour contribution," *Journal of Economic Study*, vol. 10, pp. 62–68, 1999.

[9] World Bank, *China 2020: Development Challenges in the New Century*, World Bank, Washington, DC, USA, 1997.

[10] T. Hertel and F. Zhai, "Labor market distortions, rural-urban inequality and the opening of China's economy," *Economic Modelling*, vol. 23, no. 1, pp. 76–109, 2006.

[11] C. J. Liu and J. L. Xu, "A study on the second generation peasant w orkers and their citizenization," *Population, Resources and Environment*, vol. 1, pp. 22–26, 2007.

[12] J. C. Hu, "Studies of citizenization of rural migrant workers," *Lanzhou Academic Journal*, vol. 8, pp. 91–95, 2010.

[13] K. Huang, "Empirical analysis of the impact on the citizenization of rural migrant workers from urban-rural dual institution," *China Population Resource and Environment*, vol. 21, pp. 76–81, 2011.

[14] Y. L. Dong, C. J. Liu, and M. Hu, "Urbanization in the context of citizenizing new generation peasant workers," *Population Research*, vol. 1, pp. 65–73, 2011.

[15] Research Group of Development Research Center of the State Council, "The effect of citizenization of rural migrant workers on the domestic demand and economic growth," *Economic Research Journal*, vol. 6, pp. 4–16, 2010.

[16] J. Lise, S. Seitz, and J. Smith, "Equilibrium policy experiments and the evaluation of social programs," NBER Working Paper Series no. 10283, 2004, http://www.nber.org/papers/w10283.

[17] R. Blundell, C. Meghir, M. C. Dias, and J. van Reenen, "Evaluating the employment impact of a mandatory job search program," *Journal of the European Economic Association*, vol. 2, no. 4, pp. 569–606, 2004.

[18] P. B. Dixon, B. R. Parmenter, J. Sutton, and D. P. Vincent, *ORANI: A Multisectoral Model of the Australian Economy*, North-Holland, Amsterdam, The Netherlands, 1982.

[19] P. B. Dixon and M. T. Rimmer, *Dynamic General Equilibrium Modelling for Forecasting and Policy: A Practical Guide and Documentation of MONASH*, North-Holland, Elsevier Science, Amsterdam, The Netherlands, 2002.

[20] Y. H. Mai, P. B. Dixon, and M. T. Rimmer, "CHINAGEM: a monash-styled dynamic CGE model of China," CoPS Working Paper G-201, 2010, http://www.copsmodels.com/ftp/workpapr/g-201.pdf.

[21] N. Tran, L. Roos, and J. Giesecke, "DIAC-TERM: a multi-regional model of the Australian economy with migration detail," CoPS Working Paper no. G-238, 2012, http://www.copsmodels.com/ftp/workpapr/g-238.pdf.

[22] G. A. Meagher, P. D. Adams, and J. M. Horridge, "Applied general equilibrium modeling and labour market forecasting," CoPS Working Paper n o.IP-76, 2000, http://www.copsmodels.com/ftp/workpapr/ip-76.pdf.

[23] P. B. Dixon and D. Jorgenson, *Handbook of Computable General Equilibrium Modeling*, North-Holland, Amsterdam, The Netherlands, 2011.

[24] Y. H. Mai, "The MONASH-Multi-Country (MMC) model and the investment liberalisation in China's Oil Industry," CoPS Working Paper no. G-150, 2005, http://www.copsmodels.com/ftp/workpapr/g-150.pdf.

[25] J. L. Xiao, "Theoretical structure of the FAGE model," CoPS Working Paper G-198, 2010, http://www.copsmodels.com/ftp/workpapr/g-198.pdf.

[26] M. Horridge, "The TERM model and its data base," CoPS Working Paper no. G-219, 2011, http://www.copsmodels.com/ftp/workpapr/g-219.pdf.

[27] C. Sussangkarn, "Macroeconomic impacts of migrant workers: analyses with a CGE model," *TDRI Quarterly Review*, vol. 11, no. 3, pp. 3–11, 1996.

[28] D. G. Johnson, "Can agricultural labour adjustment occur primarily through creation of rural non-farm jobs in China?" *Urban Studies*, vol. 39, no. 12, pp. 2163–2174, 2002.

[29] Y. H. Mai, X. J. Peng, P. B. Dixon, and M. T. Rimmer, "The effects of facilitating the flow of rural labour to urban employment in China," CoPS Working Paper G-188, 2009, http://www.copsmodels.com/ftp/workpapr/g-188.pdf.

[30] P. B. Dixon, J. Martin, and M. T. Rimmer, "Economy-wide effects of reducing illegal immigrants in U.S. employment," *Contemporary Economic Policy*, vol. 29, no. 1, pp. 14–30, 2011.

[31] ACFTU, *The Report about New Generation of Migrant Workers*, Workers' Daily, 2010.

[32] Research Group of Development Research Center of the State Council, "Policy framework and basic thinking of china's rural reform and development in the twelfth five-year plan period," *Reform*, vol. 5, pp. 5–20, 2010.

Hindawi Publishing Corporation
Discrete Dynamics in Nature and Society
Volume 2014, Article ID 802429, 8 pages
http://dx.doi.org/10.1155/2014/802429

Research Article

Linear Control of Fractional-Order Financial Chaotic Systems with Input Saturation

Junhai Luo,[1] Guanjun Li,[2] and Heng Liu[2]

[1] *School of Electronic Engineering, University of Electronic Science and Technology of China, Chengdu 611731, China*
[2] *Department of Mathematics and Computational Sciences, Huainan Normal University, Huainan 232038, China*

Correspondence should be addressed to Junhai Luo; junhai_luo@uestc.edu.cn

Received 12 March 2014; Accepted 17 July 2014; Published 6 August 2014

Academic Editor: Taishan Yi

In this paper, control of fractional-order financial chaotic systems with saturated control input is investigated by means of state-feedback control method. The saturation problem is tackled by using Gronwall-Bellman lemma and a memoryless nonlinearity function. Based on Gronwall inequality and Laplace transform technique, two sufficient conditions are achieved for the asymptotical stability of the fractional-order financial chaotic systems with fractional orders $0 < \alpha \leq 1$ and $1 < \alpha < 2$, respectively. Finally, simulation studies are carried out to show the effectiveness of the proposed linear control method.

1. Introduction

In the past two decades, studies of chaotic systems have received more and more attention in various fields of natural sciences. This is because chaotic systems are rich in dynamics and possess great sensitivity to initial conditions. Up to now, econophysics has been raised to an alternative scientific methodology to comprehend the highly complex dynamics in economic and financial systems. Many economists are working hard to explain the central features of economic data, including erratic macroeconomic fluctuations (business cycles), irregular microeconomic fluctuations, irregular growth, structural changes, and overlapping waves of economic development [1, 2]. Representative effects, that is, treated as random shocks, are political events, weather variables, and other human factors [3–7]. Compared with the opinion discussed above, chaos supports an endogenous explanation of the complexity appeared in economic series.

Since chaos in financial systems was firstly studied in 1985, great impact has been put on the prominent economics recently, because the occurrence of the chaotic phenomenon in the economic system indicates that the macroeconomic operation has in itself the inherent indefiniteness. Studies on the complicated financial systems by using nonlinear method are fruitful [2, 8, 9]. Controlling chaos in fractional-order financial systems is also studied in recent years [10–18]. In [15], an active sliding mode controller is constructed to synchronize fractional-order financial chaotic systems in master-slave structure. In [16], a necessary condition is introduced to confirm the existence of 1-scroll, 2-scroll, or multiscroll chaotic attractors in a fractional-order financial system and a sliding mode controller is proposed. Active control method is also used in [17], and the variable-order fractional derivative is defined in Caputo type. Wang et al. investigate impulsive synchronization and adaptive-impulsive synchronization of a novel financial hyperchaotic system [18]. In above literatures, the stability analysis is carried out based on fractional-order linear system stability theorem and only the situation where fractional order $0 < \alpha \leq 1$ is concerned.

Most of real world technical systems are subjected to input constraints, especially in financial systems. In financial systems, input saturation does exist due to a limited size of weather variables, political events, and other human factors. The existence of input saturation may decrease the control performance or cause oscillations and even lead to instability of the system [19–21]. It is advisable for us to consider the control of financial systems with input saturation. For the integer-order linear and nonlinear systems, input saturation has received much attention from researchers in the past decade. The sector bounded condition associated with input nonlinearities is useful for analysis and synthesis of control systems subject to input saturation. Then the stability of the system can be formulated using Lyapunov stability theory and invariant theory.

Though many research efforts have been put to the fractional-order financial chaotic systems, the financial systems with saturated control input have rarely been investigated in literatures. Here, with the help of Laplace transform, Mittag-Leffler function, and Gronwall inequality, a linear controller will be derived for fractional-order financial chaotic systems in this paper. There are some main contributions that are worth to be emphasized as follows.

(1) Two sufficient conditions are derived for the asymptotical stability of fractional-order financial chaotic systems with fractional orders $0 < \alpha \leq 1$ and $1 < \alpha \leq 2$, respectively.

(2) A linear controller is given to control the fractional-order financial chaotic system.

(3) A memoryless nonlinearity function is employed to handle the input saturation problem in fractional-order chaotic systems.

2. Preliminaries and System Description

2.1. Preliminaries. The Caputo definition of fractional-order derivatives can be expressed as [21–24]

$$ {}_{0}^{C}D_{t}^{\alpha}x(t) = \frac{1}{\Gamma(n-\alpha)}\int_{0}^{t}\frac{x^{(n)}(\tau)}{(t-\tau)^{\alpha-n+1}}d\tau, \quad n-1<\alpha<n, \tag{1} $$

where α represents the fractional order and the Euler function $\Gamma(\cdot)$ is defined as $\Gamma(\tau) = \int_0^\infty t^{\tau-1}e^{-t}d\tau$.

The Laplace transform of Caputo fractional derivative can be given as

$$ \int_{0}^{\infty} e^{-st}\, {}_{0}^{C}D_{t}^{\alpha}\, x(t)\, dt = s^{\alpha} - \sum_{k=0}^{n-1} s^{\alpha-k-1}x^{(k)}(0). \tag{2} $$

The following definition and lemmas will be used.

Definition 1. The Mittag-Leffler function with two parameters can be written as

$$ E_{\alpha,\beta}(z) = \sum_{k=0}^{\infty}\frac{z^k}{\Gamma(\alpha k+\beta)}, \tag{3} $$

where $\alpha, \beta > 0$ and $z \in C$, and its Laplace transform can be given as

$$ \mathscr{L}\left\{t^{\beta-1}E_{\alpha,\beta}(-\lambda t^{\alpha})\right\} = \frac{s^{\alpha-\beta}}{s^{\alpha}+\lambda}. \tag{4} $$

Lemma 2 (see [22]). *If $A \in R^{n\times n}$, $0<\alpha\leq 1$, β is an arbitrary real number, and $C>0$ is a real constant, then*

$$ E_{\alpha,\beta}(A) \leq \frac{C}{1+\|A\|}, \tag{5} $$

where $\mu \leq |\arg(\mathrm{eig}(A))| \leq \pi$ with $\mu \in R$ satisfying $\pi\alpha/2 < \mu < \min\{\pi, \pi\alpha\}$.

Lemma 3 (see [24]). *If $t \in [0,T]$ and*

$$ x(t) \leq h(t) + \int_0^t k(\tau)x(\tau)d\tau, \tag{6} $$

where $k(t) \geq 0$ and all the functions involved are continuous on the interval $[0,T]$, then we can obtain

$$ x(t) \leq h(t) + \int_0^t k(\tau)h(\tau)\exp\left[\int_\tau^t k(u)du\right]d\tau. \tag{7} $$

Definition 4 (see [18]). A memoryless nonlinearity $\varphi(t,x) : [0,\infty)\times R^p \to R^p$ is said to satisfy a sector condition if the following inequality holds:

$$ \left(\varphi(t,x) - K_1x\right)^T\left(\varphi(t,x)-K_2x\right) \leq 0, \quad \forall x \in S \tag{8} $$

for constant matrices K_1 and K_2, where K_2-K_1 is a symmetric positive matrix and S contains the origin.

Based on the Definition 4, the following lemma holds.

Lemma 5 (see [18]). *Let*

$$ S(LK,u_0) = \left\{x(t)\in R^n \mid -u_0 \leq LKx(t) \leq u_0\right\}, \tag{9} $$

where $L = \mathrm{diag}[l_1, l_2, \ldots, l_n]$ with $0<l_i\leq 1, \forall i = 1,2,\ldots,n$, and

$$ \varphi(t,x(t)) = \mathrm{sat}(Kx(t)) - LKx(t); \tag{10} $$

then the following inequalities are equivalent:

(1) $(\mathrm{sat}(Kx(t)) - LKx(t))^T(\mathrm{sat}(Kx(t)) - Kx(t)) \leq 0$;

(2) $\varphi(t,x(t))^T(\varphi(t,x(t)) - (K-LK)x(t)) \leq 0$;

(3) $\|\varphi(t,x(t))\| \leq \|K-LK\|\|x(t)\|$.

Lemma 6. *The autonomous dynamic system*

$$ D^{\alpha}x(t) = Ax(t), \qquad x(0) = x_0 \tag{11} $$

is asymptotically stable if the following condition holds:

$$ \left|\arg\left(\mathrm{eig}\ (A)\right)\right| > \frac{\pi\alpha}{2}. \tag{12} $$

The stability region for $0<\alpha<1$ is depicted in Figure 1.

2.2. Description of Fractional-Order Financial Chaotic Systems. The fractional-order financial chaotic systems are proposed by [1]. The mathematical model describes a fractional-order financial system including three nonlinear differential equations. The states, $x_1(t)$, $x_2(t)$, and $x_3(t)$, represent the interest rate, the investment demand, and the price index, respectively. The fractional-order model of the system can be described as

$$ \begin{aligned} {}_{0}^{C}D_{t}^{\alpha}x_1(t) &= x_3(t) + \left(x_2(t)-a\right)x_1(t), \\ {}_{0}^{C}D_{t}^{\alpha}x_2(t) &= 1 - bx_2(t) - x_1^2(t), \\ {}_{0}^{C}D_{t}^{\alpha}x_3(t) &= -x_1(t) - cx_3(t), \end{aligned} \tag{13} $$

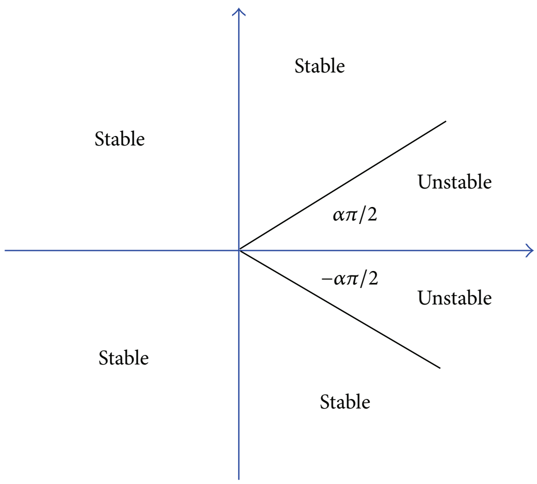

Figure 1: Stability region of linear system (11) with fractional order $0 < \alpha < 1$.

where a denotes the saving amount, b is the cost per investment, and c is the elasticity of demand of commercial market. $0 < \alpha < 2$ is the fractional-order derivative.

3. State-Feedback Controller Design and Stability Analysis

3.1. Fractional Order α: $0 < \alpha \leq 1$. Let us rewrite the controlled system (13) as the following compact form:

$$\begin{aligned} {}_0^C D_t^\alpha x(t) &= Px(t) + f(x(t)) + [0,1,0]^T + \operatorname{sat}(u(t)), \\ x(0) &= x_0, \end{aligned} \tag{14}$$

where $x(t), u(t) \in R^3$, represent the state variables and the control input, respectively. Consider that

$$\begin{gathered} P = \begin{bmatrix} -a & 0 & 1 \\ 0 & -b & 0 \\ -1 & 0 & -c \end{bmatrix}, \\ f(x) = \begin{bmatrix} x_1(t)\,x_2(t) \\ -x_1^2(t) \\ 0 \end{bmatrix} \\ \operatorname{sat}(u) = [\operatorname{sat}(u_1), \operatorname{sat}(u_2), \operatorname{sat}(u_3)]^T \end{gathered} \tag{15}$$

is the vector-valued saturation function with

$$\operatorname{sat}(u_i) = \operatorname{sign}(u_i)\min(u_{0i}, |u_i|), \quad i = 1,2,3, \tag{16}$$

where u_{0i} represents the symmetric saturation level of the ith control input.

Noting that in chaotic systems the states are bounded, the nonlinear function $f(x)$ satisfies

$$\|f(x(t))\| = |x_1(t)| \sqrt{x_1^2(t) + x_2^2(t)} \leq M \|x(t)\|, \tag{17}$$

where $M > |x_1(t)|$ is a constant.

Let us define the state-feedback control input as

$$u(t) = Kx(t) + [0,-1,0]^T, \tag{18}$$

where $K \in R^{3\times 3}$ is the control gain matrix. Then we have

$$\begin{aligned} {}_0^C D_t^\alpha x(t) &= Px(t) + [0,1,0]^T + f(x(t)) \\ &\quad + \operatorname{sat}\left(Kx(t) + [0,-1,0]^T\right) \\ &= Ax(t) + f(x(t)) + \varphi(t, x(t)), \end{aligned} \tag{19}$$

where $A = P + LK$.

Theorem 7. *Consider system* (14). *If we choose matrices L and K such that $|\arg(\operatorname{eig}(A))| > \alpha\pi/2$ and $\alpha\|A\| > d$, then system* (14) *is asymptotically stable. d is a positive constant and will be defined later.*

Proof. Taking Laplace transform on (19), we can obtain

$$s^\alpha X(s) = s^{\alpha-1}x_0 + AX(s) + \mathscr{L}\{f(x)\} + \mathscr{L}\{\varphi(t,x)\}, \tag{20}$$

where $X(s)$ represents the Laplace transform of $x(t)$. Let I denote the 3×3 identity matrix; we have

$$X(s) = (Is^\alpha - A)^{-1}\left(s^{\alpha-1}x_0 + \mathscr{L}\{f(x)\} + \mathscr{L}\{\varphi(t,x)\}\right). \tag{21}$$

By taking Laplace inverse transform on (21), we get the solution of system (14):

$$\begin{aligned} x(t) &= E_{q,1}\left(A(t)^\alpha\right)x_0 + \int_0^t (t-\tau)^{\alpha-1} \\ &\quad \times E_{\alpha,\alpha}\left(A(t-\tau)^\alpha\right) f(x)\,d\tau \\ &\quad + \int_0^t (t-\tau)^{\alpha-1} E_{\alpha,\alpha}\left(A(t-\tau)^\alpha\right)\varphi(t,x)\,d\tau. \end{aligned} \tag{22}$$

According to Lemma 2, we know there exist some constants $c_i > 0$, $i = 1,2$, such that

$$\begin{aligned} \|x(t)\| &\leq \frac{c_1\|x_0\|}{1 + \|A\|t^\alpha} + \int_0^t \frac{(t-\tau)^{\alpha-1}c_2}{1 + \|A\|(t-\tau)^\alpha}\|f(x)\|\,d\tau \\ &\quad + \int_0^t \frac{(t-\tau)^{\alpha-1}c_2}{1 + \|A\|(t-\tau)^\alpha}\|\varphi(t,x)\|\,d\tau. \end{aligned} \tag{23}$$

Then (23) can be rewritten as

$$\begin{aligned} \|x(t)\| &\leq \frac{c_1\|x_0\|}{1 + \|A\|t^\alpha} + M\int_0^t \frac{(t-\tau)^{\alpha-1}c_2}{1 + \|A\|(t-\tau)^\alpha}\|x(t)\|\,d\tau \\ &\quad + \int_0^t \frac{(t-\tau)^{\alpha-1}c_2}{1 + \|A\|(t-\tau)^\alpha}\|\varphi(t,x)\|\,d\tau. \end{aligned} \tag{24}$$

From Definition 4 and Lemma 5, we know that $\varphi(t, x(t))$ satisfies

$$\|\varphi(t, x(t))\| \leq \|K - LK\|\,\|x(t)\|. \tag{25}$$

Let $d = Mc_2 + c_2\|K - LK\|$; we can obtain

$$\|x(t)\| \leq \frac{c_1\|x_0\|}{1+\|A\|t^{\alpha}} + d\int_0^t \frac{(t-\tau)^{\alpha-1}}{1+\|A\|(t-\tau)^{\alpha}}\|x(t)\|\,d\tau. \tag{26}$$

By using Lemma 3, we have

$$\begin{aligned}
\|x(t)\| \leq{}& \frac{c_1\|x_0\|}{1+\|A\|t^{\alpha}} \\
&+ \int_0^t \frac{dc_1(t-\tau)^{\alpha-1}\|x_0\|}{(1+\|A\|(t-\tau)^{\alpha})(1+\|A\|\tau^{\alpha})} \\
&\times \exp\left(\int_\tau^t \frac{d(t-y)^{\alpha-1}}{1+\|A\|(t-y)^{\alpha}}dy\right)d\tau \\
={}& \frac{c_1\|x_0\|}{1+\|A\|t^{\alpha}} \\
&+ \int_0^t \frac{dc_1(t-\tau)^{\alpha-1}\|x_0\|}{(1+\|A\|\tau^{\alpha})(1+\|A\|(t-\tau)^{\alpha})^{1-c/\alpha\|A\|}}d\tau \\
\leq{}& \frac{c_1\|x_0\|}{1+\|A\|t^{\alpha}} \\
&+ dc_1\|x_0\|\|A\|^{d/\alpha\|A\|-2}\int_0^t (t-\tau)^{d/\|A\|-1}\tau^{-\alpha}d\tau \\
={}& \frac{c_1\|x_0\|}{1+\|A\|t^{\alpha}} + dc_1\|x_0\|\|A\|^{c/\alpha\|A\|-2} \\
&\times \frac{\Gamma(d/\|A\|)\Gamma(1-\alpha)}{\Gamma(1+d/\|A\|-\alpha)}t^{d/\|A\|-\alpha}.
\end{aligned} \tag{27}$$

Since $\alpha\|A\| > d$, from (27) we can conclude that

$$\lim_{t\to\infty}\|x(t)\| = 0, \tag{28}$$

and this ends the proof. □

3.2. Fractional Order α: $1 < \alpha < 2$. Let the initial conditions be $x^{(i)}(0) = x_i$, $i = 1, 2$. Then we have the following results.

Theorem 8. *Consider system* (14)*. If we choose matrices L and K such that* $|\arg(\operatorname{eig}(A))| > \alpha\pi/2$ *and* $(\alpha - 1)\|A\| > d$*, then system* (14) *is asymptotically stable. d is a positive constant.*

Proof. Similar to the proof of Theorem 8, taking the Laplace transform and Laplace inverse transform on (14) gives

$$\begin{aligned}
x(t) ={}& E_{q,1}(A(t)^{\alpha})x_1 + \int_0^t (t-\tau)^{\alpha-1}E_{\alpha,\alpha}(A(t-\tau)^{\alpha})f(x)\,d\tau \\
&+ \int_0^t (t-\tau)^{\alpha-1}E_{\alpha,\alpha}(A(t-\tau)^{\alpha})\varphi(t,x)\,d\tau \\
&+ tE_{\alpha,2}(At^{\alpha})x_2.
\end{aligned} \tag{29}$$

According to Lemma 2, there exist positive constants c_i, $i = 1, 2, 3$, such that

$$\begin{aligned}
\|x(t)\| \leq{}& \frac{c_1\|x_1\|}{1+\|A\|t^{\alpha}} + \int_0^t \frac{(t-\tau)^{\alpha-1}c_2}{1+\|A\|(t-\tau)^{\alpha}}\|f(x)\|\,d\tau \\
&+ \int_0^t \frac{(t-\tau)^{\alpha-1}c_2}{1+\|A\|(t-\tau)^{\alpha}}\|\varphi(t,x)\|\,d\tau + \frac{c_3t\|x_2\|}{1+\|A\|t^{\alpha}}.
\end{aligned} \tag{30}$$

From Definition 4 and Lemma 5, we know that $\varphi(t, x(t))$ satisfies

$$\|\varphi(t,x(t))\| \leq \|K-LK\|\,\|x(t)\|. \tag{31}$$

Let $d = Mc_2 + c_2\|K - LK\|$; we can obtain

$$\begin{aligned}
\|x(t)\| \leq{}& \frac{c_1\|x_1\| + c_3t\|x_1\|}{1+\|A\|t^{\alpha}} \\
&+ d\int_0^t \frac{(t-\tau)^{\alpha-1}}{1+\|A\|(t-\tau)^{\alpha}}\|x(t)\|\,d\tau.
\end{aligned} \tag{32}$$

Then we have

$$\begin{aligned}
\|x(t)\| \leq{}& \frac{c_1\|x_1\| + c_3t\|x_1\|}{1+\|A\|t^{\alpha}} \\
&+ \int_0^t \frac{d(t-\tau)^{\alpha-1}(c_1\|x_1\| + c_3t\|x_2\|)}{(1+\|A\|(t-\tau)^{\alpha})(1+\|A\|\tau^{\alpha})} \\
&\times \exp\left(\int_\tau^t \frac{d(t-y)^{\alpha-1}}{1+\|A\|(t-y)^{\alpha}}dy\right)d\tau \\
={}& \frac{c_1\|x_1\| + c_3t\|x_1\|}{1+\|A\|t^{\alpha}} \\
&+ \int_0^t \frac{d(t-\tau)^{\alpha-1}(c_1\|x_1\| + c_3\|x_2\|)}{(1+\|A\|\tau^{\alpha})(1+\|A\|(t-\tau)^{\alpha})^{1-c/\alpha\|A\|}}d\tau \\
\leq{}& \frac{c_1\|x_1\| + c_3t\|x_1\|}{1+\|A\|t^{\alpha}} \\
&+ dc_1\|x_1\|\|A\|^{d/\alpha\|A\|-2}\int_0^t (t-\tau)^{1/\|A\|-1}\tau^{-\alpha}d\tau \\
&+ dc_3\|x_2\|\|A\|^{d/\alpha\|A\|-2}\int_0^t (t-\tau)^{1/\|A\|-1}\tau^{1-\alpha}d\tau \\
={}& \frac{c_1\|x_1\| + c_3t\|x_1\|}{1+\|A\|t^{\alpha}} + dc_1\|x_1\|\|A\|^{d/\alpha\|A\|-2} \\
&\times \frac{\Gamma(d/\|A\|)\Gamma(1-\alpha)}{\Gamma(1+d/\|A\|-\alpha)}t^{d/\|A\|-\alpha} \\
&+ dc_3\|x_2\|\|A\|^{d/\alpha\|A\|-2} \\
&\times \frac{\Gamma(d/\|A\|)\Gamma(2-\alpha)}{\Gamma(2+d/\|A\|-\alpha)}t^{d/\|A\|+1-\alpha}.
\end{aligned} \tag{33}$$

Since $(\alpha - 1)\|A\| > d$, from (33) we know that

$$\lim_{t\to\infty} \|x(t)\| = 0, \tag{34}$$

and this ends the proof. □

4. Simulation Studies

The system (14) has 3 equilibriums:

$$E_1 = \left(0; \frac{1}{b}; 0\right),$$
$$E_2 = \left(\sqrt{\frac{c-b-abc}{c}}; \frac{1+ac}{c}; -\frac{1}{c}\sqrt{\frac{c-b-abc}{c}}\right), \tag{35}$$
$$E_3 = \left(-\sqrt{\frac{c-b-abc}{c}}; \frac{1+ac}{c}; \frac{1}{c}\sqrt{\frac{c-b-abc}{c}}\right).$$

The Jacobian matrix of the fractional-order chaotic system (14), at the equilibrium $E^* = [x^*, y^*, z^*]^T$, can be given as

$$J_E = \begin{bmatrix} -a+y^* & x^* & 1 \\ -2x^* & -b & 0 \\ -1 & 0 & -c \end{bmatrix}. \tag{36}$$

Let $a = 1$, $b = 0.1$, and $c = 1$. The eigenvalues for the system equilibrium $E_1 = (0;\ 10;\ 0)$ are $\lambda_1 = 8.8990$, $\lambda_2 = -0.8990$, and $\lambda_3 = -0.1$. And it is a saddle point. For equilibrium points $E_2 = (0.8944;\ 2; -0.8944)$ and $E_3 = (-0.8944;\ 2;\ 0.8944)$ they are $\lambda_1 = -0.7609$ and $\lambda_{2,3} = 0.3304 \pm 1.4112i$. It is a saddle-focus point. Since it is an unstable equilibrium, the condition for chaos is satisfied and the system (14) can show chaotic behavior. We can easily get the minimal commensurate order of the system which is $\alpha > 0.8537$.

Case 1 ($0 < \alpha \le 1$). Assume the fractional order is $\alpha = 0.9$. The characteristic equation of the linearized system for the equilibrium E_1 is

$$\lambda^{27} - 7.9\lambda^{18} - 8.8\lambda^{9} - 0.8 = 0. \tag{37}$$

The characteristic equation of the linearized system for the equilibriums E_2 and E_3 is

$$\lambda^{27} + 0.1\lambda^{18} + 1.6\lambda^{9} + 1.6 = 0 \tag{38}$$

and the unstable eigenvalues are $\lambda_{1,2} = 1.0306 \pm 0.1547i$.

Let the initial condition be $x(0) = [2, -1, 1]^T$. The chaotic behavior of uncontrolled fractional-order financial system (13) is shown in Figure 2.

The control gain matrices are chosen as $L = \mathrm{diag}[0.9, 0.9, 0.9]$.

Let

$$A = \begin{bmatrix} 0 & 1 & 0 \\ 0 & 0 & 1 \\ -2 & -2 & -3 \end{bmatrix}; \tag{39}$$

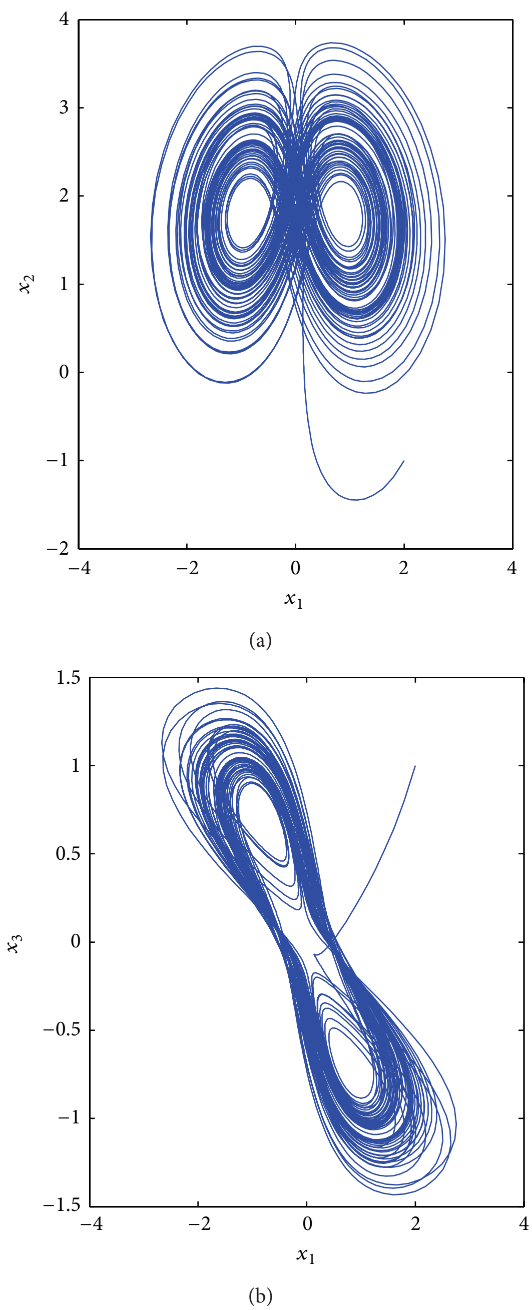

Figure 2: Chaotic attractor of fractional-order financial system with fractional order $\alpha = 0.90$: (a) x_1-x_2 plane; (b) x_1-x_3 plane.

then we have $\|A\| = 4.2160$. From simulation results (see Figure 2), we know $|x_1(t)| \le 3$. From $A = P + LK$, we have

$$K = \begin{bmatrix} 1.1111 & 1.1111 & -1.1111 \\ 0 & 0.1111 & 1.1111 \\ -1.1111 & -2.2222 & -2.2222 \end{bmatrix}. \tag{40}$$

From above discussion, we know $\|A\| = 4.2160$ and $|\arg(\mathrm{eig}(A))| = [3.1416, 1.8428, 1.8428]^T$. Then we can easily test that the conditions $|\arg(\mathrm{eig}(A))| > \alpha\pi/2$ and $\alpha\|A\| > d$ are satisfied.

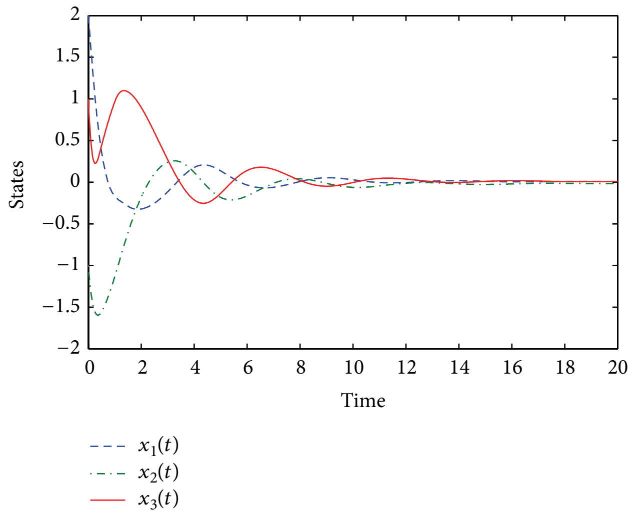

Figure 3: Time response of the state variables with fractional order $\alpha = 0.90$.

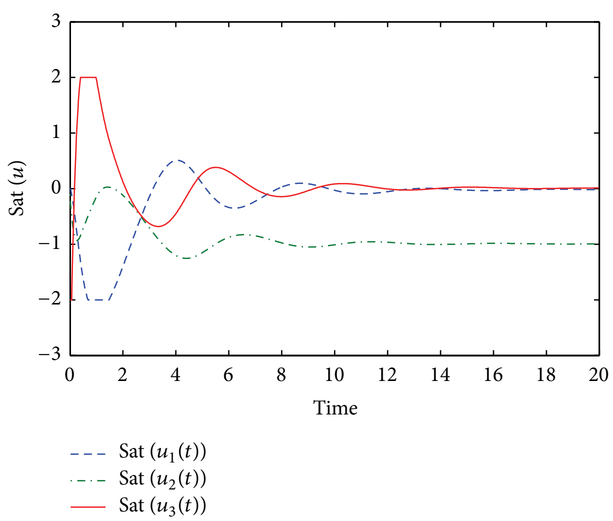

Figure 4: Time response of the control inputs with fractional order $\alpha = 0.90$.

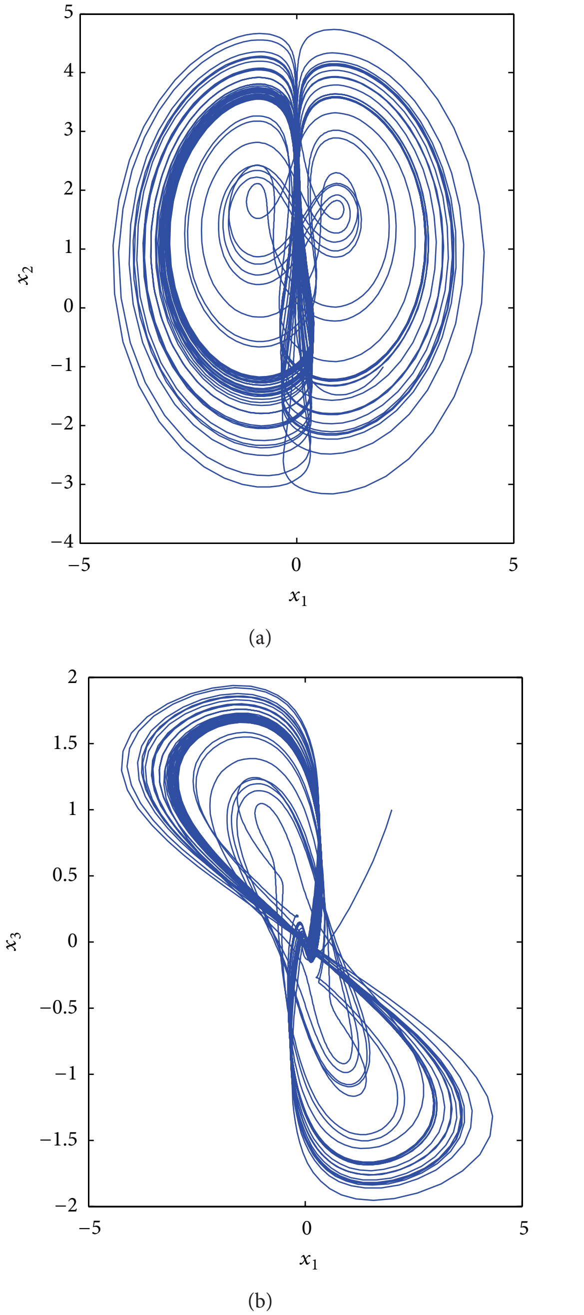

Figure 5: Chaotic attractor of fractional-order financial system with fractional order $\alpha = 1.04$: (a) x_1-x_2 plane; (b) x_1-x_3 plane.

Let $u_{01} = u_{02} = u_{03} = 2$. The simulation results can be seen in Figures 3 and 4. From the results, we can see that the states variables converge rapidly. The involved system is asymptotic stable. Figure 4 shows the boundedness and smoothness of the saturated control inputs. It can be concluded that good control performance has been achieved.

Case 2 ($1 < \alpha < 2$). Let the fractional order be $\alpha = 1.04$. The chaotic behavior is depicted in Figure 5. In the simulation, the control gain matrices are chosen as $L = \operatorname{diag}[0.9, 0.9, 0.9]$,

$$K = \begin{bmatrix} 1.1111 & 1.1111 & -1.1111 \\ 0 & 0.1111 & 1.1111 \\ -4.4444 & -6.6667 & -6.6667 \end{bmatrix}; \tag{41}$$

then we have

$$A = P + LK = \begin{bmatrix} 0 & 1 & 0 \\ 0 & 0 & 1 \\ -5 & -6 & -7 \end{bmatrix}. \tag{42}$$

From above discussion, we know $\|A\| = 10.5249$ and $|\arg(\operatorname{eig}(A))| = [3.1416, 2.0573, 2.0573]^T$. Then we have $|\arg(\operatorname{eig}(A))| > \alpha\pi/2$ and $\alpha\|A\| > d$.

Let $u_{01} = u_{02} = u_{03} = 2$. The simulation results can be seen in Figures 6 and 7. From the simulation results we can conclude that good control performance has been achieved.

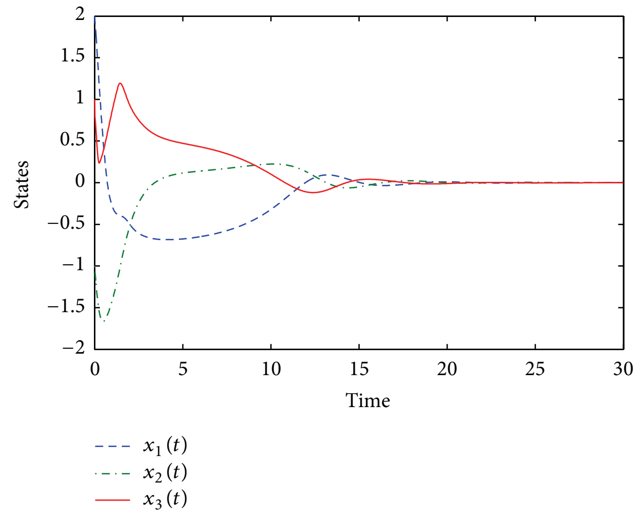

FIGURE 6: Time response of the state variables with fractional order $\alpha = 1.04$.

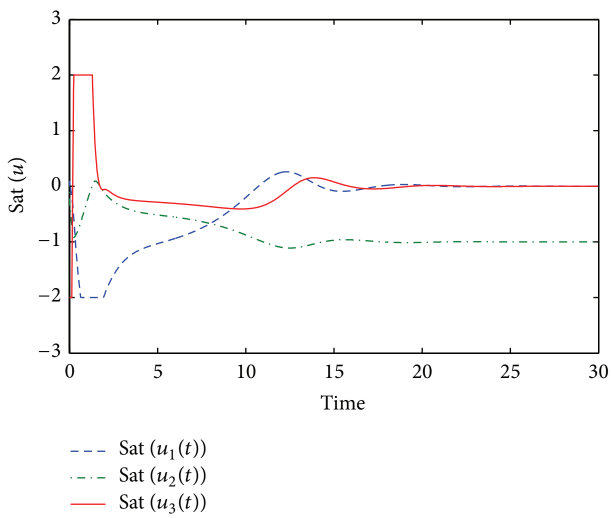

FIGURE 7: Time response of the control inputs with fractional order $\alpha = 1.04$.

5. Conclusions

We investigate the control problem for fractional-order financial chaotic systems subject to input saturation by means of linear control. Two sufficient conditions are given for the stabilization of such systems with fractional orders $0 < \alpha \le 1$ and $1 < \alpha < 2$, respectively. A state-feedback controller is designed and the asymptotical stability of the involved system is guaranteed. It is shown that state-feedback controller can be designed to control the fractional-order financial chaotic systems. Simulation studies confirm the results of this paper.

Conflict of Interests

The authors do not have a direct financial relation with any commercial identity mentioned in their paper that might lead to a conflict of interests for any of the authors.

Acknowledgments

This work is supported by the National Natural Science Foundation of China (Grant no. 61001086) and the Fundamental Research Funds for the Central Universities (Grant no. ZYGX2011X004).

References

[1] W. C. Chen, "Nonlinear dynamics and chaos in a fractional-order financial system," *Chaos, Solitons and Fractals*, vol. 36, no. 5, pp. 1305–1314, 2008.

[2] G. Cai and J. Huang, "A new finance chaotic attractor," *International Journal of Nonlinear Science*, vol. 3, no. 3, pp. 213–220, 2007.

[3] F. Wen and X. Yang, "Skewness of return distribution and coefficient of risk premium," *Journal of Systems Science & Complexity*, vol. 22, no. 3, pp. 360–371, 2009.

[4] C. Huang, C. Peng, X. Chen, and F. Wen, "Dynamics analysis of a class of delayed economic model," *Abstract and Applied Analysis*, vol. 2013, Article ID 962738, 12 pages, 2013.

[5] C. Huang, X. Gong, X. Chen, and F. Wen, "Measuring and forecasting volatility in Chinese stock market using HAR-CJ-M model," *Abstract and Applied Analysis*, vol. 2013, Article ID 143194, 13 pages, 2013.

[6] F. Wen and Z. Liu, "A copula-based correlation measure and its application in chinese stock market," *International Journal of Information Technology and Decision Making*, vol. 8, no. 4, pp. 787–801, 2009.

[7] F. Wen, X. Gong, Y. Chao, and X. Chen, "The effects of prior outcomes on risky choice: evidence from the stock market," *Mathematical Problems in Engineering*, vol. 2014, Article ID 272518, 8 pages, 2014.

[8] M. Rivero, J. J. Trujillo, L. Vázquez, and M. P. Velasco, "Fractional dynamics of populations," *Applied Mathematics and Computation*, vol. 218, no. 3, pp. 1089–1095, 2011.

[9] Z. Wang, X. Huang, and H. Shen, "Control of an uncertain fractional order economic system via adaptive sliding mode," *Neurocomputing*, vol. 83, pp. 83–88, 2012.

[10] J. Cao, D. W. C. Ho, and Y. Yang, "Projective synchronization of a class of delayed chaotic systems via impulsive control," *Physics Letters. A*, vol. 373, no. 35, pp. 3128–3133, 2009.

[11] J. D. Cao and L. L. Li, "Cluster synchronization in an array of hybrid coupled neural networks with delay," *Neural Networks*, vol. 22, no. 4, pp. 335–342, 2009.

[12] J. Cao, A. Alofi, A. Al-Mazrooei, and A. Elaiw, "Synchronization of switched interval networks and applications to chaotic neural networks," *Abstract and Applied Analysis*, vol. 2013, Article ID 940573, 11 pages, 2013.

[13] H. Zhang, J. Cao, and W. Jiang, "Controllability criteria for linear fractional differential systems with state delay and impulses," *Journal of Applied Mathematics*, vol. 2013, Article ID 146010, 9 pages, 2013.

[14] J. D. Cao and Y. Wan, "Matrix measure strategies for stability and synchronization of inertial BAM neural network with time delays," *Neural Networks*, vol. 53, pp. 165–172, 2014.

[15] M. S. Tavazoei and M. Haeri, "Synchronization of chaotic fractional-order systems via active sliding mode controller," *Physica A: Statistical Mechanics and Its Applications*, vol. 387, no. 1, pp. 57–70, 2008.

[16] M. S. Tavazoei and M. Haeri, "Chaotic attractors in incommensurate fractional order systems," *Physica D: Nonlinear Phenomena*, vol. 237, no. 20, pp. 2628–2637, 2008.

[17] Y. F. Xu and Z. M. He, "Synchronization of variable-order fractonal financial systems via active control method," *Central European Journal of Physics*, vol. 11, no. 6, pp. 824–835, 2013.

[18] Z. Wang, X. Huang, and G. D. Shi, "Analysis of nonlinear dynamics and chaos in a fractional order financial system with time delay," *Computers & Mathematics with Applications*, vol. 62, no. 3, pp. 1531–1539, 2011.

[19] Y.-H. Lim, K.-K. Oh, and H.-S. Ahn, "Stability and stabilization of fractional-order linear systems subject to input saturation," *IEEE Transactions on Automatic Control*, vol. 58, no. 4, pp. 1062–1067, 2013.

[20] T. Gußner, M. Jost, and J. Adamy, "Controller design for a class of nonlinear systems with input saturation using convex optimization," *Systems and Control Letters*, vol. 61, no. 1, pp. 258–265, 2012.

[21] J. Luo, "State-feedback control for fractional-order nonlinear systems subject to input saturation," *Mathematical Problems in Engineering*, vol. 2014, Article ID 891639, 8 pages, 2014.

[22] I. Podlubny, *Fractional Differential Equations*, vol. 198, Mathematics in Science and Engineering, Academic Press, San Diego, Calif, USA, 1999.

[23] H. S. Ahn and Y. Q. Chen, "Necessary and sufficient stability condition of fractional-order interval linear systems," *Automatica*, vol. 44, no. 11, pp. 2985–2988, 2008.

[24] L. Chen, Y. Chai, R. Wu, and J. Yang, "Stability and stabilization of a class of nonlinear fractional-order systems with caputo derivative," *IEEE Transactions on Circuits and Systems II: Express Briefs*, vol. 59, no. 9, pp. 602–606, 2012.

Hindawi Publishing Corporation
Discrete Dynamics in Nature and Society
Volume 2014, Article ID 308626, 6 pages
http://dx.doi.org/10.1155/2014/308626

Research Article

Analysis on the Impact of the Fluctuation of the International Gold Prices on the Chinese Gold Stocks

Jiankang Jin,[1] Chen Jie,[2] and Quanda Zhang[2]

[1] *School of Economics & Management, Northwest University, Xian 710127, China*
[2] *School of Finance, Zhejiang University of Finance and Economics, Hangzhou 310018, China*

Correspondence should be addressed to Jiankang Jin; jiankangjin760@126.com

Received 14 March 2014; Revised 18 June 2014; Accepted 30 June 2014; Published 21 July 2014

Academic Editor: Fenghua Wen

Five gold stocks in Chinese Shanghai and Shenzhen A-share and Comex gold futures are chosen to form the sample, for the purpose of analysing the impact of the fluctuation of the international gold prices on the gold stocks in Chinese Shanghai and Shenzhen A-share. Using the methods of unit root test, Granger causality test, VAR model, and impulse response function, this paper has analysed the relationship between the price change of the international gold futures and the price fluctuation of gold stocks in Chinese Shanghai and Shenzhen comprehensively. The results suggest the fluctuation of the international gold futures has a strong influence on the domestic futures.

1. Introduction

Gold futures are a future contract which chooses the gold as subject, and it is a standardized protocol that the seller and the buyer agree to deal in a specific time in the future based on their agreement. In an efficient market, the gold futures market and spot market, however, will respond to innovation at the same time, and there is no lead-lag relationship between the two markets. Product design, trading mechanism, and different investors are the main differences between the gold futures market and spot market. Because of the great risk when investing in the gold futures, many investors prefer gold stock instead of gold futures to be their first choice. Therefore, it is important to understand the relationship between the gold futures and gold stocks. For many investors, it is rather meaningful to predict the trend of the value of listed gold companies and thus make more accurate price estimate when the trend of the gold futures is analyzed and available. This paper has analyzed the relationship between the price change of the international gold futures and the price fluctuation of gold stocks in Chinese Shanghai and Shenzhen comprehensively. Section 2 gives out a review of the literature on the gold futures research, Section 3 explains the research design and innovation, Section 4 introduces the empirical methods, and Section 5 is the empirical process. The results of this paper are given in the last section.

2. Review of the Literature

Both the domestic and foreign scholars have studied the relationship between the gold spot and gold futures from many aspects. Using the methods of correlation analysis, unit root test, cointegration test, and Granger Causality test and impulse response function, Jiaming [1] chooses Chinese gold futures as the research object to study the effectiveness of the gold market in China and the United States, respectively. His research suggests there are noneffective factors in gold futures market, and gold spot price has an unidirectional guide to gold futures. Some scholars have researched the relative content from the market viewpoint, such as [2, 3]. Based on the impulse response function, variance decomposition in vector autoregression model, cointegration test, and Granger causality test, Zhipeng and Guoyan [4] adopt the daily closing price of gold futures 0806 contract, which is the latest issue due between January 9, 2008, and May 16, 2008, traded in Shanghai futures exchange, to be their research object. With the bivariate EC-EGARCH model built, they study the price relationship between gold futures market and gold spot market in China empirically. The result shows that there is no guide relationship in gold futures market and gold spot market in China, which is caused by the weak efficiency of market information transformation, and the gold futures market is not smooth enough in the early stage of Chinese gold futures. Using the autoregressive distributed lag model combined with GARCH models, Di and Jiangming [5] study the dynamic relationship between the price volatility of New York gold futures and the price volatility of copper futures, zinc futures, and natural rubber futures traded in Shanghai futures exchange to measure the effect of macroeconomic performance on Chinese futures market. They find part of futures has showed the financial attributes and is linked closely with macroeconomic volatility in China. Besides, some scholars have researched the investors' risk preference aspect, such as [6, 7], and other scholars have researched risk premium viewpoint, such as [8].

Using the daily data of New York mercantile exchange, Shawky et al. [9] study the dynamic relationship between the futures market price and the spot market price by EGARCH model; they also study the inverse relationship between the two markets by building the vector autoregression (VAR) model. Choosing the data of daily yield of gold and silver between 1982 and 2002 to be the sample, Lucey and Tully [10] study the condition and unconditional mean and variance of daily yield based on the frame of GARCH model. Their research shows that daily average yield cyclical characteristic is not obvious, but the cyclical change characteristic of variance is obvious. Hillier et al. [11] study the function of gold futures in securities market, they find 1976–2004 gold and S&P500 index are negatively correlated, and the portfolio which contains 5%–10% gold has a better performance than other ones which contain no gold. Lin et al. [12] employ a bivariate GARCH model to examine the dynamic relationship between two gold futures markets. Their results show that the performance of Comex is better than TOCOM. Volatility transmission effects exist in both Comex and TOCOM. While the responses to good news and bad news are symmetrical in TOCOM, they are asymmetric in Comex. Cretien [13] offers information about the importance of gold and silver on futures trades in the USA. The paper states the differences and similarities of both precious metals make them a target for options on trade. It mentions that the futures market for gold and silver produces best measure of how well the country currently is protecting the value of dollar. Based on the smooth transition regression model, Lee and Lin [14] investigate the nonlinear dynamic relationship between USD/yen and gold futures in the commodity exchange. The empirical results show the transition function is a logistic type. Gold is both a hedge and a safe haven for developing countries but not for emerging countries; the relationships between gold and emerging market index are positive.

3. Research Design

Through the review of the literature above, we find both domestic and foreign scholars choose the gold spot as the corresponding sample when they investigate the gold futures, and the research theme mostly concentrates on the dynamic relationship between gold futures and gold spot instead of the dynamic relationship of gold futures and stocks. Therefore, this paper is aimed at studying the relationship between gold futures and gold stocks. In this paper, we select the Zhongjin Gold (600489), which enjoys the fame—China No. 1 gold stock in Shanghai and Shenzhen A-share, the Shandong Gold (600547), which is the No. 2 listed company in Chinese gold industry and its corporation size nearly reaches the level of government, the Zijin Mining (600189), which is among the gold producing corporation in China and is evaluated as "Chinese largest gold mine" by China Gold Association, the Chenzhou Mining (002155), which is one of the domestic top ten gold mine development companies, the Shanghai gold exchange consolidated class member and the provider of standard gold bullion, and the Hengbang Stock (002237), which has the gold output that ranked the forefront of the Chinese gold enterprises. The above five gold stocks form the sample (there are more than five gold stocks in Shanghai and Shenzhen A-share, but after a lot of contrast, we found choosing five stocks is most suitable for presentation, not eight or ten), and the Comex gold futures traded in New York form the future sample.

On the data processing, both the domestic and foreign scholars tend to use the raw data or the raw data in logarithmic in their research. And then they will conduct a series of empirical analyses on this basis. However, in this paper, the daily revenue growth rate is calculated on the basis of daily data in the process of gold stock data, and then the weighted average of 5-daily-revenue growth rate of the stock can be counted, what we get is the daily price volatility of Shanghai and Shenzhen gold stocks (the weighted average of the 5-gold-stock daily growth rate of revenue, the following JPS). On the international gold future data processing, the calculated daily growth rate of Comex gold future prices (following Comex) forms the analytical sample, and the time range of the two sets of data starts from January 1, 2010, to December 31, 2012. Considering the effects of time differences caused by the geographical location (New York in West Area 5 while Beijin in East Area 8), we lag the gold futures data a day, contrast the gold stocks and gold futures, and then delete the day data the two sides stop plate and off plate, and then the data we get have the same timeline of gold stock and futures.

On the empirical analysis, the raw data is transferred to weight percentage data. Based on the unit root test, we find both of the two sets of the data are stationary; thus, we can direct use the methods of Granger causality test, to build the VAR model as well as to do the impulse response functions analysis to determine the correlation between the data.

4. Research Methods

4.1. ADF Test. ADF test is an augmented version of the Dickey-Fuller test for a larger and more complicated set of time series models. ADF test consists of the following three models:

Model 1: $\Delta X_t = \delta X_{t-1} + \sum_{i=1}^{m} \beta_i \Delta X_{t-i} + \varepsilon_t$.

Model 2: $\Delta X_t = \alpha + \delta X_{t-1} + \sum_{i=1}^{m} \beta_i \Delta X_{t-i} + \varepsilon_t$.

Model 3: $\Delta X_t = \alpha + \beta_t + \delta X_{t-1} + \sum_{i=1}^{m} \beta_i \Delta X_{t-i} + \varepsilon_t$.

In the model, $\Delta X_t = X_t - X_{t-1}$, Δ is the first order difference operation factor and the residual term ε_t is the white noise (ε_t is the random item with zero mean, constant variance, and no autocorrelation). The null hypothesis of three models above is $H_0 : \delta = 0$, which means there is a unit root. If the ADF test value exceeds the critical value, the null hypothesis H_0 cannot be rejected, which means the time series X_t contains a unit root and it is not stationary.

4.2. Granger Causality Test. For the two variables X and Y, Granger causality test requires an estimation of the following regression:

$$Y_t = \beta_0 + \sum_{i=1}^{m} \beta_i Y_{t-i} + \sum_{i=1}^{m} \alpha_i X_{t-i}, \quad (1)$$

$$X_t = \delta_0 + \sum_{i=1}^{m} \delta_i X_{t-i} + \sum_{i=1}^{m} \lambda_i Y_{t-i}. \quad (2)$$

We use the assumption that X is not Y Granger cause as example, which is equal to the assumption that the parameter before the X lag items all equals zero, and we make regression which contains the X lag items and regression which does not contain the X lag items. Using RSS_U to represent the former residual sum of squares and RSS_R to represent the latter residual sum of squares, then calculate the F statistic as follows:

$$F = \frac{(\text{RSS}_R - \text{RSS}_U)/m}{\text{RSS}_U/(n-k)}. \quad (3)$$

In the equation, m is the number of the X lag items, n is the number of sample, and k is the number of the unconstrained regression model parameters to be estimated which may contain constant and other variables. If the calculated F value exceeds the corresponding the critical value $F_\alpha(m, n-k)$ under the given significance level α, then the null hypothesis will be rejected and the X is the Granger cause of Y.

4.3. VAR Model. VAR model is used to predict and analyze interrelated time series and the dynamic effects that the random perturbations have on the variable system. There is no need to specify whether some variables are endogenous or exogenous. Besides, VARs allow the value of a variable to depend on its own lags and the lags of other variables. Models thus offer a structure which may be able to capture more characteristics of the data. VAR model is defined as follows.

If $Y_t = (y_{1t}, \ldots, y_{Nt})^T$ is the $N \times 1$ order time series variable column vector, then the P order VAR model (the following VAR (P)) is as follows:

$$\begin{aligned} Y_t &= \sum_{i=1}^{P} \prod_i Y_{t-i} + U_t \\ &= \prod_1 Y_{t-1} + \prod_2 Y_{t-2} \cdots + \prod_P Y_{t-p} \\ &\quad + U_t U_T \sim IID(0, \Omega), \end{aligned} \quad (4)$$

where $U_t = (u_{1t}, \ldots, u_{Nt})^T$ is $N \times 1$ order random error column vector, P is the maximum lag order of the model, and Ω is $N \times N$ order covariance matrix. VAR (P) model is the equations model which chooses the t period variable $y_{1t}, y_{2t}, \ldots, y_{Nt}$ as dependent variables and the maximum P order lag variables of dependent variables $y_{1t}, y_{2t}, \ldots, y_{Nt}$ as independent variables, and the equations models have N equations.

4.4. Impulse Response Function. It is absolutely necessary to do the impulse response function analysis to investigate the dynamic characteristics of the Comex and JPS. What the impulse response function concern is the impact that the dependent variables on each variables, it is used to analyze the effect of the information to the system. By applying a unit shock to the disturbance term of each equation, we can get the impact of unit shocks on VAR system in a period of time. We use VAR (2) model which contains two variables as an example to explain. Set two-variable VAR (2) model as follows:

$$\begin{aligned} \begin{pmatrix} \text{GDP}_t \\ M_t \end{pmatrix} &= \begin{pmatrix} \alpha_{11} & \alpha_{12} \\ \alpha_{21} & \alpha_{22} \end{pmatrix} \begin{pmatrix} \text{GDP}_{t-1} \\ M_{t-1} \end{pmatrix} \\ &\quad + \begin{pmatrix} \beta_{11} & \beta_{12} \\ \beta_{21} & \beta_{22} \end{pmatrix} \begin{pmatrix} \text{GDP}_{t-2} \\ M_{t-2} \end{pmatrix} + \begin{pmatrix} \mu_{1t} \\ \mu_{2t} \end{pmatrix}. \end{aligned} \quad (5)$$

In the above equation, M is the money supply. If the system is subject to some kind of disturbance, making μ_{1t} change in one standard deviation, the GDP_t not only change immediately (response), but also influence the value of M_t through $\text{GDP}_{t-1}, \text{GDP}_{t-2}$, and it will affect the subsequent value of GDP and M (lag response). Impulse response function describes the response trajectory of the interaction between the variables in the system, showing the entire chain reaction process of how any disturbances affect other variables through model.

5. The Process of Empirical Study

5.1. ADF Test. In the aspect of testing the stationary of time series, the ADF test is used in this paper. Table 1 is the ADF test results of both JPS and Comex.

As we can see the t-statistic of the daily return growth rate of the Comex gold future and the weight average daily return growth rate of 5 stocks are less than the t-statistic under the significance at 1% level, and the P value is 0, which means the null hypothesis should be rejected. Therefore, the JPS and Comex are stationary.

5.2. Granger Causality Test. Table 2 shows the result of the Granger causality test.

The F-statistic of the first line is significantly greater than the critical value of F at 99% confidence level, and its P value is a near-zero constant, so the null hypothesis that the price change of the international gold future does not guide the price change of the Chinese gold stocks is rejected. And the price change of the international gold future guides the price change of the Chinese gold stocks at 99% confidence level.

The F-statistic of the second line is less than the critical value at 99% confidence level and P value is 0.5874, which is

Table 1: The result of the unit root test.

ADF test statistic	t-statistic	P value
JPS	−25.5933	0.000
Comex	−24.4506	0.000
The critical value		
1% level	−2.5684	
5% level	−1.94129	
10% level	−1.61638	

Note. JPS means the weight average daily return growth rate of 5 stocks. Comex means the daily return growth rate of the Comex gold future.

Table 2: The result of the Granger causality test.

Null hypothesis	F-statistic	P value
Comex does not Granger cause JPS	33.1689	1.80E − 14
JPS does not Granger cause Comex	0.53249	0.58739

Note. JPS means the weight average daily return growth rate of 5 stocks. Comex means the daily return growth rate of the Comex gold future.

Table 3: The selection of the VAR model optimal lag period.

Period	AIC	SC
0	−10.8977	−10.7222
1	−10.8299	−10.8164
2	−10.91258*	−10.87208*
3	−10.9037	−10.8361
4	−10.9086	−10.8141

Note. * stands for the optimal period.

relatively great, so the null hypothesis that the price change of Chinese gold stocks does not guide the price change of international gold future should be accepted. The conclusion here is consistent with the findings of many scholars.

5.3. VAR Model. First, it is necessary to determine the lag period. Based on the smallest AIC and SC values, the lag period P is the optimal lag period. According to Table 3, the smallest AIC and SC values appear when P equals 2. Therefore, we select $P = 2$ as the optimal lag period.

Second, the stable test of the VAR. Using AR root table test method, we get the result (Table 4).

The test shows there is no root that lies outside the unit circle, so the VAR model meets the stability requirements. We get the matrix form of VAR model as follows:

$$\begin{pmatrix} \text{JPS} \\ \text{Comex} \end{pmatrix} = \begin{pmatrix} -0.062 & 0.675 \\ 0.016 & 0.6467 \end{pmatrix} \begin{pmatrix} \text{JPS}_{t-1} \\ \text{Comex}_{t-1} \end{pmatrix} + \begin{pmatrix} 0.003 & -0.06 \\ 0.013 & -0.055 \end{pmatrix} \begin{pmatrix} \text{JPS}_{t-2} \\ \text{Comex}_{t-2} \end{pmatrix} + \begin{pmatrix} -0.0002 \\ 0.0006 \end{pmatrix}. \quad (6)$$

From the equation above, we can see that the coefficient of the stock lag term is rather small in the JPS equation, while the coefficient of gold future lag term is relatively great, which

Table 4: AR root.

Root	Modulus
−0.076204 − 0.200863i	0.214833
−0.076204 + 0.200863i	0.214833
0.069731 − 0.094652i	0.117564
0.069731 + 0.094652i	0.117564

illustrates that the fluctuation of gold stocks in Shanghai and Shenzhen A-share is influenced by external price change more than themselves. In the gold future equation, its lag coefficient is significantly greater than that of the gold stock, but the coefficient is greater than the one in the JPS equation, which shows the Comex gold future is affected by stock price change to some degree. And this result is consistent with the conclusion of Granger causality test.

5.4. Impulse Response Function. Impulse response functions describe how the economy reacts over time to exogenous impulses, which economists usually call shocks, and are often modeled in the context of a VAR. In this paper, we use impulse response function to analyze the price volatility of gold stocks in Shanghai and Shenzhen stock and the international gold futures. Selecting 10 as the impulse function tracking period, we can conduct impulse analysis to the daily return growth rate of JPS and Comex from January 1, 2010, to December 31, 2012, and the results are shown as in Figure 1.

In Figure 1, abscissa indicates the follow-up period, the vertical axis represents the level of impulse response, Figure 1 shows Comex, the price of international gold futures, impact price fluctuations on their own in the first follow-up period are 1.14%, the impact in the second follow-up period rapidly decreases to 0.1%, it decreases to 0.1% below zero in the third follow-up period, and the impact gradually converges to 0 from the fourth follow-up period. The impact of the JPS on the international gold futures is 0 in the first follow-up period, the impact increases to 0.04% from the second follow-up period, the impact in the third follow-up period is almost the same to the second follow-up period, it is 0.03%, and the impact starts converging to 0 in the fourth follow-up period.

From Figure 2, the impact of JPS on the price fluctuations on their own in the first follow-up period is 2.3%, and it decreases to 1.4% below zero in the second follow-up period and then rises in third follow-up period to 0.02%. And then it gradually converges to 0 in the fourth follow-up period. The impact of Comex on JPS is 6.3% in the first follow-up period, and then it increases to 7.2% in the second follow-up period. It decreases to 0.6% below zero in the third follow-up period, and then it decreases and gradually converges to 0 in the fourth follow-up period.

In summary, the effect of the price change of international gold futures on the price change of gold stocks in Shanghai and Shenzhen is obvious, and the guiding impact of the price change of the gold stocks to the international gold futures is not obvious. The impulse response efficiency of the international gold futures to gold stocks in Shanghai and Shenzhen stock surpasses the gold stocks in Shanghai and Shenzhen stock to international gold futures. This illustrates

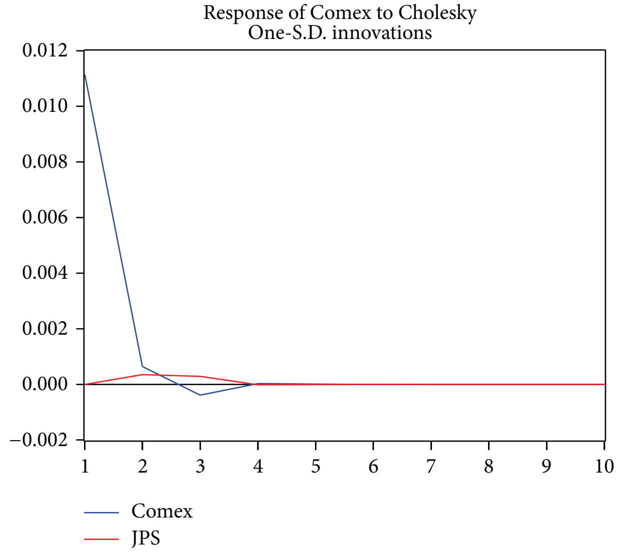

Figure 1: The impulse response function analysis graph of Comex.

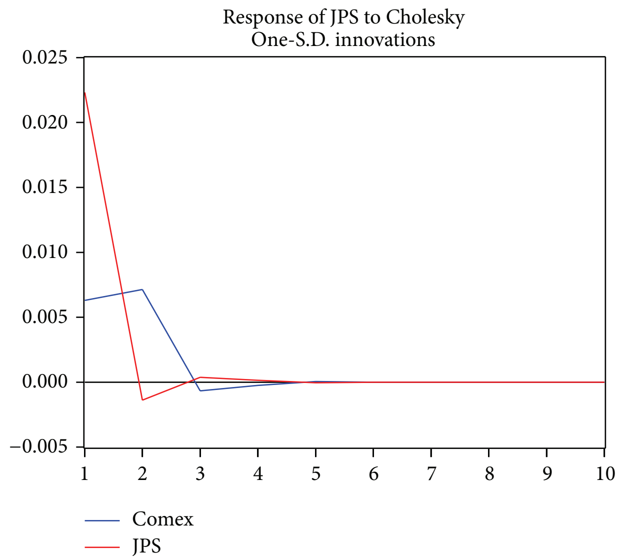

Figure 2: The impulse response function analysis graph of JPS.

the influence and authority of the international gold futures is much greater than the gold stocks in Shanghai and Shenzhen stocks. There is long-term equilibrium relationship between the foreign and domestic futures and spot, but the guiding force of the foreign futures and spot to domestic futures and spot is greater than that of the latter to the former.

6. Conclusion

Based on the empirical analysis above, we can get the main conclusions of this paper.

(1) As the foreign financial market will bring about the fluctuations to the domestic market price, it is necessary to examine the impact that international market price movements have on the domestic market.

(2) Granger causality test shows the price change of the international gold futures is the reason which causes the price change of the gold stocks in Shanghai and Shenzhen A-share, but in the reverse situation it is much less. It illustrates the international gold futures have an unidirectional guiding role on the gold stocks in Shanghai and Shenzhen A-share. By impulse response function, we can further clearly understand that the fluctuation of the foreign gold futures and spot has much stronger effect on the domestic market. It suggests we must continue to foster our markets both stocks, futures, and spot.

Conflict of Interests

The authors declare that they have no conflict of interests.

Acknowledgments

This research was supported by the National Natural Science Foundation of China (Grant no. 71171176) and the Program of Humanities and Social Sciences of Ministry of Education of China (Grant no. 12YJC910011).

References

[1] X. Jiaming, “The empirical study of the China and America gold futures market efficiency,” *Journal of Shanghai Commercial College*, vol. 9, no. 5, pp. 18–24, 2009.

[2] F. Wen, X. Cong, Y. Chao, and X. Chen, “The effects of prior outcomes on risky choice: evidence from the stock market,” *Mathmatical Problems in Engineering*, vol. 2014, Article ID 272518, 8 pages, 2014.

[3] F. Wen and Z. Liu, “A copula-based correlation measure and its application in chinese stock market,” *International Journal of Information Technology and Decision Making*, vol. 8, no. 4, pp. 787–801, 2009.

[4] T. Zhipeng and Z. Guoyan, “The empirical study of the price relation of Chinese gold market futures and spot,” *Journal of Shandong Institute of Business*, vol. 23, no. 2, pp. 76–81, 2009.

[5] W. Di and H. Jiangming, “The study of the impact that the price volatility of New York gold futures price on China futures market yield,” *Economic Survey*, vol. 2, no. 2, pp. 22–27, 2010.

[6] F. Wen, Z. He, X. Gong, and A. Liu, “Investors' risk preference characteristics based on different reference point,” *Discrete Dynamics in Nature and Society*, vol. 2014, Article ID 158386, 9 pages, 2014.

[7] F. Wen, Z. He, and X. Chen, “Investors' risk preference characteristics and conditional skewness,” *Mathmatical Problems in Engineering*, vol. 2014, Article ID 814965, 14 pages, 2014.

[8] F. Wen and X. Yang, “Skewness of return distribution and coefficient of risk premium,” *Journal of Systems Science & Complexity*, vol. 22, no. 3, pp. 360–371, 2009.

[9] H. A. Shawky, A. Marathe, and C. L. Barrett, “A first look at the empirical relation between spot and futures electricity prices in the United States,” *Journal of Futures Markets*, vol. 23, no. 10, pp. 931–955, 2003.

[10] B. M. Lucey and E. Tully, "Seasonality, risk and return in daily COMEX gold and silver data 1982–2002," *Applied Financial Economics*, vol. 16, no. 4, pp. 319–333, 2006.

[11] D. Hillier, P. Draper, and R. Faff, "Do precious metals shine? An investment perspective," *Financial Analysts Journal*, vol. 62, no. 2, pp. 98–106, 2006.

[12] H.-N. Lin, S.-M. Chiang, and K.-H. Chen, "The dynamic relationships between gold futures markets: evidence from COMEX and TOCOM," *Applied Financial Economics Letters*, vol. 4, no. 1, pp. 19–24, 2008.

[13] P. D. Cretien, "Gold & silver: always good options," *Futures: News, Analysis & Strategies for Futures, Options, Derivative Traders*, vol. 40, no. 5, pp. 28–30, 2011.

[14] W.-C. Lee and H.-N. Lin, "Threshold effects in the relationships between USD and gold futures by panel smooth transition approach," *Applied Economics Letters*, vol. 19, no. 11, pp. 1065–1070, 2012.

Hindawi Publishing Corporation
Discrete Dynamics in Nature and Society
Volume 2014, Article ID 453458, 6 pages
http://dx.doi.org/10.1155/2014/453458

Research Article

Estimation of the Treatment Effects of Ownership on the Indirect Financing of Small- and Medium-Sized Enterprises

Xiuzhen Wang,[1] Yi Hu,[2] Xiaohua Xia,[3] and Ying Deng[4]

[1] *School of Economics and Management, Beijing Jiaotong University, Beijing 100044, China*
[2] *School of Management, University of Chinese Academy of Sciences, Beijing 100190, China*
[3] *Institute of China's Economic Reform and Development, Renmin University of China, Beijing 100872, China*
[4] *School of International Trade and Economics, University of International Business and Economics, Beijing 100029, China*

Correspondence should be addressed to Yi Hu; huyi@ucas.ac.cn

Received 17 April 2014; Accepted 7 July 2014; Published 16 July 2014

Academic Editor: Chuangxia Huang

Small- and medium-sized enterprises (SMEs) are the important driving forces for the growth of China's economy. However, financing difficulty has always been the important problem besetting the development of SMEs for a long time. In particular, in recent years, US subprime crisis in 2008 caused a heavy blow to the development of some externally oriented SMEs. Thus, how to effectively overcome financing predicament for the SMEs is crucial for Chinese government. In this paper, based on microdata from China Industrial Enterprise Database, propensity score matching (PSM) method is adopted to conduct empirical analysis about the treatment effects of indirect financing level of SMEs under different systems. Empirical results reveal that state-owned enterprises enjoy indirect financing advantages compared with other enterprises and there is certain ownership discrimination against foreign-funded enterprises and private enterprises. In particular, the indirect financing rate of state-owned enterprises is 1.4% higher than that of other enterprises, and the indirect financing rate of foreign-funded enterprises is 6% lower than that of other enterprises; private enterprises are advantageous in indirect financing compared with other enterprises; however, indirect financing rate of private enterprises is 1.8% lower than that of state-owned enterprises, which also reveals ownership discrimination to certain extent.

1. Introduction

Small- and medium-sized enterprises (SMEs) play a decisive role in developing national economy. However, their development is confronted with many difficulties. In particular US subprime crisis in 2008 triggered global economic recession, causing a heavy blow to the survival, operation, and development of some externally oriented SMEs [1–3]. Thus how to help SMEs resolve economic difficulty, enable healthy growth of SMEs, especially how to effectively overcome financing predicament for them, remove financing barriers, and improve financing efficiency is currently one important subject and pressing task for China.

Financing difficulty has always been the important problem baffling the development of SMEs for a long time [4–6]. Though the government and financial institutions have made great efforts in improving financing services for SMEs, financial resources from formal financial system, for example, stock market, for SMEs are still much lower than economic contributions made by SMEs [7–10]. According to statistical data from National Development and Reform Commission, the number of SMEs registered with industrial and commercial department in China has exceeded 4.80 million, while total number of SMEs including individual businesses in China has surpassed 42 million, accounting for more than 99% of aggregate number of enterprises nationwide. Jobs provided by SMEs account for more than 75% of total jobs in cities and towns nationwide and GDP created by SMEs represents 59% of national GDP; commodities produced by these enterprises make up 60% of total social sales, while tax payment from them constitutes 51% of total national tax amount; these enterprises stand for half of national economy. In addition, SMEs also play an important role in scientific and technical innovation activities and have become the main body for technologies and innovations in China. Currently, in China, 66% of patents are invented by SMEs, more than 75% of technical innovations are completed by SMEs, and new products researched and developed by these enterprises account for 82% of total ones in China. However, according to *2012 Blue Book of Chinese SMEs*, estimation made by China Banking Regulatory Commission showed that bank credit covered 100% of large enterprises, 90% of medium-sized enterprises, and only 20% of small enterprises and almost no microenterprises. Given current economic downturn, commercial banks are more prudential in offering loans and 10%–15% of SMEs actually obtain loans. Furthermore, according to data from People's Bank of China, as of September, 2010, only 239,000 SMEs nationwide had acquired banks' intent for credit extension and bank credit covered less than 1% of SMEs.

Many SMEs cannot but secure financing from informal financial channels in order to address the shortage of capital in China; thus private finance rapidly grows and considerable quantity of bank credit and capital from listed companies also flow to private lending market through various channels. In recent years, with rising labor and land costs in China and unfolding adverse impact from exchange rate reform and international financial crisis on export market for Chinese SMEs, profit margin for SMEs has been narrowed, while high cost of private financing has further exacerbated the difficulties for survival and development of SMEs with relatively low profit margin, which has not only affected continuously stable growth of China's economy but also exerted negative impact on employment, income distribution, economy, and social stability.

Large number of SMEs have gone bankrupt and been closed in China since financial crisis; thus the contradiction in financing difficulty for SMEs has become more acute. The State attaches great importance to the problems for SMEs as the State Council, ministries, and commissions under the State Council have intensively released series of policy measures. In March, 2012, the State Council established pilot financial reform zone in Wenzhou City, Zhejiang Province, with the purpose of exploring the realistic path for further promoting China's financial reform. The State Council promulgated *the Opinions on Further Supporting Healthy Development of Small and Microenterprises* on April 19, 2012, which intensified support for small and microenterprises. Afterwards, China Banking Regulatory Commission issued *the Implementation Opinions on Encouraging and Guiding Entry of Private Capital into the Banking Industry* in May, 2012, with the aim of supporting private capital to be invested in financial institutions together with other capitals under equal conditions.

Many scholars take ownership discrimination as one important cause for financing difficulty surrounding SMEs. However, existing research is subject to the following restrictions: firstly, research sample is derived from either questionnaire survey on local areas or annual reports of listed SMEs, data size is very limited, and research conclusions are also exposed to certain limitations. Secondly, the method is dominated by direct regression without considerations for possible endogeneity issue in model and with failure to effectively identify the real causal relationship. Therefore, this paper uses Industrial Enterprise Survey Database of National Bureau of Statistics since this database includes all state-owned enterprises and nonstate-owned industrial enterprises with main business revenue exceeding five million Yuan and extensively covers enterprises, adopts many survey indicators, and can better reflect current situation of Chinese SMEs. Moreover, in this paper, propensity score matching method is employed to study indirect financing for SMEs under different ownerships so as to draw more accurate research conclusions.

The remainder of the paper proceeds as follows: Section 2 introduces the data and variables. Section 3 discusses the propensity score matching method and empirical analysis. Section 4 concludes.

2. Data and Variables

2.1. Data. This paper derives data from China Industrial Enterprise Database of National Bureau of Statistics in 2007. This database is developed by National Bureau of Statistics on the basis of statistics concerning all state-owned enterprises and nonstate-owned industrial enterprises with main business revenue exceeding five million Yuan each year. However, part of statistical samples in this database includes mistakes and omissions; thus this paper conducts preliminary screening of data samples under the screening principle: samples "under operation" (namely, operation state = 1) and organizations which are "enterprises" (namely, organization type = 1) are retained, while samples with "annual average number of all employees" less than 5, those with "total assets" less than or equal to 0, and those with "total current liabilities" less than or equal to 0 as well as those with "total industrial output value (current year's prices)" less than 0 are eliminated.

Reference is made to the standard for classification of SMEs implemented in 2003 so that the screened data is sorted out, and enterprises which concurrently satisfy the conditions that total assets and sales volume do not exceed 400 million and 300 million and the number of employees is not more than 3,000 are classified as SMEs, namely, small- and medium-sized industrial enterprises above the designated scale. This treatment embodies the real meaning of national standard and controls enterprises above certain level as well as is the common way for addressing such issue in relevant domestic and foreign researches.

2.2. Variables. This paper is mainly designed to study indirect financing for enterprises under different ownerships and focuses research on ownership discrimination against state-owned, foreign-funded, and private holding enterprises among SMEs. In this paper, propensity score matching method is used to examine the impact from ownerships on financing for SMEs. This method needs to be based on the following variables.

(1) *Independent Variable.* Indirect financing rate (Y) is closely related to current liability rate; numerical value of indirect financing cannot be directly

Table 1: Descriptive statistics.

Ownership		State-owned	Foreign	Private	Others	Total
Obs		5124	20661	126752	22502	163972
Y	Mean	0.569	0.475	0.533	0.545	0.528
	S.D	0.437	0.346	0.294	0.339	0.31
	Min	0.001	0	0	0	0
	Max	8.851	12.998	8.787	8.138	12.998
X_1	Mean	0.659	0.499	0.574	0.597	0.569
	S.D	0.483	0.351	0.29	0.346	0.312
	Min	0.001	0	0	0	0
	Max	14.662	12.998	8.787	8.144	14.662
X_2	Mean	19.294	6.818	6.348	14.151	7.356
	S.D	15.731	4.781	6.385	10.133	7.601
	Min	0	0	0	0	0
	Max	100	107	169	69	169
X_3	Mean	218.024	237.323	297.727	277.132	286.189
	S.D	325.562	288.706	293.513	1088.525	404.459
	Min	0.069	0.353	0.167	0.273	0.069
	Max	9008.5	11301.176	8944.077	112290	112290
X_4	Mean	236.331	216.215	195.298	204.726	199.873
	S.D	306.038	279.792	221.966	241.806	234.618
	Min	1.333	1.022	0.452	1.473	0.452
	Max	7805.4	6782.2	6986	5080	7805.4

obtained; this paper adopts the ratio of current liabilities to total assets as indirect financing rate.

(2) *Treatment Variables.* This paper considers the following three treatment variables: dummy variables as to whether they are state-owned holding enterprises (D_1), foreign-funded holding enterprises (D_2), and private holding enterprises (D_3).

(3) *Characteristic Variables.* The following control variables concerning enterprise characteristics are considered: asset-liability ratio (X_1, ratio of total liabilities to total assets), enterprise age (X_2, years from enterprise establishment to 2007), labor productivity (X_3, ratio of total industrial output value to the number of employees), and capital intensity (X_4, ratio of total assets to number of employees).

Table 1 provides the result of descriptive statistics about the above variables grouped on the basis of actual holding.

According to the result of descriptive statistics in Table 1, enterprises under different ownerships show marked differences in production and operation. State-owned holding enterprises enjoy relatively high indirect financing rate, while foreign-funded holding enterprises have relatively low indirect financing rate. Meanwhile, state-owned holding enterprises indicate the highest asset-liability ratio, while foreign-funded holding enterprises present the lowest asset-liability ratio. Current liabilities form the important part of total liabilities and serve as the important yardstick for measuring indirect financing; thus asset-liability ratio and indirect financing rate have exactly the same size relationship among enterprises under different ownerships. From the perspective of labor productivity, state-owned holding enterprises reveal the lowest efficiency, while private holding enterprises exhibit relatively high efficiency. Foreign-funded holding enterprises have the highest capital intensity, while private enterprises show the lowest capital intensity, which also reflect the disadvantages of private holding enterprises in capital.

Table 1 only gives expression to differences in simple average values of indirect financing rates among enterprises under different ownerships and does not control the impact from other factors. Subsequently, ordinary least squares (OLS) regression is performed for basic econometrical models composed of the above variables; the models are given in the following:

$$Y_i = C + X_{1i}\beta_1 + X_{2i}\beta_2 + X_{3i}\beta_3 + X_{4i}\beta_4 + T_{1i}\gamma_1 + \varepsilon_i, \quad (1)$$

$$Y_i = C + X_{1i}\beta_1 + X_{2i}\beta_2 + X_{3i}\beta_3 + X_{4i}\beta_4 + T_{2i}\gamma_2 + \varepsilon_i, \quad (2)$$

$$Y_i = C + X_{1i}\beta_1 + X_{2i}\beta_2 + X_{3i}\beta_3 + X_{4i}\beta_4 + T_{3i}\gamma_3 + \varepsilon_i \quad (3)$$

in which, γ_1, γ_2, and γ_3 measure the magnitudes of treatment effect.

The ordinary least squares regression result shown in Table 2.

As indicated by estimation results (1), (2), and (3) in Table 2, subject to controlling asset-liability ratio, enterprise age, labor productivity and capital intensity, and so forth, indirect financing rate of foreign-funded holding enterprises is higher than that of nonforeign-funded holding enterprises, while that of state-owned holding enterprises is lower than that of nonstate-owned holding enterprises, and estimation

Table 2: Ordinary least squares estimation (1).

	Model (1)	Model (2)	Model (3)
X_1	0.921***	0.921***	0.920***
	(973.07)	(969.86)	(970.12)
X_2	−0.412***	−0.641***	−0.653***
	(−10.17)	(−16.49)	(−16.27)
X_3	0.0555***	0.0665***	0.0597***
	(7.11)	(8.5)	(7.63)
X_4	−0.152***	−0.172***	−0.164***
	(−11.29)	(−12.83)	(−12.17)
T_1	−0.0380***		
	(−21.57)		
T_2		0.0123***	
		(13.84)	
T_3			6.72E − 05
			(0.09)
Constant	0.00987***	0.00864***	0.0109***
	(13.62)	(11.65)	(11.49)
N	163972	163972	163972

***,**,*indicates statistical significance at the 1%, 5%, and 10% significance level, respectively. The t statistics are given in parenthesis.

Table 3: Ordinary least squares estimation (2).

	Model (4)	Model (5)	Model (6)
X_2	2.43***	2.44***	3.01***
	(23.16)	(24.22)	(29.05)
X_3	−0.0174	−0.0509**	−0.0414**
	(−0.86)	(−2.51)	(−2.04)
X_4	−0.270***	−0.225***	−0.225***
	(−7.74)	(−6.44)	(−6.43)
T_1	0.0130***		
	(2.84)		
T_2		−0.0592***	
		(−25.69)	
T_3			0.0373***
			(19.8)
Constant	0.515***	0.523***	0.483***
	(392.15)	(388.66)	(228.98)
N	163972	163972	163972

***,**,*indicates statistical significance at the 1%, 5%, and 10% significance level, respectively. The t statistics are given in parenthesis.

results about private holding enterprises are insignificant. This means that state-owned holding enterprises are subject to ownership discrimination from indirect financing. Such results are exactly opposite to descriptive statistical analysis in Table 1. Furthermore, given possible endogeneity in asset-liability ratio, regressions are reconducted after such variable is deleted; the modified models are given by

$$Y_i = C + X_{2i}\beta_2 + X_{3i}\beta_3 + X_{4i}\beta_4 + T_{1i}\gamma_1 + \varepsilon_i, \quad (4)$$

$$Y_i = C + X_{2i}\beta_2 + X_{3i}\beta_3 + X_{4i}\beta_4 + T_{2i}\gamma_2 + \varepsilon_i, \quad (5)$$

$$Y_i = C + X_{2i}\beta_2 + X_{3i}\beta_3 + X_{4i}\beta_4 + T_{3i}\gamma_3 + \varepsilon_i. \quad (6)$$

With the estimation results shown in Table 3.

It is observed that, after enterprise age, labor productivity, capital intensity, and so forth are controlled; indirect financing rate of state-owned holding enterprises is higher than that of nonstate-owned holding enterprises, while indirect financing rate of foreign-funded holding enterprises is lower than that of nonforeign-funded holding enterprises and that of private enterprises is significantly higher than that of nonprivate enterprises. Results are exactly contrary to (1), (2), and (3). Given instability of results, the following section of this paper adopts propensity score matching method to accurately estimate the impact from ownership factor on indirect financing rates of SMEs.

3. Propensity Score Matching Method and Empirical Analysis

3.1. Propensity Score Matching Method. Econometrical analysis in the above section indicates that difference in ownership form indeed results in changes in indirect financing rates of enterprises. However, we should also pay attention to possible endogeneity issue between ownership form and indirect financing rate. In order to eliminate sample selectivity bias, this section uses propensity score matching (PSM, [11–14]) method to address such issue. Take whether enterprises are state-owned holding ones as an example, core philosophy of this method lies in identifying the difference in indirect financing rates of one enterprise between "state-owned holding" and "nonstate-owned holding"; given that such difference involves one enterprise under different ownership forms, we can confirm that such difference is caused by change in ownership form and there is no endogeneity issue that indirect financing rate of state-owned holding enterprise itself is relatively high or relatively low. However, as no "nonstate-owned holding" condition exists in state-owned holding enterprises, we need to find nonstate-owned holding enterprises "similar" to state-owned holding enterprises and study nonstate-owned holding enterprises to judge whether indirect financing rate of state-owned holding enterprises is increased so as to obtain average treatment effect (ATE) concerning the impact of different ownership forms on indirect financing rates of enterprises. Specifically, we firstly estimate the determining equation as to whether enterprises are state-owned ones:

$$\mathrm{PS}(X) = P(D = 1 \mid X) = E(T \mid X), \quad (7)$$

where D is indicative variable, if it is 1, it means state-owned holding, and if it is 0, it represents nonstate-owned holding; X means the factor which affects whether enterprise selects state-owned holding. PS is the probability that enterprise selects state-owned holding, namely, propensity score. Based on (1), propensity score $\mathrm{PS}(X_i)$ of each enterprise i can be

Table 4: Average treatment effects (matching estimators).

		Treated	Controls	ATT	S.E.	t-stat
D_1	Unmatched	0.569	0.527	0.042^{***}	0.004	9.570
	ATT	0.569	0.555	0.014^{**}	0.007	2.020
D_2	Unmatched	0.475	0.536	-0.061^{***}	0.002	−26.420
	ATT	0.475	0.535	-0.060^{***}	0.003	−20.910
D_3	Unmatched	0.533	0.509	0.024^{***}	0.002	13.220
	ATT	0.533	0.501	0.033^{***}	0.003	12.550
${D_3}^*$	Unmatched	0.533	0.569	-0.035^{***}	0.004	−8.250
	ATT	0.533	0.552	-0.018^{*}	0.011	−1.660

***,**,*indicates statistical significance at the 1%, 5%, and 10% significance level, respectively.

calculated. Based on Becker and Ichino [11], average treatment effect concerning state-owned holding and nonstate-owned holding for indirect financing rates of enterprises can be obtained:

$$\begin{aligned} \mathrm{ATT} &= E\left[Y_{1i} - Y_{0i} \mid D_i = 1\right] \\ &= E\left\{E\left[Y_{1i} - Y_{0i} \mid D_i = 1, p\left(X_i\right)\right]\right\}, \end{aligned} \tag{8}$$

where Y_{1i} and Y_{0i} separately represent indirect financing rates of individual i under both conditions: state-owned holding and nonstate-owned holding.

In actual analysis, average treatment effect is generally calculated through the following three steps.

Step 1. Logit model is used to estimate propensity score:

$$\mathrm{PS}\left(X_i\right) = P\left(D_i = 1 \mid X_i\right) = \frac{\exp\left(X_i'\beta\right)}{1 + \exp\left(X_i'\beta\right)}. \tag{9}$$

Fitted value $\widehat{\mathrm{PS}}(X_i)$ (namely, propensity score) is obtained.

Step 2 (Matching). PS(X) is continuous variable; thus it is very difficult to conduct exact matching for it. Common inexact matching methods include one-to-one matching, k-nearest neighbors matching, radius matching, and kernel matching. As sample size in this paper is very large, it takes excessively long time to adopt the latter two ones which are unfeasible in practice. This paper uses k-nearest neighbors matching. Matching rules are shown below:

$$\left|\mathrm{PS}_i - \mathrm{PS}_j\right| = \min_{k\in\{D=0\}} \left\{\left|\mathrm{PS}_i - \mathrm{PS}_k\right|\right\}. \tag{10}$$

Step 3. According to the matching results, average treatment effect is calculated as follows:

$$\mathrm{ATT} = \frac{1}{N^T}\sum_{i\in T}\left[Y_i^T - \sum_{j\in C(i)} \omega_{ij} Y_j^C\right] \tag{11}$$

in which Y_i^T and Y_j^C are the outcomes of treated individual i and control individual j, respectively. ω_{ij} is the weight.

3.2. Empirical Analysis. After nonstate-owned holding enterprises which match with state-owned holding enterprises are identified through the above method, propensity score matching method is adopted to calculate the difference in average indirect financing rates between two groups of enterprises; final results are shown in D_1 in Table 4. The matching processes for foreign-funded holding and private holding enterprises are similar to the above process; their final results are indicated in D_2 and D_3 in Table 4. The estimation results to which we mainly pay attention in these tables are average treatment effects on the treated (ATT) which means the difference in indirect financing rates of enterprises between treatment group and control group.

According to Table 4, with respect to D_1, in terms of state-owned and nonstate-owned enterprises, indirect financing rate of state-owned enterprises is 4.2% higher than that of nonstate-owned enterprises before treatment; after treatment, indirect financing rate of state-owned enterprises is still but only 1.4% higher than that of nonstate-owned enterprises. With respect to D_2, in terms of foreign-funded and nonforeign-funded enterprises, indirect financing rate of foreign-funded enterprises is 6% lower than that of nonforeign-funded enterprises both before and after treatment, which suggests that foreign-funded enterprises are disadvantageous in indirect financing. With regard to D_3, in terms of private and nonprivate enterprises, indirect financing rate of private enterprises is 2.4% and 3.3% higher than that of nonprivate enterprises before and after treatment.

However, it is worth noting that indirect financing rate of private enterprises is 3.5% lower before treatment. In order to further study whether there is discrimination against private enterprises compared with state-owned enterprises, sample size is limited to state-owned enterprises and private enterprises, and propensity score matching estimation is reconducted, with the result shown in ${D_3}^*$, which shows that indirect financing rate of private enterprises is 1.8% lower than that of state-owned enterprises after treatment. The corresponding value t is −1.66, and it is significant at 10% significant level. This means that private enterprises are also subject to certain ownership discrimination in indirect financing compared with state-owned enterprises.

4. Conclusions

This paper utilizes China Industrial Enterprise Database of National Bureau of Statistics and makes reference to the standard for classification of SMEs implemented in 2003 for screening samples of SMEs and studying the difference in indirect financing among SMEs under different ownership systems. As indicated by regression result, results greatly vary with different control variables. Propensity score matching method is further adopted to perform estimation and discover that state-owned enterprises enjoy advantages in indirect financing compared with other enterprises, and indirect financing rate is 1.4% higher than that of other enterprises. Foreign-funded enterprises are faced with ownership discrimination in indirect financing, and their indirect financing rate is 6% lower than that of other enterprises. Private enterprises are advantageous in indirect financing compared with other enterprises. However, indirect financing rate of private enterprises is 1.8% lower than that of state-owned enterprises, which also reveals ownership discrimination to certain extent.

Conflict of Interests

The authors declare that there is no conflict of interests regarding the publication of this article.

Acknowledgment

This work was partially supported by the National Natural Science Foundation of China (Grant nos. 71301160 and 71203224) and China Postdoctoral Science Foundation funded project (Grant nos. 2012M520420).

References

[1] F. H. Wen, Z. F. He, and X. H. Chen, "Investors risk preference characteristics and conditional skewness," *Mathematical Problems in Engineering*, vol. 2014, Article ID 814965, 14 pages, 2014.

[2] C. Huang, C. Peng, X. Chen, and F. Wen, "Dynamics analysis of a class of delayed economic model," *Abstract and Applied Analysis*, vol. 2013, Article ID 962738, 12 pages, 2013.

[3] F. H. Wen, Z. F. He, X. Gong, and A. M. Liu, "Investors'risk preference characteristics based on different reference point," *Discrete Dynamics in Nature and Society*, vol. 2014, Article ID 158386, 9 pages, 2014.

[4] J. Lopez-Gracia and C. Aybar-Arias, "An empirical approach to the financial behaviour of small and medium sized companies," *Small Business Economics*, vol. 14, no. 1, pp. 55–63, 2000.

[5] D. Czarnitzki, "Research and development in small and medium-sized enterprises: the role of financial constraints and public funding," *Scottish Journal of Political Economy*, vol. 53, no. 3, pp. 335–357, 2006.

[6] D. Czarnitzki and H. Hottenrott, "R&D investment and financing constraints of small and medium-sized firms," *Small Business Economics*, vol. 36, no. 1, pp. 65–83, 2011.

[7] F. Wen and Z. Liu, "A copula-based correlation measure and its application in Chinese stock market," *International Journal of Information Technology and Decision Making*, vol. 8, no. 4, pp. 787–801, 2009.

[8] F. Wen and X. Yang, "Skewness of return distribution and coefficient of risk premium," *Journal of Systems Science & Complexity*, vol. 22, no. 3, pp. 360–371, 2009.

[9] C. X. Huang, X. Gong, X. H. Chen, and F. H. Wen, "Measuring and forecasting volatility in Chinese stock market using HAR-CJ-M model," *Abstract and Applied Analysis*, vol. 2013, Article ID 143194, 13 pages, 2013.

[10] F. H. Wen, X. Gong, Y. C. Chao, and X. H. Chen, "The effects of prior outcomes on risky choice: evidence from the stock market," *Mathematical Problems in Engineering*, vol. 2014, Article ID 272518, 8 pages, 2014.

[11] S. Becker O and A. Ichino, "Estimation of average treatment effects based on propensity scores," *The Stata Journal*, vol. 2, no. 4, pp. 358–377, 2002.

[12] R. H. Dehejia and S. Wahba, "Propensity score-matching methods for nonexperimental causal studies," *Review of Economics and Statistics*, vol. 84, no. 1, pp. 151–161, 2002.

[13] A. Abadie and G. W. Imbens, "Large sample properties of matching estimators for average treatment effects," *Econometrica*, vol. 74, no. 1, pp. 235–267, 2006.

[14] M. Caliendo and S. Kopeinig, "Some practical guidance for the implementation of propensity score matching," *Journal of Economic Surveys*, vol. 22, no. 1, pp. 31–72, 2008.

Hindawi Publishing Corporation
Discrete Dynamics in Nature and Society
Volume 2014, Article ID 262384, 7 pages
http://dx.doi.org/10.1155/2014/262384

Research Article

An Extended SISa Model for Sentiment Contagion

Zhifeng Liu,[1] Tingting Zhang,[1] and Qiujun Lan[2]

[1] *College of Management and Economics, Tianjin University, Tianjin 300072, China*
[2] *Business School, Hunan University, Changsha 410082, China*

Correspondence should be addressed to Qiujun Lan; lanqiujun@hnu.edu.cn

Received 17 April 2014; Accepted 2 July 2014; Published 16 July 2014

Academic Editor: Chuangxia Huang

One of the main differences between sentiment and infectious diseases is that the former one has two opposite infectious states: positive (optimistic) and negative (pessimistic), while the latter one has not. In this paper, based on the SISa model, we consider this issue and propose a new model of sentiment contagion called the SOSa-SPSa model. The results of both numerical and agent-based simulations show that our model could explain the process of sentiment contagion better than that of Hill et al. (2010). Further analysis shows that both the numbers of optimistic and pessimistic individuals will increase with the probability of spontaneity or contagion and decrease with the probability of recovery. Potential applications of this model in financial market have also been discussed.

1. Introduction

Social emotion (or sentiment) is the result of the interaction between individuals, but how does this interaction take place and ultimately form the social emotion? Maybe the study of emotional contagion can give an answer for this question. Emotional contagion can be simply defined as a situation where every individual's emotion could be affected by others' emotion, and the whole process is usually spontaneous, unconscious, and uncontrolled [1]. The previous studies on emotional contagion are mainly concentrated in the field of psychology and sociology [2–5]; however, in recent years, this issue has been also discussed in financial market.

In the field of psychology and sociology, the behavior of emotional contagion has been studied in many papers [6, 7]. The most representative works are SIS and SIR models [8–11], which belong to the classic epidemic models and are designed to study the infection of diseases. But now these models have been used to solve the problem of emotion contagion. Dodds and Watts (2005) discuss these two models in a unified framework [12]. Hill et al. (2010), who have considered the spontaneous generation process of emotion, explore the issues of emotional contagion on the basis of SISa model and use the data from the Framingham Heart Study to estimate the model parameters [13]. As we all know, social networks are very complex [14–17], and the research of the complex networks is also the new trend of research on emotion contagion [18–20]. For example, Zhao et al. (2014) establish an emotion contagion model in complex networks and find that the tendency of emotion variation in the BA scale-free network is almost the same as that in the homogeneous network [21]. Another research method called computational model has been in use recently [5, 22, 23]. For example, Fu et al. (2014) simulate the dynamic process of emotion contagion based on the SIR model and find that infection frequency will increase with the average crowd density [24].

Investor sentiment is a special kind of individual emotion, which originates in people's psychological behavior, such as risk preference [25, 26]. Sentiment contagion in the financial field is also a promising research topic (the sentimental process is similar to the emotional process, both of which have some common characteristics, but when we use the word "sentiment" in financial market, it contains more meanings related to asset prices. However, we are indeed not to distinguish the difference between these two words in this paper, and in the next part, we use the word "sentiment" instead of "emotion"). In recent years, scholars' understanding of investor sentiment contagion has already been developed to a certain scope on the macro level [27–29]. Baker et al.'s (2012) research about contagion of investor sentiment is a representative work [30]. Chang et al. (2012) have also studied the problem of global sentiment contagion and the influencing factors of it, and they find the capital flow is a channel of contagion, but not the only one [31]. Overall, the research on sentiment contagion still needs further study, especially on the contagion mechanism and channel.

Using classical epidemic models to mathematically describe the sentimental contagion process can help us to understand and predict generation and spread of sentiment. But this method at least has a defect at present; that is, when treating sentiment as infectious disease, we need to mention that sentiment in real life has two opposite contagious states: positive (optimistic) and negative (pessimistic), but the disease only has one infectious state, which is the "infected" status in SIS or SIR model. For this reason, the usual epidemic model is not very suitable to be used to describe the process of sentiment contagion directly. Being different from the existing researches, this paper extends the SISa model with considering the two states of sentiment and builds a new model called SOSa-SPSa model. The main reason why we choose the SISa model is that, comparing with the classic SIS model, the SISa model involves an automatic process of sentiment generation, which is consistent with our intuition that sentiment can arise spontaneously. In our new model, both of the two opposite sentiment states are similar to the infectious state in SISa model. By treating optimism and pessimism as contagious, we divide the process of sentiment contagion into two processes: susceptible-optimistic-susceptible (SOS) and the susceptible-pessimistic-susceptible (SPS), and each of these processes is similar to the susceptible-infected-susceptible (SIS) process.

The rest of this paper is divided into 3 sections. After providing some background information about sentimental contagion and giving a literature review in Section 1, we introduce our model in Section 2. Section 3 analyzes the equilibrium solutions of the new model by using both numerical and agent-based simulations. Finally, Section 4 summarizes the main conclusions of this paper and outlines some potential applications in further studies.

2. The SOSa-SPSa Model

According to whether the infector can become immune to the virus, the most classic epidemic models can be divided into two categories: one is SIS model; the other is SIR model. In the classic SIS model, an individual only switches between the two states: the susceptible (S) and infected (I). If considering the immune status which exists after some diseases' recovery, then the model can be transformed to SIR model. In this paper, we will regard sentiment as one kind of diseases, which can be transmitted among people. As we all know, individual sentiment is innate, spontaneous, and susceptible, and people face difficulty in being immune to others' sentiment. Therefore, we discuss the problem of sentimental contagion based on the SISa model, which is an extend model of SIS model with an automatic sentiment generation process.

The SISa model is proposed by Hill et al. (2010), and it considers the spontaneous generation process of sentiment [13]. The basic framework of the model is as in Figure 4, where S and I represent the susceptible people and the infected people, respectively, q is the probability of the process of the susceptible transform into the infected, including both the spontaneous and infectious processes, and g is the probability that the infected can recover back to the susceptible.

The characteristics of sentiment are very complex, and simply treating sentiment as a single status is not good enough for us to understand sentiment well. So, based on the SISa model above, this paper divides the infected status into two states: the optimistic (O) and the pessimistic (P).

And both the classic SIS model and SIR model have two assumptions (Hill et al., 2010): first, the more the susceptible are exposed to the infected, the more the probability the susceptible become to the infected; second, the probability of the infected people's recovery is irrelevant to the number of infected individuals. Hill et al. (2010) further consider the probability that the susceptible spontaneously convert to the infected, which means that no matter whether contacted with the infected or not, the susceptible will automatically transform into the infected at a certain probability, and it is consistent with the spontaneously generated pattern of sentiment. When considering dividing the sentiment into optimism and pessimism, the two assumptions discussed above are still applicable but not complete. Therefore, we add some other assumptions as follows.

(1) There are three kinds of sentiment states: the optimistic, the pessimistic, and the susceptible.

(2) The more the number of the optimistic whom the susceptible contacted with, the greater the probability that it will become optimistic; the more the number of the pessimistic whom the susceptible contacted with, the greater the probability that it will become pessimistic.

(3) The probability that the optimistic or the pessimistic recover back to the susceptible is irrelevant to the number of the optimistic or the pessimistic.

(4) The susceptible will spontaneously transform into the optimistic or the pessimistic at a certain probability.

In addition, because of the lack of understanding the transmission mechanism between optimism and pessimism, and for simplified analysis too, this paper assumes that the optimistic and the pessimistic can only transform into the susceptible but cannot transform into each other directly.

Based on the assumptions above, this paper analyzes the sentimental contagion process by considering the opposite sentiment states, and similar to Hill et al. (2010) [13], the processes can be mainly described in Figure 5.

In Figure 5(a), the model depicts the process of the transformation between the optimistic and the susceptible. (1) The susceptible will not change to the optimistic due to their connections with the pessimistic. (2) When the susceptible one contacts with the optimistic ones, there is a probability of β_O for him or her to become an optimistic one. (3) Regardless of whom the susceptible one contacts with, there is a probability of α_O for him or her to become optimistic spontaneously. (4) Regardless of whom the optimistic one contacts with, there is a probability of g_O for him or her to revert to the susceptible status.

Similarly, as we can see in Figure 5(b), the model describes the transformation process between the pessimistic and the susceptible. (1) The susceptible will not become pessimistic due to their connections with the optimistic. (2) When the susceptible one contacts with the pessimistic ones, there is a probability of β_P for him or her to become a pessimistic one. (3) Regardless of whom the susceptible one contacts with, there is a probability of α_P for him or her to become pessimistic automatically. (4) Regardless of whom the pessimistic one contacts with, there is a probability of g_P for him or her to recover to the susceptible status.

In brief, the individual mainly experiences two conversion processes: susceptible-optimistic-susceptible (SOS) and susceptible-pessimistic-susceptible (SPS), both of which include an automatic process of sentiment generation. Therefore, this paper names the new model as SOSa-SPSa model.

Figure 6 is a simple description for the basic framework of the SOSa-SPSa model, and different from the SISa model, the parameters q_O and q_P, which express the probabilities that the susceptible transform into the optimistic and the pessimistic, respectively, have new features. When considering the optimistic or pessimistic status of sentiment, the susceptible can contact with the optimistic and the pessimistic simultaneously, but in this situation, which status the susceptible will transform into? And how large the probability is? In order to discuss these problems conveniently, this paper assumes that the total number of individuals is N, and among them, the number of the optimistic is O, the number of the pessimistic is P, and the number of the susceptible is S, which satisfy the equation $O + P + S = N$. We also simply assume that the processes of the susceptible transform into the optimistic and the pessimistic are independent; thus the SOSa-SPSa model can be written as follows:

$$\begin{aligned} \frac{dS}{dt} &= g_O O + g_P P - (\alpha_O + \alpha_P) S - (\beta_O O + \beta_P P) S. \\ \frac{dO}{dt} &= -g_O O + \alpha_O S + \beta_O O S \\ \frac{dP}{dt} &= -g_P P + \alpha_P S + \beta_P P S \\ O + P + S &= N. \end{aligned} \tag{1}$$

Let $dS/dt = 0$, $dO/dt = 0$, and $dP/dt = 0$, and we can get the equilibrium points of these differential equations. If $\alpha_O + \beta_O O \neq 0$ and $\alpha_P + \beta_P P \neq 0$, it is easy to obtain that $S = g_O O/(\alpha_O + \beta_O O)$ and $S = g_P P/(\alpha_P + \beta_P P)$. Thus, in the equilibrium state, the quantity relation between the number of the optimistic and the number of the pessimistic is given by

$$\frac{g_O O}{\alpha_O + \beta_O O} = \frac{g_P P}{\alpha_P + \beta_P P}. \tag{2}$$

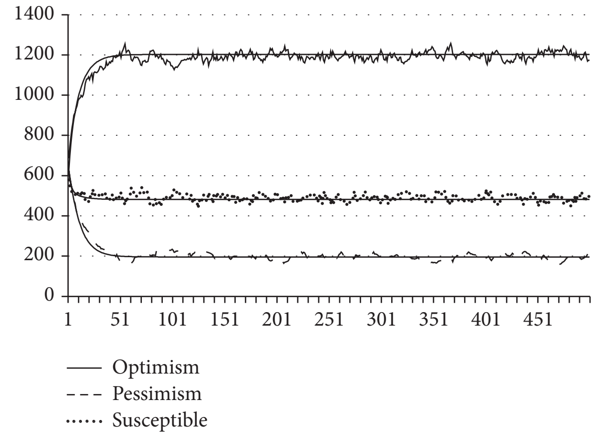

Figure 1: Equilibrium process of sentiment contagion.

3. Model Simulations

3.1. Equilibrium: Numerical and Agent-Based Simulations. The differential equation is popular in the relevant theory, but the solutions of these differential equations are usually complicated [32–34]; therefore we analyze the process of sentiment contagion by using the numerical and agent-based simulations. At first, we have to set the parameters, which usually depend on the specific situation. In this paper, according to the estimated results from Hill et al. (2010), we set the key parameters as follows: $\alpha_O = 0.18$, $\beta_O = 0.02$, $g_O = 0.088$, $\alpha_P = 0.04$, $\beta_P = 0.04$, and $g_P = 0.13$. And we set the initial values of the number of three statuses as $O = 626$, $P = 626$, and $S = 628$, so $N = 1880$. In fact, the choice of initial values has no effect on the final results. Additionally, it is important to note that we do not assume the population as well mixed, but it has an average degree of 4.

The final equilibrium states from numerical and agent-based simulations are shown in Figure 1, and we can find that the number of each state reaches a constant value by using numerical simulation ($O = 1202.21(63.95\%)$, $P = 196.13(10.43\%)$, and $S = 481.66(25.62\%)$), which is nearly identical to the results of the agent-based simulation. These results are almost consistent with the results from Hill et al. (2010), who have reported the proportion of each status. And these results show that our model is reasonable and can explain the process of sentiment contagion well.

3.2. The Effect of Different Parameters on the Equilibrium. There are six parameters in our model, which makes the equilibrium results very complex. Therefore, in order to facilitate the follow discussion, we assume that there is no difference between the optimistic and the pessimistic sentiment contagion processes. In fact, when the corresponding parameters are equal, the results of the two processes are symmetric. That is to say, when the equilibrium state has been reached, there will be the same number of the optimistic and the pessimistic. Therefore, at the beginning of the analysis in this section, we only discuss the related characteristics about the pessimistic. It means that this paper only discusses how

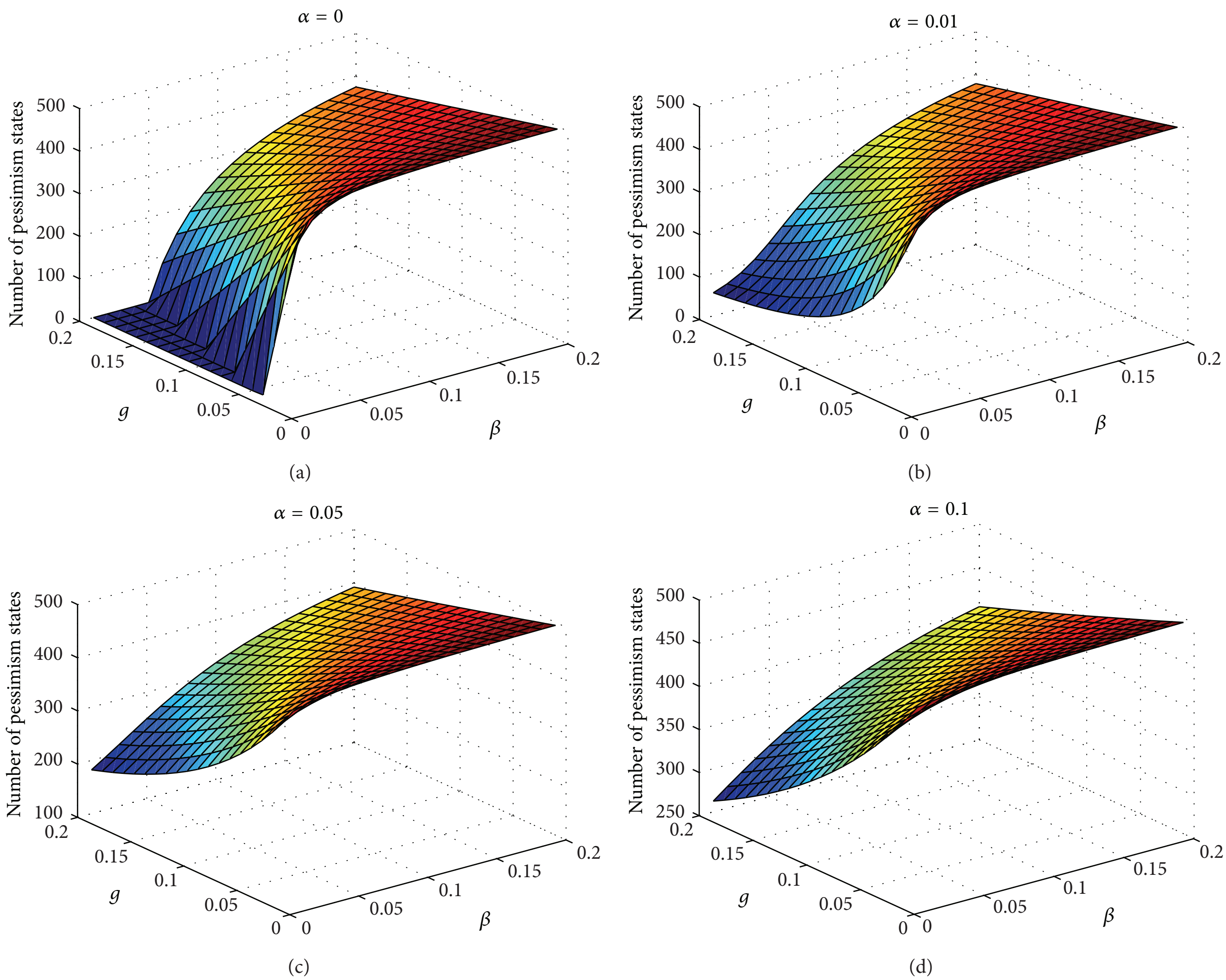

Figure 2: The influence of main parameters on the equilibrium.

the change of key parameters, which is associated with the pessimistic sentiment, affects the quantity of the pessimistic. In other words, we will discuss how the change of α_P, β_P, and g_P affects the equilibrium results. Meanwhile, in order to make the simulation results more intuitive, we set $N = 1000$. In fact, we find that in the process of the simulation, the setting of other parameters has no effect on the basic conclusions of this paper.

Figure 2 shows how the pessimism's recovery speed and its transmission speed influence the equilibrium number of the pessimistic under different parameters. Simply speaking, the faster the speed of the spontaneous generation is, the higher the equilibrium number of the pessimistic is. And the number of the pessimistic in equilibrium is positively related to the transmission speed but negatively related to the recovery speed. This is the same with our intuition. The interesting thing is that when the speed of the spontaneous generation and the probability of the susceptible getting infected are both at a low level, the speed of recovery in different intervals may have obvious different effects on equilibrium quantity.

In practice, the contagion rate of pessimism is often bigger than that of optimism, but how does this difference influence the equilibrium? In order to further study this issue, we relax the assumptions above and take the unequal contagion rates into consideration. From Figure 3, we can find that when the speed of spontaneous generation is very small or even near 0 (it is also close to the SIS model which does not consider the spontaneous generation of sentiment), the tiny difference between the contagion speeds of pessimism and optimism may lead to a huge difference between the numbers of the final equilibrium quantity of each sentiment state. It means that when the contagion speed of pessimism is bigger than that of optimism, the former one will hold the dominant position quickly. But when the mechanism of sentiment's spontaneous generation exists, the above phenomenon would not be so obvious. This can be understood as follows: the mechanism of sentiment's spontaneous generation would do an important and stable job to avoid the unlimited spread

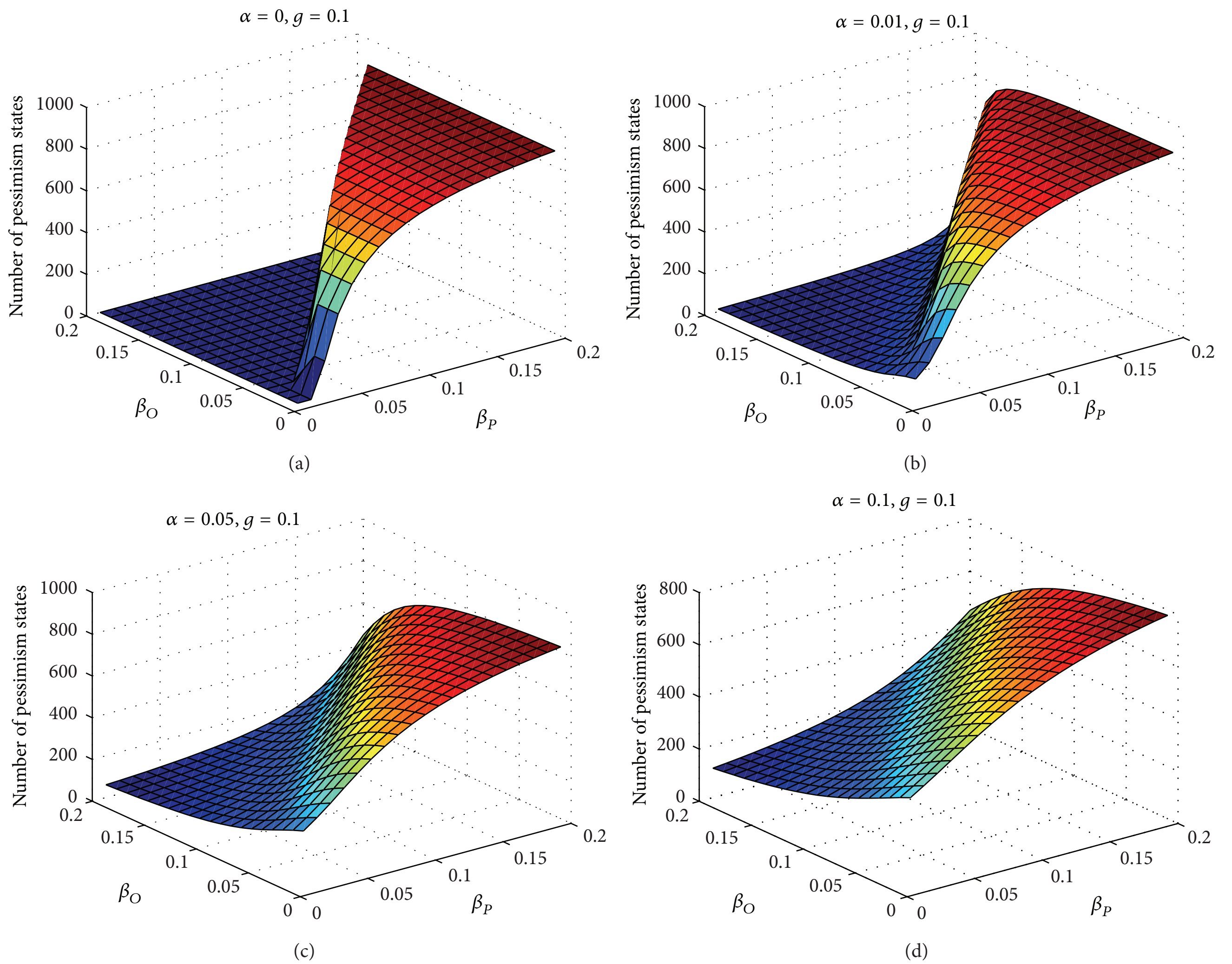

Figure 3: The influence of different infection probabilities on the equilibrium.

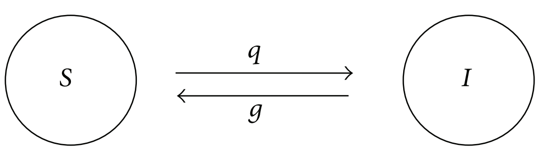

Figure 4

of single sentiment, especially the negative sentiment. It also enlightens us about the importance of cultivating a good generation mechanism of optimistic sentiment in our society.

We also simulate our model by using agent-based model, and the limited experimental results show that the above numerical solutions are also stable.

4. Discussions and Conclusions

This paper extends the classic SISa model, proposes a new framework model considering both the optimistic and pessimistic states, and constructs a SOSa-SPSa model. The simulations of the new model show that the results can match with the experimental data of Hill et al. (2010) well. From the further analysis of the equilibrium results affected by the key parameters, we can discover that the equilibrium quantity of the pessimistic is only related to the pivotal parameters, while irrelevant to the initial values of each sentiment group.

The SOSa-SPSa model proposed by this paper can well portray the process of sentiment contagion involving both the optimistic and pessimistic states, and the results are also consistent with the limited experimental data. However, the lack of the stability analysis of the equilibrium of this model is the limitation of this paper. Although this paper already analyzes the equilibrium of the SOSa-SPSa model, the stability of the equilibrium has not been discussed mathematically yet. Actually, the SOSa-SPSa model has six key parameters, which makes the analysis of the stability of the equilibrium point become a very difficult job. And we just have some infinite tests to observe the stability of this model under the different parameters settings, which show that the above equilibrium points are stable. The simulation results of agent-based model also suggest that the equilibrium

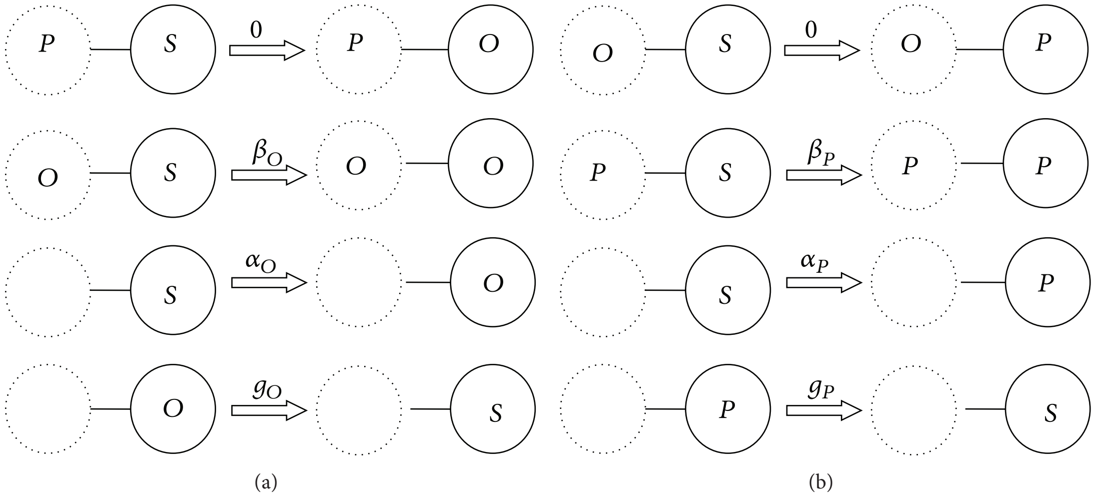

Figure 5

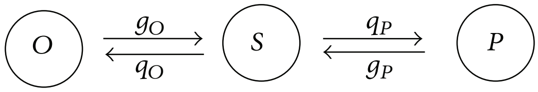

Figure 6

solution is stable, but it is still necessary to discuss the stability of the equilibrium model in a strict framework. We also have not considered the transformation mechanism between the optimistic and the pessimistic, which will be included in the next step of our work.

This SOSa-SPSa model can be used to study the investor sentiment contagion in the field of behavioral finance, but if you want to apply it to this topic, there are still some difficulties exist. We argue that the general sentiment contagion model in the field of psychology and sociology can only be used as a base model for investor sentiment contagion, but the deeper study of the characteristics of investor sentiment contagion is also very important and therefore necessary [35, 36]. If you want to further consider the issue of the investor sentiment contagion based on our model, you will need to think deeply about the commonness and differences between the definition of "emotion" and "investor sentiment" in both fields of social psychology and behavioral finance. This is because the investor sentiment not only has some common features of social mood but also could be profoundly affected by many market factors, such as the special operation mechanism of financial markets [37], the diffusion pattern of market information, the characteristic of complex network among investors, and the people's risk attitude [38, 39], and the presence of these factors may lead the contagion process of investor sentiment to present different characteristics from those in the field of sociology and psychology. Therefore, in our future research, we will further study the contagion characteristics of investor sentiment based on the microscopic model, which helps us to understand the generation mechanism of the investor sentiment and the relationship between investor sentiment and asset price more profoundly.

Conflict of Interests

The authors declare that there is no conflict of interests regarding the publication of this paper.

Acknowledgment

This research is supported by the National Science Foundation of China (NSFC) (no. 71171076).

References

[1] K. R. Olson, "A literature review of social mood," *The Journal of Behavioral Finance*, vol. 7, no. 4, pp. 193–203, 2006.

[2] B. Parkinson and G. Simons, "Affecting others: Social appraisal and emotion contagion in everyday decision making," *Personality and Social Psychology Bulletin*, vol. 35, no. 8, pp. 1071–1084, 2009.

[3] S. D. Pugh, "Service with a smile: emotional contagion in the service encounter," *Academy of Management Journal*, vol. 44, no. 5, pp. 1018–1027, 2001.

[4] U. Hess and S. Blairy, "Facial mimicry and emotional contagion to dynamic emotional facial expressions and their influence on decoding accuracy," *International Journal of Psychophysiology*, vol. 40, no. 2, pp. 129–141, 2001.

[5] T. Bosse, R. Duell, A. Z. Memon et al., "A multi-agent model for emotion contagion spirals integrated within a supporting ambient agent model," in *Principles of Practice in Multi-Agent Systems*, pp. 48–67, Springer, 2009.

[6] E. Hatfield and J. T. Cacioppo, *Emotional Contagion*, Cambridge University Press, Cambridge, UK, 1994.

[7] S. G. Barsade, "The ripple effect: emotional contagion and its influence on group behavior," *Administrative Science Quarterly*, vol. 47, no. 4, pp. 644–768, 2002.

[8] R. M. Anderson, R. M. May, and B. Anderson, *Infectious Diseases of Humans: Dynamics and Control*, Wiley, 1992.

[9] H. W. Hethcote and P. van den Driessche, "An SIS epidemic model with variable population size and a delay," *Journal of Mathematical Biology*, vol. 34, no. 2, pp. 177–194, 1995.

[10] B. Shulgin, L. Stone, and Z. Agur, "Pulse vaccination strategy in the SIR epidemic model," *Bulletin of Mathematical Biology*, vol. 60, no. 6, pp. 1123–1148, 1998.

[11] E. Beretta and Y. Takeuchi, "Global stability of an SIR epidemic model with time delays," *Journal of Mathematical Biology*, vol. 33, no. 3, pp. 250–260, 1995.

[12] P. S. Dodds and D. J. Watts, "A generalized model of social and biological contagion," *Journal of Theoretical Biology*, vol. 232, no. 4, pp. 587–604, 2005.

[13] A. L. Hill, D. G. Rand, M. A. Nowak, and N. A. Christakis, "Emotions as infectious diseases in a large social network: the SISa model," *Proceedings of the Royal Society B: Biological Sciences*, vol. 277, no. 1701, pp. 3827–3835, 2010.

[14] R. M. May and A. L. Lloyd, "Infection dynamics on scale-free networks," *Physical Review E*, vol. 64, no. 6, Article ID 066112, 2001.

[15] R. Pastor-Satorras and A. Vespignani, "Epidemic spreading in scale-free networks," *Physical Review Letters*, vol. 86, no. 14, pp. 3200–3203, 2001.

[16] V. M. Eguíluz and K. Klemm, "Epidemic threshold in structured scale-free networks," *Physical Review Letters*, vol. 89, no. 10, Article ID 108701, 2002.

[17] M. Boguñá and R. Pastor-Satorras, "Epidemic spreading in correlated complex networks," *Physical Review E*, vol. 66, no. 4, Article ID 047104, 2002.

[18] D. Centola and M. Macy, "Complex contagions and the weakness of long ties," *The American Journal of Sociology*, vol. 113, no. 3, pp. 702–734, 2007.

[19] P. S. Dodds and J. L. Payne, "Analysis of a threshold model of social contagion on degree-correlated networks," *Physical Review E*, vol. 79, no. 6, Article ID 066115, 2009.

[20] R. Pastor-Satorras and A. Vespignani, "Epidemic dynamics and endemic states in complex networks," *Physical Review E*, vol. 63, no. 6, Article ID 066117, 2001.

[21] L. Zhao, J. Wang, R. Huang et al., "Sentiment contagion in complex networks," *Physica A: Statistical Mechanics and Its Applications*, vol. 394, pp. 17–23, 2014.

[22] J. Tsai, E. Bowring, S. Marsella, and M. Tambe, "Empirical evaluation of computational emotional contagion models," in *Proceedings of the 10th International Conference on Intelligent Virtual Agents (IVA '11)*, pp. 384–397, 2011.

[23] G. Pereira, J. Dimas, R. Prada, P. A. Santos, and A. Paiva, "A generic emotional contagion computational model," *Lecture Notes in Computer Science*, vol. 6974, no. 1, pp. 256–266, 2011.

[24] L. Fu, W. Song, W. Lv, and S. Lo, "Simulation of emotional contagion using modified SIR model: a cellular automaton approach," *Physica A: Statistical Mechanics and Its Applications*, vol. 405, pp. 380–391, 2014.

[25] F. Wen, Z. He, and X. Chen, "Investors' risk preference characteristics and conditional skewness," *Mathematical Problems in Engineering*, vol. 2014, Article ID 814965, 14 pages, 2014.

[26] F. Wen, Z. He, X. Gong, and A. Liu, "Investors'risk preference characteristics based on different reference point," *Discrete Dynamics in Nature and Society*, vol. 2014, Article ID 158386, 9 pages, 2014.

[27] Y. Hudson and C. J. Green, "Born in the USA? Contagious investor sentiment and UK equity returns," Working Paper, 2013.

[28] Y. Lee, A. L. Tucker, D. K. Wang, and H.-T. Pao, "Global contagion of market sentiment during the US subprime crisis," *Global Finance Journal*, vol. 25, no. 1, pp. 17–26, 2014.

[29] Y. Bai, "Cross-border sentiment: an empirical analysis on EU stock markets," *Applied Financial Economics*, vol. 24, no. 4, pp. 259–290, 2014.

[30] M. Baker, J. Wurgler, and Y. Yuan, "Global, local, and contagious investor sentiment," *Journal of Financial Economics*, vol. 104, no. 2, pp. 272–287, 2012.

[31] C. Chang, R. Faff, and C. Y. Hwang, "Local and global sentiment effects, and the role of legal, information and trading," Working Paper, 2012.

[32] C. Huang, C. Peng, X. Chen, and F. Wen, "Dynamics analysis of a class of delayed economic model," *Abstract and Applied Analysis*, vol. 2013, Article ID 962738, 12 pages, 2013.

[33] C. Huang, H. Kuang, X. Chen, and F. Wen, "An LMI approach for dynamics of switched cellular neural networks with mixed delays," *Abstract and Applied Analysis*, vol. 2013, Article ID 870486, 8 pages, 2013.

[34] G. Qin, C. Huang, Y. Xie et al., "Asymptotic behavior for third-order quasi-linear differential equations," *Advances in Difference Equations*, vol. 2013, no. 1, article 305, 2013.

[35] N. S. Tay, "Social network characteristics and the evolution of investor sentiment," in *Agent-Based Approaches in Economic and Social Complex Systems V*, vol. 6 of *Springer Series on Agent Based Social Systems*, pp. 207–217, Springer, 2009.

[36] L. Cen, H. Lu, and L. Yang, "Investor sentiment, disagreement, and the breadth-return relationship," *Management Science*, vol. 59, no. 5, pp. 1076–1091, 2013.

[37] J. Liu, L. Yan, and C. Ma, "Pricing options and convertible bonds based on an actuarial approach," *Mathematical Problems in Engineering*, vol. 2013, Article ID 676148, 9 pages, 2013.

[38] F. Wen and X. Yang, "Skewness of return distribution and coefficient of risk premium," *Journal of Systems Science & Complexity*, vol. 22, no. 3, pp. 360–371, 2009.

[39] F. Wen, X. Gong, Y. Chao, and X. Chen, "The effects of prior outcomes on risky choice: evidence from the stock market," *Mathematical Problems in Engineering*, vol. 2014, Article ID 272518, 8 pages, 2014.

Hindawi Publishing Corporation
Discrete Dynamics in Nature and Society
Volume 2014, Article ID 917913, 4 pages
http://dx.doi.org/10.1155/2014/917913

Research Article

Dynamics of Third-Order Nonlinear Neutral Equations

Hua Wang,[1] Li Liu,[1] and Yanxiang Tan[2]

[1] *School of Mathematics and Computing Science, Changsha University of Science and Technology, Changsha, Hunan 410114, China*
[2] *College of Mathematics and Econometrics, Hunan University, Changsha, Hunan 410082, China*

Correspondence should be addressed to Li Liu; babaley@163.com

Received 12 March 2014; Accepted 18 June 2014; Published 14 July 2014

Academic Editor: Taishan Yi

The aim of this paper is to study oscillatory and asymptotic properties of the third-order nonlinear neutral equation with continuously distributed delays of the form $(r(t)([x(t)+\int_a^b p(t,\mu)x[\tau(t,\mu)]\,d\mu]'')^{\alpha})'+\int_c^d q(t,\xi)f^{\alpha}(x[g(t,\xi)])\,d\xi=0$. Applying suitable generalized Riccati transformation and integral averaging technique, we present new criteria for oscillation or certain asymptotic behavior of nonoscillatory solutions of this equation. Obtained results essentially improve and complement earlier ones.

1. Introduction

In recent years, the dynamics theory such as oscillation theory and asymptotic behavior of differential equations and their applications have been and still are receiving intensive attention [1–4]. In fact, in the last few years several monographs and hundreds of research papers have been written; see, for example, the monograph [5]. Determining oscillation criteria for particular second-order differential equations has received a great deal of attention in the last few years [6–8]. For example, [9] considered

$$\left(r(t)\left[x(t)+p(t)x(t-\tau)\right]'\right)' + \int_a^b q(t,\xi)\,x\left[g(t,\xi)\right]d\sigma(\xi)=0 \tag{1}$$

and obtained oscillatory criteria of Philos type. In [10], by means of Riccati transformation technique, Han et al. established some new oscillation criteria for the second-order Emden Fowler delay dynamic equations on a time scale T:

$$x''(t)+p(t)x^{\gamma}(\tau(t))=0. \tag{2}$$

However, compared to second-order differential equations, the study of oscillation and asymptotic behavior of third-order differential equations has received considerably less attention in the literature [11–15]. In [16], Qiu investigated the oscillation criteria for the third-order neutral differential equations taking the following form:

$$\left(r(t)\left[x(t)+p(t)x(t)\right]''\right)' + \int_a^b q(t,\xi)\,x\left[g(t,\xi)\right]d\sigma(\xi)=0,\quad t\ge t_0. \tag{3}$$

By using a generalized Riccati transformation and integral averaging technique, Zhang et al. [17] established some new sufficient conditions which ensure that every solution of the following equation oscillates or converges to zero:

$$\left(r(t)\left(\left[x(t)+\int_a^b p(t,\mu)\,x\left[\tau(t,\mu)\right]d\mu\right]''\right)\right)' + \int_c^d q(t,\xi)\,f\left(x\left[g(t,\xi)\right]\right)d\xi=0. \tag{4}$$

As we know, the dynamics theory such as oscillation theory and asymptotic behavior of the following equation have not been investigated up to now:

$$\left(r(t)\left(\left[x(t)+\int_a^b p(t,\mu)\,x\left[\tau(t,\mu)\right]d\mu\right]''\right)^{\alpha}\right)' + \int_c^d q(t,\xi)\,f^{\alpha}\left(x\left[g(t,\xi)\right]\right)d\xi=0. \tag{5}$$

With the help of a generalized Riccati transformation and integral averaging technique, this paper aims to establish some new sufficient conditions of Philos type which ensure that every solution of (5) oscillates or converges to zero. Our results improve and complement the corresponding results in [6, 11–17]. We should point out that, in this paper, α is any quotient of odd positive integers and $\alpha \le 1$; it is more general than that reported in [17] where $\alpha = 1$.

We are interested in (5) in the case of $t \ge t_0$. Throughout this paper, we assume that the following hypotheses hold:

(H_1) $r(t) \in C^1([t_0,\infty),(0,\infty))$, $\int_{t_0}^{\infty}(1/r(t))dt = \infty$;

(H_2) $P(t,\mu) \in C([t_0,\infty)\times[a,b],R)$, $0 \le p(t) \equiv \int_a^b p(t,\mu)d\mu \le p < 1$;

(H_3) $\tau(t,\mu) \in C([t_0,\infty)\times[a,b],R)$ is not a decreasing function for ξ, and $\tau(t,\mu) \le t$, $\lim_{t\to\infty}\min_{\xi\in[a,b]}\tau(t,\mu) = \infty$;

(H_4) $q(t,\xi) \in C([t_0,\infty)\times[c,d],(0,\infty))$;

(H_5) $g(t,\xi) \in C([t_0,\infty)\times[c,d],R)$ is not a decreasing function for ξ, such that $g(t,\xi) \le t$, $\lim_{t\to\infty}\min_{\xi\in[c,d]}g(t,\xi) = \infty$;

(H_6) $f(x) \in C(R,R), (f(x)/x^{\alpha}) \ge \delta >, \ x \ne 0$.

We also define the following function:

$$z(t) = x(t) + \int_a^b p(t,\mu)\, x[\tau(t,\mu)]\, d\mu. \tag{6}$$

As far as a solution of (5) is concerned, we mean a nontrivial function $x(t) \in C'([T_x,\infty),R)$, $T_x \ge t_0$, which has the property $r(t)z''(t) \in C'([T_x,\infty))$ and satisfies (5) on $[T_x,\infty)$.

We restrict our attention to those solutions of (5) which satisfy $\sup\{|x(t)| : t \ge T\} > 0$ for all $T > T_x$. A solution of (5) is said to be oscillatory on $[T_x,\infty)$ if it is neither eventually positive nor eventually negative. Otherwise it is called nonoscillatory.

The rest of this paper is organized as follows. In Section 2, we will present some lemmas which are useful for the proof of our main results. In Section 3, we present new criteria of Philos type for oscillation or certain asymptotic behavior of nonoscillatory solutions of (5).

2. Several Lemmas

Lemma 1. *Let $x(t)$ be a positive solution of* (5), *and* $r'(t) \ge 0$, $z'''(t) < 0$. *Then $z(t)$ which is defined as in* (6) *has only one of the following two properties:*

(*I*) $z(t) > 0,\ z'(t) >,\ z''(t) > 0$;

(*II*) $z(t) > 0,\ z'(t) < 0,\ z''(t) > 0$.

Proof. Letting $x(t)$ be a positive solution of (5) on $[t_0,\infty)$, from (6), we have $z(t) > x(t) > 0$ and $(r(t)(z''(t))^{\alpha})' = -\int_c^d q(t,\xi)f^{\alpha}(x[g(t,\xi)])d\xi < 0$. Then $r(t)(z''(t))^{\alpha}$ is a decreasing function and of one sign, and following $\alpha \in (0,1)$ and $\alpha = p/q$ where p and q are odd positive integers, we have that $(z''(t))^{\alpha}$ and $z''(t)$ have the same sign, so $z''(t)$ is either eventually positive or eventually negative on $t \ge t_1 \ge t_0$; that is, $z''(t) < 0$ or $z''(t) > 0$. If $z''(t) < 0$, then there exists a constant $M > 0$, such that $r(t)z'' \le -M < 0$. By integrating from t_1 to t, we get

$$z'(t) \le z'(t_1) - M\int_{t_1}^{t}\frac{1}{r(s)}ds. \tag{7}$$

Letting $t \to \infty$ and using (H_1), we have $z'(t) \to -\infty$. Thus $z'(t) < 0$ eventually; since $z''(t) < 0$ and $z'(t) < 0$, we have $z(t) < 0$, which contradicts assumption $z(t) > 0$, so $z''(t) > 0$. Therefore, $z(t)$ has only one of the two properties (I) and (II). □

Lemma 2. *Let $x(t)$ be a positive solution of* (5), *and correspondingly $z(t)$ has property* (*II*). *Assume that*

$$\int_{t_0}^{\infty}\int_{v}^{\infty}\left[\frac{1}{r(u)}\int_u^{\infty}\left(\int_c^d q(s,\xi)\,d\xi\right)ds\right]^{1/\alpha} du\, dv = \infty. \tag{8}$$

Then

$$\lim_{t\to\infty} x(t) = \lim_{t\to\infty} z(t) = 0. \tag{9}$$

Proof. Let $x(t)$ be a positive solution of (5). Since $z(t)$ has property (II), then there exists finite limit $\lim_{t\to\infty}z(t) = l$. We assert that $l = 0$. Assuming that $l > 0$, then we have $l < z(t) < l + \epsilon$, for all $\epsilon > 0$. Choosing $\epsilon \in (0, l(1-p)/p)$, we obtain

$$\begin{aligned} x(t) &= z(t) - \int_a^b p(t,\mu)\,x[\tau(t,\mu)]\,d\mu \\ &> l - \int_a^b p(t,\mu)\,x[\tau(t,\mu)]\,d\mu \\ &\ge l - p(t)\,z[\tau(t,a)] \\ &\ge l - p(l+\epsilon) \\ &= k(l+\epsilon) \\ &> kz(t), \end{aligned} \tag{10}$$

where $k = (l - p(l+\epsilon))/(l+\epsilon) > 0$. Using ($H_6$) and $x(t) > kz(t)$, from (5), we find that

$$\left(r(t)\left(z''(t)\right)^{\alpha}\right)' \le -k\delta\int_c^d q(t,\xi)\, z^{\alpha}(x[g(t,\xi)])\, d\xi. \tag{11}$$

Note that $z(t)$ has property (II) and (H_5); we have

$$\left(r(t)\left(z''(t)\right)^{\alpha}\right)' \le -k\delta z^{\alpha}(x[g(t,d)])\int_c^d q(t,\xi)\,d\xi \tag{12}$$

$$= -q_1(t)\, z^{\alpha}[g_1(t)], \tag{13}$$

where $q_1(t) = k\delta\int_c^d q(t,\xi)d\xi$, $g_1(t) = g(t,d)$. Integrating inequality (13) from t to ∞, we get

$$\begin{aligned} \left(r(t)\left(z''(t)\right)^{\alpha}\right) &\ge \int_t^{\infty} q_1(s)\, z^{\alpha}[g_1(s)]\, ds, \\ z''(t) &\ge \left[\frac{1}{r(t)}\int_t^{\infty} q_1(s)\, z^{\alpha}[g_1(s)]\, ds\right]^{1/\alpha}. \end{aligned} \tag{14}$$

Using $z[g_1(t)] \geq l$, then we have

$$z''(t) \geq \left[\frac{l^\alpha}{r(t)} \int_t^\infty q_1(s)\, ds\right]^{1/\alpha}. \quad (15)$$

Integrating inequality (15) from t to ∞, we have

$$-z'(t) \geq l \int_t^\infty \left[\frac{1}{r(u)} \left(\int_u^\infty q_1(s)\, ds\right)\right]^{1/\alpha} du. \quad (16)$$

Integrating the last inequality from t_1 to ∞, we obtain

$$z(t_1) \geq l \int_{t_1}^\infty \int_v^\infty \left[\frac{1}{r(u)} \left(\int_u^\infty q_1(s)\, ds\right)\right]^{1/\alpha} du\, dv; \quad (17)$$

we have a contradiction with (8) and so it follows that $\lim_{t\to\infty} x(t) = 0$. □

Lemma 3 (see [18]). *Let $z(t) > 0, z'(t) > 0, z''(t) \leq 0, t > t_0$. Then, for each $\beta \in (0,1)$, there exists $T_\beta \geq t_0$ such that*

$$z(g(t)) \geq \beta \frac{g(t)}{t} \cdot z(t), \quad t \geq T_\beta. \quad (18)$$

Lemma 4 (see [19]). *Letting $z(t) > 0$, $z'(t) > 0$, $z'' \geq 0$, $r' > 0$, $z'''(t) \leq 0$, $t \geq T_\beta$, then there exist $\gamma \in (0,1)$ and $T_\gamma \geq T_\beta$ such that*

$$z(t) \geq \gamma t z'(t), \quad t \geq T_\gamma. \quad (19)$$

Lemma 5. *For all $\alpha > 0$, then for all $A > 0, B > 0$, one has*

$$Bu - Au^{(\alpha+1)/\alpha} \leq \frac{\alpha^\alpha}{(\alpha+1)^{\alpha+1}} \cdot \frac{B^{\alpha+1}}{A^\alpha}. \quad (20)$$

Proof. Let $u \geq 0$, $\alpha > 0$. We investigate the maximal value and minimal value of the function $f(u) = Bu - Au^{(\alpha+1)/\alpha}$.

At first, for all $A > 0$, $B > 0$, the derivative of function $f(u) = Bu - Au^{(\alpha+1)/\alpha}$ is $f'(u) = B - A((\alpha+1)/\alpha)u^{1/\alpha}$. It is clear that when $u > (B/A)^\alpha \cdot (\alpha/(\alpha+1))^\alpha$, we have $f'(u) < 0$, and when $u < (B/A)^\alpha \cdot (\alpha/(\alpha+1))^\alpha$, we have $f'(u) > 0$. Hence the function $f(u) = Bu - Au^{(\alpha+1)/\alpha}$ attains its maximum value $(\alpha^\alpha/(\alpha+1)^{\alpha+1}) \cdot (B^{\alpha+1}/A^\alpha)$ at $u = (B/A)^\alpha \cdot (\alpha/(\alpha+1))^\alpha$. This completes the proof. □

3. Main Result

Theorem 6. *Assume that the condition of Lemma 2 holds, and there exists $\rho \in C^1([t_0,\infty),(0,\infty))$, such that $\rho' > 0$ and*

$$\lim_{t\to\infty} \int_T^t \left[Q(s) - \frac{\alpha^\alpha}{(\alpha+1)^{\alpha+1}} \cdot \frac{B^{\alpha+1}(s)}{A^\alpha(s)}\right] ds = \infty, \quad (21)$$

where

$$Q(s) = [\beta\gamma\delta(1-p)]^\alpha \cdot \frac{\rho(t)}{t^\alpha} g^{2\alpha}(t,c) \int_c^d q(t,\xi)\, d\xi,$$
$$B(s) = \frac{\alpha}{[\rho(s) r(s)]^{1/\alpha}}, \quad (22)$$
$$A(s) = \frac{\rho'(s)}{\rho(s)}.$$

Then every solution $x(t)$ of (5) *either is oscillatory or converges to zero.*

Proof. Assume that (5) has a nonoscillatory solution $x(t)$. Without loss of generality we may assume that $x(t) > 0, t \geq t_1$, $x[\tau(t,\mu)] > 0$, $(t,\mu) \in [t_1,\infty) \times [a,b]$; $x[g(t,\xi)] > 0$, $(t,\xi) \in [t_1,\infty) \times [c,d]$, and $z(t)$ is defined as in (6). By Lemma 1, we have that $z(t)$ has property (I) or property (II). At first, when $z(t)$ has property (I), we obtain

$$\begin{aligned} x(t) &= z(t) - \int_a^b p(t,\mu) x[\tau(t,\mu)]\, d\mu \\ &\geq z(t) - \int_a^b p(t,\mu) z[\tau(t,\mu)]\, d\mu \\ &\geq z(t) - z[\tau(t,b)] \int_a^b p(t,\mu)\, d\mu \\ &\geq \left(1 - \int_a^b p(t,\mu)\, d\mu\right) z(t) \\ &\geq (1-p) z(t). \end{aligned} \quad (23)$$

Using (H_5) and (H_6), we get

$$\begin{aligned} &\left(r(t)\left(z''(t)\right)^\alpha\right)' \\ &\quad \leq -\delta^\alpha (1-p)^\alpha \int_c^d q(t,\xi) z^\alpha[g(t,\xi)]\, d\xi \\ &\quad \leq -\delta^\alpha (1-p)^\alpha z^\alpha[g(t,c)] \int_c^d q(t,\xi)\, d\xi \\ &\quad \equiv -q_2(t) z^\alpha[g_2(t)], \end{aligned} \quad (24)$$

where

$$q_2(t) = \delta^\alpha (1-p)^\alpha \int_c^d q(t,\xi)\, d\xi, \qquad g_2(t) = g(t,c). \quad (25)$$

Let

$$w(t) = \rho(t) r(t) \left(\frac{z''(t)}{z'(t)}\right)^\alpha, \quad t \geq t_1. \quad (26)$$

Then

$$\frac{w(t)\left(z'(t)\right)^\alpha}{\rho(t)} = r(t)\left(z''(t)\right)^\alpha, \quad (27)$$

so

$$\begin{aligned} &\left(\frac{w(t)\left(z'(t)\right)^\alpha}{\rho(t)}\right)' = \left(r(t)\left(z''(t)\right)^\alpha\right)' \leq -q_2(t) z^\alpha[g_2(t)], \\ &w'(t) \leq -q_2(t)\rho(t)\left[\frac{z[g_2(t)]}{z'}\right]^\alpha \\ &\qquad + \frac{\rho'(t)}{\rho(t)} w(t) - \frac{\alpha}{[\rho(t) r(t)]^{1/\alpha}} w^{(\alpha+1)/\alpha}(t). \end{aligned} \quad (28)$$

Letting $u(t) = z'(t)$, from Lemma 3, we obtain

$$\frac{1}{z'(t)} \geq \frac{\beta g_2(t)}{tz'[g_2(t)]}, \quad t \geq T_\beta \geq t_1. \tag{29}$$

Using Lemma 4, we get

$$z[g_2(t)] \geq \gamma g_2(t) z'[g_2(t)], \quad t \geq T_\gamma \geq T_\beta. \tag{30}$$

Hence

$$w'(t) \leq -Q(t) + \frac{\rho'(t)}{\rho(t)} w(t) - \frac{\alpha}{[\rho(t) r(t)]^{1/\alpha}} w^{(\alpha+1)/\alpha}(t), \quad t \geq T_\gamma, \tag{31}$$

where $Q(t)$ is defined as (21). Letting $A(t) = \rho'(t)/\rho(t)$, $B(t) = \alpha/(\rho(t)r(t))^{1/\alpha}$, we have that

$$w'(t) \leq -Q(t) + A(t) w(t) - B(t) w^{(\alpha+1)/\alpha}(t), \tag{32}$$

and, from Lemma 5, we obtain

$$w'(t) \leq -Q(t) + \frac{\alpha^\alpha}{(\alpha+1)^{\alpha+1}} \cdot \frac{B^{\alpha+1}(t)}{A^\alpha(t)}. \tag{33}$$

Integrating inequality (33) from T to t,

$$\int_T^t w'(s)\, ds \leq -\int_T^t \left(Q(s) - \frac{\alpha^\alpha}{(\alpha+1)^{\alpha+1}} \cdot \frac{B^{\alpha+1}(s)}{A^\alpha(s)} \right) ds, \tag{34}$$

we obtain

$$0 < w(t) \leq w(T) - \int_T^t \left(Q(s) - \frac{\alpha^\alpha}{(\alpha+1)^{\alpha+1}} \cdot \frac{B^{\alpha+1}(s)}{A^\alpha(s)} \right) ds, \tag{35}$$

which contradicts (21). If $z(t)$ has property (II), since (8) holds, then the conditions in Lemma 2 are satisfied. Hence $\lim_{t\to\infty} x(t) = 0$.

This completes the proof. □

Conflict of Interests

The authors declare that there is no conflict of interests regarding the publication of this paper.

Acknowledgments

This work is supported by the Scientific Research Funds of Hunan Provincial Science and Technology Department of China (no. 12FJ4252 and no. 2013SK3143), National Natural Science Foundation of China (nos. 11101053, 11326116).

References

[1] C. Huang, Z. Yang, T. Yi, and X. Zou, "On the basins of attraction for a class of delay differential equations with non-monotone bistable nonlinearities," *Journal of Differential Equations*, vol. 256, no. 7, pp. 2101–2114, 2014.

[2] C. Huang, C. Peng, X. Chen, and F. Wen, "Dynamics analysis of a class of delayed economic model," *Abstract and Applied Analysis*, vol. 2013, Article ID 962738, 12 pages, 2013.

[3] G. Qin, C. Huang, Y. Xie, and F. Wen, "Asymptotic behavior for third-order quasi-linear differential equations," *Advances in Difference Equations*, vol. 2013, article 305, 2013.

[4] C. Huang, H. Kuang, X. Chen, and F. Wen, "An LMI approach for dynamics of switched cellular neural networks with mixed delays," *Abstract and Applied Analysis*, vol. 2013, Article ID 870486, 8 pages, 2013.

[5] R. P. Agarwal, S. Grace R, and D. O'Regan, *Oscillation Theory for Difference and Functional Differential Equations*, Kluwer Academic, Dordrecht, The Netherlands, 2000.

[6] A. Tiryaki and M. F. Aktaş, "Oscillation criteria of a certain class of third order nonlinear delay differential equations with damping," *Journal of Mathematical Analysis and Applications*, vol. 325, no. 1, pp. 54–68, 2007.

[7] R. P. Agarwal, S. R. Grace, and D. O'Regan, *Oscillation Theory for Second Order Dynamic Equations*, vol. 5, Taylor and Francis, London, UK, 2003.

[8] L. H. Erbe, Q. Kong, and B. G. Zhang, *Oscillation Theory for Functional-Differential Equations*, Marcel Dekker, New York, NY, USA, 1995.

[9] P. G. Wang, "Oscillation criteria for second-order neutral equations with distributed deviating arguments," *Computers & Mathematics with Applications*, vol. 47, no. 12, pp. 1935–1946, 2004.

[10] Z. L. Han, S. R. Sun, and B. Shi, "Oscillation criteria for a class of second-order Emden-Fowler delay dynamic equations on time scales," *Journal of Mathematical Analysis and Applications*, vol. 334, no. 2, pp. 847–858, 2007.

[11] M. F. Aktas, A. Tiryaki, and A. Zafer, "Oscillation criteria for third-order nonlinear functional differential equations," *Applied Mathematics Letters*, vol. 23, no. 7, pp. 756–762, 2010.

[12] S. R. Grace, R. P. Agarwal, R. Pavani, and E. Thandapani, "On the oscillation of certain third order nonlinear functional differential equations," *Applied Mathematics and Computation*, vol. 202, no. 1, pp. 102–112, 2008.

[13] S. R. Grace, R. P. Agarwal, and M. F. Aktas, "On the oscillation of third order functional differential equations," *Indian Journal of Pure and Applied Mathematics*, vol. 39, no. 6, pp. 491–507, 2008.

[14] N. Parhi and S. Padhi, "Asymptotic behaviour of solutions of third order delay-differential equations," *Indian Journal of Pure and Applied Mathematics*, vol. 33, no. 10, pp. 1609–1620, 2002.

[15] A. Tiryaki and S. Yaman, "Asymptotic behaviour of a class of nonlinear functional differential equations of third order," *Applied Mathematics Letters*, vol. 14, no. 3, pp. 327–332, 2001.

[16] Y. Qiu, "Philos Oscillation theorems for third-order neutral equations," *Mathematics in Practice and Theory*, vol. 41, pp. 247–252, 2011.

[17] Q. Zhang, L. Gao, and Y. Yu, "Oscillation criteria for third-order neutral differential equations with continuously distributed delay," *Applied Mathematics Letters*, vol. 25, no. 10, pp. 1514–1519, 2012.

[18] L. Erbe, "Oscillation criteria for second order nonlinear delay equations," *Canadian Mathematical Bulletin*, vol. 16, pp. 49–56, 1973.

[19] I. T. Kiguradze, "On the oscillation of solution of the equation $d^m u/dt^m + a(t)|u|^m signu = 0$," *Matematicheskii Sbornik*, vol. 65, pp. 172–187, 1964.

Hindawi Publishing Corporation
Discrete Dynamics in Nature and Society
Volume 2014, Article ID 964654, 10 pages
http://dx.doi.org/10.1155/2014/964654

Research Article

Forecasting Return Volatility of the CSI 300 Index Using the Stochastic Volatility Model with Continuous Volatility and Jumps

Xu Gong, Zhifang He, Pu Li, and Ning Zhu

School of Business, Central South University, Changsha, Hunan 410083, China

Correspondence should be addressed to Ning Zhu; zhuning@csu.edu.cn

Received 13 April 2014; Accepted 12 June 2014; Published 9 July 2014

Academic Editor: Chuangxia Huang

The logarithmic realized volatility is divided into the logarithmic continuous sample path variation and the logarithmic discontinuous jump variation on the basis of the SV-RV model in this paper, which constructs the stochastic volatility model with continuous volatility (SV-CJ model). Then, we use high-frequency transaction data for five minutes of the CSI 300 stock index as the study sample, which, respectively, make parameter estimation on the SV, SV-RV, and SV-CJ model. We also comparatively analyze these three models' prediction accuracy by using the loss functions and SPA test. The results indicate that the prior logarithmic realized volatility and the logarithmic continuous sample path variation can be used to predict the future return volatility in China's stock market, while the logarithmic discontinuous jump variation is poor at its prediction accuracy. Besides, the SV-CJ model has an obvious advantage over the SV and SV-RV model as to the prediction accuracy of the return volatility, and it is more suitable for the research concerning the problems of financial practice such as the financial risk management.

1. Introduction

Recent papers (such as Corsi [1], Wen and Yang [2], Liu et al. [3], Andersen et al. [4, 5], Dai et al. [6], Wen et al. [7], Bollerslev et al. [8, 9], and Liu et al. [10–12]) have showed that the financial risk management, financial asset pricing, and financial derivatives pricing play more and more important roles in the analysis of the problems in financial practices. What is more, the research on the asset volatility of the financial market is the basis of the analysis of the problems in financial practices like the financial risk management, financial asset pricing, and financial derivatives pricing. Therefore, the measurement and forecast of financial asset volatility have become hot topics.

In order to accurately measure and predict the financial asset volatility, Engle [13] proposed an ARCH model according to "clustering" and "long-memory" features of the return volatility; Bollerslev [14], on the basis of the ARCH model, established a GARCH model. Taylor [15] first proposed a stochastic volatility (SV) model. Then, many scholars study the SV model and comparatively analyze the measurement and forecast accuracy for financial asset volatility between the GARCH model and SV model. Among them, there are many literatures about the comparison of SV model and GARCH model on asset volatility measurement and sample fitting ability. Danielsson [16] studied the S&P 500 index of American stock markets, and he found that the fitting ability of SV model for the S&P 500 index volatility is stronger than the ARCH (5), GARCH (1, 2), IGARCH, and EGARCH (2, 1) model. Wang et al. [17], the empirical study on the application of China's stock market data, found that the SV model can better describe the heteroscedasticity in the return of stock market and the serial correlation of volatility than GARCH model. Kim et al. [18] also found that the SV model have a better sample fitting ability for the financial asset volatility than the GARCH model. In addition, there exist some literatures about the prediction accuracy of the future financial asset volatility as to the comparative study on SV model and GARCH model. Yu [19], the comparative study on the SV model and GARCH model, found that the SV model showed much better out-of-sample forecasting performance than the ARCH and GARCH (1, 1) and GARCH (3, 2) model in New Zealand stock market. Sadorsky [20] (in the US stock market), Pederzoli [21] (in the UK stock market), and Wei [22] (in the crude oil futures market) came to a similar conclusion with Yu [19], that is to say, the SV model's prediction accuracy is stronger than the GARCH model's.

Although the SV model has good forecasting performance for the future return volatility, higher accuracy is more favorable to the analysis of practical financial problems such as financial risk measuring, financial asset pricing, and financial derivatives pricing. In order to improve the prediction and measurement accuracy of the model, Koopman et al. [23] introduced realized volatility (RV; Andersen and Bollerslev [24]) as an exogenous variable into the volatility equation of SV model so as to construct the SV-RV model. After applying the S&P 100 index in American stock markets, Koopman et al. found the measuring and forecasting accuracy for return volatility of SV-RV model is stronger than the SV model. Then, Geweke et al. [25] found that the SV-RV model has a good ability to predict financial asset volatility. Jacquier and Miller [26] also found that the realized volatility (RV) contained certain prediction information for the future volatility, and the SV-RV model's prediction ability is superior to the SV model. However, in the real financial market, because of the impact of the abnormal information and the existence of the irrational investors, the financial asset volatility is not only a continuous process but also there are some jumps in it. Therefore, while we study the SV-RV model, it is more reasonable to divide the RV into the continuous sample path variation (C) and the discontinuous jump variation (J) and add the two factors into the volatility equation of SV model. Hence, after learning from Barndorff-Nielsen and Shephard [27, 28] and Andersen et al. [5], on the basis of the SV-RV model, we divide the RV into C and J and establish the SV-CJ model so as to further improve the model's ability to measure and forecast financial asset volatility. Then, we use the high-frequency data for five minutes of CSI 300 index in China's stock market as the research sample to make parameter estimation on the SV, SV-RV, and SV-CJ model, respectively, and use the loss functions and SPA test proposed by Hansen [29] to comparatively analyze forecasting performance for the future return volatility of the three models. By this way, we look for the best model for forecasting financial asset volatility.

The remainder of this paper is organized as follows. In Section 2, we discuss three volatility models, the SV, SV-RV, and SV-CJ model. In Section 3, we introduce estimation and evaluation method of the models. In Section 4, the estimating and forecasting results are presented. Section 5 is the conclusion of this paper.

2. Volatility Models

2.1. The SV and SV-RV Model. In the existing literature, there exist many forms about the SV model; one of the common forms can be expressed as follows:

$$\begin{aligned} y_t &= \varepsilon_t e^{h_t/2}, \\ h_t &= \alpha + \beta h_{t-1} + \eta_t, \end{aligned} \tag{1}$$

where y_t is a return. $\{\varepsilon_t\}$ and $\{\eta_t\}$ are mutual dependent. In this paper, we suppose $\varepsilon_t \sim i.i.N(0,1)$, $\eta_t \sim i.i.N(0,\sigma_\eta^2)$, and σ_η^2 is unknown. α and β are constant. β, as continuous parameter, reflects the impact of the prior volatility on the current volatility, and when $|\beta| < 1$, it stands for covariance stationary of the SV model. h_t is the logarithm of return volatility; supposing $h_0 \sim N(\alpha, \sigma_\varepsilon^2)$, we can conclude that for given h_{t-1}, α, β, h_t obeys normal distribution with mean $\alpha + \beta h_{t-1}$ and variance σ_ε^2; that, is $h_t \mid h_{t-1}, \alpha, \beta \sim N(\alpha + \beta h_{t-1}, \sigma_\varepsilon^2)$, $t = 1, 2, \ldots, T$.

To enhance the model's accuracy for volatility measurement and prediction, according to Koopman et al. [23], we add $\ln(\mathrm{RV}_{t-1})$ as an exogenous variable to the volatility equation of SV model; we establish the SV-RV model

$$\begin{aligned} y_t &= \varepsilon_t e^{h_t/2}, \\ h_t &= \alpha + \beta h_{t-1} + \gamma \ln(\mathrm{RV}_{t-1}) + \eta_t, \end{aligned} \tag{2}$$

where RV_{t-1} is a realized volatility at time $t-1$; the volatility used in this paper is identical to that in Martens [30] and Koopman et al. [23]; taking the overnight return variance into consideration, RV_{t-1} can be expressed as follows:

$$\mathrm{RV}_t = \sum_{i=1}^{N} r_{t,j}^2 + r_{t,n}^2 = \sum_{j=1}^{M} r_{t,j}^2, \quad M = N + 1, \tag{3}$$

where $r_{t,1}$ and $r_{t,n}$ stand for the overnight return, $r_{t,1} = r_{t,n} = 100(\ln P_{t,o} - \ln P_{t-1,c})$, $P_{t,o}$ represents the open price at time t, and $P_{t-1,c}$ denotes the closing price of phase $t-1$; $r_{t,2}$ is the 1st return after the opening of time t, $r_{t,2} = 100(\ln P_{t,1} - \ln P_{t,o})$; $P_{t,1}$ is the 1st close price after the opening of time t; $r_{t,3}$ shows the 2nd return after the opening of time t, $r_{t,3} = 100(\ln P_{t,2} - \ln P_{t,1})$;...; $r_{t,M}$ is the $(M-1)$th return after the opening of time t, and $r_{t,M} = 100(\ln P_{t,M-1} - \ln P_{t,M-2})$.

2.2. The SV-CJ Model. In the real financial market, since the impact of information and irrational behavior of investors, the volatility of return on asset is no longer continuous,while there are some jumps. Andersen et al. [31] have shown that the separation of the realized volatility into the continuous sample path variation and the discontinuous jump variation will enhance the accuracy to predict future volatility. Therefore, in order to further improve the accuracy to predict the future volatility of the model, we transform the logarithmic realized volatility $\ln(\mathrm{RV}_t)$ of model (2) to the logarithmic continuous sample path variation $\ln(C_t)$ and the discontinuous jump variation $\ln(J_t + 1)$.

When the realized volatility is divided into the continuous sample path variation and the discontinuous jump variation, we need to understand several important concepts. Please assume that return on assets is a continuous process; when we use the quadratic variation (quadratic variation, QV) to describe the total variation of the return volatility on financial assets and the integrated variation (IV) to depict the continuous part of the total variation, we can conclude that the difference between quadratic variation and integrated variation is the jump variation. In fact, the observed data are discrete, when they are used by the scholars to estimate the quadratic variation and integrated variation; the realized volatility and realized bipower variation (RBV) can be renamed. Barndorff-Nielsen and Shephard [27, 28] used the quadratic variation theory to separate realized volatility into the continuous sample path variation and the discontinuous jump variation. A mathematical description of this decomposition approach is given as follows.

Let $p_t = \ln(P_t)$ denote a logarithmic financial asset price at time t. The continuous-time jump diffusion process traditionally used in financial asset pricing is conveniently expressed in stochastic differential equation form as

$$dp_t = \mu_t dt + \sigma_t dW_t + \kappa_t dq_t, \quad 0 \le t \le T, \tag{4}$$

where μ_t is a continuous and locally bounded variation process. σ_t is a strictly positive stochastic volatility process with a sample path that is right continuous and has well-defined left limits (allowing for occasional jumps in volatility). W_t is a standard Brownian motion. κ_t refers to the size of the corresponding discrete jumps in the logarithmic price process. q_t represents Poisson counting process of λ_t, and λ_t is a time-varying intensity variable, so $P(dq_t = 1) = \lambda_t dt$.

For discrete prices from a continuous time process, the logarithmic return volatility at time t is a compound volatility including jump volatility rather than an unbiased estimator of integrated volatility. The log return rate from $t-1$ to t is quadratic variation:

$$\mathrm{QV}_t = [r, r]_t = \int_{t-1}^{t} \sigma_s^2 ds + \sum_{t-1<s\le t} \kappa_s^2, \tag{5}$$

where $\int_{t-1}^{t} \sigma_s^2 ds < \infty$ is called an integrated variation, representing the continuously altering part of variation of the return rate. Besides, $\sum_{t-1<s\le t} \kappa_s^2$ is called a jump volatility, representing the cumulative amount of jump variation of return rates in $[t-1, t]$.

Andersen and Bollerslev [24] argued that for quadratic variation, which cannot be observed directly, RV_t is a consistent estimator of QV_t, when using the discrete data to calculate quadratic variation with M converging to infinite

$$\mathrm{RV}_t \xrightarrow{M\to\infty} \mathrm{QV}_t = \int_{t-1}^{t} \sigma_s^2 \mathrm{ds} + \sum_{t-1<s\le t} \kappa_s^2. \tag{6}$$

Besides, integrated volatility can be estimated by realized bipower variation (Barndorff-Nielsen and Shephard [27, 28]), which is consistent estimator of the continuous sample path variation, with M converging to infinite

$$\mathrm{RBV}_t = z_1^{-2} \frac{M}{M-2} \sum_{j-3}^{M} \left|r_{t,j-2}\right| \left|r_{t,j}\right|, \tag{7}$$

where $z_1 = E(Z_t) = \sqrt{\pi/2}$; Z_t is a random variable subjecting to standardized normal distribution. $M/(M-2)$ is the correction of the sample size. According to Barndorff-Nielsen and Shephard [27, 28], when $M \to \infty$, the difference between RV_t and RBV_t is consistent estimator of the discontinuous jump variation:

$$\mathrm{RV}_t - \mathrm{RBV}_t \xrightarrow{M\to\infty} J_t. \tag{8}$$

However, the discontinuous jump variation mentioned above cannot guarantee the result to be nonnegative for finite-sized sample. Therefore, to ensure the nonnegativity of the discontinuous jump variation, this paper handles the discontinuous jump variation J_t as follows:

$$J_t = \max\left[\mathrm{RV}_t - \mathrm{RBV}_t, 0\right]. \tag{9}$$

In the computational process of the discontinuous jump variation, the arithmetic error varies with the frequency of sample selection. To improve the accuracy of the discontinuous jump variation, we use some estimator to test the level of significance of it. This paper applies Z_t (Barndorff-Nielsen and Shephard [27, 28]; Huang et al. [32]) to identify the factors of discontinuous jump variation:

$$Z_t = \frac{\left(\mathrm{RV}_t - \mathrm{RBV}_t\right) \mathrm{RV}_t^{-1}}{\sqrt{\left(\mu_1^{-4} + 2\mu_1^{-2} - 5\right)(1/M) \max\left(1, \mathrm{RTQ}_t/\mathrm{RBV}_t^2\right)}} \longrightarrow N(0,1), \tag{10}$$

where $\mu_1 = \sqrt{2/\pi}$ and RTQ_t is realized tri-power quarticity:

$$\mathrm{RTQ}_t = M\mu_{4/3}^{-3} \left(\frac{M}{M-4}\right) \sum_{j=4}^{M} \left|r_{t,j-4}\right|^{4/3} \left|r_{t,j-2}\right|^{4/3} \left|r_{t,j}\right|^{4/3},$$
$$\mu_{4/3} = E\left(\left|Z_T\right|^{4/3}\right) = 2^{\frac{2}{3}} \Gamma\left(\frac{7}{6}\right) \Gamma\left(\frac{1}{2}\right)^{-1}. \tag{11}$$

Because of the remarkable relativity between the result of RBV and the possibility of high-frequency sample, with the increase of sampling frequency, the estimator of RBV can not be converged to the integrated volatility under the impact of the market microstructure. Therefore, it is biased to exploit RBV as the estimator of the robust test of discontinuous jump variation and thus this paper chooses the new estimator MedRV_t (Andersen et al. [5]), which is

$$\mathrm{MedRV}_t = \frac{\pi}{6 - 4\sqrt{3} + \pi} \left(\frac{M}{M-2}\right) \times \sum_{i=2}^{M-1} \mathrm{Med}\left(\left|r_{t,i-1}\right| \left|r_{t,i}\right| \left|r_{t,i+1}\right|\right)^2. \tag{12}$$

Correspondingly, $\mathrm{RTQ}_{1,t}$ of statistics Z_t in (10) is also replaced by MedRTQ_t, which is proposed by Andersen et al. [6] and can be defined by

$$\mathrm{MedRTQ}_t = \frac{3\pi M}{9\pi + 72 + -52\sqrt{3}} \left(\frac{M}{M-2}\right) \times \sum_{i=2}^{M-1} \mathrm{Med}\left(\left|r_{t,i-1}\right|, \left|r_{t,i}\right|, \left|r_{t,i+1}\right|\right)^4. \tag{13}$$

In (7), we replace RBV_t, MedRTQ_t by MedRV_t after the calculation of statistic Z_t, under the significance level of $1-\alpha$; we can get the estimator of the discontinuous jump variation:

$$J_t = I\left(Z_t > \phi_\alpha\right)\left(\mathrm{RV}_t - \mathrm{MedRV}_t\right). \tag{14}$$

Correspondingly, the estimator of the continuous sample path variation is

$$C_t = I\left(Z_t \le \phi_\alpha\right)\mathrm{RV}_t + I\left(Z_t > \phi_\alpha\right)\mathrm{MedRV}_t. \tag{15}$$

In the actual computational process, we need to select the sound confidence level α. In this paper, based on previous researches (such as Andersen et al. [4, 31]; Huang and Tauchen [32], Huang et al. [33]), confidence level α is set at 0.99. In addition, through the above inspection of statistic Z_t and based on the quadratic variation theory, we can get the logarithmic volatility estimator of the continuous sample path variation C_t and the discontinuous jump variation J_t.

According to the decomposition method of realized volatility, we decompose RV_{t-1} into the continuous sample path variation C_{t-1} and the discontinuous jump variation J_{t-1}. Referenced to the research of Andersen et al. [31], we can, respectively, transform C_{t-1} and J_{t-1} to logarithmic form $\ln(C_{t-1})$ and $\ln(J_{t-1}+1)$. Then, adding $\ln(C_{t-1})$ and $\ln(J_{t-1}+1)$ as exogenous variables followed the way of SV-RV model into the volatility equation of SV model; we can get the SV-CJ model:

$$\begin{aligned} y_t &= \varepsilon_t e^{h_t/2}, \\ h_t &= \alpha + \beta h_{t-1} + \lambda \ln\left(C_{t-1}\right) + \theta \ln\left(J_{t-1}+1\right) + \eta_t. \end{aligned} \tag{16}$$

3. Estimation and Evaluation Method

3.1. Estimation Method. In the SV model, using maximum likelihood estimation method for parameter estimation is difficult, so there are many alternative methods produced, such as the moment method (Taylor, [15]), the pseudomaximum likelihood method (Ruiz [34]), the Markov Chain Monte Carlo method (MCMC; Jacquier et al. [35]), the generalized moment method (Andersen and Sørensen [36]), and the nonlinear filtering maximum likelihood method (Watanabe [37]). However, Jacquier [35], Kim et al. [18], and Durbin and Koopman [38] show that the MCMC method estimates in estimation performance are the best. Bauwens and Lubrano [39] pointed out that when using the MCMC method to estimate model parameters, using Gibbs sampling is better than importance sampling and Metropolis Hastings algorithm. The MCMC with the Gibbs sampling method can make full use of the advantages of computer simulation technology and get a large number of state samples. It uses elementary method to estimate model parameters and avoids the complicated calculation in E-M algorithm, so it improves the success rate of the estimate. Therefore, in this paper, using the MCMC method to estimate the parameters of SV, SV-RV, and SV-CJ model, the sampling method is the Gibbs sampling; the used software is the Open BUGS.

3.2. Evaluation Method

3.2.1. DIC Criterion. The SV, SV-RV, and SV-CJ model have many unknown variables, and the unknown variables are not independent of each other, and we are not able to determine the number of independent parameters in advance. In order to make a comparison among the goodness of SV, SV-RV, and SV-CJ model, we select the deviance information criterion (DIC) mentioned by Spiegelhalter et al. [40] to be the criterion of model evaluation. Mathematics form of DIC can be expressed as follows.

Dempster [41] considered that posterior distribution inspecting the classical deviation can employ Bayesian model, that is:

$$D(\omega) = -2\ln\left(L\left(y \mid \omega\right)\right) + 2\ln\left(g\left(y\right)\right), \tag{17}$$

where ω can represent $\alpha, \beta, \gamma, \lambda, \theta$, and logarithmic potential volatility sequences $\{\omega_t\}$. y refers to a list of data distribution, $y = (y_1, \ldots, y_n)$. $L(y \mid \omega)$ means likelihood function. $\ln(g(y))$ is the standardized form of independent data function. Bauwens and Lubrano [39] based on (17) develop into an important model selection criterion of DIC. DIC includes two parts, the specific expression as follows:

$$\mathrm{DIC} = \overline{D} + p_D. \tag{18}$$

In this formula, the first part $\overline{D}$ is minus twice the posterior mean log-likelihood; a natural choice for a suitable model is one that minimizes the DIC. The posterior mean deviation is defined as a parameter. Consider

$$\overline{D} = E_{\omega|y}\left[D(\omega)\right] = E_{\omega|y}\left[-2\ln\left(L\left(y\omega\right)\right)\right]. \tag{19}$$

The second part p_D is defined as the difference between the posterior mean of the deviance and the deviance evaluated at the posterior mean or mode of the relevant parameters. Consider

$$\begin{aligned} p_D = \overline{D} - D(\overline{\omega}) &= E_{\omega|y}\left[D(\omega)\right] - D\left(E_{\omega|y}(\omega)\right) \\ &= E_{\omega|y}\left[-2\ln\left(L\left(y \mid \omega\right)\right)\right] + 2\ln\left(L\left(y\overline{\omega}\right)\right). \end{aligned} \tag{20}$$

$\overline{\omega}$ is the posterior mean of ω. $L(y \mid \overline{\omega})$ is the known parameters and logarithmic potential fluctuations of the likelihood function of average cases.

AIC is similar to AIC or BIC; the smaller the value of DIC, the better the model. But if we consider the model for the complexity of the data fitting ability, DIC has better comparative superiority and inferiority complex model than the AIC and BIC. In this paper, the SV, SV-RV, and SV-CJ model are complicated, so using DIC is more suitable.

3.2.2. Loss Functions. In this paper, we use the loss functions and SPA test with the "Bootstrap" to analyze the predictive accuracy of SV, SV-RV, and SV-CJ model both in sample and out of sample. According to Bollerslev et al. [42] and Hansen and Lunde [43], we choose six common loss functions. They are the mean absolute error (MAE, denoted by L_1), the heteroskedastic adjusted mean absolute error (HMAE, denoted by L_2), the mean squared error (MSE, denoted by L_3), the heteroskedastic adjusted mean squared error (HMSE, denoted by L_4), QLIKE (denoted by L_5), and R^2LOG (We can refer the details of loss functions QLIKE and R2LOG to Bollerslev et al. [43] and Hansen and Lunde [43]) (denoted by L_6). If the values of the six functions are smaller,that means the corresponding predictive accuracy of volatility models are stronger. The computation expression of MAE, HMAE, MSE, HMSE, QLIKE, and R^2LOG is as formulas (21). Because the volatility in the stock market cannot be observed, scholars (such as Koopman et al. [23]; Corsi [1]) often use RV_t to replace the real volatility at time t; therefore, we also use RV_t to replace the real volatility in stock market. Consider

$$\begin{aligned}
L_1&: \mathrm{MAE} = \frac{1}{n}\sum_{t=1}^{n}\left|\sigma_t^2 - \widehat{\sigma}_t^2\right| \\
L_2&: \mathrm{HMAE} = \frac{1}{n}\sum_{t=1}^{n}\left|\frac{\sigma_t^2 - \widehat{\sigma}_t^2}{\sigma_t^2}\right| \\
L_3&: \mathrm{MSE} = \frac{1}{n}\sum_{t=1}^{n}\left(\sigma_t^2 - \widehat{\sigma}_t^2\right)^2 \\
L_4&: \mathrm{HMSE} = \frac{1}{n}\sum_{t=1}^{n}\left[\frac{\sigma_t^2 - \widehat{\sigma}_t^2}{\sigma_t^2}\right]^2 \\
L_5&: \mathrm{QLIKE} = \frac{1}{n}\sum_{t=1}^{n}\left[\ln\left(\widehat{\sigma}_t^2\right) + \frac{\sigma_t^2}{\widehat{\sigma}_t^2}\right] \\
L_6&: R^2\mathrm{LOG} = \frac{1}{n}\sum_{t=1}^{n}\left[\ln\left(\frac{\sigma_t^2}{\widehat{\sigma}_t^2}\right)\right]^2,
\end{aligned} \tag{21}$$

where n is the number of predicted samples. σ_t^2 is real volatility, that is, RV_t. $\widehat{\sigma}_t^2$ represents the prediction value of volatility obtained by the SV, SV-RV, or SV-CJ model.

3.2.3. SPA Test. On the basis of the loss functions, Hansen [29] proposed a superior predictive ability (SPA). Then, there are many researchers (such as Hansen and Lunde [43], Martin et al. [44], Wang and Wu [45], and Hung et al. [46]) who used this method to compare prediction accuracy of the models. Hansen [29] found that, due to SPA test with "Bootstrap," it has better model discriminated ability than RC test mentioned in White [47], and the SPA test has better robustness.

The SPA test can be simply described as follows. Firstly, we need to compare $J + 1$ types of volatility models, denoted by M_k, $k = 0, 1, \ldots, J$. Every volatility model M_k predict the future of volatility for a day as $\widehat{\sigma}_{k,t}^2$, $t = 0, 1, \ldots, n$. For each prediction, formula (21) can be calculated, as defined by the six loss functions, denoted by $L_{m,k,t}$, $m = 1, 2, \ldots, 6$. Using M_0 to be the inspection benchmark model of the SPA, M_k $(k = 1, 2, \ldots, J)$ is compared model. So we can calculate that M_0 are relative to compared model; the "relative loss function values" can be expressed as

$$\begin{gathered}
X_{k,t} = L_{m,0,t} - L_{m,k,t}; \\
m = 1, 2, \ldots, 6;\ k = 1, 2, \ldots, J;\ t = 1, 2, \ldots, n.
\end{gathered} \tag{22}$$

In order to determine whether there is a better prediction model than M_0 in M_k $(k = 1, 2, \ldots, J)$, we define a null hypothesis "M_0 is the best prediction model, compared with M_k $(k = 1, 2, \ldots, J)$." This null hypothesis can be expressed in mathematical expressions as follows:

$$\max \lambda_k = E\left(X_{k,t}\right), \quad k = 1, 2, \ldots, J. \tag{23}$$

Hansen [29] proved that the hypothesis test statistics are

$$\begin{gathered}
T = \max \frac{\sqrt{n}\overline{X}_{k,t}}{\widehat{\omega}_{kk}}, \quad k = 1, 2, \ldots, J, \\
\text{in that} \quad \overline{X}_{k,t} = n^{-1}\sum_{t=1}^{t=n} X_{k,t}, \quad \widehat{\omega}_{kk} = \mathrm{var}\left(\sqrt{n}\overline{X}_{k,t}\right).
\end{gathered} \tag{24}$$

In order to get formula (24) of the distribution of the T statistic and P value of Hansen [29] using "Bootstrap" to obtain the value is recommended. Firstly, we need to get a new sample $X_{k,t}$ of length n. To get a new sample, we need to randomly take a new subsample from the original collection $\{X_{k,t}\}$, and the length of the subsample from a obey averages q geometric distribution of random numbers, and at the same time control the combination of these sub sample length required for n.

Repeating the Bootstrap process B, B $X_{k,t}$ of length n can be obtained; that is, $X_{k,t}^i$, $i = 1, 2, \ldots, B$. In this paper, $q = 0.5$ and $B = 5000$ times are used as the Bootstrap process control parameters. So each Bootstrap sample mean can be expressed as

$$\overline{X}_k^i = n^{-1}\sum_{t=1}^{t=n} X_{k,t}^i, \quad i = 1, 2, \ldots, B. \tag{25}$$

The estimator of B Bootstrap samples mean variance can be expressed as

$$\widehat{\omega}_{kk} = B^{-1}\sum_{i=1}^{i=B}\left(\overline{X}_k^i - \overline{\overline{X}}_k\right)^2, \quad \overline{\overline{X}}_k = B^{-1}\sum_{i=1}^{i=B}\overline{X}_k^i. \tag{26}$$

Define $\overline{Z}_k^i$ as

$$\begin{gathered}
\overline{Z}_k^i = \left(\overline{X}_k^i - \overline{\overline{X}}_k\right) \times I\left(\overline{\overline{X}}_k > -A_k\right), \\
\text{in that,} \quad A_k = \frac{1}{4}n^{-1/4}\widehat{\omega}_{kk}.
\end{gathered} \tag{27}$$

$I\{\cdot\}$ is an indicator function; as the conditions of the $\{\cdot\}$, $I\{\cdot\}$ is 1, otherwise is 0. In the end, we can get the new T^i statistical magnitude:

$$T^i = \max \frac{\sqrt{n}\overline{Z}_k^i}{\widehat{\omega}_{kk}}, \quad i = 1, 2, \ldots, B. \tag{28}$$

Hansen [29] showed that under the null hypothesis in (23), formula (28) T^i statistical magnitude converges to formula (24), as defined by the T statistic. Therefore, the P values can be obtained directly from the type

$$P = B^{-1}\sum_{i=1}^{i=B} I\left\{T^i > T\right\}. \quad (29)$$

When comparing the quality prediction model and the test of SPA (the closer to 1), if the P value is greater, we cannot refuse the null hypothesis of formula (27) any more. That is to say, compared with other models, the accuracy of the baseline model is much higher.

4. Empirical Evidence

4.1. Data and Summary Statistics. This paper uses the CSI 300 index in China's stock market to empirical evidence. The data derived from the WIND financial database. The time span of samples is April 20, 2007, to April 20, 2012, and is a total of 1199 days. In the calculation of realized volatility, the daily sample data extracting frequency greatly affects the result of the study. On the one hand, the lower sampling frequency cannot describe the wave information well. On the other hand, the higher sampling frequency will produce micronoise that influenced the results. Therefore, this paper, based on the research of previous scholars (such as Andersen et al. [4, 31] and Huang and Tauchen [32], Huang et al. [33]) and the influence of both hands, uses the CSI 300 index of 5 minutes high frequency data. After eliminating the trading time related data and supplementing the missing data using moving average interpolation method, there are 58751 data, that is, 49 data everyday. (including 1 overnight trading data and 48 intraday trading data). In this paper, we need to use the variables; the rate of return R_t, the logarithmic realized volatility $\ln(\mathrm{RV}_t)$, the logarithmic continuous sample path variation $\ln(C_t)$, and the logarithmic discontinuous jump variation $\ln(J_t + 1)$ are all obtained by Matlab 2013a or Excel 2007.

Table 1 is descriptive statistics results of R_t, $\ln(\mathrm{RV}_t)$, $\ln(C_t)$, and $\ln(J_t + 1)$. From Table 1, we can find that $\ln(\mathrm{RV}_t)$ sequence shows the phenomenon of "High Kurtosis and Fat Tail" and does not obey the normal distribution; this shows that China's stock market volatility is large. In addition, the unit root test (ADF test) shows that every sequence in the 99% confidence interval significantly declined to unit root of null hypothesis, so each sequence is stationary, and we can further analyze the models.

4.2. Parameter Estimation. In Section 2, we introduce Bayesian estimation results of the SV, SV-RV, and SV-CJ model using the MCMC methods through the OpenBUGS software. In order to ensure the convergence of the estimated parameters, 50000 iterations are performed on each parameter in the process of Gibbs sampling; by observing the orbit of the parameters iterations and the autocorrelation function, we found that after 10,000 iterations, the iterative process has converged. Hence, we anneal by using the first 10,000 samples and estimate the model by using the last 40,000 samples in this paper.

Table 2 lists the results of the Bayesian parameter estimation of the SV, SV-RV, and SV-CJ model, including the mean, standard deviation, MC error (the error of Monte Carlo simulation value), 95% confidence interval for the posterior, the median, and the value of the deviation information criterion (DIC) of the parameter estimation. Firstly, we analyze the results of Bayesian estimation of the SV and SV-RV model. The estimation value of the parameter β is close to 1, explaining that there is a strong persistence and autocorrelation with the return volatility of China's stock market, in accord with mature capital markets (such as the US and UK) and emerging capital markets (such as South Korea and New Zealand). If the standard deviation and MC error of the parameter are small, the accuracy of the parameter estimation is much higher. In the SV-RV model, estimation of parameter γ is positive; its standard deviation and MC errors are relatively small and 95% confidence interval for the posterior does not contain the value 0, which proves that the prior logarithmic realized volatility $\ln(\mathrm{RV}_{t-1})$ has a significant impact on the current volatility. $\ln(\mathrm{RV}_{t-1})$ contains certain volatility forecast information. Comparing the DIC of SV model and SV-RV model, we find that the DIC of SV-RV model is smaller than that of SV model, which shows that the SV-RV model has a better measuring accuracy to the volatility and agrees with the research results of Koopman et al. [23] and Jacquier and Miller [26].

We focus on the estimation results of SV-CJ model; the coefficient λ of the logarithmic continuous sample path variation $\ln(C_{t-1})$ in the model is positive; its standard deviation and MC errors are relatively small and 95% confidence interval for the posterior does not contain the value 0, which proves that the prior logarithmic continuous sample path variation $\ln(C_{t-1})$ has a certain prediction on the current volatility. However, the coefficient θ of the logarithmic discontinuous jump variation $\ln(J_{t-1} + 1)$ in the model is comparatively large and 95% confidence interval for the posterior contains the value 0, proving that the previous logarithmic discontinuous jump variation $\ln(J_{t-1} + 1)$ has little effect on the current volatility. In addition, comparing the DIC of the models, we can find that the DIC of SV-CJ model is smaller than that of the SV-RV model, which shows that the SV-CJ model has a better measuring accuracy to the volatility and shows that adding the decomposition of the logarithmic realized volatility to the volatility equation SV model can improve the measurement capability to the return volatility. Therefore, when measuring the return volatility, it is more reasonable to use the SV-CJ, SV and SV-RV model.

4.3. Forecasting

4.3.1. In-Sample Forecasts. Figure 1 contains a real volatility sequence and three in-sample forecast volatility sequences that are obtained by the SV, SV-RV, and SV-CJ model. To comparatively analyze the predictive accuracy for future volatility of the SV, SV-RV, and SV-CJ model, we use the loss functions and SPA test to compare the predictive accuracy of

Table 1: Descriptive statistics for each variable.

	Mean	Std. dev.	Skewness	Kurtosis	Jarque-Bera	ADF-t statistic
R_t	−0.0152	2.1141	−0.2647	4.9345	200.95***	−32.901***
$\ln(RV_t)$	0.9600	0.9323	0.5180	3.2163	55.961***	−4.9183***
$\ln(C_t)$	0.7650	0.8992	0.3525	2.8382	26.138***	−5.3556***
$\ln(J_t + 1)$	0.2825	0.6209	3.0445	14.085	7990.6***	−16.266***

*** Indicates significance at the 1% level.

Table 2: The estimation results of the SV, SV-RV, and SV-CJ model.

Model	Parameter	Mean	Standard deviation	MC error	2.5% quantile	Median	97.5% quantile	DIC
SV	α	0.0377	0.0178	0.0011	0.0136	0.0347	0.0798	4961.0
	β	0.9694	0.0141	0.0009	0.9356	0.9860	0.9894	
SV-RV	α	0.2053	0.0594	0.0037	0.1085	0.1982	0.3381	4951.0
	β	0.6063	0.0886	0.0057	0.4152	0.6175	0.7541	
	γ	0.2870	0.0587	0.0037	0.1855	0.2823	0.4132	
SV-CJ	α	0.2927	0.06966	0.0046	0.1665	0.2865	0.4581	4938.0
	β	0.5206	0.08546	0.0059	0.3548	0.5149	0.7192	
	λ	0.3566	0.05807	0.0038	0.2208	0.3623	0.4602	
	θ	0.0389	0.04991	0.0030	−0.06129	0.03955	0.1409	

these three models in this paper. Table 3 lists the statistical results of the loss functions (the MAE, HMAE, MSE, HMSE, QLIKE, and R^2LOG) about the SV, SV-RV, and SV-CJ model in the in-sample forecasts. Table 4 lists the SPA test results of SV, SV-RV, and SV-CJ model in the sample in the in-sample forecasts. In Table 3, comparing the size of the loss functions, we find that apart from one point that the QLIKE of SV-RV model is slightly smaller than that of SV-CJ model, the other loss functions of SV model are greater than those of SV-RV model, and the loss functions of SV-RV model are greater than the loss functions of SV-CJ model. In Table 4, the first column represents the baseline model M_0. Numerical values in the table are the P value of SPA test; the larger the P value, the stronger the predictive accuracy of the baseline model M_0, compared with the other two comparison models. In this table, there are four P values of SPA test treating the SV-CJ model as a baseline model larger than those of SV-RV model. Similarly, there are four P values of SPA test treating SV-RV model as a baseline model larger than those of SV model.

Analyzing the results of the loss functions in Table 3 and the results of SPA test in Table 4, we can get the following conclusions. The in-sample forecast accuracy of SV model for return volatility is weaker than that of SV-RV model, and the in-sample forecast ability of SV or SV-RV model for return volatility is weaker than that of SV-CJ model.

4.3.2. Out-of-Sample Forecasts. Compared with the in-sample predictive accuracy of the model, we are more concerned with the out-of-sample forecasting accuracy, because the out-of-sample forecasting is more meaningful to financial practical issues like the financial risk management, financial asset pricing, financial derivatives pricing, and so on. In order to effectively evaluate the out-of-sample forecasting accuracy

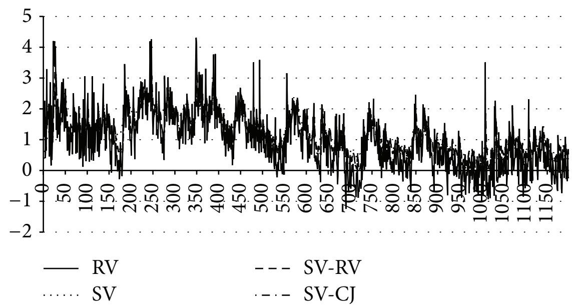

Figure 1: Comparison of the in-sample forecasting performance of the SV, SV-RV, and SV-CJ model. In the figure, RV represents the true volatility; SV, SV-RV, and SV-CJ represent the forecast volatility of the SV, SV-RV, and SV-CJ model, respectively.

of the models, we use the rolling time windows method to test the volatility forecasting accuracy of the SV, SV-RV, and SV-CJ model. We select 999 samples as the fixed time windows and the last 200 samples (May 31, 2011–April 20, 2012) as the prediction and evaluation interval. Figure 2 contains a real volatility sequence and three out-of-sample forecast volatility sequences that are obtained by the SV, SV-RV, and SV-CJ model. The analysis approach is consistent with the in-sample forecasting part, still using the loss functions and SPA test to compare the predicting accuracy of each model. The results are shown in Tables 5 and 6. In Table 5, comparing the loss functions, in these three models, apart from one point that the MSE of SV-CJ model is slightly larger than that of SV Model, the other loss functions of SV-CJ are smaller than those of SV and SV-RV model, and the loss functions of SV-RV model are greater than those of SV-CJ model. In addition, comparing the loss functions about the SV and SV-RV models, the loss

Table 3: The loss functions of in-sample forecasts.

	MAE	HMAE	MSE	HMSE	QLIKE	R^2LOG
SV	2.3879	0.7237	1.0140	34.830	2.2034	0.4572
SV-RV	2.3197	0.7104	0.9862	32.099	**2.1941**	0.4377
SV-CJ	**2.2951**	**0.6736**	**0.8440**	**31.167**	2.1983	**0.4203**

The bold part is the minimum value of each loss function.

Table 4: The SPA test results of in-sample forecasts.

	MAE	HMAE	MSE	HMSE	QLIKE	R^2LOG
SV	0.0780	0.2056	0.1330	0.0538	0.1882	**0.7944**
SV-RV	0.0408	**0.8562**	0.1382	0.0648	0.3784	0.5798
SV-CJ	**0.5816**	0.5456	**0.6730**	**0.6412**	**0.7220**	0.2504

Numerical values in the table represent P value of SPA test obtained by 5000 Bootstrap simulation; the larger the P value, the stronger the in-sample predictive accuracy of the baseline model, compared with the other two comparison models. The bold part is the maximum P value of each model's SPA test.

Table 5: The loss functions of out-of-sample forecasts.

	MAE	HMAE	MSE	HMSE	QLIKE	R^2LOG
SV	1.3145	1.9953	1.0463	**7.0803**	1.4152	0.6488
SV-RV	1.4186	3.1494	1.1515	8.2392	1.4127	0.7103
SV-CJ	**1.2636**	**1.4354**	**0.8932**	7.6884	**1.3878**	**0.5871**

The bold part is the minimum value of each loss function.

Table 6: The SPA test results of out-of-sample forecasts.

	MAE	HMAE	MSE	HMSE	QLIKE	R^2LOG
SV	0.2324	0.0300	0.0256	**0.8558**	0.0616	0.1048
SV-RV	0.0262	0.0106	0.0248	0.0386	0.2538	0.0092
SV-CJ	**0.7720**	**0.6616**	**0.7970**	0.0208	**0.8862**	**0.5442**

Numerical values in the table represent the P values of SPA test obtained by 5000 Bootstrap simulation; the larger the P value, the stronger out-of-sample predictive accuracy of the baseline model, compared with the other two comparison models. The bold part is the maximum P value of each model's SPA test.

functions of SV model are smaller than those of the SV-RV model apart from the HMSE value. In Table 6, there are five P values of SPA test treating SV-CJ model as a baseline model larger than those of SV-RV model and five P values of SPA test treating SV model as a baseline model larger than those of SV-RV model.

Analyzing the results of loss functions in Table 5 and the results of SPA test in Table 6, we can get the following conclusions. The out-of-sample forecasting accuracy of SV-CJ model for return volatility is stronger than that of SV or SV-RV model. The out-of-sample forecast ability of SV model return volatility is stronger than that of SV-RV model.

All in all, by analyzing Sections 4.3.1 and 4.3.2, we know that the predictive accuracy for future volatility of SV-CJ model is the strongest in the above three volatility models. Therefore, adding the logarithmic realized volatility $\ln(\mathrm{RV}_{t-1})$ to the SV volatility model and decomposing $\ln(\mathrm{RV}_{t-1})$ into the logarithmic continuous sample path variation $\ln(C_{t-1})$ and the logarithmic discontinuous jump variation $\ln(J_{t-1}+1)$, we can improve the model's performance to predict future volatility. Therefore, this decomposition is meaningful.

5. Conclusion

In this paper, we first construct the SV-CJ model based on SV-RV model. Then, we estimate the parameters of SV, SV-RV, and SV-CJ models through MCMC methods, using the 5 minutes frequency data in CSI 300 Index of China's stock market. Finally, using the loss functions and SPA test analyzes the return volatility forecasting accuracy of each model both in-sample and out-of-sample.

According to the parameter estimation results of the models, we find that the measuring accuracy for Chinese stock market volatility of SV-CJ model is significantly stronger than that of SV or SV-RV model. The prior logarithmic realized volatility and the prior logarithmic continuous sample path variation contain much predictive information on future volatility while the logarithmic discontinuous jump variation contains little predictive information. Moreover, comparative analysis of the predictive accuracy about the three models indicates that the in-sample forecasting accuracy for return volatility of SV-RV model is stronger than that of SV model. This conclusion may be different from the results of Koopman et al. [23], Jacquier and Miller [26]. It

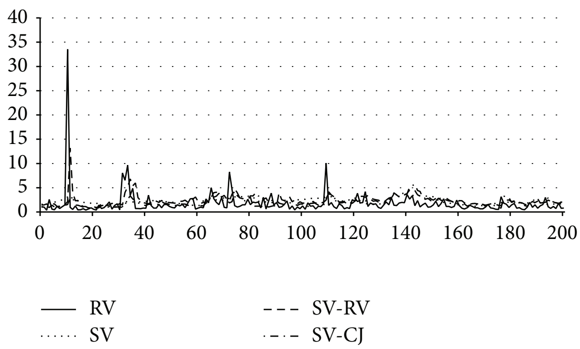

Figure 2: Comparison of the out-of-sample forecasting performance of the SV, SV-RV, and SV-CJ model. In the figure, RV represents the true volatility; SV, SV-RV, and SV-CJ represent the forecast volatility of the SV, SV-RV, and SV-CJ model, respectively.

may be due to the inconsistency with the model predictive accuracy of future volatility in different markets. In the Chinese stock market, the performance of SV-RV model added RV as the exogenous variables to predict the stock volatility are not significantly stronger than the SV model. However, the volatility forecasting accuracy of SV-CJ model is significantly stronger than the other two models, which shows that using SV-CJ model to measure and predict the volatility is more reasonable in financial practical issues like the financial risk management, financial asset pricing, and financial derivatives pricing. While the SV-CJ model has a better accuracy on volatility measuring and forecasting, it is still necessary to improve the measuring precision and forecasting precision of the volatility model. Therefore, we will further focus on the study to improve the measuring accuracy and forecasting accuracy of the volatility models on the basis of SV-CJ model.

Conflict of Interests

The authors declare that there is no conflict of interests regarding the publication of this paper.

Acknowledgment

This work was supported in part by the Natural Science Foundation of China (no. 71171024, no. 71371195, and no. 71221061).

References

[1] F. Corsi, "A simple approximate long-memory model of realized volatility," *Journal of Financial Econometrics*, vol. 7, no. 2, pp. 174–196, 2009.

[2] F. Wen and X. Yang, "Skewness of return distribution and coefficient of risk premium," *Journal of Systems Science & Complexity*, vol. 22, no. 3, pp. 360–371, 2009.

[3] J. Liu, C. Ma, and F. Wen, "An Actuarial approach to option pricing under O-U process and stochastic interest rates," in *Proceedings of the International Joint Conference on Computational Sciences and Optimization (CSO '09)*, pp. 549–553, IEEE, Sanya, China, April 2009.

[4] T. G. Andersen, T. Bollerslev, and X. Huang, "A reduced form framework for modeling volatility of speculative prices based on realized variation measures," *Journal of Econometrics*, vol. 160, no. 1, pp. 176–189, 2011.

[5] T. G. Andersen, D. Dobrev, and E. Schaumburg, "Jump-robust volatility estimation using nearest neighbor truncation," *Journal of Econometrics*, vol. 169, no. 1, pp. 75–93, 2012.

[6] Z. Dai, D. Li, and F. Wen, "Robust conditional value-at-risk optimization for asymmetrically distributed asset returns," *Pacific Journal of Optimization*, vol. 8, no. 3, pp. 429–445, 2012.

[7] F. Wen, Z. Li, C. Xie, and D. Shaw, "Study on the fractal and chaotic features of the Shanghai composite index," *Fractals*, vol. 20, no. 2, pp. 133–140, 2012.

[8] T. Bollerslev, D. Osterrieder, N. Sizova, and G. Tauchen, "Risk and return: long-run relations, fractional cointegration, and return predictability," *Journal of Financial Economics*, vol. 108, no. 2, pp. 409–424, 2013.

[9] T. Bollerslev, V. Todorov, and S. Z. Li, "Jump tails, extreme dependencies, and the distribution of stock returns," *Journal of Econometrics*, vol. 172, no. 2, pp. 307–324, 2013.

[10] J. Liu, L. Yan, and C. Ma, "Pricing options and convertible bonds based on an actuarial approach," *Mathematical Problems in Engineering*, vol. 2013, Article ID 676148, 9 pages, 2013.

[11] J. Liu, M. Tao, C. Ma, and F. Wen, "Utility indifference pricing of convertible bonds," *International Journal of Information Technology & Decision Making*, vol. 13, no. 2, pp. 429–444, 2014.

[12] J. Liu, J. Xiao, L. Yan, and F. Wen, "Valuing catastrophe bonds involving credit risks," *Mathematical Problems in Engineering*, vol. 2014, Article ID 563086, 6 pages, 2014.

[13] R. F. Engle, "Autoregressive conditional heteroscedasticity with estimates of the variance of United Kingdom inflation," *Econometrica*, vol. 50, no. 4, pp. 987–1007, 1982.

[14] T. Bollerslev, "Generalized autoregressive conditional heteroskedasticity," *Journal of Econometrics*, vol. 31, no. 3, pp. 307–327, 1986.

[15] J. S. Taylor, *Modeling Financial Time Series*, John Wiley & Sons, Chichester, UK, 1986.

[16] J. Danielsson, "Stochastic volatility in asset prices estimation with simulated maximum likelihood," *Journal of Econometrics*, vol. 64, no. 1-2, pp. 375–400, 1994.

[17] F. C. Wang, L. X. Jiang, and G. Li, "Estimating volatility of Chinese stock market by stochastic volatility model," *Journal of Management Sciences in China*, vol. 4, pp. 63–72, 2003.

[18] S. Kim, N. Shephard, and S. Chib, "Stochastic volatility: likelihood inference and comparison with ARCH models," *Review of Economic Studies*, vol. 65, no. 3, pp. 361–393, 1998.

[19] J. Yu, "Forecasting volatility in the New Zealand stock market," *Applied Financial Economics*, vol. 12, no. 3, pp. 193–202, 2002.

[20] P. Sadorsky, "A comparison of some alternative volatility forecasting models for risk management," in *Proceedings of the 2nd IASTED International Conference: Financial Engineering and Applications*, 2004.

[21] C. Pederzoli, "Stochastic volatility and GARCH: a comparison based on UK stock data," *The European Journal of Finance*, vol. 12, no. 1, pp. 41–59, 2006.

[22] Y. Wei, "Forecasting volatility of fuel oil futures in China: GARCH-type, SV or realized volatility models?" *Physica A: Statistical Mechanics and its Applications*, vol. 391, no. 22, pp. 5546–5556, 2012.

[23] S. J. Koopman, B. Jungbacker, and E. Hol, "Forecasting daily variability of the S&P 100 stock index using historical, realised and implied volatility measurements," *Journal of Empirical Finance*, vol. 12, no. 3, pp. 445–475, 2005.

[24] T. G. Andersen and T. Bollerslev, "Answering the critics: yes, ARCH models do provide good volatility forecasts," *International Economic Review*, vol. 4, pp. 885–905, 1998.

[25] J. Geweke, G. Koop, and H. Dijk, *The Oxford Handbook of Bayesian Econometrics*, Oxford University Press, 2011.

[26] E. Jacquier and S. Miller, "The information content of realized volatility," Working Paper, HEC Montreal, 2013.

[27] O. E. Barndorff-Nielsen and N. Shephard, "Power and bipower variation with stochastic volatility and jumps," *Journal of Financial Econometrics*, vol. 2, pp. 1–37, 2004.

[28] O. E. Barndorff-Nielsen and N. Shephard, "Econometrics of testing for jumps in financial economics using bipower variation," *Journal of Financial Econometrics*, vol. 4, pp. 1–30, 2006.

[29] P. R. Hansen, "A test for superior predictive ability," *Journal of Business & Economic Statistics*, vol. 23, no. 4, pp. 365–380, 2005.

[30] M. Martens, "Measuring and forecasting S&P 500 index-futures volatility using high-frequency data," *Journal of Futures Markets*, vol. 22, no. 6, pp. 497–518, 2002.

[31] T. G. Andersen, T. Bollerslev, and F. X. Diebold, "Roughing it up: including jump components in the measurement, modeling, and forecasting of return volatility," *The Review of Economics and Statistics*, vol. 89, no. 4, pp. 701–720, 2007.

[32] X. Huang and G. Tauchen, "The relative contribution of jumps to total price variance," *Journal of Financial Econometrics*, vol. 3, no. 4, pp. 456–499, 2005.

[33] C. Huang, X. Gong, X. Chen, and F. Wen, "Measuring and forecasting volatility in Chinese stock market using HAR-CJ-M model," *Abstract and Applied Analysis*, vol. 2013, Article ID 143194, 13 pages, 2013.

[34] E. Ruiz, "Quasi-maximum likelihood estimation of stochastic volatility models," *Journal of Econometrics*, vol. 63, no. 1, pp. 289–306, 1994.

[35] E. Jacquier, N. G. Polson, and P. E. Rossi, "Bayesian analysis of stochastic volatility models," *Journal of Business and Economic Statistics*, vol. 12, no. 4, pp. 371–417, 1994.

[36] T. G. Andersen and B. E. Sørensen, "GMM estimation of a stochastic volatility model: a Monte Carlo study," *Journal of Business and Economic Statistics*, vol. 14, no. 3, pp. 328–352, 1996.

[37] T. Watanabe, "A non-linear filtering approach to stochastic volatility models with an application to daily stock returns," *Journal of Applied Econometrics*, vol. 14, no. 2, pp. 101–121, 1999.

[38] J. Durbin and S. J. Koopman, *Time Series Analysis by State Space Methods*, vol. 38, Oxford University Press, Oxford, UK, 2nd edition, 2012.

[39] L. Bauwens and M. Lubrano, "Bayesian inference on GARCH models using Gibbs sampler," *Econometrics Journal*, vol. 1, pp. 23–46, 1998.

[40] D. J. Spiegelhalter, N. G. Best, B. P. Carlin, and A. van der Linde, "Bayesian measures of model complexity and fit," *Journal of the Royal Statistical Society B*, vol. 64, no. 4, pp. 583–639, 2002.

[41] A. P. Dempster, "The direct use of likelihood for significance testing," in *Proceedings of Conference on Foundational Questions in Statistical Inference*, pp. 335–352, Department of Theoretical Statistics, University of Aarhus, 1974.

[42] T. Bollerslev, R. F. Engle, and D. Nelson, "ARCH models," in *Handbook of Econometrics*, D. L. McFadden, Ed., vol. 4, pp. 2961–3038, Elsevier Science B.V., Amsterdam, The Netherlands, 1994.

[43] P. R. Hansen and A. Lunde, "A forecast comparison of volatility models: does anything beat a GARCH (1, 1)?" *Journal of Applied Econometrics*, vol. 20, no. 7, pp. 873–889, 2005.

[44] G. M. Martin, A. Reidy, and J. Wright, "Does the option market produce superior forecasts of noise-corrected volatility measures?" *Journal of Applied Econometrics*, vol. 24, no. 1, pp. 77–104, 2009.

[45] Y. Wang and C. Wu, "Forecasting energy market volatility using GARCH models: can multivariate models beat univariate models?" *Energy Economics*, vol. 34, no. 6, pp. 2167–2181, 2012.

[46] J. C. Hung, T. W. Lou, Y. H. Wang, and J. Lee, "Evaluating and improving GARCH-based volatility forecasts with range-based estimators," *Applied Economics*, vol. 45, no. 28, pp. 4041–4049, 2013.

[47] H. White, "A reality check for data snooping," *Econometrica*, vol. 68, no. 5, pp. 1097–1126, 2000.

Hindawi Publishing Corporation
Discrete Dynamics in Nature and Society
Volume 2014, Article ID 232516, 11 pages
http://dx.doi.org/10.1155/2014/232516

Research Article

Incorporating Overconfidence into Real Option Decision-Making Model of Metal Mineral Resources Mining Project

Jian-bai Huang,[1,2] Na Tan,[1,2] and Mei-rui Zhong[1,2]

[1] *School of Business, Central South University, Changsha, Hunan 410083, China*
[2] *Institute of Metal Resources Strategy, Changsha, Hunan 410083, China*

Correspondence should be addressed to Mei-rui Zhong; zmr726@163.com

Received 14 April 2014; Revised 18 June 2014; Accepted 18 June 2014; Published 3 July 2014

Academic Editor: Fenghua Wen

As for uncertainties and decision-makers' overconfidence psychological bias, overconfidence has been incorporated into real option decision-making model of metal mineral resources mining to estimate its effect on decision-making of the project and thus a behavioral real option decision-making model of metal mineral resources mining based on overconfidence has been established. Furthermore, numerical simulation and sensitivity analysis have been conducted to verify the practicality of the model. Results show that model in this paper has greatly changed trigger value and option value of mineral resources mining project compared with traditional real option model, thus greatly changing optimal decision results. Incorporating overconfidence into real option decision-making model of metal mineral resources development is a crucial extension of project evaluation theory.

1. Introduction

Metal mineral resources are essential base material and important strategic supplies in economic development. Metal mineral resources mining project bears large budget, long construction cycle, and high risks and it is influenced by external factors including metal mineral market supply and demand, technological progress and policies, and internal factors including decision-maker's working capacity and psychological bias, which could take effect on evaluation of metal mineral resources mining project [1]. This makes it difficult to evaluate metal mineral resources mining project by traditional DCF method accurately. Recently, with considerable researches in this field, real option approach (ROA), which is firstly brought up by Myers and Turnbull [2] and Ross [3], has been generally accepted as an appropriate method to help make decisions of metal mineral resources mining under uncertain circumstances. Brennan and Schwartz [4] initiated ROA into copper mining project, Smith and Nau [5] and Smith and McCardle [6] analyzed hydrocarbon resource development project by using dynamic programming and option pricing. Lately, scholars tend to investigate relationship between investment decision making and uncertain factors, operation cost uncertainty [7], production uncertainty [8], full-cost uncertainty [9], and exchange rate uncertainty [10, 11], have become vital factors which have expanded ROA model.

In the literature, ROA is increasingly applied to study metal mineral resources mining by scholars, but there still exists a widespread problem. In real option theory, scholars generally presume investment decision-makers are completely rational; ROA model only considers external uncertainties and ignores internal uncertainties factors including overconfidence, risk preference, and herd effect existing in economic activities [12, 13]. On the premise of investors' limited rationalities, real market scenes can hardly be simulated through experiment and results of investors' transaction accounts are often not representative [14]. Therefore, incorporating heterogeneous beliefs into real option model is of great significance, amongst which overconfidence is a prior. In fact, a great number of behavioral finance literatures have demonstrated that overconfidence bias of decision-makers takes great effect on investment decisions. Cooper et al. [15] and Russo and Schoemaker [16] proved that both entrepreneurs and managers showed overconfidence; Odean [17] made a comparison between investment decisions made by rational and overconfident managers and it turned out that overconfident managers tended to accept earlier investment; Hao et al. [18] through empirical approach analyzed relationship between overconfident CEO and investment. Results showed that overconfident CEO was more likely to conduct inefficient allocation of overinvestment. In incorporating overconfidence to real option theory, Hu and Ye [19] concentrated on uncertainties caused by the managers and revised the "approximate twin securities" approach, thus improving traditional real option evaluation. Throughout the abovementioned literatures, researches which incorporated overconfidence bias into real option model are at premium. A few studies have focused on qualitative analysis and very few scholars conducted quantitative analysis on impacts of overconfidence exerted by real option evaluation.

Therefore, aiming at this relatively blank field, overconfidence is incorporated into a real option decision-making model of metal mineral resources mining project in this paper and "twin security" is applied to build a connection between real option and overconfidence psychological bias. Since the ubiquitous overconfidence in decision-makers can change their estimation of expected growth rate and volatility of project value, the changes will take effect on the option pricing through the abovementioned key factors. On these premises, this paper establishes a behavioral real option price model and lists the numerical result of the model. In the context of China's metal mineral resources mining projects, overconfidence of decision-makers ought to be incorporated into real option model, which could help make metal mineral resources investment decisions more precisely.

This paper is organized as follows. Section 2 establishes the model; Section 3 provides numerical results and discussions; Section 4 presents the concluding comments and final discussion.

2. Establishment of Model

2.1. Basic Assumptions. Uncertainties such as irreversibility and capability to defer contribute to real option value. But since there exists no real option trading market, it is impossible to apply a standard financial option pricing model to price real option. Fortunately, theoretical study by Mason and Merton [20] indicates once a "twin security" which bears the same risk features as the project can be found in the stock market, method of a standard option pricing model can be applied to derive real option pricing model under the same assumptions as standard DCF method. Since the existence of a "twin security" requires a standardized market and the same risk and distribution features as the project to be evaluated, it is difficult to find a "twin security" for a project whose underlying asset is not tradable [21]. But as for metal mineral resources mining project, its underlying asset is tradable in standardized active stock market, for example, "LME copper futures market," which makes the metal mineral products standardized and tradable; additionally, the price volatility of metal mineral future is consistent with the value of the mining project, which exhibits the same risk features. Furthermore, the price motion of metal mineral future is similar to the value of the mining project; that is, they follow geometric Brownian motion; thus, metal mineral futures can be applied as the "twin security" of the metal mineral mining project as evidenced by Hu and Ye [19] and Trigeorgis [22] and Zhu [23]. By using the combination of "twin security" and risk-free security, the yield features of relevant real option can be copied. Consequently, the real option model can be solved by the same way of option pricing initiated by Black-Scholes [24–26].

In addition, as a form of risky security, twin security will inevitably meet the basic features of the risky securities and traditional behavioral asset pricing theory based on overconfidence is generally built on the premise of risk stock market [27] and assumes price of risk security is a normal random variable. On the abovementioned analysis, we take metal mineral futures as the "twin security" of the metal mineral mining project, through which contact between twin security market volatility and cognitive volatility of overconfident investors can be established. Ultimately, information of twin security can be used to indicate the value and volatility of metal mineral resources mining projects under investors' overconfidence conditions.

On these premises, it is reasonable to assume that (1) the project to be decided is at a perfect competition market and there exists a tradable "twin security" θ, which shows the same risk features with the project and follows normal distribution $N(0, \sigma_\theta^2)$, so the project value is affected by the equivalent uncertain factors of "twin security"; (2) the initial cost I of the project is fixed; (3) decision-makers of the project are overconfident; (4) price of the metal mineral product follows geometric Brownian motion:

$$\frac{dP}{P} = \mu_1 dt_1 + \sigma_1 dz_1, \tag{1}$$

where μ_1 stands for expected rate of growth, σ_1 stands for volatility, and dz_1 is a standard Wiener process. Since value of the project is mainly affected by price, the value of project is also follows:

$$\frac{dV}{V} = \alpha dt + \sigma dz. \tag{2}$$

Malmendier and Tate pointed out that entrepreneurs and business managers show overconfidence and investment decision-makers of metal mining projects are often middle-senior managers; these managers are often faced with a variety of complex issues and thus they are more likely to exhibit higher overconfidence bias than the ordinary group. Numerous studies [28, 29] documented overconfident investment decision-makers estimated expected growth rates and project value volatility with error. Therefore, they estimate α as α_o and σ as σ_o. So (2) turns to (3) under the condition of investment decision-makers' overconfidence:

$$\frac{dV_o}{V_o} = \alpha_o dt + \sigma_o dz, \tag{3}$$

where V_o stands for the value of metal mineral mining project when taking overconfidence of investment decision-makers into consideration, α_o shows the cognitive expectation when investment decision-makers are overconfident, σ_o is the cognitive volatility when decision-makers are overconfident, and dz is a standard Wiener process. Copying the project value by "twin security" in the metal mineral futures market, "twin security" under investment makers' overconfidence follows geometric Brownian motion as well:

$$\frac{d\theta}{\theta} = \alpha_o dt + \sigma_o dz. \tag{4}$$

Mathematical description of overconfidence in the model is particularly important so as to make real option decision-making model of mineral resources development based on overconfidence which is more persuasive in explaining reality of economic phenomena. Representative overconfidence measurement methods are as follows: Gervais and Goldstein defined overconfidence level $d = A - a$, in which d was overconfidence level, A was the cognitive capability of the overconfident, a meant the actual capability of the overconfident decision-maker, and $A > a$. Keiber figured out that, when analyzing relationship between variables in stock market, it can be inevitably affected by random variables; the distribution of the random variable ε was assumed to meet normal distribution $N(0, \sigma_\theta^2)$. The existence of overconfidence decreased the variance of the random variable ε to $k\sigma^2$ $(0 < k < 1)$; k stood for overconfidence level because of their own experiences and ability. But the measurement method of overconfidence in DHS model is most generally accepted and widely used, where it was assumed that overconfident investment decision-makers were influenced by private signals in the stock market and overconfidence coefficient ϕ $(0 < \phi < 1)$ indicated that noise factor variance was underestimated. Based on the above theories, overconfidence can be incorporated into real option model of mineral resources mining.

2.2. Model Construction. When starting to make decisions on the metal mineral resources mining project, overconfident investment decision-makers will receive private signal S which is related to "twin security" in stock market and the signal is random which follows

$$S = \theta + \varepsilon, \tag{5}$$

where θ follows normal distribution $(\overline{\theta}, \sigma_\theta^2)$, ε is a noise factor which follows normal distribution $(0, \sigma_\varepsilon^2)$ and it is a one-dimensional random variable, and θ and ε are independent of each other. According to features of one-dimensional random variables, variance of signal S is as follows:

$$\operatorname{Var}(S) = \sigma_\theta^2 + \sigma_\varepsilon^2. \tag{6}$$

σ_θ^2 could be understood as the market risk of "twin security" of metal mineral product which would not be affected by capability of decision-makers, σ_ε^2 is a risk relevant with the effort of the decision-makers' capability; namely, it is dominantly affected by the capability and overconfidence level of the decision-makers. According to Gervais and Odean [27] and Daniel et al. [29], overconfident decision-makers will overestimate the accuracy of the information and underestimate risk that is facing them, namely, underestimation of noise variance σ_ε^2. Assume that there exists a coefficient ϕ $(0 < \phi < 1)$ which turns the estimation of noise variance under investment decision-makers' overconfidence into

$$\sigma_\varepsilon'^2 = \phi\sigma_\varepsilon^2. \tag{7}$$

The lower the ϕ is, the higher the overconfidence level is. In order to facilitate the following context, we also take $\phi = 1$ into account and in this circumstance equation (7) turns into a situation when investment decision-makers are completely rational with no overconfidence bias. The "twin security" that is affected by private signals $(\theta \mid S)$ also follows normal distribution; the expected value and cognitive volatility under investment decision-maker's overconfidence condition are, respectively, [30]

$$\begin{aligned} E(\theta \mid S) &= E(\theta) + \operatorname{cov}(\theta, S)^T \operatorname{cov}(S, S)^{-1} \{S - E(S)\} \\ &= \frac{\phi\sigma_\varepsilon^2}{\sigma_\theta^2 + \phi\sigma_\varepsilon^2}\theta + \frac{\sigma_\theta^2}{\sigma_\theta^2 + \phi\sigma_\varepsilon^2}(\theta + \varepsilon), \end{aligned} \tag{8}$$

$$\begin{aligned} \operatorname{Var}(\theta \mid S) &= \operatorname{Var}(\theta) - \operatorname{cov}(\theta, S)^T \operatorname{cov}(S, S)^{-1} \operatorname{cov}(\theta, S) \\ &= \sigma_\theta^2 - \sigma_\theta^2 \cdot \frac{1}{\sigma_\theta^2 + \phi\sigma_\varepsilon^2} \cdot \sigma_\theta^2 = \frac{\phi\sigma_\theta^2\sigma_\varepsilon^2}{\sigma_\theta^2 + \phi\sigma_\varepsilon^2}. \end{aligned} \tag{9}$$

It is easy to prove that $\operatorname{Var}(\theta \mid S) < \sigma_\theta^2$, so the overconfident investment decision-makers underestimate the volatility of metal mineral resources mining project, thus generating great impact on decision-making.

As for overconfident decision-maker of metal mineral resources mining project, generally we can assume his utility function is [31]

$$U(W) = -e^{-aw}, \tag{10}$$

where risk averse coefficient $a > 0$; in order to simplify the following analysis, we take $a = 1$; W is the wealth hold by the decision-maker. Under such conditions, when the overconfident decision-maker tends to make optimal decision in the "twin security" market of metal mineral resources mining project, the following requirements need to be met:

$$\begin{aligned} &\operatorname*{Max}_{Q_{r1}} \quad E\left(-e^{-w} \mid S\right) \\ &\text{s.t.} \quad P \cdot Q_{r1} + Q_{f1} = P \cdot Q_{r0} + Q_{f0} \\ &\qquad\; W_1 = Q_{f1} + \theta \cdot Q_{r1}, \end{aligned} \tag{11}$$

where Q_{r0} stands for the quantity of "twin security" hold by overconfident decision-maker before decision making, Q_{r1} is the quantity of "twin security" hold by overconfident decision-maker after decision making, Q_{f0} is the quantity of the risk-free security hold by overconfident decision-maker before decision-making, and Q_{f1} is the quantity of the risk-free security hold by overconfident decision-maker after decision-making. The first constraint condition means, as for overconfident decision-maker, the investment capitals before decision-making equals that after decision-making and the second constraint condition stands for the total wealth after decision-making.

Derive the solution of the abovementioned problem, we arrive at

$$\begin{aligned} E\left(-e^{-w} \mid S\right) &= E\left(-e^{-(Q_{f1}+\theta\bullet Q_{r1})} \mid S\right) \\ &= -e^{-Q_{f1}} \cdot E\left(-e^{-\theta\bullet Q_{r1}} \mid S\right) \\ &= -e^{-Q_{f1}} \cdot \int_{-\infty}^{+\infty} -e^{-Q_{r1}x} \cdot \frac{1}{\sqrt{2\pi \operatorname{Var}(\theta \mid S)}} \\ &\qquad \cdot e^{-[x-E(\theta|S)]^2/2\operatorname{Var}(\theta|S)} dx \\ &= -e^{-(P\cdot Q_{r0}+Q_{f0})+PQ_{r1}-E((\theta|S))Q_{r1}+(1/2)\operatorname{Var}(\theta|S)Q_{r1}^2}. \end{aligned} \tag{12}$$

Therefore, the optimal solution is

$$Q_{r1} = \frac{E(\theta \mid S) - P}{\operatorname{Var}(\theta \mid S)}. \tag{13}$$

When the twin security market is at the equilibrium state, the supply equals demand at metal mineral futures market; that is,

$$\sum Q_{r1} = Q_1. \tag{14}$$

Combine (8), (9), (13), and (14); the equilibrium price of the twin security θ when taking decision-maker's overconfidence into account can be written as

$$P = \frac{\phi\sigma_\varepsilon^2\overline{\theta} - \phi\sigma_\theta^2\sigma_\varepsilon^2\overline{Q}_1}{\sigma_\theta^2 + \phi\sigma_\varepsilon^2} + \frac{\sigma_\theta^2}{\sigma_\theta^2 + \phi\sigma_\varepsilon^2}S, \tag{15}$$

where $\overline{Q}_1$ stands for average holding quantity of twin security. Therefore, the cognitive expectation of the metal mineral's twin security when taking decision-maker's overconfidence into account turns to

$$\begin{aligned} \alpha_o = E(P) &= E\left(\frac{\phi\sigma_\varepsilon^2\overline{\theta} - \phi\sigma_\theta^2\sigma_\varepsilon^2\overline{Q}_1}{\sigma_\theta^2 + \phi\sigma_\varepsilon^2} + \frac{\sigma_\theta^2}{\sigma_\theta^2 + \phi\sigma_\varepsilon^2}S\right) \\ &= \overline{\theta} - \frac{\phi\sigma_\theta^2\sigma_\varepsilon^2\overline{Q}_1}{\sigma_\theta^2 + \phi\sigma_\varepsilon^2}. \end{aligned} \tag{16}$$

It is easy to prove that overconfidence coefficient and the cognitive expectation of the metal mineral's twin security show negative correlation, which means when overconfidence coefficient decreases, the cognitive expectation of the metal mineral's twin security increases. In order to facilitate the following analysis, we take $\overline{Q}_1 = 1$. Put (9) and (16) into (3); the value of metal mineral resources mining project under decision-makers' overconfidence condition can be described as follows:

$$\frac{dV_o}{V_o} = \left(\overline{\theta} - \frac{\phi\sigma_\theta^2\sigma_\varepsilon^2}{\sigma_\theta^2 + \phi\sigma_\varepsilon^2}\right)dt + \sqrt{\frac{\phi\sigma_\theta^2\sigma_\varepsilon^2}{\sigma_\theta^2 + \phi\sigma_\varepsilon^2}}dz. \tag{17}$$

2.3. Model Solution. According to Dixit and Pindyck [32], $F(V)$ stands for investment option value and V stands for value of metal mineral resources development project. Assume that there is no time boundary in decision making of mining investment. When investment decision-makers are overconfident, the Bellman equation of investment option value in continuous time can be presented as

$$\frac{1}{2}\frac{\phi\sigma_\theta^2\sigma_\varepsilon^2}{\sigma_\theta^2 + \phi\sigma_\varepsilon^2}V_o^2F''(V_o) + (r-\delta)V_oF'(V_o) - rF(V_o) = 0. \tag{18}$$

With boundary conditions,

$$\begin{aligned} F(V_o^*) &= V_o^* - I, \\ F'(V_o^*) &= 1, \end{aligned} \tag{19}$$

where ϕ is overconfidence coefficient, σ_θ^2 is volatility of "twin security", σ_ε^2 is volatility of noise factor which stands for investment cost of investing the project, r is discount rate, and δ is dividend, it could be interpreted as the convenience yield of metal mineral resources mining project or the opportunity cost to delay the project. According to option pricing method given by Dixit and Pindyck, investment option value and value of the project are, respectively, as follows:

$$F(V_o) = AV_o^{\beta_1}. \tag{20}$$

A and V^* can be obtained with the boundary conditions and V^* stands for trigger value in optimal investment timing:

$$V = \begin{cases} K_1P^{\beta_1}, & P < C \\ B_2P^{\beta_2} + q\left(\dfrac{P}{\delta} - \dfrac{C}{r}\right), & P \geq C, \end{cases} \tag{21}$$

where C stands for operation cost of investment project. Substituting the parameters into differential equation, parameters β_1 and β_2 can be obtained:

$$\begin{aligned} \beta_1 &= \frac{1}{2} - \frac{(r-\delta)\left(\sigma_\theta^2 + \phi\sigma_\varepsilon^2\right)}{\phi\sigma_\theta^2\sigma_\varepsilon^2} \\ &\quad + \sqrt{\left(\frac{(r-\delta)(\sigma_\theta^2 + \phi\sigma_\varepsilon^2)}{\phi\sigma_\theta^2\sigma_\varepsilon^2} - \frac{1}{2}\right)^2 + \frac{2r\left(\sigma_\theta^2 + \phi\sigma_\varepsilon^2\right)}{\phi\sigma_\theta^2\sigma_\varepsilon^2}}, \\ &\qquad \beta_1 > 1, \\ \beta_2 &= \frac{1}{2} - \frac{(r-\delta)\left(\sigma_\theta^2 + \phi\sigma_\varepsilon^2\right)}{\phi\sigma_\theta^2\sigma_\varepsilon^2} \\ &\quad - \sqrt{\left(\frac{(r-\delta)\left(\sigma_\theta^2 + \phi\sigma_\varepsilon^2\right)}{\phi\sigma_\theta^2\sigma_\varepsilon^2} - \frac{1}{2}\right)^2 + \frac{2r\left(\sigma_\theta^2 + \phi\sigma_\varepsilon^2\right)}{\phi\sigma_\theta^2\sigma_\varepsilon^2}}, \\ &\qquad \beta_2 < 0. \end{aligned} \tag{22}$$

According to boundary conditions and $V(P)$, $V'(P)$ is continuous at $P = C$; we arrive at

$$K_1 = \frac{C^{1-\beta_1} q}{\beta_1 - \beta_2}\left(\frac{\beta_2}{r} - \frac{\beta_2 - 1}{\delta}\right),$$
$$B_2 = \frac{C^{1-\beta_2} q}{\beta_1 - \beta_2}\left(\frac{\beta_1}{r} - \frac{\beta_1 - 1}{\delta}\right). \quad (23)$$

Based on value matching and smooth paste conditions of Pindyck, we get to

$$A = \frac{(1-\beta_2) P^{*(1-\beta_1)}}{(\beta_1 - \beta_2)\delta} q - \frac{\beta_2 P^{*-\beta_1}}{\beta_1 - \beta_2}\left(\frac{Cq}{r} + I\right). \quad (24)$$

And P^* is the solution of (24):

$$(\beta_1 - \beta_2) B_2 (P^*)^{\beta_2} + (\beta_1 - 1)\frac{q}{\delta} P^* - \beta_1\left(\frac{q}{r} C + I\right) = 0. \quad (25)$$

Using numerical method, we can get value of P^*. The abovementioned equations give the option value, project value, and boundary conditions in optimal investment; we can get trigger value to carry out the investment when investment decision-makers are overconfident.

3. Numerical Results and Discussions

3.1. Main Parameters. In order to apply the model to estimate the effect of overconfidence on trigger value V^* and option value, a domestic copper mining project has been considered with the value of technical and economic parameters as those presented in Table 1. The life span of the project is 20 years, initial investment cost is 9.3 billion yuan, the cost of production is 8967.54 yuan per ton, yearly production is 1,010,000 ton, and risk free rate is 3.48%.

On the premise of the analysis, the copper futures in LME futures market are adopted as the "twin security" of the copper mining project and as for the projects that can find "twin securities" in stock market, the volatility of "twin securities" is often used to substitute that of real assets projects [22, 23]. Therefore, the volatility of copper futures in LME is applied to present the project twin security's volatility σ_θ of copper mining project. σ_θ is extracted from LME copper price on daily basis from October 2003 to October 2013 [33]; from the data we get standard deviation of copper price during these ten years 22.46%; risk-free rate is one-year treasury rate in 2013 and convenience yield is 1.48%. The estimation of noise factor's volatility σ_ε is more subjective, since there is no publicly available information regarding it. Consequently, in this case, assume that $\sigma_\varepsilon = 31.4\%$ is just a first approximation.

3.2. Numerical Results and Discussions. Since only when the project value exceeds the trigger value can the investment of the project be carried out, trigger value is the prior evaluation criteria. Additionally, option value presents the value to delay the project; it has also been taken into consideration as key evaluation criteria. The following data and analysis show how overconfidence coefficient affects optimal decision timing in the copper mining project.

Table 1: Main technical and economic parameters of the copper mining project.

Input parameters	Units	Value
Initial investment (I)	RMB billion yuan	9.3
Cost of production (C)	RMB yuan/ton	8967.54
Yearly production of copper ore (q)	Ton	1010000
Risk-free interest rate (r)	%	3.48
Twin security's volatility (σ_θ)	%	22.46
Noise factor's volatility (σ_ε)	%	31.4
Overconfidence coefficient (ϕ)	Dimensionless	0.5
Yearly convenience yield (δ)	%	1.48
Life span of the project (L)	Year	20
Initial price of copper	RMB yuan/ton	28950

3.2.1. Effects of Overconfidence Coefficient on Decision-Making. Impacts of overconfidence on project trigger value and option value are mainly focused in this paper; part of the numerical data is shown from Tables 2, 3, and 4. In order to decrease the possible error caused by subjective estimation, simulation results under different σ_ε value are given as follows.

Since the metal mineral resources mining project is faced with great uncertainty, the trigger condition of the project is that the value of metal mineral mining project exceeds the trigger value. Therefore, according to Table 2 to Table 4, we can figure out the following.

(1) Owing to the existence of overconfidence, investment decision-makers are too optimistic about market price and thus they will carry out the project when project value is beneath proper trigger value. The model also echoes from another perspective that overconfident investment decision-makers tend to implement project earlier which has been proved by Odean [17] and Sarkar [34], thus increasing the possibility of failure.

(2) As overconfidence coefficient grows, namely, overconfidence level decreases, trigger value of the project is increasingly getting close to 5.351×10^{11} (when $\sigma_\varepsilon = 0.314$); in other words, the conclusion can be interpreted as with increase of overconfidence level; overconfident decision-makers will underestimate the trigger value to a greater extent; possibility to carry out the project earlier is growing as well as the risk of fault investment decision.

(3) The estimation of option value by overconfident decision-maker is lower than that of rational decision-maker, which means that overconfident decision-maker bears the belief that the present metal mineral price is high so the option value to defer the project is relatively low and there is no need in waiting for new opportunities.

(4) The overconfidence coefficient shows positive correlation with project option value. As the overconfidence coefficient increases, the investment decision-maker will

Table 2: Simulation result under different overconfidence coefficient ($\sigma_\varepsilon = 0.214$).

Overconfidence coefficient	Trigger value	Option value
0.05	3.995×10^{11}	3.902×10^{11}
0.10	4.144×10^{11}	4.051×10^{11}
0.15	4.258×10^{11}	4.165×10^{11}
0.20	4.353×10^{11}	4.260×10^{11}
0.25	4.434×10^{11}	4.341×10^{11}
0.30	4.505×10^{11}	4.412×10^{11}
0.35	4.568×10^{11}	4.475×10^{11}
0.40	4.625×10^{11}	4.532×10^{11}
0.45	4.677×10^{11}	4.584×10^{11}
0.50	4.724×10^{11}	4.631×10^{11}
0.55	4.767×10^{11}	4.674×10^{11}
0.60	4.807×10^{11}	4.714×10^{11}
0.65	4.843×10^{11}	4.750×10^{11}
0.70	4.878×10^{11}	4.785×10^{11}
0.75	4.909×10^{11}	4.816×10^{11}
0.80	4.939×10^{11}	4.846×10^{11}
0.85	4.967×10^{11}	4.874×10^{11}
0.90	4.993×10^{11}	4.900×10^{11}
0.95	5.017×10^{11}	4.924×10^{11}
1.00	5.040×10^{11}	4.947×10^{11}

Table 3: Simulation result under different overconfidence coefficient ($\sigma_\varepsilon = 0.314$).

Overconfidence coefficient	Trigger value	Option value
0.05	4.163×10^{11}	4.070×10^{11}
0.10	4.378×10^{11}	4.286×10^{11}
0.15	4.534×10^{11}	4.442×10^{11}
0.20	4.657×10^{11}	4.564×10^{11}
0.25	4.757×10^{11}	4.664×10^{11}
0.30	4.841×10^{11}	4.748×10^{11}
0.35	4.911×10^{11}	4.818×10^{11}
0.40	4.973×10^{11}	4.880×10^{11}
0.45	5.026×10^{11}	4.933×10^{11}
0.50	5.073×10^{11}	4.980×10^{11}
0.55	5.115×10^{11}	5.022×10^{11}
0.60	5.152×10^{11}	5.059×10^{11}
0.65	5.186×10^{11}	5.093×10^{11}
0.70	5.216×10^{11}	5.123×10^{11}
0.75	5.244×10^{11}	5.151×10^{11}
0.80	5.270×10^{11}	5.176×10^{11}
0.85	5.292×10^{11}	5.199×10^{11}
0.90	5.313×10^{11}	5.220×10^{11}
0.95	5.333×10^{11}	5.240×10^{11}
1.00	5.351×10^{11}	5.258×10^{11}

underestimate the option value to a greater extent. Overconfident decision-maker thinks that the project's delay option value is not high; they tend to give up waiting for new market

Table 4: Simulation result under different overconfidence coefficient ($\sigma_\varepsilon = 0.414$).

Overconfidence coefficient	Trigger value	Option value
0.05	4.330×10^{11}	4.237×10^{11}
0.10	4.597×10^{11}	4.504×10^{11}
0.15	4.776×10^{11}	4.683×10^{11}
0.20	4.908×10^{11}	4.815×10^{11}
0.25	5.010×10^{11}	4.917×10^{11}
0.30	5.092×10^{11}	4.999×10^{11}
0.35	5.158×10^{11}	5.065×10^{11}
0.40	5.213×10^{11}	5.120×10^{11}
0.45	5.260×10^{11}	5.167×10^{11}
0.50	5.300×10^{11}	5.207×10^{11}
0.55	5.335×10^{11}	5.242×10^{11}
0.60	5.366×10^{11}	5.273×10^{11}
0.65	5.393×10^{11}	5.300×10^{11}
0.70	5.417×10^{11}	5.324×10^{11}
0.75	5.439×10^{11}	5.346×10^{11}
0.80	5.458×10^{11}	5.365×10^{11}
0.85	5.476×10^{11}	5.383×10^{11}
0.90	5.492×10^{11}	5.399×10^{11}
0.95	5.506×10^{11}	5.413×10^{11}
1.00	5.520×10^{11}	5.427×10^{11}

Note: when overconfidence coefficient is 1, it means that investment decision-maker bears no overconfidence. Since it has no negative effect on the model, the data has been kept for further illustration.

opportunity and carry out the metal mineral resource mining project earlier.

Figures 1 and 2 show, respectively, impact of overconfidence coefficient on trigger value and option value under different noise factor volatilities. From Figure 1, it can be concluded that, when overconfidence coefficient increases or decreases 1% from 0.1, trigger value will change −0.845% and 0.794%, respectively; when overconfidence coefficient increases or decreases 1% from 0.5, trigger value will change −0.176% and 0.172%, respectively; when overconfidence coefficient increases or decreases 1% from 0.9, trigger value will change −0.077% and 0.076%, respectively. Therefore, in the interval where the overconfidence level is high, the overconfident investment decision-makers will underestimate the trigger value to a greater extent and thus overconfidence generates greater impacts on decision-making. When overconfidence coefficient gets close to 1, estimation error is approximately 0.

Figure 2 indicates that overconfidence coefficient and the option value show positive correlation. When overconfidence coefficient increases or decreases 1% from 0.1, the option value will change −0.86293% and 0.81135%; when overconfidence coefficient increases or decreases 1% from 0.5, the option value will change −0.17967% and 0.17546%; when overconfidence coefficient increases or decreases 1% from 0.9, the option value will change −0.07906% and 0.07782%. This on the one hand shows that, due to investment decision-maker's overconfidence, option value of project is

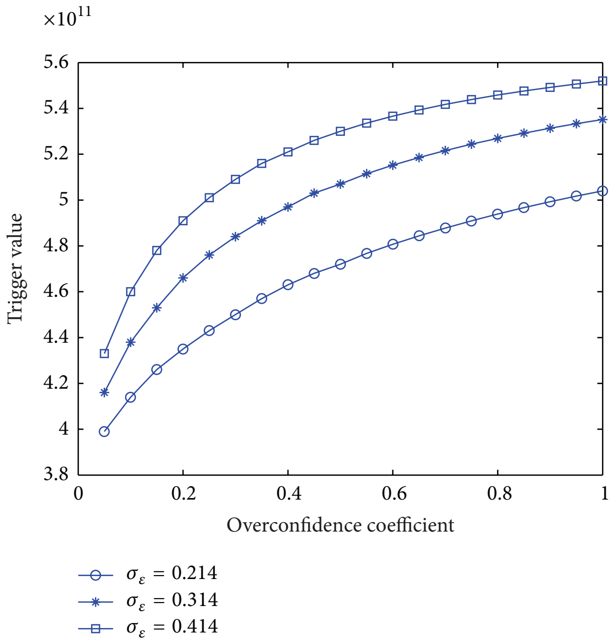

Figure 1: Impact of overconfidence coefficient on critical investment value.

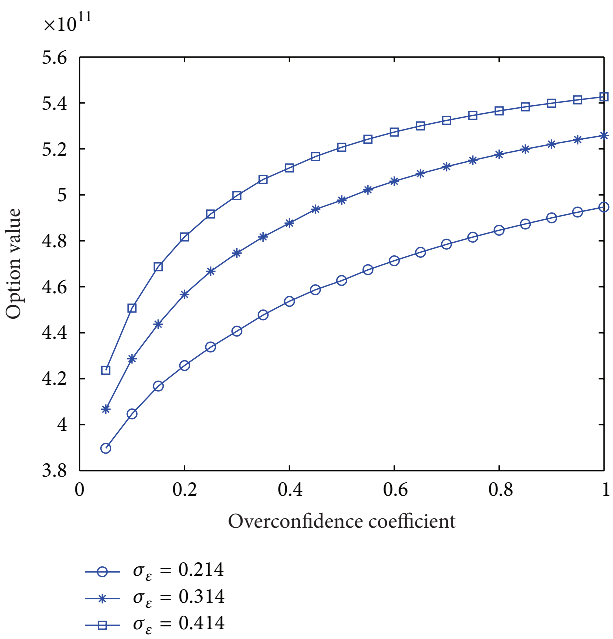

Figure 2: Impact of overconfidence coefficient on option value.

underestimated by the decision-maker; on the other hand, it indicates that in the interval where the overconfidence level is high, impact of overconfidence to option value is greater and vice versa. When overconfidence coefficient gets close to 1, the option value of the model gets close to the value when the investment decision-maker is not overconfident.

3.2.2. A Comparison Analysis of Numerical Results between the Proposed and DCF Approach. In order to clarify the different effects of the proposed and classic approaches on decision-making and exhibit the superior performance of the proposed model, comparison studies of the real option decision-making model which incorporates overconfidence and classic DCF method, Black-Scholes formula based model, Monte Carlo based model has been presented.

According to market information, the expected growth rate of copper product is 0.005. Applying (1) and Ito's Lemma, the copper price P_t in the year t follows lognormal distribution, based on the features of which the expected value of P_t can be described as in the following expression:

$$E(P_t) = P_0 \exp\left(\mu_1 t + \frac{1}{2}\sigma_1^2 t\right). \tag{26}$$

Therefore, the net present value (NPV) of the copper mining project is presented by

$$\begin{aligned}
\text{NPV} \\
&= q\sum_{t=1}^{L}\frac{E(P_t)-E(C_t)}{(1+r)^t} - I \\
&= q\left[\sum_{t=1}^{L}\frac{P_0\exp\left(\mu_1 t+(1/2)\sigma_1^2 t\right)-C}{(1+r)^t}\right] - I = 1.01\times 10^6 \\
&\quad\times\left[\sum_{t=1}^{20}\left(\left(57729\exp\left(0.005t+\frac{1}{2}\times 0.2246^2 t\right)\right.\right.\right. \\
&\qquad\left.\left.\left. - 8967.54\right)\left(\left(1+0.0348\right)^t\right)^{-1}\right)\right] \\
&\quad - 9.3\times 10^9 \\
&= 7.95969\times 10^{11} - 9.3\times 10^9 = 7.867\times 10^{11}.
\end{aligned} \tag{27}$$

Table 5 shows evaluation results between the DCF and the real option method. The net present value of copper mining project by traditional DCF method is 7.867×10^{11}; therefore the project is feasible and should be immediately carried out. Conversely, the evaluation result by RO method indicates that immediate investment is not an optimal decision, because it means the investment decision-maker gives up the delay option value 4.980×10^{11}. Even if price uncertainty and overconfidence brings up the project value, a delay investment is an optimal decision.

Therefore, DCF method cannot reflect the uncertainty and investment flexibility, which means an ignorance of the option value of the copper mining project, while, as for the proposed model which takes the price uncertainty and overconfidence into the real option model, the delay option value reflects such added value brought by these uncertainties.

3.2.3. A Comparison Analysis of Numerical Results between Traditional Black-Scholes Formula Based and the Proposed

Table 5: The comparison of the evaluation results between the DCF and the proposed model.

Method	Feature	Trigger value V_o^*	Option value $F(V_o^*)$	Investment decision
Traditional DCF	Ignoring uncertainty and investment flexibility	9.300×10^9	—	Make investment immediately
Proposed model ($\phi = 0.5$)	Incorporating uncertainty and investment flexibility into the model	5.073×10^{11}	4.980×10^{11}	Delay investment

Table 6: The comparison of the evaluation results between traditional BS based formula and the proposed model.

Method	Feature	Trigger value V_o^*	Option value $F(V_o^*)$	Investment decision
Traditional BS model	Ignoring investment maker's overconfidence bias	5.838×10^{11}	5.745×10^{11}	Wait and delay investment
Proposed model ($\phi = 0.5$)	Incorporating overconfidence into the model	5.073×10^{11}	4.980×10^{11}	Early investment*

Note: *denotes that the evaluation result is compared with the investment decision made through traditional BS approach.

Model. The simulation results of traditional BS formula based and the proposed model of this copper mining project are shown in Table 6.

Table 6 exhibits the evaluation results of traditional BS based formula and the proposed model. As can be seen in Table 6, option value of the model which incorporates overconfidence is beneath that of the traditional real option model with no overconfidence bias (5.745×10^{11}); therefore the proposed model proves that overconfident decision-maker usually underestimates the delay option value and loses the opportunity to wait for better market information, thus resulting in early investment compared with the evaluation results of traditional BS approach. On the other hand, the trigger value of the project in new model is below that of traditional BS model since overconfidence bias contributes to the optimistic estimation of the market price of metal mineral so overconfident decision-maker often exercises the project when the value does not exceed proper trigger value. Overconfident decision-maker bears higher risks in making fault investment decisions.

3.2.4. A Comparison Analysis of Numerical Results between the Proposed and Monte Carlo Based Model. The copper mining project can be understood as an American option; the following part gives the option pricing results based on Monte Carlo simulation [34]. According to the previous parameters and results, the initial price of the real option is 7.87×10^{11} yuan and the exercise price of the real option is 9.3×10^9; all the other necessary parameters can be obtained in Table 1. We take 1000 simulation sample paths and divide each discrete time interval into 20 steps which added to 400 steps for each path. Part of the simulation result is shown in Figure 3.

Comparison of the evaluation results between Monte Carlo based model and the proposed model is presented in Table 7. It shows that overconfident decision-maker underestimates the option value of the copper mining investment project, which means an underestimation of the value to wait for new market information. This evaluation result is consistent with the results in previous part. In addition, the comparison shows that our proposed model can determine the optimal timing of copper mining investment project,

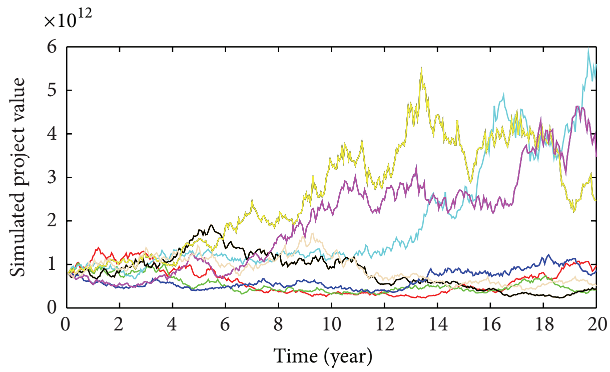

Figure 3: Monte Carlo simulation result of copper mining project value in the following 20 years.

while the traditional Monte Carlo simulation cannot solve it, which also reflects the superiority of the proposed model.

3.3. Sensitivity Analysis. In order to ensure the stability of model, sensitivity of main parameters in this paper is conducted; results are shown in Figures 4 and 5. From the two figures, trigger value is the most sensitive to convenience yield, which is consistent with traditional conclusion and this ensures the stability of the model. In this paper, when convenience yield decreases or increases 1% from 3.48%, it will contribute to 83.2% and −38.73% change in the trigger value; it should be noted that, as convenience yield goes up, its impact on trigger value goes down. The newly incorporated parameters in this paper, that is, overconfidence coefficient, noise factor volatility, and twin security volatility, also take effect on trigger value as analyzed in the previous chapter. When noise volatility goes up or down 1% from 31.4%, the trigger value changes −0.176% and 0.172%, respectively, while the sensitivity of trigger value to twin security volatility falls in the interval between overconfidence coefficient and noise factor volatility.

Figure 6 exhibits that, when risk free rate increases, trigger value increases and vice versa. When risk-free rate decreases or increases 1% from 2.48%, the trigger value

Table 7: The comparison of the evaluation results between Monte Carlo based model and the proposed model.

Method	Feature	Trigger value V_0^*	Option value $F(V_o^*)$	Investment decision
Monte Carlo based model	Optimal investment timing cannot be obtained	—	5.562×10^{11}	Wait and delay investment
Proposed model ($\phi = 0.5$)	Optimal investment timing can be obtained	5.073×10^{11}	4.980×10^{11}	Early investment*

Note: * denotes that the evaluation results are compared with the investment decision made through traditional Monte Carlo based approach.

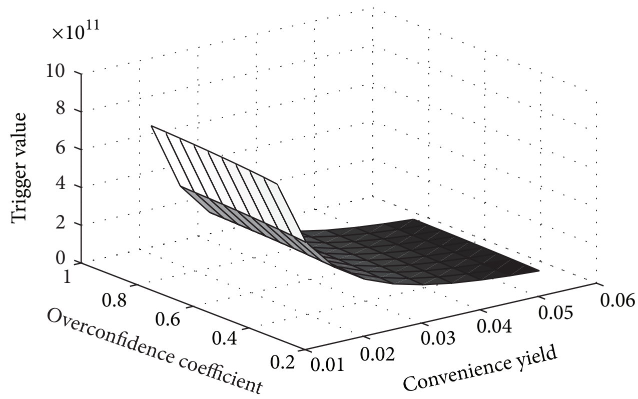

Figure 4: Sensitivity analysis of trigger investment value to convenience yield and overconfidence coefficient.

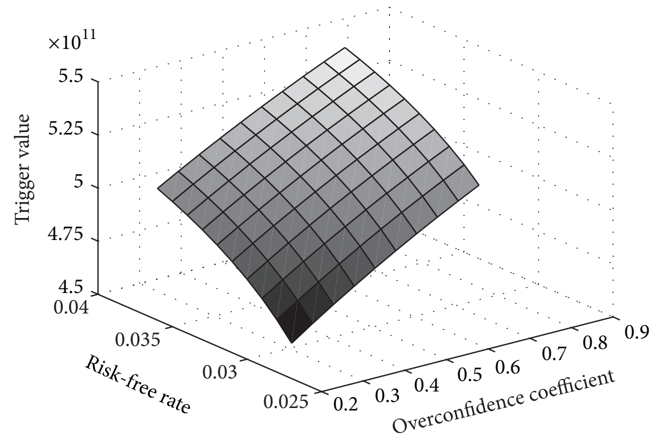

Figure 6: Sensitivity analysis of trigger investment value to overconfidence coefficient and risk-free rate.

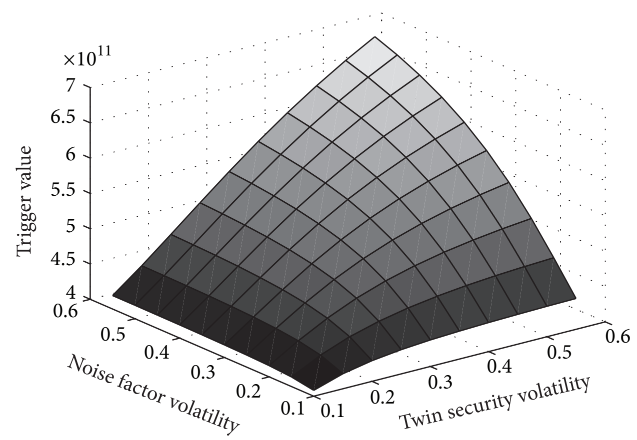

Figure 5: Sensitivity analysis of trigger investment value to noise factor volatility and twin security volatility.

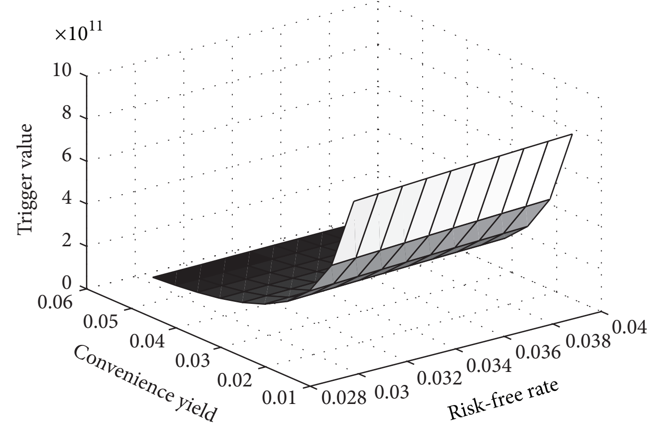

Figure 7: Sensitivity analysis of trigger investment value to risk-free rate and convenience yield.

changes −19.056% and 13.7214%, respectively; when risk-free rate decreases or increases 1% from 4.48% the trigger value changes −7.87% and 5.7385%, respectively. Comparatively, the sensitivity of trigger value to overconfidence coefficient is lower than that to convenience yield. Figure 7 also shows that the sensitivity of trigger value to risk-free rate is lower than that to convenience yield.

In order to estimate the effect of main parameters to option value of the model, the sensitivity analysis of option value to overconfidence coefficient, convenience yield, noise factor volatility, and twin security volatility has been given. Results show that option value presents the greatest sensitivity to convenience yield among the input parameters. Figure 8 shows relatively higher convenience yield can decrease the option value to defer. When overconfidence coefficient takes 0.5, convenience yield decreases or increases 1% from 2% and option value changes 164.22% or −50.61%; while when convince yield is 1.48%, when overconfidence coefficient decreases or increases 1% from 0.1, the option value just changes −0.86293% and 0.81135%, respectively. Figure 9 shows that both higher noise factor volatility and twin security volatility add the delay option value in the proposed model, which is consistent with traditional research

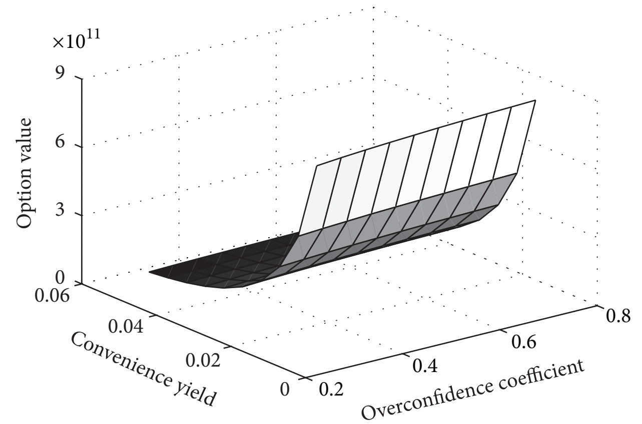

Figure 8: Sensitivity analysis of option value to convenience yield and overconfidence coefficient.

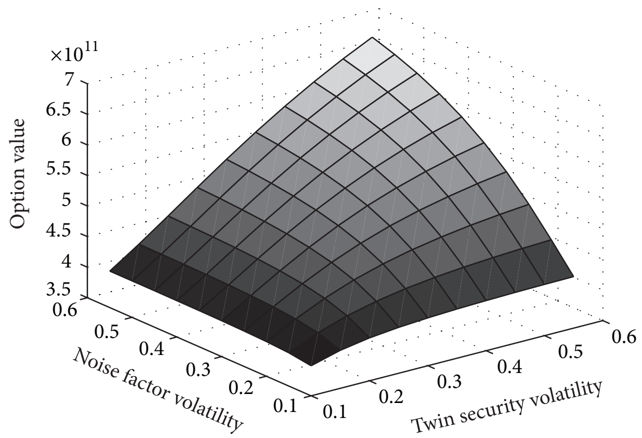

Figure 9: Sensitivity analysis of option value to noise factor volatility and twin security volatility.

findings, while the sensitivity levels to the two factors are quite close.

4. Conclusion

This paper considers the shortage of traditional real option approach when making investment decisions of metal mineral resources mining project and establishes a behavioral real option decision-making model which is incorporated with overconfidence. Finally, analytical solution of the model has been given. To further illustrate the theoretical value and practical significance of the model, we use the data of a domestic copper mining project to conduct example and sensitivity analysis; results show the following. (1) Overconfidence is an important factor in decision making of metal mineral resources mining projects and, according to the results of the model, overconfident investment decision-makers will underestimate trigger value of the implementation of the project and the greater the degree of overconfidence is, the greater the degree of underestimation of the trigger value will be. Therefore when decision-makers show overconfidence bias in reality, optimal investment value of project should be higher than the trigger value assessed by the overconfident investment decision-makers so as to effectively avoid the risk brought by overconfidence. (2) Presence of overconfidence decreases uncertainty of metal mineral resources development investment since the overconfident decision-maker generally underestimates the volatility of the project value; consequently, the delay option value in metal mineral resources development investment increases as overconfidence coefficient increases. These findings echo previous study of Sarkar [34]. (3) Convenience yield of metal mineral resources is an important factor for evaluation of metal mineral resources project. Through sensitivity analysis of the model, it can be figured out that convenience yield generates the greatest impact on the valuation of metal mineral resource projects; relatively higher convenience yield will reduce the trigger value of mineral resources investment projects. While the convenience yield reflects the abundance of metal mineral resources, so it is important for overconfident decision-makers to consider the abundance of mineral resources when making a metal mineral resources development decision. Because high resource abundance of the project can bring higher investment income and offset the risk brought by decision-makers' overconfidence to some extent.

Existence of overconfidence contributes to investment in advance and overinvestment into metal mineral resources market. These findings also provide a theoretical basis for phenomenon of excess investment in metal mining industry of iron and steel. But model in this paper shows some deficiencies; the paper fails to take cost uncertainty of metal mineral resources development and measurement of overconfidence into account. In future studies, it is not only meaningful to build a more realistic and accurate metal mineral resources investment decision-making model with the consideration of cost and other uncertainties, but also of theoretical value and realistic significance by incorporating overconfidence into real option models.

Conflict of Interests

The authors declare that there is no conflict of interests regarding the publication of this paper.

Acknowledgments

This work was partially supported by National Natural Science Foundation of China (NSFC) under Grant no. 71073177, Ministry of Education of International Financial Crisis Emergency Response Project under Grant no. 2009JYJR035, the National Natural Science Foundation of China (Grant no. 71171203), Major Project of National Social Science Foundation (Grant nos. 13 and ZD024 and nos. 13 and ZD169), the Ph.D. Programs Foundation of Ministry of Education of China (Grant no. 20130162110076), the Research Project in Humanities and Social Sciences of Chinese Ministry of Education (Grant nos. 13YJAZH149 and 09YJC90261), the Emergency Project of Chinese Ministry of Education (Grant no. 2009JYJR035), the Postgraduate Autonomous Exploration Innovation Fund of Central South University (Grant no. 2013zzts141), the China Postdoctoral Science Foundation (Grant no. 20110491264), the Special Project of Postdoctoral Research Funds of Hunan Province (Grant no. S2011R1040), and the Project of Soft Science of Hunan Province (Grant no. 2009ZK3193).

References

[1] M. R. Zhong, J. Y. Chen, X. H. Zhu, and J. B. Huang, "Strategic equilibrium price analysis and numerical simulation of preponderant high-tech metal mineral resources," *Transactions of Nonferrous Metals Society of China*, vol. 23, no. 10, pp. 3153–3160, 2013.

[2] S. C. Myers and S. M. Turnbull, "Capital budgeting and the capital asset pricing model: good news and bad news," *The Journal of Finance*, no. 32, pp. 321–333, 1977.

[3] S. A. Ross, "A simple approach to the valuation of risky income streams," *Journal of Business*, vol. 51, pp. 453–475, 1978.

[4] M. J. Brennan and E. S. Schwartz, "Evaluation natural resource investments," *Journal of Business*, vol. 58, no. 2, pp. 135–149, 1985.

[5] J. E. Smith and R. F. Nau, "Valuing risky projects: option pricing theory and decision analysis," *Management Science*, vol. 41, no. 5, pp. 795–816, 1995.

[6] J. E. Smith and K. F. McCardle, "Valuing oil properties: integrating option pricing and decision analysis approaches," *Operations Research*, vol. 46, no. 2, pp. 198–217, 1998.

[7] C. Lima, A. Gabriel, and B. S. Suslick, "Estimating the volatility of mining projects considering price and operating cost uncertainties," *Resources Policy*, vol. 31, no. 2, pp. 86–94, 2006.

[8] G. W. Evatt, M. O. Soltan, and P. V. Johnson, "Mineral reserves under price uncertainty," *Resources Policy*, vol. 37, no. 3, pp. 340–345, 2012.

[9] H. Dehghani and M. Ataee-pour, "Determination of the effect of operating cost uncertainty on mining project evaluation," *Resources Policy*, vol. 37, no. 1, pp. 109–117, 2012.

[10] L. Zhu and Y. Fan, "A real options-based CCS investment evaluation model: case study of China's power generation sector," *Applied Energy*, vol. 88, no. 12, pp. 4320–4333, 2011.

[11] Y. Fan, J. Mo, and L. Zhu, "Evaluating coal bed methane investment in China based on a real options model," *Resources Policy*, vol. 38, no. 1, pp. 50–59, 2013.

[12] F. Wen, Z. He, and X. Chen, "Investors' risk preference characteristics and conditional skewness," *Mathematical Problems in Engineering*, vol. 2014, Article ID 814965, 14 pages, 2014.

[13] F. Wen, Z. He, X. Gong, and A. Liu, "Investors' risk preference characteristics based on different rEFerence POInt," *Discrete Dynamics in Nature and Society*, vol. 2014, Article ID 158386, 9 pages, 2014.

[14] F. Wen, X. Gong, Y. Chao, and X. Chen, "The effects of prior outcomes on risky choice: evidence from the stock market," *Mathematical Problems in Engineering*, vol. 2014, Article ID 272518, 8 pages, 2014.

[15] A. C. Cooper, C. Y. Woo, and W. C. Dunkelberg, "Entrepreneurs' perceived chances for success," *Journal of Business Venturing*, vol. 3, no. 2, pp. 97–108, 1988.

[16] J. E. Russo and P. J. Schoemaker, "Managing overconfidence," *Sloan Management Review*, vol. 33, pp. 7–17, 1992.

[17] T. Odean, "Volume, volatility, price, and profit when all traders are above average," *Journal of Finance*, vol. 53, no. 6, pp. 1887–1934, 1998.

[18] Y. Hao, X. Liu, and C. Lin, "Executives of listed companies and investment decisions overconfidence empirical research," *China Management Science*, vol. 10, no. 13, pp. 142–147, 2005.

[19] W. Hu and G. Ye, "Influence on the valuation of options of risky project put by Project manager," *Operations Research and Management*, vol. 2, no. 12, pp. 105–109, 2003.

[20] S. P. Mason and R. C. Merton, *The Role of Contingent Claims Analysis in Corporate Finance*, Division of Research, Graduate School of Business Administration, Harvard University, 1984.

[21] M. J. Brennan and L. Trigeorgis, Eds., *Project Flexibility, Agency, and Competition: New Developments in the Theory and Application of Real Options*, Oxford University Press, 2000.

[22] L. Trigeorgis, *Real Options: Managerial Flexibility and Strategy in Resource Allocation*, MIT Press, 1996.

[23] D. Zhu, "Project investment decision-making methods research based on real options," Tech. Rep. no. 6, Northeastern University, 2009.

[24] J. B. Huang and M. R. Zhong, "Real options theory and its applications," *Economic Management*, vol. 12, pp. 30–33, 2002.

[25] S. Li and Y. Liu, "Mining investment decision model based on real options delayed," *Systems Engineering*, vol. 3, pp. 124–126, 2008.

[26] M. He and J. Liu, "Outsourcing opportunity decision-making model based on real options," *Systems Engineering*, vol. 5, pp. 38–42, 2011.

[27] S. Gervais and T. Odean, "Learning to be overconfident," *The Review of Financial Studies*, vol. 14, no. 1, pp. 1–27, 2001.

[28] U. Malmendier and G. Tate, "CEO overconfidence and corporate investment," *Journal of Finance*, vol. 60, no. 6, pp. 2661–2700, 2005.

[29] K. D. Daniel, D. Hirshleifer, and A. Subrahmanyam, "Investor psychology and security market under-and overreactions," *The Journal of Finance*, vol. 53, no. 6, pp. 1839–1885, 1998.

[30] H. Gui, M. Cai, and W. Wu, "A commentary overconfidence research model approach," *Financial Research*, vol. 2, pp. 98–109, 2007.

[31] Q. Chen, G. Gao, and H. Chen, "Pricing model of Chinese stock market based on individual investors overconfidence," *China Management Science*, vol. 4, no. 8, pp. 38–46, 2011.

[32] A. Dixit and R. Pindyck, *Investment under Uncertainty*, Princeton University Press, Princeton, NJ, USA, 1994.

[33] F. Wen and X. Yang, "Skewness of return distribution and coefficient of risk premium," *Journal of Systems Science and Complexity*, vol. 22, no. 3, pp. 360–371, 2009.

[34] S. Sarkar, "On the investment-uncertainty relationship in a real options model," *Journal of Economic Dynamics and Control*, vol. 24, no. 2, pp. 219–225, 2000.

Hindawi Publishing Corporation
Discrete Dynamics in Nature and Society
Volume 2014, Article ID 260484, 7 pages
http://dx.doi.org/10.1155/2014/260484

Research Article

Model for Dynamic Multiple of CPPI Strategy

Guangyuan Xing,[1] Yong Xue,[2] Zongxian Feng,[1] and Xiaokang Wu[3]

[1] *School of Finance and Economics, Xi'an Jiaotong University, Xi'an 710061, China*
[2] *Financial Market Department, Bank of Xi'an, Xi'an 710075, China*
[3] *School of Management, Xi'an Jiaotong University, Xi'an 710049, China*

Correspondence should be addressed to Zongxian Feng; zxfeng@mail.xjtu.edu.cn

Received 13 March 2014; Accepted 28 May 2014; Published 24 June 2014

Academic Editor: Chuangxia Huang

Focusing on the parameter "Multiple" of CPPI strategy, this study proposes a dynamic setting model of multiple for gap risk management purpose. First, CPPI gap risk is measured as the probability that the value loss of active asset exceeds its allowed maximum drop determined by a given multiple setting. Moreover, according to the statistical estimation using SV-EVT approach, a dynamic choice of multiple is detailed as a function of time-varying asset volatility, expected loss, and the possibility of occurrence of extreme events in the active asset returns illustrated empirically on Shanghai composite index data. This study not only enriches the literature of dynamic proportion portfolio insurance, but also provides a practical reference for CPPI investors to choose a moderate risky exposure achieving gap risk management, which promotes CPPI's application in emerging capital market.

1. Introduction

Portfolio insurance strategy can help investors control downside risk of asset value on retention of upward market opportunities; it mainly includes dynamic strategies like OBPI based on replication options, CPPI and TIPP based on parameter setting, and static strategies like stop-loss and buy-hold, in which CPPI (constant proportion portfolio insurance) strategy is based on parameter setting. Black and Jones [1] described basic execution procedure as follows: the initial investment volume is V_0, the period of ensuring not to lose capital investment is T, terminal guaranteed value G is proportional to the initial investment volume V_0, $G = \lambda V_0$, and the required terminal asset value $V_T \geq G$. In CPPI strategy, we define the bottom-line value of the asset portfolio $F_t = G \cdot e^{-r(T-t)}$ $(0 \leq t \leq T)$ in every moment. r is risk-free interest rate; the difference between portfolio value and bottom-line value is a cushion; $C_t = V_t - F_t$. We set the multiple and multiply it by the cushion, invest the amount of capital on risky assets and the remainder on risk-free assets, dynamically allocate the risky and risk-free assets in the time horizon, and achieve the goal of portfolio insurance. CPPI strategy which is initially put forward by Black and Jones shows considerable simplicity and flexibility compared with other portfolio insurance strategies; for example, with no maturity date limit, risk exposure can be chosen according to risk appetite of investors. Meanwhile, CCPPI strategy has solid theoretical foundation. Kingston [2] demonstrates that CPPI strategy is optimal when and only when the investors have decreasing absolute and relative risk aversion. Black and Perold [3] studied the impact of transaction cost and borrowing constraints on portfolio insurance strategy under CPPI strategy. They find that when there is no transaction cost, CPPI strategy is equivalent to permanent American buy right investment, and piecewise HARA utility function is optimal under the restriction of minimum consumption. With the increasing of the multiple, the payoffs of CPPI strategy are close to those of stop-loss strategy; the relationship between expected payoffs in holding period and multiplier is monotonous; expected payoffs of CPPI strategy are larger than those of stop-loss strategy [1–3]. Different from portfolio insurance strategy based on option replication, which needs complicated option pricing technology, CPPI strategy is much easier in operation because it is only based on parameter setting. Therefore, it is widely used as an important investment technology in guaranteed fund [4]. All the guaranteed funds in China have been using CPPI strategy or other investment strategies with CPPI strategy at the core since southern safe-haven growth fund, the first guaranteed fund, came into existence.

The setting of multiple (denoted by m in the following model) is crucial in the operation of CPPI strategy, since it directly determines the risk exposure. The bigger the multiple m, the stronger the portfolio participates in the growing market. But it is also accompanied by much bigger risks. When the risky assets fall, the portfolio value falls quickly. Thus the research on CPPI strategy mainly focused on the setting of the multiple m. In traditional CPPI strategy, m was preestablished as a fixed value, and it never changes with the market conditions. Some scholars make an improvement by putting forward variable ratio portfolio insurance strategy, which means dynamic parameter settings in CPPI strategy.

Chen et al. believe that the fixed multiple in CPPI strategy should rectify with the market conditions. They put forth dynamic constant proportion portfolio insurance (DPPI) by using genetic algorithm considering several factors related to the market volatility. The empirical results show that DPPI strategy is more profitable than CPPI strategy [5]. Chen and Liao believe that the investor has his implicit or explicit goal in an investment; thus they proposed goal-directed strategy to describe the trading behavior of investors which, being integrated with CPPI strategy, got a staged goal-directed CPPI strategy (GDCPPI) and was further extended into staged nonlinear goal-directed CPPI strategy [6]. Lee et al. proposed variable proportion portfolio insurance (VPPI) strategy, which enlarges or lessens the multiple when share price rises or falls. They believe portfolio insurance strategy based on this principle will produce better performance [7].

Different multiple dynamic setting principles make the CPPI strategy more profitable or more in line with the investor' targets. Unfortunately, the previous study ignored a real problem in operation: the continuous adjustment of assets in theory leads to some gap risks. Under continuous time frame, CPPI portfolio value at any moment is shown in formula (1) [3], in which V_t is portfolio value at t; F_t is bottom-line value at t; S_t is risky assets value at t; m is multiple in CPPI strategy; r is risk-free interest rate; σ is volatility of risk assets value; $0 \leq t \leq T$; V_0, F_0, and S_0 denote initial values ($t = 0$) of variables. V_t is not less than F_t regardless of m, and terminal guaranteed value can always be achieved. It suggests that when setting the multiple in the research on DPPI, we need only to take into consideration the risk preference and expected return rate of investors:

$$V_t = F_t + (V_0 - F_0)\left(\frac{S_t}{S_0}\right)^m \times \exp\left\{\left(r - m\left(r - \frac{\sigma^2}{2}\right) - \frac{1}{2}m^2\sigma^2\right)t\right\}. \quad (1)$$

In the real market conditions, because of the existence of market friction factors like transaction cost, rebalancing happens on the discrete adjustment point. It is possible that portfolio value drops below bottom-line value because of the

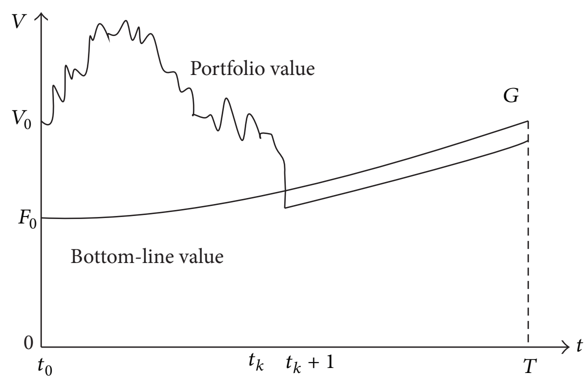

Figure 1: Gap risk of CPPI.

sharp fall of risky assets value between two adjustment points, facing the risk that CPPI portfolio value cannot achieve its guaranteed value on the due day. Figure 1 shows the situation in which gap risk happens between two adjustment points t_k and t_{k+1} possibly because risky assets value falls sharply before CPPI investors rebalance assets. Meanwhile, CPPI portfolio value V_t falls under bottom-line value F_t. The whole funds can only be invested on risk-free assets.

Therefore, Balder et al. defined discrete CPPI strategy and its gap risk which is more congruent to the market environment [8]. In terms of the management of gap risk in CPPI strategy, Cont and Tankov [9] studied the situation of downward jump of object portfolio and its CPPI strategy, the possibility of portfolio value reaching the bottom-line value, the expected loss and distribution of the loss, and the measure of gap risk they took to study the problem of hedging the gap risk in CPPI strategy by option. Considering transaction cost and borrowing constraints, Jessen studied CPPI strategy under the condition of discrete transactions. He believed that gap risk can be avoided by charging, hedging, or setting a "mendacious" guaranteed value, but the latter two cost less for investors [10].

Although the study above considered gap risk in CPPI strategy, it mainly concentrated on extracting the administrative cost and managing the gap risk by option hedging without any attention to the setting of the multiple. In this paper, based on the discrete CPPI strategy by Balder et al. [8], we built a dynamic multiple setting model according to the estimation of extreme changes in risky assets, aiming at studying gap risk management in CPPI strategy from "dynamic proportion." Different from mature capital markets, financial derivatives and their trading are not that abundant in China or in other developing countries. No financial products can be used directly to hedge gap risks in CPPI strategy; thus a multiple setting perspective is needed to handle gap risks. No research has been done on how to dynamically set the multiple in order to avoid gap risks and improve the venture capital in fluctuating market environment. Additionally, dynamic multiple setting model in this paper enriched theoretical system in dynamic proportion portfolio insurance strategy. The basis of dynamic multiple setting is given from the gap risk management perspective, which reveals that multiple setting is not simply to enlarge or lessen the multiple according to the rise or fall of share price [7] but is a complex decision based on risky assets value fluctuation, the frequency of occurrence of extreme prices, and expected loss. Since the dynamic multiple setting provides a basis for gap risk management, the conclusion in this paper offered upper limit of multiple setting in CPPI strategy; further research may consider investment preference and object of investors under this constraint.

2. Model

2.1. Gap Risks and Modeling Basis. In discrete CPPI strategy, asset allocation happens on equally spaced time series [8], defined as $\{t_0^n = 0 < t_1^n \cdots < t_k^n < t_{k+1}^n \cdots < t_n^n = T, t_{k+1}^n - t_k^n = T/n\}$, where n denotes times number of assets allocation in break-even period. In the practice, it has always been adjusted week by week according to the fixed cycle adjustment principle; since risky assets equal to the multiple m multiply the cushion in CPPI strategy, the largest tolerable drop of risky assets value is $1/m$. If risky assets value drop is $1/m$ between two discrete adjustment points t_k and t_{k+1}, r is risk-free interest rate between t_k and t_{k+1}, as shown in

$$\begin{aligned} V_{t_{k+1}} &= mC_{t_k}\left(1 - \frac{1}{m}\right) + \left(V_{t_k} - mC_{t_k}\right)(1+r) \\ &= \left(V_{t_k} - C_{t_k}\right) + \left(V_{t_k} - mC_{t_k}\right) r \\ &= F_{t_k} + \left(V_{t_k} - mC_{t_k}\right) r \\ &\le F_{t_{k+1}}. \end{aligned} \tag{2}$$

Portfolio value $V_{t_{k+1}}$ will be less than or equal to bottom-line value $F_{t_{k+1}}$ at t_{k+1}, and the whole CPPI portfolio assets invested in risk-free assets increase with risk-free interest rate. Therefore, $1/m$ provides the largest drop of risky assets in an adjustment period (t_k, t_{k+1}); we take the probability of risky assets value loss more than $1/m$ in adjustment period as a measurement of gap risks; the probability of risky assets value loss more than $1/m$ should be very small when setting m in the management of this risk. The measurement of gap risk is shown in

$$P\left(x_k > \frac{1}{m}\right) = \alpha, \tag{3}$$

where x_k denotes risky assets value loss in adjustment period (t_k, t_{k+1}) and α denotes the probability of risky assets value loss more than $1/m$. Formula (3) demonstrates the relationship between multiple and the change of risky assets value under the requirement of gap risk management; α is given based on the requirement of CPPI investors. The smaller α means a stronger risk control requirements. In this paper, $\alpha = 0.1\%$. Multiple setting based on the probability of gap risk offers an upper limit of the multiple for CPPI investors. In this way, we increased risky assets investment under the premise of gap risk avoiding and thus a higher expected value.

2.2. Multiple Dynamic Setting Model in CPPI Strategy. Due to the constant fluctuations in the value of assets, dynamic multiplier set is needed to meet the requirements of formula (3). Firstly, we must describe the characteristics of the movements of the risk asset value. Based on the SV-EVT description of the extreme price behavior of the market, this paper gives model to dynamically set the multiplier. Against the price fluctuations and volatility clustering time-varying of the risk asset, the autoregressive conditional heteroscedasticity (ARCH) models [11, 12] and stochastic volatility (SV) model [13] are applicative. ARCH model introduces conditional variance to analyze the variance variability and the fluctuation in the course is a linear function of the past observations and the square of the hysteretic disturbance. But in view of the financial time series "fat tail," the ARCH model seems fragile with the weak leverage and lasting square sequence [14]. Besides, the SV model is considered more suitable for describing the characteristics of the actual financial market volatility because the fluctuation is decided by a random process. Therefore, this paper uses the SV model to describe the risk assets yield characteristics with the following form:

$$\begin{gathered} x_k = \mu + \sigma_k z_k, \quad z_k \sim \text{i.i.d} \\ \ln \sigma_k^2 = \upsilon + \phi\left(\ln \sigma_{k-1}^2 - \upsilon\right) + \eta_k, \quad \eta_k \sim \text{i.i.d}N\left(0, \tau^2\right), \end{gathered} \tag{4}$$

where x_k denotes risky assets value loss in adjustment period (t_k, t_{k+1}), the loss can be defined as negative return, and $x_k = -(p_{t_{k+1}} - p_{t_k})/p_{t_k}$. Corresponding to formula (2), we use hundred yields. $p_{t_{k+1}}$ and p_{t_k} are assets value in adjustment time point; μ denotes expected loss of risky assets; z_k denotes residual items of independent identically distribution; σ_k denotes potential fluctuations; υ is constant terms of wave equation, and it denotes mean value of logarithmic fluctuations; η_k denotes wave disturbance level of independent identically distribution, which follows normal distribution with 0 mean and τ^2 variance; error term η_k and z_k are mutually independent; ϕ is continuous parameter, reflecting the influence of current fluctuation on the future, for $|\phi| < 1$; SV model is covariance stationary.

According to formula (3), we control gap risk less than α, namely, guarantee portfolio insurance with confidence level $1 - \alpha$, equivalent to

$$P\left\{x_k < \frac{1}{m_k}\right\} = \int_{-\infty}^{1/m_k} f\left(x_k\right) dx_k = 1 - \alpha, \tag{5}$$

where $f(x_k)$ is probability density function of loss x_k; the standard form of the above Formula (5) is

$$\begin{aligned} P\left\{x_k < \frac{1}{m_k}\right\} &= P\left\{\frac{x_k - \mu}{\sigma_k} < \frac{m_k^{-1} - \mu}{\sigma_k}\right\} \\ &= P\left\{z_k < g\left(m_k\right) = \frac{m_k^{-1} - \mu}{\sigma_k}\right\} \\ &= \int_{-\infty}^{g(m_k)} f\left(z_k\right) dz_k = 1 - \alpha. \end{aligned} \tag{6}$$

Therefore,

$$m_k = g^{-1}\left(F_Z^{-1}(1-\alpha)\right) = \left[\mu + \sigma_k F_Z^{-1}(1-\alpha)\right]^{-1}, \quad (7)$$

where σ_k can be obtained from SV modeling estimation and $F_Z^{-1}(1-\alpha)$, high fractal of $f(z_k)$ under confidence level $1-\alpha$, still needs to be estimated; $f(z_k)$ is probability density function of residual term z_k.

In the standard model, z_k is independent of identically distributed white noise, following normal distribution. In the application of SV modeling, because of the fact that return on assets series does not follow normal distribution, we always assume that z_k follows t distribution, generalized error distribution (GED), and mixed normal distribution to describe the kurtosis, fat tail, and skewness of return on assets. We introduce extreme value theory (EVT) to describe the characters of z_k from formula (7). We are interested in extreme risk of gap risks in CPPI strategy, that is, high score sites of loss distribution. We do not have to estimate the entire loss distribution because EVT can describe the tail of loss, accordingly avoid assumption of loss distribution, and reduce the risk of the model. Additionally, extreme value rarely occurs in real data, and estimate efficiency will be affected when estimating quantile by estimating distribution. However, EVT makes the extrapolation based on practice distribution smooth and thereby shows the entire shape of the tail rather than several losses in the tail. It suits the estimation under high confidence level involved in CPPI gap risk management.

Extreme value theory is used specifically for abnormal phenomena and small probability event. It is not modeled for the entire distribution but concentrates on the approximate expression of the tail distribution. Two types of model mainly include traditional block maxima and peaks over threshold (POT) model. POT model can use the original data more effectively when observed value exceeds a certain big enough threshold, especially for the financial risk measurement and modeling [15]. It is suitable for the description of extreme risk of gap risk in CPPI strategy. Thus, POT modeling was used to describe tail area of z_k distribution.

$F(x)$ denotes cumulative distribution function (CDF) of variable X; x_+ is upper extreme point of F. u denotes the big enough threshold value; the number of samples exceeding the threshold is N_u; $x_1, \ldots, x_{N_u}$ denotes sample observations of exceeding samples; let $y = x - u$; the exceeding loss distribution $F_u(y)$ is shown in

$$F_u(y) = P(X - u \le y \mid X > u) = \frac{F(y+u) - F(u)}{1 - F(u)}. \quad (8)$$

$F_u(y)$ defines probability distribution of exceeding loss on the right end, which is also cumulative probability distribution of variable exceeding u under the condition of $x > u$. According to Pickands III theorem [16], when $u \to x_+$, for a wide range probability distribution $F(x)$

$$\lim_{u \to x+} \sup_{0 \le y \le x_+ - u} \left|F_u(y) - G_{\xi,\beta(u)}(y)\right| = 0 \quad (9)$$

holds for certain ξ and $\beta(u)$. In other words, for a large enough threshold u, $F_u(y)$ tends to be generalized Pareto distribution (GPD) $G_{\xi,\beta(u)}(\cdot)$. Its function is as follows:

$$G_{\xi,\beta}(y) = \begin{cases} 1 - \left(1 + \dfrac{\xi y}{\beta}\right)^{-1/\xi} & \text{if } \xi \ne 0, \\ 1 - \exp\left(-\dfrac{y}{\beta}\right) & \text{if } \xi = 0. \end{cases} \quad (10)$$

ξ denotes shape parameter; β denotes scale parameter. After having the distribution function of exceeding loss, let $x = y + u$; the tail distribution function is shown as

$$F(x) = (1 - F(u))\, G_{\xi,\beta}(x-u) + F(u). \quad (11)$$

N denotes the total number of observed samples; N_u denotes the number of samples exceeding the threshold u. From empirical data, we get the estimated value of $F(u)$, $(N - N_u)/N$, which means that when x is large enough, the estimation of tail cumulative distribution is

$$\begin{aligned} F(x) &= \frac{N_u}{N}\left[1 - \left(1 + \frac{\xi}{\beta}(x-u)\right)^{-1/\xi}\right] + \left(1 - \frac{N_u}{N}\right) \\ &= 1 - \frac{N_u}{N}\left(1 + \frac{\xi}{\beta}(x-u)\right)^{-1/\xi}; \end{aligned} \quad (12)$$

and thus,

$$F_Z^{-1}(1-\alpha) = u + \frac{\beta}{\xi}\left[\left(\frac{N}{N_u}\alpha\right)^{-\xi} - 1\right]. \quad (13)$$

Putting it into formula (7), we get

$$m_k = \frac{1}{\mu + \sigma_k u + \sigma_k(\beta/\xi)\left[\left((N/N_u)\alpha\right)^{-\xi} - 1\right]}. \quad (14)$$

Formula (14) reveals the function relationship of multiple m and risky assets value, frequency of extreme price, or expected loss under the requirement of gap risk management. When risky assets value fluctuated wildly, reduce the multiple to reduce the risk exposure; when ξ is increasingly larger, corresponding multiple gets smaller and smaller. Parameter ξ depends on distribution shape and denotes the heaviness of tail distribution. It indicates that when there is more frequent extreme price, the risk exposure of CPPI portfolio should be reduced. μ denotes the expected loss of risky assets. When expected loss is small, enlarge multiple to increase risk exposure. It is intuitive that the proportion of risky assets in CPPI portfolio should be increased in bull market, but formula (14) reveals that multiple setting should consider other factors from a gap risk management perspective, not to overincrease risk exposure in bull market.

3. Empirical Studies

This paper selects the Shanghai composite index as a risky asset investment portfolio (from January 02, 1997, to December 31, 2010), for the following reasons. (1) From

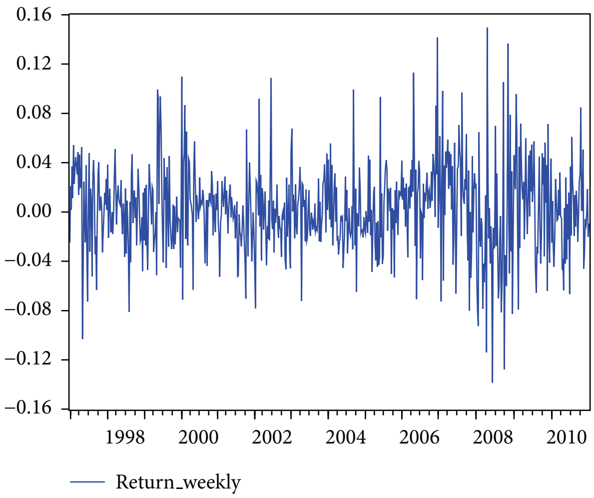

FIGURE 2: Time series of Shanghai composite index returns.

the perspective of risk measurement, the change of the Shanghai composite index can reflect system risk. Moreover, it covers the influence of extreme events such as Asian financial crisis that happened in 1997 and the United States financial crisis of 2008. (2) From the perspective of model estimation, the Shanghai composite index has been compiled for the longest time, which guarantees that there are enough samples, especially plenty of weekly return data. (3) From the perspective of the time span, because it was not until December 16, 1996, that the price limit regime began to be implemented, we choose the time span which is from January 1997 on so as to eliminate the abnormal samples resulting from the unsound regulations, such as a 105.27% boom in a single day on May 21, 1992. Corresponding to week by week fixed cycle adjustment principle, we analyze assets value changing by weekly return rate. 700 samples are included, with percentile return rate.

3.1. Data Description. Firstly, basic statistical description of return series is given. Figure 2 shows time series of Shanghai composite index returns, in which wave agglomeration effect can be seen in the series. Basic statistical description of return series can be seen in Table 1; P values of corresponding statistics are shown in brackets. Compared with the normal distribution (skewness 0 and kurtosis 3), skewness and kurtosis characteristics can be shown in return series. Meanwhile, Jarque-Bera normality test also shows a remarkable difference from normal distribution. Moreover, ADF test of unit root shows stability of return series, and Ljung-Box test shows a noticeable autocorrelation. Thus, time series of Shanghai composite index returns shows the characteristics of kurtosis, skewness, and aggregation, which is suitable for SV modeling and analysis.

3.2. Results. Secondly, dynamic multiple is set by model parameter estimation in formula (14). It is achieved by estimating the SV model by loss series of Shanghai composite index returns. Fluctuation in SV model is a latent variable,

TABLE 1: Statistical characteristics of shanghai composite index returns.

Statistical indicators	Value
Mean	0.002
Maximum	0.149
Minimum	−0.138
Standard deviation	0.035
Skewness	0.194
Kurtosis	4.570
J-B statistic	76.36 (0.000)
ADF test	−13.030 (0.000)
L-B $Q(5)$	14.006 (0.016)
L-B $Q(10)$	22.238 (0.014)

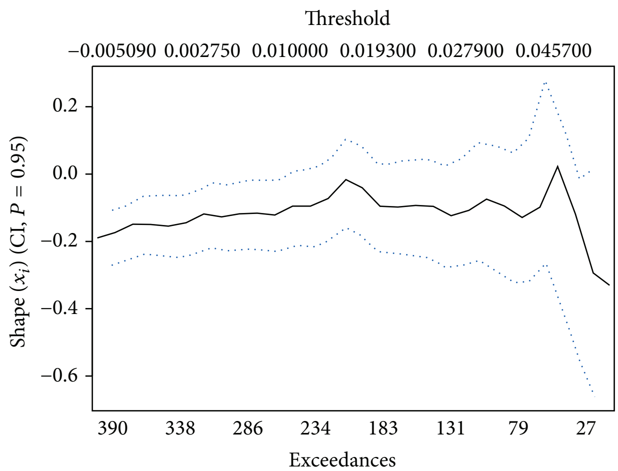

FIGURE 3: Estimates of shape parameter as a function of the threshold value.

and it is difficult to estimate the parameters by maximum likelihood method; thus, Bayesian principle and MCMC method are used in this paper [17]. By constructing a Markov chain for the sampling of given multivariate probability density, statistical inference is made with the help of ergodicity of Markov chain. Programmed and computed in Winbugs [18], the expected estimation values of Bayesian posterior distribution in SV modeling parameter are $\hat{\upsilon} = 0.007, \hat{\phi} = 0.859$, and $\hat{\tau} = 0.119$.

After that we estimate high fractal $F_Z^{-1}(1-\alpha)$ of residual sequence z_k. First of all, we choose an appropriate threshold value estimate generalized Pareto distribution parameter. Since shape parameter ξ is the limited index of distribution independent of threshold value u, an effective way to choose the threshold value (Figure 3) is to observe the shape parameter ξ estimation curve in different threshold value. Generally, we choose threshold value when shape parameter ξ is relatively stable.

$$F(x) = \frac{N_u}{N}\left[1 - \left(1 + \frac{\xi}{\beta}(x-u)\right)^{-1/\xi}\right] + \left(1 - \frac{N_u}{N}\right). \quad (15)$$

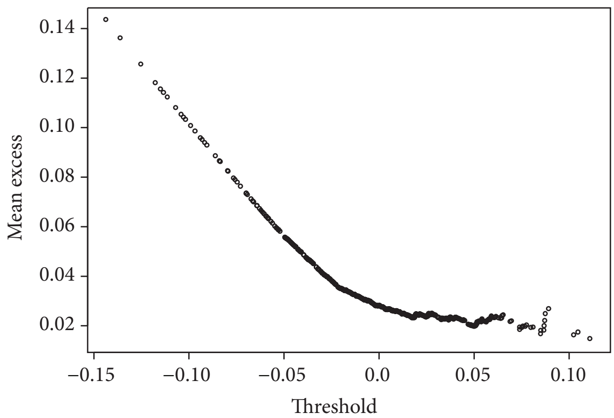

Figure 4: Empirical mean excess plot.

Table 2: Estimates of GPD parameters and quantile of residuals z_k.

u	$\hat{\xi}$	$\hat{\beta}$	N_u/N	$F_Z^{-1}(1-\alpha)$
0.045	−0.101	0.024	9.714%	0.133

Here, $u = 0.045$. We can also confirm through empirical mean excess function plot (EMEF), which is the curve of points $(u, e_N(u))$. The definition of $e_N(u)$ can be seen in formula (16). The basis for the selection is whether a linear trend is shown after exceeding a certain threshold. Figure 4 shows that threshold should be about 0.05. Considering the judgment from Figures 3 and 4, we choose the threshold value $u = 0.045$:

$$e_N(u) = \frac{\sum_{i=a}^{N}(x_i - u)}{N - a - 1}, \qquad a = \min\{i \mid x_i > u\}. \tag{16}$$

After u is given, we can have estimated value of parameters ξ and $\beta(u)$ based on maximum likelihood method estimation. For a given generalized Pareto distribution sample, $\{y_1, \ldots, y_{N_u}\}$, GPD log-likelihood function of GPD can be seen in formula (17). When $1-\alpha = 99.9\%$, calculate $F_Z^{-1}(1-\alpha)$; the results are shown in Table 2:

$$L(\xi, \beta \mid y) = \begin{cases} -N_u \ln\beta - \left(1 + \dfrac{1}{\xi}\right)\displaystyle\sum_{i=1}^{N_u} \ln\left(1 + \dfrac{\xi}{\beta} y_i\right) & \xi \neq 0, \\ -N_u \ln\beta - \dfrac{1}{\beta}\displaystyle\sum_{i=1}^{N_u} y_i & \xi = 0. \end{cases} \tag{17}$$

Figure 5 shows the sensitivity of 99.9% quantile estimates to changes in the threshold. Obviously, when the threshold value is large enough, the estimated value of $F_Z^{-1}(1-\alpha)$ is not sensitive to the change of u. This indicates that the estimation result has strong stability. Putting σ_k and parameter estimation results in Table 2 into formula (14), we have dynamic setting of multiple m in CPPI strategy (see Figure 6). The selection range of multiple is about 5~10,

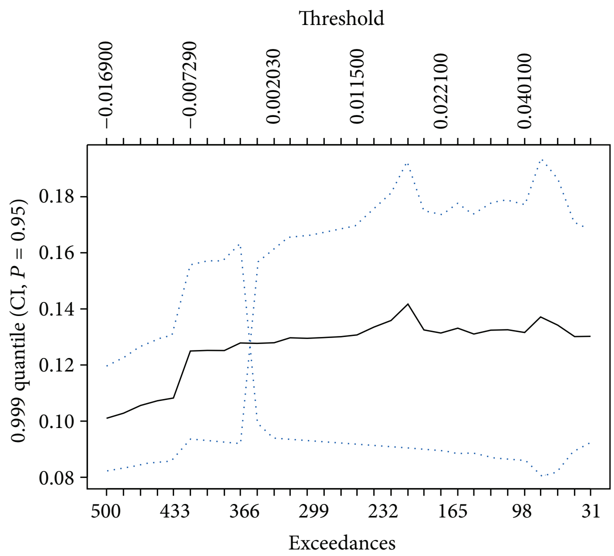

Figure 5: The sensitivity of 99.9% quantile estimates to changes in the threshold.

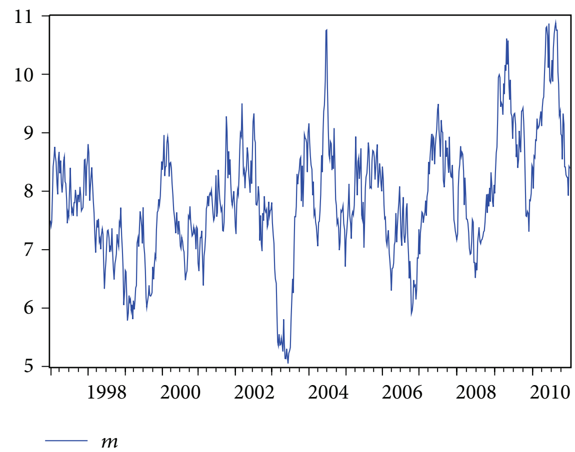

Figure 6: Determination of dynamic CPPI multiple.

and the mean and the median are both 7.8. This range is a little larger than the static multiple setting from Jessen [10]. Apart from different research methods, it is probably because dynamic multiple setting increased risky assets investment under the premise of gap risk avoiding, thus achieving a higher expected value.

4. Conclusions

From a perspective of gap risk management, this paper proposes a dynamic setting model of the parameter "Multiple" of CPPI strategy. According to the statistical estimation of extreme value change of risky asset by using SV-EVT approach, a dynamic choice of multiple is detailed as a function of time-varying asset volatility, expected loss, and the possibility of occurrence of extreme events in the active asset returns. The empirical illustration on Shanghai composite index data shows that the multiple should be chosen dynamically in the interval 5~10, which is larger than the static results in prior studies. Our research promotes the applicability of CPPI strategy in emerging capital market by providing useful reference and tools for CPPI investors to manage gap risk and choose a proper risk exposure level. The model demonstrates the effect of time-varying asset volatility, expected loss, and the possibility of occurrence of extreme events in the active asset returns on multiple setting. Therefore, investors can make decisions on changing multiple to manage gap risk based on analyzing market conditions from the above-mentioned three dimensions. Moreover, the model allows investors to choose a moderate risk control level according to their specific management target and risk preference.

Conflict of Interests

The authors declare that there is no conflict of interests regarding the publication of this paper.

Acknowledgment

This work is supported by the National Natural Science Foundation of China (Project no. 71073124).

References

[1] F. Black and R. Jones, "Simplifying portfolio insurance for corporate pension plans," *The Journal of Portfolio Management*, vol. 14, no. 4, pp. 33–37, 1988.

[2] G. Kingston, "Theoretical foundations of constant-proportion portfolio insurance," *Economics Letters*, vol. 29, no. 4, pp. 345–347, 1989.

[3] F. Black and A. F. Perold, "Theory of constant proportion portfolio insurance," *Journal of Economic Dynamics and Control*, vol. 16, no. 3-4, pp. 403–426, 1992.

[4] H. P. Huang and Y. F. Tang, "The application of CPPI strategy in guaranteed fund," *Management Review*, vol. 18, no. 4, pp. 10–13, 2006.

[5] J. S. Chen, C. L. Chang, J. L. Hou, and Y. T. Lin, "Dynamic proportion portfolio insurance using genetic programming with principal component analysis," *Expert Systems with Applications*, vol. 35, no. 1-2, pp. 273–278, 2008.

[6] J. S. Chen and B. P. Liao, "Piecewise nonlinear goal-directed CPPI strategy," *Expert Systems with Applications*, vol. 33, no. 4, pp. 857–869, 2007.

[7] H. I. Lee, M. H. Chiang, and H. Hsu, "A new choice of dynamic asset management: the variable proportion portfolio insurance," *Applied Economics*, vol. 40, no. 16, pp. 2135–2146, 2008.

[8] S. Balder, M. Brandl, and A. Mahayni, "Effectiveness of CPPI strategies under discrete-time trading," *Journal of Economic Dynamics & Control*, vol. 33, no. 1, pp. 204–220, 2009.

[9] R. Cont and P. Tankov, "Constant proportion portfolio insurance in the presence of jumps in asset prices," *Mathematical Finance*, vol. 19, no. 3, pp. 379–401, 2009.

[10] C. Jessen, "Constant proportion portfolio insurance: discrete-time trading and gap risk coverage," in *Proceedings of the 23rd Australasian Finance and Banking Conference*, Sydney, Australia, December 2010.

[11] R. F. Engle, "Autoregressive conditional heteroscedasticity with estimates of the variance of United Kingdom inflation," *Econometrica*, vol. 50, no. 4, pp. 987–1007, 1982.

[12] T. Bollerslev, "Generalized autoregressive conditional heteroskedasticity," *Journal of Econometrics*, vol. 31, no. 3, pp. 307–327, 1986.

[13] S. J. Taylor, "Modeling stochastic volatility: a review and comparative study," *Mathematical Finance*, vol. 4, no. 2, pp. 183–204, 1994.

[14] S. Kim, N. Shephard, and S. Chib, "Stochastic volatility: likelihood inference and comparison with ARCH models," *The Review of Economic Studies*, vol. 65, no. 3, pp. 361–393, 1998.

[15] A. J. McNeil and R. Frey, "Estimation of tail-related risk measures for heteroscedastic financial time series: an extreme value approach," *Journal of Empirical Finance*, vol. 7, no. 3-4, pp. 271–300, 2000.

[16] J. Pickands III, "Statistical inference using extreme order statistics," *The Annals of Statistics*, vol. 3, no. 1, pp. 119–131, 1975.

[17] S. Chib, F. Nardari, and N. Shephard, "Markov chain Monte Carlo methods for stochastic volatility models," *Journal of Econometrics*, vol. 108, no. 2, pp. 281–316, 2002.

[18] R. Meyer and J. Yu, "BUGS for a Bayesian analysis of stochastic volatility models," *Econometrics Journal*, vol. 3, no. 2, pp. 198–215, 2000.

Hindawi Publishing Corporation
Discrete Dynamics in Nature and Society
Volume 2014, Article ID 301282, 9 pages
http://dx.doi.org/10.1155/2014/301282

Research Article

Valuing Convertible Bonds Based on LSRQM Method

Jian Liu,[1] Lizhao Yan,[2] and Chaoqun Ma[3]

[1] *School of Economics and Management, Changsha University of Science and Technology, Changsha 410004, China*
[2] *Press, Hunan Normal University, Changsha 410081, China*
[3] *Business School, Hunan University, Changsha 410082, China*

Correspondence should be addressed to Jian Liu; ljorg@126.com

Received 11 March 2014; Accepted 23 May 2014; Published 24 June 2014

Academic Editor: Chuangxia Huang

Convertible bonds are one of the essential financial products for corporate finance, while the pricing theory is the key problem to the theoretical research of convertible bonds. This paper demonstrates how to price convertible bonds with call and put provisions using Least-Squares Randomized Quasi-Monte Carlo (LSRQM) method. We consider the financial market with stochastic interest rates and credit risk and present a detailed description on calculating steps of convertible bonds value. The empirical results show that the model fits well the market prices of convertible bonds in China's market and the LSRQM method is effective.

1. Introduction

Convertible bond is a hybrid financial derivative with the properties of the bond and option which can be converted to the underlying common stocks. The outstanding US convertible bond market stood at $240 billion in 2012 while the accumulative issuance was $404 billion from 1980 to 2011. The pricing problem is the key to the convertible bonds research, for the prices of convertible bonds immediately influence both the profits of the investors and the financing costs of the issuers.

The convertible bonds are difficult to be priced due to embedded American-style options from the provisions, such as callability and puttability, where the ability of the issuing firm to exercise its options depends on the path of the underlying stock price. Due to the uncertainty of the optimal exercise time, the problem of American option pricing cannot be solved with analytical solution methods such as B-S formula but can be solved with numerical methods, such as binary tree method, finite difference method, and finite element method. The binary tree method introduced by Cox et al. [1] is one of the most influential numerical methods to price American options. However, it is likely to increase the computation amount and may cause the curse of dimensionality when there are multiple stochastic factors in the market model. The finite difference method also hardly disposes the situation with two or more stochastic factors. Another choice is the Monte Carlo simulation method. Ammann et al. [2] show that the relationship between the number of stochastic factors and computing time is almost linear in the Monte Carlo framework. But the normal Monte Carlo method usually only suits the European options pricing, because the optimal exercise strategy algorithm to American options is backward while the Monte Carlo method is forward, which may cause incompatibility and generate deviation.

Longstaff and Schwartz [3] present the Least-Squares Monte Carlo (LSM) approach for pricing American options by simulation. Stentoft [4] makes a detailed analysis of the LSM approach and shows that the LSM method is computationally more efficient than finite difference methods and the Binomial Model when the number of assets is high. However, the pseudorandom number generated by Monte Carlo (MC) method in the LSM approach shows aggregation so that the convergence is very slow, the simulation variance is large, and the pricing efficiency is low. For that, an alternative method, namely, the quasi-Monte Carlo (QMC) method, is widely used in pricing financial derivatives [5–9]. The basic idea of QMC method is using more uniformly distributed points instead of random points. The QMC method is applied to evaluate the expectation of a random function path generated by a stochastic process and the convergence of QMC is asymptotically better than MC. However, the convergence order is related to the dimension, and the efficiency reduces for high-dimensional integrals. Some researchers present a Randomized Quasi-Monte Carlo (RQMC) method which overcomes the disadvantage of QMC. This paper uses a Least-Squares Randomized Quasi-Monte Carlo (LSRQM) method, which combines the LSM approach with RQMC method, to price the convertible bond.

Furthermore, as a kind of corporate bonds, the convertible bonds with long duration may involve credit risk. There are two methods to model the credit risk. One is using the credit risk premium to describe the credit risk, so the discount rate of the bond part value in convertible bonds equals the risk-free interest rate plus the credit risk premium, and the equity value is discounted by the risk-free interest rate. Details can be found in Ammann et al. [2]. The other one is using the default probability to reflect the credit risk. The value of convertible bonds turns to be the recovery value when bonds default, details can be found in Jarrow and Turnbull [10], Hung and Wang [11], Donald and Qin [12], Liu et al. [13], and Xu [14]; the latter uses the no-arbitrage principle to get the probability of default, and it is simple and convenient. So we use the latter method to model the credit risk involved in convertible bonds.

This paper prices convertible bonds with call and put provisions. Firstly, we model the financial market with the stochastic interest rates and the credit risk with suitable stochastic differential equations. Then, we describe the credit risk with Jarrow and Turnbull model. Furthermore, we present detailed calculation steps of convertible bonds values with LSRQM approach. Based on the theoretic analysis, we make a numerical simulation under determinate parameters and an empirical analysis using the data from China's market.

2. Market Model

2.1. Stock Price. Suppose the financial market is frictionless, efficient, and continuous in the time interval $[0, T]$, which is characterized by the probability space $(\Omega, \mathscr{F}, \{\mathscr{F}_t\}_{t\geq 0}, P)$. Ω denotes the state space, $\mathscr{F}$ is the σ-algebra of measurable events, $\{\mathscr{F}_t\}_{t\geq 0}$ is the σ-algebra filtration generated by a two-dimensional Brownian motion $\{\widetilde{B}^1, \widetilde{B}^2; t \leq T\}$, and P is the physical probability measure. Considering a convertible bond with callable and puttable provisions, the process of the underlying stock price satisfies the stochastic differential equation given by [15]

$$\begin{aligned} d\widetilde{S}_s &= \mu\left(\widetilde{r}_s, \widetilde{S}_s, s\right)\widetilde{S}_s ds \\ &\quad + \sigma_1\left(\widetilde{r}_s, \widetilde{S}_s, s\right)\widetilde{S}_s d\widetilde{B}_s^1 + \sigma_2\left(\widetilde{r}_s, \widetilde{S}_s, s\right)\widetilde{S}_s d\widetilde{B}_s^2, \\ \widetilde{S}_0 &= S_0 > 0, \end{aligned} \tag{1}$$

where $\widetilde{r}_s$ denotes the short rate at time s, μ denotes the drift, and the coefficients σ_1 and σ_2 are positive and describe the volatility of the stock price. All of the parameters are $\mathscr{F}_t$-adapted. As we will see, $\widetilde{B}_s^2$ represents the price fluctuation due to stock-specific randomness.

Table 1: Short-term interest rate models.

Model	a_0	b_0	$c(t)$	$d(t)$
Vasicek	$-a_0$	b_0	0	σ^2
Cox-Ingersoll-Ross	$-a_0$	b_0	σ^2	0
Ho-Lee	0	b_0	0	σ^2
Hull-White 1	$-a_0$	b_0	0	$\sigma(t)^2$
Hull-White 2	$-a_0$	b_0	$\sigma(t)^2$	0

2.2. Interest Rate. Assume that the process of risk-free short interest rate follows the stochastic differential equation:

$$\begin{gathered} d\widetilde{r}_s = \left(a_0(s) + b_0(s)\widetilde{r}_s\right)ds + \sqrt{c(s)\widetilde{r}_s + d(s)}d\widetilde{B}_s^1, \\ \widetilde{r}_0 = r_0. \end{gathered} \tag{2}$$

The parameters a_0, b_0, c, d are the deterministic functions of time t. This interest rate model is a general model which can be changed into classical interest rate models such as Vasicek and CIR model as choosing different form of parameters. See details in Table 1.

Models 1 and 2 are built in the real probability space which should be transformed into the risk-neutral probability space. So, define

$$\begin{gathered} u_{1t} = \frac{\left(a_0(t) - a(t)\right) + \left(b_0(t) - b(t)\right)\widetilde{r}_t}{\sqrt{c(t)\widetilde{r}_t + d(t)}}, \\ u_{2t} = \frac{\mu_t - \widetilde{r}_t - \sigma_1 u_{1t}}{\sigma_2(t)}, \\ M_t = \exp\left(-\int_0^t u_{1t} d\widetilde{B}_t^1 - \int_0^t u_{2t} d\widetilde{B}_t^2 \right. \\ \left. -\frac{1}{2}\int_0^t u_{1t}^2 d\widetilde{B}_t^1 - \frac{1}{2}\int_0^t u_{2t}^2 d\widetilde{B}_t^2\right). \end{gathered} \tag{3}$$

Let $dQ(\omega) = M_T(\omega)dP(\omega)$, $\omega \in \mathscr{F}_T^2$; then by Girsanov Theorem, Q is the risk-neutral probability measure in $\mathscr{F}_T$. Define $B_t^1 = \widetilde{B}_t^1 + \int_0^t u_{1s} ds$, $B_t^2 = \widetilde{B}_t^2 + \int_0^t((\mu_t - \widetilde{r}_t - \sigma_1 u_{1s})/\sigma_2)ds$, and then (B_t^1, B_t^2) is a two-dimensional Brownian motion with respect to Q, and the process of risk-free interest rate satisfies the following stochastic differential equation under Q:

$$\begin{gathered} dr_s = \left(a(s) - b(s)r_s\right)ds + \sqrt{c(s)r_s + d(s)}dB_s^1, \\ r_t = r_0. \end{gathered} \tag{4}$$

The process of the stock price satisfies the following stochastic differential equation under Q:

$$\begin{gathered} dS_s = r_s S_s ds + \sigma_1\left(r_s, S_s, s\right)S_s dB_s^1 + \sigma_2\left(r_s, S_s, s\right)S_s dB_s^2, \\ S_0 = S_0 > 0. \end{gathered} \tag{5}$$

So far the pricing space is transformed into the risk-neutral probability space that ensures that the convertible bond value is no-arbitrage and unique.

2.3. Credit Risk. We account for credit risk in the spirit of the methodology in Jarrow and Turnbull [10], where the credit risk is described by the default probability and the recovery value of the convertible bond by arbitrage-free valuation techniques. As the actual payoff in default is a complex problem, we take the recovery rate to the convertible bond in the event of default as an exogenously given constant like much literature does [10]. The recovery rate is assumed to be the same for all bonds in a given credit risk class. In this case, we can discount the cash flows both in the bond part and the equity part with the risk-free rate but not have to discount the bond part with the risk rate showing the credit spread as the usual practice. Actually, the probability of default has reflected the credit risk in the bond part, so the uncertainty is only from the fluctuation of the stock price and the risk-free rate.

As for the probability of default, many researchers have discussed its modeling. One method is to obtain the probability of default by calculating the corresponding intensity function of default which describes the default of the corporation. The intensity function model is developed by Litterman and Iben [16], Jarrow and Turnbull [10], and Duffie [17]. There are kinds of representations to the intensity function of default, such as the negative-exponential intensity model presented by Andersen and Buffum [18] and Linetsky [19], where the intensity function follows:

$$h(S) = \frac{e}{S^f}, \tag{6}$$

for some $e > 0$, $f > 0$, and they are both constants. The negative-exponential intensity model reflects the fact that the credit risks of corporations with high stock prices are less than the corporations with low stock prices. In order to describe the positive correlation between the default risk and the fluctuation, Carr and Linetsky [20] suppose that the intensity function of default is an affine function with respect to the spot volatility of the stock price given by

$$h(S) = g(t) + \frac{q\sigma_S^2}{S^{2(1-\alpha)}}, \tag{7}$$

where $g(t)$ is a nonnegative function of time and q is positive integer. Duffie et al. [21] discover that the probability of default depends on the stock price index and the interest rate.

Denote the probability of default in time interval $[i-1, i]$ by λ_i. When the interest rate is r_i and the stock price is S_i, the probability of default λ_{t_i} at time t_i can be expressed as

$$\lambda_{t_i} = 1 - e^{h(r_i, S_i)\Delta t}. \tag{8}$$

This method is complicated for application in that it relates to the parameter estimation problem in default intensity function. If the estimation is not accurate, the reliability of default probability is directly affected.

Another method is using the no-arbitrage principle to get the probability of default, such as Jarrow and Turnbull [10]. This method is simple and convenient and can fit the existing term structure of interest rate better. The paper uses this no-arbitrage method to calculate the probability of default. Denote the probability of default in each time interval $[i-1, i]$ by λ_{t_i}, $i = 1, 2, \ldots, n$, and the optimal stopping time of the convertible bond by τ; let

$$\lambda_\tau^* = -\frac{1}{\tau}\sum_{t=t_1}^{\tau} \ln(1 - \lambda_t). \tag{9}$$

Then

$$\prod_{t=t_1}^{\tau}(1 - \lambda_t) = e^{-\lambda_\tau^* \cdot \tau}. \tag{10}$$

When λ_i is small, we can obtain

$$\lambda_\tau^* \approx \frac{\sum_{t=t_1}^{\tau} \lambda_t}{\tau}. \tag{11}$$

Expression (11) means that λ_τ^* is the average intensity of default in the time interval $[0, \tau]$.

With the no-arbitrage principle, we get

$$e^{-r_\tau^*} = \left[1 \cdot (1 - \lambda_\tau^*) + \delta_\tau \cdot \lambda_\tau^*\right] e^{-R_\tau}, \tag{12}$$

where r_τ^* is the interest rate of the risky bond in the time interval $[0, \tau]$, R_τ is the risk-free interest rate, and δ_τ is the recovery rate of the convertible bond.

Then we have

$$\lambda_\tau^* = \frac{1 - e^{R_\tau - r_\tau^*}}{1 - \delta_\tau}. \tag{13}$$

So, we can firstly obtain the average intensity of default λ_τ^* with expression (13) and then deduce the probability of default in each time interval $\lambda_{t_i}, i = 1, 2, \ldots, n$ with expression (11). Furthermore, we assume that the recovery rate of the convertible bond is a constant δ.

2.4. General Expression of Convertible Bond Value. We consider the convertible bond with call and put provisions (see Table 2). The call provision allows the issuer to demand premature redemption for the call price applicable and to announce the intention to call a certain period in advance which is known as the call notice period. The put provision allows the investor to force the issuer to prematurely repurchase the bond for a certain predefined price. Consequently, the payoff of the convertible bond depends on the optimal strategies of the investor and the issuer which relate to the holding value and the intrinsic value. In each exercise time t_k, the convertible bond has four possible strategies, hold, conversion, redemption, and put-back. If the optimal strategy is held at time t_k, the cash flow of the convertible bond is 0 or the current interest. While if the optimal strategy is conversion, redemption, or put-back, the cash flow of the convertible bond is the conversion value, redemption value, and puttable value, respectively. After careful analysis, the value of convertible bond is given by

$$\begin{aligned}\max&\left[\min(\text{holding value}, \text{call value}),\right.\\ &\left.\text{put value}, \text{conversion value}\right].\end{aligned} \tag{14}$$

Let τ be the optimal exercise time, let ω be the path of state variables, and let $V(\omega;\tau)$ be the value of the convertible bond at time τ. Then in accordance with no-arbitrage principle, the value of the convertible bond at time 0 is given by [22]

$$V_0 = E^Q\left[e^{-\int_0^\tau r(\omega,t)dt}V(\omega;\tau)\right], \tag{15}$$

where Q is the risk-neutral probability.

3. Pricing Convertible Bond with LSRQM Method

3.1. Calculating Steps. Suppose there are n exercise times for the convertible bond for the duration T; that is, $0 < t_1 \le t_2 \le t_3 \le \cdots \le t_n = T$, respectively. The time interval $\Delta t = T/n$. In the spirit of Tsiveriotis and Femandes [23], the value of the convertible bond can be divided into two parts. One part is the equity value which involves the value converted to stock and exercising the embedded options. The other part is the bond value which involves the present value of the convertible bond with the principal plus interest and the residual value when the convertible bond defaults [24]. Let the face value of the convertible bond be F, let the probability of default at the time interval $[t_k, t_{k+1}]$ be $\lambda_{t_{k+1}}$, let the annual interest rate be $r(\omega;t_k)$, let the recovery rate be $\delta_{t_{k+1}}$, and let the recovery value be $\delta_{t_{k+1}}F$.

At any given time, the convertible bond has the possibility of default. That is to say, there are three kinds of cash flow prior to the due time, interest, equity value, and recovery value, and there are principals at the end. The interest promised in the contract is usually fixed and will be paid if the bond does not default. The equity value related to the optimal exercise time is the bond value when the bond is redeemed, sold back, and converted if the bond does not default. The bond value only has the recovery value when the bond defaults. If the bond does not default, the holding value of the convertible bond at time t_{k+1} for every path can be expressed by

$$\begin{aligned} h(\omega;t_k) &= e^{-r(\omega;t_k)\cdot\Delta t}\cdot\left[\left(1-\lambda_{t_{k+1}}\right)\cdot C(\omega;t_{k+1}) + D(\omega;t_{k+1})\right.\\ &\left.\quad\cdot\prod_{t=t_{k+1}}^{t^*}(1-\lambda_t) + \lambda_{t_{k+1}}\delta_{t_{k+1}}F\right]. \end{aligned} \tag{16}$$

In general, the holding value of the convertible bond at time t_{k+1} for every path can be expressed by

$$\begin{aligned} h(\omega;t_k) &= e^{-r(\omega;t_k)\cdot\Delta t}\cdot\left\{\prod_{t=t_{k+1}}^{t_\tau}(1-\lambda_t)\cdot C(\omega;t_{k+1})\right.\\ &\quad + \prod_{t=t_{k+1}}^{t^*}(1-\lambda_t)D(\omega;t_\tau) + \lambda_{t_{k+1}}\delta_{t_{k+1}}F\\ &\quad + \sum_{n=k+1}^{\tau-1}e^{-\sum_{m=k+1}^{n}r(\omega;t_m)\cdot\Delta t}\\ &\quad\left.\times\left(\prod_{m=k+1}^{n}\left(1-\lambda_{t_m}\right)\right)\lambda_{t_{n+1}}\delta_{t_{n+1}}F\right\}. \end{aligned} \tag{17}$$

t_τ is the optimal stopping time at which it is optimal for either the issuer or the investor to terminate the convertible bond, if the bond is not exercised before time t_k. t^* denotes time points of paying interest, and $C(\omega;t_{k+1})$ denotes the time-t_{k+1} discounted value of the equity part value if the bond does not default at time t_{k+1}. $D(\omega;t_\tau)$ denotes the time-t_{k+1} discounted value of the interest at the time interval $[t_k, t_\tau)$.

Accordingly, the value of the convertible bond at time t_k is given by

$$\begin{aligned} V(\omega;t_k) = \max&\left[\min\left(EH(\omega;t_k), V^{\text{call}}(\omega;t_k)\right),\right.\\ &\left.V^{\text{con}}(\omega;t_k), V^{\text{put}}(\omega;t_k)\right], \end{aligned} \tag{18}$$

where $V^{\text{call}}(\omega;t_k)$, $V^{\text{con}}(\omega;t_k)$, $V^{\text{put}}(\omega;t_k)$ denote the values of redemption, conversion, and put-back, respectively, $EH(\omega;t_k)$ is the expected holding value. We can determine the optimal strategy of the convertible bond with (18).

Based on the above discussion, we get the calculation steps for the convertible bond with call and put provisions and the credit risk as follows.

(1) Simulate M paths of state variables (stock and interest rate).

(2) At the last time t_n, the cash flow of the convertible bond for every path is given by

$$C(\omega;t_n) = \max\left[h(\omega;t_n), V^{\text{con}}(\omega;t_n)\right], \tag{19}$$

where $h(\omega;t_n)$ is the face value plus the interest at the maturity. Denote $t_\tau = t_n$, $\tau = n$.

(3) At time t_{n-1}, we get the holding value for every path as follows:

$$\begin{aligned} h(\omega;t_{n-1}) &= e^{-r(\omega;t_{n-1})\cdot\Delta t}\cdot\left\{\left(1-\lambda_{t_n}\right)\cdot\left[C(\omega;t_n)+D(\omega;t_n)\right]\right.\\ &\quad\left.+\lambda_{t_n}\delta_{t_n}F\right\}. \end{aligned} \tag{20}$$

(4) With the least square method, we regress $h(\omega;t_{n-1})$ on basis function of the time-t_{n-1} state variables $(S(\omega;t_{n-1}), r(\omega;t_{n-1}))$ denoted by $L_j(S(\omega;t_{n-1}), r(\omega;t_{n-1}))$, $j = 1\cdots K$, and get the regression coefficients $\{a_1(\omega;t_{n-1}), a_2(\omega;t_{n-1}),\ldots,a_K(\omega;t_{n-1})\}$, so the conditional expectation function is represented as a linear combination of basis functions denoted by $H(\omega;t_{n-1})$ as follows:

$$H(\omega;t_{n-1}) = \sum_{j=0}^{K}a_j(\omega;t_{n-1})\cdot L_j\left(S(\omega;t_{n-1}), r(\omega;t_{n-1})\right). \tag{21}$$

(5) Substituting the state variables $(S(\omega; t_{n-1}), r(\omega; t_{n-1}))$ into regression (21), we get the estimated expected holding value for each path ω denoted by $E\widehat{H}(\omega; t_{n-1})$.

(6) Comparing the $E\widehat{H}(\omega; t_{n-1})$ with other kinds of value, the value of convertible bond at time t_{n-1} for each path ω can be expressed as

$$V(\omega; t_{n-1}) = \max\Big[\min\Big(E\widehat{H}(\omega; t_{n-1}), V^{\text{call}}(\omega; t_{n-1})\Big), V^{\text{con}}(\omega; t_{n-1}), V^{\text{put}}(\omega; t_{n-1})\Big]. \tag{22}$$

Then, the optimal strategy and the cash flow at time t_{n-1} for each path are given as follows.

(a) If $V(\omega; t_{n-1}) = E\widehat{H}(\omega; t_{n-1})$, the investor will keep holding the convertible bond, and the equity value at time t_{n-1} is $C(\omega; t_{n-1}) = C(\omega; t_n)e^{-r(\omega; t_{n-1})\Delta t}$.

(b) If $V(\omega; t_{n-1}) = V^{\text{call}}(\omega; t_{n-1})$, the issuer will redeem the convertible bond, and the investor will obtain the call value. Then the equity value at time t_{n-1} is $C(\omega; t_{n-1}) = V^{\text{call}}(\omega; t_{n-1})$.

(c) If $V(\omega; t_{n-1}) = V^{\text{con}}(\omega; t_{n-1})$, the investor will convert the bond into the underlying stock under the agreed conversion price and get the conversion value. Then the equity value at time t_{n-1} is $C(\omega; t_{n-1}) = V^{\text{con}}(\omega; t_{n-1})$.

(d) If $V(\omega; t_{n-1}) = V^{\text{put}}(\omega; t_{n-1})$, the investor will sell back the bond to the issuer under the agreed price and get the put value. Then the equity value at time t_{n-1} is $C(\omega; t_{n-1}) = V^{\text{put}}(\omega; t_{n-1})$.
If the convertible bond is redeemed, converted, and sold back, denote $t_\tau = t_{n-1}$, $\tau = n-1$.

(7) Work backwards, and repeat step 3 to step 6 for the time $t_{n-2}, t_{n-3}, \ldots, t_1$. The discounted value of the cash flow calculated with the optimal strategy after time t_k can be expressed as

$$\begin{aligned} h(\omega; t_k) &= e^{-r(\omega; t_k)\cdot\Delta t} \\ &\quad \cdot \Bigg\{ \prod_{t=t_{k+1}}^{t_\tau} (1-\lambda_t)\cdot C(\omega; t_{k+1}) \\ &\quad + \prod_{t=t_{k+1}}^{t^*} (1-\lambda_t) D(\omega; t_\tau) + \lambda_{t_{k+1}} \delta_{t_{k+1}} F \\ &\quad + \sum_{n=k+1}^{\tau-1} e^{-\sum_{m=k+1}^{n} r(\omega; t_m)\cdot\Delta t} \\ &\quad \times \left(\prod_{m=k+1}^{n} (1-\lambda_{t_m}) \right) \lambda_{t_{n+1}} \delta_{t_{n+1}} F \Bigg\}. \end{aligned} \tag{23}$$

With the least square method, we get the regression function $H(\omega; t_k)$ and the estimated expected holding value $E\widehat{H}(\omega; t_k)$. Then, we get the equity value of the convertible bond at each time for each path $C(\omega; t_k)$, $t_1 \le t_k \le t_n = T$.
If the convertible bond is redeemed, converted, and sold back, update the optimal stopping time by $t_\tau = t_k$, $\tau = k$.

(8) Finally, the price of convertible bond at time 0 is the mean of the discounted value of time-t_1 cash flow for all M paths, which can be expressed as

$$\begin{aligned} V_0 &= E_Q \Bigg\{ e^{-r(\omega;\,0)\cdot\Delta t} \\ &\quad \cdot \Bigg[\prod_{t=t_1}^{t_\tau} (1-\lambda_t)\cdot C(\omega; t_1) \\ &\quad + \prod_{t=t_1}^{t^*} (1-\lambda_t) D(\omega; t_\tau) + \lambda_{t_1} \delta_{t_1} F \\ &\quad + \sum_{n=1}^{\tau-1} e^{-\sum_{m=1}^{n} r(\omega; t_m)\cdot\Delta t} \\ &\quad \times \left(\prod_{m=1}^{n} (1-\lambda_{t_m}) \right) \lambda_{t_{n+1}} \delta_{t_{n+1}} F \Bigg] \mid \mathcal{F}_0 \Bigg\} \\ &= \frac{1}{M} \sum_{i=1}^{M} e^{-r(\omega_i;\,0)\cdot\Delta t} \\ &\quad \cdot \Bigg[\prod_{t=t_1}^{t_\tau(\omega_i)} (1-\lambda_t)\cdot C(\omega_i; t_1) \\ &\quad + \prod_{t=t_1}^{t^*(\omega_i)} (1-\lambda_t) D(\omega_i; t_\tau) + \lambda_{t_1} \delta_{t_1} F \\ &\quad + \sum_{n=1}^{\tau(\omega_i)-1} e^{-\sum_{m=1}^{n} r(\omega; t_m)\cdot\Delta t} \\ &\quad \times \left(\prod_{m=1}^{n} (1-\lambda_{t_m}) \right) \lambda_{t_{n+1}} \delta_{t_{n+1}} F \Bigg]. \end{aligned} \tag{24}$$

3.2. RQMC Method. For the numerical method of the convertible bond pricing, an important problem is to simulate the path of state variables. The distribution of state variables is generally related to a normal distribution, so the simulation needs to generate the random numbers of normal distribution which is generated by the random numbers of uniform distribution at the interval $[0, 1]$. Therefore, the simulation of random numbers with uniform distribution at the interval $[0, 1]$ plays an important role in simulation. The MC method used in the LSM approach employs the pseudorandom numbers which show aggregation and make the convergence too slow. QMC method uses low-discrepancy sequences which generate more uniformly distributed points in order to have high accuracy. The main low-discrepancy sequences are Halton sequences, Faure sequences, Sobol sequences, and so on. Halton sequences are sensitive to the dimensions, while Faure sequences and Sobol sequences are not, so the latter two are employed in the high-dimensional situation.

Based on the Koksma-Hlawka inequality, the asymptotic convergence order of QMC method is $O((\log N)^d/N)$, which is generally better than the $O(1/\sqrt{N})$ of MC method. However, $(\log N)^d/N$ may be smaller than $1/\sqrt{N}$ when the dimension is high enough. In order to improve the QMC method in the high-dimensional situation, dimension reduction techniques are specially designed, such as the linear transformation method, the ordinary Brownian bridge [25, 26], and the principal component analysis (PCA). The linear transformation method is not easy to implement for some complex optimization problems in it. The PCA method outperforms the ordinary Brownian bridge method in most examples, so we use PCA method to conduct the high-dimensional problem in the QMC. Furthermore, to get better convergence and reduce the actual error in QMC, we employ the RQMC method instead of QMC.

Based on the above analysis, this paper uses the Randomized Quasi-Monte Carlo (RQMC) method to simulate the paths of state variables. That means step 1 of the convertible bond pricing in Section 3.1 can be refined as the following steps.

(a) Generate d-dimensional Sobol sequence in $[0,1]^d$ denoted by

$$\left\{x^{(i)}\right\}, \quad i = 1, 2, \ldots, M. \tag{25}$$

(b) Generate the stochastic variables with uniform distribution in $[0,1]^d$ denoted by $\varepsilon^{(i)}$. Let

$$z^{(i)} = \operatorname{mod}\left\{x^{(i)} + \varepsilon^{(i)}, 1\right\}. \tag{26}$$

(c) Convert the $z^{(i)}$ into random numbers of normal distribution with Moro algorithm.

(d) Reduce the dimension with PCA method; then get the two-dimensional Brownian motion $(B^1_{t_i}, B^2_{t_i})$.

(e) Obtain M paths of each state variable with the corresponding difference equation.

4. Numerical Experiment

This section makes a numerical experiment for the convertible bond pricing in risk-neutral space and explores the influence of stochastic interest rate and credit risk on convertible bond prices. Firstly, with the stock price model of (5) and Ito's formula, we get

$$\begin{aligned} d\ln S_t &= \frac{1}{S_t} dS_t - \frac{1}{2}\frac{1}{S_t^2}(dS_t)^2 \\ &= \left[r_t - \frac{1}{2}\left(\sigma_1^2 + \sigma_2^2\right)\right] dt + \sigma_1 dB^1_t + \sigma_2 dB^2_t. \end{aligned} \tag{27}$$

Then the stock price process satisfies the following difference equation:

$$\begin{aligned} S_{t+\Delta t} = S_t \times \exp\bigg\{ & \left[r_t - \frac{1}{2}\left(\sigma_1^2 + \sigma_2^2\right)\right]\Delta t \\ & + \sigma_1\left(B^1_{t+\Delta t} - B^1_t\right) + \sigma_2\left(B^2_{t+\Delta t} - B^2_t\right)\bigg\}, \end{aligned} \tag{28}$$

and with the interest rate model of (4), the process of interest rate satisfies the following difference equation:

$$r_{t+\Delta t} = r_t + (a - br_t)\Delta t + \sqrt{cr_t + d}\left(B^1_{t+\Delta t} - B^1_t\right). \tag{29}$$

We consider a three-year convertible bond with call and put provisions. Assume that the face value of the convertible bond is 100, the annual interest rate is 2.5%, the interest is paid at the end of each year, and the initial conversion price is $p = 28$; then the convertible value for time t is $V_t^{\text{con}} = (S_t/P) \times 100$. Other parameters in the given model are as follows:

$$\begin{gathered} S_0 = 22, \qquad r_0 = 0.06, \\ a = 0.05, \qquad b = 0.012, \\ c = 0.054, \qquad d = 0.036, \\ \sigma_1 = 0.08, \qquad \sigma_2 = 0.11, \\ \Delta t = \frac{1}{100}, \\ V^{\text{call}} = 120, \qquad V^{\text{put}} = 102, \\ \lambda = 0.08, \qquad \delta = 0.5. \end{gathered} \tag{30}$$

On Matlab software, we get the price of the convertible bond which is 97.86. Figure 1 shows the optimal exercise time of the convertible bond with call and put provisions. When there is no restrictive period to call and put provisions, the optimal exercise time of the convertible bond will centralize in the earlier stage. As a matter of fact, convertible bonds existing in the financial market have some banned puttable period.

5. Empirical Analysis

5.1. Data. In this section, we make an empirical study using the data of China's stock market. In recent years, the convertible bond market in China has developed rapidly. In 2012, the issuance of convertible bonds in China is nearly 100 billion Yuan. By the end of 2012, there are 21 convertible bonds traded in Shanghai stock exchange and Shenzhen stock exchange, 15 of which are in Shanghai stock exchange. The credit ratings of convertible bonds in China are all above AA-, and 10 of them are AAA, and only 2 are AA-. In China's market, the face value of all the convertible bonds is 100 Yuan, with maturities of generally 5-6 years, annual interest rates less than one-year bank deposit interest rate which is 3% now, and the interest paid once each year. Convertible bonds existing in China's market have four additional provisions, namely, general call provisions, conditional call provisions

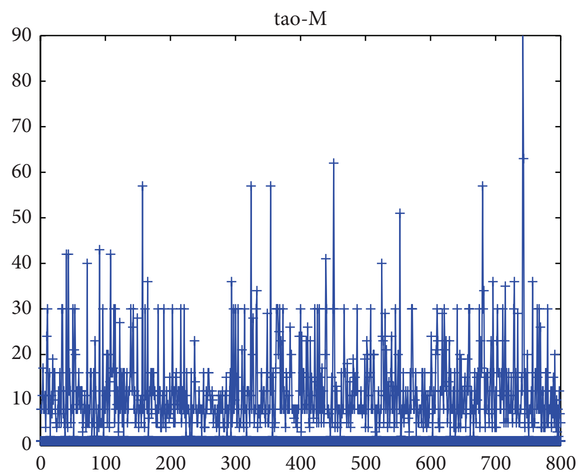

Figure 1: Optimal exercise time of convertible bond.

(soft call provisions), conditional put provisions, and general put provisions. Considering that the credit risk is involved in the pricing model of the convertible bond, we choose two convertible bonds, XGZZ and BHZZ, with different credit ratings as the sample, whose additional provisions both are the call provision and the general put provision.

The time interval of the sample data is from October 2009 to October 2012, the stock price is the daily closing price, and the interest rate model is estimated based on the closing yield to maturity of treasury. The data of convertible bonds prices, underlying stocks prices, and yield to maturity of treasury are taken from China Stock Market Accounting Research (CSMAR) database.

5.2. Stock Price and Interest Rate. Now, we estimate the parameters in stock price model and interest rate model with MLE method, and the likelihood function needs to be deduced firstly. We assume that the market price of risk equals 0. With difference equation (28), we get

$$(\ln S_{t+\Delta t} \mid \ln S_t) \sim N\left(\ln S_t + \left[r_t - \frac{1}{2}\left(\sigma_1^2 + \sigma_2^2\right)\right]\Delta t, \left(\sigma_1^2 + \sigma_2^2\right)\Delta t\right). \quad (31)$$

With difference equation (29), one has

$$(r_{t+\Delta t} \mid r_t) \sim N\left(r_t + (a - br_t)\Delta t, (cr_t + d)\Delta t\right). \quad (32)$$

So the joint distribution of $(\ln S_{t+\Delta t}, r_{t+\Delta t} \mid \ln S_t, r_t)$ follows the bivariate normal distribution $N_2(\mu, \Sigma)$, where

$$\mu = \begin{pmatrix} \ln S_t + \left[r_t - \frac{1}{2}\left(\sigma_1^2 + \sigma_2^2\right)\right]\Delta t \\ r_t + (a - br_t)\Delta t \end{pmatrix},$$
$$\Sigma = \begin{pmatrix} \left(\sigma_1^2 + \sigma_2^2\right)\Delta t & \sigma_1\sqrt{cr_t + d}\Delta t \\ \sigma_1\sqrt{cr_t + d}\Delta t & (cr_t + d)\Delta t \end{pmatrix}, \quad (33)$$

and the correlation coefficient is $\rho = \sigma_1 / \sqrt{\sigma_1^2 + \sigma_2^2}$.

We divide the time interval $[0, T]$ into n equal parts, then $\Delta t = T/n$, and the stock price and interest rate of the kth part are S_k and r_k. Based on the above analysis, we get the likelihood function as follows:

$$\begin{aligned} L(a, b, c, d, \sigma_1, \sigma_2) &= P(\ln S_1, \ln S_2, \ldots, \ln S_n;\ r_1, r_2, \ldots, r_n) \\ &= \prod_{k=1}^{n-1} P(\ln S_{k+1}, r_{k+1} \mid \ln S_k, r_k), \end{aligned} \quad (34)$$

where $P(\ln S_{k+1}, r_{k+1} \mid \ln S_k, r_k)$ can be obtained with the joint density function of $(\ln S_{t+\Delta t}, r_{t+\Delta t} \mid \ln S_t, r_t)$. On Matlab software and with historical data, we get the above parameter estimates, which are denoted by $\hat{a}, \hat{b}, \hat{c}, \hat{d}, \hat{\sigma}_1, \hat{\sigma}_2$.

After obtaining the parameter estimates $\hat{a}, \hat{b}, \hat{c}, \hat{d}, \hat{\sigma}_1, \hat{\sigma}_2$, we can use the RQMC method to simulate the process of stock prices and interest rates with difference equations (28) and (29).

5.3. Default Rate and Recovery Value. For each path, we can obtain the optimal exercise time τ for convertible bonds with the LSROM method, and the interest rate of a risky bond is r_τ^* and the interest rate of risk-free bonds is R_τ. Both of them can be obtained with the term structure of interest rate. The recovery rate is a constant of δ when the bond defaults; then the average default intensity at time interval $[0, \tau]$ is

$$\lambda_\tau^* = \frac{1 - e^{R_\tau - r_\tau^*}}{1 - \delta}. \quad (35)$$

So, the price of the convertible bond at time 0 can be written as

$$\begin{aligned} V_0 = \frac{1}{M}\sum_{i=1}^{M} e^{-r(\omega_i;\,0)\cdot\Delta t} \cdot \Bigg[&\prod_{t=t_1}^{t_\tau(\omega_i)} (1 - \lambda_t) \cdot C(\omega_i; t_1) \\ &+ \prod_{t=t_1}^{t^*(\omega_i)} (1 - \lambda_t) D(\omega_i; t_\tau) + \lambda_{t_1}\delta_{t_1}F \\ &+ \sum_{n=1}^{\tau(\omega_i)-1} e^{-\sum_{m=1}^{n} r(\omega; t_m)\cdot\Delta t} \\ &\times \left(\prod_{m=1}^{n}\left(1 - \lambda_{t_m}\right)\right)\lambda_{t_{n+1}}\delta F \Bigg]. \end{aligned} \quad (36)$$

5.4. Basis Functions. Stentoft [27] made numerical analysis to the deviation of American option price which is obtained with the LSM method through choosing a different number of basis functions. The results show that there is no monotonous relationship between the number of basis functions and the pricing deviation. That is to say, increasing the number of basis functions does not always decrease the pricing

Table 2: Sample of convertible bonds.

Item	Issuing date	Maturity date	Conversion price	Provision	Credit rating
XGZZ	2008.8.21	2013.8.21	5.88 Yuan	Call, put	AA+
BHZZ	2009.9.23	2014.9.23	6.16 Yuan	Call, put	AA−

Table 3: Estimates of parameters in convertible bond pricing model.

Name	$\hat{a}$	$\hat{b}$	$\hat{c}$	$\hat{d}$	$\hat{\sigma}_1$	$\hat{\sigma}_2$
XGZZ	0.0351	0.1264	0.0693	0.05694	0.2534	0.1053
BHZZ	0.0492	0.0588	0.1042	0.1257	0.3291	0.0859

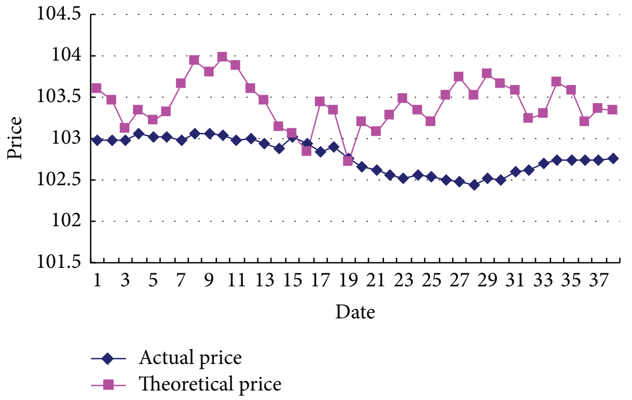

Figure 2: Comparison of theoretical price with actual price of XGZZ.

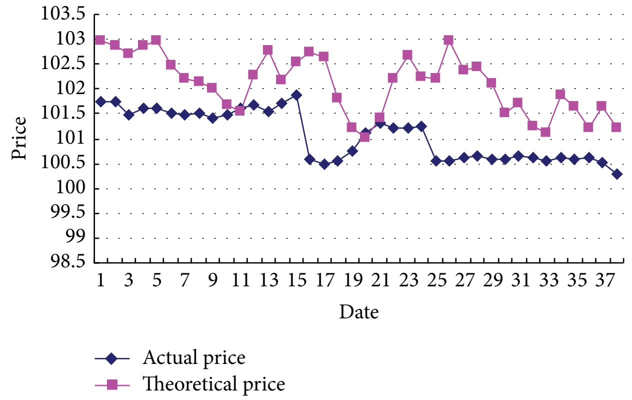

Figure 3: Comparison of theoretical price with actual price of BHZZ.

deviation, especially in the case of the out-of-the-money option. However, increasing the paths of simulation and basis functions will contribute to the pricing deviation reduction.

As to numerical stability, Laguerre polynomial is not the optimal choice for basis functions, but the converted Legendre polynomial is more effective than the general Chebyshev polynomial. Considering the calculation time and the computational accuracy, the better choice is the ordinary monomial for regressor. Since an increase in the number of basis functions cannot reduce the pricing deviation significantly but increase the computational amount greatly, we select ordinary monomials as basis functions with the number $K = 5$, that is, $S_t, r_t, S_t^2, r_t^2, S_t r_t$, respectively.

5.5. Results. This paper selects the data from October, 2009, to September, 2012, as the sample and obtains the estimate parameters of the convertible bond pricing models with the MLE method as shown in Table 3. Furthermore, we obtain the comparison between theoretical prices and real market prices of the two convertible bonds, XGZZ and BHZZ, from October to November, 2012, as shown in Figures 2 and 3, respectively. The average pricing deviation of XGZZ is 2.72%, and the average pricing deviation of BHZZ is 1.86%. Obviously, the pricing of BHZZ is better than XGZZ's. The different deviations between the two convertible bonds may be due to the different terms to maturity; XGZZ is closer to the maturity date than BHZZ.

6. Conclusions

This paper studies the pricing problem of convertible bonds with LSRQM method. Extending existing approaches, the method is capable of accounting for the complex convertible bond with call and put provisions. Pricing convertible bonds with Randomized Quasi-Monte Carlo simulation is more flexible than previous Monte Carlo methods because it is effective for high-dimensional cases.

We model the financial market with stochastic interest rates and credit risk with suitable stochastic differential equations and describe the credit risk with Jarrow and Turnbull model. Furthermore, we present detailed calculation steps of convertible bonds values with LSRQM approach. Based on the theoretical analysis, we make a numerical simulation under determinate parameters and an empirical analysis using data in China's market. The results verify the validity of the proposed method.

Conflict of Interests

The authors declare that there is no conflict of interests regarding the publication of this paper.

Acknowledgments

The authors would like to express their gratitude to the supports given by the Natural Science Foundation of China (no. 71201013), the National Natural Science Innovation Research Group of China (no. 71221001), and the Innovation Platform Open Funds for Universities in Hunan Province of China (no. 13K059).

References

[1] J. C. Cox, S. A. Ross, and M. Rubinstein, "Option pricing: a simplified approach," *Journal of Financial Economics*, vol. 7, no. 3, pp. 229–263, 1979.

[2] M. Ammann, A. Kind, and C. Wilde, "Simulation-based pricing of convertible bonds," *Journal of Empirical Finance*, vol. 15, no. 2, pp. 310–331, 2008.

[3] F. A. Longstaff and E. S. Schwartz, "Valuing American options by simulation: a simple least-squares approach," *Review of Financial Studies*, vol. 14, no. 1, pp. 113–147, 2001.

[4] L. Stentoft, "Assessing the Least Squares Monte-Carlo approach to American option valuation," *Review of Derivatives Research*, vol. 7, no. 2, pp. 129–168, 2004.

[5] P. A. Acworth, M. Broadie, and P. Glasserman, "A comparison of some Monte Carlo and quasi Monte Carlo techniques for option pricing," in *Monte Carlo and Quasi-Monte Carlo Methods 1996*, pp. 1–18, Springer, New York, NY, USA, 1998.

[6] J. Imai and K. S. Tan, "Minimizing effective dimension using linear transformation," in *Monte Carlo and Quasi-Monte Carlo Methods 2002*, pp. 275–292, Springer, Berlin, Germany, 2004.

[7] W. J. Morokoff, "Generating quasi-random paths for stochastic processes," *SIAM Review*, vol. 40, no. 4, pp. 765–788, 1998.

[8] B. Moskowitz and R. E. Caflisch, "Smoothness and dimension reduction in quasi-Monte Carlo methods," *Mathematical and Computer Modelling*, vol. 23, no. 8-9, pp. 37–54, 1996.

[9] F. Wen, Z. He, and X. Chen, "Investors'risk preference characteristics and conditional skewness," *Mathematical Problems in Engineering*, vol. 2014, Article ID 814965, 14 pages, 2014.

[10] R. A. Jarrow and S. M. Turnbull, "Pricing derivatives on financial securities subject to credit risk," *Journal of Finance*, vol. 50, no. 1, pp. 53–85, 1995.

[11] M. W. Hung and J. Y. Wang, "Pricing convertible bonds subject to default risk," *The Journal of Derivatives*, no. 4, pp. 75–87, 2002.

[12] R. C. Donald and L. Qin, "A tree model for pricing convertible bonds with equity, interest rate, and default risk," *The Journal of Derivatives*, no. 2, pp. 25–46, 2007.

[13] J. Liu, J. Xiao, L. Yan, and F. Wen, "Valuing catastrophe bonds involving credit risks," *Mathematical Problems in Engineering*, vol. 2014, Article ID 563086, 6 pages, 2014.

[14] R. Xu, "A lattice approach for pricing convertible bond asset swaps with market risk and counterparty risk," *Economic Modelling*, vol. 28, no. 5, pp. 2143–2153, 2011.

[15] J. Liu, M. Tao, C. Ma, and F. Wen, "Utility indifference pricing of convertible bonds.," *International Journal of Information Technology & Decision Making*, vol. 13, no. 2, pp. 429–444, 2014.

[16] R. Litterman and T. Iben, "Corporate bond valuation and the term structure of credit spreads," *Journal of Portfolio Management*, pp. 52–64, 1991.

[17] D. Duffie, "Credit swap valuation," *Financial Analysts Journal*, vol. 55, no. 1, pp. 73–87, 1999.

[18] L. Andersen and D. Buffum, "Calibration and implementation of convertible bond models," *Journal of Computational Finance*, vol. 7, no. 2, pp. 1–34, 2004.

[19] V. Linetsky, "Pricing equity derivatives subject to bankruptcy," *Mathematical Finance*, vol. 16, no. 2, pp. 255–282, 2006.

[20] P. Carr and V. Linetsky, "A jump to default extended CEV model: an application of Bessel processes," *Finance and Stochastics*, vol. 10, no. 3, pp. 303–330, 2006.

[21] D. Duffie, L. Saita, and K. Wang, "Multi-period corporate default prediction with stochastic covariates," *Journal of Financial Economics*, vol. 83, no. 3, pp. 635–665, 2007.

[22] J. Liu, L. Yan, and C. Ma, "Pricing options and convertible bonds based on an actuarial approach," *Mathematical Problems in Engineering*, vol. 2013, Article ID 676148, 9 pages, 2013.

[23] K. Tsiveriotis and C. Femandes, "Valuing convertible bonds with default risk," *Journal of Fixed Income*, vol. 8, no. 2, pp. 95–102, 1998.

[24] C. Huang, C. Peng, X. Chen, and F. Wen, "Dynamics analysis of a class of delayed economic model," *Abstract and Applied Analysis*, vol. 2013, Article ID 962738, 12 pages, 2013.

[25] J. Lin and X. Wang, "New Brownian bridge construction in quasi-Monte Carlo methods for computational finance," *Journal of Complexity*, vol. 24, no. 2, pp. 109–133, 2008.

[26] L. Yu, S. Wang, F. Wen, and K. K. Lai, "Genetic algorithm-based multi-criteria project portfolio selection," *Annals of Operations Research*, vol. 197, pp. 71–86, 2012.

[27] L. Stentoft, "Assessing the least squares Monte-Carlo approach to American option valuation," *Review of Derivatives Research*, vol. 7, no. 2, pp. 129–168, 2004.

Hindawi Publishing Corporation
Discrete Dynamics in Nature and Society
Volume 2014, Article ID 821463, 9 pages
http://dx.doi.org/10.1155/2014/821463

Research Article

The Relations between QFII Holdings and Company Performance: Evidence from China's A-Share Listed Companies

Xiong Wang,[1] Shuanghong Zhou,[1] and Wenqian Fang[2]

[1] *School of Business, Central South University, Changsha, Hunan 410083, China*
[2] *School of Economics, Fudan University, Shanghai 200433, China*

Correspondence should be addressed to Shuanghong Zhou; shzhou7230@sohu.com

Received 13 March 2014; Revised 4 June 2014; Accepted 6 June 2014; Published 23 June 2014

Academic Editor: Fenghua Wen

In order to investigate the relations between qualified foreign institutional investors (QFII) holdings and the performance of the A-share listed companies and effectively distinguish between QFIIs' ability to identify value companies and their ability to enhance company value, this paper empirically examines the relations between QFII holdings and company performance using Chinese annual report data from 2010 to 2012. The results show that QFIIs have strong ability in identifying value companies. However, the effect of QFII holdings on company performance improvement is mainly manifested in the short term, and the long-term effect is insignificant. In the long run, QFIIs may not be considered as "value boosters," implying that it is unlikely for QFIIs to greatly enhance company value and help the invested companies to improve the level of governance and their long-term performance.

1. Introduction

After nearly two decades of development, China's securities market has been remarkably enhanced either in terms of scale and levels or in terms of functions and efficiency and has become one of Asia's most promising markets. However, due to the QFII investment restriction ratios and QFII investment range limitations, there is still a lot of room for QFIIs to enhance operational efficiency in China's securities market. Early in 2001, both academic experts and practitioners began to suggest that Chinese government introduces QFII scheme as soon as possible in order to compensate for the absence of domestic institutional investors. As China's capital and monetary items are not yet fully open, the QFII scheme is a temporary institutional arrangement that allows licensed foreign institutional investors to invest in China's securities market. The QFIIs may remit a certain amount of foreign currency and convert it into local currency through special channels with the approval of relevant authorities. The capital gains and dividends received can be converted back into foreign currency for repatriation upon approvals. With the continuous development and improvement of this scheme, QFIIs have gradually grown into important investors in China's securities market. According to the latest data released by China's State Administration of Foreign Exchange, as of December 31, 2012, China has awarded a combined $37.443 billion of QFII quotas to 169 foreign institutions. The active participation of QFIIs in China's securities market is good for the country's interest rate liberalization and foreign exchange market reformation. It also promotes the opening of China's capital market, the convertibility of RMB capital item, and the backward flow mechanism of offshore RMB as well. Eventually it helps the internalization of RMB. Meanwhile, through holding shares, QFIIs also play an important role in improving governance and performance levels of the invested listed companies.

The analysis of the relations between QFII holdings and the performance of those selected listed companies is really about examining the roles of QFIIs. Are QFIIs "value discoverers" who are good at spotting the best-performing companies or "value boosters" who help improve the governance and performance of the relevant listed companies? Or, do QFIIs act as both? Theoretically speaking, QFIIs as institutional investors with advanced investment philosophy can improve the performance of the invested companies. Compared with the small investors, QFIIs can effectively supervise the listed companies to avoid "moral hazard" and reduce the cost of commissions, which helps improve corporate governance and performance. Nevertheless, practically in the not-so-mature Chinese capital market, there are still different voices about whether QFIIs are able to improve corporate performance.

As far as the relevant research at home and abroad is concerned, the relation between QFII holdings and company performance is still a relatively new topic. Most studies have focused on the impact of the general institutional investors on company performance. Based on Pound's study on institutional investors, there are three hypotheses regarding the correlation between QFII holdings and company performance: Efficient Monitoring Hypothesis, Conflict of Interest Hypothesis, and Strategy Alignment Hypothesis [1]. The latter two both hold that QFIIs are unable to improve company performance through enhancing company governance. Whether in the Western countries with matured capital markets or in newly industrialized China in transition, the results of both theoretical and empirical studies are mixed like Pound's three hypotheses. The first category of views believes QFIIs can enhance company governance and thus help to enhance company value [2, 3]. This viewpoint agrees with Pound's Efficient Monitoring Hypothesis. Most studies on the performance of the listed companies invested by QFIIs show that, compared with the stocks without QFII holdings, companies with QFII participation tend to perform better. Lin and Chen studied the Taiwan stock market and selected 10 stocks with the highest QFII investment ratios and another 10 with the lowest in three different industry sectors as samples and found out that all the 20 stocks showed a significant difference in earnings after the introduction of QFII program. The stocks with higher QFII investment ratios tended to perform much better than the ones with lower ratios [4]. Huang and Shiu conducted another empirical study using Taiwan data and also found out that when factors such as company size and transparency were under control, stocks with higher QFII investment ratios did perform better than those with lower proportions [5]. Khanna and Palepu made use of the data in the 1990s from India and came to the conclusion that QFII holdings and company performance were significantly positively related [6]. Furthermore, Douma et al. found out that, in the Indian stock market, QFIIs who were long-term investors would have positive impact on the performance of the listed companies [7]. Wu et al. collected the information about the top ten shareholders as well as the top ten holders of negotiable stocks released by the A-share listed companies in their semiannual reports and annual reports for years from 2006 to 2009 [8]. They analyzed the role played by QFIIs in A-share market in terms of financial characteristics and company governance. The results of this study showed that companies with QFII holdings did better than those without them in profitability, operational capability, and governance quality. A further regression analysis has proved that QFII holdings could help to enhance company performance to a certain degree. All the above-mentioned studies showed that QFIIs might act as value discoverers. However, the second category of views questions the positive impact of QFII program on company governance [9–12]. They hold that QFII holdings cannot add any value to the selected listed companies. Such a viewpoint applauds Pound's Conflict of Interest Hypothesis and Strategy Alignment Hypothesis. For example, Tan conducted research using data on the listed companies in China and concluded that QFIIs so far had not directly taken part in company governance at all and therefore had only limited positive impact on improving company governance [13].

The limitations of the existing studies mainly lie in three areas. First, most of them narrowly focused on general institutional investors and only a few analyzed directly the relations between QFII holdings and company performance. There is no consistent answer so far to the question about what specific functions QFIIs actually have. Second, the existing studies on the impact of QFII holdings on company performance were mostly based on direct regression analyses with the sum of QFII holdings and company performance in order to test whether QFIIs are able to identify value companies and enhance company value, which has in fact mixed up value discovery and value enhancement. Even if there exists positive relation between them, we cannot conclude that QFIIs are able to discover value or enhance value. Third, chances are that QFII holdings and company performance may be mutually dependent. On the one hand, QFIIs may be involved in company governance and thus help to improve company performance; on the other hand, the best-performing companies may attract more QFIIs and thus help to increase the proportion of shares held by QFIIs. This means that there is reciprocal causality between the two to some extent, which may lead to a serious endogenous problem in the model.

This paper makes an empirical study on the relationship between QFII holdings and company performance using the data for years from 2010 to 2012 released by listed companies in their annual reports. Compared with past studies, the paper bears two unique characteristics. First, studies are performed on the impact of QFII holdings on company performance and on performance enhancement, respectively. This helps to differentiate more effectively between QFII investors' ability to identify value companies and their ability to enhance company value. Second, lag treatment is considered, which to some degree helps to alleviate the so-called endogenous problem that widely existed in prior studies so that the conclusions of the paper are more reliable.

The rest of the paper is organized as follows. In Section 2, we make an introduction of the empirical models. Then we provide data and descriptive statistics in Section 3. In Section 4, we present the empirical evidence and the analyses. Finally, the conclusions will be shown in Section 5.

2. The Model

This paper selects company performance and performance improvement as dependent variables. Company performance refers to the operational performance and efficiency of a company which reflects its operating results. While there are many variables used to evaluate company performance, this paper selects three: TOBIN's Q, ROA (return on assets), and ROE (return on equity). They look at company performance,

Table 1: List of study variables.

Variable types	Variable names and symbols	Definition	Calculating method
Dependent variables	ROA	Return on assets	Net profit/average total assets
	ROE	Return on equity	Net profit/average net assets
	TOBIN_Q	Tobin's Q	Company's market price/company's replacement cost
	CROA	Improvement of ROA	ROA of current period minus ROA of last period
	CROE	Improvement of ROE	ROE of current period minus ROE of last period
	CTOBIN_Q	Improvement of Tobin's Q	Tobin's Q of current period less than the value of last period
Explanatory variables	MaxQFII	Proportion of QFII holdings	Sum of QFII investment ratios among the top ten shareholders
Control variables	Size	Company size	Period-end total assets
	Lev	Debt levels	Liabilities/total Assets
	Share	Ownership concentration	Investment ratio of the largest shareholder
	Sal	Growth	Main business revenue growth
	Tat	Operational capacity	Total assets turnover rate
	Industry	Industries, sectors	Dummy variables, 11 variables representing 12 industries
	Year	Years	Dummy variable, two variables representing three years

respectively, from three aspects: capital expansion capability, core achievements, and share price performance.

QFII investment ratio is treated as an independent variable as institutional investors do not have the ability or the incentive to be involved in company governance unless they hold a certain proportion of its shares. According to Giannetti and Laeven, only institutional investors with big scale and strong independence are able to add value to a listed company [14]. Therefore, this paper uses QFII investment ratio among the top ten largest shareholders as an independent variable rather than QFII ratio among all holders.

In addition to QFII investment ratios, some other variables may also influence the performance of a listed company. Based on prior literature in this regard, in order to control the influence of other characteristics of a company, this paper selects such control variables as company size, debt levels, ownership concentration, growth, operational capability, industry sectors, operating years, and so on.

Definitions and symbols for the main variables are shown in Table 1.

Based on the selected samples and regression variables, the intrinsic link between QFII holdings and company performance is examined through establishing regression models. Generally speaking, there are two ways for institutional investors to participate in company governance. First, they buy and sell shares of the listed company but do not involve much in company governance or company decision making. In this situation, institutional investors mainly focus on stock selection and try to identify value companies. They do not intend to help the invested company to enhance value. Second, institutional investors may choose to hold shares for long and thus will actively participate in company governance in order to protect their gains. In this situation, they not only identify value companies but also help to enhance company value. A lot of studies have proved that institutional investors tend to favor the second practice. They try to influence and improve company governance and enhance company value. The paper tries to separate QFIIs' ability to identify value companies and their ability to enhance company value through the following steps.

Step 1. Since the investment decision of QFIIs in period t is made based on company performance in the same and previous periods and the potential company value as well, QFIIs ability to identify value companies can be seen by whether the corresponding listed companies can perform better after QFII involvement. Therefore, this paper makes regression analyses of performance level in period t and QFII investment ratios in lag periods, namely, period $(t-1)$ and period $(t-2)$, in order to examine QFII investors' ability to identify value companies. The established regression models named MODEL I and MODEL II are written as follows:

MODEL I:

$$\begin{aligned} Z_t = {} & \alpha_0 + \alpha_1 \mathrm{MaxQFII}_{j,t-1} + \alpha_2 \mathrm{Size}_{jt} + \alpha_3 \mathrm{Share}_{jt} \\ & + \alpha_4 \mathrm{Tat}_{jt} + \alpha_5 \mathrm{Sal}_{jt} + \cdots + \alpha_6 \mathrm{Lev}_j \\ & + \sum_{i=1}^{11} \alpha_{6+i} \mathrm{Industry}_i + \sum_{k=1}^{2} \alpha_{17+k} \mathrm{Year}_k + \varepsilon; \end{aligned} \tag{1}$$

MODEL II:

$$\begin{aligned} Z_t = {} & \alpha_0 + \alpha_1 \mathrm{MaxQFII}_{j,t-2} + \alpha_2 \mathrm{Size}_{jt} + \alpha_3 \mathrm{Share}_{jt} \\ & + \alpha_4 \mathrm{Tat}_{jt} + \alpha_5 \mathrm{Sal}_{jt} + \cdots + \alpha_6 \mathrm{Lev}_j \\ & + \sum_{i=1}^{11} \alpha_{6+i} \mathrm{Industry}_i + \sum_{k=1}^{2} \alpha_{17+k} \mathrm{Year}_k + \varepsilon, \end{aligned} \tag{2}$$

Table 2: Industry distribution of sample companies.

Sectors	Number of companies	The proportion
Manufacturing	135	54.66%
Nonmanufacturing	112	45.34%
Agriculture, forestry, animal husbandry, and fishery	2	0.81%
Mining	6	2.43%
Electricity, gas, and water production and supply	8	3.24%
Building industry	6	2.43%
Transportation, storage, and postal	13	5.26%
Information transmission, computer services, and software industry	18	7.29%
Wholesale and retail	19	7.69%
Accommodation and catering	9	3.64%
Financial sector	15	6.07%
Real estate	11	4.45%
Scientific research, technical services, and geological prospecting	5	2.02%

Source: eastern wealth network, GTA database.

where Z_t represents performance indicators, ROA, ROE, and TOBIN's Q in period t, $\mathrm{MaxQFII}_{j,t-1}$ and $\mathrm{MaxQFII}_{j,t-2}$ stand for QFII investment ratios in period $(t-1)$ and period $(t-2)$, respectively, $j = 1, 2, 3, \ldots, 247$, α_0 indicates a constant, $\alpha_1, \alpha_2, \ldots, \alpha_{19}$ represent the regression coefficients for corresponding variables, and ε indicates residuals. MODEL I mainly observes the relation between QFII holdings and performance of invested companies in period $(t-1)$ while MODEL II mainly observes their relation in period $(t-2)$.

Step 2. After having studied QFII investors' ability to identify value companies, the paper selects performance improvement as a dependent variable and makes regression analyses of QFII investment ratios in period $(t-1)$ and period $(t-2)$ in order to examine QFII investors' ability to enhance company value. As for the evaluation of performance improvement, we use such an equation (taking CROE as an example): $\mathrm{CROE}_{t,i} = (\mathrm{ROE}_{t,i} - \mathrm{ROE}_{t,I}) - (\mathrm{ROE}_{t-1,i} - \mathrm{ROE}_{t-1,I})$, where $\mathrm{CROE}_{t,i}$ represents ROE improvement of company i in year t, $\mathrm{ROE}_{t,i}$ indicates ROE for company i in year t, and $\mathrm{ROE}_{t,I}$ stands for the mean of the whole industry in year t. Such treatment can effectively remove the influence of differences in industry and year on performance improvement and thus makes the evaluation of performance improvement more accurate. The regression models are written as MODEL III and MODEL IV as follows:

MODEL III:

$$\begin{aligned} CZ_t = {} & \alpha_0 + \alpha_1 \mathrm{MaxQFII}_{j,t-1} + \alpha_2 \mathrm{Size}_{jt} + \alpha_3 \mathrm{Share}_{jt} \\ & + \alpha_4 \mathrm{Tat}_{jt} + \alpha_5 \mathrm{Sal}_{jt} + \cdots + \alpha_6 \mathrm{Lev}_j \\ & + \sum_{i=1}^{11} \alpha_{6+i} \mathrm{Industry}_i + \sum_{k=1}^{2} \alpha_{17+k} \mathrm{Year}_k + \varepsilon; \end{aligned} \tag{3}$$

MODEL IV:

$$\begin{aligned} CZ_t = {} & \alpha_0 + \alpha_1 \mathrm{MaxQFII}_{j,t-2} + \alpha_2 \mathrm{Size}_{jt} + \alpha_3 \mathrm{Share}_{jt} \\ & + \alpha_4 \mathrm{Tat}_{jt} + \alpha_5 \mathrm{Sal}_{jt} + \cdots + \alpha_6 \mathrm{Lev}_j \\ & + \sum_{i=1}^{11} \alpha_{6+i} \mathrm{Industry}_i + \sum_{k=1}^{2} \alpha_{17+k} \mathrm{Year}_k + \varepsilon, \end{aligned} \tag{4}$$

where CZ_t represents company performance indicators, CROA, CROE, and CTOBIN's Q in period t, $\mathrm{MaxQFII}_{j,t-1}$ and $\mathrm{MaxQFII}_{j,t-2}$ represent, respectively, QFII investment ratios in period $(t-1)$ and period $(t-2)$, $j = 1, 2, 3, \ldots, 247$, α_0 indicates a constant, $\alpha_1, \alpha_2, \ldots, \alpha_{19}$ are the regression coefficients for corresponding variables, and ε refers to residuals. MODEL III mainly observes the relation between QFII holdings and performance improvement of the invested companies in lag period $(t-1)$, whereas MODEL IV mainly observes their relation in lag period $(t-2)$.

3. Data and Descriptive Statistics

The samples selected for this paper are from the listed companies with QFII holdings annually disclosed by Shanghai Stock Exchange and Shenzhen Stock Exchange in years from 2010 to 2012. Four types of companies are excluded, companies listed in and after 2010, companies without full record of financial data, companies which have also issued B shares, H shares, or S shares, and companies with abnormal data values. Eventually, a total of 247 listed companies are qualified as samples and their industry distribution is shown in Table 2. The industries are classified according to Industry Classification Standard publicized by China's National Bureau of Statistics (http://www.stats.gov.cn/).

As shown in Table 2, of all the selected companies, the number of companies in manufacturing sector amounts to 135 or 54.66%, whereas the number of companies in

Table 3: Statistical descriptions.

	2010		2011		2012	
	QFII invested companies	A-share listed companies	QFII invested companies	A-share listed companies	QFII invested companies	A-share listed companies
ROA	4.86	2.26	5.08	2.16	3.30	1.87
ROE	18.10	16.28	16.01	15.25	17.13	13.32
Tobin_Q	2.15	2.09	1.61	1.62	1.45	1.47
Tat	0.68	0.23	0.70	0.24	0.67	0.22
Sal	50.97	33.86	41.40	20.81	148.74	7.67
Lev	48.82	85.59	50.04	85.64	50.33	85.80
Share	21.86	55.79	26.42	47.63	28.51	44.82
Size	11.73	3.54	13.79	4.19	15.50	4.83

Source: GTA database.

Table 4: Pearson correlation coefficients.

	ROA	ROE	Tobin_Q	MaxQFII	Tat	Sal	Lev	Share	Size
ROA	1.0000								
ROE	0.3153	1.0000							
Tobin_Q	0.0149	−0.0039	1.0000						
MaxQFII	0.0018	0.0034	0.0017	1.0000					
Tat	0.0102	0.0030	−0.0341	−0.0182	1.0000				
Sal	0.0005	0.0001	−0.0033	0.0034	−0.0042	1.0000			
Lev	−0.0076	−0.0027	0.0088	−0.0013	0.0056	0.0004	1.0000		
Share	−0.0038	−0.0009	−0.0131	−0.0100	0.0303	−0.0013	0.0076	1.0000	
Size	−0.0096	0.0011	−0.0001	−0.0021	0.0025	0.0000	−0.0056	0.0075	1.0000

Source: GTA database.

nonmanufacturing sector amounts to 112 or 45.34%. In nonmanufacturing sector, three industries with the highest proportions are wholesale and retail (7.69%), information transmission, computer services and software (7.29%), and financial sector (6.07%).

Data used in this study mainly come from five sources: annual reports of the listed companies with QFII holdings released by the websites of Shanghai Stock Exchange and Shenzhen Stock Exchange, annual QFII investment ratios disclosed by Eastern Wealth Network, financial data of listed companies with QFII holdings released by GTA database, financial data provided by Wind Information, and China's National Bureau of Statistics.

Table 3 compares the mean values of relevant financial indicators for companies with QFII holdings and those for all A-share listed companies. As shown in the table, in terms of company performance, mean ROA and mean ROE of companies with QFII holdings are both substantially higher than the mean values for all A-share listed companies. This clearly shows that companies invested by QFIIs tend to perform better and QFIIs tend to select value companies. The total assets of companies invested by QFIIs tend to be much more than the mean value of all A-share listed companies, which means QFIIs favor larger companies.

Besides, the proportion of the largest shareholders in companies invested by QFIIs is lower than the mean value of all A-share listed companies. If the proportion of the largest shareholder is used to measure company governance level, we can see that companies invested by QFIIs tend to govern better. Meanwhile, the higher growth rate and operating level of companies invested by QFIIs also prove that they enjoy better governance. Finally, the debt levels of companies invested by QFIIs are smaller than the corresponding mean value of all A-share listed companies, which serves as one of the factors leading to better company performance.

The Pearson correlation coefficients between selected main variables are shown in Table 4.

We can see clearly from Table 4 that the correlation coefficients between the three performance indicators, ROA, ROE, and TOBIN's Q, are relatively larger and the QFII investment ratios have positive relationship with all the three performance indicators although their correlation coefficients are not big (with the correlation coefficient between QFII and ROE the most significant at 0.0034).

4. Empirical Results

Table 5 shows the regression results of MODEL I using QFII investment ratio in lag period $(t-1)$ as an independent variable examines QFII investors' ability to identify value companies.

From Table 5 we can see that the independent variable of QFII investment ratio in lag period $(t-1)$ is notably

Table 5: Regression results of QFII investment ratio in period $(t-1)$ and company performance according to MODEL I.

Variables	ROA	ROE	Tobin's Q
Constant	0.11531^{***}	0.17056^{**}	1.86739^{***}
	4.41143	2.03436	11.04490
MaxQFII(−1)	0.00849^{***}	0.02662^{**}	0.06213^{**}
	3.42647	2.55455	2.46714
Size	0.00000^{**}	0.00000^{**}	0.00000
	2.21042	2.24849	0.09737
Share	0.00047^{***}	0.00075^{**}	0.00320
	2.94002	2.29432	1.40466
Lev	-0.21255^{***}	−0.35712	-1.24395^{***}
	−3.45720	−1.57304	−4.10290
Sal	0.00008	0.00051	0.00425^{***}
	0.54543	0.86615	7.63855
Tat	0.01797^{***}	0.03794^{***}	0.21312^{*}
	2.85683	3.01675	1.90997
Industry	Yes	Yes	Yes
Year	Yes	Yes	Yes
Sample	247	247	247
R^2	0.34122	0.03430	0.11295
Adjusted R^2	0.33309	0.02233	0.10200
F-statistic	41.95437	2.86483	10.31351
Prob. F	0.00000	0.00943	0.00000

Notes. ***,**,*denote statistical significance at the 1%, 5%, and 10% levels, respectively. The upper values of the regression results are regression coefficients while the lower ones are corresponding T statistics.

Table 6: Regression results of QFII investment ratio in period $(t-2)$ and company performance according to MODEL II.

Variables	ROA	ROE	Tobin's Q
Constant	0.12674^{***}	0.06946^{***}	1.66543^{***}
	3.14283	3.16050	8.63443
MaxQFII(−2)	0.00993^{***}	0.01666^{***}	0.05709^{**}
	2.80691	5.14342	2.05416
Size	0.00000^{**}	0.00000^{***}	0.00000
	2.10072	5.66414	−0.17631
Share	0.00056^{**}	0.00077^{**}	0.00277
	2.44543	2.15816	1.26991
Lev	-0.26210^{***}	-0.11981^{***}	-0.94633^{***}
	−2.72848	−3.42330	−2.60462
Sal	0.00011	0.00031	0.00432^{***}
	0.62405	1.03791	8.51312
Tat	0.01506^{***}	0.02775^{*}	0.17935
	2.92032	1.87526	1.59534
Industry	Yes	Yes	Yes
Year	Yes	Yes	Yes
Sample	247	247	247
R^2	0.36985	0.11315	0.08934
Adjusted R^2	0.35403	0.09070	0.06648
F-statistic	23.37894	5.03950	3.90792
Prob. F	0.00000	0.00007	0.00096

Notes. ***,**,*denote statistical significance at the 1%, 5%, and 10% levels, respectively. The upper values of the regression results are regression coefficients while the lower ones are corresponding T statistics.

positively related to each performance indicator, ROA, ROE, and Tobin's Q. At significance level of 1%, one percentage of increase in QFII investment ratio in lag period $(t-1)$ leads to an ROA increase by 0.00849; at significance level of 5%, one percentage of increase in QFII investment ratio in lag period $(t-1)$ leads to an ROE increase by 0.02662 and Tobin's Q increase by 0.06213. Of the control variables, company size, ownership concentration, operational capabilities, and growth rate are positively related to performance indicators but negatively related to liability/asset ratio. The F statistics of the regression equations for ROA, ROE, and Tobin's Q stand at 41.95437, 2.86483, and 10.31351, respectively. In all three equations, Prob. F representing significance level is smaller than 0.001, which means the regression equations are significant.

According to MODEL II, we take QFII investment ratio in lag period $(t-2)$ as an independent variable to further examine QFII investors' ability to identify long-term company value and the regression results are shown in Table 6.

As shown in Table 6, the independent variable of QFII investment ratio in lag period $(t-2)$ is significantly positively related to each performance indicator, ROA, ROE, and Tobin's Q. At significance level of 1%, one percentage of increase in QFII investment ratio in lag period $(t-2)$ leads to an ROA increase of 0.00993 and ROE increase of 0.01666; at significance level of 5%, one percentage of increase in QFII investment ratio in lag period $(t-2)$ leads to a Tobin's Q increase by 0.05709. The regression results show that QFII ratio in period $(t-2)$ is positively related to company performance and the larger the ratio, the better the performance. Of the control variables, company size, ownership concentration, operational capabilities, and growth rate are positively related to performance indicators but negatively related to liability/asset ratio. The F statistics for the three regression equations stand at 23.37894, 5.03950, and 3.90792, respectively. In all three equations, Prob. F representing significance level is smaller than 0.001, which means the regression equations are significant.

Overall, results from both MODEL I and MODEL II show that QFIIs are capable of identifying value companies. That is to say, QFIIs as "value discoverers" are able to select better-performing companies. However, whether QFIIs are "value boosters" and can also help to enhance company performance through active participation in company governance still remains to be seen.

According to MODEL III, we select QFII investment ratio in period $(t-1)$ as an independent variable and the performance improvement indicators of QFII invested companies as dependent variables to examine QFII investors' ability to enhance company value. Regression results are presented in Table 7.

We can see, from Table 7 that except for CTobin's Q, QFII ratio does not have any significant correlation with the other two performance improvement indicators, CROA and

Table 7: Regression results of QFII ratio in period ($t-1$) and company performance improvement according to MODEL III.

Variables	CROA	CROE	CTobin's Q
Constant	0.02217	0.25365	-0.67125^{***}
	0.84817	1.18952	−6.56337
MaxQFII(−1)	0.00309	−0.01657	-0.04722^{**}
	1.36791	−0.55919	−2.10425
Size	0.00000	0.00000	0.00000
	1.42781	−0.25222	0.56848
Share	−0.00003	−0.00490	0.00221
	−0.17379	−1.00645	1.32378
Lev	−0.07030	0.01079	0.65454^{***}
	−1.15191	0.03470	4.09037
Sal	0.00025^{***}	−0.00023	0.00300^{***}
	3.31425	−0.25646	3.38701
Tat	0.00385	−0.07649	−0.04019
	1.08949	−0.89436	−1.01220
Industry	Yes	Yes	Yes
Year	Yes	Yes	Yes
Sample	247	247	247
R^2	0.03474	0.00297	0.05507
Adjusted R^2	0.02282	−0.00942	0.04341
F-statistic	2.91490	0.23960	4.72068
Prob. F	0.00840	0.96329	0.00011

Notes. ***,**,*denote statistical significance at the 1%, 5%, and 10% levels, respectively. The upper values of the regression results are regression coefficients while the lower ones are corresponding T statistics.

Table 8: Regression results of QFII ratio in period ($t-2$) and performance improvement indicators according to MODEL IV.

Variables	CROA	CROE	CTobin's Q
Constant	0.03032	−0.03107	-0.42509^{***}
	0.74699	−1.39079	−5.03189
MaxQFII(−2)	0.00493	−0.00199	−0.00827
	1.44008	−0.45074	−0.70662
Size	0.00000	0.00000	0.00000
	1.59043	0.20419	−1.29006
Share	0.00016	−0.00021	0.00163
	0.78211	−0.60593	1.09693
Lev	−0.12202	0.03209	0.49343^{***}
	−1.25216	0.46746	3.41901
Sal	0.00027^{**}	0.00038^{**}	0.00263^{***}
	2.06836	2.55080	3.69150
Tat	0.00277	−0.00455	−0.01835
	0.56454	−0.48566	−0.40938
Industry	Yes	Yes	Yes
Year	Yes	Yes	Yes
Sample	247	247	247
R^2	0.12444	0.00548	0.06806
Adjusted R^2	0.10246	−0.01970	0.04466
F-statistic	5.66113	0.21763	2.90893
Prob. F	0.00002	0.97093	0.00934

Notes. ***,**,*denote statistical significance at the 1%, 5%, and 10% levels, respectively. The upper values of the regression results are regression coefficients while the lower ones are corresponding T statistics.

CROE. At significance level of 5%, QFII ratio is negatively related to CTobin's Q. Therefore, it can be concluded that QFII holdings do not generate significant performance improvement in short term (one year). In some cases, they may even destroy value.

Next, according to MODEL IV, we use QFII ratio in period ($t-2$) as an independent variable to examine the performance improvement effect of QFIIs on listed companies in longer term (two years). The regression results are presented in Table 8.

We can see from the regression results shown in Table 8 that QFII ratio does not have any significant correlation with any of the three performance improvement indicators, CROA, CROE, and CTobin's Q. Therefore, QFII holdings do not help much in performance improvement in relatively longer term (two years).

We also find out from Tables 7 and 8 that all listed companies invested by QFII do not show significant performance improvement regardless of short term or long term. It is known that QFIIs may have different expectations behind shareholding. Some may pursue short-term gains through frequent transactions on shares of undervalued listed companies, while others may well look for long-term returns through active participation in company governance which then helps to improve company performance. In order to exclude the influence from short-term gain expectations and further study QFII investors' ability to improve company performance, the paper selects 88 listed companies with QFII holdings either in two successive years from 2010 to 2011 or in three successive years from 2010 to 2012. The objective is to examine whether QFIIs are able to enhance company value. First, we use QFII ratio in period ($t-1$) as an independent variable and the regression results are presented in Table 9.

As shown in Table 9, at significance level of 1%, QFII ratio in period ($t-1$) is positively related to the three performance improvement indicators except CTobin's Q. One percentage of increase in QFII investment ratio in lag period ($t-1$) leads to a CROA increase of 0.00200 and CROE increase of 0.00467. The regression results show that QFII ratio in period ($t-1$) is positively related to performance improvement, and the larger the ratio, the more significant the performance improvement. In the first two equations, Prob. F representing significance level is smaller than 0.05, which means the regression equations are significant. It shows that QFII investors do have positive impact on performance improvement in the short term (one year) and thus act as the so-called role of "value boosters" in the short run.

Then, according to MODEL IV, we select QFII ratio in period ($t-2$) as an independent variable and the regression results are presented in Table 10.

We can see from Table 10 that the independent variable of QFII investment ratio in period ($t-2$) is notably related to performance improvement indicators, CROA and CROE. At significance level of 10%, one percentage of increase in QFII

Table 9: Regression results of continuous QFII investment in period $(t-1)$ and company performance improvement according to MODEL III.

Variables	CROA	CROE	CTobin's Q
Constant	-0.01755^{**}	-0.01479	-0.87958^{***}
	-2.18180	-1.03486	-4.34624
MaxQFII(−1)	0.00200^{***}	0.00467^{***}	-0.00511
	3.04878	2.78349	-0.35149
Size	0.00000^{***}	0.00000^{***}	0.00000
	4.02036	3.24496	-0.59170
Share	-0.00007	-0.00027	0.00538^{*}
	-0.73445	-1.14166	1.93553
Lev	-0.01048	-0.03748^{*}	0.74865^{**}
	-1.07672	-1.66090	2.44204
Sal	0.00046^{***}	0.00177^{***}	-0.00524^{**}
	4.39394	7.82854	-2.00151
Tat	0.02136^{***}	0.02249^{*}	-0.11674
	3.51361	1.83851	-1.04473
Industry	Yes	Yes	Yes
Year	Yes	Yes	Yes
Sample	88	88	88
R^2	0.07784	0.05540	0.09094
Adjusted R^2	0.04510	0.02167	0.05866
F-statistic	2.37751	2.64230	2.93642
Prob. F	0.03130	0.01839	0.01042

Notes. ***,**,*denote statistical significance at the 1%, 5%, and 10% levels, respectively. The upper values of the regression results are regression coefficients while the lower ones are corresponding T statistics.

Table 10: Regression results of continuous QFII investment in period $(t-2)$ and performance improvement according to MODEL IV.

Variables	CROA	CROE	CTobin's Q
Constant	-0.02653^{**}	-0.01873	-0.68215^{***}
	-2.15342	-0.74761	-2.95152
MaxQFII(−2)	0.00179^{*}	0.00630^{**}	-0.01386
	1.73844	2.18170	-1.03571
Size	0.00000^{***}	0.00000^{***}	0.00000
	2.81223	3.13358	-1.35747
Share	-0.00004	0.00002	0.00112
	-0.31899	0.05548	0.39436
Lev	-0.00121	-0.08530^{*}	0.87797^{**}
	-0.06856	-1.88554	2.61655
Sal	0.00054^{***}	0.00234^{***}	-0.00789^{***}
	3.62545	6.09090	-3.85868
Tat	0.01526^{**}	0.01489	-0.05486
	2.30065	0.82115	-0.39137
Industry	Yes	Yes	Yes
Year	Yes	Yes	Yes
Sample	88	88	88
R^2	0.05947	0.09093	0.12806
Adjusted R^2	0.01020	0.02359	0.06348
F-statistic	1.98277	2.81754	0.85362
Prob. F	0.07763	0.01223	0.53266

Notes. ***,**,*denote statistical significance at the 1%, 5%, and 10% levels, respectively. The upper values of the regression results are regression coefficients while the lower ones are corresponding T statistics.

investment ratio in lag period $(t-2)$ leads to a CROA increase of 0.00179 and at significance level of 5% one percentage of increase in QFII investment ratio in lag period $(t-2)$ leads to a CROE increase of 0.00630. In the first two equations, Prob. F representing significance level is less than 0.10, which means the regression equations are significant. It shows that QFII holdings also help improve company performance in the relatively longer term (two years).

Overall, QFII holdings can help to improve company performance in the first two years. Therefore, we can state that QFIIs do play the role of "value boosters." Nevertheless, in the periods after $(t-2)$ the significance level of the independent variable declines sharply, which means that QFII holdings show strong effect of improving company performance in the short term but not in the long term.

5. Conclusions

This paper quantitatively analyzes the relations between QFII holdings and company performance and attempts to make an effective distinction between QFIIs' ability to identify value companies and their ability to enhance company value. We come to the following main conclusions.

First, after performing the regression analyses of QFII investment ratio in lag periods and each of the three performance indicators one by one, ROA, ROE, and Tobin's Q, we can observe that QFII ratios in periods $(t-1)$ and $(t-2)$ are positively related to all the performance indicators. This implies that QFII investors have strong capability to identify value companies and tend to perform well in investing those companies whose shares have been held following due diligence given to the companies' performance level and potential value. Therefore, we can state that QFIIs have done well identifying value companies.

Second, after performing the regression analyses of QFII investment ratio in lag periods and each of the three performance improvement indicators (CTobin's Q, CROA, and CROE), we find that both QFII ratios in periods $(t-1)$ and $(t-2)$ do not have any significant correlation with any of the three performance improvement indicators, which means in full sample QFIIs play less significant roles in performance improvement of the selected companies.

Third, it is known that QFIIs may have different expectations behind shareholding. Some may pursue short-term gains through frequent transactions on shares of undervalued listed companies, while others may look for long-term returns through active participation in company governance which then helps to improve company governance and performance. In order to discard the influence of the short-term gain expectation and further study QFII investors' ability to improve company performance, the paper selects 88 listed companies with QFII holdings either in two successive years from 2010 to 2011 or in three successive years from 2010 to 2012. The objective is to examine whether QFIIs are able to boost company value. The results show that both QFII investment ratios in periods $(t-1)$ and $(t-2)$ have remarkably positive impact on company performance. Nevertheless, in periods after $(t-2)$ the significance level of the independent variable declines sharply, which means that QFII holdings show strong effect of improving company performance in the short term but not in the long term.

From the above conclusions, we can see that QFIIs, as qualified foreign institutional investors with advanced investment philosophy and mature investment experience, have shown strong ability to identify value companies. However, QFIIs have shown much less influence on midterm and long-term performance of the listed companies in terms of enhancing company value. The lack of influence of QFIIs on company performance in China can be explained in three aspects.

Firstly, because QFIIs haven not been in China's capital market for very long, they are still at the exploration stage getting to know the country's macroenvironment and how the listed companies are operating here. QFIIs so far do not get much involved in company governance and have limited influence on company value enhancement. Secondly, China's securities market is still in early development without complete and sound governing laws and regulations. Issues brought by allocation of shares are not fully resolved and there are many more speculators on the sidelines than real investors in China's stock market. All these factors inevitably make QFIIs unable to fully play their roles. Lastly, the administrative authorities in China still implement rigid regulations on QFII program, which leads to low QFII investment ratios and high cost in participating in company administration and governance. Therefore, QFII investors generally do not have great interest for participation in company governance.

Conflict of Interests

The authors declare that there is no conflict of interests regarding the publication of this paper.

Acknowledgment

This research was supported by the Natural Science Foundation of China under Grant no. 71203241.

References

[1] J. Pound, "Proxy contests and the efficiency of shareholder oversight," *Journal of Financial Economics*, vol. 20, pp. 237–265, 1988.

[2] S. Gillan and L. Starks, "Corporate governance, corporate ownership, and the role of institutional investors: a global perspective," *Journal of Applied Finance*, vol. 13, pp. 4–22, 2003.

[3] M. M. Cornett, A. J. Marcus, A. Saunders, and H. Tehranian, "The impact of institutional ownership on corporate operating performance," *Journal of Banking & Finance*, vol. 31, no. 6, pp. 1771–1794, 2007.

[4] A. Lin and C. Chen, "The impact of qualified foreign institutional investors on Taiwan's stock market," *Journal of Chinese Management Review*, vol. 9, no. 2, pp. 1–27, 2006.

[5] R. D. Huang and C.-Y. Shiu, "Local effects of foreign ownership in an emerging financial market: evidence from qualified foreign institutional investors in Taiwan," *Financial Management*, vol. 38, no. 3, pp. 567–602, 2009.

[6] T. Khanna and K. Palepu, "Emerging market business groups, foreign investors, and corporate governance," NBER Working Paper 6955, 1999.

[7] S. Douma, R. George, and R. Kabir, "Foreign and domestic ownership, business groups, and firm performance: evidence from a large emerging market," *Strategic Management Journal*, vol. 27, no. 7, pp. 637–657, 2006.

[8] W. Wu, D. Wan, and D. Cai, "Are qualified foreign institutional investors real investors or speculators? Evidence from China," SSRN Working Paper Series, 2011.

[9] A. Bhide, "The hidden costs of stock market liquidity," *Journal of Financial Economics*, vol. 34, no. 1, pp. 31–51, 1993.

[10] M. P. Smith, "Shareholder activism by institutional investors: evidence from CalPERS," *Journal of Finance*, vol. 51, no. 1, pp. 227–252, 1996.

[11] H. Short and K. Keasey, "Institutional voting in the UK: is mandatory voting the answer?" *Corporate Governance*, vol. 5, no. 1, pp. 37–44, 1997.

[12] D. D. Guercio and J. Hawkins, "The motivation and impact of pension fund activism," *Journal of Financial Economics*, vol. 52, no. 3, pp. 293–340, 1999.

[13] M. N. T. Tan, "Has the QFII scheme strengthened corporate governance in China?" *China*, vol. 7, no. 2, pp. 353–369, 2009.

[14] M. Giannetti and L. Laeven, "Pension reform, ownership structure, and corporate governance: evidence from a natural experiment," *Review of Financial Studies*, vol. 22, no. 10, pp. 4091–4127, 2009.

Hindawi Publishing Corporation
Discrete Dynamics in Nature and Society
Volume 2014, Article ID 721635, 13 pages
http://dx.doi.org/10.1155/2014/721635

Research Article

Realized Jump Risk and Equity Return in China

Guojin Chen,[1] Xiaoqun Liu,[2] Peilin Hsieh,[1] and Xiangqin Zhao[2]

[1] *School of Economics and The Wang Yanan Institute for Studies in Economics, Xiamen University, Xiamen, Fujian 361005, China*
[2] *School of Economics, Xiamen University, Xiamen, Fujian 361005, China*

Correspondence should be addressed to Peilin Hsieh; peilin.h@gmail.com

Received 2 March 2014; Revised 10 May 2014; Accepted 11 May 2014; Published 23 June 2014

Academic Editor: Fenghua Wen

We utilize the realized jump components to explore a new jump (including nonsystematic jump and systematic jump) risk factor model. After estimating daily realized jumps from high-frequency transaction data of the Chinese A-share stocks, we calculate monthly jump size, monthly jump standard deviation, and monthly jump arrival rate and then use those monthly jump factors to explain the return of the following month. Our empirical results show that the jump tail risk can explain the equity return. For the large capital-size stocks, large cap stock portfolios, and index, one-month lagged jump risk factor significantly explains the asset return variation. Our results remain the same even when we add the size and value factors in the robustness tests.

1. Introduction

Jump is a source which attributes to the fat tail of a return distribution. If a market is incomplete and thus investors cannot form a market portfolio to diversify the nonsystematic risk away, firm-specific and industry-level risk may have the influence over return premium and affect asset prices, making the classical capital asset pricing model (CAPM) unable to explain the returns as perfectly as the theory says. Inspired by this idea, this paper considers the jump, the tail risk, and a good supplemental factor to explain the asset returns.

After CAPM model was proposed, how well this model performs has been always challenged. Fama and French [1, 2] demonstrate that the CAPM model is unable to explain cross-sectional stock returns well and find that value premium (HML) and size (SMB) factors outperform the market model. As a result, they proposed the well-known Fama-French three-factor model which subsequently was extended to the models with liquidity and momentum factors. Further, Harvey and Siddique [3] and Wen and Yang [4] argue that conditional coskewness, which could capture similar information contained in the size and book-to-market ratio, complements market beta to explain the return. Merton [5] also supplements a theoretical argument to market model. As CAPM model does not price idiosyncratic risk (IV), he claims that incomplete information, which hinders the investors to diversify their portfolios, leads to the positive relation between idiosyncratic risk and expected stock return.

According to the studies, the empirical results of cross-sectional relation between the idiosyncratic volatility and expected return are mixed. Ang et al. [6] show that high idiosyncratic volatility in one lagged month predicts abysmally low average returns in the next month. Similarly, Guo and Robert [7] propose that, in addition to stock market volatility, the aggregate idiosyncratic volatility (IV) could be the source of risk that determines the equity return. In their preposition, IV may be considered as a proxy for variance of the risk factors of a multiple-factor or intertemporal capital asset pricing model (ICAPM). Guo and Robert [8] further used the average idiosyncratic volatility (AV-IV) as proxy for investment opportunity cost on G7 countries and concluded that IV contributes, as well as the book-to-market factor, to explaining the cross-sectional stock returns. In addition to empirical works, Campbell et al. [9] also provide a very noticeable argument for the declining explanatory power of traditional market model. In their paper, they find the increase of firm-level volatility level and market volatility level, making correlations between the stock returns lower and diversification difficult. Therefore, seeking firm-specific or aggregate level risk factors becomes a more important issue for asset pricing.

Recently, several studies have presented the empirical evidence in favor of jump risk effects on financial asset prices by using nonparametric method and high-frequency database. Since the realized volatility (RV), the realized range volatility (RRV), and realized jump volatility (RJV) were proposed, those nonparametric measures have been applied extensively, even for the researches in volatility parametric models, for example, GARCH-RV and the heterogeneous autoregressive with realized volatility (HAR-RV) model. Those nonparametric measures not only can be used to depict the volatility dynamic nature, such as clustering, long memory, asymmetric leverage effect, and the price-volume relation in financial market microstructure theory [10–18], but also can be considered as the risk indications. Therefore, investigating those risks' influences on asset pricing is of great interest. Adrian and Rosenberg [19] explore a new three-factor pricing model, including the long-run volatility component, the short-run volatility component, and the market return, and they conclude that their model outperforms the Fama-French model through reducing the pricing biased errors. Apparently, volatility can be a risk factor which accounts the return premium. Following Adrian and Rosenberg [19], Kelly and Jiang [20] develop a tail risk factor model. Both models are based on the structural model by theoretical derivation with explicit economical meanings. For tail risk model by Kelly, the bivariate calibration of tail risk factors with macrovariables can be based on the long-run risk model proposed by Bansal and Yaron [21] and the disaster risk model proposed by Rietz [22] and Barro [23].

Though there are a large number of researches seeking different risk factors for the returns, all of them focus on the returns of index, bond market, and credit spread. Moreover, most of those works are using high-frequency data in the United States. Inspired by those works, we propose a jump-based model to examine the relations between the realized jump components and equity returns at China market. We will begin with an illustration of the nonparametric jump estimation method. After daily realized jump volatility is estimated from 5-minute high-frequency trading data, we then calculate monthly jump size, jump standard deviation, and jump arrival intensity. Finally, these jump components are used to investigate their predicting and explaining power over one-month-ahead equity return.

The remaining parts of this paper are organized as follows. Section 2 introduces the identification method for the high-frequency realized jump and presents the jump risk factor model, and Section 3 describes our sample data and its descriptive statistics. Empirical results are demonstrated in Section 4, and Section 5 is robustness tests analysis. Finally, the conclusion is in Section 6.

2. Preliminaries and Theories

2.1. Realized Jump Risk. While jumps are known to be very crucial in the asset pricing [32], estimation of jump components by parametric model has been questioned for the stability over different sample time periods. With the availability of high-frequency data, nonparametric estimation method has been developed rapidly. Andersen and Bollerslev [33], Barndorff-Nielsen and Shephard [34, 35], and Meddahi [36] have presented the use of the so-called realized variance measures by utilizing the information in the intraday data for measuring and forecasting volatilities. Barndorff-Nielsen and Shephard [37, 38] developed a series of the seminal work on bipower variation measure, which is then used to divide the RV into continuous diffusion volatility and jump volatility (see Andersen et al. [39] and Huang and Tauchen [40]). Under the reasonable presumption that jumps on financial markets are usually rare and large, we follow Huang and Tauchen [40] to assume that there is at most one jump per day and that the jump size dominates the daily return when a jump occurs. These assumptions allow us to extract the daily realized jumps and further to explicitly calculate the monthly jump intensity, size, and standard deviation. Tauchen and Zhou [29] have demonstrated that jump parameters can be precisely estimated and that the statistic inference is reliable.

Compared to parametric models, in which jump is estimated by the maximum likelihood, MCMC or GMM methods, nonparametric estimation has merit of convenient estimation without assuming specifying underlying drift, diffusion, and jump functions. The assumption of one jump per day fits to the compound Poisson jump process ([41] also utilizes the Poisson jump process to describe rare and large return jumps which are presumably the responses to the arrivals of important news), and it should be pointed out that bipower variation also works for the infinite activity jumps despite the fact that we focus only on the case of rare and large jumps. The following presents the details of jump estimation and detection.

Let $p_t = \log(P_t)$ denote the time t logarithmic price of the asset, and assume that it evolves in continuous time as a jump-diffusion process:

$$dp_t = \mu_t dt + \sigma_t dW_t + J_t dq_t, \tag{1}$$

where dq_t is a Poisson jump process with intensity λ_J and J_t is the corresponding log jump size distribution following normal (μ_J, σ_J). Consider

$$\mathrm{RV}_t = \sum_{j=1}^{M} r_{t,j}^2 \longrightarrow \int_{t-1}^{t} \sigma_s^2 ds + \int_{t-1}^{t} J_s^2 dq_s, \tag{2}$$

where M is the total number of trades during time t and $t+1$ and j is the indication for each trade. In the realistic financial markets, the price volatility of financial asset is not continuous but contains jumps due to the influence aroused by information shock on market. Barndorff-Nielsen and Shephard [37, 38] proposed two general measures for the quadratic variation process-realized variance and realized bipower variation; this is presented in the following:

$$\mathrm{BV}_t \equiv \frac{\pi}{2} \frac{M}{M-1} \sum_{j=2}^{M} \left| r_{t,j} \right| \left| r_{t,j-1} \right| \longrightarrow \int_{t-1}^{t} \sigma_s^2 ds, \tag{3}$$

where $\sqrt{\pi/2} = \mathrm{E}(\Pi_t)$, Π_t is a standardized normal distribution random variable, and $M/(M-1)$ is the amendment to sample size. According to Barndorff-Nielsen and Shephard, the difference between RV_t and BV_t is just the consistent estimator of the discrete jump variation when $M \rightarrow \infty$; that is,

$$\mathrm{RV}_t - \mathrm{BV}_t \xrightarrow{M \rightarrow \infty} \mathrm{RJV}_t. \tag{4}$$

A variety of jump detection techniques are proposed and studied by Barndorff-Nielsen and Shephard [37], Huang and Tauchen [40], and Andersen et al. [14]. In fact, in the process of calculating the discrete jump variation, the existence of different intraday sampling frequency may lead to some kind of calculation errors. Here, we adopt the ratio statistic favored by their findings:

$$Z_t = \frac{\left(\mathrm{RV}_t - \mathrm{BV}_t\right)/\mathrm{RV}_t}{\sqrt{\left(\pi^2/4 + \pi - 5\right)\left(1/M\right)\max\left(1, \mathrm{TP}_t/\mathrm{BV}_t^2\right)}}, \tag{5}$$

where TP_t is the tripower quarticity that Barndorff-Nielsen and Shephard [37] define as

$$\mathrm{TP}_t = \frac{M}{M-2} \cdot \frac{M}{4\left[\Gamma\left(7/6\right)/\Gamma\left(1/2\right)\right]^3} \cdot \sum_{i=3}^{M} \left|r_{t,i}\right|^{4/3} \left|r_{t,i-1}\right|^{4/3} \left|r_{t,i-2}\right|^{4/3}. \tag{6}$$

The test statistic has an asymptotical normal distribution. Under the significance level, $1 - \alpha$, we can get the estimate of the discrete jump variation:

$$\mathrm{RJV}_t = I\left(Z_t > \Phi_\alpha^{-1}\right)\sqrt{\left[\mathrm{RV}_t - \mathrm{BV}_t\right]}, \tag{7}$$

where Φ is the cumulative distribution function of a standard normal and $I(Z_t > \Phi_\alpha^{-1})$ is the resulting indicator function on whether there is a jump during the day; $I(Z_t > \Phi_\alpha^{-1})$ equals 1 when a jump is detected at day t and 0 otherwise. In the process of actual operation, we need to choose an appropriate α, and Tauchen and Zhou [29] propose that when jump contributions are 10% and 80%, the significance level should be 0.99 and 0.999, respectively.

With the above test of Z_t statistic and the related bipower variation theory, we can get the estimator of RJV_t and then calculate the monthly jump size ($\mathrm{Size\_RJV}_{\mathrm{month}}$), monthly jump size mean ($\mathrm{Mean\_RJV}_{\mathrm{month}}$), monthly jump arrival rate ($\mathrm{Arr\_RJV}_{\mathrm{month}}$), and monthly jump size standard deviation ($\mathrm{Std\_RJV}_{\mathrm{month}}$). The jump components are defined as follows:

$$\mathrm{Size\_RJV}_{\mathrm{month}} = \sum \mathrm{Size\_RJV}_{\mathrm{day}}, \tag{8}$$

$$\mathrm{Mean\_RJV}_{\mathrm{month}} = \frac{\mathrm{Size\_RJV}_{\mathrm{month}}}{N\mathrm{\_RJV\_days}}, \tag{9}$$

$$\mathrm{Arr\_RJV}_{\mathrm{month}} = \frac{N\mathrm{\_RJV\_days}}{\mathrm{days}}, \tag{10}$$

$$\mathrm{Std\_RJV}_{\mathrm{month}} = \left[\sum\left(\left(\mathrm{Size\_RJV}_{\mathrm{day}} - \mathrm{Mean\_RJV}_{\mathrm{day}}\right)^2\right)\right]^{1/2}, \tag{11}$$

where N_RJV_days is the total number of days when realized jump occurs and "days" denotes the trading days in a month. We follow the previous studies of China stock market to set the confidence level α at 0.95 in this paper. Our results show that, among 5 different capital-size portfolios, monthly jump size for the largest-cap portfolio is 8%, and it is 9% for the smallest-cap portfolio. The jump size mean is significantly larger than 0 for all portfolios. Standard deviation is about 0.32~0.36%, and jump arrival rate is about 19% for all portfolios.

2.2. Jump Components Risk Factor Model under the Incomplete Market. There are a few methods for measuring time-varying tail risk. First, Kelly and Jiang [20] devise a panel approach to estimate economy-wide conditional tail risk by using common fluctuation of the stocks. The framework is based on the long-run risk literature by Bansal and Yaron [21] and time-varying rare disaster model by Gabaix [24] as well as by Wachter [25]. Secondly, Bollerslev et al. [26] examine how the variance risk premium (VRP) implied in index option prices relates to the equity premium. As VRP is an ex-ante measure that represents investors' expectation for future risk, the realized jump is ex-post measure for tail risk.

Owing to the trading constraints, including short-selling constraint, liquidity issue, and budget constraint, the investors are not able to form market portfolio effectively and cannot diversify the nonsystematic risk away. As a result, the risk of the individual stock may need to be priced, and the risk information could be contained in the historical return characteristics (e.g., skewness and kurtosis.). This paper considers the jump the resource of stock risk and should affect the asset prices. We thus do an extensive investigation on the relation between jump risk and equity returns. Our empirical works cover the index returns, return of portfolios, and stock returns.

Guo and Robert [8] argue that it is the omitted variables problem that results in the failure of the CAPM, and they derive the equation about the effect of the idiosyncratic volatility on risk premium. Their argument is analogous to our reasoning on the tail risk of individual stock and can be expressed in following expression:

$$\begin{aligned} E_t\left(r_{i,t+1}\right) &= \gamma_M \mathrm{Cov}_t\left(r_{i,t+1}, r_{M,t+1}\right) + \gamma_H \mathrm{Cov}_t\left(r_{i,t+1}, r_{H,t+1}\right) \\ &= \gamma_M \frac{\mathrm{Cov}_t\left(r_{i,t+1}, r_{M,t+1}\right)}{\mathrm{Var}_t\left(r_{M,t+1}\right)} \mathrm{Var}_t\left(r_{M,t+1}\right) \\ &\quad + \gamma_H \frac{\mathrm{Cov}_t\left(r_{i,t+1}, r_{H,t+1}\right)}{\mathrm{Var}_t\left(r_{H,t+1}\right)} \mathrm{Var}_t\left(r_{H,t+1}\right) \\ &= \gamma_M \beta_{i,M,t} \mathrm{Var}_t\left(r_{M,t+1}\right) + \gamma_H \beta_{i,H,t} \mathrm{Var}_t\left(r_{H,t+1}\right). \end{aligned} \tag{12}$$

It says that the expected return on any asset is a function of conditional variances of stock market returns, $r_{M,t+1}$, and the risk factor, $r_{H,t+1}$, is omitted in the CAPM.

Under some moderate conditions, average idiosyncratic volatility (IV_t) is the proxy for volatility of $r_{H,t+1}$, and MV_t is the proxy of aggregate market volatility at time $t+1$; therefore, we can write

$$r_{i,t+1} = \alpha_{i,t} + \gamma_M \beta_{i,M} \mathrm{MV}_t + \gamma_H \beta_{i,H} \mathrm{IV}_t + \zeta_{i,t+1}. \quad (13)$$

For simplicity, we assume constant betas in (13), as Bollerslev et al. [27] do. Suppose that the intercept is zero; in (13), the loading on stock market volatility is equal to the market beta scaled by the price of market risk, γ_M. Similarly, the loading on idiosyncratic volatility is equal to the beta on the omitted risk factor scaled by its risk price, γ_H. Therefore, we can use (13) to explain the cross-sectional stock returns, even though we do not observe the risk factor, $r_{H,t+1}$. This method provides a direct link between time series and cross-sectional stock return predictability. If the value premium is an omitted risk factor, as argued by Fama and French [28], we can expect that its volatility should have predictive power for the stock returns similar to that of average idiosyncratic volatility.

Jump volatility risk shares similar characteristics regarding what generates IV. For example, Bollerslev et al. [27] provide a new framework for estimating the systematic and idiosyncratic jump tail risks in financial asset pricing. In their paper, the opinion dispersion is subsequently related to the jump, and it should be pointed out that their concept is also relevant to incomplete market hypothesis. Therefore, the theoretical argument over idiosyncratic volatility and jump volatility risk on equity returns is based on incomplete market foundation.

For an individual stock, the jump could result from nonsystematic information as well as systematic information. According to the theory, the index jump carries the systematic information, which also leads to the jump of individual stocks. Therefore, when investigating the nonsystematic jump effect on the returns, we also do both regressions with market jumps as well as without market jumps separately. In Section 4, we examine the nonsystematic and systematic jump effects on the returns of index, portfolios, and stocks. Our regression models for the stock return and portfolio are the following:

$$\begin{aligned} r_{i,m+1} = {} & C + \beta_{i,\mathrm{Size}} \mathrm{Size\_RJV}_m + \beta_{i,\mathrm{Std}} \mathrm{Std\_RJV}_m \\ & + \beta_{i,\mathrm{Arr}} \mathrm{Arr\_RJV}_t + \zeta_{M,m+1}, \end{aligned} \quad (14)$$

$$\begin{aligned} r_{i,m+1} = {} & C + \beta_{i,\mathrm{Size}} \mathrm{Size\_RJV}_m + \beta_{i,\mathrm{Std}} \mathrm{Std\_RJV}_m \\ & + \beta_{i,\mathrm{Arr}} \mathrm{Arr\_RJV}_m + \beta_{P,\mathrm{Size}} P\mathrm{Size\_RJV}_m \\ & + \beta_{P,\mathrm{Size}} P\mathrm{Size\_RJV}_m + \beta_{P,\mathrm{Std}} P\mathrm{Std\_RJV}_m \\ & + \zeta_{M,t+1}. \end{aligned} \quad (15)$$

As for index return, the estimation model is given as follows:

$$\begin{aligned} r_{P,m+1} = {} & \alpha_P + \beta_{P,\mathrm{size}} P\mathrm{Size\_RJV}_m + \beta_{P,\mathrm{std}} P\mathrm{Std\_RJV}_m \\ & + \beta_{P,\mathrm{Arr}} P\mathrm{Arr\_RJV}_m + \zeta_{P,m+1}. \end{aligned} \quad (16)$$

For each individual stock, Size_RJV, Std_RJV, and Arr_RJV denote monthly jump size, jump standard deviation, and jump arrival rate, respectively. PSize_RJV, PStd_RJV, and PArr_RJV represent monthly market index jump size, index jump standard deviation, and index jump arrival rate. m is the indication of month. i and p are notations for individual stock (portfolio) and index (market portfolio). In the robustness tests, we run the regression models incorporating Fama-French factors and regression models with nonlinear jump components. Those models are given as follows:

$$\begin{aligned} r_{i,m+1} = {} & C + \beta_{i,\mathrm{Size}} \mathrm{Size\_RJV}_m + \beta_{i,\mathrm{Std}} \mathrm{Std\_RJV}_m \\ & + \beta_{i,\mathrm{Arr}} \mathrm{Arr\_RJV}_m + \gamma_{i,\mathrm{size}} \mathrm{Size\_RJV}_m * \mathrm{Arr\_RJV}_m \\ & + \gamma_{i,\mathrm{std}} \mathrm{Std\_RJV}_m * \mathrm{Arr\_RJV}_m + \zeta_{i,t+1}, \end{aligned} \quad (17)$$

$$\begin{aligned} r_{i,m+1} = {} & C + \beta_{i,\mathrm{Size}} \mathrm{Size\_RJV}_m \\ & + \beta_{i,\mathrm{Std}} \mathrm{Std\_RJV}_m + \beta_{i,\mathrm{Arr}} \mathrm{Arr\_RJV}_m \\ & + \gamma_{i,\mathrm{size\_Arr}} \mathrm{Size\_RJV}_m * \mathrm{Arr\_RJV}_m \\ & + \gamma_{i,\mathrm{std\_Arr}} \mathrm{Std\_RJV}_m * \mathrm{Arr\_RJV}_m \\ & + \beta_{P,\mathrm{Size}} P\mathrm{Size\_RJV}_m + P\mathrm{Std\_RJV}_m \\ & + \beta_{P,\mathrm{Arr}} P\mathrm{Arr\_RJV}_m + \zeta_{i,m+1}, \end{aligned} \quad (18)$$

$$\begin{aligned} r_{i,m+1} = {} & C + \beta_{i,\mathrm{Size}} \mathrm{Size\_RJV}_m + \beta_{i,\mathrm{Std}} \mathrm{Std\_RJV}_m \\ & + \beta_{i,\mathrm{Arr}} \mathrm{Arr\_RJV}_m + \beta_{P,\mathrm{Size}} P\mathrm{Size\_RJV}_m \\ & + \beta_{P,\mathrm{Std}} P\mathrm{Std\_RJV}_m + \beta_{P,\mathrm{Arr}} P\mathrm{Arr\_RJV}_m \\ & + \gamma_{\mathrm{SMB}} \mathrm{SMB}_m + \gamma_{\mathrm{HML}} \mathrm{HML}_m + \zeta_{i,m+1}. \end{aligned} \quad (19)$$

When (17) expands (14) to include the nonlinear jump multiple terms, $\mathrm{Size\_RJV}_m * \mathrm{Arr\_RJV}_m$, $\mathrm{Std\_RJV}_m * \mathrm{Arr\_RJV}_m$, into repressors, (18) extends (17), so we can test nonlinearity effect of jump components under the control of the index jump components. Finally, (19) is used to investigate the nonlinear jump effect on return with control of Fama-French factors.

3. Estimation of Jump Components

3.1. Data and Summary Statistics. Intraday high-frequency trading contains noises. On the one hand, low sampling frequency may fail to depict the actual volatility information on that day. On the other hand, high sampling frequency may lead to the problem of micronoise which may affect the results. As suggested by the former literature, we use five-minute high-frequency data for return calculation. To minimize the noise, we then divide 200 randomly selected stocks into 5 portfolios based on the stock market value and then use the equally weighted return for realized jump estimation. The data comes from the CSMAR high-frequency database, and sampling period begins from January 4, 2007, and ends on October 31, 2013. There are 82 months and 49 transactions per day (including one overnight trading data and 48 intraday trading data). The individual stocks' monthly returns and the index returns are directly from the CSMAR financial database. We calculate all monthly jump components from high-frequency transaction and run the

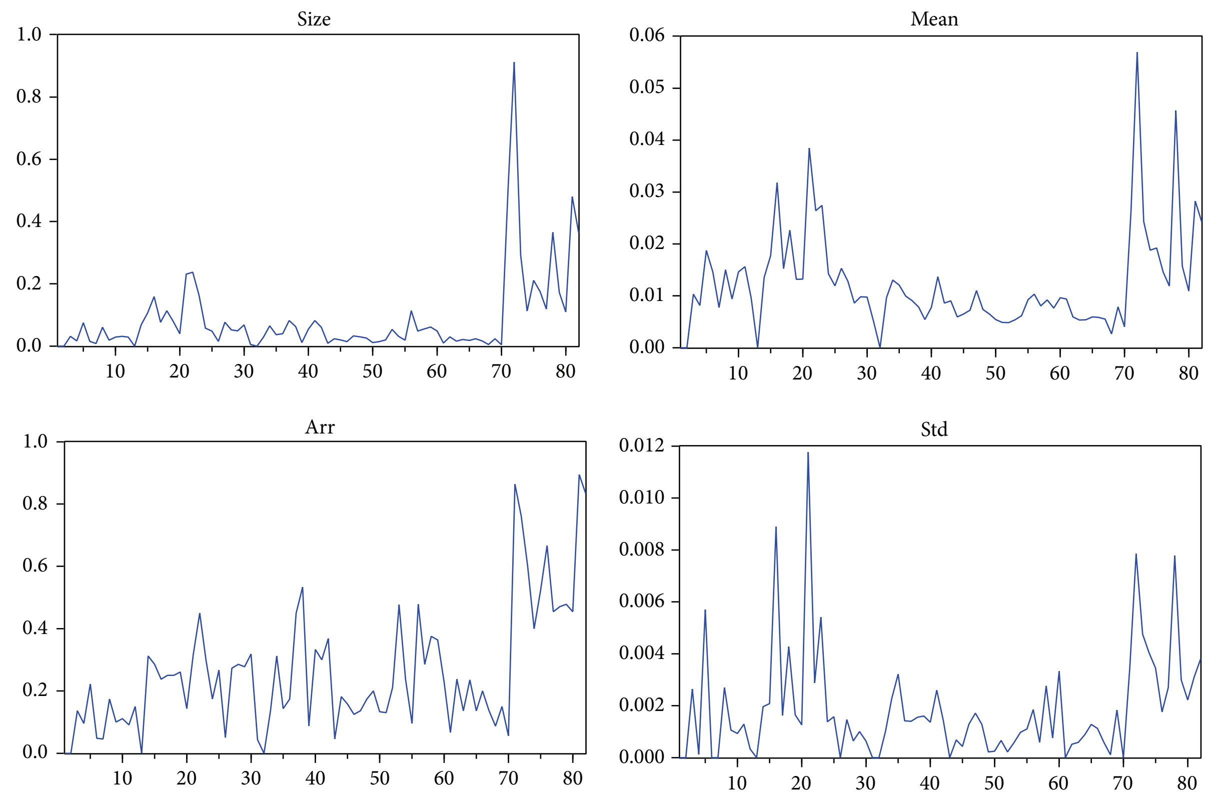

Figure 1: Time series characteristic of index jump components.

Table 1: Descriptive statistics for index jump components.

Index 000002	Size	Mean	Arr	Std
Mean	0.0864	0.0124	0.2608	0.0019
Median	0.0437	0.0096	0.2247	0.0013
Maximum	0.9120	0.0570	0.8947	0.0118
Minimum	0.0000	0.0000	0.0000	0.0000
Std. dev.	0.1361	0.0096	0.1990	0.0021
Skewness	3.6540	2.1444	1.2761	2.2811
Kurtosis	19.4318	9.0465	4.5444	9.2647
Jarque-Bera	1104.99	187.76	30.40	205.21
Probability	0.0000	0.0000	0.0000	0.0000

regression on monthly return over monthly jump components.

For market-level (systematic) realized jump estimation, our sample data is high-frequency return of Shanghai composite index. Table 1 demonstrates descriptive statistics of index jump components, and Figure 1 shows the time series of index jump components.

In comparison with the study of Tauchen and Zhou [29] on S&P, the A-share index jump size mean is 1.24%, while it is 6.5% for S&P index. The jump arrival rates are 26.08% for Shanghai index and 13.3% for S&P index; standard deviations are 0.19% for Shanghai index and 0.525% for S&P index. The difference is mainly due to the different significant level selected for jump filtration. Our paper sets α equal 0.95, allowing smaller jumps and increasing the jump arrival rate. Therefore, we have a larger sample size of realized jumps, and larger sample size leads to lower jump size variance. Additionally, as self-evident in Figure 1, the jump components are apparently time varying.

Table 2 shows the jump statistics of the largest-cap and second largest-cap portfolios, each of which contains 40 stocks. And Figure 2 demonstrates time series of jump components for size 1 portfolio.

Compared with jump components of index return, the magnitude of monthly jump size mean is larger for portfolios, and the arrival rate tends to be lower. The way we sort the portfolios by the size of capitalization is inspired not only by traditional cross-sectional return researches but also by Bollerslev et al. works in [27, 30], in which they show that their model works better for large cap stocks or for stocks traded actively (descriptive statistics for other portfolios are listed in the appendix). While the statistics of portfolio with smaller size stocks are shown in the appendix, we find very interesting pattern over jump components of 5 portfolios. As seen in Table 3 and Figure 3, monthly jump size, jump mean, jump intensity, and jump size variance tend to be lower for larger capitalization stocks. Therefore, jump components may capture the similar information of the size factor.

3.2. Jump Components of the Index and of the Individual Stock. In Figure 4, we compare jump components of individual stock, the largest-cap portfolio, and index over our sample

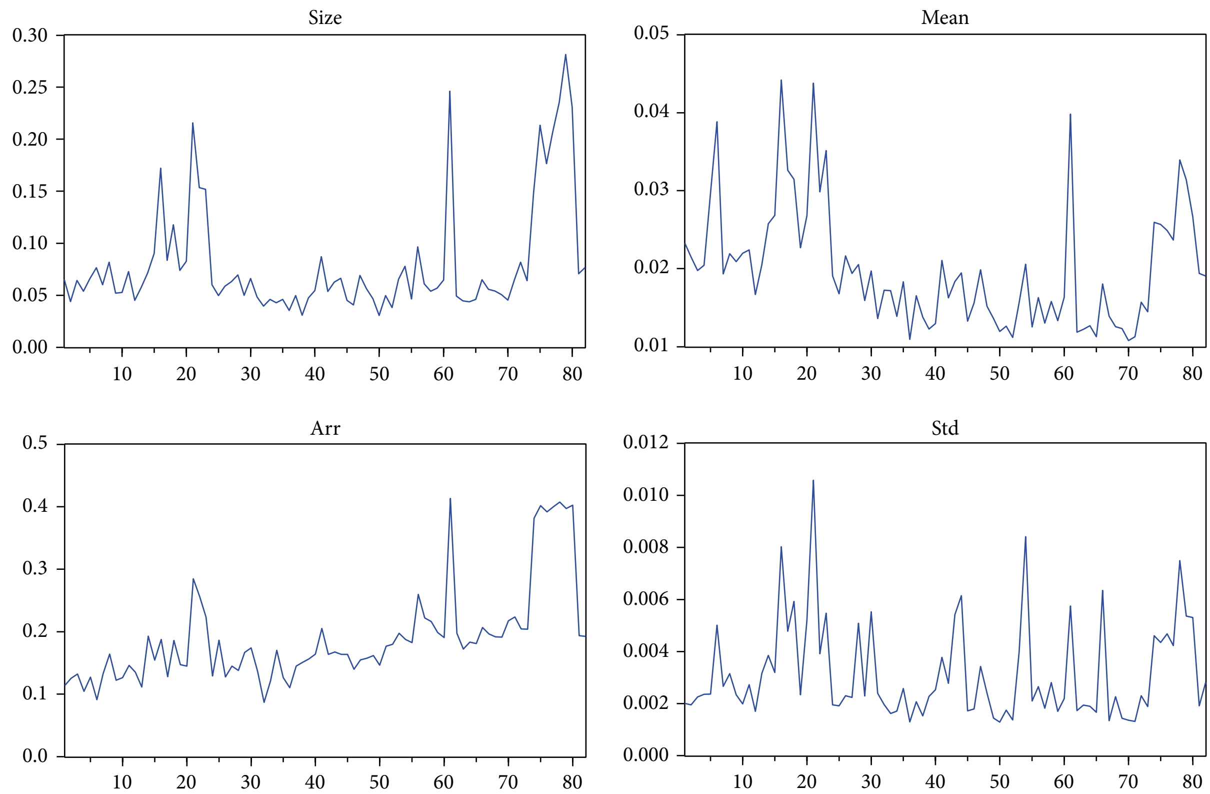

Figure 2: Time series characteristic of individual-based portfolio.

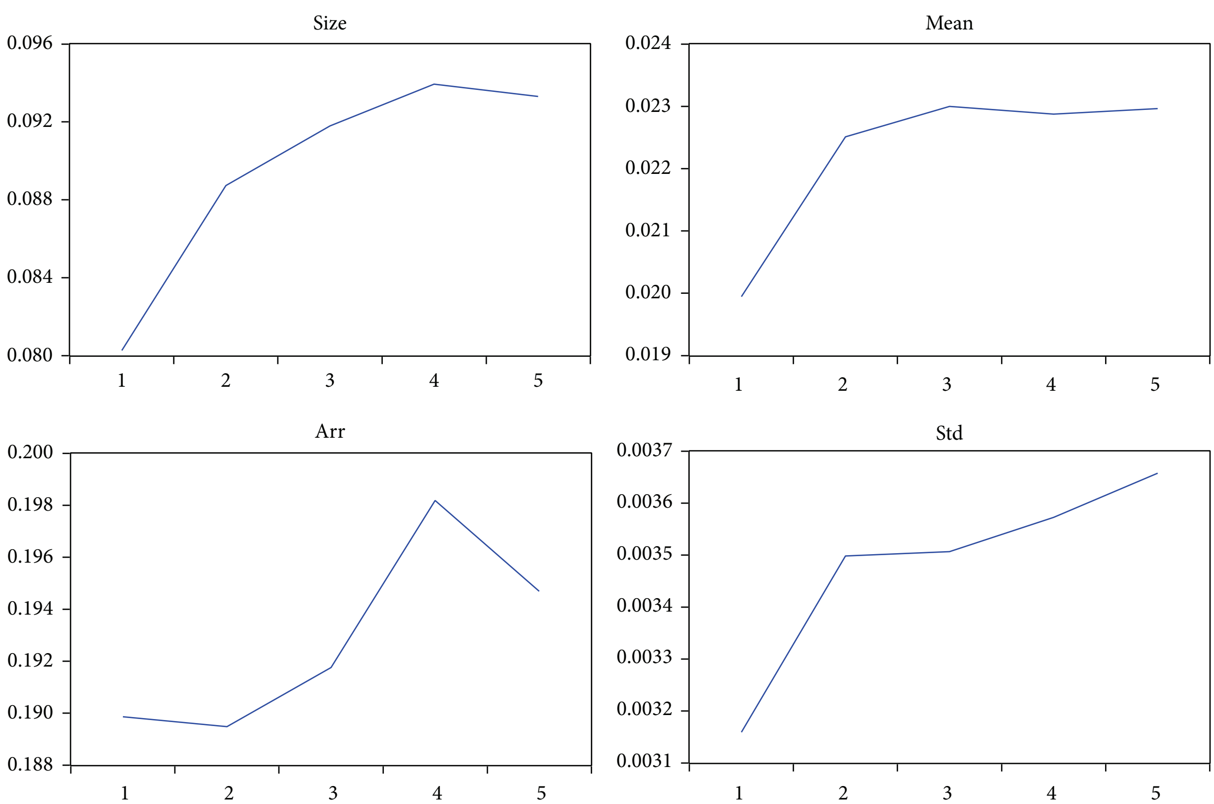

Figure 3: Trend of jump components for portfolios.

Table 2: Descriptive statistics of jump components for size 1 and size 2 portfolios.

SZ1	Size	Mean	Arr	Std	SZ2	Size	Mean	Arr	Std
Mean	0.0803	0.0199	0.1899	0.0032	Mean	0.0887	0.0225	0.1895	0.0035
Median	0.0617	0.0187	0.1713	0.0023	Median	0.0656	0.0202	0.1707	0.0029
Maximum	0.2813	0.0442	0.4134	0.0106	Maximum	0.3011	0.0488	0.4264	0.0097
Minimum	0.0304	0.0108	0.0870	0.0013	Minimum	0.0429	0.0119	0.1065	0.0014
Std. dev.	0.0553	0.0077	0.0786	0.0019	Std. Dev.	0.0596	0.0082	0.0744	0.0018
Skewness	2.0477	1.2664	1.7262	1.5554	Skewness	2.0234	1.1964	1.9767	1.3557
Kurtosis	6.2403	4.3168	5.3520	5.3717	Kurtosis	6.0927	4.1452	6.1131	4.5256
Jarque-Bera	93.181	27.843	59.623	52.283	Jarque-Bera	88.634	24.043	86.513	33.071
Probability	0.0000	0.0000	0.0000	0.0000	Probability	0.0000	0.0000	0.0000	0.0000

Table 3: Descriptive statistics of jump components for portfolios.

Portfolio mean	Size	Mean	Arr	Std
SZ1	0.0803	0.0199	0.1899	0.0032
SZ2	0.0887	0.0225	0.1895	0.0035
SZ3	0.0918	0.0230	0.1918	0.0035
SZ4	0.0939	0.0229	0.1982	0.0036
SZ5	0.0933	0.0230	0.1947	0.0037
Observations	82	82	82	82

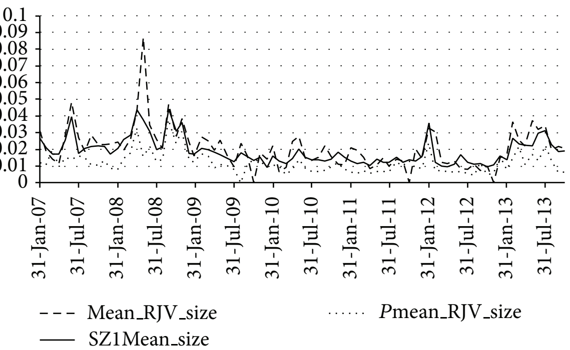

Figure 4: Jump size mean for a stock, a size 1 portfolio, and an A-share index.

Table 4: Forecasting one-month-ahead index returns using realized jump risk factor model.

Variables	C	PSize	PArr	PStd	Adj.R^2
Coefficients	0.027	0.278^{**}	−0.055	-18.695^{***}	0.080

Note: The numbers in the table are coefficients, and "∗", "∗∗", "∗∗∗" represents 10%, 5% and 1% significance level, same for the following tables.

Table 5: Forecasting one-month-ahead individual stock returns using realized jump volatility-based factor model.

Stock	C	Size_RJV	Arr_RJV	Std_RJV	Adj.R^2
600362	0.115^{***}	0.977^{*}	-0.760^{**}	−9.494	0.047
600100	0.044	0.533	−0.357	-3.494^{*}	0.010
600859	0.037	0.602^{*}	−0.206	-14.241^{**}	0.039

period. The stock is one randomly picked stock in size 1 portfolio, and we can find the jump comovements between the stock, portfolio, and index. In this quick glance, the monthly jump size mean is the largest for the individual stock and the lowest for the index. The figure strongly implies that index jump components could also be a proxy for the systematic risk.

4. Forecasting One-Month-Ahead Equity Returns

Realize that jump components have been applied for predicting and explaining the return of market in the USA and China. However, for the return of stock and portfolio, no empirical work has been done by using the realized jump measure. The existing researches for stock market in China mainly have been focusing on either macroeconomic variables or Fama-French multifactor models. Our paper thus makes the contribution of applying jump components to study the equity return and exploring their power to predict the return. By aggregating the daily realized jump into monthly jump size, we then use the monthly realized jump components as risk factors to explain one-month-ahead equity return. Meanwhile, we also consider index jump components systematic risks and add them as control variables in our tests.

4.1. Forecasting One-Month-Ahead Index Return. For the market-level realized jump, our sample is the return of Shanghai composite A-share index (000002). Because the calculations of monthly jump size and monthly jump size mean are highly related, we use monthly jump size as one of the explanatory variables. Table 4 shows the results of regression. In linear model, the monthly jump size (Psize)

Table 6: Forecasting one-month-ahead individual stock portfolio returns using realized jump volatility-based factor model with market-level jump components.

Stock	C	Size_RJV	Arr_RJV	Std_RJV	Psize	PStd	PArr	Adj.R^2
600362	−0.04	6.024**	−0.02	−12.957**	5.045	−0.042	−33.608**	0.113
600100	0.072**	0.654*	−0.39	−3.818*	0.305	−0.108	−15.798	0.015
600859	0.057*	0.890**	−0.251	−15.176***	0.135	−0.014	−22.315***	0.104

Table 7: Forecasting one-month-ahead individual-based portfolio returns using realized jump volatility-based factor model.

Size	C	Size_RJV	Std_RJV	Arr_RJV	Adj.R^2
1	0.073**	0.725	−13.634*	−0.379	0.011
2	0.120**	1.390**	−20.060	−0.823**	0.024
3	0.107**	1.132*	−26.017*	−0.539	0.016
4	0.099	1.117	−19.607	−0.588*	—
5	0.079	0.848	−11.404	−0.517	—

and monthly jump standard deviation (Pstd) are significant, while the coefficients are positive for the jump size and negative for jump standard deviation. It is quite intuitive that the larger jump size implies higher tail risk such that investors require higher return. However, the negative sign for jump standard deviation is not easy to comprehend.

While Guo and Robert [7, 8] also find that the average idiosyncratic volatility has negative coefficients on future index return, they claim that the average idiosyncratic volatility may capture the information of opportunity cost. When higher opportunity lowers the return, the increase of idiosyncratic volatility decreases the returns. We thus conjecture that the jump standard deviation may also catch the information of opportunity cost.

4.2. Forecasting One-Month-Ahead Stock Return. Following Bollerslev et al. [27, 30], using top 40 large cap stocks or stocks traded actively for empirical analysis, we also pick up large cap stocks among our randomly selected stocks for predicting power tests. For each stock, we first regress the individual stock's return on its realized jump components and then add market components into explanatory variables for advanced investigation. Tables 5 and 6 demonstrate the results of two regressions for 3 large cap stocks. The results of more stocks listed in our largest-cap portfolio are shown in the appendix. According to the results for stock, we find that jump size is commonly a tail risk factor in explaining the future return, and at least one jump component is a significant factor in regression.

Moreover, the coefficient signs for jump size and jump standard deviation are consistent with the results of index return. From the general equilibrium perspective, if the tail risk cannot be diversified away, higher jump size implies higher tail risk and requires higher return for compensation. As for negative relation between return and jump standard deviation, we think that the jump standard deviation is highly negatively correlated with book-to-market ratio for the success or failure of a project, leading to the jump, has stronger impact on stocks with lower book-to-market ratio. Hence, higher jump size deviation implies lower book-to-market ratio. While Gou and Robert [7, 8] empirically show the negative correlation between idiosyncratic volatility and book-to-market ratio, we are collecting more accounting information for another further work. Table 6 shows the results with the control of market jump components. The Adj.R^2 increases after we include index jump components into the regression model.

4.3. Forecasting One-Month-Ahead Portfolio Return. For portfolio return analysis, we apply the convention of cross-section return research which divides the total sample into 5 portfolios based on the stock market capital size. Using the portfolio return helps us to reduce the trading noise of the individual stock. As a few researches apply realized jump to study the index return, we supplement the first empirical study of realized jump effect on the portfolio and the stock return. Similar to our empirical work on stocks, we first estimate portfolio return over the portfolio jump components and show the results in Table 7. Then, we include the market index jump components as the control variables and list the results in Table 8.

According to Table 7, the jump components work better to explain the future return for larger-cap portfolios, including size 1 to size 3. For smaller size portfolios (size 4 and size 5), the jump components perform marginally in predicting return. The Adj.R^2 is also very low for small cap portfolio. Those results are consistent with the paper by Bollerslev et al. [27, 30], in which they show that their model performs better for large cap stocks. In addition, the signs of the coefficients agree with results of index and stocks. Our conclusion does not alter if we add market-level jump components into the regression model; however, the explaining power of the model increases greatly. With the control of market jump components, all of jump components, including monthly jump size (Size_RJV), jump standard deviation (Std_RJV), and arrival rate (Arr_RJV), become significant for size 2 portfolios. Finally, we find that jump arrival rate also has significantly negative impact on return for large cap portfolio. However, the role of jump arrival rate should not be overemphasized, because size has correlations with jump arrival rate owing to jump detection statistics design. In this paper, we set α equal to 0.95, leading to jump size mean ranging from

Table 8: Forecasting one-month-ahead individual-based portfolio returns using realized jump volatility-based factor model with market-level jump components.

Size	C	Size_RJV	Arr_RJV	Std_RJV	Psize	PArr	PStd	Adj.R^2
1	0.083**	1.237*	−0.581*	−9.260	−0.170	0.033	0.033	0.047
2	0.139**	2.022**	−1.092**	−16.304**	−0.171	0.042**	0.042**	0.108
3	0.099*	1.184	−0.597	−12.683	0.246	−0.036*	−0.036*	0.040
4	0.088	1.649*	−0.728	−7.980	−0.272	−0.009	−0.009	0.057
5	0.088	1.389	−0.620	−7.020	0.112	−0.086	−0.086	0.015

Table 9: Forecasting one-month-ahead individual returns using realized jump volatility-based factor model with FF factors.

	C	Size_RJV	Arr_RJV	Std_RJV	Psize	PArr	PStd	SMB	HML	Adj.R^2
600362	0.150***	1.280**	−0.806**	−11.864	0.484*	−0.089	−35.944***	−0.049	−0.671	0.103
600100	0.067*	0.643*	−0.382	−3.764*	0.300	−0.110	−14.427	0.258	0.027	0.015
600859	0.047	0.882*	−0.260	−15.119**	0.118	−0.011	−19.235**	0.597*	0.133	0.123

Table 10: Forecasting one-month-ahead individual returns using realized jump volatility-based factor model with cross-term.

	C	Size_RJV	Arr_RJV	Std_RJV	Psize	PArr	PStd	Std $*$ Arr	Size $*$ Arr	Adj.R^2
600362	0.167***	1.842**	−0.837**	−40.387*	0.513*	−0.112	−40.058**	129.012	−2.333	0.115
600100	0.087**	−0.185	−0.31	3.484	0.256	−0.113	−8.573	−51.175	2.044	0.018
600859	0.047	0.761	−0.249	−2.221	0.138	−0.009	−22.127***	−69.190	1.124	0.096

Table 11: Forecasting one-month-ahead index returns using realized jump volatility-based factor model with cross-term of its jump components.

Index	C	Psize	PArr	PStd	Std $*$ Arr	Size $*$ Arr	Adj.R^2
	0.015	0.691	−0.042	−8.972	−56.573	−0.162	0.058
000002	C	Psize	PArr	PStd			Adj.R^2
	0.027	0.278**	−0.055	−18.695***			0.080

1 to 3% and jump arrival rate ranging from 15 to 25%. If the confidence level α increases to 0.99, the stricter criteria naturally discriminate against smaller jumps. As a result, out data contains only larger jumps, leading to lower arrival rate. This paper follows the previous study, using the ease criteria to filter the jump. Compared with Tauchen and Zhou [29], documenting 6% jump size mean, our jump size mean is 2% and is more practical for nature of jump dynamics.

In summary of 4.1, 4.2, and 4.3, the monthly jump size (Size_RJV) is a significant risk factor which positively influences one-month-ahead return, while the jump size standard deviation (Std_RJV) has negative impact on the return. After including market jump components, we derive the same conclusion and find the increased Adj.R^2. Overall, as shown in the appendix, even for the individual stock, at least one jump component is a significant factor for return with or without the control of market jump components.

5. Robustness Tests

In this section, we proceed with the robustness tests from two perspectives. First, because many empirical works use Fama-French factor models to explain cross-sectional returns, this paper thus compares jump risk factors together with size and book-to-market ratio for stock return. Secondly, we consider jump components' nonlinear effect on return; therefore, the multiples of jump risk factors are added to regression models for advanced tests. If those multiple terms are significant and greatly improve the predicting power, then the effect of jump risk factors on return is probably nonlinear.

Table 9 shows the jump risk factors regression with control of size (SMB) and book-to-market ratio (HML) for stocks. The jump size and standard deviation remain significant, and Adj.R^2 does not increase. Additionally, Fama-French factors are not significant. In other words, the one-month-ahead return is influenced by the jump effect rather than FF factors.

Table 10 demonstrates the results of regressions which incorporate the multiples of jump risk factors. Though Adj.R^2 improves slightly, the multiple terms are not significant.

Table 11 shows the robustness results for index jump effect on the returns. As seen, not only nonlinear terms, Std $*$ Arr and Size $*$ Arr, are insignificant, but also Adj.R^2 drops.

Table 12 shows the robustness results for 5 portfolios. After adding control variables of multiple terms, all jump components became insignificant for size 1 portfolio. While Adj.R^2 does not increase, the nonlinear terms are not significant.

Table 12: Forecasting one-month-ahead individual-based portfolio returns using realized jump volatility-based factor model with cross-term of its jump components.

Size	C	Size_RJV	Arr_RJV	Std_RJV	Psize	PArr	PStd	Std ∗ Arr	Size ∗ Arr	Adj.R^2
1	0.091	1.139	−0.612	−10.041	−0.146	0.028	−15.147	5.862	0.194	0.020
2	0.146	4.829*	−1.439*	−74.502	−0.734	0.156	−27.168**	295.313	−9.148	0.103
3	0.058	2.062	−0.491	−18.227	0.070	0.000	−23.763*	8.667	−2.071	0.017
4	0.111	3.156	−0.946	−45.107	−0.560	0.032	−23.857*	146.138	−4.150	0.040
5	0.099	2.762	−0.756	−40.191	−0.021	−0.054	−28.734**	145.713	−4.528	0.042

Size 1 to size 5 portfolios are arranged in the order of capitalization. Size 1 is the largest-cap portfolio, while size 5 is the smallest-cap portfolio. The numbers in the table are coefficients, and "∗", "∗∗", and "∗∗∗" represent 10%, 5%, and 1% significance levels.

Table 13: Descriptive statistics of jump components for size 3 to size 5 portfolios.

SZ3	Size	Mean	Arr	Std	SZ4	Size	Mean	Arr	Std	SZ5	Size	Mean	Arr	Std
Mean	0.0918	0.0230	0.1918	0.0035	Mean	0.0939	0.0229	0.1982	0.0036	Mean	0.0933	0.0230	0.1947	0.0037
Median	0.0690	0.0212	0.1756	0.0030	Median	0.0719	0.0200	0.1778	0.0030	Median	0.0712	0.0210	0.1727	0.0033
Maximum	0.3286	0.0508	0.4283	0.0090	Maximum	0.3002	0.0505	0.4330	0.0089	Maximum	0.2663	0.0499	0.4324	0.0095
Minimum	0.0326	0.0131	0.0855	0.0012	Minimum	0.0447	0.0140	0.1032	0.0018	Minimum	0.0386	0.0147	0.1085	0.0011
Std. dev.	0.0604	0.0081	0.0779	0.0016	Std. dev.	0.0568	0.0079	0.0759	0.0016	Std. dev.	0.0552	0.0077	0.0762	0.0016
Skewness	2.0464	1.3540	1.6768	1.3756	Skewness	1.9224	1.5546	1.7292	1.5800	Skewness	1.6370	1.5211	1.5507	1.4567
Kurtosis	6.6092	4.6886	5.3955	4.5527	Kurtosis	5.8266	5.1466	5.4538	5.1632	Kurtosis	4.8022	5.0022	4.7581	5.1850
Jarque-Bera	101.74	34.799	58.033	34.099	Jarque-Bera	77.807	48.773	61.438	50.105	Jarque-Bera	47.720	45.318	43.423	45.311
Probability	0.0000	0.0000	0.0000	0.0000	Probability	0.0000	0.0000	0.0000	0.0000	Probability	0.0000	0.0000	0.0000	0.0000
										Observations	82	82	82	82

Table 14: Descriptive statistics for individual stock average jump components.

600362	Size	Mean	Arr	Std
Mean	0.106062	0.023454	0.216076	0.003758
Median	0.074818	0.023504	0.195238	0.002885
Maximum	0.528641	0.063170	0.733333	0.018655
Minimum	0.000000	0.000000	0.000000	0.000000
Std. dev.	0.090047	0.011790	0.135851	0.003497
Skewness	1.740065	0.680288	0.938441	1.552614
Kurtosis	7.637096	3.866075	4.460514	6.301100
Jarque-Bera	114.8477	8.887622	19.32393	70.17733
Probability	0.000000	0.011751	0.000064	0.000000

In short, after controlling size and value factors, we find that the realized jump risk can explain and predict the equity return. Therefore, jump is an important risk factor needed to be considered for asset pricing and risk management. We also find that nonlinear models do not work better than linear models [31].

6. Conclusion

For risk-aversion investors, jump risk, which leads to return distribution with fat tail, can greatly affect investors' perception about how risky a company is or how it captures the risk information. As long as nonsystematic risk of the individual stock cannot be diversified away, the firm-level and industry-level risk should be priced into the return. This paper applies the realized jump, considers a measure of tail risk, and uses high-frequency data to estimate jump components including jump size mean, jump size standard deviation, and jump intensity. We argue that trading constraints make investors unable to diversify nonsystematic risk away; hence, the tail risk should be priced, and jump should be able to explain the asset return.

Our data contain high-frequency trades of 200 randomly selected stocks which are the composite stocks for Shanghai composite index. Our empirical works are divided into 3 parts, including index return, portfolio returns, and stock returns. Under the control of Fama-French factors, our results show that jump factors can explain one-month-ahead return for index, high cap portfolio, and high cap stocks. Moreover, we also try to use nonlinear combinations of jump components to explain and predict the returns. However, no evidence supports that the nonlinear models are better than linear models.

In our research, the monthly jump size and jump size standard deviation are generally significant factors for equity return. The positive coefficient for jump size is quite intuitive as it is directly linked to the tail risk. However, the negative coefficient for jump size standard deviation is for the first time documented in the literature. We claim that the jump standard deviation is positively related to opportunity cost which decreases the returns, as similar argument was made for the idiosyncratic volatility. Obviously, further theoretical models are needed after we find that jump components can explain the return. We are also looking forward to the theory model delivering the insights about how jump components are prices and looking forward to seeing more empirical

Table 15

	C	Size_RJV	Arr_RJV	Std_RJV						Adj.R^2
600066	0.039	−0.162	0.069	−4.371						0.051
	C	Size_RJV	Arr_RJV	Std_RJV	Psize	PArr	PStd			Adj.R^2
600066	0.056*	0.145	−0.058	−5.543*	0.165	0.017	−17.954*			0.069
	C	Size_RJV	Arr_RJV	Std_RJV	Psize	PArr	PStd	Std ∗ Arr	Size ∗ Arr	Adj.R^2
600066	0.028	0.601	−0.024	5.626	0.147	0.051	−19.204**	−68.284	−0.303	0.062
	C	Mean_RJV	Arr_RJV	Std_RJV						Adj.R^2
600276	0.003	−1.517	0.138*	4.749*						0.045
	C	Mean_RJV	Arr_RJV	Std_RJV	Pmean	PArr	PStd			Adj.R^2
600276	0.009	−1.856	0.122	4.901*	4.206*	−0.117*	−9.39			0.064
	C	Mean_RJV	Arr_RJV	Std_RJV	Pmean	PArr	PStd	Std ∗ Arr	Mean ∗ Arr	Adj.R^2
600276	0.025	−1.484	0.03	−3.703	4.598**	−0.121*	−10.859	42.980**	−2.751	0.148
	C	Size_RJV	Arr_RJV	Std_RJV						Adj.R^2
600377	0.115***	0.977*	−0.760**	−9.494						0.047
	C	Size_RJV	Arr_RJV	Std_RJV	Psize	PArr	PStd			Adj.R^2
600377	−0.04	6.024**	−0.02	−12.957**	5.045	−0.042	−33.608**			0.113
	C	Size_RJV	Arr_RJV	Std_RJV	Psize	PArr	PStd	Std ∗ Arr	Size ∗ Arr	Adj.R^2
600377	0.055	−0.711	−0.268	22.229*	0.247*	−0.043	−16.372**	−141.272*	5.712*	0.115
	C	Mean_RJV	Arr_RJV	Std_RJV						Adj.R^2
600079	−0.015	5.303**	−0.181	−11.173*						0.073
	C	Mean_RJV	Arr_RJV	Std_RJV	Pmean	PArr	PStd			Adj.R^2
600079	−0.04	6.024**	−0.02	−12.957**	5.045	−0.042	−33.608**			0.112
	C	Mean_RJV	Arr_RJV	Std_RJV	Pmean	PArr	PStd	Std ∗ Arr	Mean ∗ Arr	Adj.R^2
600079	−0.116*	9.884**	0.504*	−2.751	4.86	−0.063	−27.503*	−34.662	−27.183	0.146
	C	Size_RJV	Arr_RJV	Std_RJV						Adj.R^2
601006	−0.004	0.177	0.110	−9.650*						0.052
	C	Size_RJV	Arr_RJV	Std_RJV	Psize	PArr	PStd			Adj.R^2
601006	0.015	0.358	0.067	−7.748*	0.188	−0.071	−12.002			0.053
	C	Size_RJV	Arr_RJV	Std_RJV	Pmean	PArr	PStd	Std ∗ Arr	Size ∗ Arr	Adj.R^2
601006	0.031	0.002	0.020	−14.181	0.192	−0.082	−9.975	40.557	0.393	0.044
	C	Size_RJV	Arr_RJV	Std_RJV						Adj.R^2
600748	0.049	−0.004	−0.178	0.717						—
	C	Size_RJV	Arr_RJV	Std_RJV	Psize	PArr	PStd			Adj.R^2
600748	0.111**	0.536	−0.187	−2.107	0.642**	−0.253	−47.805***			0.101
	C	Size_RJV	Arr_RJV	Std_RJV	Psize	PArr	PStd	Std ∗ Arr	Size ∗ Arr	Adj.R^2
600748	0.119*	−0.019	−0.226	9.983	0.608**	−0.225	−47.241***	−66.184	2.291	0.087

researches on what information is contained in the jump components.

Appendix

Tables 13, 14, and 15 show the descriptive statistics of individual-based portfolio 3 to portfolio 5 and individual stock, respectively. Figure 5 shows the time series of individual stock's jump components.

We forecast one-month-ahead stock return using the following:

$$r_{i,m+1} = C + \beta_{i,\mathrm{Size}}\mathrm{Size\_RJV}_m + \beta_{i,\mathrm{Std}}\mathrm{Std\_RJV}_m + \beta_{i,\mathrm{Arr}}\mathrm{Arr\_RJV}_t + \zeta_{M,m+1},$$

$$\begin{aligned} r_{i,m+1} = {} & C + \beta_{i,\mathrm{Size}}\mathrm{Size\_RJV}_m + \beta_{i,\mathrm{Std}}\mathrm{Std\_RJV}_m \\ & + \beta_{i,\mathrm{Arr}}\mathrm{Arr\_RJV}_m + \beta_{P,\mathrm{Size}}P\mathrm{Size\_RJV}_m \\ & + \beta_{P,\mathrm{Size}}P\mathrm{Size\_RJV}_m + \beta_{P,\mathrm{Std}}P\mathrm{Std\_RJV}_m \\ & + \zeta_{M,t+1}, \end{aligned}$$

$$\begin{aligned} r_{i,m+1} = {} & C + \beta_{i,\mathrm{Size}}\mathrm{Size\_RJV}_m \\ & + \beta_{i,\mathrm{Std}}\mathrm{Std\_RJV}_m + \beta_{i,\mathrm{Arr}}\mathrm{Arr\_RJV}_m \\ & + \gamma_{i,\mathrm{size\_Arr}}\mathrm{Size\_RJV}_m * \mathrm{Arr\_RJV}_m \\ & + \gamma_{i,\mathrm{std\_Arr}}\mathrm{Std\_RJV}_m * \mathrm{Arr\_RJV}_m \end{aligned}$$

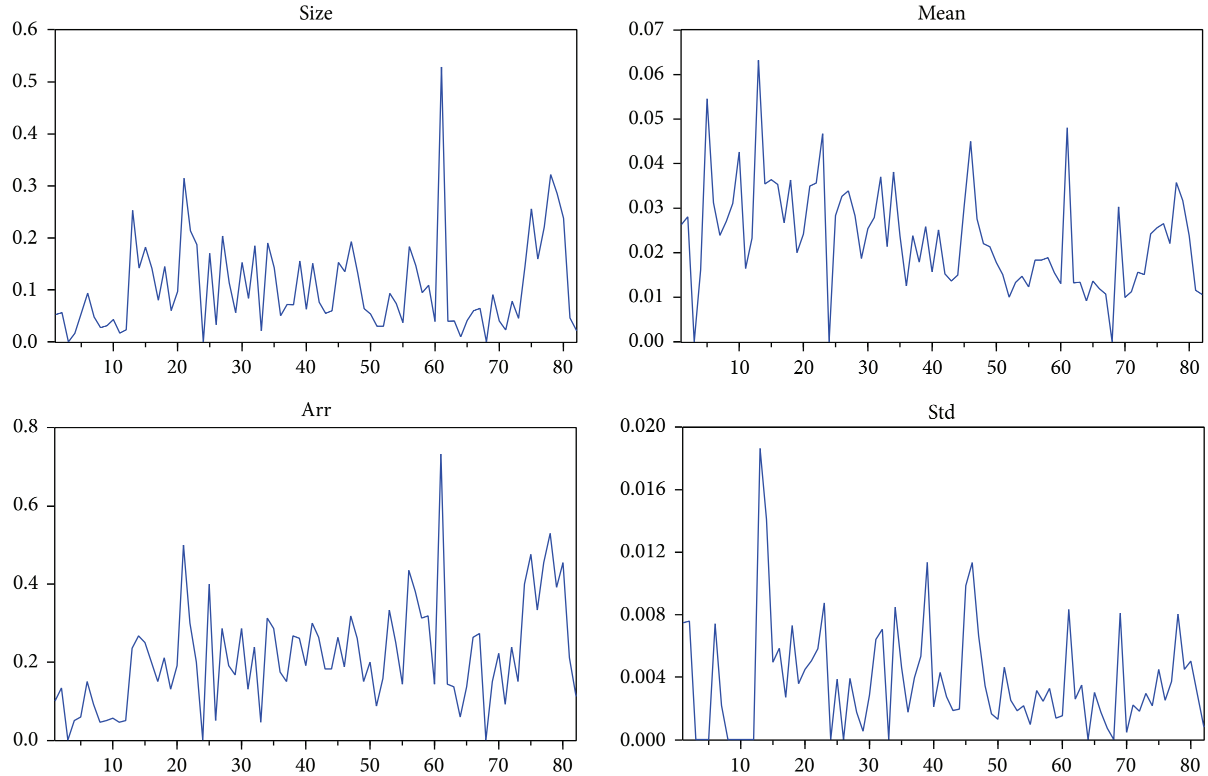

Figure 5: Time series characteristic of individual stock.

$$+ \beta_{P,\mathrm{Size}} P\mathrm{Size\_RJV}_m + P\mathrm{Std\_RJV}_m + \beta_{P,\mathrm{Arr}} P\mathrm{Arr\_RJV}_m + \zeta_{i,m+1}. \tag{A.1}$$

Conflict of Interests

The authors declare that there is no conflict of interests regarding the publication of this paper.

Acknowledgment

This work was partly supported by National Science Foundation of China (Grant no. 71071132).

References

[1] E. F. Fama and K. R. French, "The cross-section of expected stock returns," *The Journal of Financial*, vol. 47, no. 2, pp. 427–465, 1992.

[2] E. F. Fama and K. R. French, "Common risk factors in the returns on stocks and bonds," *Journal of Financial Economics*, vol. 33, no. 1, pp. 3–56, 1993.

[3] C. R. Harvey and A. Siddique, "Conditional skewness in asset pricing tests," *The Journal of Finance*, vol. 6, no. 3, pp. 1263–1295, 2000.

[4] F. Wen and X. Yang, "Skewness of return distribution and coefficient of risk premium," *Journal of Systems Science and Complexity*, vol. 22, no. 3, pp. 360–371, 2009.

[5] R. C. Merton, "A simple model of capital market equilibrium with incomplete information," *The Journal of Finance*, vol. 42, no. 3, pp. 483–510, 1987.

[6] A. Ang, R. Hodrick, Y. Xing, and X. Zhang, "High idiosyncratic volatility and low returns: international and further U.S. evidence," Working Paper, Columbia Univerity, 2006.

[7] H. Guo and S. Robert, "Idiosyncratic volatility, stock market volatility, and expected stock returns," *Journal of Business & Economic Statistics*, vol. 24, no. 1, pp. 43–56, 2006.

[8] H. Guo and S. Robert, "Average idiosyncratic volatility in G7 countries," *The Review of Financial Studies*, vol. 21, no. 3, pp. 1259–1296, 2008.

[9] J. Y. Campbell, M. Lettau, B. G. Malkiel, and Y. Xu, "Have individual stocks become more volatile? An empirical exploration of idiosyncratic risk," *The Journal of Finance*, vol. 56, no. 1, pp. 1–43, 2001.

[10] T. G. Andersen, T. Bollerslev, F. X. Diebold, and P. Labys, "The distribution of realized exchange rate volatility," *Journal of the American Statistical Association*, vol. 96, no. 453, pp. 42–55, 2001.

[11] T. G. Andersen, T. Bollerslev, F. Diebold, and H. Ebens, "The distribution of realized stock return volatility," *Journal of Financial Economics*, vol. 61, no. 1, pp. 43–76, 2001.

[12] S. J. Koopman, B. Jungbacker, and E. Hol, "Forecasting daily variability of the S&P 100 stock index using historical, realised and implied volatility measurements," *Journal of Empirical Finance*, vol. 12, no. 3, pp. 445–475, 2005.

[13] F. Corsi, "A simple approximate long-memory model of realized volatility," *Journal of Financial Econometrics*, vol. 7, no. 2, pp. 174–196, 2009.

[14] T. G. Andersen, T. Bollerslev, and F. X. Diebold, "Roughing it up: including jump components in the measurement, modeling, and forecasting of return volatility," *The Review of Economics and Statistics*, vol. 89, no. 4, pp. 701–720, 2007.

[15] T. G. Andersen, T. Bollerslev, and X. Huang, "A reduced form framework for modeling volatility of speculative prices based on realized variation measures," *Journal of Econometrics*, vol. 160, no. 1, pp. 176–189, 2011.

[16] F. Wen and Z. Liu, "A copula-based correlation measure and its application in chinese stock market," *International Journal of Information Technology & Decision Making*, vol. 8, no. 4, pp. 787–801, 2009.

[17] C. Huang, X. Gong, X. Chen, and F. Wen, "Measuring and forecasting volatility in Chinese stock market using HAR-CJ-M model," *Abstract and Applied Analysis*, vol. 2013, Article ID 143194, 13 pages, 2013.

[18] C. Huang, C. Peng, X. Chen, and F. Wen, "Dynamics analysis of a class of delayed economic model," *Abstract and Applied Analysis*, vol. 2013, Article ID 962738, 12 pages, 2013.

[19] T. Adrian and J. Rosenberg, "Stock returns and volatility: pricing the short-run and long-run components of market risk," *The Journal of Finance*, vol. 63, no. 6, pp. 2997–3030, 2008.

[20] B. Kelly and H. Jiang, "Tail Risk and Asset Prices," Working Paper no. 19375, The National Bureau of Economic Research, 2013.

[21] R. Bansal and A. Yaron, "Risks for the long run: a potential resolution of asset pricing puzzles," *The Journal of Finance*, vol. 59, no. 4, pp. 1481–1509, 2004.

[22] T. A. Rietz, "The equity risk premium a solution," *Journal of Monetary Economics*, vol. 22, no. 1, pp. 117–131, 1988.

[23] R. Barro, "Rare disasters and asset markets in the twentieth century," *Quarterly Journal of Economics*, vol. 121, no. 3, pp. 823–866, 2006.

[24] X. Gabaix, "Variable rare disasters: an exactly solved framework for ten puzzles in macro-finance," *Quarterly Journal of Economics*, vol. 127, no. 2, pp. 645–700, 2012.

[25] J. A. Wachter, "Can time-varying risk of rare disasters explain aggregate stock market volatility," *The Journal of Finance*, vol. 63, no. 3, pp. 987–1035, 2013.

[26] T. Bollerslev, M. Gibson, and H. Zhou, "Dynamic estimation of volatility risk premia and investor risk aversion from option-implied and realized volatilities," *Journal of Econometrics*, vol. 160, no. 1, pp. 235–245, 2011.

[27] T. Bollerslev, V. Todorov, and S. Z. Li, "Jump tails, extreme dependencies, and the distribution of stock returns," *Journal of Econometrics*, vol. 172, no. 2, pp. 307–324, 2013.

[28] E. Fama and K. French, "Multifactor explanations of asset pricing anomalies," *The Journal of Finance*, vol. 51, no. 1, pp. 55–84, 1996.

[29] G. Tauchen and H. Zhou, "Realized jumps on financial markets and predicting credit spreads," *Journal of Econometrics*, vol. 160, no. 1, pp. 102–118, 2011.

[30] T. Bollerslev, T. H. Law, and G. Tauchen, "Risk, jumps, and diversification," *Journal of Econometrics*, vol. 144, no. 1, pp. 234–256, 2008.

[31] G. Qin, C. Huang, Y. Xie, and F. Wen, "Asymptotic behavior for third-order quasi-linear differential equations," *Advances in Differential Equations*, vol. 2013, article 305, pp. 1–8, 2013.

[32] A. R. Jarrow and E. R. Rosenfeld, "Jump risks and the intertemporal captial asset pricing model," *The Journal of Business*, vol. 57, no. 3, pp. 337–351, 1984.

[33] T. G. Andersen and T. Bollerslev, "Answering the skeptics: yes, standard volatility models do provide accurate forecasts," *International Economic Review*, vol. 39, no. 4, pp. 885–905, 1998.

[34] O. Barndorff-Nielsen and N. Shephard, "Econometric analysis of realized volatility and its use in estimating stochastic volatility models," *Journal of the Royal Statistical Society B: Statistical Methodology*, vol. 64, no. 2, pp. 253–280, 2002.

[35] O. Barndorff-Nielsen and N. Shephard, "Estimating quadratic variation using realized variance," *Journal of Applied Econometrics*, vol. 17, no. 5, pp. 457–477, 2002.

[36] N. Meddahi, "A theoretical comparison between integrated and realized volatility," *Journal of Applied Econometrics*, vol. 17, no. 5, pp. 479–508, 2002.

[37] O. E. Barndorff-Nielsen and N. Shephard, "Power and bipower variation with stochastic volatility and jumps," *Journal of Financial Econometrics*, vol. 2, no. 1, pp. 1–37, 2004.

[38] O. E. Barndorff-Nielsen and N. Shephard, "Econometrics of testing for jumps in financial economics using bipower variation," *Journal of Financial Econometrics*, vol. 4, no. 1, pp. 1–30, 2006.

[39] T. G. Andersen, T. Bollerslev, and F. Diebold, "Some like it smooth, and some like it rough: untangling continuous and jump components in measuring, modeling, and forecasting asset return volatility," Working Paper, Department of Economics, University of Pennsylvania, 2003.

[40] X. Huang and G. Tauchen, "The relative contribution of jumps to total price variance," *Journal of Financial Econometrics*, vol. 3, no. 4, pp. 456–499, 2005.

[41] R. Merton, "Option pricing when underlying stock returns are discontinuous," *Journal of Financial Economics*, vol. 3, no. 1-2, pp. 125–144, 1976.

Hindawi Publishing Corporation
Discrete Dynamics in Nature and Society
Volume 2014, Article ID 803073, 11 pages
http://dx.doi.org/10.1155/2014/803073

Research Article

Project Capital Allocation Combination Equilibrium Decision Model Based on Behavioral Option Game

Meirui Zhong,[1,2] Anqi Zeng,[1] Jianbai Huang,[1,2] and Kairong Hong[1,2]

[1] *School of Business, Central South University, Changsha 410083, China*
[2] *Institute of Metal Resources Strategy, Changsha 410083, China*

Correspondence should be addressed to Anqi Zeng; kiddy77@qq.com

Received 13 March 2014; Accepted 20 May 2014; Published 18 June 2014

Academic Editor: Fenghua Wen

Aiming at option value of the project and fairness preference psychological utility features, this paper modified objective function between players by option game equilibrium and utility function of project managers by inequity aversion. Therefore, under the symmetric and asymmetric information conditions, a project capital allocation combination equilibrium decision model has been built. It draws a conclusion that the option value of projects has changed the utility function of shareholders and managers in capital allocation, whereas fairness preferences of the project managers have changed the way of allocation through psychological utility. These two effects have influenced the trigger point of capital allocation decision-making. One is the decrease of trigger point owing to capital allocation decision-making of a CEO affected by the option value; the other is the reaction due to the crowding-out and crowding-in effect of the project manager's fairness preference, which restrains the severity of underinvestment. Therefore, a good incentive plan should be a balance among insurance, incentive, and fairness, not only a balance between insurance and incentive.

1. Introduction

Project capital allocation decision-making is a dynamic process, which owns characteristics such as multistage, investment irreversibility, flexibility, and complexity in management. Meanwhile in the capital allocation process, the project capital allocation can be analyzed in principal analysis framework, after asymmetric distribution of key factors involved in the project is considered, such as project quality, fluctuations in cash flow, return rate, and project investment costs. When faced with the complex market, information, and value structure in project capital allocation, it is of great significance to create a project capital allocation analytical framework which integrates option value and asymmetric information in the process of making a breakthrough in this field.

Traditional project capital allocation theory mainly concentrates on solving basic capital allocation issues such as the project's future cash flow projections and discount rates. Capital allocation based on real option aims to solve the multistaged capital allocation, investment irreversibility, flexible management, and other issues; it usually takes the value of options which result from the future cash flows of the projects fluctuations into consideration.

Capital allocation based on the game equilibrium mainly aims to figure out the effect that the project participants' interactions have on project value and to seek strategic equilibrium. Therefore, Ziegler [1] indicates that capital allocation decision analysis based on option game solved difficulties, such as the value of the uncertainty neglected by standard game theory analysis paradigm, flexible investment decisions under uncertainty, and dealing with competition inherent of real options, and added the condition of embedded option value in agent analysis paradigm. The decision-making models which can enrich the option game capital allocation include continuous-time options game model [2, 3], discrete-time option game model [4, 5], discrete-time and continuous-time model of combining option game expressed in binomial [6, 7], and model of decision-making behavior of investment projects containing option value [8–10]. All of these studies have highlighted the significance of project capital allocation based on option game equilibrium analysis.

As for agency problems of capital allocation decisions, Antle and Eppen [11], Wen et al. [12], and Wen and Yang [13] have built capital allocation decision model under the hypothesis that project managers prefer private information on technology and capital; Harris and Raviv [14] and Wen et al. [15] have launched capital allocation model with moral hazard, but they treat the compensation contract as exogenous variables; Milbourn et al. [16] have built a capital allocation model with asymmetric information, moral hazard, and endogenous compensation plans; however, this model did not consider manager's preference for capital, causing the incompetence in solving the capital flexibility of optimal allocation and predicting underinvestment problem.

Recently, however, game experiments such as the ultimatum game, dictatorial game, gift exchange game, public goods games, trust game, and other games have confirmed the prevalent ignorance of fairness preference in traditional agency theory [17–23]. This preference can affect the capital allocation decision-making behavior through the utility function. The models which utilize the fairness beliefs mainly include reciprocal fairness model [20] (Rabin), the revised sequential interactive equilibrium model [21] (Dufwenberg and Kirchsteiger), the revised reciprocal fairness equilibrium model (Falk and Fischbacher [22]), and inequity-aversion model based on allocation results (Fehr and Schmidt [23] and Bolton and Ockenfels [24]). All the models above extended the utility function, added different social preference, and used the game theory as a basic tool.

Different from the abovementioned models, this paper attempts to analyze the behavior of CEO (shareholder agent) and project managers from a new perspective in the process of capital allocation decision-making under asymmetric information and put the various option values of project capital allocation into the optimal capital allocation decision-making process so that it can build an expected utility maximization framework which is embedded in option value analysis. Meanwhile, according to principal-agent theory which is currently being expanded, this paper puts emotion factors which are opposite to selfishness, such as fairness and reciprocity, utilizes social preference in decision-making, and adds the condition of embedded option value in agent analysis paradigm.

Because of capital allocation, the project's value will depend on not only material benefits brought by projects development but also social and psychological effects contained by fairness beliefs, as long as the related project subjects are given fairness beliefs. In this way, it can lead to a relevant thinking between fairness equilibrium and capital allocation. Therefore, we can build an option behavioral game analysis framework which can optimize capital allocation of embedded option value and psychological utility.

2. The Description of the Model

The firm is run by the CEO who is risk neutral and stands for the benefits of the shareholders who have the rights to allocate the capital and make decisions of the investment. The optimal amount of the investment depends on the quality of the project. The CEO is not quite clear about the quality, but he hires project manager who is risk neutral and knows it well. Once the manager is hired, he has to report the quality of the project to the CEO, according to which the CEO will allocate the capital. The project manager owns not only private information of the quality of the project but also that of some key factors such as the volatility of the cash flow and effort level. Project manager has the intention to exaggerate the project cash flow volatility to obtain high payment and to reduce the cost by lowering down the effort level. So, in the allocation of capital in the principal-agent, the task of the CEO is to set capital allocation plan and remuneration packages for project managers to induce a variety of key project manager's private information and appropriate effort level.

Function form of project cash flows which does not consider the option value is basically the same as the one showed in the literature of Bernardo et al. [25], and, so forth, it mainly depends on the quality of the project q, capital k allocated to the project, and the cost of capital r; thus, the initial value of cash flow of the project when not considering the option value is

$$V_0 = nk + \delta qk - rk + \varepsilon. \tag{1}$$

In the equation above, n stands for regular cash flow which is affected by factors except the quality of the project, effort level, and the fluctuation of the project; ε stands for the noise disturbance of the cash flow of the project and is the subject to Gaussian distribution; δ measures the contribution margin of the quality to cash flow of the project. Marginal capital output is an increasing function of project quality q, which means that the project's CEO would like to configure more capital for high quality project. In the project capital allocation, project participants are risk neutral. The CEO of the project does not know the true quality of q but knows that the project quality distribution interval is $[0, \overline{q}]$, according to a distribution function $F(t)$ with density function $f(t)$ in the distribution interval. In mechanism design literature, risk distribution function is assumed to be $g(t) = f(t)/(1 - F(t))$.

In the implementation of the project, the cash flow is volatile; if the conditions are good, then the initial value of cash flow is uV_0 ($u \geq 1$) (u stands for the increase probability of cash flow according to the binary tree option pricing mechanism); otherwise, it comes to dV_0 ($d < 1$) (d stands for the decrease probability of cash flow according to the binary tree option pricing mechanism). Meanwhile, many engineering project investments present periodic characteristics. Due to the natural state, there is an uncertainty in decreasing and expanding the scale as well as waiting for the investment opportunity in the process of the multistage investment, which is embodied in the option value.

The premise condition for the next-stage investment is $dV_o - K_1 \leq 0$ and $uV_o - K_1 \leq 0$, and the capital allocation in the next stage is K_1 and lets the project cash flow increase x ($x > 1$) times (it will not affect the analysis under the condition of $x = 2$) [26]. Under the risk neutral assumption of the company, which can scatter unsystematic risk through portfolio diversification, portfolio return rate is r_o which only contains systematic risk.

According to the calculation formula of binary tree option value, the probability of initial value of cash flow fluctuating upward uV_o $(u > 1)$ is $p(u)(p(u) = [(1 + r_f) - d]/(u - d))$, and all the parties involved in the project share the same belief that the distribution interval of u is $(\underline{u}, \overline{u})$ and the distribution function is $g(u) = f(u)/(1 - F(u))$. According to the discounted value of expected presence of cash flow with option value $((p(u) \cdot \mathrm{Max}(2uV_0 - K_1, uV_0) + (1 - p(u)) \cdot \mathrm{Max}(2dV_0 - K_1, dV_0))/(1 + r_0)) - K_0$, in which K_0 stands for initial investment, the total expectation value at the beginning of the project can be simplified into

$$V_0 - K_0 + \frac{1}{1 + r_0} \left(p(u) \left(uV_0 - K_1 \right) \right). \tag{2}$$

The part of project cash flow implied options value is

$$p(u) \left(uV_0 - K_1 \right). \tag{3}$$

Because the project cash flow volatility is reported to the CEO by the project manager as private information and project managers generally have control preference (the preference for capital can enhance reputation and increase invisible income in the process of on-the-job consumption), the project manager has a high motivation in exaggerating project cash flow volatility.

Since information report such as project quality, project information, and the choice of effort level all need an incentive mechanism, the incentive mechanism can result in a widespread fairness preference confirmed by game theory, neuroeconomics, and psychology in the implementation of the project.

If the CEO launches a higher incentive compensation plan, the project manager will report real key personal information such as project quality and volatility and choose the appropriate level of efforts to repay CEO. In information economy era, heterogeneous human capital obtaining certain skills becomes scarcer. And owing to the specificity of heterogeneous human capital investment, project managers would contribute more to the project. In addition, their exit cost would grow and risk tolerance would be weakened.

Therefore, the negotiation ability of project managers and shareholders is enhanced, which contributes to higher requirement of surplus sharing of the project of project managers. They will compare the surplus sharing with that of the project owner, which embodies a kind of fairness preference based on allocation result. The fairness preference will turn into a kind of psychological effect, which can change capital allocation decision-making utility function. In the project capital allocation decisions, the psychological utility function form takes the measure of Fehr and Schmidt [23]:

$$U_M = -a \max \left\{ \pi_S - \pi_M, 0 \right\} - \theta \max \left\{ \pi_M - \pi_S, 0 \right\}. \tag{4}$$

In the equation, π_S stands for the income of the owner of the project, π_M means the income of the manager of the project, $a > 0$ is the jealousness preference parameter which measures the negative unfairness, and $\theta > 0$ is sympathy preference parameter which measures positive unfairness. The function assumes that $a \geq \theta$, namely, the negative unfairness, encounters greater loss than the positive unfairness does, which is consistent with loss aversion raised by Tversky and Kahneman [27]. So, for a given fairness preference of project managers, if $\pi_s > \pi_M$, the project managers who have the awareness of fairness will make the least effort $e = \underline{e}$; it can only provide positive effect, when $e = \underline{e}$ and $\pi_s > \pi_M$; the project managers who have the awareness of fairness will make greater effort to bridge the income gap between the project owner and himself.

Project managers improve their operating skills through the continuous variable selection of efforts so as to enhance the project value, but they also bear the corresponding costs. The cost function of project managers can be set as $c(e) = 0.5\gamma e^2$, where γ is the effort-aversion parameter. When the scale is increased during the investment, the effort of the project managers can bring down the investment cost to $\eta\alpha e K_1$; α stands for the marginal contribution of project quality to the project cash flow; $\eta \in [0, 1]$ is the capital preference intensity parameter of the project managers; then the option value of the project turns into $p(u)(uV_0 + \eta\alpha e K_1 - K_1)$. The expected utility function of the project managers is

$$\begin{aligned} U = {} & E \left[w \left(\hat{q}, \hat{u}, V \right) \right] \\ & + bp(u) \left(uV_0 + \eta\alpha e K_1 - K_1 \right) - 0.5\gamma e^2 - \theta \left(\pi_M - \pi_S \right). \end{aligned} \tag{5}$$

In (5), b measures the control preference of the project managers; at the same time, it is assumed that the project managers have external opportunities to be hired, thus making the reservation utility of the project managers $\overline{U} \geq 0$.

The task of the project CEO is to maximize shareholders' expected profits; shareholders are residual claimants to project cash flow. Assume that in the project there is no conflict of interest between CEO and shareholders. Project chief executive can use two tools (manager compensation plan and capital allocation plan) to provide incentives for project managers; the incentive plans make managers report true project quality and project fluctuation and make appropriate effort. Project CEO set the optimal mechanism, including capital allocation policy $k(\hat{q})$, which mainly depends on the reports of project quality $\hat{q}$ and project cash flow volatility $\hat{u}$. Compensation plans $w(\hat{q}, \hat{u}, V)$ mainly depend on the various key reported information and project value. And it is assumed that project quality is q, cash flow volatility is u, and the effort level of project managers cannot be directly observed or later confirmed by CEO; as a result, contracts cannot be resigned through the observation to the project quality of q, the cash flow volatility u, and effort level. So faced with risks of hidden information and hidden action, the game sequence of both sides is as follows.

Firstly, the CEO will provide an incentive $\{w(\hat{q}, \hat{u}, V), k(\hat{q})\}$ for the project manager, and then the project manager will make a promise of the effort level $e(\hat{q})$ and report the quality of the project $\hat{q}$ and cash flow volatility $\hat{u}$. Then, the CEO allocates capital to each department; the project manager will make corresponding effort and perform his programs, and finally he can get the project cash flow; one part of them will be assigned to the project manager in the form of linear performance payment and the remaining to shareholders. The objective function of shareholders and managers is, respectively, as follows when considering the option value and the fairness psychological utility:

$$EU_S = V_0 - K_0 + \frac{1}{1+r_0}\int_0^{\overline{q}}\int_{\underline{u}}^{\overline{u}} [p(u)(uV_0 + \eta\alpha e K_1 - K_1) - s(u,q)] f(u,q)\,dq\,du, \tag{6}$$

$$\begin{aligned} U_M(u,\widehat{u};q,\widehat{q}) = {} & E[s(u,q)] + bp(u)(uV_0 + \eta\alpha e K_1 - K_1) - \frac{1}{2}\gamma e^2 - \theta(\pi_M - \pi_S) \\ = {} & (1-2\theta)E[s(u,q)] + (1-2\theta)[bp(u)(uV_0 + \eta\alpha e K_1 - K_1)] \\ & + \theta p(u)[2uV_0 + \eta\alpha e K_1 - K_1 - K_0(1+r_0)] - \frac{1}{2}\gamma e^2 \\ = {} & (1-2\theta) \times \{\alpha(\widehat{u},\widehat{q}) + \beta(\widehat{u},\widehat{q})p(u) \times [2uV_0 + \eta\alpha e K_1 - K_1 - K_0(1+r_0)]\} \\ & - \frac{1}{2}\gamma e^2 + (1-2\theta)[bp(u)(uV_0 + \eta\alpha e K_1 - K_1)] \\ & + \theta p(u)[2uV_0 + \eta\alpha e K_1 - K_1 - K_0(1+r_0)]. \end{aligned} \tag{7}$$

From (7), we can figure out that the utility function U is made up of four parts. The first part is the fixed income and income expectations which does not include option value performance-sharing income; it is related to the project quality and project cash flow volatility that are reported by the project managers; the second part is expectation value of the option value $bp(\widehat{u})(\widehat{u}V_0 + \eta\alpha e K_1 - K_1)$, which is formed because the investment scale is exaggerated and it mainly reflects the transformation from control power turning into utility; the third part is negative effect caused by the cost of the project manager's effort, but the increase of the effort level will help reduce investment costs and increase the part of option value, thus contributing to positive effect $\eta\alpha e K_1$. The fourth part is the negative effects of unfairness that the project manager believes.

In (6) and (7), because the managers have external opportunities to be hired, the project managers will keep the reservation utility $\overline{U} \geq 0$. Since the CEO expects that the project managers can accurately report the quality and the upward volatility u of the project, the participation constraint has to assure that the utility they get by reporting information accurately exceeds or equals that they get by reporting false information of project quality and volatility. Therefore, in the process of capital allocation and contract design, the participation constraint (PC) and incentive compatible constraint (IC) are as follows:

$$\begin{aligned} \max_{s(q,u)} EU_S = {} & V_0 - K_0 + \frac{1}{1+r_0} \times \int_0^{\overline{q}}\int_{\underline{u}}^{\overline{u}} [p(u)(uV_0 + \eta\alpha e K_1 - K_1) - s(u,q)] f(q,u)\,dq\,du, \\ U_M(u,\widehat{u};q,\widehat{q}) = {} & E[s(u,q)] + bp(u)(uV_0 + \eta\alpha e K_1 - K_1) - \frac{1}{2}\gamma e^2 - \theta(\pi_M - \pi_S) \\ = {} & (1-2\theta)E[s(u,q)] + (1-2\theta)[bp(u)(uV_0 + \eta\alpha e K_1 - K_1)] \\ & + \theta p(u)[2uV_0 + \eta\alpha e K_1 - K_1 - K_0(1+r_0)] - \frac{1}{2}\gamma e^2 \\ = {} & (1-2\theta)\{\alpha(\widehat{u},\widehat{q}) + \beta(\widehat{u},\widehat{q})p(u) \times [2uV_0 + \eta\alpha e K_1 - K_1 - K_0(1+r_0)]\} - \frac{1}{2}\gamma e^2 \\ & + (1-2\theta)[bp(u)(uV_0 + \eta\alpha e K_1 - K_1)] \\ & + \theta p(u)[2uV_0 + \eta\alpha e K_1 - K_1 - K_0(1+r_0)] \\ & U(q,\widehat{q};u,\widehat{u}) \geq 0 \quad (\mathrm{PC}) \\ & U(q,q;u,u) \geq U(q,\widehat{q};u,\widehat{u}) \quad (\mathrm{IC}). \end{aligned} \tag{8}$$

3. The Equilibrium Solution and Discussion of the Model

Equations (8) are analysis paradigm of behavioral option game theory of optimal capital allocation which are based on embedded option value and psychological utility and it is an extension of the optimal expected utility analysis paradigm under traditional capital allocation theory. First, we will begin with optimal capital allocation decision-making behavior when considering project volatility belief; the decision-making model is as follows:

$$\max_{s(u)} EU_S = V_0 - K_0 + \frac{1}{1+r_0} \times \int_{\underline{u}}^{\overline{u}} [p(u)(uV_0 + \eta\alpha e K_1 - K_1) - s(u)] f(u)\,du, \tag{9}$$

$$\begin{aligned}
U_M(u,\hat{u}) &= E[s(u)] + bp(u)(uV_0 + \eta\alpha e K_1 - K_1) \\
&\quad - \frac{1}{2}\gamma e^2 - \theta(\pi_M - \pi_S) \\
&= (1-2\theta)E[s(u)] + (1-2\theta) \\
&\quad \times [bp(u)(uV_0 + \eta\alpha e K_1 - K_1)] \\
&\quad + \theta p(u)[2uV_0 + \eta\alpha e K_1 - K_1 - K_0(1+r_0)] \\
&\quad - \frac{1}{2}\gamma e^2 \\
&= (1-2\theta) \\
&\quad \times \{\alpha(\hat{u}) + \beta(\hat{u}) p(u) \\
&\qquad \times [2uV_0 + \eta\alpha e K_1 - K_1 - K_0(1+r_0)]\} \\
&\qquad - \frac{1}{2}\gamma e^2 \\
&\quad + (1-2\theta)[bp(u)(uV_0 + \eta\alpha e K_1 - K_1)] \\
&\quad + \theta p(u)[2uV_0 + \eta\alpha e K_1 - K_1 - K_0(1+r_0)] \\
&\qquad U(u,\hat{u}) \geq 0 \quad (\text{PC}) \\
&\qquad U(u,u) \geq U(u,\hat{u}) \quad (\text{IC}).
\end{aligned} \tag{10}$$

In order to analyze capital allocation behavior when the shareholders are faced with risk of hidden information and hidden action, the situations of symmetric and asymmetric information are comparatively analyzed in the following part.

(1) Pareto optimality decision-making of capital allocation under symmetric information condition.

It is assumed that the CEO and project manager have common belief on key information of project quality and volatility; that is to say, the information between them follows symmetrical distribution and the project CEO can notice the effort level of the project manager. At this time, manager who bears the belief of fairness cannot repay the CEO through effort strategic choice and interactive fairness intention in the game; while effort levels can be observed by CEO, the contract signed by project managers and the CEO of projects at this time is complete; incentive mechanism will be replaced by a deterministic scheme which can make up for the project manager's effort cost and has nothing to do with the effort level, and capital allocation behaviors belong to Pareto optimality. This kind of Pareto optimal solution is the maximization of the utility sum of shareholders and the project managers:

$$\begin{aligned}
\max_{e_{\text{best}}}(EU) &= \max_{e_{\text{best}}}(EU_P + U_M) \\
&= V_0 - K_0 + \frac{1}{1+r_0} \\
&\quad \times \Big[p(u)(uV_0 + \eta\alpha e K_1 - K_1) \\
&\qquad + bp(u)(uV_0 + \eta\alpha e K_1 - K_1) - \frac{1}{2}\gamma e^2\Big].
\end{aligned} \tag{11}$$

Calculating the derivative of the effort e, we arrive at the optimal effort level of the project manager:

$$e_{\text{best}} = \frac{p(u)\eta a K_1(1+b)}{\gamma}. \tag{12}$$

Under the condition that the optimal effort level of the project manager is known, the CEO will set the optimal decision-making point of capital allocation according to the optimal effort level; at this optimal decision-making point $u = u_{\text{best}}$, $(EU_P + U_M) = 0$, the CEO will accept the project that meet the requirement $u = u_{\text{best}}$:

$$\begin{aligned}
&p(u)\left(uV_0 + \frac{p(u)\eta a^2 K_1^2(1+b)}{\gamma} - K_1\right) \\
&\quad + bp(u)\left(uV_0 + \frac{p(u)\eta a^2 K_1^2(1+b)}{\gamma} - K_1\right) \\
&\quad - \frac{p^2(u)\eta a^2 K_1^2(1+b)^2}{2\gamma} \geq (K_0 - V_0)(1+r_0).
\end{aligned} \tag{13}$$

So the decision-making point of Pareto is

$$\begin{aligned}
u_{\text{best}} &= \frac{(K_0 - V_0)(1+r_0)\, p(u)\eta a K_1(1+b)}{p(u)V_0(1+b)} \\
&\quad + \frac{K_1}{V_0} - \frac{p(u)\eta a^2 K_1^2(1+b)}{2\gamma V_0}.
\end{aligned} \tag{14}$$

When $u = u_{\text{best}}$, the CEO will allocate 0 to the project; namely, the shareholders will invest nothing in the project, because even if the option value is considered, the expanded NPV of the project is negative; when $u = u_{\text{best}}$, since the sum of the option value and the NPV-based static value is positive, the CEO will allocate K_0 to the project.

(2) Optimal decision-making of capital allocation under asymmetric information condition.

Under the asymmetric information condition, as for principal-agent problems in capital allocation based on embedded option value and the fairness psychological utility, the project manager maximizes his expected utility through the selection of the optimal effort level under the condition that incentive contracts and investment decisions are definite. And then the CEO will provide the manager with incentive $\{w(\hat{u}, V)\}$, which can ensure that the manager will report accurate information. Since the information reported at that time can maximize the utility of the manager, otherwise, the manager is irrational. Consider $\hat{u} = u$, which meets the demand that $(\partial U_M(\hat{u}, u)/\partial u)|_{\hat{u}=u} = 0$, so that we get incentive mechanism which meets incentive compatibility constraint and participation constraint of project manager, and then we put the incentive mechanism in the objective function of the shareholders to obtain the optimal incentive contracts.

(i) According to (10), it can be obtained that, under the condition of asymmetric information, the optimal effort level under option and fairness equilibrium combination is as follows (refer to Appendix A):

$$e^{*}(u,\theta)=\frac{p(u)\,\eta a K_1\left[(1-2\theta)(\beta(u)+b)+\theta\right]}{\gamma}. \tag{15}$$

From (15), we can figure out that the suboptimal effort level of the manager has something to do with the fairness preference of himself (or herself) besides the incentive level $\beta(u,\theta)$ in the traditional principal-agent paradigm. Under the condition that project manager has the preference of control right ($b > 0.5$), the suboptimal effort level of the manager is the reduction function of the fairness preference, which is caused by the unfairness premium of fairness preference. It is namely that the more unfairness-averse the manager is, the lower effort level the manager will make when the sharing gap is comparatively huge, which is consistent with the empirical data in real life. Meanwhile, behavioral experimental economists Fehr and Schmidt [23], Charness and Rabin [28], and Teyssier [29] by game experiments proved that about 85% of the population falls in θ distribution in the range $(0.15, 0.50)$, so suboptimal effort level of project managers is affected by option value; namely, the larger the b is, the greater option utility value the project manager will obtain and the more willing they are to pay the effort level. This is a change of the effort level decision of the project manager when the option value is considered.

(ii) Comparing (15) and (12), we can find that the gap between suboptimal effort level in asymmetric information and suboptimal effort level in mechanism within symmetric information condition is

$$\begin{aligned}\Delta e&=e^{*}-e_{\text{best}}\\&=\frac{p(u)\,\eta a K_1\left[(1-2\theta)\beta(u)+(1-2b)\theta-1\right]}{\gamma}.\end{aligned} \tag{16}$$

Under manager's strong control power preference for capital and in the interval distribution of θ, $e^{*}-e_{\text{best}} < 0$ is established. That is, when the effort cannot be observed, project with inequity aversion will minimize his effort, which is consistent with the conclusion of classical agency problems. For (16), we can see that Δe is decreasing in θ since we can get the derivation of the inequity aversion coefficients. Thus, managerial function of effort in the suboptimal mechanism with asymmetric information is more close to the optimal solution with symmetric information while the inequity aversion of project manager is intensive, which means that equity preference can improve the managerial effort. As specific human capital investment is growing, the project manager shares behind the owner, which will result in a negative unfairness loss. In order to reduce or even eliminate the loss, the project will make a greater level of effort, which creates the incentive effect of the inequity aversion.

(iii) We can drive the compensation contract package from (12) (the proof is in Appendix B) as follows:

$$\begin{aligned}s(u,\theta)&\\&=\left(2p(u)\beta(u)V_0H(u)-(1-2\theta)\right.\\&\quad\times\left.\left[bp(u)\left(uV_0+\eta\alpha eK_1-K_1\right)\right]\right)\\&\quad\times(1-2\theta)^{-1}\\&\quad-\frac{\theta p(u)\left[2uV_0+\eta\alpha eK_1-K_1-K_0\left(1+r_0\right)\right]+(1/2)\gamma e^2}{(1-2\theta)}.\end{aligned} \tag{17}$$

Substituting the compensation contract package and optimal effort level into (9), we get the suboptimal sharing coefficient from derivation (the proof is in Appendix B):

$$\beta^{*}(u,\theta)=\frac{2v_0H(u)\gamma}{(1-2\theta)\,p(u)\,\eta^2a^2K_1^2}-1-\frac{\theta\gamma}{1-2\theta}. \tag{18}$$

We can draw a conclusion from (18) that option value and fairness preference have negative effect on sharing coefficient. With asymmetric information, the project manager will get more incentive effects due to the misrepresented project volatility while the project volatility is higher. Thus, he will make greater level of effort; sharing coefficient is approximately in the interval $(0.3, 0.6)$ while θ is in the interval $(0.15, 0.50)$, which is consistent with the evidence in game experimental. When sharing coefficient is too low or too high, jealousy preference or sympathy preferences exist, and inequity aversion has crowding-out effect on explicit incentive contracts.

(iv) Substituting the compensation contract package, optimal effort level, and sharing coefficient into (9), we get the fixed sharing coefficient (the proof is in Appendix B) as follows:

$$\begin{aligned}\alpha^{*}(u,\theta)&=\frac{\int_{\underline{u}}^{u}2\beta(u,\theta)\,p(u)\,dz}{1-2\theta}-bp(u)\left(uV_0-K_1\right)\\&\quad-\beta(u,\theta)\,p(u)\left[2uV_0-K_1-K_0\left(1+r_0\right)\right]\\&\quad-\frac{\theta p(u)\left[2uV_0-K_1-K_0\left(1+r_0\right)\right]}{1-2\theta}\\&\quad+\left[p(u)\,\eta\alpha K_1\right]^2\left[(1-2\theta)\left(\beta(u,\theta)+b\right)\right]\\&\quad\times\left[\frac{\left(\beta(u,\theta)+b\right)\left(\gamma^2-2\right)}{2\gamma}+\frac{\gamma\theta}{2(1-2\theta)}\right].\end{aligned} \tag{19}$$

As can be seen from (19), in the condition of asymmetric information, the fixed part of the contract is no longer decided by the industry level, local minimum wage standards, and the option and inequity aversion; when it comes to the option, the fixed part is decreasing in b and it will be negative while b is large. Giving that, it must be subject to a certain margin in the process of building our operating annual salary system or option compensation system, in order to allow the manager to obtain the risk income and mitigate the incentive for manager to overstate option value. The more the manager is inequality averse, the larger the proportion of fixed part will be required, and the effect of crowding-out on incentive effort will be greater. The fixed part can no longer insure the project manager at this situation. Therefore, the capital allocation of incentive contracts should balance the three factors: insurance, incent, and fairness, but not insurance and incent, while taking option and fairness preference into account.

(v) Substituting (15), (18), and (19) into the equation, we can solve out the cash flow volatility, when taking options factors into account (the proof is in Appendix B) as follows:

$$\begin{aligned} u^{*} = {} & \frac{(K_0 - V_0)(Hr_0)(1-2\theta)}{[(1+b)(1-2\theta)+2\theta]\,p(u)} + \frac{K_1 + K_0(1+r_0)}{(1+b)(1-2\theta)+2\theta} \\ & + \frac{(1+b)K_1(1-2\theta)}{(1+b)(1-2\theta)+2\theta} \\ & + \frac{2\beta(u)V_0 + H(u)}{(1+b)(1-2\theta)+2\theta} \\ & - \frac{(1-2\theta)\,p(u)\,\eta^2 a^2 K_1^2\left[(1-2\theta)(\beta(u)+b)+\theta\right]}{(1+b)(1-2\theta)+2\theta} \\ & * \left[\frac{1+b}{\gamma} + \frac{\theta}{\gamma(1-2\theta)} + \frac{\gamma\left[(1-2\theta)(\beta(u)+b)+\theta\right]}{2(1-2\theta)}\right]. \end{aligned} \tag{20}$$

It is from the derivation of control preference of project manager and inequity aversion coefficient. As we can see, u^{*} is decreasing in b (control preference of project manager). Due to advantage of private information of project quality, project manager can get more utilities through understating project quality. In assumption of rationality, the CEO, who is acting in the interest of the shareholders, knows that project manager may report a higher cash flow volatility to increase their effectiveness. So the CEO will reduce the investment critical point to get the real cash flow volatility. u^{*} is increasing in θ (inequity aversion coefficient of project manager, which means that project manager with hinger inequity aversion coefficient has a greater incentive to overstate the cash flow volatility.In the interval of $\theta(0.15, 0.50)$, comparing (20) with (14), we find $\Delta u > 0$. Consequently, there is underinvestment of capital in the suboptimal mechanism relative to the optimal solution since the hurdle rates of return required by CEO are higher than those predicted with symmetric information. This capital underinvestment result is consistent with inequity aversion of project manager; project manager with fairness preference will reduce the incentive of understate cash flow volatility through crowding-out effect. Thereby, the utility brought by option value reduced, and the capital underinvestment is inhibited as well.

(vi) If project manager has no control preference to the project, the optimal effort level of the project manager and optimal investment point are as follows:

$$e_1(u,\theta) = \frac{p(u)\,\eta a K_1\left[(1-2\theta)\beta(u)+\theta\right]}{\gamma}, \tag{21}$$

$$\begin{aligned} u_1 = {} & \frac{(K_0 - V_0)(Hr_0)(1-2\theta)}{p(u)} + K_1 + K_0(1+r_0) \\ & + K_1(1-2\theta) + 2\beta(u)V_0 + H(u) \\ & - (1-2\theta)\,p(u)\,\eta^2 a^2 K_1^2\left[(1-2\theta)\beta(u)+\theta\right] \\ & * \left[\frac{1-\theta}{\gamma(1-2\theta)} + \frac{\gamma\left[(1-2\theta)\beta(u)+\theta\right]}{2(1-2\theta)}\right]. \end{aligned} \tag{22}$$

As we can see from (21), while project manager has no control preference to the project, he will report a lower quality to minimize his effort, which will be canceled out by crowding-out effect of fairness preference. Project manager will improve his level of effort if he is of great fairness preference. Comparing (15) with (21), we get that $e_1(u,\theta) < e^{*}(u,\theta)$. If project manager has no control preference to the project in the condition of asymmetric information, he will have no interest in the cash flow. He will improve his utility by reducing his level of effort. That is to say, the project manager should make more effort if he can improve his utility by reporting a higher project option value.

Comparing (20) with (22), we find $u_1 > u^{*}$. While project manager has no control preference to the project, he has no incentive to misrepresent the cash flow volatility. The CEO will improve the point of capital allocation in order to prevent project manager of fairness preference from making less effort due to the underreporting of project volatility.

4. Conclusions

The research describes an option game analysis framework of capital allocation optimization, which takes option value and psychological utility into account. It integrates option value generated by uncertainty and psychological utility generated by fairness preference into the analysis framework of capital allocation and agent relationship. The conclusions are as follows.

(1) There is volatility in project investment in the analysis of project capital allocation and agent relationship and the volatility implies option value. The greater the volatility is, the greater the value of option is. It changes the manager's utility function of capital

allocation. The effort of incentive will be affected by the fairness preference of project manager if considering option value in the incentive program. Project manager has an incentive to misrepresent project volatility due to the existence of option value. It is because the effort of incentive will be better while the volatility and option value are greater. We draw a conclusion that project value is increasing in project risks, which is contrary to the result of Holmstrom [30]. However, the positive relationship is consistent with the degree of project manager's fairness preference. Inequity aversion has a crowding-out effect on explicit incentive contracts. The utility function of project manager is affected not only by his income level but also by his relative income level.

(2) In the classical capital allocation agent analytical framework, the fixed part is only for insurance; it has no impact on the level of project manager's effort. But it has an incentive effect after taking option value and fairness preference into account. In the option game model of capital allocation optimization described in this research, the fixed part can inhibit project manager from misrepresented option value. The degree of inequity aversion is greater; the fixed part required is larger. It will have a crowding-out effect on incentive effect. Therefore, analysis paradigm of capital allocation incentive is expanded. An excellent incentive plan in capital allocation should balance the three factors: insurance, incentive, and fairness.

(3) The model in our research analyzed the capital allocation optimization and incentive plan to project manager. The CEO should not naively apply the NPV rule when deciding how much capital to allocate to a project manager, because they must depend on the reports of project manager with fairness preference to get the information of project volatility. Because manager with fairness preference has a preference for larger capital allocations, they have an incentive to overstate project volatility to CEO to secure more capital. The option value generated from overstating project volatility motivates project manager to provide a high level of effort as well, which is partially offset by fairness preference.

There are many paths for further research in our paper. First of all, there are many kinds of options in project and each option is specific. We have no idea about whether the specification will have an impact on the heterogeneity and stability of project manager's fairness preference, which will lead to a different capital allocation decision. Secondly, we should consider the stability of the capital allocation decision-making model based on option game. We assume that project manager is risk neutral. It is more costly for CEO to offer profit-sharing incentives if project manager is risk aversion. The CEO will decrease the sharing part of incentive contracts. The underinvestment problem in capital allocation and effort will be more severe due to the crowding-in effect of fairness preference, which decreases the level of effort and suboptimal capital allocation. Finally, the relationship between fairness preference and risk preference is complicated. In the research of Traub et al. [31] about social preference, they find the correlation between risk aversion and social preference. In the model of capital allocation agent with risk aversion, risk aversion has an effect on the utility while applying the certainty equivalent method. Considering fairness preference, the capital allocation agent model measures the fairness preference by utility. So the two kinds of psychological preferences have repeated impacts on the utility function. These issues are worth further study in the future research.

Appendices

A. The Optimal Effort Level under Option and Fairness Equilibrium Combination

Considering option value and inequity aversion, the utility of project manager with asymmetric information is

$$\begin{aligned}
U(u,\hat{u}) &= E[s(u)] + bp(u)\left(uV_0 + \eta\alpha e K_1 - K_1\right) \\
&\quad - \frac{1}{2}\gamma e^2 - \theta\left(\pi_M - \pi_S\right) \\
&= (1-2\theta)E[s(u)] \\
&\quad + (1-2\theta)\left[bp(u)\left(uV_0 + \eta\alpha e K_1 - K_1\right)\right] \\
&\quad + \theta p(u)\left[2uV_0 + \eta\alpha e K_1 - K_1 - K_0\left(1+r_0\right)\right] \\
&\quad - \frac{1}{2}\gamma e^2 \\
&= (1-2\theta)\left\{\alpha(\hat{u}) + \beta(\hat{u})\,p(u)\right. \\
&\qquad \left.\times\left[2uV_0 + \eta\alpha e K_1 - K_1 - K_0\left(1+r_0\right)\right]\right\} \\
&\quad - \frac{1}{2}\gamma e^2 \\
&\quad + (1-2\theta)\left[bp(u)\left(uV_0 + \eta\alpha e K_1 - K_1\right)\right] \\
&\quad + \theta p(u)\left[2uV_0 + \eta\alpha e K_1 - K_1 - K_0\left(1+r_0\right)\right].
\end{aligned} \tag{A.1}$$

Solving from (A.1), the suboptimal effort choice with asymmetric information is

$$\begin{aligned}
\frac{\partial U}{\partial e} &= (1-2\theta)\,\beta(\hat{u})\,p(u)\,\eta\alpha K_1 - \gamma e \\
&\quad + (1-2\theta)\,bp(u)\,\eta\alpha K_1 + \theta p(u)\,\eta\alpha K_1 = 0,
\end{aligned} \tag{A.2}$$

$$e^* = \frac{p(u)\,\eta\alpha K_1\left[(1-2\theta)\left(\beta(u)+b\right)+\theta\right]}{\gamma}. \tag{A.3}$$

B. The Compensation Contract Package and the Suboptimal Sharing Coefficient

With asymmetric information, the suboptimal equation of payment contract package is

$$\left.\frac{\partial U(u,\hat{u})}{\partial u}\right|_{\hat{u}=u} = \left.\frac{\partial U(u,\hat{u})}{\partial u}\right|_{\hat{u}=u} + \left.\frac{\partial U(u,\hat{u})}{\partial \hat{u}}\right|_{\hat{u}=u}. \tag{B.1}$$

The functional form of the first term on the right-hand side of (B.1) is as follows:

$$\Longrightarrow \left.\frac{\partial U(u,\hat{u})}{du}\right|_{\hat{u}=u} = 2\beta(u)\,p(u)\,V_0. \tag{B.2}$$

Integration by utility function gives

$$U(u,\hat{u}) = \int_{\underline{u}}^{\overline{u}} 2\beta(u)\,p(u)\,V_0 dz. \tag{B.3}$$

Solving from (B.3), we arrive at

$$\begin{aligned}
&\int_{\underline{u}}^{\overline{u}}\int_{\underline{u}}^{u} 2\beta(u)\,p(u)\,v_0 dzd(F(u)) \\
&\quad = F(u)\int_{\underline{u}}^{u} 2\beta(u)\,p(u)\,V_0 dz\Big|_{\underline{u}}^{\overline{u}} \\
&\qquad - \int_{\underline{u}}^{\overline{u}} 2\beta(u)\,p(u)\,V_0 F(u)\,du \\
&\quad = \int_{\underline{u}}^{\overline{u}} 2\beta(u)\,p(u)\,V_0 du - \int_{\underline{u}}^{\overline{u}} 2\beta(u)\,p(u)\,V_0 F(u)\,du \\
&\quad = \int_{\underline{u}}^{\overline{u}} 2\beta(u)\,p(u)\,V_0\,[1-F(u)]\,du \\
&\quad = \int_{\underline{u}}^{\overline{u}} 2\beta(u)\,p(u)\,V_0 H(u)\,f(u)\,du\left(H(u) = \frac{1-F(u)}{f(u)}\right).
\end{aligned} \tag{B.4}$$

Plugging (A.3) and (B.4) into the objective function of the principal-agent gives

$$\begin{aligned}
&\max_{s(u)} EU_S \\
&\quad = V_0 - K_0 + \frac{1}{1+r_0} \\
&\qquad \times \int_{\underline{u}}^{\overline{u}}\Bigg[p(u)\left(uV_0 + \eta\alpha e^* K_1 - K_1\right) \\
&\qquad\qquad - \Big(\big(2p(u)\,\beta(u)\,V_0 H(u) \\
&\qquad\qquad\quad + (1-2\theta)\left[bp(u)\left(uV_0 + \eta\alpha e^* K_1 - K_1\right)\right]\big) \\
&\qquad\qquad\quad \times (1-2\theta)^{-1}\Big) \\
&\qquad\qquad + \Big(\big(\theta p(u)\left[2uV_0 + \eta\alpha e^* K_1 - K_1 - K_0(1+r_0)\right]\big) \\
&\qquad\qquad\quad \times (1-2\theta)^{-1}\Big) \\
&\qquad\qquad + \frac{+(1/2)\,\gamma[e^*]^2}{(1-2\theta)}\Bigg] f(u)\,du.
\end{aligned} \tag{B.5}$$

Solving the suboptimal payment contract package from (B.5), we arrive at

$$\begin{aligned}
&s(u) \\
&\quad = \Big(\big(2p(u)\,\beta(u)\,V_0 H(u) - (1-2\theta) \\
&\qquad \times \left[bp(u)\left(uV_0 + \eta\alpha e K_1 - K_1\right)\right]\big) \\
&\qquad \times (1-2\theta)^{-1}\Big) \\
&\qquad - \frac{\theta p(u)\left[2uV_0 + \eta\alpha e K_1 - K_1 - K_0(1+r_0)\right] + (1/2)\,\gamma e^2}{(1-2\theta)}.
\end{aligned} \tag{B.6}$$

Get the derivation of incentive factors from (B.6); the first-order condition is

$$\begin{aligned}
\frac{dEU_s}{d\beta} &= \frac{p^2(u)\,\eta^2 a^2 K_1^2 (1-2\theta)}{\gamma} \\
&\quad - \frac{2p(u)\,V_0 H(u)}{1-2\theta} \\
&\quad - \frac{bp^2(u)\,\eta^2 a^2 K_1^2 (1-2\theta)}{\gamma} \\
&\quad + \theta p^2(u)\,\eta^2 a^2 K_1^2 \\
&\quad + \frac{p^2(u)\,\eta^2 a^2 K_1^2 (\beta(u)+b)}{\gamma} = 0.
\end{aligned} \tag{B.7}$$

Therefore, the suboptimal incentive factor is

$$\beta^*(u) = \frac{2V_0 H(u)\,\gamma}{(1-2\theta)\,p(u)\,\eta^2 a^2 K_1^2} - 1 - \frac{\theta\gamma}{1-2\theta}. \tag{B.8}$$

Plugging (B.8) into (B.6), we get the insurance part of the incentive contract as follows:

$$\begin{aligned}
\alpha^*(u,\theta) &= \frac{\int_{\underline{u}}^{u} 2\beta(u,\theta)\,p(u)\,dz}{1-2\theta} - bp(u)\left(uV_0 - K_1\right) \\
&\quad - \beta(u,\theta)\,p(u)\left[2uV_0 - K_1 - K_0(1+r_0)\right] \\
&\quad - \frac{\theta p(u)\left[2uV_0 - K_1 - K_0(1+r_0)\right]}{1-2\theta} \\
&\quad + \left[p(u)\,\eta\alpha K_1\right]^2\left[(1-2\theta)\left(\beta(u,\theta)+b\right)\right] \\
&\quad \times \left[\frac{\left(\beta(u,\theta)+b\right)\left(\gamma^2-2\right)}{2\gamma} + \frac{\gamma\theta}{2(1-2\theta)}\right].
\end{aligned} \tag{B.9}$$

By definition and (A.3), (B.8), and (B.9), the first-order condition of volatility on option factors of project with inequity aversion is

$$\begin{aligned}
&\partial^{*}(u) \\
&\quad = p(u) V_0 u + \frac{p^2(u)\eta^2 a^2 K_1^2 \left[(1-2\theta)\left(\beta(u)+b\right)+\theta\right]}{\gamma} \\
&\qquad - \frac{2p(u)\beta(u) v_0 H(u)}{1-2\theta} - p(u) K_1 \\
&\qquad + bp(u) V_0 u - bp(u) K_1 \\
&\qquad + \frac{bp^2(u)\eta^2 a^2 K_1^2 \left[(1-2\theta)\left(\beta(u)+b\right)+\theta\right]}{\gamma} \\
&\qquad + \frac{2\theta p(u) V_0}{1-2\theta} * u \\
&\qquad + \frac{\theta p^2(u)\eta^2 a^2 K_1^2 \left[(1-2\theta)\left(\beta(u)+b\right)+\theta\right]}{\gamma(1-2\theta)} \\
&\qquad - \frac{\theta p(u) K_1}{1-2\theta} - \frac{p(u) K_0 \left(Hr_0\right)}{1-2\theta} \\
&\qquad + \frac{\gamma p^2(u)\eta^2 a^2 K_1^2 \left[(1-2\theta)\left(\beta(u)+b\right)+\theta\right]^2}{2(1-2\theta)} \\
&\quad \geq \left(K_0 - V_0\right)\left(1+r_0\right).
\end{aligned} \tag{B.10}$$

Solving for the suboptimal volatility on option factors of project with inequity aversion from the first-order condition in (B.10) gives

$$\begin{aligned}
u^{*} &= \frac{\left(K_0 - V_0\right)\left(Hr_0\right)(1-2\theta)}{\left[(1+b)(1-2\theta)+2\theta\right] p(u)} \\
&\quad + \frac{K_1 + K_0\left(1+r_0\right)}{(1+b)(1-2\theta)+2\theta} \\
&\quad + \frac{(1+b) K_1 (1-2\theta)}{(1+b)(1-2\theta)+2\theta} \\
&\quad + \frac{2\beta(u) V_0 + H(u)}{(1+b)(1-2\theta)+2\theta} \\
&\quad - \frac{(1-2\theta) p(u)\eta^2 a^2 K_1^2 \left[(1-2\theta)\left(\beta(u)+b\right)+\theta\right]}{(1+b)(1-2\theta)+2\theta} \\
&\quad \cdot \left[\frac{1+b}{\gamma} + \frac{\theta}{\gamma(1-2\theta)} + \frac{\gamma\left[(1-2\theta)\left(\beta(u)+b\right)+\theta\right]}{2(1-2\theta)}\right].
\end{aligned} \tag{B.11}$$

Conflict of Interests

The authors declare that there is no conflict of interests regarding the publication of this paper.

Acknowledgments

This work was partially supported by the National Natural Science Foundation of China (Grant no. 71171203), the major Project of National Social Science Foundation (Grants nos. 13&ZD024 and 13&ZD169), the Ph.D. Programs Foundation of Ministry of Education of China (Grant no. 20130162110076), the Research Project in Humanities and Social Sciences of Chinese Ministry of Education (Grants nos. 13YJAZH149 and 09YJC90261), the Emergency Project of Chinese Ministry of Education (Grant no. 2009JYJR035), the China Postdoctoral Science Foundation (Grant no. 20110491264), the Special Project of Postdoctoral Research Funds of Hunan Province (Grant no. S2011R1040), and the Project of Soft Science of Hunan Province (Grant no. 2009ZK3193).

References

[1] A. Ziegler, *A Game Theory Analysis of Options—Contributions to the Theory of Financial Intermediation in Continuous Time*, vol. 468 of *Lecture Notes in Economics and Mathematical Systems*, Springer, New York, NY, USA, 1999.

[2] F. Smets, "Exporting versus FDI: the effect of uncertainty, irreversibilities and strategic interactions," Working Paper, Yale University, 1991.

[3] A. K. Dixit and R. S. Pindyck, *Investment under Uncertainty*, Princeton University Press, Princeton, NJ, USA, 1994.

[4] H. T. J. Smit and L. A. Ankum, "A real options and game-theoretic approach to corporate investment strategy under competition," *Financial Management*, vol. 22, no. 3, pp. 241–250, 1993.

[5] H. T. J. Smit and L. Trigeorgis, "R&D option strategies," Working Paper, University of Chicago, 1997.

[6] I. Junichi and T. Watanabe, "A two-stage investment game in real option analysis," in *Proceedings of the 8th Annual Conference on Real Options Theory*, Discussion Paper, Tokyo Metropolitan University, March 2004.

[7] I. Junichi and T. Watanabe, "A numerical approach for real option values and equilibrium strategies in a Duopoly," in *Proceedings of the 10th Annual Conference on Real Options Theory*, May 2006.

[8] Q. H. Zhong and Z. R. Tian, "The strategic analysis framework for project investment portfolio based on real option," *Chinese Journal of Management Science*, vol. 12, no. 3, pp. 18–21, 2004.

[9] X. L. Wang and S. G. Zhang, "Option games in finite investment project life," *System Engineering Theory and Practice*, vol. 31, no. 2, pp. 247–251, 2011.

[10] J. B. Huang and B. Bai, "The study of investment decision under the technology collaborative innovation mode of electric vehicle enterprise," *System Engineering Theory and Practice*, vol. 31, no. 9, pp. 1707–1717, 2011.

[11] R. Antle and G. Eppen, "Capital rationing and organizational slack in capital budgeting," *Management Science*, vol. 31, no. 2, pp. 163–174, 1985.

[12] F. Wen, X. Gong, Y. Chao, and X. Chen, "The effects of prior outcomes on risky choice evidence from the stock market," *Mathematical Problems in Engineering*, vol. 2014, Article ID 272518, 8 pages, 2014.

[13] F. Wen and X. Yang, "Skewness of return distribution and coefficient of risk premium," *Journal of Systems Science and Complexity*, vol. 22, no. 3, pp. 360–371, 2009.

[14] M. Harris and A. Raviv, "The capital budgeting process: incentives and information," *Journal of Finance*, vol. 51, no. 4, pp. 1139–1174, 1996.

[15] F. Wen, Z. He, and X. Chen, "Investors' risk preference characteristics and conditional skewness," *Mathematical Problems in Engineering*, vol. 2014, Article ID 814965, 14 pages, 2014.

[16] T. T. Milbourn, A. W. A. Boot, and A. V. Thakor, "Megamergers and expanded scope: theories of bank size and activity diversity," *Journal of Banking and Finance*, vol. 23, no. 2, pp. 195–214, 1999.

[17] R. Antle, P. Bogetoft, and A. W. Stark, "Incentive problems and investment timing options," Working Paper, 2002.

[18] S. R. Grenadier and N. E. Wang, "Incentives and investment timing: real option in a principle-agent setting," Working Paper, 2003.

[19] C. Osakwe, "Real option and adverse incentives: determining the incentive compatible cost-of-capital," Working Paper, 2002.

[20] M. Rabin, "Incorporating fairness into game theory and economics," *The American Economic Review*, vol. 83, no. 5, pp. 1281–1302, 1993.

[21] M. Dufwenberg and G. Kirchsteiger, "A theory of sequential reciprocity," *Games and Economic Behavior*, vol. 47, no. 2, pp. 268–298, 2004.

[22] A. Falk and U. Fischbacher, "A theory of reciprocity," *Games and Economic Behavior*, vol. 54, no. 2, pp. 293–315, 2006.

[23] E. Fehr and K. M. Schmidt, "A theory of fairness, competition, and cooperation," *Quarterly Journal of Economics*, vol. 114, no. 3, pp. 817–868, 1999.

[24] G. E. Bolton and A. Ockenfels, "ERC: a theory of equity, reciprocity, and competition," *The American Economic Review*, vol. 90, no. 1, pp. 166–193, 2000.

[25] A. E. Bernardo, H. Cai, and J. Luo, "Capital budgeting and compensation with asymmetric information and moral hazard," *Journal of Financial Economics*, vol. 61, no. 3, pp. 311–344, 2001.

[26] J. N. Zhou and D. S. Huang, "Investment decision behavior on project with expand option," *Journal of Management Sciences*, vol. 9, no. 2, pp. 28–35, 2006.

[27] A. Tversky and D. Kahneman, "Advances in riskless choice: a reference-dependent model," *Quarterly Journal of Economics*, vol. 106, no. 5, pp. 1039–1061, 1992.

[28] G. Charness and M. Rabin, "Understanding social preferences with simple tests," *Quarterly Journal of Economics*, vol. 117, no. 3, pp. 817–869, 2002.

[29] S. Teyssier, "Experimental evidence on inequity aversion and self-selection between incentive contracts," Working Paper, University of Lyon, 2008.

[30] B. Holmstrom, "Moral hazard and observability," *Journal of Economics*, vol. 10, pp. 74–91, 1979.

[31] S. Traub, C. Seidl, and U. Schmidt, "An experimental study on individual choice, social welfare, and social preferences," *European Economic Review*, vol. 53, no. 4, pp. 385–400, 2009.

Hindawi Publishing Corporation
Discrete Dynamics in Nature and Society
Volume 2014, Article ID 216057, 11 pages
http://dx.doi.org/10.1155/2014/216057

Research Article

Pricing Scheme of Ocean Carrier for Inbound Container Storage for Assistance of Container Supply Chain Finance

Mingzhu Yu,[1] Xin Tian,[2] and Lean Yu[3]

[1] *Department of Transportation Engineering, College of Civil Engineering, Shenzhen University, Shenzhen 518060, China*
[2] *Research Center on Fictitious Economy and Data Science, Chinese Academy of Sciences, Beijing 100190, China*
[3] *School of Economics and Management, Beijing University of Chemical Technology, Beijing 100029, China*

Correspondence should be addressed to Lean Yu; yulean@amss.ac.cn

Received 12 February 2014; Revised 21 May 2014; Accepted 22 May 2014; Published 15 June 2014

Academic Editor: Chuangxia Huang

The aim of this paper is to investigate the pricing scheme of ocean carrier for inbound container storage so as to assist container supply chain finance. In this paper, how an ocean carrier should set price of inbound container storage to the customer while facing the contract from the container terminal operator is first analyzed. Then, two different contract systems, the free-time contract system which is widely used in practice and the free-space contract system which is newly developed recently, are considered. In the two different contract systems, inbound container storage pricing models are constructed, and accordingly optimal solution approaches for the ocean carrier are provided. For comparison purpose, some numerical experiments for the two different contract systems are conducted to investigate the effects of the container terminal operator's decision on the system outcomes. Numerical experiments show that (1) the carrier is more flexible in the free-space contract system and can receive more profit by using the free-storage-space as a pooling storage system and (2) the free-space contract system benefits both the carrier in profit and the busy terminal in traffic control.

1. Introduction

The ocean transportation business leads to the scarcity of resources in the container terminal. Therefore, operational efficiency improvement is now one of the main concerns of container terminal operators. The container terminal yard operation plays a critical role in integrated terminal operations because efficiency improvement in the container terminal yard accelerates both the waterside operations and the landside operations. Traditionally, terminal operators try to optimize the schedule of the yard crane and the allocation of containers. Nowadays, they are paying more attention to strategic decisions. Take the inbound container storage for example; if the customer stores an inbound container in a container terminal yard for longer than the so-called free-time-limit, the storage fee will be linear to the container dwell time in the terminal yard and will be charged by the container terminal operator.

Fransoo and Lee [1] find that the operational relationship may not be aligned with the contractual relationship in ocean transportation system. Though there is no direct contractual relationship between the customer and the terminal operator, the operational interaction exists. The inbound container storage reflects the unaligned operational and contractual relationship. Customers store their inbound containers in the container terminal yard. Container terminal operator first charges the storage fee from the ocean carrier, and ocean carrier charges this fee from the customer later. The fees paid to the terminal operator and paid from the customer are not necessarily the same amount. That is, the customer pays the container storage fees to the terminal operator through the ocean carrier.

This paper aims to investigate the pricing scheme of ocean carrier's inbound container storage facing two kinds of contracts from the container terminal operator: the free-time contract and the free-space contract. In the free-time contract setting, the container terminal operator provides a contract consisting of "free-time-limit" and storage fee to the ocean carrier. If the customer's containers stay in the terminal yard for longer than the free-time-limit, each container will be charged by container terminal operator per extra day. Given this free-time contract from the terminal operator, the ocean carrier provides a similar contract to the customer with the same free-time-limit value and higher storage fee rate than provided by the container terminal operator. In the free-space contract setting, the container terminal operator provides a contract which includes free-storage-space and storage fee to the ocean carrier. If the storage space occupied by the customers' inbound containers exceeds the free space, the ocean carrier needs to pay the container storage fee for per day per unit container to the container terminal operator. Facing this contract from the container terminal operator, the carrier still provides a free-time contract to the customer. In the free-space contract system, the carrier does not operate the terminal storage yard directly. Hence, it is impossible for the carrier to track the space occupied in the container terminal yard. Therefore, the carrier provides free-time contract rather than free-space contract to the customers.

In the ocean transportation system, the free-time contract system is quite popular. For example, in Hong Kong port and many other Chinese ports, container terminal operators provide the free-time contract to carriers. However, the free-space contract system is newly developed and is not well studied. Some container terminals in South Korea are using the free-space contracts now. In order to fill the gap in the inbound container storage pricing area, we explore the ocean carrier's inbound container storage price schemes with the free-time and free-space contracts from the container terminal operator.

In the context of supply chain finance, solutions and technics are adopted to optimize capital for the buyer and enhanced cash flow for the supplier and to minimize risk in the supply chain. The pricing problems we studied involve three parties: the container terminal operator, the carrier, and the customers, in the container supply chain. We investigate the contractual relations between them, which helps to build the basis for further studies on the container supply chain finance.

2. Literature Review

There are extensive studies concerning efficiency improvement of various container terminal operations. Comprehensive reviews could be found in Günther and Kim [2] and Stahlbock and Voß [3]. It is hard to find existing studies on the container storage pricing schemes in supply chain finance. Fransoo and Lee [1] mentioned that extensive research questions need to be answered in the ocean transportation area, where the unaligned contractual and operational relationship in the container supply chain is a critical topic.

de Castilho and Daganzo [4] firstly discussed the effect of the remote warehouse's existence on the customer behavior. In order to minimize the total storage cost, customers between the container terminal and the remote warehouse should be considered. Their paper investigates the pricing issue for the cargo's temporary storage in the container ports under discriminatory and nondiscriminatory schemes. K. H. Kim and K. Y. Kim [5] considered the real practice of the container terminal operator's inbound container storage price, which consists of a free-time-limit and an extra storage fee after the free-time-limit. In their paper, they assumed that a remote container storage yard is located near the terminal. Different models are provided to maximize the container terminal profit which is under a certain customer service constraint or to minimize the total public cost. Lee and Yu [6] focus on the inbound container storage price competition problem and consider the competition relationship between the container terminal operator and the remote container storage yard operator. The container terminal operator provides the free-time-limit and an off-time storage fee in their pricing scheme, and the remote container yard operator sets the storage price as linear to the container storage time. Both the random container storage time and the sensitive container storage time are considered. They proved the uniqueness and existence of the price equilibrium.

Holguín-Veras and Jara-Díaz [7] studied a joint problem of optimal space allocation as well as storage pricing. The priority price scheme where a different class of containers get different storage charge and neutral price scheme where a unique price is utilized for all types of containers are considered. They extended their research by considering that the container arrival rate is sensitive to the terminal storage charge in Holguín-Veras and Jara-Díaz [8]. Saurí et al. [9] proposed a new import container storage pricing model which has a flat storage fee (a nonzero constant) before the free-time-limit.

Our paper contributes to the literature by considering the unaligned situation in the ocean transportation system. Different from the traditional study, we focus on the pricing scheme of the ocean carrier rather than the container terminal operator.

3. Model Formulation

In this paper, an inbound container storage pricing problem, which includes one carrier, one terminal operator, and related customers, is considered. After unloading from vessels, inbound containers of the customers may stay in the container terminal yard (CTY) until the external trucks come to collect them. The inbound container dwell time T (random variable) is the time interval between the container arrival time at the terminal and the time when the customer calls the inbound container. In the free-time contract system, if the container dwell time in the terminal yard is longer than F_0 days, the free-time-limit provided by the CTY, the carrier needs to pay the terminal operator p_0 per container per day. In the free-space contract system, if the occupied space in the container terminal yard exceeds K (unit of K is TEU$*$day), the carrier needs to pay the container terminal operator p_1 per container per day. We assume that there is an alternative storage place for the inbound containers C, a remote container storage yard (RCY) near the container terminal. The RCY provides storage space for the inbound containers and charges a storage fee s_0 per container per day: $s_0 < p_0$ and $s_0 < p_1$. However, the carrier needs to pay additional handling and transportation costs c_0 per container to move a container from the CTY to the RCY.

The average number of arriving inbound containers at the terminal every day is n TEU. It is widely accepted that the average number of inbound containers is independent of the storage price. For the simplicity, we assume that the average number of arriving containers at the container terminal every day is stable. Due to information asymmetry, the ocean carrier, CTY, and RCY do not know the exact inbound container dwell time; they only know the distribution $f(T)$ (probability density function). Following the analysis in the literature (K. H. Kim and K. Y. Kim [5]; Watanabe [10]), we assume that the inbound container dwell time follows exponential distribution $f(T) = \lambda e^{-\lambda T}$.

In the free-time contract system, facing the inbound container storage price scheme (F_0, p_0), the ocean carrier decides the container storage fee w and provides the price contract (F_0, w) to the customer. It is assumed that $w > p_0$. In the free-space contract system, facing the inbound container storage price scheme (K, p_1), the ocean carrier decides price contract (F, s) to the customer. It is assumed that $s > p_1$.

Besides the container terminal yard, the customer has an alternative container storage place, that is, the RCY. Firstly, the ocean carrier and RCY will simultaneously provide their storage price schemes, (F, s) (or (F_0, w) for the free-time contract system) and s_0. After the storage price schemes are announced, the customer determines whether to transfer the inbound container from the CTY to the RCY after the free-time-limit. Figure 1 demonstrates the customer payment function. Here, we define $t_s = c_0/(s-s_0)$ (or $t_w = c_0/(w-s_0)$ for the free-time contract system) as the indifference time. If the inbound container's dwell time is shorter than $F+t_s$ (or F_0+t_w for the free-time contract system), the customer will leave the container in the CTY till it is needed. If the container dwell time is longer than $F + t_s$ (or $F_0 + t_w$), then the customer will move the container to the RCY after the free-time-limit and then collect it when it is needed.

In the following two sections, we will study the ocean carrier's storage price schemes in the free-time contract system, (F_0, w), and in the free-space contract system, (F, s). In the free-time contract system, the free-time-limit value, F_0, is given by the container terminal. Hence, the ocean carrier only needs to determine the inbound container storage fee per day per TEU, w. In the free-space contract system, the two decisions of the ocean carrier are the free-time-limit F and the inbound container storage fee s.

4. Free-Time Contract System

In the free-time contract system, the container terminal operator provides a free-time-limit F_0 and the inbound container extra storage fee rate p_0 to the ocean carrier. The ocean carrier offers the same free-time-limit F_0 to the customer but will add an additional storage fee. Namely, the ocean carrier's inbound container storage fee for the customer, w, is higher than p_0. It is assumed that the upper limit of the ocean carrier's charge is $\overline{w}$. Therefore, we have $p_0 \le w \le \overline{w}$.

Based on the customer behavior analysis in Section 3, the containers, whose dwell time is less than F_0+t_w, will be stored

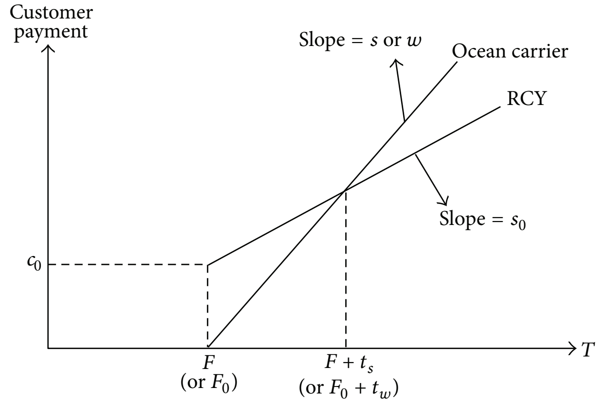

Figure 1: The payment function of the customer.

in the container terminal after the free-time-limit. Hence, the ocean carrier's profit is the following:

$$\Pi(w) = n\int_{F_0}^{F_0+t_w} (w - p_0)(t - F_0) f(t)\,dt, \tag{1}$$

where $(w - p_0)$ is the extra money the ocean carrier earns per TEU, besides paying the container terminal.

We can get the first and second derivatives of the ocean carrier's objective function as follows:

$$\begin{aligned}\frac{\partial \Pi}{\partial w} &= n\int_{F_0}^{F_0+t_w} (t - F_0) f(t)\,dt \\ &\quad - n(w - p_0)\frac{c_0^2}{(w - s_0)^3} f(F_0 + t_w),\end{aligned} \tag{2}$$

$$\begin{aligned}\frac{\partial^2 \Pi}{\partial w^2} &= -\frac{2nc_0^2}{(w - s_0)^3} f(F_0 + t_w) + \frac{3nc_0^2(w - p_0)}{(w - s_0)^4} f(F_0 + t_w) \\ &\quad + \frac{nc_0^3(w - p_0)}{(w - s_0)^5}\frac{\partial f(F_0 + t_w)}{\partial t_w}.\end{aligned} \tag{3}$$

Proposition 1. *In the free-time contract system, the ocean carrier's objective function is concave if the following assumption is satisfied.*

Assumption 2. $\overline{w} \le 3p_0 - 2s_0$.

Proof. By (3), to prove the concavity of the ocean carrier's objective function, we need to show that

$$\begin{aligned}\frac{\partial^2 \Pi}{\partial w^2} &= -\frac{2nc_0^2}{(w - s_0)^3} f(F_0 + t_w) + \frac{3nc_0^2(w - p_0)}{(w - s_0)^4} f(F_0 + t_w) \\ &\quad + \frac{nc_0^3(w - p_0)}{(w - s_0)^5}\frac{\partial f(F_0 + t_w)}{\partial t_w} \le 0.\end{aligned} \tag{4}$$

Since we have $f(T) = \lambda e^{-\lambda T}$, then

$$\frac{\partial^2 \Pi}{\partial w^2} = -\frac{2nc_0^2}{(w-s_0)^3}\lambda e^{-\lambda(F_0+t_w)} + \frac{3nc_0^2(w-p_0)}{(w-s_0)^4}\lambda e^{-\lambda(F_0+t_w)} - \frac{nc_0^3(w-p_0)}{(w-s_0)^5}\lambda^2 e^{-\lambda(F_0+t_w)}. \quad (5)$$

We have $w > p_0$ and $w > s_0$; hence, the third part in the right side of the above expression is less than zero. If we have the assumption $\overline{w} \le 3p_0 - 2s_0$, then we can get the first and second parts:

$$-\frac{2nc_0^2}{(w-s_0)^3}\lambda e^{-\lambda(F_0+t_w)} + \frac{3nc_0^2(w-p_0)}{(w-s_0)^4}\lambda e^{-\lambda(F_0+t_w)} \le 0. \quad (6)$$

Therefore, we have $\partial^2\Pi/\partial w^2 \le 0$. □

Assumption 2 indicates that, given the RCY storage fee and the container terminal storage fee, the ocean carrier's storage price upper limit should not be too high. Otherwise, the container terminal could set pretty high storage price (even though there exists threat from the RCY), which is not fair to the customer.

Letting (2) equal zero, we can find the stationary point for the objective function. From Proposition 1, we know that if Assumption 2 is satisfied, then the objective function is concave in the feasible region $(p_0, \overline{w})$ and there exists at most one stationary point in this region. If there is no stationary point in the feasible region, then the objective function either increases or decreases in $(p_0, \overline{w})$. We summarize the solution steps as follows.

Step 1. Let (2) equal zero and use the line search method to find the stationary point. Go to Step 2.

Step 2. Check the w value region $(p_0, \overline{w})$; if there is one stationary point in this region, then let this point value be w^*, the optimal storage price, and stop. Otherwise, go to Step 3.

Step 3. If there is no stationary point in region $(p_0, \overline{w})$ and the objective function is increasing in this region, then let $w^* = \overline{w}$ be the optimal storage price. On the other hand, if the objective function is decreasing in this region, then let $w^* = p_0$ be the optimal storage price. Stop.

5. Free-Space Contract System

In the free-space contract system, the container terminal operator provides an inbound container free-storage-space K and the inbound container extra storage fee rate p_1 to the ocean carrier. If the total amount of space occupied by the inbound containers in the terminal exceeds K, then the ocean carrier needs to pay p_1 per TEU per day. Facing this price contract from the container terminal, the ocean carrier offers a free-time-limit F and the inbound container extra storage fee rate s to the customer. If the container dwell time in the terminal is longer than F, the customer needs to pay the ocean carrier s per TEU per day. It is assumed that the ocean carrier charges more than the container terminal and the upper limit of the ocean carrier's charge is $\bar{s}$. Therefore, we have $p_1 \le s \le \bar{s}$.

The customer will leave their container in the container terminal after the free-time-limit if the dwell time is less than $F + t_s$. Therefore, the ocean carrier's profit is the following:

$$\Pi(F,s) = n\int_F^{F+t_s} s(t-F)f(t)\,dt - p_1\left(\int_0^{F+t_s} ntf(t)dt - K\right)^+, \quad (7)$$

where the first part is the ocean carrier's income from the containers whose dwell time is less than $F+t_s$. In the second part, $\int_0^{F+t_s} ntf(t)dt$ denotes the expected space occupied by containers in the container terminal yard. Hence, the second part is the ocean carrier's payment to the container terminal for the containers whose space exceeds the free-space value, K.

Proposition 3. *In the free-space contract system, the ocean carrier's optimal free-time-limit setting is zero; namely,* $F^* = 0$.

Proof. To prove $F^* = 0$, we only need to show that, for any given s, the optimal value of F is 0. We divide (7) into two parts to analyze the monotonicity. Firstly, for the first part, we take derivative with F and have

$$\frac{\partial\left(n\int_F^{F+t_s} s(t-F)f(t)\,dt\right)}{\partial F} = -ns\int_F^{F+t_s} f(t)\,dt + nst_s f(F+t_s). \quad (8)$$

Since the container dwell time follows exponential distribution, we can draw out its distribution as in Figure 2. From the figure, we can easily get $\int_F^{F+t_s} f(t)dt \ge t_s f(F+t_s)$. Therefore, we have $-ns\int_F^{F+t_s} f(t)dt + nst_s f(F+t_s) \le 0$. Namely, the first part of the objective function decreases with F. Hence, for the first part, the optimal value of F is 0.

We now investigate the second part of (7), $-p_1(\int_0^{F+t_s} ntf(t)dt - K)^+$. In the second part, $\int_0^{F+t_s} ntf(t)dt$ increases with F. Therefore, the second part decreases with F. Hence, for the second part, the optimal value of F is also 0.

Summarizing the analysis of the first and second parts, we have $F^* = 0$. □

Although the optimal value of the free-time-limit is zero, it is often set to a positive value by the ocean carrier in practice. Therefore, in the remainder of this section, we take it as given and focus on the study of the optimal storage price s.

Followed by Proposition 3, we can rewrite (7) as

$$\Pi(s) = n\int_0^{t_s} stf(t)\,dt - p_1\left(\int_0^{t_s} ntf(t)dt - K\right)^+. \quad (9)$$

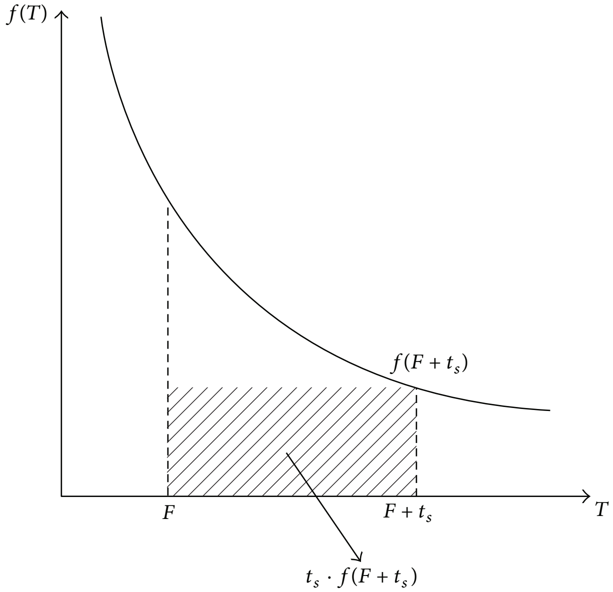

FIGURE 2: The container dwell time distribution.

Let $\int_0^{t_s} ntf(t)dt - K = 0$; then, we solve a corresponding s value and let this value be s_H. Since $t_s = c_0/(s-s_0)$, it is easy to find that $\int_0^{t_s} ntf(t)dt$ decreases with s. By this monotonic property, we can rewrite (9) to two segments and get

$$\Pi(s) = \begin{cases} \Pi_1(s) = n\int_0^{t_s} stf(t)\,dt, & \text{if } s \geq s_H, \\ \Pi_2(s) = n\int_0^{t_s} (s-p_1)\,tf(t)\,dt + p_1K, & \text{otherwise.} \end{cases} \quad (10)$$

We now derive the conditions under which $\Pi_1(s)$ and $\Pi_2(s)$ are concave. The first and second derivatives of $\Pi_1(s)$ and $\Pi_2(s)$ can be obtained as follows:

$$\frac{\partial \Pi_1(s)}{\partial s} = n\int_0^{t_s} tf(t)\,dt - \frac{c_0nst_s}{(s-s_0)^2}f(t_s), \quad (11)$$

$$\frac{\partial^2 \Pi_1(s)}{\partial s^2} = -\frac{2nc_0^2}{(s-s_0)^3}f(t_s) + \frac{3nsc_0^2}{(s-s_0)^4}f(t_s) + \frac{nsc_0^3}{(s-s_0)^5}\frac{\partial f(t_s)}{\partial t_s}, \quad (12)$$

$$\frac{\partial \Pi_2(s)}{\partial s} = n\int_0^{t_s} tf(t)\,dt - \frac{c_0n(s-p_1)t_s}{(s-s_0)^2}f(t_s), \quad (13)$$

$$\frac{\partial^2 \Pi_2(s)}{\partial s^2} = -\frac{2nc_0^2}{(s-s_0)^3}f(t_s) + \frac{3n(s-p_1)c_0^2}{(s-s_0)^4}f(t_s) + \frac{n(s-p_1)c_0^3}{(s-s_0)^5}\frac{\partial f(t_s)}{\partial t_s}. \quad (14)$$

Proposition 4. *In the free-space contract system, $\Pi_1(s)$ is concave if the following assumption is satisfied.*

Assumption 5. $\bar{s} \leq (\lambda c_0 - s_0 + \sqrt{(s_0-\lambda c_0)^2 + 8s_0^2})/2$.

Proof. To prove Proposition 4, we need to show that if $\bar{s} \leq (\lambda c_0 - s_0 + \sqrt{(s_0-\lambda c_0)^2 + 8s_0^2})/2$, then

$$\frac{\partial^2 \Pi_1(s)}{\partial s^2} = -\frac{2nc_0^2}{(s-s_0)^3}f(t_s) + \frac{3nsc_0^2}{(s-s_0)^4}f(t_s) + \frac{nsc_0^3}{(s-s_0)^5}\frac{\partial f(t_s)}{\partial t_s} \leq 0. \quad (15)$$

Since we have $f(T) = \lambda e^{-\lambda T}$, hence

$$\begin{aligned}\frac{\partial^2 \Pi_1(s)}{\partial s^2} &= -\frac{2nc_0^2}{(s-s_0)^3}\lambda e^{-\lambda t_s} + \frac{3nsc_0^2}{(s-s_0)^4}\lambda e^{-\lambda t_s} - \frac{nsc_0^3}{(s-s_0)^5}\lambda^2 e^{-\lambda t_s} \\ &= \frac{n\lambda e^{-\lambda t_s}c_0^2}{(s-s_0)^5}\left(s^2 + s_0s - \lambda c_0 s - 2s_0^2\right).\end{aligned} \quad (16)$$

If $\bar{s} \leq (\lambda c_0 - s_0 + \sqrt{(s_0-\lambda c_0)^2 + 8s_0^2})/2$, then we have $(s^2 + s_0s - \lambda c_0 s - 2s_0^2) \leq 0$. Therefore, if Assumption 5 is satisfied, then $\partial^2\Pi_1(s)/\partial s^2 \leq 0$. □

Proposition 6. *In the free-space contract system, $\Pi_2(s)$ is concave if Assumption 5 and the following assumption are satisfied.*

Assumption 7. $p_1 \geq (\lambda c_0 + 3p_1 - s_0 - \sqrt{(s_0 - \lambda c_0 - 3p_1)^2 + 8s_0^2 - 12p_1s_0 - 4\lambda c_0 p_1})/2$.

Proof. To prove Proposition 6, we need to show that if Assumption 5 is satisfied and $p_1 \geq (\lambda c_0 + 3p_1 - s_0 - \sqrt{(s_0 - \lambda c_0 - 3p_1)^2 + 8s_0^2 - 12p_1s_0 - 4\lambda c_0 p_1})/2$, then

$$\frac{\partial^2 \Pi_2(s)}{\partial s^2} = -\frac{2nc_0^2}{(s-s_0)^3}f(t_s) + \frac{3n(s-p_1)c_0^2}{(s-s_0)^4}f(t_s) + \frac{n(s-p_1)c_0^3}{(s-s_0)^5}\frac{\partial f(t_s)}{\partial t_s} \leq 0. \quad (17)$$

Since we have $f(T) = \lambda e^{-\lambda T}$, hence

$$\begin{aligned}\frac{\partial^2 \Pi_2(s)}{\partial s^2} &= -\frac{2nc_0^2}{(s-s_0)^3}\lambda e^{-\lambda t_s} + \frac{3n(s-p_1)c_0^2}{(s-s_0)^4}\lambda e^{-\lambda t_s} \\ &\quad - \frac{n(s-p_1)c_0^3}{(s-s_0)^5}\lambda^2 e^{-\lambda t_s} \\ &= \frac{n\lambda e^{-\lambda t_s} c_0^2}{(s-s_0)^5}\left[s^2 + (s_0 - \lambda c_0 - 3p_1)s - 2s_0^2 \right. \\ &\quad \left. +3p_1 s_0 + \lambda c_0 p_1\right].\end{aligned} \tag{18}$$

We only need to show that $s^2 + (s_0 - \lambda c_0 - 3p_1)s - 2s_0^2 + 3p_1 s_0 + \lambda c_0 p_1 \le 0$. From the property of the quadratic formula, we know that if the following inequations are satisfied,

$$\begin{aligned}&\left(\lambda c_0 + 3p_1 - s_0 \right. \\ &\quad \left. - \sqrt{(s_0 - \lambda c_0 - 3p_1)^2 + 8s_0^2 - 12p_1 s_0 - 4\lambda c_0 p_1}\right) \times \frac{1}{2} \\ &\quad \le s \le \left(\lambda c_0 + 3p_1 - s_0 \right. \\ &\qquad \left. + \sqrt{(s_0 - \lambda c_0 - 3p_1)^2 + 8s_0^2 - 12p_1 s_0 - 4\lambda c_0 p_1}\right) \\ &\quad \times \frac{1}{2} = A(p_1),\end{aligned} \tag{19}$$

then $s^2 + (s_0 - \lambda c_0 - 3p_1)s - 2s_0^2 + 3p_1 s_0 + \lambda c_0 p_1 \le 0$.

We now prove the right inequation of (19). It is easy to find that $\partial A(p_1)/\partial p_1 > 0$. Since we have $p_1 > 0$, we get $A(p_1 > 0) > A(p_1 = 0) = (\lambda c_0 - s_0 + \sqrt{(s_0 - \lambda c_0)^2 + 8s_0^2})/2$. Because $s \le \bar{s}$, if Assumption 5 is satisfied, then the right inequation of (19) is satisfied.

Because $s \ge p_1$, if Assumption 7 is satisfied, then the left inequation of (19) is also satisfied. □

Assumption 5 reveals that, given other parameters, the ocean carrier should not set the storage price too high (namely, the storage price upper limit is constrained). Otherwise, the unreasonable high storage price is unfair to the customer. Assumption 7 indicates that the ocean carrier could not choose too low storage price (namely, the storage price lower limit is also constrained). Otherwise, the inbound containers stay too long in the container terminal and occupy a large amount of space, which hurts both the container terminal (in space control) and the carrier (in storage payment).

From Propositions 4 and 6, we know that if Assumptions 5 and 7 are satisfied, then there exists at most one stationary point of the objective function in the feasible region $(p_1, \bar{s})$ for both $\Pi_1(s)$ and $\Pi_2(s)$. If the feasible region contains no stationary point, then the objective function either increases or decreases in this region. We summarize the solution steps as follows.

Step 1. Solve $\int_0^{t_s} ntf(t)dt - K = 0$ and get a corresponding s value. Let this value be s_H.

Step 2. If $s_H \ge \bar{s}$, we have the objective function $\Pi(s) = \Pi_2(s)$, let (13) be equal to zero, and use the line search method to find the stationary point, and then we go to Step 3. If $s_H \le p_1$, we have the objective function $\Pi(s) = \Pi_1(s)$, let (11) be equal to zero to find the stationary point, and then go to Step 3. If $p_1 < s_H < \bar{s}$, then go to Step 4.

Step 3. Check the region $(p_1, \bar{s})$.

(1) If there is one stationary point in this region, then let this point value be s^*.

(2) If there is no stationary point in region $(p_1, \bar{s})$ and the objective function is increasing in this region, then let $s^* = \bar{s}$ be the optimal storage price.

(3) If there is no stationary point in region $(p_1, \bar{s})$ and the objective function is decreasing in this region, then let $s^* = p_1$ be the optimal storage price.

Stop.

Step 4. Separate the region $(p_1, \bar{s})$ into two parts: (p_1, s_H) and $(s_H, \bar{s})$.

Step 5. For part $(s_H, \bar{s})$, we have the objective function $\Pi(s) = \Pi_1(s)$. Let (11) be equal to zero and find the stationary point.

(1) If the stationary point is in region $(s_H, \bar{s})$, let the s_1^* be this stationary point.

(2) If there is no stationary point in region $(s_H, \bar{s})$ and $\Pi_1(s)$ is increasing in this region, then let $s_1^* = \bar{s}$ be the optimal storage price.

(3) If there is no stationary point in region $(s_H, \bar{s})$ and $\Pi_1(s)$ is decreasing in this region, then let $s_1^* = s_H$ be the optimal storage price.

Step 6. For part (p_1, s_H), we have the objective function $\Pi(s) = \Pi_2(s)$. Let (13) be equal to zero and find the stationary point.

(1) If the stationary point is in region (p_1, s_H), let the s_2^* be this stationary point.

(2) If there is no stationary point in region (p_1, s_H) and $\Pi_2(s)$ is increasing in this region, then let $s_2^* = s_H$ be the optimal storage price.

(3) If there is no stationary point in region (p_1, s_H) and $\Pi_2(s)$ is decreasing in this region, then let $s_2^* = p_1$ be the optimal storage price.

Step 7. Let $s^* = \operatorname{argmax}\{\Pi_1(s_1^*), \Pi_2(s_2^*)\}$. Stop.

6. Numerical Experiments

In order to verify the effectiveness of the proposed models and their solution methods, several numerical experiments are conducted. The analysis in this section lies in the following threefold: (1) the effect of the container terminal's contract

Table 1: Parameters setting for numerical experiments.

Parameters	Applied value
Average number of arriving inbound containers every day, n	1000 TEU
Inbound container dwell time distribution parameter, λ	0.6
The container transportation cost from the CTY to the RCY, c_0	\$100
The container storage fee in the RCY, s_0	\$45
The carrier's storage fee uplimit in free-time system, $\overline{w}$	\$70
The carrier's storage fee uplimit in free-space system, $\overline{s}$	\$70

settings on the three parties (e.g., the carrier, the container terminal, and the customer) is studied; (2) the sensitivity analysis with respect to the parameter changes (e.g., the container dwell time distribution, the container transportation cost from the CTY to the RCY, and the storage fee in the RCY) is conducted; (3) the two contract systems are compared under the same conditions so as to investigate the carrier's profit, the container terminal's income, and the customer's cost.

Before presenting the numerical results, we first provide the parameter and condition settings in the following subsection.

6.1. Preliminary Setting. In order to guarantee that the two contract systems are compared under the same condition, we set the container terminal's two kinds of contract parameters as follows.

(1) The storage fees charged by the container terminal to the carrier under the two systems are set the same: $p_0 = p_1$. Similarly, the carrier's storage fee uplimits are set the same: $\overline{w} = \overline{s}$.

(2) The free-storage-space K offered by the container terminal in the free-space contract system equals the equivalent space accumulated in the free-time-limit F_0 in the free-time system. Namely, we have $K = \int_0^{F_0} ntf(t)dt$.

For the container terminal parameter effect analysis and the comparison of the two contract systems, we set the common parameters as in Table 1. All parameters are set such that Assumptions 2, 5 and 7 are satisfied. In each instance, we change one parameter and keep other parameters unchanged. In order to better demonstrate the effect of different parameters on carrier's price, customer's cost, carrier's profit, container terminal operator's income, and the average storage space in the container terminal at the same time, we use tables rather than figures to show the results.

For the sensitivity analysis, we change the value of c_0, s_0, and λ, so as to study the system outcomes. Parameters settings are described later in Tables 3 and 4.

6.2. The Effect of the Container Terminal Contract Parameters. In this subsection, the effect of the container terminal's storage contract parameter change on the system outcomes under the two contract systems is first investigated. We keep other parameters unchanged and only adjust the free-time-limit F_0 (or the free-storage-space K) and the container terminal storage fee p_0 (or p_1). The results are summarized in Table 2. We use "FT" and "FS" to denote the free-time and free-space contract systems in the table. By these numerical analyses, we intend to figure out the container terminal's reasonable decisions on the free-time-limit, the free-storage-space value, and the storage fee.

From the numerical results in Table 2, we summarize the insights from three angles: the container terminal, the carrier, and the customers.

6.2.1. Container Terminal (CT)

(1) In the free-time contract system, with the rise of the free-time-limit F_0, the average storage space in the container terminal occupied by the inbound containers will increase. Moreover, the longer free-time-limit leads to lower income to the container terminal. Therefore, it is suggested that the container terminal should not set too long free storage time in the free-time contract system. Practically, the container terminal often provides a nonzero free-time-limit directly to the carrier (or indirectly to the customer). Although this value could be different among different carriers, depending on the relationship between the carrier and the terminal operator, the container terminal operator should not set the value too high according to our analysis.

(2) In the free-space contract system, when the free-storage-space value K is relatively small, the container terminal's income (and its percentage of the customer's total payment) increases with the terminal's storage fee (p_1). When the free space value K is large, the carrier takes away all of the customer's payment and the container terminal gets no income. In addition, with the increase of K, the average storage space in the terminal occupied by the containers increases. Hence, the container terminal should not set too large K value, for the sake of traffic control and income enhancement.

(3) The container terminal and the carrier share the customer's storage payment (namely, each one takes a proportion). In the free-time contract system, the container terminal's income (and its percentage) increases with the terminal's storage fee (p_0). This result is intuitive, because the higher the storage charge, the higher the container terminal's income.

6.2.2. Carrier and Customer

(1) In the free-time contract system, the carrier's profit and the customer's cost decrease with the free-time-limit (F_0) set by the container terminal, which is quite

Table 2: Numerical results under different container terminal storage contract parameter settings.

CT storage contract parameters F_0	p_0 (p_1)	K	Carrier price ($) FT	FS	Customer cost ($) (carrier revenue) FT	FS	Carrier profit ($) FT	FS	CT income ($) FT	FS	Average storage space (TEU∗day) FT	FS
3	55	895.3	70	70	13346.7	80681.8	2860.0 (21.4%)	66528.9 (82.5%)	10486.7 (78.6%)	14152.9 (17.5%)	1537.1	1152.6 > K
3	60	895.3	70	70	13346.7	80681.8	1906.7 (14.3%)	65242.2 (80.9%)	11440.0 (85.7%)	15439.6 (19.1%)	1537.1	1152.6 > K
3	65	895.3	70	70	13346.7	80681.8	953.3 (7.1%)	63955.6 (79.3%)	12393.4 (92.9%)	16726.2 (20.7%)	1537.1	1152.6 > K
5	55	1335.5	70	65	4019.9	86807.3	861.4 (21.4%)	86807.3 (100%)	3158.5 (78.6%)	0 (0%)	1618.5	1335.5 = K
5	60	1335.5	70	65	4019.9	86807.3	574.3 (14.3%)	86807.3 (100%)	3445.6 (85.7%)	0 (0%)	1618.5	1335.5 = K
5	65	1335.5	70	65	4019.9	86807.3	287.1 (7.1%)	86807.3 (100%)	3732.8 (92.9%)	0 (0%)	1618.5	1335.5 = K
7	55	1537.1	70	59.3	1210.8	91130.6	259.5 (21.4%)	91130.6 (100%)	951.3 (78.6%)	0 (0%)	1649.5	1537.1 = K
7	60	1537.1	70	60	1210.8	90842.0	173.0 (14.3%)	90842.0 (100%)	1037.8 (85.7%)	0 (0%)	1649.5	1514.0 < K
7	65	1537.1	70	65	1210.8	86807.3	86.5 (7.1%)	86807.3 (100%)	1124.3 (92.9%)	0 (0%)	1649.5	1335.5 < K

[1]FT = free-time contract system; FS = free-space contract system.
[2]The percentages in the table denote the proportions of the carrier's profits or container terminal's incomes to the customer payment costs.

Table 3: Sensitivity analysis of free-time system under different c_0, s_0, and λ.

Parameters c_0	s_0	λ	Carrier price ($)	Customer cost ($) (carrier revenue)	Carrier profit ($)	CT income ($)	Average storage space (TEU∗day)
25	45	0.2	66.7	4164.2	732 (17.6%)	3432.2 (82.4%)	1010.3
35	45	0.2	67.5	7302.8	1352.7 (18.5%)	5950.1 (81.5%)	1157.8
45	45	0.2	68.3	10855.0	2113.4 (19.5%)	8741.6 (80.5%)	1296.0
45	35	0.2	70	5360.0	1148.6 (21.4%)	4211.4 (78.6%)	1059.4
45	40	0.2	70	7094.9	1520.3 (21.4%)	5574.6 (78.6%)	1137.6
45	45	0.2	68.3	10855.0	2113.4 (19.5%)	8741.6 (80.5%)	1296.0
25	45	0.2	66.7	4164.2	732.0 (17.6%)	3432.2 (82.4%)	1010.3
25	45	0.3	67.7	4035.3	756.0 (18.7%)	3279.3 (81.3%)	1161.5
25	45	0.4	68.7	3500.5	696.6 (19.9%)	2803.9 (80.1%)	1207.1

[1]The parameters are set as follows: $F_0 = 7$ days; $p_0 = \$55$; $\overline{w} = \$70$.
[2]The percentages in the table denote the proportions of the carrier's profits or container terminal's incomes to the customer payment costs.

intuitive. But in the free-space contract system, the carrier's profit and the customer's cost increase (or at least do not decrease) with the free-storage-space (K) provided by the terminal. This is because the increase of the free-space value makes the carrier have more freely controllable space, storing more containers freely in the terminal but still charging the customers.

(2) The carrier earns less with the increase of the storage fee (p_0 or p_1) of the container terminal, which is intuitive. The customer pays less (or at least not more) if the storage fee (p_0 or p_1) set by the container terminal increases. The reason lies in the fact that the increase of the container terminal storage fee makes the carrier raise his price, which further drives the containers to the RCY. Therefore, the customer pays less by the container transfer.

6.3. Sensitivity Analysis. We now analyze how the change of the parameters (besides the container terminal's contract parameter) affects the system outcomes. The results are shown in Tables 3 and 4. Notations "FT" and "FS" are utilized to denote the free-time and free-space contract systems in the tables. The parameters are set as described in the footnotes of the tables. Assumptions 2, 5 and 7 are satisfied.

We summarize the results as follows.

6.3.1. Effect of c_0. In both the free-time and free-space contract systems, with the increase of the container transportation cost from the CTY to the RCY, c_0, the containers are more likely to be stored in the CTY. Therefore, the carrier has motivation to raise the storage price. The carrier and the terminal gain more incomes. The customer suffers both high transportation cost and high total storage payment.

6.3.2. Effect of s_0. In both the free-time and free-space contract systems, if the storage fee in the RCY rises, then customers are willing to store the containers in the CTY. Therefore, the profits of the carrier and the terminal increase.

6.3.3. Effect of λ. If there are more inbound containers to be collected early by the customer (namely, λ increases),

TABLE 4: Sensitivity analysis of free-space system under different c_0, s_0, and λ.

Parameters c_0	s_0	λ	Carrier price ($)	Customer cost ($) (carrier revenue)	Carrier profit ($)	CT income ($)	Average storage space (TEU∗day)
100	45	0.6	59.3	91130.6	91130.6 (100%)	0 (0%)	$1537.1 = K$
110	45	0.6	60.7	93326.5	93326.5 (100%)	0 (0%)	$1537.1 = K$
120	45	0.6	62.1	95522.4	95522.4 (100%)	0 (0%)	$1537.1 = K$
100	45	0.6	59.3	91130.6	91130.6 (100%)	0 (0%)	$1537.1 = K$
100	47	0.6	61.3	94204.9	94204.9 (100%)	0 (0%)	$1537.1 = K$
100	50	0.6	64.3	98816.3	98816.3 (100%)	0 (0%)	$1537.1 = K$
100	45	0.6	59.3	91130.6	91130.6 (100%)	0 (0%)	$1537.1 = K$
100	45	0.7	61.1	81247.8	81247.8 (100%)	0 (0%)	$1329.2 < K$
100	45	0.8	64.4	73846.9	73846.9 (100%)	0 (0%)	$1145.9 < K$
100	45	0.6	70	80681.8	66528.9 (82.5%)	14152.9 (17.5%)	$1152.6 > K$
110	45	0.6	70	86361.8	67746.0 (78.4%)	18615.8 (21.6%)	$1233.7 > K$
120	45	0.6	70	91256.2	68794.8 (75.4%)	22461.4 (24.6%)	$1303.7 > K$
100	45	0.6	70	80681.8	66528.9 (82.5%)	14152.9 (17.5%)	$1152.6 > K$
100	47	0.6	70	85667.1	67597.2 (78.9%)	18069.9 (21.1%)	$1223.8 > K$
100	50	0.6	70	93484.8	69272.4 (74.1%)	24212.4 (25.9%)	$1335.5 > K$
100	45	0.6	70	80681.8	66528.9 (82.5%)	14152.9 (17.5%)	$1152.6 > K$
100	45	0.7	70	76892.1	65221.4 (84.8%)	11670.7 (15.2%)	$1098.5 > K$
100	45	0.8	70	72519.8	63084.6 (87.0%)	9435.2 (13.0%)	$1036.0 > K$

[1]The parameters are set as follows: $p_1 = \$55$; $\bar{s} = \$70$. In the first 9 instances, $K = 1537.1$ TEU∗day, and in the second 9 instances, $K = 895.3$ TEU∗day.
[2]The percentages in the table denote the proportions of the carrier's profits or container terminal's incomes to the customer payment costs.

then the customer totally pays less in both the free-time and free-space contract systems. This is because the earlier the containers are collected, the shorter the storage time is, which makes the customer pay less. In the free-space contract system, if the containers are to be collected earlier (λ increases), the carrier's profit percentage to the customer's payment increases (or at lease does not decrease). It is due to the reason that, facing a given free space from the container terminal, the earlier the containers are collected, the more free space to utilize the carrier has. Therefore, the carrier's profit percentage increases.

6.4. Comparison of the Two Contract Systems. The free-time contract system is widely used in the ocean transportation network. However, the free-space contract system is newly developed. Currently, there is no related research concerning the comparison of the two systems. After analyzing the two models in the previous sections, we now use the numerical experiments results (refer to Table 2) to quantitatively compare these two contract systems. We analyze the system outcomes from three aspects: the carrier, the customer, and the container terminal. The percentages in Table 2 denote the proportions of the carrier's profits or the terminal's incomes to the customer's payments.

6.4.1. Carrier

(1) The carrier makes more profit in the free-space contract system than in the free-time one. In the free-time system, the carrier only adds a small extra fee based on the price provided by the container terminal. However, in the free-space system, the carrier treats the free-storage-space provided by the container terminal as a pooling storage system. Although the dwell times of different containers vary from short to long, as long as the total storage space in the terminal is below the free-storage-space value K, the carrier pays nothing to the terminal. Therefore, the free-space contract system alleviates the container dwell time varying risk for the carrier and brings him a high profit.

(2) In the free-time contract system, the carrier receives a smaller proportion of the customer's payment than the container terminal, while, in the free-space contract system, the carrier takes larger proportion of the customer's payment than the terminal. In some cases, the carrier even sets suitable storage price such that the storage space occupied by the containers in the terminal is no more than K. Hence, the carrier earns 100% of the customer's storage payment.

Based on the analysis above, the carrier prefers the free-space contract system to the free-time one, because it brings him higher profit.

6.4.2. Container Terminal (CT)

(1) If the free-storage-space K is small, then the container terminal earns more in the free-space contract system than in the free-time system, while if K is relatively

large, in the free-space contract system, the container terminal's income is zero. This is because, facing the large free-storage-space value, the carrier will set suitable storage price such that the container space in the terminal is less than or equal to K.

(2) Although the container terminal has the risk of no income from the container storage in the free-space contract system, this contract system can help to reduce the space occupied by the inbound containers in the CT. Therefore, for a busy container terminal, the free-space contract system is preferred by the terminal operator. After all, the container storage income is not the terminal's main focus. The terminal operators are eager to control the traffic congestion because the terminal yard crane operation cost quadratically increases with the number of containers in the yard [11]. Moreover, the terminal yard efficiency helps to increase the waterside quay crane operation speed.

(3) If the terminal operator has choice, he would rather not use either of the two contract systems but would directly provide the free-time contract to the customer because, in the free-time contract system and the free-space contract system, the carrier takes away all or part of the customer's payment, while if the direct free-time contract is signed between the container terminal and the customer, the terminal operator seizes 100% of the customer's storage payment.

From the discussion above, we know that, in the unaligned relationship ocean transportation network, the free-space contract system is a "win-win" strategy for both the carrier and the busy container terminal.

6.4.3. Customer. The customers pay more storage fee in the free-space contract system than in the free-time contract system. This is due to the fact that, in the free-space contract system, the carrier provides zero free-time-limit for the customer. Hence, the customers need to pay the storage fee from the beginning of the container dwell period. Therefore, customers prefer the free-time contract system.

7. Conclusion

In this paper, the ocean carrier's pricing schemes for the inbound container storage in the container terminal are investigated from the perspective of supply chain finance. Besides the container terminal, the customer has another container storage place, that is, the RCY. The ocean carrier faces two different charge contracts from the container terminal: the free-time contract and free-space contract. We propose two models to analyze the ocean carrier's price decisions under these two charge contracts.

In the free-time contract system and free-space contract system, we derive the assumptions under which the objective function of the ocean carrier is concave. With these assumptions, we propose the solution approaches for the optimal price schemes. It is shown that, in the free-space contract system, the optimal free-time-limit value in the ocean carrier's price scheme is zero.

The numerical studies compare the two models and show that the carrier is more flexible in the free-space contract system and receives more profit by using the free-storage-space as a pooling storage system. It is found that the free-space contract system benefits both the carrier in profit and the busy terminal in traffic control.

Although we made some assumptions in the model basic settings to let the problem be tractable, the results and insight achieved in this paper may provide a valuable managerial guide for the ocean carriers. We also raise, for the first time, the pricing scheme problem in the unaligned ocean transportation system, which provides impetus for future research.

A possible extension about this paper is the research concerning the three-tier contract system which involves both the contract between the container terminal and the ocean carrier and the contract between the ocean carrier and the customer. Moreover, the priority pricing scheme and stochastic container arrival pattern could also be future research directions.

Conflict of Interests

The authors declare that there is no conflict of interests regarding the publication of this paper.

Acknowledgments

The authors would like to express their sincere appreciation to the three independent referees in making valuable comments and constructive suggestions to the paper. Their comments have improved the quality of the paper immensely. The work described in this paper was fully supported by the National Science Fund for Distinguished Young Scholars (Grant no. 71025005), the National Natural Science Foundation of China (Grants nos. 71302109, 71202114, and 91224001), and the President Fund of UCAS (Y35101KY00).

References

[1] J. C. Fransoo and C.-Y. Lee, "Ocean container transport: an underestimated and critical link in global supply chain performance," *Production and Operations Management*, 2010.

[2] H.-O. Günther and K.-H. Kim, "Container terminals and terminal operations," *OR Spectrum*, vol. 28, no. 4, pp. 437–445, 2006.

[3] R. Stahlbock and S. Voß, "Operations research at container terminals: a literature update," *OR Spectrum*, vol. 30, no. 1, pp. 1–52, 2008.

[4] B. de Castilho and C. F. Daganzo, "Optimal pricing policies for temporary storage at ports," *Transportation Research Record*, vol. 1313, pp. 66–74, 1991.

[5] K. H. Kim and K. Y. Kim, "Optimal price schedules for storage of inbound containers," *Transportation Research B: Methodological*, vol. 41, no. 8, pp. 892–905, 2007.

[6] C.-Y. Lee and M. Yu, "Inbound container storage price competition between the container terminal and a remote container

yard," *Flexible Services and Manufacturing Journal*, vol. 24, no. 3, pp. 320–348, 2012.

[7] J. Holguín-Veras and S. Jara-Díaz, "Optimal pricing for priority service and space allocation in container ports," *Transportation Research B: Methodological*, vol. 33, no. 2, pp. 81–106, 1998.

[8] J. Holguín-Veras and S. Jara-Díaz, "Preliminary insights into optimal pricing and space allocation at intermodal terminals with elastic arrivals and capacity constraint," *Networks and Spatial Economics*, vol. 6, no. 1, pp. 25–38, 2006.

[9] S. Saurí, J. Serra, and E. Martín, "Evaluating pricing strategies for storage in import container terminals," *Transportation Research Record*, no. 2238, pp. 1–7, 2011.

[10] I. Watanabe, *Container Terminal Planning: A Theoretical Approach*, World Cargo News (WCN), Great Britain, UK, 2001.

[11] C.-Y. Lee and M. Yu, "Inbound Container Storage Price Competition between the Container Terminal and a Remote Yard," *Flexible Services and Manufacturing Journal*, vol. 24, no. 3, pp. 320–348, 2012.

Hindawi Publishing Corporation
Discrete Dynamics in Nature and Society
Volume 2014, Article ID 564213, 9 pages
http://dx.doi.org/10.1155/2014/564213

Research Article

Credit Risk Evaluation with a Least Squares Fuzzy Support Vector Machines Classifier

Lean Yu[1,2]

[1] *Alibaba Business College, Hangzhou Normal University, Hangzhou 310036, China*
[2] *School of Economics and Management, Beijing University of Chemical Technology, Beijing 100029, China*

Correspondence should be addressed to Lean Yu; yulean@amss.ac.cn

Received 12 February 2014; Accepted 27 May 2014; Published 12 June 2014

Academic Editor: Fenghua Wen

A least squares fuzzy support vector machine (LS-FSVM) model that integrates advantages of fuzzy support vector machine (FSVM) and least squares method is proposed for credit risk evaluation. In the proposed LS-FSVM model, the purpose of incorporating the concepts of fuzzy sets is to add generalization capability and outlier insensitivity, while the least squares method is adopted to reduce the computational complexity. For illustrative purposes, a real-world credit risk dataset is used to test the effectiveness and robustness of the proposed LS-FSVM methodology.

1. Introduction

Credit risk evaluation has been a major area of focus for financial and banking industries due to recent financial crises as well as the Basel III regulations. Since the seminal work of Altman [1] was published, many different techniques such as discriminant analysis [1], logit analysis [2], probit analysis [3], linear programming [4], integer programming [5], k-nearest neighbor (KNN) classifiers [6], and classification trees [7] have widely been applied to credit risk assessment tasks. With the advance of modern computing technology, some artificial intelligence (AI) tools such as artificial neural networks (ANN) [8, 9], genetic algorithms (GAs) [10, 11], self-organizing learning [12], support vector machines (SVMs) [13–18], and some variants of SVMs [19–22] have also been employed for credit risk evaluation. Empirical results have revealed that these AI techniques offer advantages over traditional statistical models and optimization techniques in credit risk evaluation.

According to the literature review, it is easy to find that almost all classification methods can be used for credit risk assessment. However, some hybrid and combined (or ensemble) classifiers, which integrate two or more single classification methods, have shown higher predictability than individual methods. Research on combined or ensemble classifiers is currently flourishing in credit risk evaluation. Recent examples are neural discriminant technique [23], neurofuzzy [16, 24], fuzzy SVM [25], rough set based SVM [26], evolving neural network [27], neural network ensemble [28, 29], support vector machine based multiagent ensemble learning [30], and AI-based fuzzy group decision making (GDM) model [31]. Two recent surveys [32, 33] and one monograph [34] cover credit risk analysis in more detail.

In this study, a new credit classification technique, least squares fuzzy SVM (LS-FSVM), is proposed to discriminate good from bad customers in customer credit evaluation. In the existing studies, the fuzzy SVM (FSVM) proposed by Lin and Wang [35] has been shown to be suitable for customer credit assessment [34]. The main reason is that in credit risk evaluation we usually cannot label a customer as absolutely good one who is sure to repay in time or absolutely bad one who will default certainly, while the FSVM treats every sample as belonging to good and bad classes to some extent. This enables the FSVM to offer a higher generalization capability without losing the merits of insensitivity to outliers. Although the FSVM has good generalization capabilities and outlier insensitivity, computational complexity of the FSVM makes its use rather difficult because the final solution of FSVM is derived from a quadratic programming (QP) problem [35]. To reduce the computational complexity of FSVM, this study applies the least squares method to reduce the computational complexity of FSVM and to formulate a new classification method—least squares FSVM (LS-FSVM). In the proposed LS-FSVM model, equality constraints instead of inequality constraints are used. As a result, the solution is obtained from a set of linear equations, instead of QP presenting in the classical FSVM approach [35], thereby reducing the computational complexity, relative to the FSVM.

From the above descriptions, the main advantage of the proposed LS-FSVM can be summarized with regard to the following two aspects. On the one hand, fuzzification processing can increase the generalization capability and improve the suitability of SVM due to the fact that the same uncertainties can be well treated by fuzzy membership. On the other hand, the least squares method can reduce the computational complexity of FSVM because the solution of least squares FSVM can be obtained from a set of linear equations instead of a QP problem, thus increasing the computational speed of FSVM which is attractive in solving fuzzy information engineering problems. In the existing literature, Tsujinishi and Abe [36] proposed a fuzzy LS-SVMs method to solve the multiclass problems. Regrettably, the performance of the proposed fuzzy LS-SVMs model is inferior to the fuzzy SVMs. On the contrary, the proposed LS-FSVM model in this paper reported the good performance in the two-class problems due to the above features of LS-FSVM model.

The main motivation of this study is to formulate the least squares version of FSVM for binary classification problems and to compare its performance with some typical classification techniques in the area of credit risk evaluation. The rest of this study is organized as follows. Section 2 illustrates the formulation of the LS-FSVM methodology. In Section 3, a real-world credit dataset is used to test the performance of the LS-FSVM to classify different samples. Section 4 concludes the paper.

2. Methodology Formulation

In this section, a brief introduction of SVM classifiers [37] is first presented. Then a fuzzy SVM (FSVM) model [35] is briefly reviewed. Finally, the least squares FSVM (LS-FSVM) model is formulated.

2.1. SVM for Binary Classification (By Vapnik [37]). Given a training dataset $\{x_i, y_i\}$ $(i = 1, \ldots, N)$, where $x_i \in R^N$ is the ith input pattern and y_i is its corresponding observed result, which is a binary variable. In credit risk evaluation models, x_is denote the attributes of customers and y_i is the observed outcome of repayment obligations. If the customer defaults, $y_i = 1$, or else $y_i = -1$. The generic idea of SVM is first to map the input data into a high-dimensional feature space through a mapping function and then to find the optimal separating hyperplane with minimal classification errors. The separating hyperplane can be represented as

$$z(x) = w^T \phi(x) + b = 0, \tag{1}$$

where w is the normal vector of the hyperplane and b is the bias.

Suppose $\phi(\cdot)$ is a nonlinear function that maps the input space into a higher dimensional feature space. If a dataset is linearly separable in this feature space, the classifier is constructed as

$$\begin{aligned} w^T \phi(x_i) + b &\geq 1 \quad \text{if } y_i = 1 \\ w^T \phi(x_i) + b &\leq -1 \quad \text{if } y_i = -1 \end{aligned} \tag{2}$$

which is equivalent to

$$y_i \left(w^T \phi(x_i) + b\right) \geq 1 \quad \text{for } i = 1, \ldots, N. \tag{3}$$

In order to deal with dataset that is not linearly separable, the previous analysis can be generalized by introducing some nonnegative variables $\xi_i \geq 0$, such that (3) can be modified as follows:

$$y_i \left[w^T \phi(x_i) + b\right] \geq 1 - \xi_i \quad \text{for } i = 1, \ldots, N. \tag{4}$$

The nonnegative ξ_i in (4) are those for which data point x_i does not satisfy (3). Thus, the term $\sum_{i=1}^{N} \xi_i$ can be considered as a measure of the amount of misclassification, that is, tolerable misclassification errors.

According to the structural risk minimization principle [37], the risk bound is minimized by solving the following optimization problem:

$$\begin{aligned} &\text{Minimize} \quad \Phi(w, b, \xi_i) = \frac{1}{2} w^T w + C \sum_{i=1}^{N} \xi_i \\ &\text{Subject to:} \quad y_i \left(w^T \phi(x_i) + b\right) = 1 - \xi_i \quad \text{for } i = 1, \ldots, N \\ &\qquad \xi_i \geq 0 \quad \text{for } i = 1, \ldots, N, \end{aligned} \tag{5}$$

where C is a free regularization parameter controlling a tradeoff between margin maximization and tolerable misclassification errors.

Searching the optimal hyperplane in (5) is a quadratic programming (QP) problem. After introducing a set of Lagrangian multipliers α_i and β_i for constraints in (5), the primal problem in (5) is to find out the saddle point of the Lagrangian function; that is,

$$\begin{aligned} \min_{w,b,\xi_i} L(w, b, \xi_i; \alpha_i, \beta_i) = {} & \frac{1}{2} w^T w + C \sum_{i=1}^{N} \xi_i \\ & - \sum_{i=1}^{N} \alpha_i \left[y_i \left(w^T \phi(x_i) + b\right) - 1 + \xi_i \right] \\ & - \sum_{i=1}^{N} \beta_i \xi_i. \end{aligned} \tag{6}$$

Differentiating (6) with w, b, and ξ_i, one obtains

$$\frac{d}{dw}L(w,b,\xi_i;\alpha_i,\beta_i) = w - \sum_{i=1}^{N}\alpha_i y_i \phi(x_i) = 0,$$
$$\frac{d}{db}L(w,b,\xi_i;\alpha_i,\beta_i) = -\sum_{i=1}^{N}\alpha_i y_i = 0, \quad (7)$$
$$\frac{d}{d\xi_i}L(w,b,\xi_i;\alpha_i,\beta_i) = C - \alpha_i - \beta_i = 0.$$

From (7) one has $w = \sum_{i=1}^{N}\alpha_i y_i \phi(x_i)$. The key issue is how to determine the value of α_i. To obtain a solution, the dual problem of the primal problem (6) becomes

$$\text{Maximize} \quad Q(\alpha) = -\frac{1}{2}\sum_{i=1}^{N}\sum_{j=1}^{N}\alpha_i\alpha_j y_i y_j \phi(x_i)^T \phi(x_j) + \sum_{i=1}^{N}\alpha_i \quad (8)$$
$$\text{Subject to:} \quad \sum_{i=1}^{N}\alpha_i y_i = 0, \quad 0 \le \alpha_i \le C, \ i = 1,\ldots,N.$$

Function $\phi(x)$ in (8) is then related to $K(x_i, x_j)$ by imposing

$$\phi(x_i)^T \phi(x_i) = K(x_i, x_j), \quad (9)$$

which is motivated by the Mercer theorem [37]. $K(x_i, x_j)$ is the kernel function in the input space that determines the inner products of the two data points in the feature space. According to the Karush-Kuhn-Tucker (KKT) theorem [38], the KKT conditions are defined as

$$\alpha_i\left[y_i\left(w^T\phi(x)+b\right) - 1 + \xi_i\right] = 0, \quad i = 1,2,\ldots,N, \quad (10)$$
$$(C-\alpha_i)\,\xi_i = 0, \quad i = 1,2,\ldots,N. \quad (11)$$

From this equality, it is deduced that the only nonzero values, α_i, in (10), are those for which constraints in (4) are satisfied with the equality sign. Data points x_i $(i = 1,2,\ldots,s)$, corresponding to $\alpha_i > 0$, are called support vectors (SVs). But there are two types of SVs in a nonseparable case. In the case of $0 < \alpha_i < C$, the corresponding support vector x_i satisfies equalities $y_k[w^T\phi(x_k) + b] = 1$ and $\xi_i = 0$. In the case of $\alpha_i = C$, the corresponding ξ_i is not zero and the corresponding support vector x_i does not satisfy (2), which considered such SVs as misclassification errors. In terms of the above processing, data points x_i $(i = 1,2,\ldots,s)$, corresponding to $\alpha_i = 0$, are classified correctly.

Using the support vectors, the optimal solution for the weight vector in (7) can be given by

$$w = \sum_{i=1}^{N_s}\alpha_i y_i \phi(x_i), \quad (12)$$

where N_s is the number of SVs. Moreover, in the case of $0 < \alpha_i < C$, condition $\xi_i = 0$ applies to (11) in terms of the KKT theorem [38]. Thus, one may determine the optimal bias b by taking any data point in the dataset. However, from the numerical perspective, it is better to take the mean value of b, from such data points in the dataset. Once the optimal parameter p air (w, b) is determined, the decision function of the SVM classifiers can be represented as

$$z(x) = \operatorname{sign}\left(\sum_{i=1}^{N_s}\alpha_i y_i K(x_i, x_j) + b\right). \quad (13)$$

2.2. FSVM (by Lin and Wang [35]). SVM has been proved to be a powerful tool for solving classification problems [37], but it has some inherent limitations. From its formulation discussed above, each training point in the training dataset belongs to either one or the other class. But in many real-world applications, every training sample does not exactly belong to one of the two classes; it may belong to one class to the extent of 80 percent and 20 percent of it may be meaningless. That is to say, there is a membership grade $\{\mu_i\}_{i=1}^{N} \in [0,1]$ associated with each training data point x_i. In this sense, FSVM is an extension of a SVM that takes into consideration the varying significance of the training samples. For FSVM, each training sample is associated with a membership value $\{\mu_i\}_{i=1}^{N} \in [0,1]$. The membership value μ_i reflects the confidence degree of the data points. The higher the value, the higher the confidence degree of its class label. Similar to SVM, the optimization problem of the FSVM [35] is formulated as follows:

$$\text{Minimize} \quad \Psi(w,b,\xi_i,\mu_i) = \frac{1}{2}w^T w + C\sum_{i=1}^{N}\mu_i\xi_i$$
$$\text{Subject to:} \quad y_i\left(w^T\phi(x_i)+b\right) \ge 1 - \xi_i \quad \text{for } i = 1,\ldots,N$$
$$\xi_i \ge 0 \quad \text{for } i = 1,\ldots,N. \quad (14)$$

Similar to SVM, the solution of FSVM is obtained from the above quadratic programming (QP) problem. Note that error term ξ_i is scaled by membership value μ_i. The membership values used to weigh the soft penalty term reflect the relative confidence degree of the training samples during training. Important samples with larger membership values will have more impact in FSVM training than those with smaller values.

Similar to Vapnik's SVM [37], optimization problem of the FSVM can be transformed into the following dual problem:

$$\text{Maximize} \quad W(\alpha) = -\frac{1}{2}\sum_{i=1}^{N}\sum_{j=1}^{N}\alpha_i\alpha_j y_i y_j K(x_i, x_j) + \sum_{i=1}^{N}\alpha_i$$
$$\text{Subject to:} \quad \sum_{i=1}^{N}\alpha_i y_i = 0, \quad 0 \le \alpha_i \le \mu_i C, \ i = 1,\ldots,N. \quad (15)$$

In the same way, KKT conditions are defined as

$$\alpha_i\left[y_i\left(w^T\phi(x)+b\right)-1+\xi_i\right]=0,\quad i=1,2,\ldots,N,$$
$$\left(\mu_iC-\alpha_i\right)\xi_i=0,\quad i=1,2,\ldots,N. \tag{16}$$

Data point x_i, corresponding to $\alpha_i>0$, is called a support vector. There are two types of SVs. The one corresponding to $0<\alpha_i<\mu_iC$ lies on the margin of the hyperplane, and the other corresponding to $\alpha_i=\mu_iC$ is treated as misclassified.

Solving (15) leads to a decision function similar to (13), but with different support vectors and the corresponding weights α_i. An important difference between SVM and FSVM is that data points with the same value of α_i may be indicated as a different type of SVs in FSVM due to membership factor μ_i. Interested readers can refer to [35] for more details.

2.3. Least Squares FSVM. In both SVM and FSVM, the final solution can be described as an issue closely associated with quadratic programming (QP) problem. The main issue with the QP method is that it is a time-consuming process to find the solutions when handling some large-scale real-world application problems. Motivated by Lai et al. [14] and Suykens and Vandewalle [39], the least squares FSVM (LS-FSVM) model is introduced by formulating the following optimization problem:

$$\text{Minimize}\quad \varphi\left(w,b,\xi_i,\mu_i\right)=\frac{1}{2}w^Tw+\frac{C}{2}\sum_{i=1}^{N}\mu_i\xi_i^2$$
$$\text{Subject to:}\quad y_i\left(w^T\phi\left(x_i\right)+b\right)=1-\xi_i\quad \text{for } i=1,\ldots,N. \tag{17}$$

One can define the Lagrangian function as

$$\min_{w,b,\xi_i}L\left(w,b,\xi_i;\alpha_i\right)=\frac{1}{2}w^Tw+\frac{C}{2}\sum_{i=1}^{N}\mu_i\xi_i^2-\sum_{i=1}^{N}\alpha_i\left[y_i\left(w^T\phi\left(x_i\right)+b\right)-1+\xi_i\right], \tag{18}$$

where α_i is the ith Lagrangian multiplier, which can be either positive or negative, due to equality constraints in accordance with KKT conditions [38].

The optimal conditions are obtained by differentiating (18):

$$\frac{d}{dw}L\left(w,b,\xi_i;\alpha_i\right)=w-\sum_{i=1}^{N}\alpha_iy_i\phi\left(x_i\right)=0,$$
$$\frac{d}{db}L\left(w,b,\xi_i;\alpha_i\right)=-\sum_{i=1}^{N}\alpha_iy_i=0,$$
$$\frac{d}{d\xi_i}L\left(w,b,\xi_i;\alpha_i\right)=\mu_iC\xi_i-\alpha_i=0,$$
$$\frac{d}{d\alpha_i}L\left(w,b,\xi_i;\alpha_i\right)=y_i\left[w^T\phi\left(x_i\right)+b\right]-1+\xi_i=0. \tag{19}$$

From (19), one can obtain the following equations:

$$w=\sum_{i=1}^{N}\alpha_iy_i\phi\left(x_i\right),$$
$$\sum_{i=1}^{N}\alpha_iy_i=0,$$
$$\alpha_i=\mu_iC\xi_i,$$
$$y_i\left[w^T\phi\left(x_i\right)+b\right]-1+\xi_i=0. \tag{20}$$

Using a matrix form, optimal conditions in (20) can be expressed by

$$\begin{bmatrix}\mathbf{\Omega} & \mathbf{Y}\\ \mathbf{Y}^T & 0\end{bmatrix}\begin{bmatrix}\alpha\\ b\end{bmatrix}=\begin{bmatrix}\mathbf{1}\\ 0\end{bmatrix}, \tag{21}$$

where $\mathbf{\Omega}$, $\mathbf{Y}$, and $\mathbf{1}$ are (22), (23), and (24), respectively:

$$\mathbf{\Omega}_{ij}=y_iy_j\phi(x_i)^T\phi\left(x_j\right)+\left(\mu_iC\right)^{-1}I \tag{22}$$

$$\mathbf{Y}=\left(y_1,y_2,\ldots,y_N\right)^T, \tag{23}$$

$$\mathbf{1}=(1,1,\ldots,1)^T. \tag{24}$$

From (22), $\mathbf{\Omega}$ is positive definite. Thus, α can be obtained from (21); that is,

$$\alpha=\mathbf{\Omega}^{-1}\left(\mathbf{1}-b\mathbf{Y}\right). \tag{25}$$

Substituting (25) into the second matrix equation in (21), we can obtain

$$b=\frac{\mathbf{Y}^T\mathbf{\Omega}^{-1}\mathbf{1}}{\mathbf{Y}^T\mathbf{\Omega}^{-1}\mathbf{Y}}. \tag{26}$$

Here, since $\mathbf{\Omega}$ is positive definite, $\mathbf{\Omega}^{-1}$ is also positive definite. In addition, since $\mathbf{Y}$ is a nonzero vector, $\mathbf{Y}^T\mathbf{\Omega}^{-1}\mathbf{Y}>0$. Thus, b is always obtained. Substituting (26) into (25), α can be obtained.

Hence, the separating hyperplane of LS-FSVM can be found by solving the linear set of (21)–(24), instead of quadratic programming (QP), thereby reducing the computational complexity, especially for large-scale problems.

The main advantages of the LS-FSVM can be summarized into the following five aspects. First of all, the LS-FSVM requires fewer prior assumptions about the input data than those required in statistical approaches, such as normal distribution and continuity. Second, it can perform nonlinear mapping from an original input space into a high dimensional feature space, in which it constructs a linear discriminant function to replace the nonlinear function in the original input space. This characteristic also solves the dimension disaster problem because its computational complexity is not dependent on the samples' dimension. Third, it attempts to learn the separating hyperplane to maximize the classification margin, thereby implementing structural risk minimization and realizing good generalization capability.

Table 1: Variables of the dataset.

Number	Variables
1	Year of birth
2	Number of children
3	Number of other dependents
4	Is there a home phone
5	Applicant's income
6	Applicant's employment status
7	Spouse's income
8	Residential status
9	Value of home
10	Mortgage balance outstanding
11	Outgoings on mortgage or rent
12	Outgoings on loans
13	Outgoings on hire purchase
14	Outgoings on credit cards

Fourth, a distinct trait of LS-FSVM is that it can further lower computational complexity by transforming a quadratic programming problem into a linear equation set problem. Finally, an important advantage of LS-FSVM is that support values α_i in LS-FSVM are proportional to the membership degree, as well as misclassification errors at the data points, thus making LS-FSVM more suitable for some real-world problems, which is the main difference between the proposed LS-FSVM and the traditional SVM and LS-SVM models. These important characteristics also make LS-FSVM preferable in many practical applications. In the following section, some experiments are presented for verification purpose.

3. Experiment Analysis

In this section, a real-world credit dataset is used to test the performance of LS-FSVM. For comparison purposes, linear regression (LinR) [14], logistic regression (LogR) [2], artificial neural network (ANN) [8, 9], Vapnik's SVM [37], Lin and Wang's FSVM [35], and LS-SVM [39] are also used.

The dataset in this study comes from a financial services company of England, obtained from a CDROM published by Thomas et al. [40]. Each applicant has 14 characteristics or variables, listed in Table 1. The dataset includes detailed information of 1225 applicants, of which 323 are observed as bad customers.

In this experiment, LS-FSVM, FSVM, LS-SVM, and SVM models use RBF kernel for classification. In the ANN model, a three-layer back-propagation neural network with 10 sigmoidal neurons is used in the hidden layer, and one linear neuron is used in the output layer. The network training algorithm is the Levenberg-Marquardt (LM) algorithm. Besides, the learning and momentum rates are set to 0.1 and 0.15, respectively. The accepted average squared error is 0.05, and the training epochs are 1600. The above parameters are obtained by trial-and-error method. The experiment is run by MATLAB 6.1 with statistical toolbox, NNET toolbox, and LS-SVM toolbox. In addition, three evaluation criteria are used to measure the efficiency of classification:

$$\begin{gathered}\text{Type I accuracy}\\ = \frac{\text{number of both observed bad and classified as bad}}{\text{number of observed bad}}\\ \text{Type II accuracy}\\ = \frac{\text{number of both observed good and classified as good}}{\text{number of observed good}}\\ \text{Total accuracy} = \frac{\text{number of correct classification}}{\text{the number of evaluation sample}}.\end{gathered} \quad (27)$$

To show the classification capability of LS-FSVM in distinguishing potentially insolvent customers from good customers, we perform the test with LS-FSVM at the beginning. This testing process includes five steps.

First, the number of observed bad customers is tripled to make their number nearly equal to the number of observed good customers. The main purpose of such processing is to avoid the impact on performance of imbalanced samples. A similar processing method can be found in Wang et al. [25]. Of course, some other imbalanced data processing methods, for example, the information granulation based method [41], can also be used.

Second, the original data is preprocessed to impute the missing data and transform category data. In this study, interpolation method is used to impute the missing data. For category data, a numerical method is used for transformation.

Third, the original dataset is randomly separated into two parts, that is, training samples and testing samples. In this study, 1500 samples are used for training and the remaining 371 samples are used for holdout testing and performance evaluation.

Fourth, membership grades are generated by the linear transformation function proposed by Wang et al. [25], in terms of the initial score obtained by experts' experience and opinions. Of course, some new membership generation methods in [42] can also be adopted.

Finally, the LS-FSVM classifier is trained and accordingly the results can be evaluated. The above five steps are repeated 20 times to confirm the robustness of the proposed method. In this study, the efficiency and robustness of credit risk evaluation using the LS-FSVM model are shown in Table 2.

As can be seen from Table 2, the proposed LS-FSVM model exhibits significant classification capabilities. In the 20 experiments, type I accuracy, type II accuracy, and total accuracy are 81.34%, 93.41%, and 89.21%, respectively, in the mean sense. Furthermore, the standard deviation is rather small, revealing that robustness of the LS-FSVM classifier is good. These results imply that the LS-FSVM model is a promising credit risk evaluation technique.

For further illustration, the classification power of the LS-FSVM is also compared with six other commonly used classifiers: linear regression (LinR) [14], logistics regression

Table 2: Computational results of credit risk evaluation using LS-FSVM.

Experiment number	Type I (%)	Type II (%)	Total (%)
1	81.56	93.81	88.54
2	86.98	95.14	92.53
3	82.02	91.84	88.49
4	79.81	98.36	93.53
5	87.77	94.03	92.24
6	81.56	96.85	92.38
7	79.19	93.05	87.41
8	85.69	92.11	88.86
9	79.27	89.33	87.63
10	82.45	96.58	90.45
11	77.96	93.08	85.06
12	80.61	89.57	85.89
13	81.16	93.41	88.34
14	78.96	89.88	87.56
15	85.56	97.35	94.53
16	70.36	98.13	84.11
17	80.14	92.01	88.68
18	75.22	89.54	86.25
19	86.72	89.61	88.04
20	83.85	94.70	92.64
Mean	81.34	93.41	89.21
Stdev	4.20	2.98	3.02

Table 3: Results of comparisons of different classifiers.

Method	Type I (%)	Type II (%)	Overall (%)	CPU time (s)
LinR	52.87	43.48	50.22	102.45
LogR	60.08	62.29	60.66	112.87
ANN	56.57	78.36	72.24	318.72
SVM	70.13	83.49	77.02	306.33
LS-SVM	79.37	93.27	89.16	138.61
FSVM	80.08	92.86	88.38	335.24
LS-FSVM	81.34	93.41	89.21	149.49

(LogR) [2], artificial neural network (ANN) [8, 9], Vapnik's SVM [37], FSVM [35], and LS-SVM [39]. The results of the comparison are reported in Table 3.

From Table 3, several important results can be observed.

(a) For type I accuracy, LS-FSVM is the best of all the listed approaches, followed by FSVM, LS-SVM, Vapnik's SVM, logistics regression, artificial neural network model, and linear regression model, implying that the LS-FSVM is a very promising technique in credit risk assessment. Particularly, performance of the two fuzzy SVM techniques (Lin and Wang's FSVM [35] and LS-FSVM) is better than other classifiers listed in this study, implying that the fuzzy SVM classifier may be more suitable for credit risk assessment tasks than other deterministic classifiers, such as linear regression (LinR) and logit regression (LogR).

(b) From the viewpoint of type II accuracy, LS-FSVM and LS-SVM outperform the other five models, implying the strong capability of the least squares version of the SVM model in credit risk evaluation. In the meantime, the proposed LS-FSVM model seems to be slightly better than LS-SVM, revealing that the LS-FSVM is a feasible solution to improve the accuracy of credit risk evaluation. Interestingly, performance of the FSVM is slightly worse than that of the LS-SVM. The reasons for this phenomenon are worth exploring further.

(c) According to the total accuracy, performances of the two statistical models (LinR and LogR) are much worse than those of the other five models. The main reason is that the five models can effectively capture the nonlinear patterns hidden in the credit data. As is known, there are many factors that affect customer credit. Usually, the relationships between customer default and these factors are very subtle and complex. Besides some linear relationships, some nonlinear relationships often exist in the credit data. Therefore, nonlinear intelligent models can offer advantage over traditional linear models.

(d) From the perspective of computational time, two traditional classification models (i.e., LinR and LogR) are faster than all the intelligent models due to their simplicity. In all the intelligent models, LS-SVM and LS-FSVM are faster than other intelligent models due to the least squares principle. However, LS-FSVM is slightly slower than LS-SVM because the fuzzification needs some processing time, but LS-FSVM performs faster than the SVM and FSVM, indicating that the proposed LS-FSVM model is a very effective model in credit risk evaluation.

(e) In the five intelligent models, the performance of ANN and SVM models is much worse than the other three intelligent models. The main reason is that the standard ANN and SVM models have their own shortcomings, such as the sensitivity of parameters and outliers, thus affecting their classification performance. For example, ANN models often get trapped into local minima and suffer from overfitting problems, while SVM models occasionally encounter overfitting problem [43]; moreover, some fuzzy information is not handled well by the standard SVM models.

(f) LS-SVM, FSVM, and LS-FSVM models outperform the other four models listed in this study, implying that the variants of SVM have a strong classification potentiality for credit risk evaluation. The possible reason is that the improvement of SVM variants overcomes some inherent limitations of standard SVM proposed by Van Gestel [44], thereby increasing the generalization capability. From a general point of view, LS-FSVM outperforms the other six classifiers from the above three measurements, revealing that

Table 4: McNemar's test for pairwise performance comparison of different models.

Model	LS-SVM	FSVM	SVM	ANN	LogR	LinR
LS-FSVM	0.0000 [1.0000]	0.0480 [0.8262]	15.488 [0.0001]	26.881 [0.0001]	59.274 [0.0001]	92.160 [0.0001]
LS-SVM		0.0120 [0.9131]	14.675 [0.0001]	25.840 [0.0001]	57.840 [0.0001]	90.482 [0.0001]
FSVM			13.133 [0.0003]	23.842 [0.0001]	55.048 [0.0001]	87.197 [0.0001]
SVM				1.5370 [0.2501]	15.584 [0.0001]	36.300 [0.0001]
ANN					7.0840 [0.0078]	22.781 [0.0001]
LogR						4.3630 [0.0367]

the LS-FSVM is used as an effective tool for credit risk evaluation.

In terms of Table 3 and the three measurements, it is easy to judge which model is the best and which model is the worst. However, it is unclear what the differences between good models and bad ones are. For this purpose, McNemar's test [45] is conducted to examine whether the proposed LS-FSVM classifier significantly outperforms the other six classifiers listed in this study.

As a nonparametric test for the two related samples, McNemar's test is particularly useful for before-after measurement of the same subjects [46]. Taking the total accuracy results from Table 3, Table 4 shows the results of the McNemar's test for the credit dataset to statistically compare the performance in respect of testing data among the seven classifiers. It should be noted that the results listed in Table 4 are the Chi-squared values, and P values are in brackets.

According to the results reported in Table 4, some important conclusions can be drawn in terms of McNemar's statistical test.

(1) The proposed LS-FSVM classifier outperforms the standard SVM, ANN, logit regression (LogR), and linear regression (LinR) models at 1% statistical significance level. However, the proposed LS-FSVM model does not significantly outperform the LS-SVM model and the FSVM model. These results are consistent with those of Table 3.

(2) Similar to the LS-FSVM model, LS-SVM and FSVM models outperform the other four individual models (i.e., individual SVM, ANN, LogR, and LinR models) at 1% significance level. But the McNemar's test does not conclude that the LS-SVM model performs better than the FSVM model.

(3) For SVM and ANN models, we can find that these two models perform much better than the two statistical models (i.e., LogR and LinR models) at 1% significance level. Interestingly, the SVM model does not outperform the ANN model at 10% significance level, although many applications have reported that the performance of the SVM was much better than that of ANN. The possible reason lies in data samples used in this study.

(4) Comparing with LogR and LinR models, it is easy to find that the LogR model performs better than the LinR model at 5% significance level. All findings are consistent with results reported in Table 3.

In summary, according to the above experimental results and statistical testing, it is easy to conclude that the LS-FSVM model can significantly outperform some standard intelligent models (e.g., SVM and ANN) and some statistical models (e.g., LogR and LinR), revealing that the LS-FSVM can also be used as a competitive solution to credit risk evaluation.

4. Conclusions

In this paper, a powerful classification method—least squares fuzzy support vector machines (LS-FSVM)—is proposed to evaluate credit risks. Through the least squares method, a quadratic programming (QP) problem of SVM can be transformed into a set of linear equations successfully, thereby reducing the computational complexity. Furthermore, the fuzzification processing in the proposed LS-FSVM model adds generalization capability and insensitivity to outliers. Experiments with real-world dataset have produced good classification results and fast computational efficiency and have demonstrated that the proposed LS-FSVM model can provide a feasible alternative to credit risk assessment. Besides the credit risk evaluation problem, the proposed LS-FSVM model can also be extended to other applications, such as consumer credit rating and corporate failure prediction problems, which will be investigated in the future research.

Conflict of Interests

The author declares that there is no conflict of interests regarding the publication of this paper.

Acknowledgments

The author would like to express his sincere appreciation to two independent referees in making valuable comments and suggestions to the paper. His comments have improved the quality of the paper immensely. This work is partially supported by Grants from the National Science Fund for Distinguished Young Scholars (NSFC no. 71025005), the National Natural Science Foundation of China (NSFC nos. 90924024 and 91224001), Hangzhou Normal University, and the Fundamental Research Funds for the Central Universities in BUCT.

References

[1] E. I. Altman, "Financial ratios, discriminant analysis and the prediction of corporate bankruptcy," *Journal of Finance*, vol. 23, pp. 89–609, 1968.

[2] J. C. Wiginton, "A note on the comparison of logit and discriminant models of consumer credit behaviour," *Journal of Financial Quantitative Analysis*, vol. 15, pp. 757–770, 1980.

[3] B. J. Grablowsky and W. K. Talley, "Probit and discriminant functions for classifying credit applicants: a comparison," *Journal of Economic Business*, vol. 33, pp. 254–261, 1981.

[4] F. Glover, "Improved linear programming models for discriminant analysis," *Decision Science*, vol. 21, pp. 771–785, 1990.

[5] O. L. Mangasarian, "Linear and nonlinear separation of patterns by linear programming," *Operations Research*, vol. 13, pp. 444–452, 1965.

[6] W. E. Henley and D. J. Hand, "A k-nearest-neighbour classifier for assessing consumer credit risk," *Journal of the Royal Statistical Society Series D: The Statistician*, vol. 45, no. 1, pp. 77–95, 1996.

[7] P. Makowski, "Credit scoring branches out," *Credit World*, vol. 75, pp. 30–37, 1985.

[8] K. K. Lai, L. Yu, S. Y. Wang, and L. G. Zhou, "Neural network meta-learning for credit scoring," in *Intelligent Computing*, vol. 4113 of *Lecture Notes in Computer Science*, pp. 403–408, 2006.

[9] R. Malhotra and D. K. Malhotra, "Evaluating consumer loans using neural networks," *Omega*, vol. 31, no. 2, pp. 83–96, 2003.

[10] M.-C. Chen and S.-H. Huang, "Credit scoring and rejected instances reassigning through evolutionary computation techniques," *Expert Systems with Applications*, vol. 24, no. 4, pp. 433–441, 2003.

[11] F. Varetto, "Genetic algorithms applications in the analysis of insolvency risk," *Journal of Banking and Finance*, vol. 22, no. 10-11, pp. 1421–1439, 1998.

[12] Z. Zhu, H. He, J. A. Starzyk, and C. Tseng, "Self-organizing learning array and its application to economic and financial problems," *Information Sciences*, vol. 177, no. 5, pp. 1180–1192, 2007.

[13] Z. Huang, H. Chen, C.-J. Hsu, W.-H. Chen, and S. Wu, "Credit rating analysis with support vector machines and neural networks: A Market Comparative Study," *Decision Support Systems*, vol. 37, no. 4, pp. 543–558, 2004.

[14] K. K. Lai, L. Yu, L. G. Zhou, and S. Y. Wang, "Credit risk evaluation with least square support vector machine," in *Rough Sets and Knowledge Technology*, vol. 4062 of *Lecture Notes in Artificial Intelligence*, pp. 490–495, 2006.

[15] K. K. Lai, L. Yu, W. Huang, and S. Y. Wang, "A novel support vector machine metamodel for business risk identification," in *PRICAI 2006: Trends in Artificial Intelligence*, vol. 4099 of *Lecture Notes in Artificial Intelligence*, pp. 480–484, 2006.

[16] R. Malhotra and D. K. Malhotra, "Differentiating between good credits and bad credits using neuro-fuzzy systems," *European Journal of Operational Research*, vol. 136, no. 1, pp. 190–211, 2002.

[17] L. Zhou, K. K. Lai, and L. Yu, "Least squares support vector machines ensemble models for credit scoring," *Expert Systems with Applications*, vol. 37, no. 1, pp. 127–133, 2010.

[18] L. Zhou, K. K. Lai, and L. Yu, "Credit scoring using support vector machines with direct search for parameters selection," *Soft Computing*, vol. 13, no. 2, pp. 149–155, 2009.

[19] L. Yu and X. Yao, "A total least squares proximal support vector classifier for credit risk evaluation," *Soft Computing*, vol. 17, no. 4, pp. 643–650, 2013.

[20] L. Yu, X. Yao, S. Wang, and K. K. Lai, "Credit risk evaluation using a weighted least squares SVM classifier with design of experiment for parameter selection," *Expert Systems with Applications*, vol. 38, no. 12, pp. 15392–15399, 2011.

[21] L. Yu, S. Wang, and J. Cao, "A modified least squares support vector machine classifier with application to credit risk analysis," *International Journal of Information Technology and Decision Making*, vol. 8, no. 4, pp. 697–710, 2009.

[22] L. Yu, S. Wang, and K. K. Lai, "Credit risk evaluation using a c-variable least squares support vector classification model," *Communications in Computer and Information Science*, vol. 35, pp. 573–579, 2009.

[23] T.-S. Lee, C.-C. Chiu, C.-J. Lu, and I.-F. Chen, "Credit scoring using the hybrid neural discriminant technique," *Expert Systems with Applications*, vol. 23, no. 3, pp. 245–254, 2002.

[24] S. Piramuthu, "Financial credit-risk evaluation with neural and neurofuzzy systems," *European Journal of Operational Research*, vol. 112, no. 2, pp. 310–321, 1999.

[25] Y. Wang, S. Wang, and K. K. Lai, "A new fuzzy support vector machine to evaluate credit risk," *IEEE Transactions on Fuzzy Systems*, vol. 13, no. 6, pp. 820–831, 2005.

[26] L. Yu, S. Wang, F. Wen, K. K. Lai, and S. He, "Designing a hybrid intelligent mining system for credit risk evaluation," *Journal of Systems Science & Complexity*, vol. 21, no. 4, pp. 527–539, 2008.

[27] R. Smalz and M. Conrad, "Combining evolution with credit apportionment: a new learning algorithm for neural nets," *Neural Networks*, vol. 7, no. 2, pp. 341–351, 1994.

[28] K. K. Lai, L. Yu, S. Y. Wang, and L. G. Zhou, "Credit risk analysis using a reliability-based neural network ensemble model," in *Proceedings of the International Conference on Artificial Neural Networks (ICANN '06)*, vol. 4132 of *Lecture Notes in Computer Science*, pp. 682–690, 2006.

[29] L. Yu, S. Wang, and K. K. Lai, "Credit risk assessment with a multistage neural network ensemble learning approach," *Expert Systems with Applications*, vol. 34, no. 2, pp. 1434–1444, 2008.

[30] L. Yu, W. Yue, S. Wang, and K. K. Lai, "Support vector machine based multiagent ensemble learning for credit risk evaluation," *Expert Systems with Applications*, vol. 37, no. 2, pp. 1351–1360, 2010.

[31] L. Yu, S. Wang, and K. K. Lai, "An intelligent-agent-based fuzzy group decision making model for financial multicriteria decision support: the case of credit scoring," *European Journal of Operational Research*, vol. 195, no. 3, pp. 942–959, 2009.

[32] L. C. Thomas, "A survey of credit and behavioural scoring: forecasting financial risk of lending to consumers," *International Journal of Forecasting*, vol. 16, no. 2, pp. 149–172, 2000.

[33] L. C. Thomas, R. W. Oliver, and D. J. Hand, "A survey of the issues in consumer credit modelling research," *Journal of the Operational Research Society*, vol. 56, no. 9, pp. 1006–1015, 2005.

[34] L. Yu, S. Y. Wang, K. K. Lai, and L. G. Zhou, *Bio-Inspired Credit Risk Analysis—Computational Intelligence with Support Vector Machines*, Springer, Berlin, Germany, 2008.

[35] C.-F. Lin and S.-D. Wang, "Fuzzy support vector machines," *IEEE Transactions on Neural Networks*, vol. 13, no. 2, pp. 464–471, 2002.

[36] D. Tsujinishi and S. Abe, "Fuzzy least squares support vector machines for multiclass problems," *Neural Networks*, vol. 16, no. 5-6, pp. 785–792, 2003.

[37] V. N. Vapnik, *The Nature of Statistical Learning Theory*, Springer, New York, NY, USA, 1995.

[38] R. Fletcher, *Practical Methods of Optimization*, A Wiley-Interscience Publication, John Wiley & Sons, 2nd edition, 1987.

[39] J. A. K. Suykens and J. Vandewalle, "Least squares support vector machine classifiers," *Neural Processing Letters*, vol. 9, no. 3, pp. 293–300, 1999.

[40] L. C. Thomas, D. B. Edelman, and J. N. Crook, *Credit Scoring and Its Applications*, Society of Industrial and Applied Mathematics, Philadelphia, Pa, USA, 2002.

[41] M.-C. Chen, L.-S. Chen, C.-C. Hsu, and W.-R. Zeng, "An information granulation based data mining approach for classifying imbalanced data," *Information Sciences*, vol. 178, no. 16, pp. 3214–3227, 2008.

[42] A. Celikyilmaz and I. B. Turksen, "Fuzzy functions with support vector machines," *Information Sciences*, vol. 177, no. 23, pp. 5163–5177, 2007.

[43] L. Cao and F. E. H. Tay, "Financial forecasting using Support Vector Machines," *Neural Computing and Applications*, vol. 10, no. 2, pp. 184–192, 2001.

[44] T. Van Gestel, B. Baesens, J. Garcia, and P. Van Dijcke, "A support vector machine approach to credit scoring," *Bank en Financiewezen*, vol. 2, pp. 73–82, 2003.

[45] Q. McNemar, "Note on the sampling error of the difference between correlated proportions or percentages," *Psychometrika*, vol. 12, no. 2, pp. 153–157, 1947.

[46] D. R. Cooper and C. W. Emory, *Business Research Methods*, Irwin, Chicago, Ill, USA, 1995.

Hindawi Publishing Corporation
Discrete Dynamics in Nature and Society
Volume 2014, Article ID 386875, 12 pages
http://dx.doi.org/10.1155/2014/386875

Research Article

Measuring Contagion of Subprime Crisis Based on MVMQ-CAViaR Method

Wuyi Ye, Kebing Luo, and Shaofu Du

School of Management, University of Science and Technology of China, Hefei 230026, China

Correspondence should be addressed to Shaofu Du; dsoft@ustc.edu.cn

Received 13 March 2014; Accepted 8 May 2014; Published 9 June 2014

Academic Editor: Fenghua Wen

The analysis of financial contagion is a topical issue in international finance and portfolio management. In this paper, we investigate whether the global financial crisis originating from American subprime crisis spreads to China, Japan, UK, France, and Germany. Firstly, multivariate conditional autoregressive value at risk (MV-CAViaR) models are applied to the whole sample to analyze the variation of market risk among these countries. By dividing the sampling period into three important subperiods (precrisis period, crisis period, and recovery period), we examine the changes of the dependence structure of risk during each period. Comparing with the situations in precrisis period, if the estimated coefficients become significant or market risk increases during the crisis, it implies the existence of contagion from the angle of coefficient significance or risk. The findings show that the concerned coefficients are significant or the market risks of the tested countries increase during the crisis except for China. The results imply that there is contagion from the US to all other countries, except for China. Furthermore, the changes of the market risk are found to be consistent with market events and media reports during that period.

1. Introduction

An observation that stock markets behave very similarly across different continents and countries during the global financial crisis of 2008-2009 casts serious doubts on the question whether financial contagion exists and, if so, to what extent markets covary during the turmoil. The financial contagion has vital impacts on the performance of international portfolios and risk management. Investors are interested in international diversification of risks. But, if the financial markets are more closely linked during the crisis, the opportunities for international diversification are decreased. For regulators of financial markets, it is particularly important to comprehend such linkage increase among world financial markets. As a result, the topic issue has attracted a considerable amount of interest among academic researchers.

One may wonder about the existence of a contagion phenomenon across different financial markets worldwide. For this purpose, it is necessary to define the concept of contagion, despite the fact that several advanced results remain hard and complex to identify contagion. In this paper, we draw lessons from the definition of contagion introduced by Forbes and Rigobon [1], who defined it as a significant increase in the market comovement after a shock happened in a country. It suggests that the financial contagion does not occur if two markets show a high degree of comovement during both tranquil and turbulent phases. In this paper, we say that there exists financial contagion only if one of the two following conditions is satisfied. (i) The interested coefficients are statistically significant during the crisis but remain insignificant during the precrisis period. (ii) The interested coefficients are significant during both precrisis period and the crisis, but compared with precrisis period, the market risk increases during the crisis.

The literature, which focuses on changes of financial market dependence in a crisis period against a tranquil period, has grown substantially in recent years and is generally related to the terminology "contagion." Baig and Goldfajn [2] and Forbes and Rigobon [1] use a linear dependence measure. Bae et al. [3] apply a multinomial logit model to estimate coexceedances. Baur [4] proposes an alternative quantile regression framework to decompose the dependence into the degree and structure of dependence. But, the estimated quantile is static and not dynamically varying with time at some given level. To detect the dynamic characteristics of financial contagion, following from Engle and Manganelli [5] and White et al. [6, 7], we use multivariate conditional autoregressive value at risk (MV-CAViaR) framework to estimate two dynamic conditional autoregressive quantile models simultaneously. We show that MV-CAViaR model provides a flexible modeling and estimation method to identify the financial contagion between two countries.

We contribute to the existing literature in two major ways. Firstly, compared with single quantile regression model, which can only study the contagious relation from one country to another, MV-CAViaR model can study the interactional contagion between two markets in dynamic settings from the angle of risk with the help of VaR. Moreover, considering the information of two countries simultaneously, we apply MV-CAViaR model to study financial contagion between the origin of global financial crisis (the US market) and major mature equity markets, namely, Japan, UK, France, Germany, and one of the biggest emerging markets (China). In this way, we can investigate not only the existence of contagion but also the changes of risk in two markets. In order to capture the variation of risk for the whole sampling period, MV-CAViaR models are employed to the overall sample between the US and other countries. We find that there is a high increase in value at risk for all sampling countries during the crisis period.

Secondly, our research accounts for the financial contagion and changes of risk by using a comprehensive time series spanning three periods: before, during, and after the crisis. In this way, we increase the efficiency of our estimation and enable a comparison of different phases by dividing the whole sample period into three periods (i.e., precrisis, crisis, and recovery periods). Then, we consider estimation of these models for three important subsamples, just as Mollick and Assefa [8] did. The first runs from January 2006 to December 2007 which is referred to as the precrisis period. The second, namely, the crisis period, starts at the beginning of 2008, right after NBER identified December of 2007 as the start of the major recent financial crisis in the US. (The National Bureau of Economic Research (NBER) is an American private nonprofit research organization "committed to undertaking and disseminating unbiased economic research among public policymakers, business professionals, and the academic community." The NBER is well known for providing start and end dates for recessions in the United States. NBER is the largest economics research organization in the United States. Many of the American winners of the Nobel Memorial Prize in Economic Sciences were NBER research associates. Many of the chairmen of the Council of Economic Advisers have also been NBER research associates, including the former NBER president and Harvard Professor, Martin Feldstein.) The US recession officially ended in June 2009, although economic growth has since been sluggish. The third subsample stretching from July 2009 to July 2013 refers to the US economy entering a recovery phase and we call it recovery period. By comparing the coefficient significance and the changes of risk during the three different phases, we judge whether there exists financial contagion from the US to the tested countries during the crisis and the economics enter the phase of recovery. The findings show that the American subprime crisis spread to Japan, UK, France, and Germany and increased their market risk during the crisis in contrast to precrisis period. But we have not found statistically significant evidence that there is financial contagion from America to China. During the recovery period, the comovement between the US and France exists, but from the perspective of risk the market risks in two countries become small in comparison with the risk in crisis period. For UK, there is no contagion phenomenon during the recovery period. However, there are risk spillovers from both Japan and Germany to the US due to market conditions of the day.

The rest of the paper is organized as follows. Section 2 provides the literature review about financial contagion. In Section 3, the multivariate multiquantiles CAViaR (MVMQ-CAViaR) framework and its estimation are detailed. Then, in Section 4, we perform empirical analysis to examine the possible financial contagion between the US and five tested countries. Finally, Section 5 concludes.

2. Literature Review

A rapid increase in global economic integration has accelerated financial integration, spillovers, and contagion in equity markets of different countries. Current studies on financial contagion offer many methods to measure the propagation of international shocks across countries. Investigating the financial transmission, Kaminsky et al. [9] categorize the theories into three groups: contagion caused by herding behavior (e.g., Banerjee [10], Calvo and Mendoza [11]); contagion resulting from trade linkages (e.g., Lahiri and Végh [12], Gerlach and Smets [13]); and contagion accelerated by financial links (e.g., Kodres and Pritsker [14], Fratzscher [15]). There are many approaches proposed to detect and identify the financial contagion. Next, we review the main approaches about the studies on financial contagion through financial linkages.

Early work on detecting contagion is obtained mainly by comparing the traditional constant Pearson correlation coefficient between two countries in times of relative calm with that in times of unusually high volatility (see, for instance, Reinhart and Calvo [16], Bordo and Murshid [17], and Forbes and Rigobon [18]). However, Corsetti et al. [19] show how these results are flawed in the presence of heteroscedasticity. The findings show that an increase in the variance of two variables will cause an increase in the correlation coefficient even if the propagation mechanism is unaltered. Moreover, Pearson correlation coefficient is a static linear correlation measure and cannot measure the nonlinear relation. Therefore, an increase in the correlation coefficient is not necessarily a proof of contagion. Rigobon [20] introduces the DCC test, which seems to provide a way to test parameter stability in the models with simultaneous heteroscedasticity and endogeneity problems. Recently, there are many literatures using DCC model to study financial contagion (see, e.g., Chiang et al. [21], Naoui et al. [22], Celik [23], and Dimitriou et al. [24]). In addition, there are numerous traditional econometric models to investigate the dependence or change of dependence. These include the volatility spillovers methods based on ARCH and GARCH models [25–27], extreme value theory (EVT) method [28], probit/logit models [29, 30], Markov switching model [31–33], the factor model [34], the copula approach [35–39], and wavelet analysis [40, 41]. But, none of these studies analyze the financial contagion from the angle of risk with the help of VaR directly.

More recently, quantile regression methods have gained popularity in economics and finance fields due to their appealing features in describing market risk directly. The quantile regression model was firstly proposed by Koenker and Bassett in 1978. Baur and Schulze [42] apply the quantile regression framework to examine the occurrences and degrees of coexceedances, concentrating on Hong Kong, Thailand, and Malaysia as the origin countries of the Asian crisis, and test the contagion effects on the US, Latin America, Europe, and other Asian countries. Chuang et al. [43] and Lee and Li [44] apply quantile regression to model the dependence of financial variables, for example, trading volume and return volatility. Engle and Manganelli [5] develop conditional autoregressive value at risk (CAViaR) model, a class of models suitable for estimating conditional quantile in dynamic settings. Engle and Manganelli apply the approach to estimate the market risk. White et al. [6] extend CAViaR model to permit joint modeling of multiple quantiles, that is, Multi-Quantile (MQ) CAViaR. They apply MQ-CAViaR model to estimate measures of conditional skewness and kurtosis defined in terms of conditional quantiles. Furthermore, White et al. [7] extend MQ-CAViaR model to a multivariate version of MQ-CAViaR model, called MVMQ-CAViaR model. The proposed framework can simultaneously accommodate models with multiple random variables, multiple confidence levels, and multiple lags of the associated quantiles. They estimated a simple version of the model using different market returns data and then constructed impulse response functions to study how financial institution specific and system wide shocks are absorbed by the system. In this paper, MV-CAViaR model is employed to research whether there was financial contagion from the US to the tested countries or not from the angle of the coefficients significance and the variation of risk before and after the American subprime crisis in dynamic settings. Moreover, by comparing the situation in the recovery period with that in the crisis, we explain how the tested countries affect American economic recovery. So far, we find there is no literature investigating the financial contagion with the model from the perspective of coefficient significance or risk.

3. Methodology

In this section, we firstly introduce MVMQ-CAViaR model following from White et al. [7]. The framework of the model can be conveniently thought of as a vector autoregressive extension to quantile models. Secondly, we present the asymmetric Laplace distribution (see Yu and Zhang [45] for details), which is the only distribution associated with quantile regression estimation. Then, we outline the quasimaximum likelihood method for estimating MVMQ-CAViaR model parameters.

3.1. MVMQ-CAViaR Model. It is assumed that $\{(Y_t', X_t') : t = 0, \pm 1, \pm 2, \ldots\}$ is stationary and ergodic stochastic process on the complete probability space $(\Omega, \mathcal{F}, P)$, where Y_t is a finitely $n \times 1$ dimensioned vector and X_t is a countably dimensioned vector whose first element is one.

Let $\mathcal{F}_{t-1}$ be the σ-algebra generated by $\{(Y_{t-1}', X_{t-1}'), (Y_{t-2}', X_{t-2}'), \ldots\}$, that is,

$$\mathcal{F}_{t-1} \equiv \sigma\left(\left\{\left(Y_{t-1}', X_{t-1}'\right), \left(Y_{t-2}', X_{t-2}'\right), \ldots\right\}\right). \quad (1)$$

For $i = 1, 2, \ldots, n$, define $F_{i,t}(y) = P(Y_{i,t} < y \mid \mathcal{F}_{t-1})$ as the cumulative distribution function (CDF) of Y_{it} conditional on $\mathcal{F}_{t-1}$.

Let $\theta_{i,j}$ belong to $(0, 1)$ for $i = 1, 2, \ldots, n$; $j = 1, 2, \ldots, p_i$. The $\theta_{i,j}$th quantile of Y_t conditional on $\mathcal{F}_{t-1}$, denoted by $q_{i,j,t}$, is

$$q_{i,j,t} = \inf\left\{y : F_{i,t}(y) \geq \theta_{i,j} \mid \mathcal{F}_{t-1}\right\}. \quad (2)$$

For simplicity, we set $q_t = (q_{1,t}', q_{2,t}', \ldots, q_{n,t}')'$ with $q_{i,t} = (q_{i,1,t}, q_{i,2,t}, \ldots, q_{i,p_i,t})'$. For the given finite integers m and k, there exist a stationary ergodic sequence of random $k \times 1$ vectors $\{\Psi_t, t = 1, 2, \ldots, T\}$ with Ψ_t measurable $\mathcal{F}_{t-1}$ and real vectors $\beta = c(\beta_{i,j,1}, \beta_{i,j,2}, \ldots, \beta_{i,j,k})'$ and $\gamma_{i,j,\tau} = (\gamma_{i,j,\tau,1}, \gamma_{i,j,\tau,2}, \ldots, \gamma_{i,j,\tau,n})$, where each $\gamma_{i,j,\tau,k}$ is $p_i \times 1$ vector, such that for $i = 1, 2, \ldots, n$; $j = 1, 2, \ldots, p_i$ and all t,

$$q_{i,j,t} = \Psi_t' \beta_{i,j} + \sum_{\tau=1}^{m} q_{t-\tau}' \gamma_{i,j,\tau}. \quad (3)$$

The structure of (3) is a multivariate multiquantiles conditional autoregressive value at risk (MVMQ-CAViaR) model introduced by White et al. [7], itself a multivariate version of the MQ-CAViaR process of White et al. [6], which is a multiquantiles version of the CAViaR process proposed by Engle and Manganelli [5]. Under suitable restrictions on the $\gamma_{i,j,\tau}$, we get the following three situations as special cases: (1) univariate MQ-CAViaR process of each element of Y_t, (2) single quantile CAViaR process of each element of Y_t, and (3) multivariate CAViaR process in which a single quantile of each element of Y_t is dynamically related to single quantiles of the other elements of Y_t or lags of them.

It is worthwhile to note that, for MVMQ-CAViaR, the number of relevant lags can differ across the elements of Y_t and conditional quantiles. In fact, it is possible that, for given i and j, elements of $\gamma_{i,j,\tau}$ may be zero for the values of τ greater than a certain integer. For the simplicity of notation, m is not denoted by $m(i, j)$. In addition, the finitely dimensioned random vectors Ψ_t may include Y_t or the lagged values of Y_t, as well as measurable functions of X_t and lagged X_t. In special cases, Ψ_t may contain Stinchcombe and White [46] GCR transformations, as discussed in White [47].

For the analytical convenience, in terms of a particular quantile, for example, $\theta_{i,j}$, the coefficients to be estimated are $\beta_{i,j}$ and $\gamma_{i,j} = (\gamma_{i,j,1}', \gamma_{i,j,2}', \ldots, \gamma_{i,j,m}')$. Let $\alpha_{ij} = (\beta_{i,j}', \gamma_{i,j}')$ and write $\alpha = (\alpha_{11}', \alpha_{12}', \ldots, \alpha_{1p_i}', \ldots, \alpha_{n1}', \alpha_{n2}', \ldots, \alpha_{np_n}')$, an $l \times 1$ vector, where $l = \sum_{i=1}^{n} p_i(k + np_i m)$. α is called the MVMQ-CAViaR coefficient vector.

To illustrate the usefulness of the models outlined above, we give an example specifying the model as follows:

$$q_{1,t} = c_1 + a_{11}\left|Y_{1,t-1}\right| + a_{12}\left|Y_{2,t-1}\right| + b_{11}q_{1,t-1} + b_{12}q_{2,t-1},$$
$$q_{2,t} = c_2 + a_{21}\left|Y_{1,t-1}\right| + a_{22}\left|Y_{2,t-1}\right| + b_{21}q_{1,t-1} + b_{22}q_{2,t-1}. \quad (4)$$

Since $P\left(Y_{i,t} \le -\mathrm{VaR}_{it} \mid \mathcal{F}_{t-1}\right) = \theta$, $-\mathrm{VaR}_{it}$ is the θth quantile of Y_{it} conditional on $\mathcal{F}_{t-1}$. Then, we get

$$\begin{aligned}\mathrm{VaR}_{1,t} &= c_1^* + a_{11}^*\left|Y_{1,t-1}\right| + a_{12}^*\left|Y_{2,t-1}\right| \\ &\quad + b_{11}\mathrm{VaR}_{1,t-1} + b_{12}\mathrm{VaR}_{2,t-1}, \\ \mathrm{VaR}_{2,t} &= c_2^* + a_{21}^*\left|Y_{1,t-1}\right| + a_{22}^*\left|Y_{2,t-1}\right| \\ &\quad + b_{21}\mathrm{VaR}_{1,t-1} + b_{22}\mathrm{VaR}_{2,t-1},\end{aligned} \quad (5)$$

where $c_i^* = -c_i$, $\alpha_{ij}^* = -\alpha_{ij}$, $i = 1, 2$; $j = 1, 2$.

Hence, the financial contagion can be detected from the perspective of the risk transmission. The financial contagion between the two financial markets is measured by the off-diagonal coefficients, b_{12} and b_{21}, and the hypothesis of no contagion can be tested by testing $H_0 : b_{12} = b_{21} = 0$. The direction of the contagion can be captured by inspecting these two coefficients. For example, if $b_{12} = 0$ and $b_{21} \neq 0$, then the direction of financial contagion is from country 1 to country 2, not the other way around. At the same time, the degree of the contagion can be measured by the magnitude of b_{12} and b_{21}. The larger b_{12} or b_{21} are, the more serious contagion between two markets is. In a similar way, the financial contagion can also be captured from the point of risk spillovers. We can investigate the existence of financial contagion by testing the significance of coefficients, $H_0 : a_{12}^* = a_{21}^* = 0$. The directions of contagion can be determined from the hypothesis test, for example, $H_0 : a_{12}^* = 0$ and $a_{21}^* \neq 0$, which means there is contagion from country 1 to country 2 and no contagion from country 2 to county 1. Similarly, the dependence structure can be analyzed from the sign and magnitude of the coefficients a_{12}^* and a_{21}^*. The larger coefficients a_{12}^* and a_{21}^* are, the larger spillover risks are, which implies that the smaller coefficients a_{12} and a_{21} are, the larger spillover risks are.

3.2. The QMLE Estimate of MV-CAViaR Model. A possible parametric link between the minimization of the sum of absolute deviate for the estimation of quantile regression and the maximum theory is given by the asymmetric Laplace distribution. The asymmetric Laplace distribution presented here is only a kind of the asymmetric Laplace distributions. It is useful for fitting quantile or quantile regression as well as for data analysis in general; see Yu and Moyeed [48], Yu and Zhang [45] for details.

We say that a random variable X is distributed as ALD with parameters μ, σ, and p, denoted by $X \sim \mathrm{ALD}(\mu, \sigma, \tau)$, if it has the following probability density function (PDF):

$$f\left(x; \mu, \sigma, p\right) = \frac{p\left(1-p\right)}{\sigma}\exp\left\{-\frac{x-\mu}{\sigma}\left[p - I_{(x\le\mu)}\right]\right\}, \quad (6)$$

where $-\infty < \mu < +\infty$ is the location parameter, $0 < p < 1$ is the skew parameter, $\sigma > 0$ is the scale parameter, and $I_{(\cdot)}$ is the indication function, which takes the value one if the argument is true and zero otherwise.

Following from Koenker and Machado [49], we assume that the error terms in quantile regression are distributed as asymmetric Laplace distribution in this paper, that is, $Y_{i,t} - q_{i,j,t} \sim \mathrm{ALD}(0, \sigma, \theta_{ij})$. Then, we can estimate the unknown parameters by the method of quasimaximum likelihood. The likelihood function for T independent observations is

$$L\left(\alpha; Y_1, Y_2\right) \propto \sigma^{-1}\exp\left\{\sum_{t=1}^{T}\sum_{i=1}^{n}\sum_{j=1}^{p_i}\frac{\rho_{\theta_{ij}(Y_{i,t}-q_{i,j,t})}}{\sigma}\right\}, \quad (7)$$

where $\rho_\theta = e\Psi_\theta(e)$ is the standard check function (see Koenker and Basset [50]), defined by the usual quantile step function, $\Psi_\theta(e) = \theta - I_{(e\le 0)}$. Because $Y_{i,t} - q_{i,j,t}$ are not necessarily distributed as this distribution, we call it quasimaximum likelihood estimator rather than maximum likelihood estimator as described in White et al. [7]. If we consider σ as a nuisance parameter, the quasimaximum likelihood estimator $\widehat{\alpha}$ is equivalent to the solution to the following optimization problem:

$$\widehat{\alpha} = \underset{\alpha\in\mathbb{R}}{\operatorname{argmin}}\sum_{t=1}^{T}\sum_{i=1}^{n}\sum_{j=1}^{p_i}\rho_{\theta_{ij}(Y_{it}-q_{i,j,t})}. \quad (8)$$

Thus, ALD proves to be useful as unifying bridge between the likelihood and inference for QR estimation. For example, Koenker and Machado [49] introduced a goodness-of-fit process for QR and related inference process, and they also considered the likelihood ratio statistic under the parametric assumption of a Laplacean distribution for the error term. For Bayesian approach, see Yu and Moyeed [48], among others. The consistency and asymptotic normality for the estimated coefficients $\widehat{\alpha}$ are derived and detailed in White et al. [7]. Following this, we can get the significance test of coefficients.

4. Data and Empirical Analysis

4.1. Data. Our empirical study of 2008-2009 financial contagion focuses on equity market indices of six countries (S&P 500 (US), CSI300 (China), Nikkei 225 (Japan), FTSE-100 (UK), CAC-40 (France), and DAX (Germany)) from January 1, 2006, to July 25, 2013, which include the episode of the financial crisis of 2008-2009. We call China, Japan, UK, France, and Germany tested countries because their market risk is subject to the impact of the S&P 500 index return in US. The daily data were downloaded from data stream. Equity index risk during the subprime crisis is analyzed based on the methodology outlined above. Daily returns are calculated as

$$r_t = 100 \times \left(\ln\left(p_t\right) - \ln\left(p_{t-1}\right)\right). \quad (9)$$

In addition, because the US market opens later than the other countries, in order to analyze the impact of S&P 500 index returns on the tested markets, we use the returns on day $t-1$ for the S&P 500 index and the returns on day t for the tested markets when calculating Kendall tau and Pearson correlation coefficients. Meanwhile, it should be noted that

Table 1: Summary statistics of log daily index returns. This table provides summary statistics of log daily index returns for six markets, including the US (S&P 500 index), China (CSI 300 index), Japan (Nikkei 225 index), UK (FTSE-100 index), France (CAC-40 index), and Germany (DAX index) from June 1, 2006, to July 25, 2013. The Kendall tau correlation coefficient (ρ_τ) and Pearson correlation coefficient (ρ) between the US and tested countries are also reported.

	US	China	Japan	UK	France	Germany
Mean	0.01	0.0345	0.01	0.0129	$-9e-04$	0.0288
Median	0.0808	0.1176	0.048	0.0469	0.0297	0.1026
Min	−9.4695	−9.6952	−12.111	−9.2656	−9.4715	−7.335
Max	10.9572	8.9309	13.2346	9.3843	10.5946	10.7975
Stdev	1.3736	1.8993	1.6547	1.2979	1.5349	1.4629
Skewness	−0.1751	−0.3594	−0.581	−0.098	0.1327	0.1375
Kurtosis	9.5992	2.7969	8.3085	7.6485	6.1511	6.3971
KS (P value)	0	0	0	0	0	0
ρ_τ		0.0873	0.3317	0.1206	0.1086	0.1125
ρ		0.1476	0.5223	0.2542	0.2354	0.2013

Note: the overall sample period is from 1/2006 to 7/2013. Standard errors are in parentheses.

if one of the markets has a holiday, that is, when it is closed for any trading day other than the weekend, we delete the observations $t-1$ for the other markets. Hence, each of the two markets between American market and markets of tested countries has exactly the same trading days.

Summary statistics of the index returns are reported in Table 1. We find that all returns except for France and Germany are negatively skewed and the excess kurtosis of all returns is larger than zero. In terms of the Kolmogorov-Smirnov test, all the distribution of the series of six returns deviates from normal distribution. Returns from all six indices exhibit the characteristics of high kurtosis and fat tail. Table 1 also reports the Kendall correlation coefficient, ρ_τ, and Pearson correlation coefficient, ρ, between return of the S&P 500 index and lagged returns from the tested stock markets. We observed a relatively loose Kendall tau correlation coefficient between the US and China stock markets (0.0873), but tighter correlation between the US and Japan (0.3317), UK (0.1206), France (0.1086), and Germany (0.1125). Pearson correlation coefficient presents the same pattern as Kendall tau correlation coefficient. Perhaps because stock market in China is weak from efficiency and highly regulated, changes in market value of listed companies are difficult to react to those in their intrinsic value quickly and accurately.

Figure 1 illustrates the evolution of stock market returns over time. The figure indicates that all markets have trembled since 2008. Stock markets show volatility clustering, revealing the presence of heteroscedasticity. This characteristic supports the usefulness of dynamic conditional autoregressive model to analyze dynamic character in stock returns. Meanwhile, due to the effect of European debt crisis, there are high volatilities around 2011. However, there is no obvious evidence that high volatilities appear in Chinese and Japanese stock returns in Figure 1 around the period. It may be due to the little impact of the European debt crisis on China and Japan.

4.2. Model Specification. To provide evidence of the volatility clustering phenomenon in financial time series and financial contagion from the American subprime crisis to market indices of the tested countries, the MV-CAViaR models are estimated as a function of one lagged quantiles and one lagged returns of other countries. Next, we estimate the following system of equations for the conditional quantiles of the US and one of the tested countries (i.e., China, Japan, UK, France, and Germany). Consider

$$\begin{aligned} q_{1,t} &= c_1 + a_{12}\left|Y_{2,t-1}\right| + b_{11}q_{1,t-1}, \\ q_{2,t} &= c_2 + a_{21}\left|Y_{1,t-1}\right| + b_{22}q_{2,t-1}, \end{aligned} \tag{10}$$

where $Y_{1,t-1}$, $Y_{2,t-1}$ are separately denoted as the daily return on one of the indices of the tested countries and that on the index of America at time $t-1$. $q_{1,t}$, $q_{2,t}$ represent 5% quantiles of one of the returns on the indices of tested countries and American stock index return at time t, respectively. In the framework of the specified model (10), b_{11}, b_{22} can be used to test whether there are the characteristics of volatility clustering in the responding stock markets. If b_{11}, b_{22} are significantly different from zero at some given significance level, it indicates that there is volatility clustering phenomenon in the responding stock markets. Similar to the discussion above, the coefficients a_{12}, a_{21} can be used to capture financial contagion. If a_{12} is significantly different from zero, it shows that there is financial contagion from America to the tested countries. Similarly, if a_{21} is significantly different from zero, it indicates that there is risk spillover from equity markets of the tested countries to American equity market. Thus, we call a_{12}, a_{21} contagious coefficients. Meanwhile, contagious coefficients can be used to analyze the variation of market risk. From the model (10), we can see that the smaller the contagious coefficients are, the larger the risks in stock market of the infected countries are. Furthermore, the negative contagious coefficients imply that the market risks in the infected countries increase.

In addition, estimating the system of (10) is not trivial. We perform the computations in a step-wise fashion as follows.

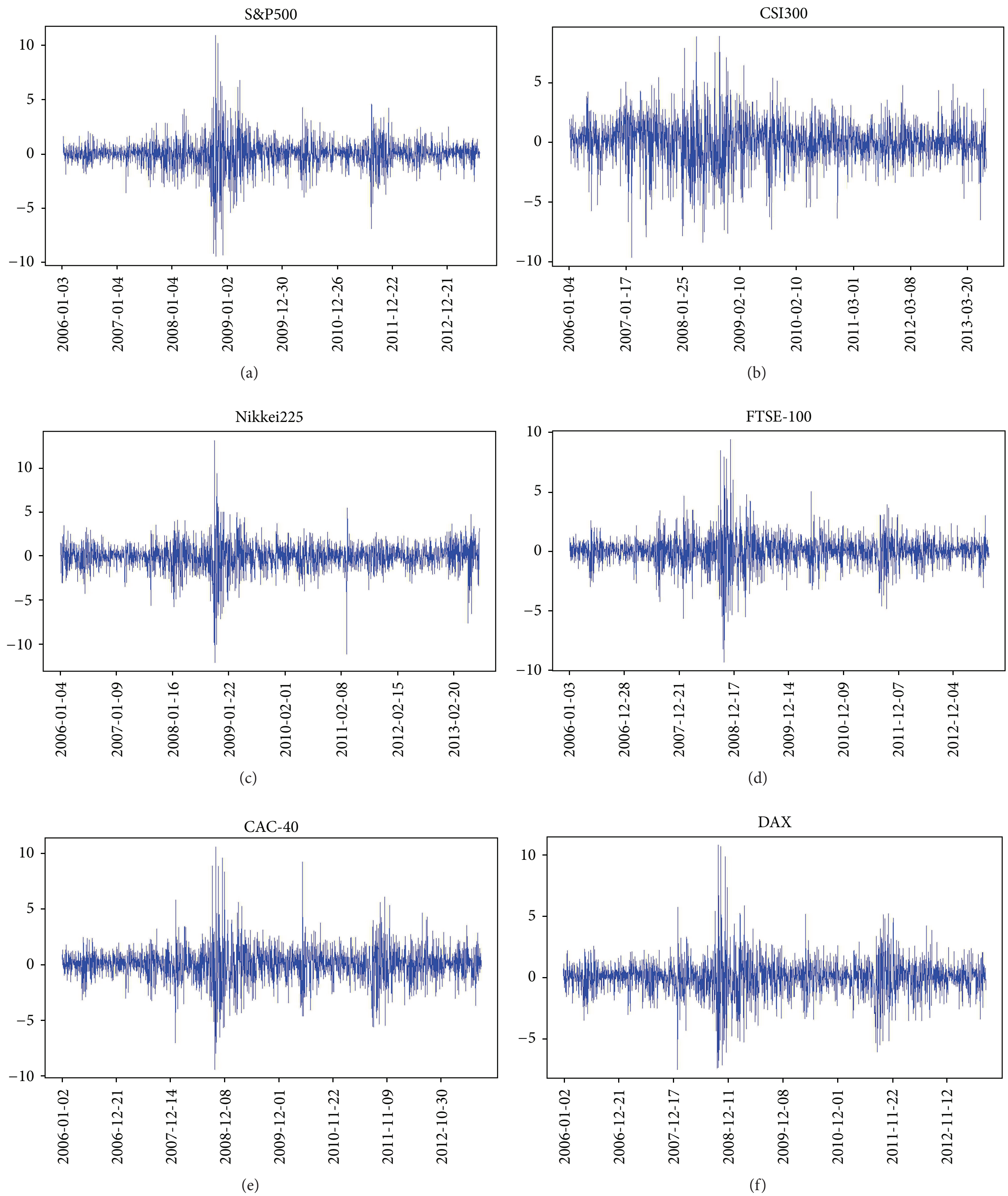

Figure 1: Daily returns of S&P500 (US), CSI300 (China), Nikkei225 (Japan), FTSE-100 (UK), CAC-40 (France), and DAX (Germany). Notes: daily data from January 2006 to July 2013.

Table 2: Estimates of MV-CAViaR model for the overall sample.

Parameters	c_1	a_{12}	b_{11}	c_2	a_{21}	b_{22}
US/China	−0.0350	−0.0157	0.9852	0.0034	−0.0116	0.9942
	(0.0107)***	(0.0047)***	(0.0041)***	(0.0015)**	(0.0016)	(0.0007)***
US/Japan	−0.7877	−1.0917	0.3103	−0.0039	0.0089	1.0045
	(0.1674)***	(0.0853)***	(0.0679)***	(0.0013)***	(0.0025)***	(0.0009)***
US/Australia	−0.4195	−0.6613	0.4356	−0.7129	−1.2766	0.2390
	(0.0740)***	(0.0769)***	(0.0575)***	(0.1552)**	(0.0862)***	(0.0758)***
US/UK	−1.6514	−0.3998	0.0293	0.0357	−0.3188	0.8806
	(0.3451)***	(0.1074)***	(0.1702)***	(0.0173)**	(0.0431)***	(0.0140)***
US/France	−0.2077	−0.3289	0.79422	−1.6113	−0.5503	0.0132
	(0.0466)***	(0.0626)***	(0.0368)***	(0.2641)***	(0.1143)***	(0.1151)
US/Germany	−0.1907	−0.2937	0.8031	−0.0022	−0.2847	0.8669
	(0.0476)***	(0.0608)***	(0.0384)***	(0.0223)	(0.0574)***	(0.0224)***

Note: the overall sample period is from 1/2006 to 7/2013. Standard errors are in parentheses.
**Significant at 5% level.
***Significant at 1% level.

Step 1. We use the QMLE method to estimate single CAViaR models: $q_{1,t} = c_1 + b_{11}q_{1,t-1}$ and $q_{2,t} = c_2 + b_{22}q_{2,t-1}$, respectively, with the initial value of c_i $(i = 1, 2)$ equal to the responding θth sample quantiles of Y_i $(i = 1, 2)$. We initialize the remaining parameters at zero.

Step 2. We use the parameter estimates of step 1 as the starting values for the optimization of the CAViaR models: $q_{1,t} = c_1 + a_{12}|Y_{2,t-1}| + b_{11}q_{1,t-1}$ and $q_{2,t} = c_2 + a_{21}|Y_{1,t-1}| + b_{22}q_{2,t-1}$, setting to zero the remaining parameters.

Step 3. We use the estimates from step 2 as the starting values for the full MV-CAViaR model (10) optimization, which contains two financial institutions of interest simultaneously.

4.3. Whole Sample Analysis. To capture the changes of market risk throughout the sampling period, we estimate the system of (10) for the entire sampling period. Table 2 displays the results of the model specified in (10) for tested countries and America.

Table 2 shows that the coefficients, b_{11} and b_{22}, are positive in each case and almost significant. It indicates that risk of stock markets is positive autocorrelation. In other words, there is volatility clustering phenomenon in stock markets. This is consistent with the conclusions of the existing research literatures, for example, Teyssiere and Kirman [51], Niu and Wang [52], and so on. Meanwhile, the contagious coefficients significantly deviate from zero in each case and are negative except for Japan. It implies that there may be financial contagion between the US and the tested countries and one country's risk increases due to another country except for Japan. It is interesting to find that the magnitude of the contagious coefficients is the smallest for China among all the examined countries. The parameter estimates of a_{12} and a_{21} are only −0.0157 and −0.0116, respectively. This means that the degree of risk spillovers for China is smallest and America has a lighter effect on China than the other investigated countries. It is consistent with the results in Table 1 that there is the smallest Kendall tau correlation coefficient between China and America.

Figure 2 illustrates the evolution of the estimated VaR at the level of 5% under the structure of the system of (10) from January 2006 to July 2013. The figure exhibits that all markets are subjected to high risks since 2008. Stock markets show the characteristics of high risk during the period of the financial crisis of 2008-2009.

However, it should be noted that estimated sampling period includes the crisis period and noncrisis period. Thus, we cannot distinguish whether the contagion is caused by the financial crisis originating from American subprime crisis. In order to overcome the defect, we consider the estimations for three important subsamples in the structure of model (10). The first runs from January 2006 to December 2007 which we refer to as the precrisis period. The second starts at the beginning of 2008, right after NBER identified December of 2007 as the start of the major recent financial crisis in the US. The US recession officially ended in June 2009, although economic growth has since been sluggish. The third subsample from July 2009 to July 2013 refers to the US economy entering a recovery phase.

4.4. Financial Contagion Analysis. As discussed in the previous section, there exists financial contagion from the US stock market to the foreign stock markets if one of the two following conditions is satisfied. (i) The contagious coefficient, a_{12}, is insignificant during the precrisis period, but it is significant during the crisis. (ii) If the contagious coefficient, a_{12}, is significant during both the precrisis and crisis period, but compared to the contagious coefficient, a_{12}, during the precrisis period, the estimated coefficient, a_{12}, during the crisis becomes smaller, which implies that there is risk increase due to America during the crisis. From the two aspects, we analyze whether there is financial contagion from one country to another. The detailed results are shown in Tables 3–7.

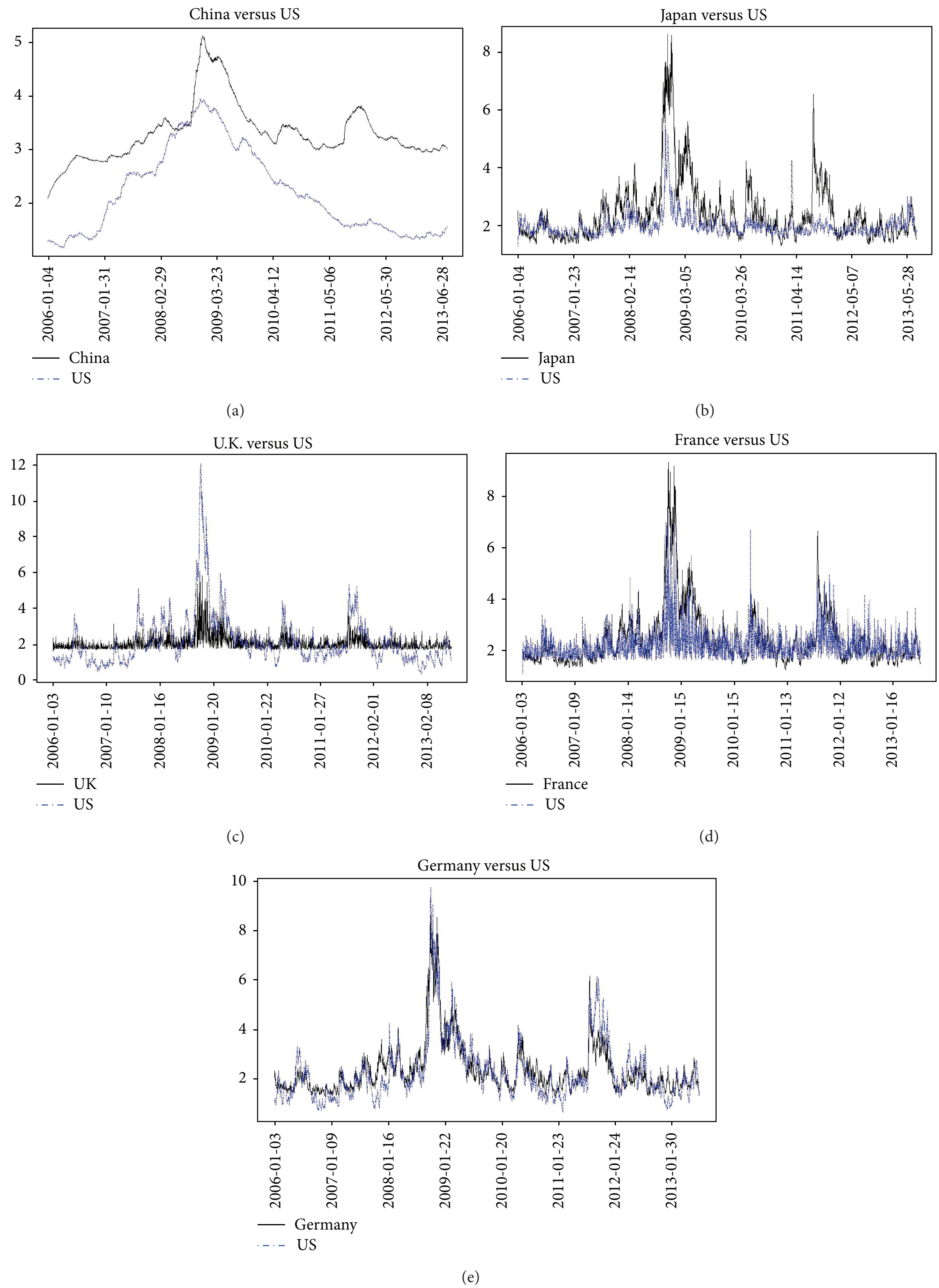

Figure 2: Estimated VaR at the level of 5% by the systems of (3). Notes: the overall sample period is from 1/2006 to 7/2013.

Table 3: Financial contagion analysis between the US and China.

Parameters	c_1	a_{12}	b_{11}	c_2	a_{21}	b_{22}
Precrisis	−0.0298	0.0580	1.0016	0.0166	−0.0015	1.0118
	(0.0078)***	(0.0193)***	(0.0019)***	(0.0046)***	(0.0032)	(0.0053)
Crisis	−0.5988	0.0294	0.8932	0.1006	−0.0537	0.9954
	(1.4327)	(0.0719)	(0.2574)***	(0.0425)***	(0.0151)***	(0.0032)***
Recovery	−4.8570	0.0554	−0.8753	−3.0359	−0.0569	−0.7033
	(0.1735)***	(0.0671)	(0.0360)***	(0.7243)***	(0.0600)	(0.3949)*

Notes: standard errors are in parentheses. The overall sample period is portioned into three subsamples: a precrisis period spanning from 1/2006 to 12/2007, a crisis period spanning from 1/2008 to 6/2009, and a recovery period spanning from 7/2009 to 7/2013.
*Significant at 10% level.
***Significant at 1% level.

Table 4: Financial contagion analysis between the US and Japan.

Parameters	c_1	a_{12}	b_{11}	c_2	a_{21}	b_{22}
Precrisis	−3.5184	−0.0866	−0.7231	−0.1383	−0.0239	0.8897
	(1.2479)***	(0.1806)	(0.6273)	(0.4116)	(0.0557)	(0.3054)***
Crisis	−0.9344	−1.0917	0.3553	−0.0333	0.0011	0.9949
	(0.2990)	(0.0956)***	(0.0872)***	(0.0059)***	(0.0094)	(0.0042)***
Recovery	−2.7990	0.3103	−0.3753	0.0161	−0.0146	1.0001
	(1.3049)**	(0.1331)	(0.6186)	(0.0047)***	(0.0049)***	(0.0010)***

Notes: standard errors are in parentheses. The overall sample period is portioned into three subsamples: a precrisis period spanning from 1/2006 to 12/2007, a crisis period spanning from 1/2008 to 6/2009, and a recovery period spanning from 7/2009 to 7/2013.
**Significant at 5% level.
***Significant at 1% level.

Table 5: Financial contagion analysis between the US and UK.

Parameters	c_1	a_{12}	b_{11}	c_2	a_{21}	b_{22}
Precrisis	0.0270	0.0292	1.0255	0.0171	0.0110	1.0208
	(0.0208)	(0.0366)	(0.0227)***	(0.0070)**	(0.0169)	(0.0107)***
Crisis	0.0148	0.0516	1.0291	0.0254	−0.0516	0.9888
	(0.0089)*	(0.0128)***	(0.0038)***	(0.0109)**	(0.0171)***	(0.0046)***
Recovery	−3.4809	−0.0129	−0.9977	−3.4290	0.0071	−0.8669
	(0.0969)***	(0.0150)	(0.0035)***	(0.7464)***	(0.0550)	(0.4042)***

Notes: standard errors are in parentheses. The overall sample period is portioned into three subsamples: a precrisis period spanning from 1/2006 to 12/2007, a crisis period spanning from 1/2008 to 6/2009, and a recovery period spanning from 7/2009 to 7/2013.
*Significant at 10% level.
**Significant at 5% level.
***Significant at 1% level.

Table 6: Financial contagion analysis between US and France.

Parameters	c_1	a_{12}	b_{11}	c_2	a_{21}	b_{22}
Precrisis	−3.0343	0.0071	−0.9769	0.0766	0.0000	1.0678
	(0.2408)***	(0.0399)	(0.0859)***	(0.0000)***	(0.0000)	(0.0000)***
Crisis	−0.2327	−0.4096	0.7474	0.0254	−0.0664	0.9751
	(0.0782)***	(0.0954)***	(0.0500)***	(0.0122)	(0.0196)***	(0.0065)***
Recovery	−0.1490	−0.2760	0.8462	−3.4290	0.2311	−0.5932
	(0.0693)**	(0.1155)**	(0.0583)***	(0.3309)***	(0.0990)**	(0.1592)***

Notes: standard errors are in parentheses. The overall sample period is portioned into three subsamples: a precrisis period spanning from 1/2006 to 12/2007, a crisis period spanning from 1/2008 to 6/2009, and a recovery period spanning from 7/2009 to 7/2013.
**Significant at 5% level.
***Significant at 1% level.

Table 7: Financial contagion analysis between the US and Germany.

Parameters	c_1	a_{12}	b_{11}	c_2	a_{21}	b_{22}
Precrisis	−3.2792	0.0204	−0.9912	0.0126	0.0019	1.0125
	(0.1669)***	(0.0152	(0.0111)***	(0.0070)*	(0.0077)	(0.0026)***
Crisis	−0.0550	−0.1400	0.9218	−0.0044	0.0863	1.0386
	(0.0336)*	(0.0477)***	(0.0266)***	(0.0162)	(0.0256)***	(0.0077)***
Recovery	−4.3511	0.0133	−0.8860	−1.4618	−0.4146	0.0097
	(1.3772)***	(0.0846)	(0.6013)	(0.4062)***	(0.1496)***	(0.2052)

Notes: standard errors are in parentheses. The overall sample period is portioned into three subsamples: a precrisis period spanning from 1/2006 to 12/2007, a crisis period spanning from 1/2008 to 6/2009, and a recovery period spanning from 7/2009 to 7/2013.
*Significant at 10% level.
***Significant at 1% level.

In Table 3, we report the results between the US and China for the three subsample periods (precrisis period, crisis period, and recovery period). The result indicates that, compared to the precrisis period, there is no evidence that there is contagion from America to China. This is consistent with the fact that the impact of the subprime crisis on China is relatively small. In reality, the Chinese government had maintained a relatively calm attitude and did not show panic that appeared in other developed countries throughout the process, which, to a large extent, relieved the negative factors brought by the stagnant international financial market. But, to some extent, Chinese market has a relationship with American market due to the economic globalization. The reason why there is only one significant contagious coefficient a_{21} during the crisis is that the linkage between the two markets increased during the crisis. Moreover, it should be noted that a_{21} is negative. This is consistent with the fact that the market risk in America increased during the crisis. As is known to all, the risk increase in America is caused by its own market conditions of the day. During the recovery period, the contagious coefficients are insignificant, which suggests that there is weaker link and no significant effect during the period.

Table 4 summarizes the financial contagion analysis between American and Japanese stock markets. We find that, during the precrisis period, the contagious coefficients a_{12} and a_{21} are not statistically significant, but during the crisis a_{12} is significant and a_{21} is insignificant. This indicates that there is financial contagion from American equity market to Japanese equity market but no contagion from Japan to America. It should be noted that during the recovery period a_{21} is the only significant contagious coefficient. This suggests that there may be contagion effect from Japanese equity market to American equity market during the recovery period. In fact, America is the second largest country for Japan and Japanese economy is affected by American economy. After the crisis, there is a strong economic resurgence in the US. However, in recent years, because the demand inside Japan is low and confused, economy is long-term backwater. As a result, American economy recovery is cumbered by Japanese sluggish economy. The significance of a_{21} cannot be explained from the perspective of financial contagion. It should be explained from the standpoint that Japan has a negative effect on American economic recovery and increases the recovery risk of American economy.

The results in Table 5 reveal the contagion effects between the US and UK. The contagion coefficients are statistically significant at the level of 1% only during the crisis. It means that there is strong financial contagion from the US to UK during the financial crisis. It is obvious that the comovements between the US and UK become stronger in contrast with noncrisis period. It is possible that there are strong historical ties between the two countries. British corporations are one of the largest foreign investors in the US. The tighter relations between the two countries may lead to the significant contagion coefficient a_{21} during the period of crisis. At last, the insignificance of the contagion coefficients suggests that the relations between the countries return to the state of the precrisis.

Table 6 shows the contagion test results between the US and France. There is strong evidence of spillover risks between the US and French markets. The contagious coefficients are statistically significant at the level of 1% during the crisis period. Moreover, they are negative and the contagious coefficient a_{12} from America to France is −0.4096, and contagious coefficient a_{21} from France to America is −0.0664. Because the financial crisis of 2008-2009 is caused by American subprime crisis, we only say that there is financial contagion from America to France. In other words, the existence of the financial contagion from the US to France leads to a stronger linkage between the two countries. In addition, from the magnitude of contagion coefficients, America has a stronger effect on France, which is consistent with the fact that the financial crisis is originating from America. At last, in comparison with the crisis period, the contagion coefficients are significant at level of 5% but larger. It means that the comovements between the two countries become weaker and risk spillovers become smaller during the recovery period. The global economy steps in a recovery phase.

In Table 7, we present estimated model parameters for the US and Germany. Estimates of the contagious coefficients, a_{12} and a_{21}, show that there is evidence of financial contagion between the US and Germany. Furthermore, in terms of the sign of the contagious coefficients, we see clearly that America increases stock market risk in Germany and Germany decreases the risk in American stock market. Similar to the discussion above, we say that the direction of contagion is from America to Germany and there exists a stronger linkage between the US and Germany. During the recovery period, only one contagion coefficient, a_{21}, is significant. Furthermore, the sign of it is negative, which implies that Germany increases the market risk in America during the period. That is to say, Germany becomes a burden on the recovery of American economy. It is possible that European debt crisis has more serious effect on German economy than on American economy and the recovery speed of American economy is faster than that of German economy.

5. Conclusions

In this paper, we examine whether the subprime crisis originating from the US led to risk spillovers in financial indices in major mature markets (Japan, UK, France, Germany) and one of the largest emerging markets (China). We apply the MV-CAViaR model to the whole sample period from 1 January 2006 to 25 July 2013. The findings show that there is a significant increase in market risk during the crisis. To investigate the changes of dependence structure during the crisis and noncrisis period, we divide the sampling period into three important subperiods: precrisis period, crisis period, and recovery period according to the announcements by NBER and government.

The piecewise estimated results show that American subprime crisis spilled over to Japan, UK, France, and Germany and increased their market risks during the crisis in comparison with the turmoil period. But, we have not found statistically significant evidence showing that there is financial contagion from America to China. During the recovery period, the strong linkages between the US and France still exist, but there is a simultaneous decrease in the market risks of both countries. As for UK, there is no contagion during the recovery period. But, it should be noted that there are spillover risks from Japan and Germany to the US due to market conditions of the day.

The findings of our paper contribute to the ongoing debate on the detection, modeling, and especially risk analysis of financial contagion. It is of great significance for investors and portfolio managers to determine the existence of financial contagion as well as risk variation before and after financial crisis. In near future, it would be interesting research areas to study how the methodology could be applied to asset and risk management despite the existing contagion in some regions.

Conflict of Interests

The authors declare that there is no conflict of interests regarding the publication of this paper.

Acknowledgments

This research is supported by National Natural Science Foundation of China (nos. 71371007 and 71271199), Program for New Century Excellent Talents in University (no. NCET-13-0538), and the Fundamental Research Funds for the Central Universities of China (no. WK2040160008).

References

[1] K. J. Forbes and R. Rigobon, "No contagion, only interdependence: measuring stock market comovements," *Journal of Finance*, vol. 57, no. 5, pp. 2223–2261, 2002.

[2] T. Baig and I. Goldfajn, "Financial market contagion in the Asian crisis," *IMF Staff Papers*, vol. 46, no. 2, pp. 167–195, 1999.

[3] K.-H. Bae, G. A. Karolyi, and R. M. Stulz, "A new approach to measuring financial contagion," *Review of Financial Studies*, vol. 16, no. 3, pp. 717–763, 2003.

[4] D. G. Baur, "The structure and degree of dependence: a quantile regression approach," *Journal of Banking and Finance*, vol. 37, no. 3, pp. 786–798, 2013.

[5] R. F. Engle and S. Manganelli, "CAViaR: conditional autoregressive value at risk by regression quantiles," *Journal of Business & Economic Statistics*, vol. 22, no. 4, pp. 367–381, 2004.

[6] H. White, T. H. Kim, and S. Manganelli, "Modeling autoregressive conditional skewness and kurtosis with multi-quantile CAViaR," European Central Bank Working Paper Series 0957, 2008.

[7] H. White, T. H. Kim, and S. Manganelli, "VAR for VaR: measuring systemic risk using multivariate regression quantiles," MPRA Paper 35372, 2010.

[8] A. V. Mollick and T. A. Assefa, "U.S. stock returns and oil prices: the tale from daily data and the 2008-2009 financial crisis," *Energy Economics*, vol. 36, pp. 1–18, 2013.

[9] G. L. Kaminsky, C. M. Reinhart, and C. A. Végh, "The unholy trinity of financial contagion," *Journal of Economic Perspectives*, vol. 17, no. 4, pp. 51–74, 2003.

[10] A. V. Banerjee, "A simple model of herd behavior," *The Quarterly Journal of Economics*, vol. 107, no. 3, pp. 797–817, 1992.

[11] G. A. Calvo and E. G. Mendoza, "Macroeconomics of emerging markets: capital-markets crises and economic collapse in emerging markets: an informational-frictions approach," *The American Economic Review*, vol. 90, no. 2, pp. 59–64, 2000.

[12] A. Lahiri and C. A. Végh, "Delaying the inevitable: interest rate defense and balance of payments crises," *Journal of Political Economy*, vol. 111, no. 2, pp. 404–424, 2003.

[13] S. Gerlach and S. Frank, "Contagious speculative attacks," CEPR Discussion Paper 1055, 1996.

[14] L. E. Kodres and M. Pritsker, "A rational expectations model of financial contagion," *Journal of Finance*, vol. 57, no. 2, pp. 769–799, 2002.

[15] M. Fratzscher, "On currency crises and contagion," *International Journal of Finance and Economics*, vol. 8, no. 2, pp. 109–129, 2003.

[16] C. Reinhart and S. Calvo, "Capital flows of Latin America: is there evidence of contagion effects?" MPRA Paper 7124, 1996.

[17] M. D. Bordo and A. P. Murshid, "Are financial crises becoming increasingly more contagious? What is historical evidence on contagion?" NBER Working Paper 7900, 2000.

[18] K. Forbes and R. Rigobon, "Contagion in Latin America: definitions, measurement, and policy implications," NBER Working Papers 7885, 2000.

[19] G. Corsetti, M. Pericoli, and M. Sbracia, "Correlation analysis of financial contagion: what one should know before running a

test," Yale University Economic Growth Center working paper 822, 2005.

[20] R. Rigobon, "On the measurement of the international propagation of shocks: is the transmission stable?" *Journal of International Economics*, vol. 61, no. 2, pp. 261–283, 2003.

[21] T. C. Chiang, B. N. Jeon, and H. Li, "Dynamic correlation analysis of financial contagion: evidence from Asian markets," *Journal of International Money and Finance*, vol. 26, no. 7, pp. 1206–1228, 2007.

[22] K. Naoui, S. Khemiri, and N. Liouane, "Crises and financial contagion: the subprime crisis," *Journal of Business Studies Quaterly*, vol. 2, no. 1, pp. 15–28, 2010.

[23] S. Celik, "The more contagion effect on emerging markets: the evidence of DCC-GARCH model," *Economic Modelling*, vol. 29, no. 5, pp. 1946–1959, 2012.

[24] D. Dimitriou, D. Kenourgios, and T. Simos, "Global financial crisis and emerging stock market contagion: a multivariate FIAPARCH-DCC approach," *International Review of Financial Anal-ysis*, vol. 30, pp. 46–56, 2013.

[25] T. Bollerslev, R. Y. Chou, and K. F. Kroner, "ARCH modeling in finance. A review of the theory and empirical evidence," *Journal of Econometrics*, vol. 52, no. 1-2, pp. 5–59, 1992.

[26] M. Billio and M. Caporin, "Market linkages, variance spillovers, and correlation stability: empirical evidence of financial contagion," *Computational Statistics & Data Analysis*, vol. 54, no. 11, pp. 2443–2458, 2010.

[27] G. Bekaert and G. Wu, "Asymmetric volatility and risk in equity markets," *Review of Financial Studies*, vol. 13, no. 1, pp. 1–42, 2000.

[28] J. A. Chan-Lau, D. J. Mathieson, and J. Y. Yao, "Extreme contagion in equity markets," *IMF Staff Papers*, vol. 51, no. 2, pp. 386–408, 2004.

[29] P. Cumperayot, T. Keijzer, and R. Kouwenberg, "Linkages between extreme stock market and currency returns," *Journal of International Money and Finance*, vol. 25, no. 3, pp. 528–550, 2006.

[30] R. Gropp, M. Lo Duca, and J. Vesala, "Cross-border bank contagion in Europe," ECB Working Paper 662, 2006.

[31] B. H. Boyer, T. Kumagai, and K. Yuan, "How do crises spread? Evidence from accessible and inaccessible stock indices," *Journal of Finance*, vol. 61, no. 2, pp. 957–1003, 2006.

[32] G. M. Gallo and E. Otranto, "Volatility spillovers, interdependence and comovements: a Markov switching approach," *Computational Statistics & Data Analysis*, vol. 52, no. 6, pp. 3011–3026, 2008.

[33] J. Chevallier, "Global imbalances, cross-market linkages, and the financial crisis: a multivariate Markov-switching analysis," *Economic Modelling*, vol. 29, no. 3, pp. 943–973, 2012.

[34] G. Corsetti, M. Pericoli, and M. Sbracia, "'Some contagion, some interdependence': more pitfalls in tests of financial contagion," *Journal of International Money and Finance*, vol. 24, no. 8, pp. 1177–1199, 2005.

[35] P. Embrechts, F. Lidskog, and A. J. McNeal, "Modelling dependence with copulas and applications to risk management," in *Handbook of Heavy Tailed Distributions in Finance*, S. T. Rachev, Ed., pp. 329–384, Elsevier, North-Holland, The Netherlands, 2003.

[36] L. Hu, "Dependence patterns across financial markets: a mixed copula approach," *Applied Financial Economics*, vol. 16, no. 10, pp. 717–729, 2006.

[37] J. C. Rodriguez, "Measuring financial contagion: a Copula approach," *Journal of Empirical Finance*, vol. 14, no. 3, pp. 401–423, 2007.

[38] S. Jayech and N. B. Zina, "A copula-based approach to financial contagion in the foreign exchange markets," *International Journal of Mathematics in Operational Research*, vol. 3, no. 6, pp. 636–657, 2011.

[39] W. Ye, X. Liu, and B. Miao, "Measuring the subprime crisis contagion: evidence of change point analysis of copula functions," *European Journal of Operational Research*, vol. 222, no. 1, pp. 96–103, 2012.

[40] M. Gallegati, "A wavelet-based approach to test for financial market contagion," *Computational Statistics & Data Analysis*, vol. 56, no. 11, pp. 3491–3497, 2012.

[41] S. Dajcman, M. Festic, and A. Kavkler, "Comovement dynamics between central and eastern European and developed European stock markets during European integration and amid financial crises—a wavelet analysis," *Engineering Economics*, vol. 23, no. 1, pp. 22–32, 2012.

[42] D. Baur and N. Schulze, "Coexceedances in financial markets—a quantile regression analysis of contagion," *Emerging Markets Review*, vol. 6, no. 1, pp. 21–43, 2005.

[43] C.-C. Chuang, C.-M. Kuan, and H.-Y. Lin, "Causality in quantiles and dynamic stock return-volume relations," *Journal of Banking and Finance*, vol. 33, no. 7, pp. 1351–1360, 2009.

[44] B. S. Lee and M.-Y. L. Li, "Diversification and risk-adjusted performance: a quantile regression approach," *Journal of Banking and Finance*, vol. 36, no. 7, pp. 2157–2173, 2012.

[45] K. Yu and J. Zhang, "A three-parameter asymmetric Laplace distribution and its extension," *Communications in Statistics. Theory and Methods*, vol. 34, no. 9-10, pp. 1867–1879, 2005.

[46] M. B. Stinchcombe and H. White, "Consistent specification testing with nuisance parameters present only under the alternative," *Econometric Theory*, vol. 14, no. 3, pp. 295–325, 1998.

[47] H. White, "Approximate nonlinear forecasting methods," in *Handbook of Economic Forecastin*, G. Elliott, C. W. J. Granger, and A. Timmermann, Eds., pp. 460–512, Elsevier, New York, NY, USA, 2006.

[48] K. Yu and R. A. Moyeed, "Bayesian quantile regression," *Statistics & Probability Letters*, vol. 54, no. 4, pp. 437–447, 2001.

[49] R. Koenker and J. A. F. Machado, "Goodness of fit and related inference processes for quantile regression," *Journal of the American Statistical Association*, vol. 94, no. 448, pp. 1296–1310, 1999.

[50] R. Koenker and G. Bassett, Jr., "Regression quantiles," *Econometrica*, vol. 46, no. 1, pp. 33–50, 1978.

[51] G. Teyssiere and A. P. Kirman, *Long Memory in Economics*, Springer, Berlin, Germany, 2007.

[52] H. Niu and J. Wang, "Volatility clustering and long memory of financial time series and financial price model," *Digital Signal Processing*, vol. 23, no. 2, pp. 489–498, 2013.

Hindawi Publishing Corporation
Discrete Dynamics in Nature and Society
Volume 2014, Article ID 492134, 5 pages
http://dx.doi.org/10.1155/2014/492134

Research Article

Pricing Chinese Convertible Bonds with Dynamic Credit Risk

Ping Li and Jing Song

School of Economics and Management, Beihang University, Beijing 100191, China

Correspondence should be addressed to Ping Li; lipingxx@126.com

Received 14 March 2014; Accepted 23 May 2014; Published 9 June 2014

Academic Editor: Chuangxia Huang

To price convertible bonds more precisely, least squares Monte Carlo (LSM) method is used in this paper for its advantage in handling the dependence of derivatives on the path, and dynamic credit risk is used to replace the fixed one to make the value of convertible bonds reflect the real credit risk. In the empirical study, we price convertible bonds based on static credit risk and dynamic credit risk, respectively. Empirical results indicate that the ICBC convertible bond has been overpriced, resulting from the underestimation of credit risk. In addition, when there is an issue of dividend, the conversion price will change in China's convertible bonds, while it does not change in the international convertible bonds. So we also empirically study the difference between the convertible bond's prices by assuming whether the conversion price changes or not.

1. Introduction

Convertible bond is an innovative and complex financial instrument which can be converted to the issuer's stock at some specified circumstance. It is hard to be valued because of its characters of both equity and bond, in addition to its varieties of terms. China's convertible bond market is an emerging market, so it is important to value the product considering some changes compared with the existed valuation methods.

Theoretical research on convertible bonds was initiated by Ingersoll [1], who applied the Black-Sholes-Merton model of pricing options. Following his work, Brennan and Schwartz [2] firstly used corporate value as the basic variable to price convertible bonds. However, corporate value was soon replaced by stock price for its simplicity of observation and measurement, which was first introduced by McConnell and Schwartz [3]. Brennan and Schwartz [4] considered stochastic interest rate firstly and constructed a two-factor pricing model for convertible bonds. Then, stochastic credit risk was introduced by Davis and Lischka [5]. From the above tendency we can see that researchers gradually added factors to increase the accuracy of valuation. To solve the more and more complex models, Monte Carlo simulation became widely used. Longstaff and Schwartz [6] firstly introduced the least squares Monte Carlo (LSM) to price American options. Following them, Moreno and Navas [7] studied the robustness of LSM method for pricing American options; Stentoft [8] studied the convergence of the LSM approach. Due to its significant advantage in pricing derivatives, LSM method was soon applied to the valuation of convertible bonds, such as the work of Crépey and Rahal [9] and Ammann et al. [10].

Credit risk is an important factor in convertible bonds valuation and is paid more attention than before in China. Currently, there are two methods to measure the credit risk. The first one is credit spread, which is firstly used by McConnell and Schwartz [3] to value convertible bonds. Following their work, Tsiveriotis and Fernandes [11] split convertible bond into two components: a cash-only part, which was discounted by risky interest rate, and an equity part, which was discounted by risk-free interest rate. The second method is to use default density, which was used by Duffie and Singleton [12] to price corporate bonds. Then, Ayache et al. [13] applied default density to convertible bonds, deriving a partial differential equation for valuation. Comparing the two methods, the first one is more widely used for its simplicity and convenience. However,the estimation of the spread is essential.

To get more accurate price, researchers began to employ dynamic credit risk. Davis and Lischka [5] supposed that hazard rate obeys a Brownian motion, with the Vasicek model of interest rate, and then established a two and a half model. But they did not verify the effect of the model using real data.

Currently, there is not any model applying dynamic credit risk to price convertible bonds. In addition, when there is a distribution of dividend, the conversion price will change in China's market, while it does not change in the international market. In this paper we will study the pricing of China's convertible bonds using dynamic credit risk and then empirically study the difference between the prices obtained by assuming whether the conversion price changes or not.

The rest of this paper is organized as follows. Section 2 gives the basic framework of convertible bond pricing by least squares Monte Carlo simulation. Section 3 derives the equation of dynamic credit spread. Section 4 is the empirical part, including the effect of dynamic credit spread and the comparison of price obtained by assuming whether the conversion price changes or not. Finally, Section 5 concludes the paper.

2. Basic Framework of Convertible Bond Pricing by LSM

Besides the common debt, convertible bonds are embedded with many options, such as conversion option, call option, put option, and option to lower the conversion price. So, we should compare the value of these options comprehensively when pricing the convertible bonds. At the expiration, the final boundary can be $V = \max(nS_T, C_T)$.

Every moment before the maturity of the convertible bond, investors and issuers will gamble over the benefit. Investors will maximize the value of convertible bonds, while the issuer will minimize the value of convertible bonds from exercising the call option. To make it clear, we use Table 1 to show the rules of option exercise.

The basic framework of convertible bonds pricing by LSM when the credit risk is static is as follows.

(1) Considering the stock volatility is one of the important parameters affecting stock path, we assume that the stock price follows the stochastic volatility model presented by Heston [14]:

$$\begin{aligned} dS_t &= S_t\left(r_f - q\right)dt + S_t\sqrt{v_t}dW, \\ dv_t &= \kappa\left(\overline{v} - v_t\right)dt + \sqrt{v_t}\sigma_v dW_v, \end{aligned} \tag{1}$$

where r_f is the risk-free interest rate, q is the dividend yield of the underlying stock, v_t is the stochastic volatility of S_t and is modeled by the second equation of (1), κ is the mean reversion coefficient of v_t, $\overline{v}$ is the long-term mean reversion level of v_t, and σ_v is the volatility of v_t, W and W_v are both Wiener processes.

We split the duration of convertible bonds into N sections on average and assume that the convertible bonds can only be exercised at these discrete times. We can generate random numbers by Monte Carlo simulation and then get N_u paths from the Heston model. Then, the stock price matrix is obtained.

(2) Applying the optimal stopping theory, we compare the value of continuation and immediate exercise. If the latter one is bigger, then we get the stopping time denoted by J and stopping value denoted by $M_i^{N_u}$.

(3) We assume (Ω, F, P) to be the complete probability space and assume $[0, T]$ to be the finite time horizon. $\mathfrak{R} = (\mathfrak{R})_{i=0,\ldots,N}$ is defined to be the augmented filtration generated by the actual market performance, and $\mathfrak{R}_0 \subset \mathfrak{R}_1 \subset \cdots \subset \mathfrak{R}_N$. The state variable S is the simulated stock price, from which we calculate the cash flow $C(\omega, j)$ on the path ω at time j and the temporary optimal stopping value $M_i^{N_u}$. Then we take the expectation of the cash flows $C(\omega, j)$ discounted by the risky interest rate $r(\omega, s)$, and get the value of continuation $Y(\omega; t)$ as follows:

$$Y(\omega; t) = E_Q\left[\sum_{j=t+1}^{N} \exp\left(-\int_t^j r(\omega, s)\,ds\right) C(\omega, j) \mid \mathfrak{R}\right]. \tag{2}$$

(4) The least square regression process is as follows. We put the value of continuation to be the dependent variable Y and the underlying stock price to be the independent variable X, and Laguerre polynomials are chosen to be the basis function to make the least square regression. The procedure to get the estimated value of Y can be described by the following equations:

$$\begin{aligned} Y_0(X) &= \exp\left(-\frac{X}{2}\right), \\ Y_1(X) &= \exp\left(-\frac{X}{2}\right)(1 - X), \\ Y_2(X) &= \exp\left(-\frac{X}{2}\right)\left(1 - 2X + \frac{X^2}{2}\right), \\ \widehat{Y}(\omega; t) &= \sum_{j=0}^{2} a_j Y_j(X). \end{aligned} \tag{3}$$

(5) Compare $\widehat{Y}(\omega; t)$ with the conversion value, call value, and the put value on the basis of the exercise rules of convertible bonds. If $\widehat{Y}(\omega; t)$ is bigger, then the optimal stopping value remains the same; if $\widehat{Y}(\omega; t)$ is smaller, then we get the new stopping time t and the new stopping value $M_i^{N_u}$.

(6) The convertible bond can be valued by discounting each $M_i^{N_u}$ back to time $t = 0$ with the risky interest rate, and averaging over all paths:

$$V = \frac{1}{N_u}\sum_{j=1}^{N_u} \exp\left(-\int_0^j r(\omega, s)\,ds\right) M_j. \tag{4}$$

It is worth noticing that not all values of continuation are estimated by the Laguerre polynomials. To increase the estimated accuracy, the following three conditions must be excluded.

(a) When the call provisions have been triggered, no matter how big the value of continuation is, the convertible bonds will be exercised and terminated, so the value of continuation does not need to be estimated.

Table 1: Rules of option exercise in convertible bonds.

Case	Payoff	Rules	Exercise restriction
Conversion	$n_t S_t$	$n_t S_t > F(\omega, t)$ and $P_t \le n_t S_t$	$t \in \Omega_{\text{conv}}$ $t \in \Omega_{\text{put}} \cap \Omega_{\text{conv}}$
Call	P_t	$P_t > F(\omega, t)$ and $n_t S_t \le P_t$	$t \in \Omega_{\text{put}}$ $t \in \Omega_{\text{put}} \cap \Omega_{\text{conv}}$
Put	C_t	$F(\omega, t) > C_t$ and $C_t > n_t S_t$	$t \in \Omega_{\text{call}}$ $t \in \Omega_{\text{call}} \cap \Omega_{\text{conv}}$
Forced conversion	$n_t S_t$	$F(\omega, t) > C_t$ and $C_t < n_t S_t$	$t \in \Omega_{\text{call}}$ $t \in \Omega_{\text{call}} \cap \Omega_{\text{conv}}$

(b) When the put provisions have been triggered, and the call value is smaller than the discounted value of the minimum payoff $V_{\min}$ until the maturity, the call action will not be exercised definitely. So, the value of continuation does not need to be estimated.

(c) When the call provisions and the put provisions have not been triggered, if the conversion value is smaller than the discounted value of the minimum payoff $V_{\min}$ until the maturity, the conversion action will not be exercised definitely. So, there is no need to estimate the value of continuation, where $V_{\min}$ is the discounted value of the call value until maturity.

3. The Dynamic Credit Risk Model

Currently, there are two main methods to describe the dynamic credit risk. The first one is the two and a half model of Davis and Lischka [5], who assumed that the hazard rate obeys a Brownian motion. The second one is of Huang et al. [15], who assume the credit spread to be linked with the asset value of the company.

In this paper, we describe the credit risk to be the dynamic credit spread linked with the stock price, because the credit risk is mostly affected by the stock price. Moreover, the conversion price can be the benchmark of the stock price, and then we can derive the equation of dynamic credit spread r_c as follows:

$$r_c = r_{mc}\left(\frac{X}{S}\right)^{\eta}, \tag{5}$$

where r_{mc} denotes the average credit spread, X is the conversion price, and S is the stock price. The equation indicates that when $S > X$, the credit spread will decrease; when $S < X$, the credit spread will increase. η denotes the adjustment speed. Finally, the risky interest rate $r(\omega, t)$ in the last section can be written to be

$$r(\omega, t) = r_f + r_{mc}\left(\frac{X}{S}\right)^{\eta}. \tag{6}$$

4. Empirical Research

To test the performance of our model, we consider ICBC convertible bond, one of the largest convertible bonds issued in China, to do the empirical study. We adopt 146 weekly data from August 12, 2011, to January 3, 2014, obtained from CSMAR. The information of ICBC convertible bond is in Table 2.

Table 2: ICBC convertible bond.

Convertible bond	ICBC convertible bond
Issue date	2010.8.31
Time horizon	6
Face value	100
Coupon (%)	0.5, 0.7, 0.9, 1.1, 1.4, 1.8
Call value till maturity	105
The first conversion price	4.2
Change of conversion price	2010.11.26, adjusted to 4.16 2010.12.27, adjusted to 4.15 2011.6.15, adjusted to 3.97 2012.6.14, adjusted to 3.77 2013.6.26, adjusted to 3.53
Reset clause	In 30 consecutive trading days, the closing stock price is smaller than 80% of conversion price in 15 trading days.
Call on condition	In 30 consecutive trading days, the closing stock price is bigger than 130% of conversion price in 15 trading days.
Call value	Face value plus the accrued interest
Put on condition	When the use of capital is changed
Put value	Face value plus the accrued interest

Before pricing we first need to estimate the related parameters. We get the term structure of risk-free interest rate based on cubic polynomial spline function using 15 treasury bonds traded in Shanghai Exchange. By minimizing the sum of squared errors between the market price and the simulated price of the underlying stock we get the three parameters in Heston's stochastic volatility model: $\sigma_v = 0.40$, $\kappa = 1.3$, and $\overline{v} = 0.04$. We employ the estimation result obtained by Zheng and Lin [16] to be China's average credit spread; that is, $r_{mc} = 0.98$.

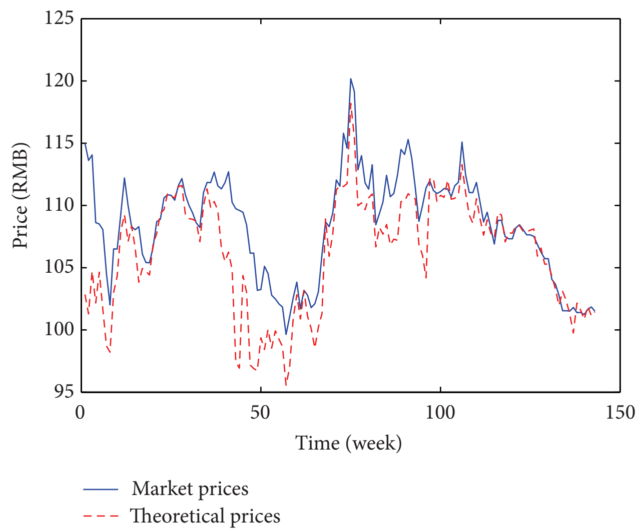

FIGURE 1: Comparison of the theoretical and market prices of ICBC convertible bond.

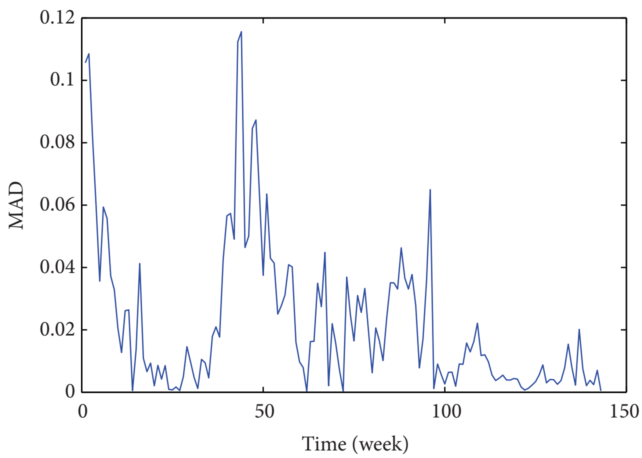

FIGURE 2: The relative deviation (AD) of ICBC convertible bond.

4.1. Pricing Results with Static Credit Risk. We first assume that the credit risk is static and get 5000 paths of the stock price by LSM. Then we get the theoretical prices of ICBC convertible bond using our pricing framework. Figure 1 is the comparison of the theoretical prices and market prices.

From Figure 1 we can see that the tendencies of the two lines fit well in the long run, so we can use this price framework to forecast market price of convertible bond and make investment decision. On the other hand, the market price is a little higher than the theoretical price, so ICBC convertible bond is a little overpriced.

We also define the variable AD to be the absolute deviation of the theoretical price from the market price as follows:

$$\mathrm{AD}_i = \frac{\left|V_i - \overline{V}_i\right|}{\overline{V}_i}. \tag{7}$$

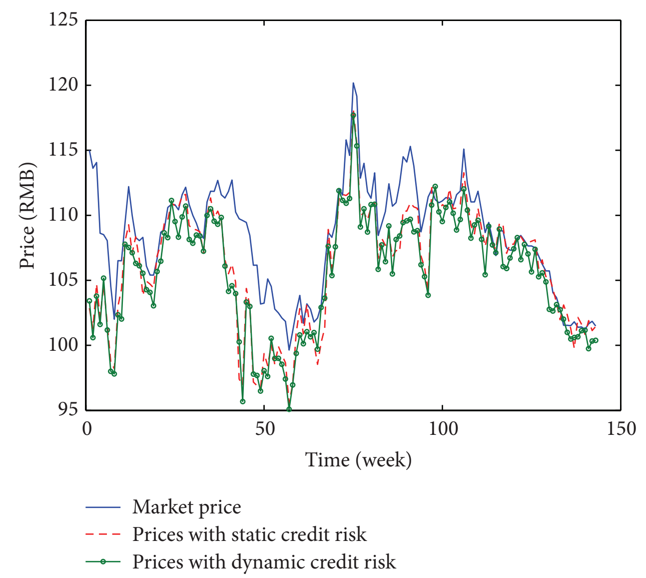

FIGURE 3: Comparison of theoretical prices with dynamic and static credit risk.

Then we get the figure of AD by Matlab and depict it in Figure 2.

The following mean absolute deviation MAD is defined to describe the integral result of our model:

$$\mathrm{MAD} = \frac{1}{146}\sum_{i=1}^{146} \mathrm{AD}_i. \tag{8}$$

Through calculation, the mean absolute deviation of ICBC convertible MAD is 2.3%, within 5%, which demonstrates that the theoretical price obtained from our model can reflect market price.

4.2. Pricing Results Using Dynamic Credit Risk. In this section, we give the pricing results of ICBC convertible bond using the dynamic credit risk modeled by (6) and with $\eta = 2$. We compare the market prices with the prices obtained from static credit risk and dynamic credit risk in Figure 3.

We can see from Figure 3 that the market price of the ICBC convertible bond is higher than the prices obtained from both the static and dynamic credit risk models, which means that the ICBC convertible bond is overestimated, resulting from the underestimation of credit risk. We can also see that the dynamic credit risk can reflect the real credit risk, since when the price of convertible bond goes downwards, the price obtained from dynamic credit risk is lower than those obtained from static credit risk. This implies that we should use dynamic credit risk to price convertible bonds.

4.3. Effect of Conversion Price. In the above empirical study we price the ICBC convertible bond based on changing conversion price (CP) resulting from two issues of dividend. Though most Chinese companies change conversion price when issuing dividend, international companies' conversion price does not change. So in this section we also give the

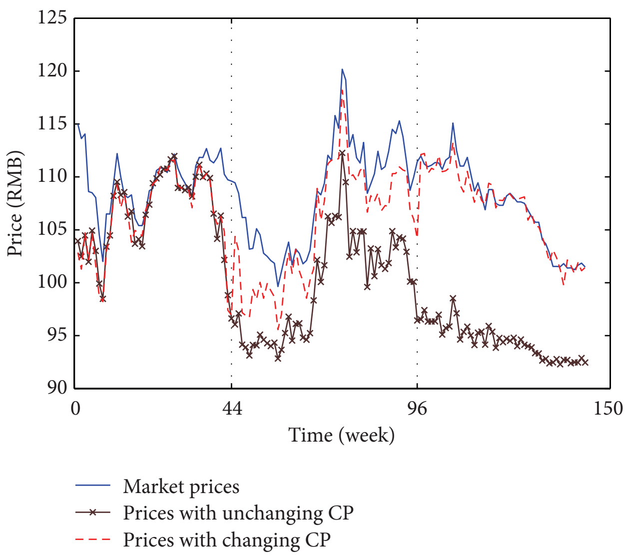

FIGURE 4: Pricing results without changing the conversion price.

prices of ICBC convertible bond assuming that the conversion price does not change. The pricing results together with those obtained from changing conversion price are shown in Figure 4.

Figure 4 indicates that, compared with the prices with changing CP obtained in Section 4.1, the obtained prices with unchanging CP have two jumps at time $t = 44$ and $t = 96$, just after the CP changed. This demonstrates that when the company issues dividend the effect of unchanging CP is significant. This can be explained by the fact that when there is an issue of dividend investors of China's convertible bonds will have an expectation of price decline which will affect the payoff of convertible bonds eventually. Therefore, Chinese companies of convertible bonds are suggested to change CP when issuing dividend. That is, we cannot copy the international experience of unchanging CP.

5. Conclusion

This paper studies the pricing of convertible bonds with dynamic credit risk using least squares Monte Carlo method. We employ the dynamic credit spread changing with stock price. In empirical study, our model is proved to be effective and the comparison test demonstrates that the dynamic credit risk is important in convertible bond pricing. The price obtained from dynamic credit risk can reflect the real credit risk. Thus, the potential risk resulting from the overestimation of convertible bonds cannot be neglected by the investors. In addition, we also study the empirical effect of changing the conversion price when the issuer distributes dividend. Consequently, the unchanged conversion price will lead to an unreasonable price. So, China's market is not mature enough to keep the conversion price constant just like international markets.

Conflict of Interests

The authors declare that there is no conflict of interests regarding the publication of this paper.

Acknowledgment

This work was supported by the National Natural Science Foundation of China (nos. 71271015 and 70971006).

References

[1] J. E. Ingersoll Jr., "A contingent-claims valuation of convertible securities," *Journal of Financial Economics*, vol. 4, no. 3, pp. 289–321, 1977.

[2] M. J. Brennan and E. S. Schwartz, "Convertible bonds: valuation and optimal strategies for call and conversion," *The Journal of Finance*, vol. 32, no. 5, pp. 1699–1715, 1977.

[3] J. J. McConnell and E. S. Schwartz, "LYON taming," *The Journal of Finance*, vol. 41, no. 3, pp. 561–576, 1986.

[4] M. J. Brennan and E. S. Schwartz, "Analyzing convertible bonds," *Journal of Financial and Quantitative Analysis*, vol. 15, pp. 907–929, 1980.

[5] M. Davis and F. R. Lischka, "Convertible bonds with market risk and credit risk," Working Paper, Tokyo-Mitsubishi International, 1999.

[6] F. A. Longstaff and E. S. Schwartz, "Valuing American options by simulation: a simple least-squares approach," *Review of Financial Studies*, vol. 14, no. 1, pp. 113–147, 2001.

[7] M. Moreno and J. F. Navas, "On the robustness of least-squares Monte Carlo (LSM) for pricing American derivatives," *Review of Derivatives Research*, vol. 6, no. 2, pp. 107–128, 2003.

[8] L. Stentoft, "Convergence of the least squares Monte Carlo approach to American option valuation," *Management Science*, vol. 50, no. 9, pp. 1193–1203, 2004.

[9] S. Crépey and A. Rahal, "Pricing convertible bonds with call protection," *Journal of Computational Finance*, vol. 15, no. 2, pp. 37–75, 2011.

[10] M. Ammann, A. Kind, and C. Wilde, "Simulation-based pricing of convertible bonds," *Journal of Empirical Finance*, vol. 15, no. 2, pp. 310–331, 2008.

[11] K. Tsiveriotis and C. Fernandes, "Valuing convertible bonds with credit risk," *The Journal of Fixed Income*, vol. 8, no. 2, pp. 95–102, 1998.

[12] D. Duffie and K. J. Singleton, "Modeling term structures of defaultable bonds," *Review of Financial Studies*, vol. 12, no. 4, pp. 687–720, 1999.

[13] E. Ayache, P. A. Forsyth, and K. R. Vetzal, "Valuation of convertible bonds with credit risk," *The Journal of Derivatives*, vol. 11, no. 1, pp. 9–29, 2003.

[14] S. L. Heston, "A closed-form solution for options with stochastic volatility with applications to bond and currency options," *Review of Financial Studies*, vol. 6, no. 2, pp. 327–343, 1993.

[15] J. G. Huang, S. C. Yang, and X. Feng, "Valuation of convertible bond with dynamic credit risk," *Mathematical Statistics and Management*, vol. 27, no. 6, pp. 1108–1116, 2008.

[16] Z. L. Zheng and H. Lin, "Estimation of the default risk premium in China," *Securities Market Herald*, vol. 13, no. 6, pp. 41–44, 2003.

Hindawi Publishing Corporation
Discrete Dynamics in Nature and Society
Volume 2014, Article ID 612064, 10 pages
http://dx.doi.org/10.1155/2014/612064

Research Article

Structural Analysis and Total Coal Demand Forecast in China

Qing Zhu,[1,2] Zhongyu Zhang,[1,2] Rongyao Li,[3] Kin Keung Lai,[2,4] Shouyang Wang,[5] and Jian Chai[2,5]

[1] *School of Finance and Economics, Xi'an Jiaotong University, Xi'an 710061, China*
[2] *International Business School, Shaanxi Normal University, Xi'an 710119, China*
[3] *College of Economics and Management, Southwest University, Chongqing 400715, China*
[4] *College of Business, City University of Hong Kong, Tat Chee Avenue, Kowloon, Hong Kong*
[5] *National Center for Mathematics and Interdisciplinary Science, Chinese Academy of Sciences, Beijing 100190, China*

Correspondence should be addressed to Jian Chai; chaijian0376@126.com

Received 7 March 2014; Accepted 16 May 2014; Published 5 June 2014

Academic Editor: Chuangxia Huang

Considering the speedy growth of industrialization and urbanization in China and the continued rise of coal consumption, this paper identifies factors that have impacted coal consumption in 1985–2011. After extracting the core factors, the Bayesian vector autoregressive forecast model is constructed, with variables that include coal consumption, the gross value of industrial output, and the downstream industry output (cement, crude steel, and thermal power). The impulse response function and variance decomposition are applied to portray the dynamic correlations between coal consumption and economic variables. Then for analyzing structural changes of coal consumption, the exponential smoothing model is also established, based on division of seven sectors. The results show that the structure of coal consumption underwent significant changes during the past 30 years. Consumption of both household sector and transport, storage, and post sectors continues to decline; consumption of wholesale and retail trade and hotels and catering services sectors presents a fluctuating and improving trend; and consumption of industry sector is still high. The gross value of industrial output and the downstream industry output have been promoting coal consumption growth for a long time. In 2015 and 2020, total coal demand is expected to reach 2746.27 and 4041.68 million tons of standard coal in China.

1. Introduction

As the basic source of energy, coal has facilitated the rapid development of the Chinese economy and has had a positive effect on the stability of the market economy. Therefore, in order to avoid indiscriminate production effectively, improving the efficiency of the coal industry and ensuring national energy security and accurate prediction of coal demand are necessary.

In the past, scholars have established a variety of energy demand forecasting models for different countries and regions as well as different kinds of energy. Traditional methods such as time series, regression, econometric, decomposition, unit root test and cointegration, ARIMA (autoregressive integrated moving average), and input-output, as well as soft computing techniques such as fuzzy logic, GA (genetic algorithm), and ANN (artificial neural networks) are being extensively used for demand side management. Support vector regression, ACO (ant colony), and PSO (particle swarm optimization) are new techniques being adopted for energy demand forecasting. Bottom up models such as MARKAL (acronym for MARKet ALlocation) and LEAP (long-range energy alternatives planning model) are also being used at the national and regional level for energy demand management [1].

For foreign energy consumption, Ediger and Akar [2] considered that estimated economic and demographic parameters usually deviate from the realizations. Time-series forecasting appears to give better results, so they used the ARIMA and SARIMA (seasonal ARIMA) methods to estimate the future primary energy demand of Turkey from 2005 to 2020. Mohr and Evans [3] considered the model of worldwide coal production developed for three scenarios (Hubbert Linearisation method scenario, reserves plus cumulative production scenario, best guess scenario). The ultimately recoverable resources (URR) estimates used in the scenarios ranged from 700 Gt to 1243 Gt. Unler [4] proposed a model to forecast the energy demand of Turkey until 2025 by using PSO-based energy demand forecasting (PSOEDF) and made a comparison with the ant colony optimization (ACO) energy demand estimation model. The result showed that the former algorithm had better accuracy. Lee and Chiu [5] applied a newly developed panel smooth transition regression model with the error-correction term (PSECM) to estimate the nonlinear relationships among energy consumption, real income, and real energy prices for 24 OECD countries.

For domestic energy consumption, various approaches to forecasting have been used in the literature, including cointegration and error correction models [6] and demand equations [7]. In 2002, Yu and Zhu [8] proposed an improved hybrid algorithm called PSO-GA (particle swarm optimization-genetic algorithm) for energy demand forecasting in China with higher precision compared with single optimization methods, such as GA, PSO or ant colony optimization, and multiple linear regressions. Results of this study show that China's energy demand will be 4.70 billion tons coal equivalent in 2015. In the same year, they also proposed mix-encoding particle swarm optimization and radial basis function (MPSO-RBF) network-based model to forecast China's energy consumption until 2020, based on GDP, population, proportion of industry in GDP, urbanization rate, and share of coal energy for the period from 1980 to 2009 [9]. Zhang et al. [10] forecast transport energy demand for 2010, 2015, and 2020 based on partial least square regression (PLSR) method under two scenarios by analyzing gross domestic product (GDP), urbanization rate, passenger-turnover, and freight-turnover for the period of 1990–2006. Crompton and Wu [11] applied the Bayesian vector autoregressive methodology to forecast China's energy consumption and to discuss potential implications. The results of this paper suggested that total energy consumption should increase to 2173 MtCE in 2010, an annual growth rate of 3.8%, which is slightly slower than the average rate in the past decade due to structural changes in the Chinese economy.

Among them, some of the latest techniques such as Bayesian vector autoregression (BVAR), support vector regression, ant colony, and particle swarm optimization models are being used in energy demand analysis. Chai et al. [12] established a VARX (vector autoregressive model with exogenous variables) model of crude oil market structure to study the effect of every variable on oil price by screening variables with price, supply, demand of oil, dollar index and China oil net import as the endogenous variables and reserve, speculative factors as the exogenous variables. Then, based on this VARX model and the Bayes theory, a MSBVAR (Markov switching bayes vector autoregression) model is established to identify and analyze the structural changing of oil price system structure within the study period. BVAR model and Granger-causality are applied to study growth in energy demand and the relationship between energy consumption and real gross domestic product per capita in selected few Caribbean countries [13]. Bayesian neural network approach is used for short term electric load forecasting [14, 15]. The BVAR model can avoid the rigid inclusion/exclusion restrictions of VAR models by allowing inclusion of many coefficients while simultaneously controlling the extent of mathematical expectation and standard deviation to which they can be influenced by the data. This reduces the spurious correlations captured by the model, thereby reducing forecast error and improving forecasting performance.

On the basis of the background and demand mentioned above, this paper attempts to analyze structural changes of coal consumption during the past 30 years and forecast future coal demand in China up to 2020. This paper includes seven parts: introduction, describing the realistic background and the academic background for research topic; variables selection and data processing, screening the core effect factors for total coal demand; methodology, introducing VAR, BVAR, and ETS models; forecast of total coal consumption, based on VAR models, applying the impulse response function and variance decomposition to portray the dynamic correlations between coal consumption and economic variables, and forecasting total coal consumption by BVAR models; structural analysis of total coal consumption, establishing ETS models based on coal consumption of seven sectors to analyze structural changes of coal consumption and forecast total coal consumption; results and discussion, comparing forecast results of total coal consumption by BVAR models and ETS models; conclusions.

2. Variables Selection and Data Processing

Many factors that affect future demand for coal, such as domestic and international price of coal, the national policy of saving energy and reducing consumption, efficiency of resource utilization, coal consumption of downstream industries, railway and highway capacity for coal transportation, technology development, urbanization, industrial growth, industrial structure, the supply and price of other alternative energy sources (such as oil, natural gas, hydropower, nuclear power, etc.), coal production cost (pollution control costs, coal mine safety production costs, exit cost, etc.), and consumer habits.

Based upon the China Statistical Yearbook, China Energy Statistical Yearbook, China Coal Industry Yearbook, and WIND Database, this paper has identified the following influence factors of coal demand from 1985 to 2011: (1) unit of coal consumption is ten thousand tons of standard coal; (2) since most coal is consumed in industry and contribution of the secondary industry to gross domestic product (GDP) fluctuates sharply, gross industrial output (100 million yuan) and industrial structure (%) are considered important factors that affect coal consumption; (3) electric power, steel, building materials, and chemical industry are four major downstream industries that consume coal, so output of thermal power (100 million kilowatt hour), crude steel (10000 tons), and cement (10000 tons) are also factors used to forecast coal consumption; (4) effect of international prices and supply position of different substitute sources of energy on domestic coal usage and consumption, such as coal price (Newcastle in Australia/Ken blah FOB), oil price

(Europe Brent Spot Price FOB), natural gas price (Louisiana spot prices), and producer price indices for domestic industrial products by sector (power, coal, and petroleum); (5) per capita GDP (yuan) and urbanization rate (%) data are collected since the improvement of consumer capacity and change of urban structure affect the energy consumption per capita in China.

First of all, in order to eliminate the heteroscedasticity of the economic time series data and to linearize its trend, the above variables are put into the natural logarithms. Then, to prevent false regression leading to an invalid conclusion, ADF (Augment Dikey-Fuller) unit root test and cointegration test are used to examine stationarity and long-run equilibrium relationship of logarithmic time series, respectively. Finally, only the following 5 groups' data meet the conditions of the VAR model: coal consumption (COAL), gross value of industrial output (IND), output of cement industrial products (CEM), output of crude steel industrial products (STE), and output of thermal power industrial products (POW).

3. Methodology

3.1. VAR. A vector autoregressive (VAR) model based on statistical properties of the data is established, without exerting a theory of a priori constraints for the data mechanism, so it is an unstructured time series model, not a structural econometric model with a theoretical foundation. Specifically, all economic variables are considered as endogenous variables in VAR model, through multistage lag regression, to estimate their relationships and for establishing forecast models.

In 1980, Sims [16] introduced the VAR model and promoted its application for dynamic analysis of the economic system extensively. VAR model is used to forecast interconnected time series system and analyze dynamic shocks from stochastic disturbances to variables, so as to explain the influence of various economic shocks on economic variables.

An unrestricted vector autoregression (UVAR) model containing n time series variables and a lag length of p has the following general form:

$$y_t = c + A_1 y_{t-1} + \cdots + A_p y_{t-p} + \mu_t, \qquad \mu_t \sim i.i.d.N\left(0, \sigma^2\right), \quad t = 1, 2, \ldots, n, \tag{1}$$

where $y_t = (y_1, y_2, \ldots, y_n)'$ is an $(n\times 1)$ vector of endogenous variables; c is an $(n \times 1)$ vector of intercept terms; A_i, $i > 1$, are $(n \times n)$ coefficient matrices; and μ_t is an $(n \times 1)$ vector of the independent normal random error vector.

Based on the VAR model, the dynamic relationship between the variables can be analyzed by impulse response function and variance decomposition.

Impulse response function describes the effect on the current and future variables from information shocks of a random disturbance which equals a standard deviation, and vividly depicts the path changes of the dynamic interaction between the variables and tests the intensity and duration of the impact of economic variables on coal consumption. This function implies that decomposition does not have to completely depend on the order of the variables in the VAR system, so as to improve the stability and reliability of the estimation results.

Variance decomposition method decomposes mean square error (MSE) of the forecast system into contributions of each variable, facilitating examination of MSE decomposition of any endogenous variables and measurement of the relative importance of random disturbances for the variables by comparing the variance contribution rate. In this paper, through the variance decomposition method, the role of the economic variables fluctuation in coal consumption growth can be determined.

3.2. BVAR. In (1), the vector c contains n intercept terms and each matrix A_i contains n^2 coefficients; hence, with the increase of variables and lag, $n + pn^2$ coefficients must be estimated, which increase exponentially with the number of variables in the system. A major problem in estimation of VAR models when p is large is over-parameterization, where too many coefficients must be estimated, relative to sample size. This can lead to an overfitting problem: the large number of coefficients in unrestricted VAR models tends to fit the data unrealistically well, while performing poorly in out-of-sample forecasting due to the effects of spurious correlations in the data set. Over-fitting of the data can distort the long-run relationships between variables in the model and inflate coefficient values on distant lags due to low degrees of freedom [17]. In addition, VAR model ignores the a priori information and presets the same importance for all estimated parameters, which can lead to the wrong model. There are many ways to overcome the over-fitting problem. By applying certain constraints on the parameters, such as reducing the lag length, or removing some of the variables in an individual equation, can solve the problem of lower degrees of freedom effectively. But from the view of Bayesian, this means that forecasters believe that the probability of removing lags whose coefficient is zero is 100%. But it is impossible to know whether this constraint is established.

An alternate approach is the BVAR method proposed by Litterman [18, 19], Doan et al. [20], Sims [21], and Sims and Zha [22]. The BVAR approach modifies the OLS estimates of (1) by treating all coefficients as random variables around their Bayesian prior mean, such that the model has the flexibility to impose these priors, to varying degrees, on the coefficient estimates.

3.3. ETS. ETS technology appeared and was used in the 1950s. After decades of development, it became mature. However, selection of "optimum" model from different models for use began few years ago. Hyndman and Khandakar [23] summed up exponential smoothing models and divided them into fifteen types. For more details, see Table 1.

Error, Trend, and Seasonal of ETS model, respectively, represent error term, trend term, and season term, in which, (Trend, Seasonal) group includes fifteen models listed in Table 1. Residual error term is classified as overlapping forms (addition forms) and multiplication forms. On the assumption of $y_t = \mu_t + \varepsilon_t$, it is an additive errors model. On the assumption of $y_t = \mu_t(1 + \varepsilon_t)$, it is a multiplication errors model. Under the circumstances of consideration of different

Table 1: Classification and summary of ETS models.

Trend component	Seasonal component		
	N (none)	A (additive)	M (multiplicative)
N (none)	N, N	N, A	N, M
A (additive)	A, N	A, A	A, M
A_d (additive damped)	A_d, N	A_d, A	A_d, M
M (multiplicative)	M, N	M, A	M, M
M_d (multiplicative damped)	M_d, N	M_d, A	M_d, M

error forms, the above fifteen models can be extended to thirty types. From the forecast results alone, addition form or multiplication form hardly influence residual error term. However, for different sampled data, various residual error forms seem superior or inferior. Because dividing by 0 is involved, attention should be paid to select different addition or multiplication forms for residual error, trend term, or season term. When samples are all positive values, using residual error multiplication form presents an advantage. However, when samples are zero value or negative value, multiplication form model is not applicable.

4. Forecast of Total Coal Consumption by BVAR Models

In order to analyze the dynamic relationship between coal consumption and economic variables, 5 d VAR model is built based on (1). According to the lag length criteria (likelihood ratio, final prediction error, AIC, SC, and Hannan-Quinn information criterion), VAR (2) is the most appropriate model. VAR models are set up as follows:

$$\begin{bmatrix} \text{LNCOAL} \\ \text{LNIND} \\ \text{LNCEM} \\ \text{LNSTE} \\ \text{LNPOW} \end{bmatrix} = \begin{bmatrix} 4.4768 \\ -20.0313 \\ 3.1506 \\ -2.4537 \\ 2.3387 \end{bmatrix} + \begin{bmatrix} 0.6785 & 0.1126 & -0.1174 & 0.0534 & 0.4913 \\ 0.1305 & 0.5586 & 1.4616 & -0.4848 & 0.6649 \\ -0.6834 & 0.0470 & 1.0756 & 0.0198 & 0.6238 \\ 0.4434 & -0.2351 & 0.0606 & 0.8957 & 0.0600 \\ -0.2571 & 0.0139 & 0.1578 & 0.3482 & 0.9504 \end{bmatrix} \times \begin{bmatrix} \text{LNCOAL}(-1) \\ \text{LNIND}(-1) \\ \text{LNCEM}(-1) \\ \text{LNSTE}(-1) \\ \text{LNPOW}(-1) \end{bmatrix} + \begin{bmatrix} -0.3453 & -0.1248 & -0.0067 & 0.1699 & -0.2082 \\ 2.0973 & -0.4018 & -0.3793 & -0.5128 & -0.4853 \\ 0.3309 & -0.0134 & -0.7911 & -0.0454 & 0.3111 \\ -0.2974 & 0.0022 & -0.0554 & -0.2683 & 0.7020 \\ -0.0600 & -0.0030 & -0.1852 & -0.1937 & 0.0594 \end{bmatrix} \times \begin{bmatrix} \text{LNCOAL}(-2) \\ \text{LNIND}(-2) \\ \text{LNCEM}(-2) \\ \text{LNSTE}(-2) \\ \text{LNPOW}(-2) \end{bmatrix} + \begin{bmatrix} \varepsilon_1 \\ \varepsilon_2 \\ \varepsilon_3 \\ \varepsilon_4 \\ \varepsilon_5 \end{bmatrix}. \tag{2}$$

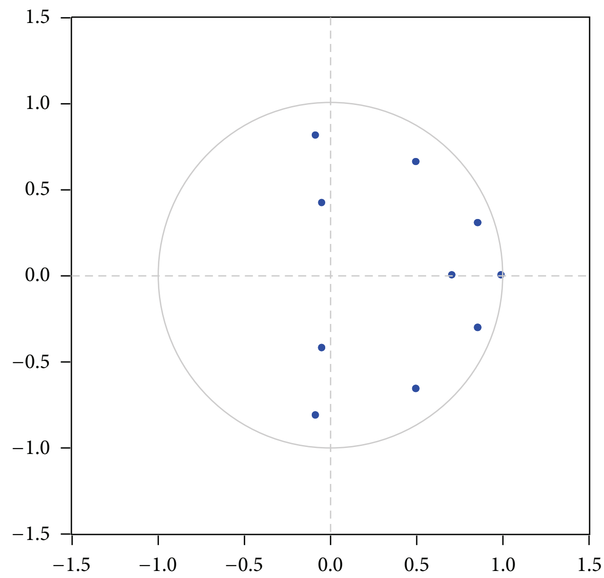

Figure 1: Inverse roots of AR characteristic polynomial.

The R-squared of the models are 0.9981, 0.9951, 0.9966, and 0.9986, which indicate good simulation results. At the same time, the reciprocals of all roots locate inside the unit circle when calculating the AR characteristic polynomial (Figure 1), which shows that the established VAR (2) model is stable. That is to say, when a variable changes in the model (i.e., to generate a shock), it leads to changes in other variables too. But as time goes on, the effect gradually disappears. In Figure 1, the horizontal axis represents the real number axis; the vertical axis represents the imaginary numbers axis; the unit circle is a circle of radius 1 and center at the origin; the points in the unit circle represent roots of the characteristic equation on VAR (2) model.

Based on the VAR model, the dynamic relationship between the variables can be analyzed by impulse response function and variance decomposition.

In Figure 2, the horizontal axis represents the lag periods of shock from innovation (unit: years); the vertical axis represents the response degree from the dependent variables to the explaining variables; the solid line is the calculated value of the impulse response function. The lag period is set to 15 years.

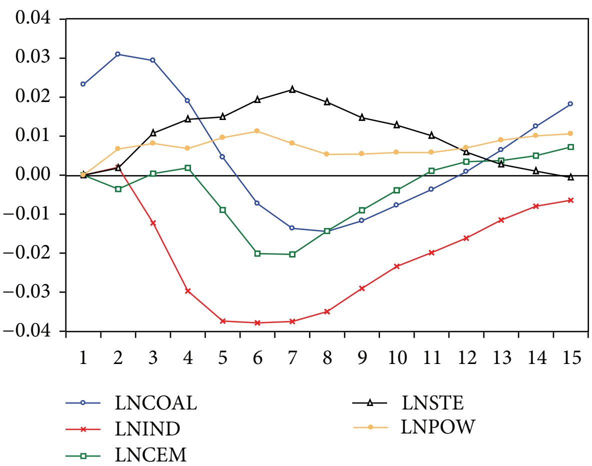

Figure 2: Responses of LNCOAL to LNCOAL, LNIND, LNCEM, LNSTE, and LNPOW.

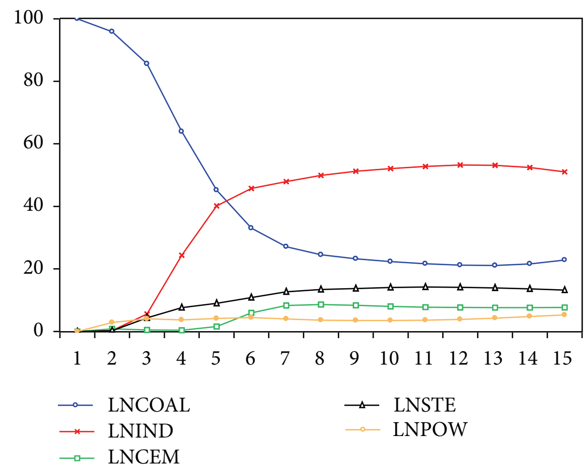

Figure 3: Factors variance decomposition on the effect of LNCOAL.

According to Figure 2, the line graph shows that when the explaining variables (coal consumption, gross value of industrial output, cement output, crude steel industrial output, and thermal power output) are shocked from innovation, respectively, how does the dependent variable (coal consumption) respond during the future 15 periods. That is to say, when these five factors change, respectively, we can forecast how much and how long will coal consumption respond.

Firstly, coal consumption volatility responds strongly to its own shock which is shown by the blue line, and in the first 15 periods it shows a fluctuating trend. Early, as a strong positive response, in the second period, it reaches the peak at 0.0310% and then plunges to the lowest point at −0.0145% in the eighth period. From this point onwards, the period between 9 and 15 experiences a gradual growth until the numbers become positive response again. This shows that coal consumption and its lagging values have a strong correlation. Secondly, after suffering a positive shock, gross value of industrial output only brings positive response to coal consumption in the second period, and then it quickly drops to a negative response, to the lowest point of −0.0379% in the sixth period. Afterwards, it rises to zero slightly. This indicates that the increase of the gross value of industrial output immediately leads to an increase in coal consumption, but in the long term it reduces consumption. The reasons may be that more output provides more capital for internal restructuring and technological progress, thus reducing coal consumption costs and increasing profits. Thirdly, coal consumption volatility responds modestly to cement output shocks in the early stage. From the fifth period to the eleventh period, the response shows a large fluctuation from negative to positive. Fourthly, coal consumption volatility has increasing positive response to crude steel industrial output shocks gradually over time, and in the seventh period that reaches the peak of 0.0219%. Fifthly, a positive shock on thermal power output brings positive response to coal consumption, which has weak intensity and stable tendency. These results indicate that the development of downstream industries drives an increase in demand for coal, whose long-term relation is in the same direction.

In Figure 3, the horizontal axis represents the lag periods of impact from innovation (unit: years); the vertical axis represents the contribution rate to coal consumption from the economic variables.

As shown in Figure 3, in the future 15 periods, coal consumption has the greatest impact during the first five periods with its own contribution rate above 40%. Since then, rates in the rest of the period level off at about 22%. The contribution rate of the gross value of industrial output to coal consumption increases steeply from the third period and then exceeds all other variables at the sixth period and remains stable and high between 51 and 53%. Thermal power industry had the highest contribution in the second period, but after that its contribution rates decline to 3-4%. Contribution rates of crude steel industry have obvious rise from the third period and make the largest contribution in the downstream industries between 12–14%. The contribution rate of cement industry has an obvious rise in the sixth period, after that, the contribution rate remains in the 7-8% level. Therefore, in the long run, industrial output has the biggest contribution to the changes of coal consumption; in a short time, coal consumption have the biggest contribution to own changes.

The system of priors commonly used in the specification of BVAR models includes conjugate prior distribution, maximum entropy prior distribution, ML-II prior distribution, and multilayer prior distribution. Different BVAR prior distributions have different impacts on the prediction results. This paper uses the *R* software to forecast coal consumption based on three kinds of prior distribution in the MSBVAR package. Command is run as follows: R > fcast < -szbvar (coal, $p = 2$, lambda 0 = 0.6, lambda 1 = 0.1, lambda 3 = 2, lambda 4 = 0.25, lambda 5 = 0, mu 5 = 0, mu 6 = 0, prior = 0). There are three different prior distributions: 0 = Normal-Wishart prior, 1 = Normal-flat prior, and 2 = flat-flat prior (i.e., akin to MLE). The forecasting results from 2012 to 2020 are shown in Table 4.

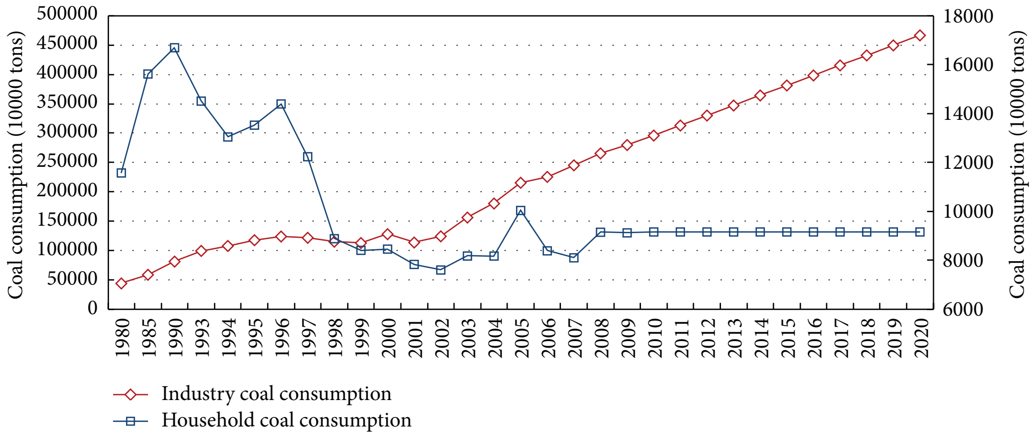

Figure 4: Changes of industry and household coal consumption.

5. Structural Analysis of Total Coal Consumption

A univariate ETS (exponential smoothing) forecast model is used to predict coal consumption of each sector in 2020 in the forecast package for *R*. Error, Trend, and Seasonal of ETS model denote error term (A, M, Z), trend term (N, A, M, Z), and season term (N, A, M, Z), respectively, in which the group includes thirty models.

From the coal balance sheet in China Statistical Yearbook and WIND Database, coal consumption data of seven sectors are selected for the period 1980–2010. The balance equation for coal consumption: Total coal consumption (TO) = Agriculture, Forestry, Animal Husbandry, Fishery and Water Conservancy (AFAFW) + Industry (IND) + Construction (CON) + Transport, Storage and Post (TSP) + Wholesale and Retail Trades, Hotels and Catering Services (WRHC) + Other Sectors (OS) + Household Consumption (HC). Unit is 10000 tons.

The final models (Table 2) are selected from thirty models by comparing information criterion (AIC, BIC, AICc) and forecast precision (mean error, root mean square error, mean absolute error, maximum permissible errors, mean absolute percentage error, mean absolute error square) (Table 3). Command is run as follows: R > fcast < -forecast(est(x)).

As can be seen from the Table 4, the total coal consumption is the sum of coal consumption in seven sectors, which is 3.9728663 billion tons in 2015. This value is similar to the goal in the development of coal industry in the twelfth five-year plan which is 3.9 billion tons in 2015. By 2020, China's total coal consumption will reach 4.83 billion tons with an annual growth rate of 4.36%, of which industry and household consumption account for the largest proportion. In Figure 4, the industry coal consumption was 438 million tons, 811 million tons, 1.278 billion tons, and 2.96 billion tons in 1980, 1990, 2000, and 2010, respectively, and it is predicted to reach 4.669 billion tons in 2020 accounting for 96.67% of total coal consumption. Therefore, to reduce coal consumption in China, industrial energy conservation and emissions reduction are the fastest and most effective breakthrough points, including the adjustment of industrial structure and optimization of technology.

However, as the second largest main channel, the proportion of household consumption is decreasing year by year. Figure 4 shows that household consumption was up to 167 million tons in 1990, which accounts for 15.83% of the total coal consumption. By 2020, household consumption will be 0.92 million tons accounting for 1.89% of the total coal consumption. In the field of household energy consumption, as the diversity of the type of energy and development of technology, electricity and heating oil are more available and convenient than coal for residents, so less and less coal is used in the household rapidly. This is beneficial to environmental protection and nonrenewable resources saving.

As shown in Figure 5, transport, storage, and post sectors were the largest coal consumption sectors in 1980, but they became the lowest coal consumption sectors after thirty years in 2010, and their coal consumption will decline constantly during the next decade by predictions. The main reason is that coal-fired steam locomotive engines have been replaced by internal combustion and electric locomotives by the railways. So, most of the raw coal has been replaced by fuel and electricity at the same time. Nowadays, road transportation mainly consumes gasoline and diesel oil; waterways transportation mainly consumes fuel oil and diesel oil; air transport mainly consumes aviation kerosene. Therefore, although the development of transport, storage, and post sectors still consumes large amounts of energy, the usage of coal is insignificant.

As the pillar industry of national economy in our country, construction sector is also an energy-intensive industry. Coal consumption increased from 5.56 to 7.1892 million tons between 1980 and 2010, representing a relatively small growth. By forecasting, the amount of coal consumption is still increasing in the future (Figure 5). At the same time, the construction sector does not have a high proportion of coal consumption and accounted for only 0.23% in 2010. That is because there are various types of energies consumed by the construction industry, including raw coal, gasoline, diesel oil, fuel oil, heat, electricity, and other petroleum products. With

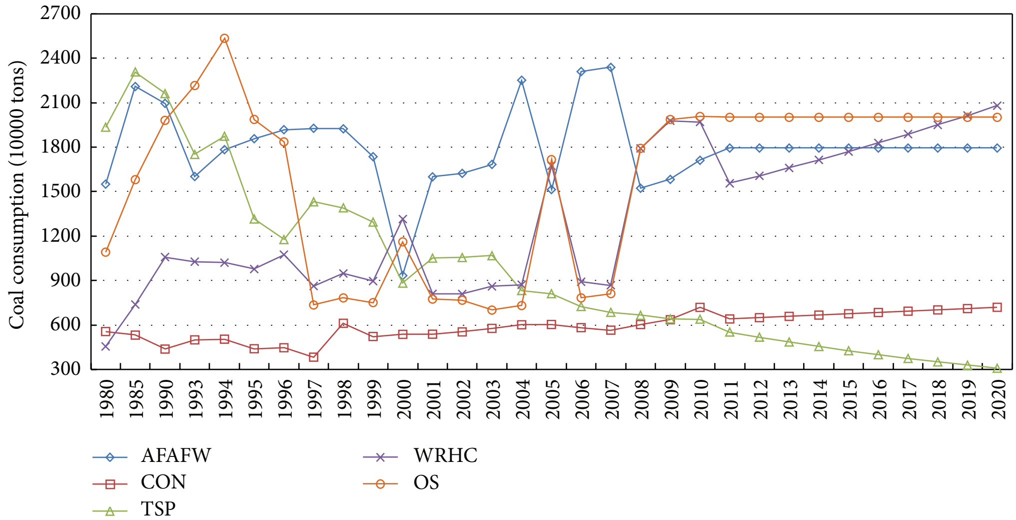

Figure 5: Changes of other sectors' coal consumption.

Table 2: Formulae for recursive calculations, point forecasts, and parametric estimated value on sector by ETS method.

Variables	Forms	Models and parameters
AFAFW	(M, N, N)	$l_t = \alpha y_t + (1-\alpha) l_{t-1}$, $\hat{y}_{t+h\|t} = l_t$, $y_{t+1} = \hat{y}_{t+1\|t}(1+\varepsilon_t)$, $\varepsilon_t \sim NID(0,\sigma^2)$, $0<\alpha<1, 0<\beta<\alpha$, $\alpha = 0.0001, l = 1793.7859, \sigma = 0.1809$
IND	(A, A, N)	$l_t = \alpha y_t + (1-\alpha)(l_{t-1}+b_{t-1})$, $b_t = \beta(l_t - l_{t-1}) + (1-\beta) b_{t-1}$, $\hat{y}_{t+h\|t} = l_t + hb_t$ $y_{t+1} = \hat{y}_{t+1\|t} + \varepsilon_t$, $\varepsilon_t \sim NID(0,\sigma^2)$, $0<\alpha<1, 0<\beta<\alpha$, $\alpha = 0.9999, \beta = 0.2697$, $l = 54782.1109, b = 9338.5498, \sigma = 12910.3600$
CON	(A, A, N)	$l_t = \alpha y_t + (1-\alpha)(l_{t-1}+b_{t-1})$, $b_t = \beta(l_t - l_{t-1}) + (1-\beta) b_{t-1}$, $\hat{y}_{t+h\|t} = l_t + hb_t$ $y_{t+1} = \hat{y}_{t+1\|t} + \varepsilon_t$, $\varepsilon_t \sim NID(0,\sigma^2)$, $0<\alpha<1, 0<\beta<\alpha$, $\alpha = 0.0009, \beta = 0.0009, l = 448.3868, b = 8.7382, \sigma = 53.6530$
TSP	(M, M, N)	$l_t = ay_t + (1-a) l_{t-1}b_{t-1}$, $b_t = \beta(l_t/l_{t-1}) + (1-\beta) b_{t-1}$, $\hat{y}_{t+h\|t} = l_t b_t^h$ $y_{t+1} = \hat{y}_{t+1\|t}(1+\varepsilon_t)$, $\varepsilon_t \sim NID(0,\sigma^2)$, $0<\alpha<1, 0<\beta<\alpha$, $\alpha = 0.0001, \beta = 0.0001, l = 2305.0531, b = 0.9371, \sigma = 0.1049$
WRHC	(M, M, N)	$l_t = ay_t + (1-a) l_{t-1}b_{t-1}$, $b_t = \beta(l_t/l_{t-1}) + (1-\beta) b_{t-1}$, $\hat{y}_{t+h\|t} = l_t b_t^h$ $y_{t+1} = \hat{y}_{t+1\|t}(1+\varepsilon_t)$, $\varepsilon_t \sim NID(0,\sigma^2)$, $0<\alpha<1, 0<\beta<\alpha$, $\alpha = 0.0001, \beta = 0.0001, l = 765.1436, b = 1.0328, \sigma = 0.2562$
OS	(A, N, N)	$l_t = ay_t + (1-a) l_{t-1}$, $\hat{y}_{t+h\|t} = l_t$ $y_{t+1} = \hat{y}_{t+1\|t} + \varepsilon_t$, $\varepsilon_t \sim NID(0,\sigma^2)$, $0<\alpha<1, 0<\beta<\alpha$, $\alpha = 0.8917, l = 1148.7978, \sigma = 497.8256$
HC	(M, N, N)	$l_t = ay_t + (1-a) l_{t-1}$, $\hat{y}_{t+h\|t} = l_t$, $y_{t+1} = \hat{y}_{t+1\|t}(1+\varepsilon_t)$, $\varepsilon_t \sim NID(0,\sigma^2)$, $0<\alpha<1, 0<\beta<\alpha$, $\alpha = 0.9999, l = 11373.6307, \sigma = 0.1327$
TO	(A, A, N)	$l_t = \alpha y_t + (1-\alpha)(l_{t-1}+b_{t-1})$, $b_t = \beta(l_t - l_{t-1}) + (1-\beta) b_{t-1}$, $\hat{y}_{t+h\|t} = l_t + hb_t$ $y_{t+1} = \hat{y}_{t+1\|t} + \varepsilon_t$, $\varepsilon_t \sim NID(0,\sigma^2)$, $0<\alpha<1, 0<\beta<\alpha$, $\alpha = 0.9999, \beta = 0.1665, l = 78421.9911, b = 9365.1674, \sigma = 14646.2100$

In the above formulae for recursive calculations and point forecasts: l_t denotes the series level at time t; b_t denotes the slope at time t; α and β are smoothness index; h denotes the lag period.

the development of technology, the construction sector will become dependent on power and all kinds of oil products increasingly instead of coal, which can improve the energy efficiency and control environmental pollution gradually.

Wholesale and retail trade and hotels and catering services consume coal, electricity, heat, gasoline, diesel oil, liquefied petroleum gas, natural gas, and other varieties of energy. Influenced by price changes and economic development, this sector has gone through booms and busts repeatedly. From 1980 to 1990, the sector had a rising trend due to adapting to the market demand quickly; from 1990 to 1997 with high price, the sector was in the integration stage; from 1997 to 1999, the sector was in a low price and low growth stage; from 2000 to 2004, the sector was in a low price and high

Table 3: Accuracy of forecast models on sector by ETS method.

	AFAFW	IND	CON	TSP	WRHC	OS	HC	TO
AIC	310.7869	469.4980	239.2015	272.4609	308.5274	328.7655	371.5486	474.7963
AICc	311.4536	471.9980	241.7015	274.9609	311.0274	329.4321	372.2153	477.2963
BIC	312.8760	473.6761	243.3796	276.6390	312.7055	330.8545	373.6377	478.9744
ME	−0.1636	1297.1479	0.2783	5.3547	−21.8557	45.5007	−105.4612	1903.6901
RMSE	324.4691	12910.3640	53.6530	154.4569	309.8943	497.8256	1540.4774	14646.2092
MAE	255.6755	10635.7804	39.6210	115.8266	272.7594	365.0402	1081.5817	11811.2234
MPE	−4.0490	−0.2898	−1.0556	−0.8693	−10.5543	−6.4377	−1.9142	−0.1609
MAPE	15.7232	9.8982	7.7865	8.7576	27.1766	30.0246	9.6963	9.3149
MASE	0.7907	0.7024	0.8702	0.7315	1.1268	0.9915	0.9609	0.7435

Table 4: Forecasting result of coal consumption on sector by ETS method.

ETS	TO	AFAFW	IND	CON	TSP	WRHC	OS	HC
2011	328820.36	1793.79	313117.60	640.68	552.60	1555.68	2000.86	9159.17
2012	345931.25	1793.79	330203.50	649.42	517.87	1606.66	2000.86	9159.17
2013	363045.90	1793.79	347289.30	658.16	485.32	1659.31	2000.86	9159.17
2014	380164.41	1793.79	364375.20	666.91	454.81	1713.68	2000.86	9159.17
2015	397286.63	1793.79	381461.10	675.65	426.23	1769.84	2000.86	9159.17
2016	414412.38	1793.79	398546.90	684.39	399.44	1827.84	2000.86	9159.17
2017	431541.82	1793.79	415632.80	693.14	374.33	1887.74	2000.86	9159.17
2018	448674.80	1793.79	432718.70	701.88	350.80	1949.61	2000.86	9159.17
2019	465811.18	1793.79	449804.50	710.62	328.75	2013.50	2000.86	9159.17
2020	482951.14	1793.79	466890.40	719.37	308.09	2079.48	2000.86	9159.17

Unit: 10000 tons.

growth stage; domestic prices began to soar in 2005 and since the American subprime crisis and the domestic policy adjustment in 2008, the sector appears to have had violent fluctuations. However, Figure 5 shows that the wholesale and retail trade, hotels, and catering services will have a growth trend of coal consumption in the future. Industry scale will continue to expand, which is consistent with our country's policy to develop the tertiary industry vigorously.

Agriculture, forestry, animal husbandry, fishery, and water conservancy are the foundation of the national economy. Coal consumption was in the second place before 1990, but in 1993, 2000, 2005, and 2008 there was a great fall (Figure 5); in contrast, coal consumption of wholesale and retail trade, hotels, and catering services, and other sectors had an obvious increase in these three years. Considerable contact with the change of the prices is guessed.

Table 5: Total coal consumption forecast.

	BVAR Prior = 0 or 1	BVAR Prior = 2	ETS aggregation	ETS forecast
2011	238033.37	238033.37	234876	234475
2012	252686.75	254034.07	247099	245921
2013	268152.68	257667.41	259324	257366
2014	284494.14	257113.39	271551	268811
2015	**301762.9**	**274627.29**	**283782**	**280256**
2016	320015.13	314720.65	296014	291701
2017	339311.96	360700.12	308250	303146
2018	359720.03	401190.03	320489	314591
2019	381312.12	444913.39	332729	326037
2020	**404167.84**	**504823.69**	**344972**	**337481**

Unit: 10000 tons of standard coal.

6. Results and Discussion

Table 5 shows prediction results of BVAR models under the three different prior distributions and the ETS models. The unit is 10000 tons in ETS models, which is 10000 tons of standard coal in BVAR models. So the results of ETS model are multiplied by the converted coefficient of 0.7143 as tons of standard coal.

The result of BVAR models under the normal-Wishart prior distribution (prior = 0) is the same as under the normal-flat prior distribution (prior = 1). Using the ETS model to predict coal consumption of every sector and then adding the seven values to get 3.44972 billion tons of standard coal in 2020; only based on the historical total coal consumption, 3.37481 billion tons of standard coal are obtained in 2020 directly. From Table 5, in 2015 forecast results of four methods have small differences. But in 2020, the results of BVAR model are larger than ETS model (Figure 6).

The reason may be that in BVAR model, the gross value of industrial output and the downstream industrial production are influencing factors, whose values are increasing over the

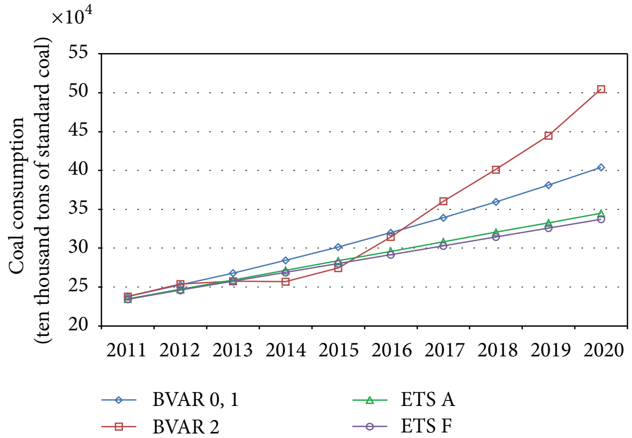

Figure 6: Total coal consumption forecast.

years. So they drive the rise in total coal consumption in the long run. However, in ETS model, total coal consumption is the sum of coal consumption in seven sectors, and the above has introduced that the coal consumption of some sectors has showed a decreasing trend, such as agriculture, forestry, animal husbandry, fishery and water conservancy, transport, storage, and post. So the ETS model prediction results are smaller.

7. Conclusions

China is a big developing country in the process of industrialization and urbanization, and therefore coal consumption will remain high in the future, for a long time. Based on guaranteeing the stability of the VAR system, coal consumption, gross industrial output value, and the downstream industrial production (crude steel, cement, thermal power) are selected as variables to establish the BVAR (2) model. At the same time, this paper analyses the changes of coal consumption structure based on sector division. The forecast models are selected through comparing information criteria and forecast accuracy comparison from thirty ETS models. By forecasting the total coal consumption and analyzing structural changes, this paper gets the following main conclusions.

(1) Results of the impulse response function indicate that the increased output of the downstream industry will become a driving force of coal consumption. In the first two periods, the same response has been there, with the increase of the gross value of industrial output. Later there will be a negative response.

(2) The variance decomposition results show that the contribution of gross value of industrial output accounted for 50% of growth in coal consumption and has long-term stable influence; in the downstream industry, the contribution rate of crude steel output is greater than that of the cement output and thermal power output.

(3) In the next decade, from a sector division point of view, industry and household consumption account for the largest proportion of total coal consumption; the proportion of industrial coal consumption will continue to rise, but the proportion of household coal consumption will continue to decline. Transport, storage, and post sectors were the largest consumers of coal consumption in 1980, which will become the lowest in the future. Construction sector, despite its lower reliance on coal, has experienced a rise in coal consumption in recent years. The scales of consumption of wholesale and retail trade, hotels and catering services, agriculture, forestry, animal husbandry, fishery, and water conservancy sectors were influenced by price fluctuations in the past few decades, causing the fluctuation of coal consumption. But in the next decade, coal consumption of both sectors will have a rising trend.

(4) The BVAR (2) forecast models predict that in 2015 coal demand will reach 2.75–3.02 billion tons of standard coal, and in 2020 it will reach 4.04–5.05 billion tons of standard coal in China. That is to say, as the momentum of rapid development of China's economy in the future, the coal consumption in 2020 is almost double that of in 2012 which is 2.46–2.53 billion tons of standard coal. However, because the unrenewable characteristics of the coal and the pollution caused by burning are bound to draw the attention of the country and the residents, how to improve the coal utilization efficiency and promote the use of clean energy will become a main research direction in the future.

Conflict of Interests

The authors declare that there is no conflict of interests regarding the publication of this paper.

Acknowledgments

This research is supported by the National Natural Science Foundation of China (no. 71103115); the China Postdoctoral Science Foundation surface of funded projects (no. 2012M510580); the Fundamental Research Funds for the Shaanxi province soft science (no. 2012KRM95). The authors would like to thank the anonymous referees.

References

[1] L. Suganthi and A. A. Samuel, "Energy models for demand forecasting—a review," *Renewable and Sustainable Energy Reviews*, vol. 16, no. 2, pp. 1223–1240, 2012.

[2] V. S. Ediger and S. Akar, "ARIMA forecasting of primary energy demand by fuel in Turkey," *Energy Policy*, vol. 35, no. 3, pp. 1701–1708, 2007.

[3] S. H. Mohr and G. M. Evans, "Forecasting coal production until 2100," *Fuel*, vol. 88, no. 11, pp. 2059–2067, 2009.

[4] A. Unler, "Improvement of energy demand forecasts using swarm intelligence: the case of Turkey with projections to 2025," *Energy Policy*, vol. 36, no. 6, pp. 1937–1944, 2008.

[5] C.-C. Lee and Y.-B. Chiu, "Modeling OECD energy demand: an international panel smooth transition error-correction model," *International Review of Economics & Finance*, vol. 25, pp. 372–383, 2013.

[6] H. Chan and S. Lee, "Forecasting the demand for energy in China," *Energy Journal*, vol. 17, no. 1, pp. 19–30, 1996.

[7] C. V. Hirschhausen and M. Andres, "Long-term electricity demand in China—from quantitative to qualitative growth?" *Energy Policy*, vol. 28, no. 4, pp. 231–241, 2000.

[8] S.-W. Yu and K.-J. Zhu, "A hybrid procedure for energy demand forecasting in China," *Energy*, vol. 37, no. 1, pp. 396–404, 2012.

[9] S. W. Yu, Y.-M. Wei, and K. Wang, "China's primary energy demands in 2020: predictions from an MPSO-RBF estimation model," *Energy Conversion and Management*, vol. 61, pp. 59–66, 2012.

[10] M. Zhang, H. L. Mu, G. Li, and Y. D. Ning, "Forecasting the transport energy demand based on PLSR method in China," *Energy*, vol. 34, no. 9, pp. 1396–1400, 2009.

[11] P. Crompton and Y. R. Wu, "Energy consumption in China: past trends and future directions," *Energy Economics*, vol. 27, no. 1, pp. 195–208, 2005.

[12] J. Chai, Z. Y. Zhang, J. L. Fu, J. E. Guo, and S. Y. Wang, "Identification and analysis of the structural mutations in oil price system," *Journal of Management Sciences*, vol. 27, no. 2, pp. 133–144, 2014 (Chinese).

[13] B. M. Francis, L. Moseley, and S. O. Iyare, "Energy consumption and projected growth in selected Caribbean countries," *Energy Economics*, vol. 29, no. 6, pp. 1224–1232, 2007.

[14] L. M. Saini, "Peak load forecasting using Bayesian regularization, Resilient and adaptive backpropagation learning based artificial neural networks," *Electric Power Systems Research*, vol. 78, no. 7, pp. 1302–1310, 2008.

[15] P. Lauret, E. Fock, R. N. Randrianarivony, and J.-F. Manicom-Ramsamy, "Bayesian neural network approach to short time load forecasting," *Energy Conversion and Management*, vol. 49, no. 5, pp. 1156–1166, 2008.

[16] C. A. Sims, "Macroeconomics and reality," *Econometrica*, vol. 48, no. 1, pp. 1–48, 1980.

[17] T. Zha, "A dynamic multivariate model for use in formulating policy," *Economic Review*, vol. 83, no. 1, pp. 16–29, 1998.

[18] R. B. Litterman, "A Bayesian procedure for forecasting with vector autoregressions," Department of Economics Working Paper, Massachusetts Institute of Technology, 1980.

[19] R. B. Litterman, "Forecasting with Bayesian vector autoregressions: five years of experience," *Journal of Business and Economic Statistics*, vol. 4, no. 1, pp. 25–38, 1986.

[20] T. Doan, R. B. Litterman, and C. A. Sims, "Forecasting and conditional projection using realistic prior distributions," *Econometric Reviews*, vol. 3, no. 1, pp. 1–100, 1984.

[21] C. A. Sims, "A nine-variable probabilistic macroeconomic forecasting model," in *Business Cycles, Indicators, and Forecasting*, J. H. Stock and M. W. Watson, Eds., University of Chicago Press, Chicago, Ill, USA, 1992.

[22] C. A. Sims and T. A. Zha, "Bayesian methods for dynamic multivariate models," *International Economic Review*, vol. 39, no. 4, pp. 949–968, 1998.

[23] R. J. Hyndman and Y. Khandakar, "Automatic time series forecasting: the forecast package for R," *Journal of Statistical Software*, vol. 27, no. 3, pp. 1–22, 2008.

Hindawi Publishing Corporation
Discrete Dynamics in Nature and Society
Volume 2014, Article ID 694568, 9 pages
http://dx.doi.org/10.1155/2014/694568

Research Article

Dynamic Pricing Based on Strategic Consumers and Substitutes in a Duopoly Setting

Gongbing Bi, Lechi Li, Feng Yang, and Liang Liang

School of Management, University of Science and Technology of China, No. 96 Jinzhai Road, Hefei, Anhui 230026, China

Correspondence should be addressed to Feng Yang; fengyang@ustc.edu.cn

Received 19 March 2014; Accepted 24 April 2014; Published 27 May 2014

Academic Editor: Fenghua Wen

Based on the rational strategic consumers, we construct a dynamic game to build a two-period dynamic pricing model for two brands of substitutes which are sold by duopoly. The solution concept of the dynamic game is Nash equilibrium. In our model, consumers have been clearly segmented into several consumption classes, according to their expected value of the products. The two competing firms enter a pricing game and finally reach the state of Nash equilibrium. In addition, decision-making process with only myopic consumers existing in the market is analyzed. To make the paper more practical and realistic, the condition, in which the myopic and strategic consumers both exist in the market, is also considered and studied. In order to help the readers understand better and make it intuitively more clearly, a numerical example is given to describe the influence of the main parameters to the optimal prices. The result indicates that, to maintain the firms' respective optimal profits, the prices of the products should be adjusted appropriately with the changes of product differentiation coefficient.

1. Introduction

Pricing and product differentiation are among the most important strategies for firms in the competitive product market. In order to increase profits, the manufactures usually apply various strategies, including selling their products in several periods.

Dynamic pricing, which means that product prices are changed periodically over time to maximize revenue, are widely applied in product market. It has received considerable attention in research and application in recent years. The benefits of dynamic pricing methods have been known in some relatively stable industries, such as airlines, hotels, and electric utilities, where the capacity is fixed in the short term and perishable. Recently, an increasing adoption of dynamic pricing methods in retail and other industries appears. Elmaghraby and Keskinocak [1] thought that three factors contributed to this phenomenon: (1) the increased availability of demand data; (2) the ease of changing prices due to new technologies; and (3) the availability of decision-support tools for analyzing demand data and dynamic pricing.

Determining the optimal prices in different periods requires the decision maker to know not only his own operating costs and the supply ability, but also how much the customers value the products and what the future demand will be. Thus, to charge a customer the right price, a company must get a wealth of information about its customer base and its competitor and also be able to set and adjust its prices at the minimal cost. Until recently, a certain amount of papers has done some research on dynamic pricing in various aspects, such as the quantity of manufactures and products, different categories of goods, and even taking inventory into account. Mitra [2] constructed a dynamic pricing model for different quality remanufactured goods in order to reach the maximum profits. Feng and Gallego [3] discussed a dynamic pricing problem of multiproducts. Federgruen and Heching [4] discussed the pricing and inventory strategy in the condition of uncertain demand. The current paper focuses on the dynamic pricing mechanisms for two brands of substitutes which are sold by duopoly with the condition that strategic consumers exist in the market.

Product differentiation is an effective way for firms to occupy the market share and increase firm's profits in a competitive market. And the strategy of product differentiation has been prevalent in many areas of our society, such as food products, electronics, and even aviation industry. In the aspect of pricing, firms in many industries often adjust their strategies to vary prices over time in order to better manage demand and increase profits. When making pricing decisions, a firm should take both the strategies of substitutes produced by their competitors and the same products sold in different cycles into consideration.

Product differentiation in the markets is often complicated by the fact that decision processes for the market participants are intrinsically dynamic. In economics and marketing, product differentiation (also known simply as differentiation) is the process of distinguishing a product offered by others and making it more attractive to a particular target market. This involves differentiating it from competitors' products as well as a firm's own goods offerings. The concept was proposed by Chamberlin [5] in his *Theory of Monopolistic Competition*. One manufacture's products are considered as the substitutes of its competitors' products. However, most durable goods are sold in several periods, so the same goods sold in different selling cycles are also regarded as substitutes. A related problem was considered by Liu and Van Ryzin [6]. They studied a two-period model with strategic consumers and quantity decisions (rather than pricing) being taken into consideration. And the model was applied to induce early purchases.

Consumer choice models are studied extensively in the marketing literature. A survey of consumer choice and strategic behavior models in retail management is found from the paper of Shen and Su [7]. The heterogeneity of consumers in the market determines that different customers have disparate valuation of different products. Consumers employ a variety of consumption patterns with actions that vary in time, even for a single brand of goods. In terms of their various psychology and behavioral characteristics, the consumers are divided into two types: myopic versus strategic customers. Elmaghraby and Keskinocak [1] had done some research on dynamic pricing in the presence of inventory considerations. They put forward a detailed expression of the two types of customers: "The purchasing behavior of the customers affects the seller's pricing decisions over time. A myopic customer is the one who makes a purchase immediately if the price is below his/her valuation (reservation price), without considering future prices. Myopic (or nonstrategic) customer's behavior allows the seller to ignore any detrimental effects of future price cuts on current customer purchases. Conversely, a strategic (or rational) customer takes into account the future path of prices when making purchasing decisions. Dynamic pricing decisions of a seller faced strategic customers is more complex, for the sake that the seller has to consider the effects of future and current prices on customers' purchasing decisions."

Although it seems that most of the ingredients in our model have been studied, one of the distinctive features and the innovation point of this paper is that it explores, in a unified model, all strategic interactions, and we combined the strategies into a special marketplace. In such a market circumstance, two competing firms sell products to a finite population of consumers in two selling periods, and each firm sells only one type of products. What is more, we also bring forth new ideas, in which all the situations of how consumers exist in the market are considered. A very important point, what our model distinguishes from others, is that it provides a dynamic game for duopoly and solved by Nash equilibrium, which is more easily understood. And this point is our core innovation. Through the analysis and simulation of our model, we derived the optimal price strategies for both firms expressed in the form of mathematical model. Executing these strategies is beneficial to both sides including the consumers. Furthermore, this framework allows us to adopt more realistic assumptions and accommodate it to the real economic market. Some of the papers we reviewed about dynamic pricing in product market setting considered only a single product, while several papers in our research studied the condition that only one manufacture exists, and their focus is mainly on static product line pricing, not dynamic pricing [8]. We hope to relax some of these limitations in our subsequent work.

The remainder of the paper proceeds as follows. In the next section, we introduce the model in a general context, and we spell out the method and hypothesis of the model. We then show in Section 3 the concept of the solution and the optimal dynamic prices are derived and presented. In the same section we also illustrate two general conditions: special condition with only myopic consumers existing in the market and myopic consumers and strategic consumers existing in the market in a certain proportion θ. In Section 4, the intuitive numerical simulation is examined in this part. We summarize our main findings of this work and outline new directions for further research in the last section. Proofs of proposition and the optimal profits are found in Appendix A.

2. Problem Descriptions and Concept of Pricing Model

With the progress of the society and the rapid development of economy, commodities in the market are stepping forward to the direction of diversification. The version, design, and even generation of the same product are changing constantly, especially in the phone market. However, facing the diversification of products, consumers are also becoming more rational and strategic. This kind of phenomenon is very common in the mobile industry. Suppose you are a potential mobile phone consumer and you want to choose one from Samsung and iPhone. As we all know, updating speed of them is faster. So you will face several choices: purchasing Samsung or iPhone, purchasing one in the current generation of them or the later one. Then the decision problem appears. The manufacturers will also have to make certain pricing sales strategies due to this reality.

2.1. Products. There are two potential brands of goods, A and B, on the market, which are substitutes for each other, and they are quality-differentiated products. Two manufactures produce and sell the products A and B in two periods, respectively. We assume that brand A is produced by firm M_1 and brand B is produced by firm M_2. At the steady limit, firm M_1 and M_2 play a pricing game and eventually converge to Nash equilibrium. The duopoly faces no capacity constraints.

All goods of each brand are of equal quality and sold in two periods: the product in the second period is sold at discount while the one in the first period is sold at normal price.

2.2. Consumers. Consumers are assumed to live forever and the population of them is a constant number N. Each consumer will buy a commodity at most; in other words, the total market demand is specified by N. The consumers are assumed to be heterogeneity and independent of each other. As usual, the heterogeneity of consumers is represented by their disparate valuation of different goods or the same ones sold in different period, while the independence of them means the valuation of goods for one consumer is not influenced by others. The valuation differences may result from many kinds of reasons. For instance, Huang et al. [9] thought that the different preferences for the old and new products lead to various consumers' valuation. We suppose that the consumers' valuation parameters of brand A in the first period are specified by v. In order to obtain the results clearly, we further assume a uniform distribution for $v \in [0, U]$. We use superscript to label the period and the subscript to label the brand. The actions a consumer takes in the whole selling lifetime are represented by the following five choices: A^1, A^2, B^1, B^2, and O, where $A^1(B^1)$ stands for purchasing the brand $A(B)$ in the first period, $A^2(B^2)$ means achieving the brand $A(B)$ in the second period, while O represents not purchasing any goods. Also the prices associated with these actions are defined analogously. For instance, $\{P_A^1, P_A^2, P_B^1, P_B^2\}$ stands for the prices of A^1, A^2, B^1, and B^2, respectively. A consumer's valuation function of different goods is constructed as follows:

$$v_A^1 = v, \qquad v_A^2 = \delta_1 v, \qquad v_B^1 = \lambda v, \qquad v_B^2 = \lambda \delta_2 v. \quad (1)$$

The constraints $0 < \lambda < 1$, $0 < \delta_i < 1$ are satisfied. This choice implies that, in the same period, all consumers have the same ordering in their consumption preferences. The exogenous parameters λ and δ_i, characterized the relative qualities of different brands in the same period and the same commodity in different periods. We restrict $\lambda \in (0, 1)$ and $\delta_i \in (0, 1)$, reflecting the chosen conventions that brand A is more desirable for any given consumer than brand B in the same period, and that goods in first period are more desirable than those in the later one. In other words, brand A has higher quality than brand B in the same selling cycle, and the earlier they purchase the same product, the more utility they will get. The consumer surplus of all the conditions is figured as follows:

$$\begin{aligned} S_A^1 &= v - P_A^1, & S_A^2 &= \delta_1 v - P_A^2, \\ S_B^1 &= \lambda v - P_B^1, & S_B^2 &= \lambda \delta_2 v - P_B^2. \end{aligned} \quad (2)$$

As we have declared above, the consumers are assumed to be rational and strategic. They will make purchasing decisions based on the consumer surplus maximization conditions.

2.3. Manufacturers: M_1 and M_2. We assume that brand A is produced by firm M_1 and brand B is produced by firm M_2. The manufacturers face no capacity constraints; in other words, the products are ample for the market. The fixed costs are ignored, which they have no effect on our model and marginal costs for brands A and B are denoted by c_A and c_B, respectively, subject to the constraint $c_A \succ c_B \succ 0$, in which the left inequality is due to the different quality and brand, while the right is obvious. In the first sales cycle, the prices of products A and B are defined by P_A^1 and P_B^1, obviously, $P_A^1 \succ P_B^1$, and in the second period, the prices of the two brands can be shown as P_A^2 and P_B^2 with the constraint $P_A^2 \succ P_B^2$. In the above context, we have presumed that, in the second sales cycle, the manufacturers will sell their products at discount, so $P_A^1 \succ P_B^1$, $P_A^2 \succ P_B^2$ are easily verified.

2.4. Concept of the Pricing Model. As in any standard game, all the players in our model are assumed to be rational and to maximize their own values (for the consumers, it is the consumer surplus, while for the manufacturers it is the profits). So faced with the two different substitutes and in order to perfect their decision-making in purchasing, the consumers will consider both the surplus of purchasing periods and the surplus of the variant brands. Based on this, we easily derive the conditions that the consumer purchases A in the first period:

$$S_A^1 \geq \max\left\{S_B^1, S_A^2, S_B^2\right\}. \quad (3)$$

Equally it means

$$v - P_A^1 \geq \max\left\{\lambda v - P_B^1, \delta_1 v - P_A^2, \lambda \delta_2 v - P_B^2\right\}, \quad (4)$$

$$v \succ \max\left\{\frac{P_A^1 - P_B^1}{1-\lambda}, \frac{P_A^1 - P_A^2}{1-\delta_2}, \frac{P_A^1 - P_B^2}{1-\lambda\delta_2}\right\}. \quad (5)$$

By the same reasoning, the conditions that consumers tend to purchase the B in the first period are specified as follows:

$$\max\left\{\frac{P_B^1 - P_B^2}{\lambda(1-\delta_2)}, \frac{P_B^1 - P_A^2}{\lambda - \delta_1}\right\} \prec v \prec \frac{P_A^1 - P_B^1}{1-\lambda}. \quad (6)$$

In the later selling period, the one who has not obtained a product has the idea that the selling cycle will end up and inaction implies zero utility, so they choose to purchase A or B only if the condition, $S_A^2 \geq \max\{S_B^2, 0\}$, $S_B^2 \geq \max\{S_A^2, 0\}$, is maintained, respectively, which equally means

$$\begin{gathered} v \succ \max\left\{\frac{P_A^2 - P_B^2}{\delta_1 - \lambda\delta_2}, \frac{P_A^2}{\delta_1}\right\} \\ \frac{P_B^2}{\lambda\delta_2} \prec v \prec \frac{P_A^2 - P_B^2}{\delta_1 - \lambda\delta_2}. \end{gathered} \quad (7)$$

There are two parts in the revenue stream of one manufacturer: sale of $A(B)$ in the first period and marketing of $A(B)$ in the second cycle. These two parts in turn depend on the aggregate consumer behaviors in the two selling cycles, in particular, the number of consumers purchase $A(B)$ in

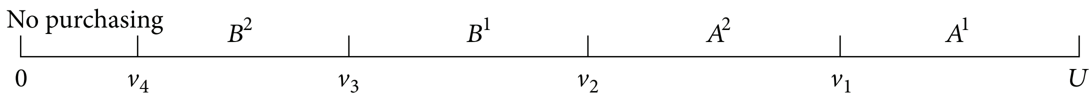

Figure 1

the first period and the later one, respectively. Here we introduce another vector,

$$Q = \left\{q_A^1, q_A^2, q_B^1, q_B^2\right\}. \tag{8}$$

The interpretation of this vector is as follows: q_i^j, with $i = A$ or B, $j = 1$ or 2, is the population of consumers in the appropriate state. Then the profit functions for $M_1(M_2)$ associated with brand $A(B)$ are given by

$$\begin{aligned}\pi_{M_1} &= \left(P_A^1 - c_A\right) * q_A^1 + \left(P_A^2 - c_A\right) * q_A^2 \\ \pi_{M_2} &= \left(P_B^1 - c_B\right) * q_B^1 + \left(P_B^2 - c_B\right) * q_B^2.\end{aligned} \tag{9}$$

3. Dynamic Pricing Based on Our Model

Our model includes two dynamic game problems. Consumers who are price takers, play the game strategically against the producers, while the manufacturer plays the game strategically against the consumers and the other producer. The manufacturers make their pricing decisions in view of consumers' strategic behaviors. This is a two-period dynamic pricing game, in which consumers with high valuation will purchase goods in the first period but not the second one, and the ones who have a comparatively low valuation will not purchase a commodity at a high price in the first selling cycle. On the other hand, as in any standard game, all the players in our model are assumed to be rational and to maximize their own values. In our research, the two manufacturers play in a dynamic pricing game to pursue the maximum profits.

According to the above context, we know that the consumers with the highest valuation will acquire A in the first period, and the ones with the lowest valuation will obtain B in the later cycle; however, the rest of them between the highest and the lowest have two choices: purchasing A in the second period or B in the first cycle, which is determined by the magnitude of the two parameters λ and δ_1. Owning to the constraints $0 < \lambda < 1$, $0 < \delta_1 < 1$, we divide them into two kinds of situations to carry on the analysis, $0 < \lambda < \delta_1 < 1$, $0 < \delta_1 < \lambda < 1$.

3.1. The Condition $0 < \lambda < \delta_1 < 1$. The present analysis shows that $v_A^1 = v$, $v_A^2 = \delta_1 v$, $v_B^1 = \lambda v$, and $v_B^2 = \lambda\delta_2 v$, in the condition $0 < \lambda < \delta_1 < 1$. We easily verify that $v_A^2 > v_B^1$. In other words, the valuation of A in the second period is higher than B in the first sales cycle, and then ordering of consumer choice is A^1, A^2, B^1, and B^2.

According to the above inequalities (5), (6), and (7), we can easily work out the class-division points and show the consumers' different purchasing states of diverse products in different cycles clearly; in addition, the market shares of substitutes are figured out (See Table 1).

Table 1: Consumers' preferences and the market shares in terms of valuation.

Valuation	Purchasing states	Market share
$v_1 \le v < U$	A^1	$N(U - v_1)/U$
$v_2 \le v < v_1$	A^2	$N(v_1 - v_2)/U$
$v_3 \le v < v_2$	B^1	$N(v_2 - v_3)/U$
$v_4 \le v < v_3$	B^2	$N(v_3 - v_4)/U$
$0 \le v < v_4$	—	—

Consumers' purchasing states are displayed in Figure 1. The class-division points are given by

$$\begin{aligned}v_1 &= \frac{P_A^1 - P_A^2}{1 - \delta_1} \\ v_2 &= \frac{P_A^2 - P_B^1}{\delta_1 - \lambda} \\ v_3 &= \frac{P_B^1 - P_B^2}{\lambda\left(1 - \delta_2\right)} \\ v_4 &= \frac{P_B^2}{\lambda\delta_2}\end{aligned} \tag{10}$$

as long as the ordering

$$0 \le v_4 \le v_3 \le v_2 \le v_1 \le U \tag{11}$$

is maintained. These expressions are found by setting the consumers' surplus functions evaluated from adjacent segments equal to one another at these indifferent points (the same theory with Huang et al., 2001). Consumers in (v_1, U) will follow the state of purchasing A^1. The same goes for other regions.

So the expected payoff functions associated with manufacturers M_1 and M_2 are expressed as follows:

$$\begin{aligned}\pi_{A_1} &= \frac{N}{U}\left(U - \frac{P_A^1 - P_A^2}{1 - \delta_1}\right)\left(P_A^1 - c_A\right) \\ \pi_{A_2} &= \frac{N}{U}\left(\frac{P_A^1 - P_A^2}{1 - \delta_1} - \frac{P_A^1 - P_B^1}{\delta_1 - \lambda}\right)\left(P_A^2 - c_A\right) \\ \pi_{M_1} &= \pi_{A_1} + \pi_{A_2}\end{aligned}$$

$$\pi_{M_1} = \frac{N}{U}\left(U - \frac{P_A^1 - P_A^2}{1-\delta_1}\right)\left(P_A^1 - c_A\right) + \frac{N}{U}\left(\frac{P_A^1 - P_A^2}{1-\delta_1} - \frac{P_A^1 - P_B^1}{\delta_1 - \lambda}\right)\left(P_A^2 - c_A\right) \tag{12}$$

$$\pi_{B_1} = \frac{N}{U}\left(\frac{P_A^1 - P_B^1}{\delta_1 - \lambda} - \frac{P_B^1 - P_B^2}{\lambda(1-\delta_2)}\right)\left(P_B^1 - c_B\right)$$

$$\pi_{B_2} = \frac{N}{U}\left(\frac{P_B^1 - P_B^2}{\lambda(1-\delta_2)} - \frac{P_B^2}{\lambda\delta_2}\right)\left(P_B^2 - c_B\right)$$

$$\pi_{M_2} = \pi_{B_1} + \pi_{B_2} \tag{13}$$

$$\pi_{M_2} = \frac{N}{U}\left(\frac{P_A^1 - P_B^1}{\delta_1 - \lambda} - \frac{P_B^1 - P_B^2}{\lambda(1-\delta_2)}\right)\left(P_B^1 - c_B\right) + \frac{N}{U}\left(\frac{P_B^1 - P_B^2}{\lambda(1-\delta_2)} - \frac{P_B^2}{\lambda\delta_2}\right)\left(P_B^2 - c_B\right).$$

3.2. The Condition $0 \prec \delta_1 \prec \lambda \prec 1$. As a similar method, in the condition $0 \prec \delta_1 \prec \lambda \prec 1$, consumers' valuation of brand B in the first period is higher than A in the second sales cycle. So it is easy to recognize that the sequence of consumer's choice of the substitutes is A^1, B^1, A^2, and B^2. Based on the preference, rational producers' pricing strategy is subject to the sequence

$$P_A^1 \succ P_B^1 \succ P_A^2 \succ P_B^2. \tag{14}$$

According to the theory in the former condition, we figure out the consumers' strategic patterns and the market shares following this condition (See Table 2).

The class-division points are given by

$$\begin{aligned} v_1 &= \frac{P_A^1 - P_B^2}{1-\lambda} \\ v_2 &= \frac{P_B^1 - P_A^2}{\lambda - \delta_1} \\ v_3 &= \frac{P_A^2 - P_B^2}{\delta_1 - \lambda\delta_2} \\ v_4 &= \frac{P_B^2}{\lambda\delta_2} \end{aligned} \tag{15}$$

as long as the sequence

$$0 \le v_4 \le v_3 \le v_2 \le v_1 \le U \tag{16}$$

is satisfied.

Table 2: Consumers' preferences and the market shares in terms of valuation.

Valuation	Purchasing states	Market share
$v_1 \le v \prec U$	A^1	$N(U - v_1)/U$
$v_2 \le v \prec v_1$	B^1	$N(v_1 - v_2)/U$
$v_3 \le v \prec v_2$	A^2	$N(v_2 - v_3)/U$
$v_4 \le v \prec v_3$	B^2	$N(v_3 - v_4)/U$
$0 \le v \prec v_4$	—	—

The expected payoff functions associated with manufacturers M_1 and M_2 are worked out with the same method of Section 3.1 as follows:

$$\pi_{M_1} = \frac{N}{U}\left(U - \frac{P_A^1 - P_B^1}{1-\lambda}\right)\left(P_A^1 - c_A\right) + \frac{N}{U}\left(\frac{P_B^1 - P_A^2}{\lambda - \delta_1} - \frac{P_A^2 - P_B^2}{\delta_1 - \lambda\delta_2}\right)\left(P_A^2 - c_A\right) \tag{17}$$

$$\pi_{M_2} = \frac{N}{U}\left(\frac{P_A^1 - P_B^1}{1-\lambda} - \frac{P_B^1 - P_A^2}{\lambda - \delta_1}\right)\left(P_B^1 - c_B\right) + \frac{N}{U}\left(\frac{P_A^2 - P_B^2}{\delta_1 - \lambda\delta_2} - \frac{P_B^2}{\lambda\delta_2}\right)\left(P_B^2 - c_B\right). \tag{18}$$

3.3. The Optimal Pricing Strategy. As we have stated in the above context, all the players in our model are assumed to be rational and maximize their own values, so as to the manufacturers. They pursuit their own profits maximization, with the common market constraints satisfied. Trade among a group of rational actors would reach a stable state if no individual had anything further to gain by making a new trade. In our model, this means that the steady limit will be the condition in which the two producers both reach their optimum. Obviously, it is a dynamic pricing game and the Nash equilibrium is then the intersection of these best responses.

To solve the Nash equilibrium, we need to find best responses with constraints appropriately imposed for both firms.

Let us sum up, finding the equilibrium solution of the above two cases amounts to solve various profit functions, defined in (13), (14) with the inequalities (10) and (12) as constraints in the whole sales cycle.

Proposition 1. *Based on the analysis above, optimal pricing strategy of the manufactures in the condition* $0 \prec \lambda \prec \delta_1 \prec 1$ *is interior solutions given by*

$$P_A^1 = \frac{\delta_1\left(4c_A(\delta_1 - \lambda) + 4U(\lambda - \delta_1)^2 + c_B(3\delta_1 - 2\lambda - 1)\right)}{\lambda(1+2\lambda) - (2+11\lambda)\delta_1 + 10\delta_1^2}.$$

$$\begin{aligned} P_A^2 = {} & \left(c_A\left(\lambda - (2+5\lambda)\delta_1 + 6\delta_1^2\right) + (\lambda - \delta_1)\right. \\ & \times \left.\left(-U\lambda + (2U + 5U\lambda - 2c_B)\delta_1 - 6U\delta_1^2\right)\right) \\ & \times \left(\lambda(1+2\lambda) - (2+11\lambda)\delta_1 + 10\delta_1^2\right)^{-1} \end{aligned}$$

$$
\begin{aligned}
P_B^1 &= \left(2U\lambda^3 - 2\lambda c_A\left(\lambda - \delta_1\right) - \left(4U\lambda^2 + c_B + 4\lambda c_B\right)\delta_1 \right.\\
&\quad \left. + \left(2U\lambda + 5c_B\right)\delta_1^2\right)\\
&\quad \times \left(\lambda(1+2\lambda) - (2+11\lambda)\delta_1 + 10\delta_1^2\right)^{-1}\\
P_B^2 &= \frac{1}{2}\left(c_B + \left(\lambda\left(-4c_A\left(\lambda - \delta_1\right)\right) + 4U \right.\right.\\
&\quad \left. \times \left(\lambda - \delta_1^2 + c_B\left(-1 - 2\lambda + 3\delta_1\right)\right)\delta_2\right)\\
&\quad \left. \times \left(\lambda\left(1+2\lambda\right) - \left(2+11\lambda\right)\delta_1 + 10\delta_1^2\right)^{-1}\right).
\end{aligned} \tag{19}
$$

The optimal profits of the two firms are too trivial and given in Appendix B.

Proposition 2. *The condition is* $0 < \delta_1 < \lambda < 1$.

The Hesse matrix of the objective function (17), (18) is shown, respectively, as follows:

$$
H_{(17)} = \begin{bmatrix} -\dfrac{2N}{U(1-\lambda)} & 0 \\ 0 & -\dfrac{2N}{U}\left(\dfrac{1}{\lambda - \delta_1} + \dfrac{1}{\delta_1 - \lambda\delta_2}\right) \end{bmatrix}
$$

$$
\begin{aligned}
&H_{(18)}\\
&= \begin{bmatrix} -\dfrac{2N}{U}\left(\dfrac{1}{1-\lambda} + \dfrac{1}{\lambda - \delta_1}\right) & 0 \\ 0 & -\dfrac{2N}{U}\left(\dfrac{1}{\delta_1 - \lambda\delta_2} + \dfrac{1}{\lambda\delta_2}\right) \end{bmatrix}.
\end{aligned} \tag{20}
$$

It is easy to verify that the Hesse matrix is negative definite. As the same reason as the first condition, the optimal pricing strategy is worked out. As analysis above, the prices of the two products in two selling cycles are figured out, and the functions of M_1 and M_2 profits are also given; then the profits are easily derived straightforwardly at least using some software packages such as Mathematica. The concept and method are absolute the same to Proposition 1 and we know that these expressions are too long and are not particularly revealing; we do not show them up.

3.4. Special Condition with Pure Myopic Consumers in the Market. From the above analysis, we assume that the consumers in a realistic market are all rational and strategic. Now we shift our hypothesis to the condition that only myopic consumers exist in the market and figure out the methods of optimal pricing strategies for two manufacturers straightforwardly. The concept of our model is as follows.

In the first period of the whole selling circle, myopic consumers will buy product $A(B)$ only if the following condition

$$
S_A^1 > \max\left\{S_B^1, 0\right\} \quad \left(S_B^1 > \max\left\{S_A^1, 0\right\}\right) \tag{21}
$$

is maintained.

As the same reason, consumers will buy $A(B)$ in the second period as long as

$$
S_A^2 > \max\left\{S_B^2, 0\right\} \quad \left(S_B^2 > \max\left\{S_A^2, 0\right\}\right). \tag{22}
$$

The preference sequence of four products is (A^1, B^1, A^2, B^2). Then we easily figure out the class-divisions:

$$
\begin{aligned}
v_1 &= \frac{P_A^1 - P_B^1}{1-\lambda}\\
v_2 &= \frac{P_B^2}{\lambda}\\
v_3 &= \frac{P_A^2 - P_B^2}{\delta_1 - \lambda\delta_2}\\
v_4 &= \frac{P_B^2}{\lambda\delta_2}
\end{aligned} \tag{23}
$$

as long as the ordering

$$
0 \le v_4 \le v_3 \le v_2 \le v_1 \le U \tag{24}
$$

is maintained.

The profit function is built as follows:

$$
\begin{aligned}
\pi_{M_1} &= \left(\frac{N}{U\left[\left(U - v_1\right)\left(P_A^1 - c_A\right) + \left(v_2 - v_3\right)\left(P_A^2 - c_A\right)\right]}\right)\\
\pi_{M_2} &= \left(\frac{N}{U\left[\left(v_1 - v_2\right)\left(P_B^1 - c_B\right) + \left(v_3 - v_4\right)\left(P_B^2 - c_B\right)\right]}\right).
\end{aligned} \tag{25}
$$

As the same theory as Propositions 1 and 2, according to the Kuhn-Tucker conditions, we reach the outcomes (the optional prices and profits) directly.

3.5. Myopic Consumers and Strategic Consumers Exist in the Market in a Certain Proportion θ. Some consumers employ a variety of consumption patterns with actions that vary in time; we call them strategic consumers, while others may only take the current period into account, and they are myopic consumers. Everyone knows that no pure market exists, and the same method applies to the consumer market. So we suppose a ratio θ exists between the quantities of myopic consumers and strategic consumers.

By using the similar theory, we add an additional parameter θ into the original model to characterize the above scenario. Then all the interesting quantities, for instance, the optimal prices, profits, and market shares, are derived straightforwardly. We assumed that in the market θN consumers are strategic, while $(1-\theta)N$ are myopic. Then the profit functions for manufactures M_1 and M_2 in the condition $0 < \lambda < \delta_1 < 1$ are shown as follows:

$$\begin{aligned}
\pi_{M_1} = {} & \frac{\theta N}{U}\left(U - \frac{P_A^1 - P_A^2}{1-\delta_1}\right)\left(P_A^1 - c_A\right) + \frac{\theta N}{U} \\
& \times \left(\frac{P_A^1 - P_A^2}{1-\delta_1} - \frac{P_A^1 - P_B^1}{\delta_1 - \lambda}\right)\left(P_A^2 - c_A\right) + \frac{(1-\theta)N}{U} \\
& \times \left(\left(U - \frac{P_A^1 - P_B^1}{1-\lambda}\right)\left(P_A^1 - c_A\right) + \left(\frac{P_B^2}{\lambda} - \frac{P_A^2 - P_B^2}{\delta_1 - \lambda\delta_2}\right)\right. \\
& \left. \times \left(P_A^2 - c_A\right)\right) \\
\pi_{M_2} = {} & \frac{\theta N}{U}\left(\frac{P_A^1 - P_B^1}{\delta_1 - \lambda} - \frac{P_B^1 - P_B^2}{\lambda(1-\delta_2)}\right)\left(P_B^1 - c_B\right) + \frac{\theta N}{U} \\
& \times \left(\frac{P_B^1 - P_B^2}{\lambda(1-\delta_2)} - \frac{P_B^2}{\lambda\delta_2}\right)\left(P_B^2 - c_B\right) + \frac{(1-\theta)N}{U} \\
& \times \left(\left(\frac{P_A^1 - P_B^1}{1-\lambda} - \frac{P_B^2}{\lambda}\right)\left(P_B^1 - c_B\right) + \left(\frac{P_A^2 - P_B^2}{\delta_1 - \lambda\delta_2} - \frac{P_B^2}{\lambda\delta_2}\right)\right. \\
& \left. \times \left(P_B^2 - c_B\right)\right).
\end{aligned} \tag{26}$$

Unfortunately, these expressions are too long and are not particularly revealing. So we will not list them here.

4. Numerical Example and Discussions

On account of the mathematical model established in the above paragraphs, we figure out that the optimal price has a certain sensitivity of each parameter in the model abstractly. In this section, we will illustrate the sensitivity through a numerical example so as to the slight change to be found out obviously.

Proposition 3. *In this paper, we assumed that the total number of consumers in the market is one hundred ($N = 100$). The maximum expect valuation of consumers is ten* ($U = 10$)*. The cost of product A(B) is five (four) ($c_A = 5$, $c_B = 4$). In this section we check the changes and figure out the sensitivity of the prices when λ varies with fixed $\delta_1 = \delta_2 = 0.8$ and $c_A = 5$, $c_B = 4$.*

λ represents the difference of two different goods A and B, while δ stands for preference difference of purchasing the same product in two different periods. The detailed prices vary as functions of λ with δ fixed are displayed in Figure 2. From Figure 2, we can see that, with the increase of λ, the four price curves changed greatly. As we know, this parameter which is becoming more and more close to 1 indicates that the differentiation between the two kinds of products is becoming smaller. Then the prices between A and B are getting closer to each other, with P_A^1 and P_A^2 getting down

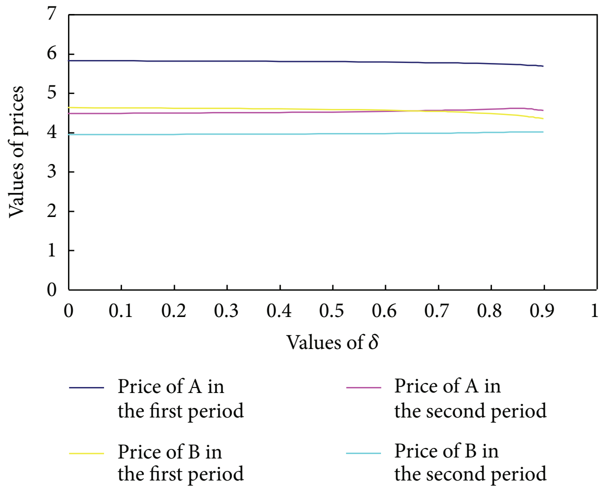

FIGURE 2: The sensitivity of optimal prices with respect to λ.

but P_B^1 and P_B^2 going up. If λ is infinitely close to δ, it means that consumers have nearly the same preference for product B in the first period and A in the later. And the price curves intersect here. In another aspect, obviously, $P_A^1(P_B^1)$ is always larger than $P_A^2(P_B^2)$. That is because the consumer preferences on the first phase of products are greater than the goods of the second stage. With the increase of λ, the quality of product B made by manufacture M_2 is getting closer to A produced in manufacture M_1. Consumer preferences for B will enhance. If M_1 does not reduce the price of A, then more and more consumers will turn to buy B. So in order to keep the profit maximization that all the manufactures will pursue and ensure a certain customers, M_1 has to adjust the prices with the optimal prices curves. Since with the continuous improvement of product quality of B, more and more consumers increase their preference for B, the same reason of pursing profit maximization, M_2 will raise prices of its products as Figure 2 shows.

From this figure, we can say that λ has a great influence on the interactions of two manufactures. Also, to combine the practical situation of realistic market, we can see that the trends of the four prices curves are consistent with the market competition environment in realistic society.

The same theory, for the purpose of having a quantitative perception on how these optimal prices are arranged on the δ-plane, we graphically display it in Figure 3. As we have already assumed, λ is fixed, and the variation of δ does not influence the interaction of product priced of two companies. Unlike the above graph, the curves variation in Figure 3 is relatively weak. However, the trend is also the same. From here, we can derive a small conclusion that differentiation of the same products sold in two phases should be smaller than different product differentiation. As δ increases, the gaps of the same products sold in the first stage and the second selling cycle are becoming smaller. If δ approaches to 1, it implies the consumers' preferences stand more stable. In other words, buying goods in different cycles does not make huge differences on consumers' decision. If δ stays away from 1,

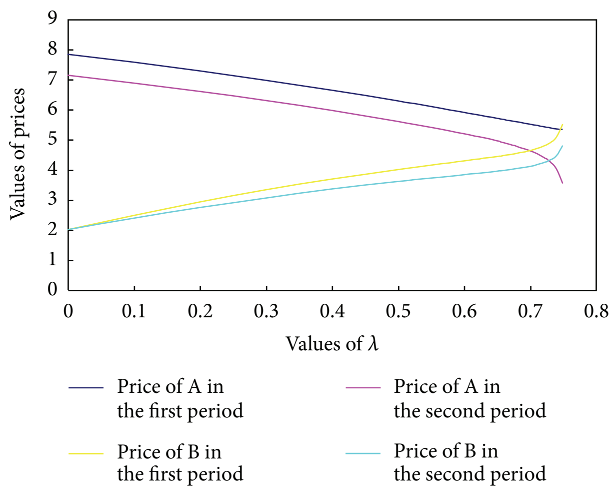

FIGURE 3: The sensitivity of optimal prices with respect to δ.

which means that the gaps of one type of goods sold in different selling cycles are large, in the competitive context, to pursue the maximize profits, each manufacture has to reduce the product prices in the second stage, just like the gaps of $P_A^1(P_B^1)$ and $P_A^2(P_B^2)$ shown in Figure 3. And, with the increase of δ, the companies have to narrow the price gaps for more customers.

5. Conclusions and Further Research

We proposed a model for differentiated durable goods and two competing manufacturers. The model treats a consumer's decision process as a process of choosing an appropriate consumption pattern, rather than an action on one period basis, based on which, the manufacturers derive their optimal prices for all their products and reach maximizing profits, respectively. The main work and conclusion of the paper are as follows:

(1) Construct different consumer surplus function for different products and profit functions for two competing manufacturers and we work out the different consumer purchasing decisions and the optimal prices for firms in the market.

(2) Through the numerical simulation, we show the sensitivity of optimal prices and decisions with respect to valuation parameters. Then we easily find out how these valuation parameters influence the pricing decision.

(3) Despite the fact that most of the consumers are strategic, we also analyze the special condition that only myopic consumers exist in the market. What is more, we proposed an assumption that myopic consumers and strategic consumers exist in the market with a certain proportion θ.

(4) Our paper is based on the previous studies but the innovation point is that the two kinds of product are produced in two different manufactures, and the Nash equilibrium will be our steady state.

Through the above conclusion, we have made some progress in this area based on previous research. However, there also exist some limitations in our paper. First of all, even in duopoly setting, we can make our model somewhat more realistic by extending the selling cycle to three or more just like the generation of iPhone. Secondly, in this paper, we just take two substitutes into consideration. As in the fact, when purchasing an item, one usually will face more than two choices, and these are all substitutes, so we can also introduce more substitute products to be more realistic. Thirdly, confronting the model with empirical data could be another limitation of our paper. In our paper, we analyzed the model and simulation with only experimental data and mathematical model. So many extensions of our model can be envisioned. And a lot work in this area deserves the effort.

Appendices

A. Proof of Proposition 1

The Hesse matrix of the objective function (12) can be shown as follow:

$$H_{(12)} = \begin{bmatrix} -\dfrac{2N}{U(1-\delta_1)} & \dfrac{N}{U}\left(\dfrac{2}{1-\delta_1} - \dfrac{1}{\delta_1 - \lambda}\right) \\ \dfrac{N}{U}\left(\dfrac{2}{1-\delta_1} - \dfrac{1}{\delta_1 - \lambda}\right) & -\dfrac{2N}{U(1-\delta_1)} \end{bmatrix}. \quad \text{(A.1)}$$

It is easy to prove that the Hesse matrix is negative definite. So the profit optimization is a problem with a quadratic objective function and linear constraints, owing to our assumption of the uniform distribution for $v \in [0, U]$. The standard way to carry out this optimal problem is to use the Kuhn-Tucker method. After some experimentation by trial and error, we choose the Lagrangian equation to investigate the equilibrium which corresponds to the best responses of the firm M_1. The relevant Lagrangian is given as follows:

$$\begin{aligned} L_A = \pi_{M_1} &+ x_1(U - v_1) + x_2(v_1 - v_2) \\ &+ x_3(v_2 - v_3) + x_4(v_3 - v_4). \end{aligned} \quad \text{(A.2)}$$

The sense of Kuhn-Tucker condition is

$$\begin{gathered} \frac{\partial L_A}{\partial P_A^1} = \frac{\partial L_A}{\partial P_A^2} = 0 \\ x_1(U - v_1) = x_2(v_1 - v_2) = x_3(v_2 - v_3) = x_4(v_3 - v_4) = 0 \\ x_i \geq 0, \quad i = 1, 2, 3, 4. \end{gathered} \quad \text{(A.3)}$$

Based on the equations given above, the closed-form expressions for all interesting quantities, such as the equilibrium prices, market, and the manufacture's profits, can be derived straightforwardly, using some software packages that can perform symbolic manipulation such as Mathematica.

For the other manufacture, the Hesse matrix of the objective function (13) is shown as follow:

$$H_{(13)} = \begin{bmatrix} -\frac{2N}{U}\left(\frac{1}{\delta_1-\lambda}+\frac{1}{\lambda(1-\delta_2)}\right) & \frac{2N}{U\lambda(1-\delta_2)} \\ \frac{2N}{U\lambda(1-\delta_2)} & -\frac{2N}{U}\left(\frac{1}{\lambda(1-\delta_2)}+\frac{1}{\lambda\delta_2}\right) \end{bmatrix}. \tag{A.4}$$

As the same reason, the relevant Lagrangian of the firm M_2's profit is given as follows:

$$\begin{aligned} L_B = {} & \pi_{M_2} + x_1(U-v_1) + x_2(v_1-v_2) \\ & + x_3(v_2-v_3) + x_4(v_3-v_4). \end{aligned} \tag{A.5}$$

The sense of Kuhn-Tucker condition is

$$\begin{gathered} \frac{\partial L_B}{\partial P_B^1} = \frac{\partial L_B}{\partial P_B^2} = 0 \\ x_1(U-v_1) = x_2(v_1-v_2) = x_3(v_2-v_3) = x_4(v_3-v_4) = 0 \\ x_i \geq 0, \quad i = 1,2,3,4. \end{gathered} \tag{A.6}$$

Solving the two Lagrange equations we can easily get the optimal prices of the four kinds of products and profits of the two firms.

B. Profits of the Manufactures in Condition $0 \prec \lambda \prec \delta_1 \prec 1$

Consider

$$\begin{aligned} \pi_{M_1} = {} & -\frac{N}{U}\Big(\Big(0 - U^2\lambda^4 + c_A^2(1+4\lambda-5\delta_1)(\lambda-2\delta_1)^2 \\ & + U\lambda\left(U\lambda^2(2+\lambda)+(1+4\lambda)c_B\right)\delta_1 \\ & + \left(U^2\lambda^2(3+14\lambda) - 2U\left(1+9\lambda+10\lambda^2\right)c_B \right. \\ & \left. + (1+4\lambda)c_B^2\right)\delta_1^2\Big) \\ & \times \left(\left(\lambda(1+2\lambda)-(2+11\lambda)\delta_1+10\delta_1^2\right)^2\right)^{-1} \\ & + \Big(\left(-U^2\lambda(8+51\lambda)+U(16+49\lambda)c_B-5c_B^2\right)\delta_1^3 \\ & + 2U(2U+28U\lambda-15c_B)\delta_1^4 - 20U^2\delta_1^5 \\ & - c_A\left(\lambda(1+4\lambda)-(2+13\lambda)\delta_1+10\delta_1^2\right) \\ & \times \left(-U\lambda+\left(U(2+5\lambda)-2c_B\right)\delta_1-6U\delta_1^2\right)\Big) \\ & \times \left(\left(\lambda(1+2\lambda)-(2+11\lambda)\delta_1+10\delta_1^2\right)^2\right)^{-1}\Big) \end{aligned}$$

$$\begin{aligned} \pi_{M_2} = {} & \Big(N\Big(16\lambda c_B\delta_1\left(\lambda(1+2\lambda)-(1+7\lambda)\delta_1+5\delta_1^2\right) \\ & \times \left(c_A+U(-\lambda+\delta_1)\right)\delta_2\Big) \\ & + 16\lambda^2(\lambda-\delta_1)\delta_1\left(c_A+U(\delta_1-\lambda)\right)^2\delta_2\Big) \\ & \times \left((2+11\lambda)\delta_1+10{\delta_1}^2\delta_2-4U\lambda(1+2\lambda)\right)^{-1} \\ & + \Big(c_B^2\Big(-100\delta_1^4+\lambda^2(1+2\lambda)^2(-1+\delta_2) \\ & + \delta_1^3(40+220\lambda-40\lambda\delta_2) - 2\lambda(1+2\lambda)\delta_1 \\ & \times (-2-11\lambda+7\lambda\delta_2) \\ & + \delta_1^2\left(-4-64\lambda-161\lambda^2+\lambda(8+65\lambda)\delta_2\right)\Big)\Big) \\ & \times \left((2+11\lambda)\delta_1+10\delta_1^2\delta_2-4U\lambda(1+2\lambda)\right)^{-1}. \end{aligned} \tag{B.1}$$

Conflict of Interests

The authors declare that there is no conflict of interests regarding the publication of this paper.

Acknowledgments

The financial supports from National Natural Science Foundation of China (Grant nos. 71171181, 71322101, 71271195, and 71110107024), Chinese Ministry of Education (NCET-10-0993), and USTC Foundation for Innovative Research Team (WK2040160008) are acknowledged.

References

[1] W. Elmaghraby and P. Keskinocak, "Dynamic pricing in the presence of inventory considerations: research overview, current practices, and future directions," *Management Science*, vol. 49, no. 10, pp. 1287–1309, 2003.

[2] S. Mitra, "Revenue management for remanufactured products," *Omega*, vol. 35, no. 5, pp. 553–562, 2007.

[3] Y. Feng and G. Gallego, "Optimal starting times for end-of-season sales and optimal stopping times for promotional fares," *Management Science*, vol. 41, no. 8, pp. 1371–1391, 1995.

[4] A. Federgruen and A. Heching, "Combined pricing and inventory control under uncertainty," *Operations Research*, vol. 47, no. 3, pp. 454–475, 1999.

[5] E. Chamberlin, *Theory of Monopolistic Competition*, The Harvard University Printing Office, 1933.

[6] Q. Liu and G. van Ryzin, "Strategic capacity rationing to induce early purchases," *Management Science*, vol. 54, no. 6, pp. 1115–1131, 2008.

[7] Z. M. Shen and X. Su, "Customer behavior modeling in revenue management and auctions: a review and new research opportunities," *Production and Operations Management*, vol. 16, no. 6, pp. 713–728, 2007.

[8] D. J. Reibstein and H. Gatignon, "Optimal product line pricing: the influence of elasticities and cross-elasticities," *Journal of Marketing Research*, vol. 21, no. 3, pp. 259–267, 1984.

[9] S. Huang, Y. Yang, and K. Anderson, "A theory of finitely durable goods monopoly with used-goods market and transaction costs," *Management Science*, vol. 47, no. 11, pp. 1515–1532, 2001.

Hindawi Publishing Corporation
Discrete Dynamics in Nature and Society
Volume 2014, Article ID 536576, 10 pages
http://dx.doi.org/10.1155/2014/536576

Research Article

Pricing Decision under Dual-Channel Structure considering Fairness and Free-Riding Behavior

Yongmei Liu, Chunjie Ding, Chen Fan, and Xiaohong Chen

Business School, Central South University, Changsha, Hunan 410083, China

Correspondence should be addressed to Yongmei Liu; liuyongmeicn@163.com

Received 3 March 2014; Accepted 7 May 2014; Published 26 May 2014

Academic Editor: Fenghua Wen

Under dual-channel structure, the free-riding behavior based on different service levels between online channel and offline channel cannot be avoided, which would lead to channel unfairness. This study implies that the dual-channel supply chain is built up by online channel controlled by manufacturer and traditional channel controlled by retailer, respectively. Under this channel structure, we rebuild the linear demand function considering free-riding behavior and modify the pricing model based on channel fairness. Then the influences of fair factor and free-riding behavior on manufacturer and retailer pricing and performance are discussed. Finally, we propose some numerical analysis to provide some valuable recommendations for manufacturer and retailer improving channel management performance.

1. Introduction

In the e-commerce era, dual-channel structure composed of direct online channel and traditional retail channel is the first choice for many manufacturers to promote products, which also attracts widespread scholars. In academia, channel pricing is one of the core decision-making problems of dual-channel researches [1, 2]. In the meantime, decision makers' behaviors are widely concerned in researches [3, 4]. Due to the differences of channel price and service and so forth, consumers' free-riding behavior based on experience service (or information service) between two channels appears which would affect the decision results of dual-channel pricing.

In dual-channel background, there are two types of free-riding behavior: one is that consumers buy product online but obtain experiential service at physical store and the other is that consumers get information service through network but finally purchase offline [5]. For instance, the experiential products, such as electronic products, household appliances, and cars, have some characteristics like being low in purchase frequency and relatively expensive in price. Consumers usually consult purchasing guiders and attempt to experience product function before they finish their shopping online at more convenient and cheaper channel [6]. As investors tend to measure the risks in the stock market [7, 8], some consumers are used to collect product information and consumers' evaluation information online and prefer traditional channel to complete their shopping with low purchase risk [9, 10]. The development of information technology is helpful for firms to use online channel to create new brands, promote new products, and organize promotional activities frequently. Meanwhile, consumers' ability to get information online is more powerful and information resources are huge online, which will also result in consumers' free-riding behavior based on information services.

In general, service level of traditional channel is higher than that of online channel. Traditional retailer provides quality experiential service offline at high expenses, but manufacturer who controls online channel is the beneficiary because of consumers' free-riding behavior under dual-channel structure. Clearly, due to the impact of free-riding behavior and double marginalization caused by dual-channel competition, retailer is faced with channel unfairness and serious decline in profits. It will increase channel pricing competition, strike a severe blow to the retailer's promotion effort, and deteriorate channels relations [11]. Kumar found that channel fairness was very important to maintain channel relationships through empirical studies [12, 13]. Fehr and Schmidt indicated that sometimes manufacturers would rather give up a portion of profits in order to achieve channel fairness [14]. Researching in supply chain performance, Wu et al. proposed a more concise fair utility form [15]. Xing et al. analyzed the effect of fairness on the optimal decision of manufacturer and retailer considering dual-channel supply chain [16]. But they ignored the influence of inevitable free-riding behavior on dual-channel pricing strategy and they did not present an appropriate coordination contract to achieve a win-win condition. By using fair utility function, Cui et al. showed that when retailer cared about fairness, manufacturer could use appropriate wholesale price to realize channel coordination [17]. Ho and Zhang [18] and Caliskan-Demirag et al. [19] studied the coordination problem of supply chain through fair utility function. Ho and Su investigated ultimatum games with participants concerning peer fairness and found that participants paid attention to both their own income and the ratio of income distribution among the partners [20].

Above all, in the context of dual-channel combined with free-riding behavior, it is worth discussing what pricing decision manufacturer should take to maximize the profits of supply chain and its own and how to coordinate dual-channel supply chain, when concerning the fact that the retailer not only is after profit maximization but also cares whether they are treated fairly.

2. Basic Assumptions

The paper assumes that the manufacturer controls the direct online channel and the traditional retailer sells the same product through distributed traditional channel at the same time. Let i be an element of a set of channels, and $i \in \{t, e\}$, where t means traditional channel and e means online channel. Based on Yue and Liu [21], we introduce free-riding behavior effect based on channel service and assume that the demand of traditional channel Q_t and online channel Q_e is linear function:

$$Q_t = (1-\phi)a - b_1 p_t + \xi_1 p_e + s_t + \mu_t s_e, \tag{1}$$

$$Q_e = \phi a - b_2 p_e + \xi_2 p_t + s_e + \mu_e s_t. \tag{2}$$

The basic hypotheses are as follows.

(1) a is the basic market demand; ϕ is the market share of online channel, which reflects best-selling extent of product online.

(2) b_1 is the price elasticity index of product at traditional channel and b_2 is the price elasticity index of product at online channel, which reflect the price sensitivity of demand for product. ξ_1 and ξ_2 are the cross-price elasticity coefficient of product, which reflect the impact of channel price on another channel demand. To simplify the analysis, we suggest that $\xi_1 = \xi_2 = \xi$. Combined with reality that the convenience of Internet search makes consumers more sensitive to the price of online channel, we suppose $b_2 > b_1 > \xi$.

(3) s_t is the service level of traditional channel, including shopping guide service, product presentation, product availability, after-sales service, and high quality shopping environment; s_e is the service level of online channel, including product information searching function, customer service online, return service, and promotional advertising service. We refer to the definition of service cost from Tsay and Agrawal [22]. Let the channel service cost C_i be

$$C_i = \frac{1}{2} s_i^2 \quad (i = \{t, e\}). \tag{3}$$

(4) Suppose that the manufacturer is a Stackelberg leader. The decision variables are wholesale price w and online selling price p_e (let $p_e \geq w$). The retailer, who is a follower, decides the traditional channel price p_t.

In order to ensure that the demand of dual-channel is positive, the online channel price should meet the following condition:

$$p_e \leq \widehat{p}_e \triangleq \frac{\xi E + b_1 F}{b_1 b_2 - \xi^2}, \tag{4}$$

where

$$E = (1-\phi)a + s_t + \mu_t s_e, \qquad F = \phi a + s_e + \mu_e s_t. \tag{5}$$

3. Channel Pricing Strategy without considering Fairness

3.1. Retailer's Pricing Decision Problem. Without the consideration of fairness, traditional retailer sets profit maximization as his decision-making goal. Given wholesale price w and online channel price p_e made by manufacturer, traditional retailer formulates an appropriate traditional channel price p_t to maximize its profit function:

$$\pi_T = Q_t (p_t - w - C_t). \tag{6}$$

Proposition 1. *The profit function π_T is the concave function of traditional channel price p_t.*

There is an optimal price p_t^* to maximize the retailer's profit, and

$$p_t^* = \frac{E + b_1 C_t + b_1 w + \xi p_e}{2b_1}. \tag{7}$$

Combining formula (1) and formula (6), we solve partial derivative condition and make it easy to prove that the profit function π_T is the concave function of traditional channel price p_t. From formula (7), we can see that optimal traditional channel price p_t^* increases in traditional channel service s_t, wholesale price w, and online channel price p_e, respectively. At the same time, the optimal price p_t^* is also a decreasing function of the price elasticity coefficient b_1. When consumers feel more sensitive to the price of traditional channel, the traditional retailer will reduce price to increase traditional channel demand.

3.2. Manufacturer's Pricing Decision Problem. Given the optimal price p_t^*, the manufacturer determines the optimal wholesale price w and online price p_e to maximize its profit function:

$$\pi_M = Q_e \cdot (p_e - C_e - c) + Q_t \cdot (w - c). \tag{8}$$

The decision-making problem can be described as formula (9), where c is manufacturer's production cost. The proof is shown in Appendix A:

$$\begin{aligned} \max_{p_e, w} \quad & \pi_M = Q_e \cdot (p_e - C_e - c) + Q_t \cdot (w - c) \\ \text{s.t.} \quad & p_e \geq w \\ & Q_t = (1 - \phi) a - b_1 p_t + \xi_1 p_e + s_t + \mu_t s_e \\ & Q_e = \phi a - b_2 p_e + \xi_2 p_t + s_e + \mu_e s_t. \end{aligned} \tag{9}$$

Proposition 2. *There is a critical value of market demand share for online channel:*

$$\begin{aligned} \widehat{\phi} = & \left((b_2 - \xi)(a + s_t + \mu_t s_e) + (\xi - b_1)(s_e + \mu_e s_t) \right. \\ & \left. + \left(\xi^2 - b_1 b_2\right)(C_t - C_e) \right) \\ & \times \left(a (b_1 + b_2 - 2\xi)\right)^{-1}. \end{aligned} \tag{10}$$

(1) When manufacturer's online market share satisfies $\phi \geq \widehat{\phi}$, the results of its optimal equilibrium pricing are

$$\begin{aligned} p_e^* &= \frac{\xi E + b_1 F + b_1 b_2 C_e}{2 (b_1 b_2 - \xi^2)} + \frac{c}{2}, \\ w^* &= \frac{b_2 E + \xi F + \left(\xi^3 / b_1\right) C_e}{2 (b_1 b_2 - \xi^2)} + \frac{c - C_t}{2}. \end{aligned} \tag{11}$$

(2) When manufacturer's online market share satisfies $\phi < \widehat{\phi}$, the results of its optimal equilibrium pricing are

$$\begin{aligned} p_e^* = w^* = & \left(\left((b_1 + \xi) E + 2 b_1 F + b_1 (\xi - b_1) C_t \right.\right. \\ & \left. + \left(2 b_1 b_2 - \xi^2 - b_1 \xi\right) C_e \right) \\ & \left. \times \left(2 \left(b_1^2 + 2 b_1 b_2 - \xi^2 - 2 b_1 \xi\right)\right)^{-1} \right) \\ & + \frac{c}{2}. \end{aligned} \tag{12}$$

From Proposition 2, we know that if online market share is larger than critical value $\widehat{\phi}$, manufacturer will set wholesale price lower than online channel price p_e; if online market share is smaller, manufacturer's wholesale price will be equal to online channel price. Put p_e^* and w^* into formula (7); we can calculate retailer's optimal equilibrium pricing. Combining the demand formulas (1) and (2) and the profit formulas (6) and (8), we can obtain the equilibrium demands of dual-channel, as well as the optimal profits of manufacturer and retailer without the consideration of channel fairness.

4. Channel Pricing Strategy considering Fairness

4.1. Retailer's Pricing Decision Problem. When retailer not only focuses on its own profit but also cares about the fairness of channel relationship, its decision-making goal turns into the perceived utility maximization. The retailer's perceived utility U_T concerning fairness is composed of two parts: profit π_T (formula (6)) and fairness utility f_T. Reviewing the existing researches of fairness utility definition [14, 17], we define fairness utility f_T function as

$$\begin{aligned} f_T = & -\alpha \max \left\{\gamma (w - c) Q_t - \pi_T, 0\right\} \\ & - \beta \max \left\{\pi_T - \gamma (w - c) Q_t, 0\right\}. \end{aligned} \tag{13}$$

γ is profit distribution ratio at traditional channel, namely, retailer's channel fairness goal. The bigger γ means that retailer is more powerful in this dual-channel supply chain. α implies that when retailer encounters disadvantageous channel unfairness, its fairness utility will decline α times of the profit difference between manufacturer and retailer in traditional channel; β means that when retailer is faced with advantageous channel unfairness, the fairness utility will decline β times of the profit difference in traditional channel. Fairness parameters (α, β, γ) satisfy $\alpha \geq \beta$, $0 \leq \beta < 1$, and $\gamma > 0$. We suppose that manufacturer and retailer all have symmetric information.

If retailer's profits do not reach γ times of manufacturer's wholesale incomes in the traditional channel, which means $\gamma(w - c)Q_t > \pi_T$, then retailer encounters disadvantageous channel unfairness. In this case, the retailer's perceived fairness utility is $-\alpha[\gamma(w-c)Q_t - \pi_T]$, and its pricing decision problem can be described as

$$\begin{aligned} \max_{p_t} \quad & U_T = \pi_T + f_T \\ \text{s.t.} \quad & \pi_T = Q_t (p_t - w - C_t) \\ & f_T = -\alpha \left[\gamma (w - c) Q_t - \pi_T\right] \\ & \gamma (w - c) Q_t \geq Q_t (p_t - w - C_t). \end{aligned} \tag{14}$$

If retailer's profits are not less than γ times of manufacturer's wholesale incomes in the traditional channel, which means $\pi_T \geq \gamma(w - c)Q_t$, then retailer is faced with advantageous channel unfairness. In this case, the retailer's perceived fairness utility is $-\beta[\pi_T - \gamma(w-c)Q_t]$ and its pricing decision problem can be described as

$$\begin{aligned} \max_{p_t} \quad & U_T = \pi_T + f_T \\ \text{s.t.} \quad & \pi_T = Q_t (p_t - w - C_t) \\ & f_T = -\beta \left[\pi_T - \gamma (w - c) Q_t\right] \\ & Q_t (p_t - w - C_t) \geq \gamma (w - c) Q_t. \end{aligned} \tag{15}$$

Proposition 3. *(1) When retailer encounters disadvantageous channel unfairness, if the wholesale price w and the online channel price p_e satisfy condition 1:*

$$w \geq \frac{(1+\alpha)(E-b_1C_t)+\gamma c b_1(2+\alpha)+(1+\alpha)\xi p_e}{b_1(1+2\gamma+\alpha+\alpha\gamma)}, \quad (16)$$

then retailer's optimal pricing strategy is $p_t^f = (E+b_1C_t+b_1w+\xi p_e)/2b_1+\alpha\gamma(w-c)/2(1+\alpha)$; if not, then the retailer's optimal pricing strategy is $p_t^f = (1+\gamma)w-\gamma c+C_t$.

(2) When retailer is faced with advantageous channel unfairness, if the wholesale price w and the online channel price p_e satisfy condition 2:

$$w \leq \frac{(1-\beta)(E-b_1C_t)+\gamma c b_1(2-\beta)+(1-\beta)\xi p_e}{b_1(1+2\gamma-\beta-\beta\gamma)} \quad (17)$$

then retailer's optimal pricing strategy is $p_t^f = (E+b_1C_t+b_1w+\xi p_e)/2b_1-\beta\gamma(w-c)/2(1-\beta)$; if not, then the retailer's optimal pricing strategy is $p_t^f = (1+\gamma)w-\gamma c+C_t$.

The proof of Proposition 3 is shown in Appendix B. To simplify the analysis, let

$$\begin{aligned} J_1 &= \frac{(1+\alpha)(E-b_1C_t)+\gamma c b_1(2+\alpha)}{b_1(1+2\gamma+\alpha+\alpha\gamma)}, \\ J_2 &= \frac{(1-\beta)(E-b_1C_t)+\gamma c b_1(2-\beta)}{b_1(1+2\gamma-\beta-\beta\gamma)}, \\ K_1 &= \frac{(1+\alpha)\xi}{b_1(1+2\gamma+\alpha+\alpha\gamma)}, \\ K_2 &= \frac{(1-\beta)\xi}{b_1(1+2\gamma-\beta-\beta\gamma)}. \end{aligned} \quad (18)$$

Then condition 1 becomes $w \geq J_1+K_1p_e$, and condition 2 becomes $w \leq J_2+K_2p_e$. It is trivial to prove that $J_j > 0$, $K_j > 0$ $(j=1,2)$, $J_1 > J_2 > 0$, and $1 > K_1 > K_2 > 0$.

According to condition 1, condition 2, and the hypothesis $p_e \leq \widehat{p}_e \triangleq (\xi E+b_1F)/(b_1b_2-\xi^2)$, retailer's pricing decision region can be divided into the following three parts:

$$\begin{aligned} &\text{Region } R_1 = \{(p_e,w) \mid w \geq J_1+K_1p_e, w \leq p_e \leq \widehat{p}_e\}; \\ &\text{Region } R_2 = \{(p_e,w) \mid J_2+K_2p_e < w < J_1+K_1p_e, \\ &\qquad w \leq p_e \leq \widehat{p}_e\}; \\ &\text{Region } R_3 = \{(p_e,w) \mid w \leq J_2+K_2p_e, w \leq p_e \leq \widehat{p}_e\}. \end{aligned} \quad (19)$$

Proposition 4. *Considering channel fairness, given manufacturer's pricing strategy (p_e, w), retailer's optimal pricing option is*

$$p_t^f = \begin{cases} \dfrac{E+b_1C_t+b_1w+\xi p_e}{2b_1}+\dfrac{\alpha\gamma(w-c)}{2(1+\alpha)}, & (p_e,w)\in R_1 \\ (1+\gamma)w-\gamma c+C_t, & (p_e,w)\in R_2 \\ \dfrac{E+b_1C_t+b_1w+\xi p_e}{2b_1}-\dfrac{\beta\gamma(w-c)}{2(1-\beta)}, & (p_e,w)\in R_3. \end{cases} \quad (20)$$

From Proposition 4 we can see that, in region R_2, when wholesale price is moderate, retailer's traditional channel pricing will not be affected by manufacturer's online price. And the optimal price of retailer is cost-based. In region R_1 as manufacturer offers high wholesale price, retailer encounters disadvantageous channel unfairness and will price p_t^f ($p_t^f = (E+b_1C_t+b_1w+\xi p_e)/2b_1+\alpha\gamma(w-c)/2(1+\alpha)$) higher than the optimal traditional channel price p_t^* without considering channel fairness ($p_t^* = (E+b_1C_t+b_1w+\xi p_e)/2b_1$) to the manufacturer; but in region R_3 with low wholesale price, retailer is faced with advantageous channel unfairness, and for the consideration of fairness, retailer will set a lower price ($p_t^f = (E+b_1C_t+b_1w+\xi p_e)/2b_1-\beta\gamma(w-c)/2(1-\beta)$) than p_t^* to compensate manufacturer with more offline sales. Overall, the effort of rewarding compensation and resisting punishment is proportional to the distribution of profits γ of traditional channel.

4.2. Manufacturer's Pricing Decision Problem. Given retailer's optimal pricing response p_t^f in the above three regions, manufacturer would determine the optimal wholesale price w^f and online direct selling price p_e^f in order to maximize its profit function $\pi_M = Q_e(p_e-C_e-c)+Q_t(w-c)$. Next, we discuss the manufacturer's pricing decision problem for each region.

(1) In region R_1, the manufacturer's pricing decision problem can be described as formula (21). Denote equilibrium price combination by (p_{e1}^f, w_1^f) and the optimal profit by π_{M1}^f:

$$\begin{aligned} \max_{p_e,w}\quad & \pi_M = Q_e\cdot(p_e-C_e-c)+Q_t\cdot(w-c) \\ \text{s.t.}\quad & p_t^f = \frac{E+b_1C_t+b_1w+\xi p_e}{2b_1}+\frac{\alpha\gamma(w-c)}{2(1+\alpha)}, \\ & w \geq J_1+K_1p_e, \quad w \leq p_e, \quad p_e \leq \widehat{p}_e. \end{aligned} \quad (21)$$

(2) In region R_2, the manufacturer's pricing decision problem can be described as formula (22). Denote equilibrium price combination by (p_{e2}^f, w_2^f) and the optimal profit by π_{M2}^f:

$$\begin{aligned} \max_{p_e,w}\quad & \pi_M = Q_e\cdot(p_e-C_e-c)+Q_t\cdot(w-c) \\ \text{s.t.}\quad & p_t^f = (1+\gamma)w-\gamma c+C_t \\ & w > J_2+K_2p_e, \quad w < J_1+K_1p_e \\ & w \leq p_e, \quad p_e \leq \widehat{p}_e. \end{aligned} \quad (22)$$

(3) In region R_3, the manufacturer's pricing decision problem can be described as formula (23). Denote equilibrium price combination by (p_{e3}^f, w_3^f) and the optimal profit by π_{M3}^f:

$$\begin{aligned} \max_{p_e,w} \quad & \pi_M = Q_e \cdot (p_e - C_e - c) + Q_t \cdot (w - c) \\ \text{s.t.} \quad & p_t^f = \frac{E + b_1 C_t + b_1 w + \xi p_e}{2b_1} - \frac{\beta\gamma (w - c)}{2(1-\beta)} \\ & w \le J_2 + K_2 p_e, \quad w \le p_e, \quad p_e \le \hat{p}_e. \end{aligned} \tag{23}$$

Ultimately, the largest global profit of manufacturer $\pi_M^f = \max\{\pi_{M1}^f, \pi_{M2}^f, \pi_{M3}^f\}$ is corresponding to the equilibrium price strategy, which decides the global optimum equilibrium strategy (p_e^f, w^f). Substituting the equilibrium solution (p_e^f, w^f) into formula (20), we get the retailer's optimal pricing strategy with the consideration of fairness. Then iterate the demand formulas (1) and (2) and retailer's profit formula (6) until the retailer's optimal profit π_T^f can be obtained.

5. Illustrative Examples

Since the objective function and the optimal decision variables contain many parameters and complex expressions, we illustrate propositions and deductions in this paper with the aid of numerical example simulations to get insight into the enlightenment of management. We set basic values of the various parameters as $a = 1$, $\phi = 0.5$, $b_1 = 0.8$, $b_2 = 1$, $\xi = 0.4$, $c = 0.5$, $s_t = 0.8$, and $s_e = 0.4$. Referring to the empirical results in Fehr and Schmidt [14] and Xing et al. [16], we set the fairness parameter values $\alpha = 1$, $\beta = 0.4$, and $\lambda = 0.7$. Considering the fairness effect on the result of supply chain members' decision-making, we select $\mu_t = \mu_e = 0.2$ and change service level to reflect the variation of free-riding effect for simplicity.

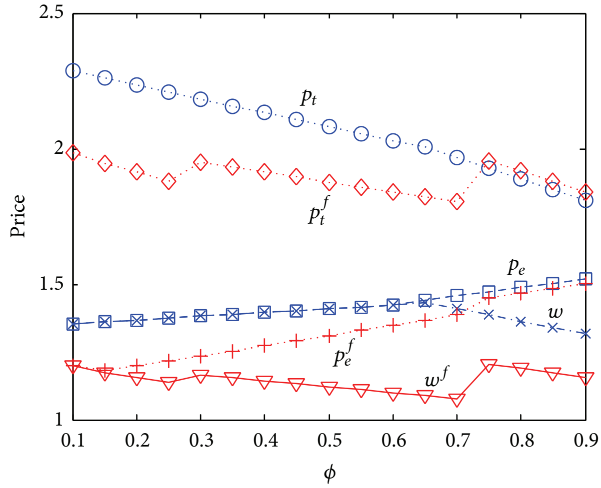

Figure 1: The effect of market share and channel on price.

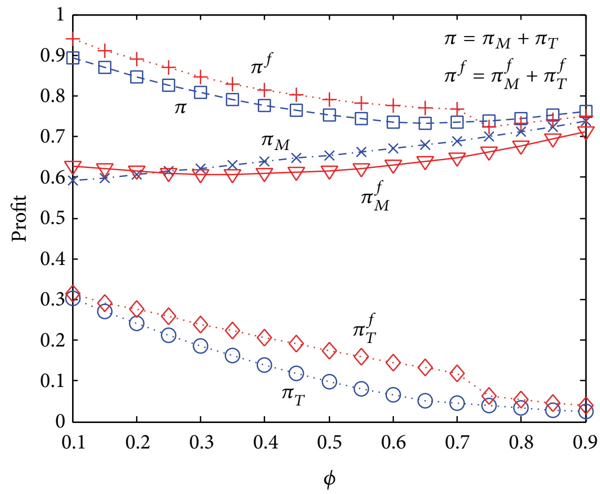

Figure 2: The effect of market share and channel fairness on profit.

5.1. Impact of Online Channel Market Share. Let the range of market share ϕ of online channel be from 0.1 to 0.9, and let other parameters be on basic values. Figures 1 and 2 reflect the effect that online market share and channel fairness have on manufacturer and traditional retailer's pricing decisions and profit results.

From Figures 1 and 2 we know that the retailer's profits in the situation of considering fairness are always higher than those of ignoring fairness $(\pi_T^f > \pi_T)$. When online market share ϕ is in the range of 0.75 to 0.9, retailer faces disadvantageous channel unfairness and will negatively increase the price $(p_t^f > p_t)$ against the manufacturer's oppression. In the end, it makes the performance of manufacturer and supply chain lower than that of the situation of not considering fairness $(\pi_M^f < \pi_M, \pi^f < \pi)$. When online market share ϕ is about 0.1 to 0.7, retailer faces advantageous channel unfairness and will reduce the price of traditional channel $(p_t^f < p_t)$ to increase the traditional channel demand. In that case, although the manufacturer's profits decline, channel fairness significantly improves the performance level of the supply chain $(\Delta\pi = \pi^f - \pi > 0)$. If manufacturer designs appropriate mechanism to coordinate dual-channel supply chain in consideration of fairness, then both the supply chain members will achieve Pareto improvement of higher income than otherwise. Among the appropriate contracts, there is a revenue sharing contract of bargaining [23] such that $\Delta\pi_T = A/(A+B)\Delta\pi > 0$ and $\Delta\pi_M = B/(A+B)\Delta\pi > 0$, where the values of A and B are determined by the bargaining power between the two sides. Finally we obtain $\pi_T' = \Delta\pi_T + \pi_T$ and $\pi_M' = \Delta\pi_M + \pi_M$ and realize win-win results of dual-channel supply chain.

From Figure 1 we can see that when online market share of manufacturer is larger, it will adopt a lower wholesale price to maintain the traditional channel operation of retailer and provide a quality experience for online consumers no matter whether they take retailer's channel fairness into account or not. Thereby, utilize free-riding behavior to further improve the attractiveness of the online channel indirectly. Overall, manufacturer's equilibrium price concerned with channel fairness will be obviously lower than that of not considering channel fairness.

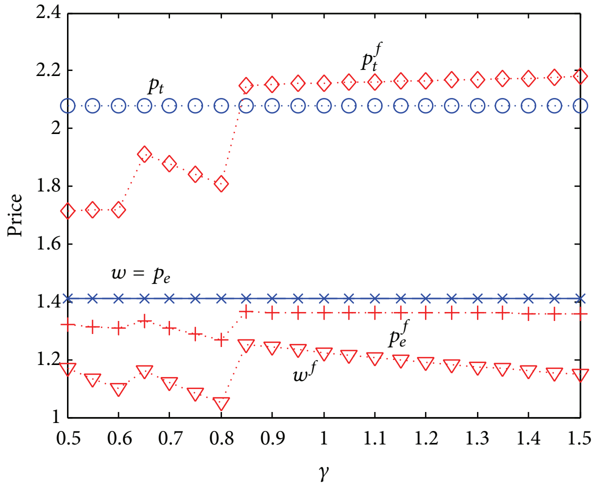

Figure 3: Effect of fairness channel profit distribution on channel pricing.

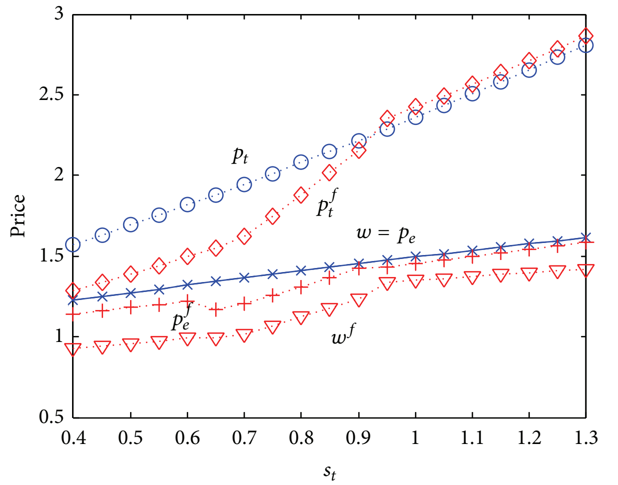

Figure 5: Effect of service level and free-riding on channel pricing.

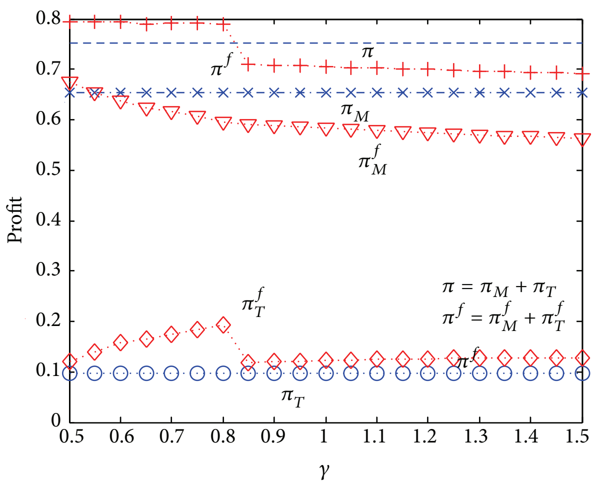

Figure 4: Effect of fairness channel profit distribution on channel profits.

5.2. Effect of Fairness Channel Profit Distribution. Figures 3 and 4 reflect the trends of equilibrium prices of manufacturer and retailer and optimal profits with the changing of fairness channel profit distribution γ.

From Figure 3 we can see that if fairness is considered, the manufacturer's equilibrium prices are always lower than otherwise ($p_e^f < p_e$). When profit distribution γ is in the range of 0.5 to 0.85, retailer faces advantageous channel unfairness. In that case, with the value of parameter γ becoming larger, retailer will increase the traditional channel price, while manufacturer reduces the wholesale price to achieve channel fairness. It makes retailer's profits in Figure 4 significantly higher than those of not considering fairness ($\pi_T^f > \pi_T$). But it causes some loss to manufacturer. However, retailer's increased profits are far more than manufacturer's decreased profits. Overall, the performance of supply chain is obviously enhanced in the end ($\pi^f > \pi$). In the above situation of considering fairness, if manufacturer designs an appropriate dual-channel contract mechanism which coordinates the profit distribution problem, then they both will achieve a win-win situation. When γ increases from 0.85 to 1.5, retailer will face disadvantageous channel unfairness. In such traditional channel profits sharing goal, manufacturer will improve its pricing level in order to suppress the retailer's ambition of earning profits in the traditional channel; at the same time retailer also increases the traditional channel price p_t^f rapidly, significantly higher than that of without considering fairness ($p_t^f > p_t$). The retailer's profits in Figure 4 are higher than its profits of not considering fairness. But due to the retailer's price increasing resistance, the demand of traditional channel reduces. Eventually it leads to the declination of manufacturer and supply chain's profits which are significantly lower than that of not considering fairness.

Overall, taking fairness into consideration, the retailer's profits are always higher than those of not considering fairness ($\pi_T^f > \pi_T$) and its maximum profit is attainable when $\gamma = 0.8$. But the comparison results of manufacturer's profits are on the contrary ($\pi_M^f < \pi_M$). But the total profits of the supply chain with considering fairness and not considering fairness have relation to the profits distribution γ which is a ratio among fairness parameters, namely, retailer's goal to reach the target profits from traditional channel compared with manufacturer. When γ is small, the total profits of the supply chain with considering fairness are bigger than those of without considering fairness. Thus manufacturer can design appropriate contract to coordinate the dual-channel for achieving win-win situation. When γ is bigger, the total profits of the supply chain without considering fairness will be bigger. In that case, the manufacturer will choose to ignore retailer's concern of channel fairness.

5.3. The Effect of Service Level and Free-Riding. Figures 5 and 6 reflect the effect of service level on equilibrium prices and profits of manufacturer and retailer. As free-riding behavior based on channel service exists between channels, we analyze

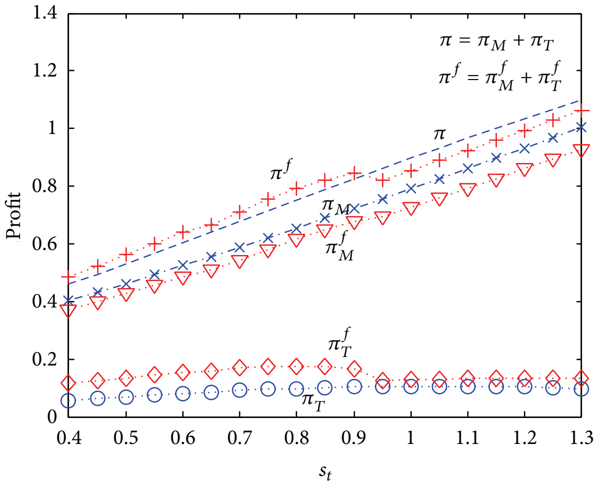

Figure 6: Effect of service level and free-riding on profit.

the impact of free-riding on dual-channel pricing decision with considering fairness through discussing the change of service level for simplicity.

Figure 5 shows that, with fairness consideration, manufacturer's equilibrium price (p_e^f, w^f) is lower than the price strategy (p_e, w) under situation of not considering channel fairness. When the service level provided by traditional retailer is lower, retailer faces advantageous channel unfairness. In that case, retailer's equilibrium price p_t^f is far lower than p_t. With the improvement of service level, p_t^f increases more precipitously than p_t. When the service level of traditional channel is high, retailer faces disadvantageous channel unfairness. Because manufacturer takes more free-riding from traditional channel to profit, retailer does not reach profits distribution goal at traditional channel. For the retailer's consideration of channel fairness, it will set p_t^f higher than p_t that not considering fairness to boycott manufacturer. This measure makes manufacturer's profits in Figure 6 decline larger and also makes the overall performance of the supply chain worse than that of not considering fairness.

Overall, from Figure 6 we know that after considering fairness, retailer's profits increase while manufacturer's profits decline. The improvement of traditional service level can increase the demand of traditional channel. But taking free-riding effect into account, the online channel free-riding effect is far beyond traditional channel's $(\mu_e s_t > \mu_t s_e)$. Thus manufacturer's profits increase with the improvement of traditional service level, while retailer's profits present the trend of first increasing and then decreasing because of the balance between service cost and benefit. When service level of traditional channel is about between 0.8 and 0.9, retailer and supply chain system both reach their peak profits. In order to achieve win-win solution among supply chain members, retailer should choose a moderate service level. In that case, with fairness consideration, if manufacturer adopts certain measures to share the additional profits with retailer, then the Pareto improvement of dual-channel supply chain will be able to be achieved.

6. Conclusions

Dual-channel structure studied in this paper includes horizontal competition between traditional channel and online channel and vertical competition between the upstream and downstream supply chain. In addition, free-riding effect that causes the imbalance of profits distribution between manufacturer and retailer is inevitable in dual-channel structure, and channel unfair phenomenon is outstanding. Combining with free-riding behavior, this paper builds a linear demand function and uses fairness revised price game model to discuss pricing strategy and revenue performance of manufacturer and retailer. Finally, from numerical analysis, we provide management recommendations for manufacturer and retailer.

Our research finds that when manufacturer's online market share is large enough, whether considering retailer's channel fairness or not, due to free-riding effect, manufacturer will always lower wholesale price in order to maintain retailer's traditional channel operation and provide quality experience service for its consumers. But as traditional channel enhances service level, online channel takes much more service free-riding from traditional channel than what traditional channel takes on the opposite. Therefore, manufacturer gains increase with the service improvement of traditional channel, the retailer profits first increase and then decrease. In short, manufacturer's equilibrium price based on channel fairness is below its equilibrium price ignoring fairness. Manufacturer is willing to lose some profits in order to achieve channel fairness, and at the same time retailer always gets more profits in fairness considering situation.

There are two channel unfairness cases that retailer faced, disadvantageous channel unfairness and advantageous channel unfairness. When retailer faces disadvantageous channel unfairness, retailer's profits gained from fairness consideration could not make up manufacturer's profits difference compared with ignoring channel fairness. In such case, taking fairness into account will make supply chain performance worse, and there is no contract that could coordinate the supply chain, so manufacturer would like to ignore channel fairness. However, when retailer encounters advantageous channel unfairness phenomenon, retailer revenue increase was significantly greater than the reduction in the earnings of manufacturers due to fairness consideration, which leads to performance improvement of supply chain. In this state, if manufacturer considers channel fairness and designs appropriate revenue sharing contract to coordinate profits distribution, the supply chain members would realize the Pareto improvement.

However, there are still some limitations in this paper. Firstly, we only analyze retailer's fairness preference and assume that manufacturer is a rational decision maker. But in reality, manufacturer may also have channel fairness preference. In addition, under certain conditions, supply chain decision performance with fairness consideration still does not reach the optimal value of centralized decision-making. Therefore, the future may continue to study how could manufacturer design appropriate contract mechanism to coordinate the dual-channel supply chain when a variety of behavioral factors are concerned. At last, the topic of this paper comes from the actual market research, but we have limitation of the availability of great empirical data. As a result of empirical data limitation, we use mathematical derivation and numerical simulation methods to solve the problem and seek management proposals. If more field research data can be collected in the future, such dual-channel management research based on behavioral factors would make a big breakthrough.

Appendices

A. The Manufacturer Equilibrium Pricing without considering Fairness

Manufacturer's decision problem is as follows:

$$\begin{aligned} \max_{p_e,w} \quad & \pi_M = Q_e \cdot (p_e - C_e - c) + Q_t \cdot (w - c) \\ \text{s.t.} \quad & p_e \geq w \\ & Q_t = (1-\phi)a - b_1 p_t + \xi_1 p_e + s_t + \mu_t s_e \\ & Q_e = \phi a - b_2 p_e + \xi_2 p_t + s_e + \mu_e s_t. \end{aligned} \tag{A.1}$$

With known $E = (1-\phi)a + s_t + \mu_t s_e$, $F = \phi a + s_e + \mu_e s_t$, to profit function π_M, the first-order partial derivatives of online channel price p_e and wholesale price w are

$$\begin{aligned} \frac{\partial \pi_M}{\partial w} &= -b_1 w + \xi p_e + \frac{(b_1 - \xi)c + E - b_1 C_t - \xi C_e}{2}, \\ \frac{\partial \pi_M}{\partial p_e} &= \xi w + \frac{\xi^2 - 2b_1 b_2}{2b_1}(2p_e - C_e) + \frac{(2b_1 b_2 - \xi^2 - b_1\xi)c + \xi E + b_1 \xi C_t}{2b_1} + F. \end{aligned} \tag{A.2}$$

The second-order partial derivatives are

$$\begin{aligned} \frac{\partial \pi_M^2}{\partial w^2} &= -b_1, \qquad \frac{\partial \pi_M^2}{\partial p_e^2} = \frac{\xi^2 - 2b_1 b_2}{b_1}, \\ \frac{\partial \pi_M^2}{\partial w \partial p_e} &= \xi, \qquad \frac{\partial \pi_M^2}{\partial p_e \partial w} = \xi. \end{aligned} \tag{A.3}$$

So the Hessian matrix of the profit function $\begin{vmatrix} -b_1 & \xi \\ \xi & (\xi^2 - 2b_1 b_2)/b_1 \end{vmatrix}$ is negative definite. Profit function is a concave function of online channel price p_e and wholesale price w and exists in unique equilibrium solution. The manufacturer decision problem is transformed into Karush-Kuhn-Tucker optimization conditions as follows:

$$\begin{aligned} & -b_1 w + \xi p_e + \frac{(b_1 - \xi)c + E - b_1 C_t - \xi C_e}{2} - \lambda = 0 \\ & \xi w + \frac{\xi^2 - 2b_1 b_2}{2b_1}(2p_e - C_e) + \frac{(2b_1 b_2 - \xi^2 - b_1\xi)c + \xi E + b_1 \xi C_t}{2b_1} + F + \lambda = 0 \\ & \lambda(p_e - w) = 0, \quad \lambda \geq 0, \quad p_e \geq w \end{aligned} \tag{A.4}$$

(1) When $\lambda = 0$,

$$\begin{aligned} p_e^* &= \frac{\xi E + b_1 F}{2(b_1 b_2 - \xi^2)} + \frac{c + C_e}{2}, \\ w^* &= \frac{b_2 E + \xi F + ((\xi^3 - b_1 b_2 \xi)/b_1) C_e}{2(b_1 b_2 - \xi^2)} + \frac{c - C_t}{2}. \end{aligned} \tag{A.5}$$

(2) When $\lambda > 0$,

$$\begin{aligned} p_e^* = w^* &= \Big(\big((b_1 + \xi)E + 2b_1 F + b_1(\xi - b_1)C_t + (2b_1 b_2 - \xi^2 - b_1\xi)C_e \big) \\ &\quad \times \left(2(b_1^2 + 2b_1 b_2 - \xi^2 - 2b_1\xi)\right)^{-1} \Big) + \frac{c}{2}, \\ \lambda &= \left((\xi^2 + b_1\xi - b_1 b_2 - b_1^2)E + b_1(\xi - b_1)F + 2b_1^2(b_2 - 2\xi)C_t + b_1(\xi^2 - b_1 b_2)C_e \right) \\ &\quad \times \left(b_1^2 + 2b_1 b_2 - \xi^2 - 2b_1\xi\right)^{-1}. \end{aligned} \tag{A.6}$$

For $\lambda > 0$ and in the text parameter assumptions conditions, we have

$$\begin{aligned} \phi < \hat{\phi} \triangleq & \Big((b_2 - \xi)(a + s_t + \mu_t s_e) + (\xi - b_1)(s_e + \mu_e s_t) \\ & + (\xi^2 - b_1 b_2)(C_t - C_e) \Big) \\ & \times \left(a(b_1 + b_2 - 2\xi)\right)^{-1}. \end{aligned} \tag{A.7}$$

B. Channel Pricing Strategy considering Fairness

(1) Retailer faces disadvantageous channel unfairness. The decision problem is

$$\begin{aligned} \max_{p_t} \quad & U_T = \pi_T + f_T \\ \text{s.t.} \quad & \pi_T = Q_t(p_t - w - C_t) \\ & f_T = -\alpha[\gamma(w - c)Q_t - \pi_T] \\ & \gamma(w - c)Q_t \geq Q_t(p_t - w - C_t). \end{aligned} \tag{B.1}$$

Using Karush-Kuhn-Tucker method, the above problem can be converted to the following optimization problem:

$$\begin{aligned}\max_{p_t,\lambda_1} \quad & L_1(p_t,\lambda_1) = Q_t(1+\alpha)(p_t - w - C_t) - \alpha\gamma Q_t(w-c) \\ & + \lambda_1[(1+\gamma)w - \gamma c + C_t - p_t] \\ \text{s.t.} \quad & Q_t = E - b_1 p_t + \xi p_e \\ & \lambda_1[(1+\gamma)w - \gamma c + C_t - p_t] = 0 \\ & (1+\gamma)w - \gamma c + C_t - p_t \ge 0 \\ & \lambda_1 \ge 0.\end{aligned} \tag{B.2}$$

The KKT conditions are as follows:

$$\begin{aligned}\frac{\partial L_1}{\partial p_t} &= (E - b_1 p_t + \xi p_e)(1+\alpha) - b_1(1+\alpha)(p_t - w - C_t) \\ &\quad + b_1\alpha\gamma(w-c) - \lambda_1 = 0, \\ & \lambda_1[(1+\gamma)w - \gamma c + C_t - p_t] = 0, \\ & (1+\gamma)w - \gamma c + C_t - p_t \ge 0, \\ & \lambda_1 \ge 0.\end{aligned} \tag{B.3}$$

(i) When $\lambda_1 = 0$, obtain $p_t^f = (E + b_1 C_t + b_1 w + \xi p_e)/2b_1 + \alpha\gamma(w-c)/2(1+\alpha)$; substituting inequality $(1+\gamma)w - \gamma c + C_t - p_t \ge 0$, get

$$w \ge \frac{(1+\alpha)(E - b_1 C_t) + \gamma c b_1(2+\alpha) + (1+\alpha)\xi p_e}{b_1(1 + 2\gamma + \alpha + \alpha\gamma)}. \tag{B.4}$$

(ii) When $\lambda_1 > 0$, obtain $p_t^f = (1+\gamma)w - \gamma c + C_t$.

Similar to the case of advantageous channel unfairness.

Conflict of Interests

The authors declare that there is no conflict of interests regarding the publication of this paper.

Acknowledgments

The authors are very grateful to the editor and the anonymous reviewers for their insightful and constructive comments and suggestions that have led to an improved version of this paper. This work was partially supported by the National Innovation Group Science Foundation, China (no. 71221061), International Major Project Supported by the National Natural Science Foundation, China (no. 71210003), the National Science Foundation of China (71271219 and 71071164), and Program for New Century Excellent Talents in University (NCET-11-0519).

References

[1] K. D. Cattani, W. G. Gilland, and J. M. Swaminathan, "Coordinating traditional and internet supply chains," in *Handbook of Quantitative Supply Chain Analysis: Modeling in the E-Business Era*, International Series in Operations Research and Management Science, Kluwer Academic, Boston, Mass, USA, 2004.

[2] A. A. Tsay and N. Agrawal, "Modeling conflict and coordination in multi-channel distribution systems: a review," in *Handbook of Quantitative Supply Chain Analysis: Modeling in the E-Business Era*, International Series in Operations Research and Management Science, Kluwer Academic, Boston, Mass, USA, 2004.

[3] F. Wen and X. Yang, "Skewness of return distribution and coefficient of risk premium," *Journal of Systems Science and Complexity*, vol. 22, no. 3, pp. 360–371, 2009.

[4] F. Wen, Z. He, and X. Chen, "Investors' risk preference characteristics and conditional skewness," *Mathematical Problems in Engineering*, vol. 2014, Article ID 814965, 14 pages, 2014.

[5] O. P. Bomsel, "Free-riding and luxury brands on the internet," *International Business Research*, vol. 7, no. 4, pp. 60–71, 2014.

[6] S. van Baal and C. Dach, "Free riding and customer retention across retailers' channels," *Journal of Interactive Marketing*, vol. 19, no. 2, pp. 75–85, 2005.

[7] F. Wen, X. Gong, Y. Chao, and X. Chen, "The effects of prior outcomes on risky choice evidence from the stock market," *Mathematical Problems in Engineering*, vol. 2014, Article ID 272518, 8 pages, 2014.

[8] C. Huang, X. Gong, X. Chen, and F. Wen, "Measuring and forecasting volatility in chinese stock market using HAR-CJ-M model," *Abstract and Applied Analysis*, vol. 2013, Article ID 143194, 13 pages, 2013.

[9] A. Rangaswamy and G. H. van Bruggen, "Opportunities and challenges in multichannel marketing: an introduction to the special issue," *Journal of Interactive Marketing*, vol. 19, no. 2, pp. 5–11, 2005.

[10] P. C. Verhoef, S. A. Neslin, and B. Vroomen, "Multichannel customer management: understanding the research-shopper phenomenon," *International Journal of Research in Marketing*, vol. 24, no. 2, pp. 129–148, 2007.

[11] D. Xing and T. Liu, "Sales effort free riding and coordination with price match and channel rebate," *European Journal of Operational Research*, vol. 219, no. 2, pp. 264–271, 2012.

[12] N. Kumar, L. K. Scheer, and J. B. E. M. Steenkamp, "The effects of supplier fairness on vulnerable resellers," *Journal of Marketing Research*, vol. 32, no. 1, pp. 54–65, 1995.

[13] N. Kumar, "The power of trust in manufacturer-retailer relationships," *Harvard Business Review*, vol. 74, no. 6, pp. 92–106, 1996.

[14] E. Fehr and K. M. Schmidt, "A theory of fairness, competition, and cooperation," *The Quarterly Journal of Economics*, vol. 114, no. 3, pp. 817–868, 1999.

[15] Y. Wu, C. H. Loch, and L. van der Heyden, "A model of fair process and its limits," *Manufacturing & Service Operations Management*, vol. 10, no. 4, pp. 637–653, 2008.

[16] W. Xing, S.-Y. Wang, Q.-H. Zhao, and G.-W. Hua, "Impact of fairness on strategies in dual-channel supply chain," *System Engineering Theory & Practice*, vol. 31, no. 7, pp. 1249–1256, 2011.

[17] T. H. Cui, J. S. Raju, and Z. J. Zhang, "Fairness and channel coordination," *Management Science*, vol. 53, no. 8, pp. 1303–1314, 2007.

[18] T. H. Ho and J. Zhang, "Designing pricing contracts for boundedly rational customers: does the framing of the fixed fee matter?" *Management Science*, vol. 54, no. 4, pp. 686–700, 2008.

[19] O. Caliskan-Demirag, Y. Chen, and J. Li, "Channel coordination under fairness concerns and nonlinear demand," *European Journal of Operational Research*, vol. 207, no. 3, pp. 1321–1326, 2010.

[20] T.-H. Ho and X. Su, "Peer-induced fairness in games," *American Economic Review*, vol. 99, no. 5, pp. 2022–2049, 2009.

[21] X. Yue and J. Liu, "Demand forecast sharing in a dual-channel supply chain," *European Journal of Operational Research*, vol. 174, no. 1, pp. 646–667, 2006.

[22] A. A. Tsay and N. Agrawal, "Channel dynamics under price and service competition," *Manufacturing & Service Operations Management*, vol. 2, no. 4, pp. 372–391, 2000.

[23] R. Yan, "Managing channel coordination in a multi-channel manufacturer-retailer supply chain," *Industrial Marketing Management*, vol. 40, no. 4, pp. 636–642, 2011.

Hindawi Publishing Corporation
Discrete Dynamics in Nature and Society
Volume 2014, Article ID 742182, 8 pages
http://dx.doi.org/10.1155/2014/742182

Research Article

How Investor Structure Influences the Yield, Information Dissemination Efficiency, and Liquidity

Hongli Che,[1] Xiong Xiong,[1,2] Juntian Yang,[1] Wei Zhang,[1,2] and Yongjie Zhang[1,2]

[1] *College of Management and Economics, Tianjin University, Tianjin 300072, China*
[2] *China Center for Social Computing and Analytics, Tianjin University, Tianjin 300072, China*

Correspondence should be addressed to Juntian Yang; 296951233@qq.com

Received 8 March 2014; Accepted 12 May 2014; Published 25 May 2014

Academic Editor: Fenghua Wen

This essay focuses on the investor structure of the stock index futures market and uses agent-based computational finance method to discuss how the volume-synchronized probability of informed trading (VPIN) affects market absolute yield, information dissemination efficiency, and liquidity with different ratios of informed traders in the market. The result shows that the higher the proportion of informed traders is, the more the volatility of the market is. Furthermore, the result indicates that when the proportion of informed traders in the stock index futures market accounts for 1/3-1/2, the transparency and liquidity of the market will be better.

1. Introduction

Looking back, there were many risky activities led by financial innovation, such as the big crash caused by the use of portfolio insurance strategies in America, in 1987, and the flash crash of Dow triggered by the e-mini futures contracts in 2010. In 2010, the CSI 300 index futures were traded officially in China, which completely changed the structure of China's capital market. The financial derivatives can play a hedge effectiveness and expand investment channels, but the risks they bring should not be ignored. How to realize liquidity risk management from the perspective of investors' structure? How investor structure influences the yield? What is the relationship between information dissemination efficiency and investor structure? To solve the mystery, regulators and academics have done much research in this field and achieved a lot.

In the commodity economy, information is mainly reflected on the price; price information is the core of economic information. The nature of market economy is using price as a signal to allocate social resources. Distribution and redistribution of social resources are actually the processes during which people play games on the price. The preemption of any kind of resources makes related profit in the game, so does the information. In order to study the price discovery, hedging, and other issues of the stock market, traditional finance researches tend to assume that traders in the market have a common set of assumptions information. However, in reality, information on the financial markets can not be completely balanced, causing the interest imbalance between both sides, which imposes adverse effect on the social principle of justice and fairness, reducing the resource allocation efficiency in the market.

The key to solve the problem of asymmetric information problem is how to measure the degree of information asymmetry. Aiming at this, many scholars have generally studied the information contained in the orders for a long time. However, in recent years, the traditional methods for measurement have too many difficulties to cope with the problem. In a framework where trades take place in milliseconds, Easley et al. (2011) [1] introduced another conception. In this paper we apply this new technique to our study. In addition, the financial system is essentially a complex system in essence (Holland, 1997 [2]), and it is nonlinear and adaptive, which makes most theoretical models ineffective even after releasing the assumption. Fortunately, agent-based computational finance provides us with new train of thoughts and tactics to study the complex adaptive system.

Based on VPIN model submitted by Easley et al. (2011), and with the help of agent-based computational finance which has real market characteristics, we study the effect of how informed traders proportion imposes on market absolute yields, information dissemination efficiency, and liquidity by setting different investor structure. As for the method, this essay uses TBS-ASIFM model, which can reproduce extreme situation of information transaction at any time by setting parameters and help market regulators prevent risk events in advance.

This essay can provide trading strategy guidance for investors on stock index futures market and offer valuable political suggestions to the market regulators to prevent liquidity risk events. To be specific, the three main topics of this essay are as follows: how informed traders' proportion affects the market; the proportion within which scope is reasonable for the whole market's transparency and liquidity; how to manage liquidity risk from the point of investor structure.

This essay includes six sections: the second part is the literature review, which systematically reviews relevant research literature at home and abroad according to the main ideas; the third part introduces the EKOP model and the VPIN model; the forth part gives a more systematical description of TBS-ASIFM artificial financial market model used later, introduces the setting of the model's parameters, and shows and analyses the results of simulation experiments; the fifth part is the conclusion; and the final part is the prospect of our study.

2. Literature Review

Earlier scholars mainly used indirect methods to calculate the degree of information asymmetry on security markets. Until 1996, Easley et al. (1996) [3] established EKOP model to calculate the degree of information asymmetry directly for the first time. Then Easley et al. (1997) [4] optimized the EKOP model by considering more comprehensive indicators, such as trading time, and built a better information transaction probability model. Researches on financial market information transaction probability of Venter and de Jongh (2004) [5], Lei and Wu (2005) [6] released the hypothesis that the traders arrival rate is constant. Venter and de Jongh (2004) assumed that traders' order arrival rates on the market followed inverse Gaussian distribution, while Lei and Wu (2005) allowed order arrival rates of uninformed traders with the behavioral characteristics of the district system to convert endogenously. In view of high frequency financial market, Easley et al. (2011) probed a method to measure the market's information transaction probability based on trading volume. This method divided trading volume into a few volume buckets and applied new estimation methods to determine the offer direction of each trade in each volume bucket. Easley et al. (2012) [7] fully expounded the significance of applying volume clock to high frequency trade, verifying the applicability of the VPIN model indirectly.

The studies mentioned above are mostly theoretical studies, and their contents are limited to the design and extension of models. In other words, they only state the characteristics and possible application theoretically and do not conduct empirical analysis on specific objects, such as stock, bonds, and futures. Nyholm (2002 [8], 2003 [9]) studied market information transaction probability through separated high frequency data, and he used regime-switching model to explain the probability of informed trades from the brokers' point of view. Easley et al. (2010) [10] applied VPIN model into "flash crash" in 2010 and studied the change of VPIN of E-Mini S&P 500 stock index futures market. The result indicates that, during the week before "flash crash," the submissions of the market orders were extremely unbalanced, information trades were very frequent, and the VPIN was also extremely unstable. Especially several hours before the "flash crash," the VPIN of the market reached an anomaly peak. Therefore, the buyers' liquidity of the market was insufficient when the "flash crash" began. Their study explained the "flash crash" theoretically, with insufficient discussion on informed traders' proportion. In the field of high-frequency trading, Huang et al. (2013) [11] took five-minute transaction data of China's CSI 300 index as the research object, established HAR-CJ-M model, and applied this model to the study of CSI 300 index volatility. The result shows that the volatility of Chinese stock market can be influenced by the past volatility components, and these different volatility components derived from behaviors of investors with different holding term limits (short term, medium term, and long term) owned by the behaviors of investors.

In recent years, agent-based computational finance, which is based on complex adaptive system theory and computer simulation modeling, has gradually risen and achieved marked achievements, combining complex adaptive system theory and behavioral finance theory and using object-oriented modeling method to construct a kind of artificial financial markets that have real market features (transaction mechanism, institutional arrangement, agent behavior patterns, and study mechanism). Using the method of ACF, researchers can extend their studies on microstructure, macroscopic properties, regular patterns, and other aspects of financial market, like Levy et al. (2000) [12]. LeBaron (2006) [13] pointed out that agent-based computational finance provided a new and exciting tool to solve problems that could not be solved by traditional models. Tesfatsion and Judd's (2006) "Agent-based computational finance" [14] indicated that the research paradigm of agent-based computational finance had taken initial shape.

In the aspect of empirical research, Lux and Marchesi (1999) [15] described a multiagent model, which classified investors into two types, namely, fundamentals and noise traders. Mike and Farmar (2008) [16] developed an agent-based model on the basis of the continuous double auction mechanism in an order-driven market, to solve liquidity and volatility problems. Gu and Zhou (2009) [17] proposed a modified version of the Mike-Farmar model by including a new ingredient, that is, long memory in the aggressiveness of incoming orders. The finding shows the memory effect of order aggressiveness has little impact on the diffusiveness of stock prices. Zhang et al. (2010) [18] used agent-based computational finance to investigate the investment yield of four kinds of investors (rational expectation strategy, BSV strategy, noise trading strategy, and passive trading strategy). The finding shows the combination of arbitrage limits, noise trading, and risk aversion; rational investors cannot "eliminate" BSV investors; all the evidence argued against the Friedman's hypothesis cannot be established. Based on Italian researcher's SUMWEB model, Xiong et al. (2011) [19] studied the impact laid by the design of cross-market risk from the view of market typical characteristics and trading mechanisms and analyzed the formation mechanism of cross-market risk. Zhang et al. (2011) [20] established two artificial financial markets, MD-ASIFM (mechanism design on artificial stock index future market) and TBS-ASIFM (trader's behavior and structure on artificial stock index future market), and then used MD-ASIFM to analyze the influence of tick size and optimal design of position limits on market quality. They also proposed a suggestion of optimal setting and used TBS-ASIFM to address the influence of investor's structure of stock index future market and programmed arbitrage strategy on market quality. It is worth noting that the empirical analysis in this paper is on the basis of the TBS-ASIFM.

3. EKOP Model and VPIN Model

3.1. EKOP Model. EKOP model was formulated based on the sequential trade model by Easley et al. (1996). It determines the probability of informed trading by calculating the proportion of informed traders in all the certain risk asset transactions. The settings of EKOP model in detail are as follows.

Market Mechanism. EKOP model is defined in the dealership market framework, and researchers assume that the market makers are risk-neutral and competitive. The price of an asset, which is calculated according to the expected price of all the past transaction information, is offered to the investors by the market makers sequentially and then promotes the trades among them.

Trading Period. The trading process of EKOP model presents a hybrid form of discrete and continuous time sequential model. Trading days as the discrete parts are expressed by i $(i = 1, \ldots I)$, and the time within a trading day as the continuous part is expressed by $t \in [0, T]$. Information events are independently distributed. At the end of each trading day, the event will be fully reflected through the asset price. Simultaneously, the hypothesis that each investor just trades once during the course of the trading day and the transaction should be accomplished timely cannot be ignored.

Investors. In this model, there are informed and uninformed traders in the market. Informed traders can know in advance the risk of asset price; they enter markets and purchase risk assets when good news appears. When bad news occurs, such traders enter the market and sell risk assets. When there is no information incident happening in a trading day, informed traders would prefer to choose to wait and see. While for the uninformed traders who are completely unable to get information in advance, they enter markets according to other purposes (liquidity, psychological bias or hedge risk, etc.). The arrival rates of informed and uninformed traders, governed by independent Poisson processes, determine trades. The arrival rates also depend on the occurrence of three types of information events, namely, no news, good news, and bad news, which are chosen by nature every day. In each trading day, arrivals of uninformed buyers and uninformed sellers are determined by independent Poisson processes. Uninformed buyers and sellers arrive at rate ε. The arrival rate of informed buyers and sellers is instead μ.

Asset. Before the beginning of each trading day, the incidence of information events is independently distributed and expressed as α. These events are divided into two types, that is, good news with probability $1-\delta$ or bad news with probability δ. After the end of trading on any day, the full information value of the asset is obtained. With the occurrence of an information event in day i, the value of the asset is either $\overline{S}_i$ with good news or $\underline{S}_i$ with bad news.

Informed Trading Probability. Define $P(t) = \{P_n(t), P_b(t), P_g(t)\}$ as the market maker's prior belief about the events, no news (n), bad news (b), and good news (g) at time t. The unconditional prior beliefs at time 0 are equal to the probabilities with which nature chooses the information regime; $P(0) = \{1 - \alpha, \alpha * \delta, \alpha * (1 - \delta)\}$. So at time t, the expected value of the risky assets of the market makers is shown as

$$E(S_i t) = P_n(t) * S_t^* + P_b(t) * \underline{S}_i + P_g(t) * \overline{S}_i. \quad (1)$$

At time t, the probability for the informed traders to sell the asset is given by $\mu * P_b(t)/(\varepsilon + \mu * P_b(t))$. Similarly, the probability for the informed traders to buy the asset is given by $\mu * P_g(t)/(\varepsilon + \mu * P_g(t))$. The bid and ask are given by the following relation:

$$\begin{aligned} B(t) &= E(S_i t) - \frac{\mu * P_b(t)}{\varepsilon + \mu * P_b(t)} * \left[E(S_i t) - \underline{S}_i\right], \\ A(t) &= E(S_i t) + \frac{\mu * P_g(t)}{\varepsilon + \mu * P_g(t)} * \left[\overline{S}_i - E(S_i t)\right]. \end{aligned} \quad (2)$$

These equations demonstrate the impact laid by arrivals of informed and uninformed traders on the market-makers quotes. If there are no informed traders ($\mu = 0$), then trade carries no information, and so the bid and ask are both equal to the prior expected value of the asset. Alternatively, if there are no uninformed traders ($\varepsilon = 0$), then the bid and ask are at the minimum and maximum prices, respectively. At these prices, no informed traders will trade either, and the market, in effect, shuts down. Generally, both informed and uninformed traders will be in the market, and so the bid is less than $E(S_i \mid t)$, and the ask is greater than $E(S_i \mid t)$.

The bid-ask spread at time t is denoted by

$$\Sigma(t) = \frac{\mu * P_g(t)}{\varepsilon + \mu * P_g(t)}\left[\overline{S_i} - E(S_i \mid t)\right] + \frac{\mu * P_b(t)}{\varepsilon + \mu * P_b(t)}\left[E(S_i t) - \underline{S_i}\right]. \tag{3}$$

The spread for the initial quotes in the period has a particularly simple form in the natural case in which good and bad events are equally likely. That is, if $\delta = 1 - \delta$, then

$$\Sigma = \frac{\alpha * \mu}{\alpha * \mu + 2\varepsilon} * \left(\overline{S_i} - \underline{S_i}\right). \tag{4}$$

So the probability that the information-based opening trade in a period is given by

$$\text{PIN} = \frac{\alpha * \mu}{\alpha * \mu + 2\varepsilon}. \tag{5}$$

Due to the indirectly observation such as the occurrence of information events or the associated arrival of informed and uninformed traders, it is difficult to estimate the parameter arise. However, knowing the daily arrivals of sell and buy is possible, which offers an excellent approach to inferring these values using maximum likelihood. Note that the trading process follows a Poisson process. Consider

$$\begin{aligned} L &= \prod_{i=1}^{n} P\left[y_t = (B_t, S_t)\right] \\ &= \prod_{i=1}^{n}\left(\alpha * (1-\delta) * e^{-(\mu+2\varepsilon)} * \frac{(\mu+\varepsilon)^{B_t} * \varepsilon^{S_t}}{B_t! * S_t!} + \alpha * \delta * e^{-(\mu+2\varepsilon)} * \frac{(\mu+\varepsilon)^{S_t} * \varepsilon^{B_t}}{B_t! * S_t!}\right) \\ &\quad + (1-\alpha) * e^{-2\varepsilon} * \frac{\varepsilon^{(B_t+S_t)}}{B_t! * S_t!}. \end{aligned} \tag{6}$$

3.2. VPIN Model. Easley et al. (2011) grouped sequential trades into equal volume bucketsof an exogenously defined size V. A volume bucket is a collection of trades with total volume V. If the last trade is in need of a complete bucket which is greater than the requirement in size, the excess size is given to the next bucket. We let $\tau = 1, \ldots, n$ be the index of equal volume buckets. If the deal is launched by the buyer, the sum of volume launches by buyers is marked as V_τ^B or marked as V_τ^S. There will be

$$\frac{1}{n}\sum_{\tau=1}^{n}\left(V_\tau^B + V_\tau^S\right) = V. \tag{7}$$

From EKOP model and Easley et al. (2008) [21], we can know the following:

$$\begin{aligned} E(V) &= \underbrace{\alpha * (1-\delta) * (\varepsilon + \mu + \varepsilon)}_{\text{volume resulting from good news}} + \underbrace{\alpha * \delta * (\mu + \varepsilon + \varepsilon)}_{\text{volume resulting from bad news}} \\ &\quad + \underbrace{(1-\alpha) * (\varepsilon + \varepsilon)}_{\text{volume without news}} = \alpha * \mu + 2\varepsilon, \\ E(OI) &= B - S \\ &= \alpha * \delta * (\varepsilon - \mu - \varepsilon) + \alpha * (1-\delta) * (\varepsilon + \mu - \varepsilon) \\ &\quad + (1-\alpha) * (\varepsilon - \varepsilon) \\ &= \alpha * \mu (1 - 2\delta). \\ E(|OI|) &= |B - S| \\ &= \alpha * \delta * (|\varepsilon - \mu - \varepsilon|) + \alpha * (1-\delta) * (|\varepsilon + \mu - \varepsilon|) \\ &\quad + (1-\alpha) * (|\varepsilon - \varepsilon|) \\ &= \alpha * \mu, \\ E[OI_\tau] &= E\left[\left|V_\tau^S - V_\tau^B\right|\right] \approx \alpha * \mu. \end{aligned} \tag{8}$$

Generally speaking, information trading can be reflected by the unbalance order. So

$$\text{VPIN} = \frac{\alpha * \mu}{\alpha * \mu + 2\varepsilon} = \frac{\alpha * \mu}{V} \approx \frac{\sum_{r=1}^{n}\left|V_\tau^S - V_\tau^B\right|}{n * V}. \tag{9}$$

4. TBS-ASIFM Artificial Financial Market and Empirical Analysis

4.1. The Introduction of TBS-ASIFM Artificial Financial Market. TBS-ASIFM artificial financial market model includes a stock market and a stock index market. We can merchandise several stocks in the stock market but merchandise only one stock index in the stock index market. The investors in the two markets can be classified into three types. The first is risky assets value informed investors, the second is risky assets uninformed investors, and the third is liquid investors. Some investors are operating in both markets. TBS-ASIFM includes multiple assets, markets, and investors. All investors are fortune-restrained, limited by risk management and market trading mechanism. Simultaneously, the artificial financial market should conform with the rules of the stock market and the stock index market.

Market mechanism includes two parts: stock market and stock index market; both of them are continuous double auction trading mechanisms. The stock market chooses $T + 1$ trading rules and the stock index market chooses the $T + 0$ one.

Assets. There are 5 stocks and 1 stock index in the market. The stock index is combined by 5 stocks. The settings of traders' transactions and trading strategies can be learned from Zhang et al. (2011).

The investors trading in the stock market can be divided into three categories: informed traders, uninformed technical traders, and uninformed noise traders. Likewise, the investors who trade in the futures market can also be classified based on this concept. However, for investors in the futures market, apart from the three categories above, we also have one special category, namely, arbitragers. The arbitragers are the investors who trade in both the stock market and the stock index futures market, making profits from the price fluctuation between these two markets. Specifically speaking, the arbitragers would open short positions in the index futures market and buy the spot stock index simultaneously when they notice that the futures price is higher than the upper limit of the nonarbitrage price. Moreover, the arbitragers would calculate their profits every single day. Both the stock and futures position will be offset; that is, if expected return is achieved, they will sell the stock index and buy the futures contract or they will not offset the position and wait until the futures contract expires. In our model, in order to execute market order promptly, the arbitragers will allocate their money properly between the stock market and futures market according to their wealth (total asset), making risk-free profits. The trading behavior and strategy for all the investors can be referred from Zhang et al. (2011) and Chiarella et al. (2009) [22].

4.2. Model Parameters Setting. There are 60522 subperiods in every experiment period, which represent 21 days. Each day has 2882 subperiods, and one subperiod stands for 5 seconds in the real world. The risk-free interest rate is 4.26%, the same number as the interbank collateral repo rate. The positions for the stock and futures market should be closed out at the end of trading day. The minimum trade requirement for the stock market is one lot, namely, 100 shares, and short selling in the stock market is prohibited. The tick size (minimum price fluctuation) is 1 cent and 20 cents for the stock market and futures market, respectively. Daily price fluctuation limit for both markets is set up as 10%. The commission fee for the stock market and futures market is 0.3% and 0.005%, respectively. The impact cost during the arbitrage is supposed to be 0.21% and 0.015% for the stock market and futures market, respectively. The maximum allowed position for the stock index futures market is 100 lots, and the margin ratio could be as low as 12%. The multiplier for the stock index futures is 300.

4.3. Simulation Experiment Results

4.3.1. Probability of Informed Trading and Market Absolute Yield. Existing empirical studies show that, in the same market investor's structural framework, with VPIN gradually increasing, the share of its subsequent market's low absolute yields reduces gradually, while the proportion of high absolute yields increases. Method of agent-based computational finance makes it possible to clarify the relationships between VPIN and market absolute yields under different proportion of informed traders. And the structure of investors in financial markets can be characterized by the proportion of various investment strategies. Proportions of informed investors in this study are designed as follows: 1/6, 1/3, 1/2, 2/3, and 5/6. In order to be consistent with the reality, experiments do not consider two extreme conditions; that is, there are no informed traders existing in the market and the proportion of informed traders reaches 100%.

Analysis of data statistics can be divided into twenty groups; each group contains 5% observations. Take the first column; for example, this row is sorted in ascending order according to the informed trading probability. The first line stands for the absolute yield, and then we divide data into eight groups according to the absolute yields from the lowest to the highest. Due to space constraints, we can not list all the statistics. Therefore, we, respectively, select the information investors' proportion between 1/6 and 5/6 as representative sample. Tables 1 and 2 show the results.

According to above-mentioned analytical results, for the same investor structure, with VPIN which is gradually increasing, the share of its subsequent market's low absolute yields gradually decreases, while the proportion of high absolute yields increases. This is consistent with empirical research findings based on the real market. Thus, for different investor structure, with the increase of informed traders in the market, the market absolute yields corresponding to larger VPIN value show a tendency of increasing. This suggests that when the market traders are usually informed traders, risk events will impact the market to a greater extent, because liquidity traders face increasing adverse selection cost when dealing with informed traders.

4.3.2. Proportion of Informed Traders and Market Quality. This section mainly studies the impacts from the proportion of informed traders on market information dissemination efficiency and market liquidity, and we choose market information dissemination efficiency from Gil-Bazo et al. (2007) [23] and Zhang et al. (2011) as the indicators. Market liquidity is represented by the turnover rate of market limit orders (a limit pay can be a market order when its price is higher than the best selling price, and a limit sell order can be a market order when its price is lower than optimal bid price. Statistical results exclude those limit orders used as market orders); the formula is as follows:

$$\mathrm{MAE} = \frac{1}{T}\sum_{t=1}^{T}\left|p_t - v_t\right|. \tag{10}$$

As can be seen from Table 3, when the proportion of informed traders is between 1/3 and 1/2, market information dissemination efficiency becomes better and the turnover rate of limit orders also rises, while in many other cases, market information dissemination efficiency and the turnover rate of limit orders are showing a deteriorating trend. This indicates that, when the proportion of informed traders is between 1/3 and 1/2, market transparency and market liquidity are better.

Table 1: Absolute yields under VPIN conditions when the proportion of informed investors is 1/6.

	0.0015	0.003	0.0045	0.006	0.0075	0.009	0.0105	>0.0105
0.00011	68.00%	24.00%	6.00%	0.00%	2.00%	0.00%	0.00%	0.00%
0.00488	40.00%	30.00%	18.00%	8.00%	4.00%	0.00%	0.00%	0.00%
0.10538	50.00%	28.00%	12.00%	4.00%	4.00%	2.00%	0.00%	0.00%
0.17095	46.00%	34.00%	10.00%	2.00%	8.00%	0.00%	0.00%	0.00%
0.29997	50.00%	24.00%	12.00%	2.00%	4.00%	2.00%	0.00%	6.00%
0.43789	50.00%	26.00%	4.00%	4.00%	10.00%	2.00%	0.00%	4.00%
0.5009	48.00%	16.00%	14.00%	6.00%	6.00%	0.00%	0.00%	10.00%
0.55039	42.00%	30.00%	12.00%	4.00%	4.00%	2.00%	0.00%	6.00%
0.58429	55.50%	20.67%	9.83%	5.33%	2.67%	1.17%	1.33%	3.50%
0.61272	55.82%	20.73%	9.64%	5.45%	2.55%	1.27%	1.27%	3.27%
0.64318	55.40%	20.80%	9.60%	5.20%	2.60%	1.40%	1.40%	3.60%
0.67021	56.67%	19.33%	9.78%	5.11%	2.89%	1.33%	1.33%	3.56%
0.69265	57.25%	19.25%	10.00%	5.00%	2.75%	1.00%	1.25%	3.50%
0.71589	56.57%	18.86%	11.14%	5.71%	2.29%	0.86%	1.43%	3.14%
0.73141	55.67%	19.33%	11.67%	5.67%	2.33%	0.67%	1.33%	3.33%
0.74439	54.80%	19.60%	11.20%	5.60%	2.40%	0.80%	1.60%	4.00%
0.75569	54.50%	19.00%	11.50%	6.50%	2.00%	1.00%	1.00%	4.50%
0.76385	51.33%	20.67%	11.33%	6.67%	2.67%	0.67%	0.67%	6.00%
0.77579	53.00%	24.00%	8.00%	8.00%	1.00%	1.00%	0.00%	5.00%
0.79111	48.00%	28.00%	10.00%	8.00%	0.00%	2.00%	0.00%	4.00%

Table 2: Absolute yields under VPIN conditions when the proportion of informed investors is 5/6.

	0.0015	0.003	0.0045	0.006	0.0075	0.009	0.0105	>0.0105
0.0053	74.00%	18.00%	8.00%	0.00%	0.00%	0.00%	0.00%	0.00%
0.029766	74.00%	20.00%	6.00%	0.00%	0.00%	0.00%	0.00%	0.00%
0.049642	56.00%	28.00%	10.00%	4.00%	2.00%	0.00%	0.00%	0.00%
0.085005	64.00%	32.00%	2.00%	0.00%	2.00%	0.00%	0.00%	0.00%
0.142565	58.00%	12.00%	14.00%	10.00%	6.00%	0.00%	0.00%	0.00%
0.242377	44.00%	22.00%	16.00%	6.00%	8.00%	4.00%	0.00%	0.00%
0.304469	52.00%	24.00%	8.00%	10.00%	0.00%	2.00%	0.00%	4.00%
0.38123	40.00%	26.00%	12.00%	8.00%	4.00%	0.00%	2.00%	8.00%
0.516074	32.00%	22.33%	14.67%	11.67%	4.83%	4.83%	3.17%	6.50%
0.61289	30.55%	21.82%	15.45%	11.82%	5.09%	5.09%	3.09%	7.09%
0.645069	30.80%	21.60%	14.20%	12.40%	5.40%	5.40%	3.00%	7.20%
0.686656	30.67%	22.00%	14.67%	12.22%	5.33%	5.56%	3.33%	6.22%
0.703128	30.50%	21.50%	15.00%	12.25%	5.75%	5.75%	3.00%	6.25%
0.726787	30.57%	22.00%	15.43%	12.29%	4.86%	5.43%	3.14%	6.29%
0.751038	31.67%	20.00%	14.67%	12.33%	4.67%	6.33%	3.33%	7.00%
0.793769	30.80%	20.40%	15.20%	12.80%	4.80%	7.20%	2.40%	6.40%
0.819723	29.50%	21.00%	16.50%	13.50%	5.50%	6.00%	3.00%	5.00%
0.84226	30.00%	18.67%	17.33%	14.67%	5.33%	6.00%	3.33%	4.67%
0.854557	29.00%	16.00%	22.00%	14.00%	4.00%	7.00%	4.00%	4.00%
0.878799	24.00%	18.00%	30.00%	10.00%	6.00%	8.00%	2.00%	2.00%

5. Conclusion

In this paper, we adopt the TBS-ASIFM model established by Zhang et al. (2011) to study probability of informed trading of stock index futures market and its effect on subsequent market absolute yields, respectively, and also give a detailed description of the market information dissemination efficiency and dynamic characteristics of liquidity under different traders structure. We find that, on one hand, as for the same traders' structure, with the probability of informed trading increasing gradually, the share of the low absolute yields in subsequent market gradually decreases, while the

Table 3: Statistical results in each experimental group.

Experimental group	Proportion of informed traders	MAE	Turnover rate of limit order
1	1/6	8.64	30.67%
2	1/3	6.06	20.45%
3	1/2	2.85	32.06%
4	2/3	12.95	12.94%
5	5/6	16.43	12.40%

proportion of high absolute yields gradually increases. As for different traders' structures, increase in informed traders on the market facilitates the increasing tendency of the market absolute yields. On the other hand, we also find that there will be better transparency and liquidity of the market when the proportion of informed traders accounts for between 1/3 and 1/2 by focusing on market information dissemination efficiency and liquidity under different trader's structures.

6. Research Prospects

In this paper, we apply VPIN model and agent-based computational finance to analyze information transactions, but there are still some issues to be further studied.

Firstly, VPIN model used in this paper is based on the market-maker market; although this model is of universal applicability and transplantability, new methods based on continuous auction market to estimate probability of informed trading are still to be drilled down into.

Secondly, VPIN model can be a warning of market liquidity risk; this paper only gives our own explanations on the most superficial level and does not explore the concrete impact mechanism.

Thirdly, we can further expand TBS-ASIFM model, invert the "flash crash" event, and study the effectiveness of market regulatory measures (e.g., transaction contracts of VPIN).

Conflict of Interests

The authors declare that there is no conflict of interests regarding the publication of this paper.

Acknowledgments

This paper was supported by NSFC (nos. 71131007 and 71271145), Program for Changjiang Scholars and Innovative Research Team in University (no. IRT1028), and Specialized Research Fund for the Doctoral Program of Higher Education (no. 20110032110031).

References

[1] D. Easley, M. M. L. de Prado, and M. O'Hara, "Flow toxicity and volatility in a high frequency world," *Review of Financial Studies*, vol. 25, no. 5, pp. 1457–1493, 2011.

[2] J. L. Holland, *Making Vocational Choices: A Theory of Vocational Personalities and Work Environments*, Psychological Assessment Resources, Odessa, Fla, USA, 1997.

[3] D. Easley, N. M. Kiefer, M. O'Hara, and J. B. Paperman, "Liquidity, information, and infrequently traded stocks," *Journal of Financeno*, vol. 51, no. 4, pp. 1405–1436, 1996.

[4] D. Easley, N. M. Kiefer, and M. O'Hara, "The information content of the trading process," *Journal of Empirical Finance*, vol. 4, no. 2-3, pp. 159–186, 1997.

[5] J. H. Venter and D. de Jongh, "Extending the EKOP model to estimate the probability of informed trading," *Studies in Economics and Econometrics*, vol. 30, no. 2, pp. 25–39, 2006.

[6] Q. Lei and G. Wu, "Time-varying informed and uninformed trading activities," *Journal of Financial Markets*, vol. 8, no. 2, pp. 153–181, 2005.

[7] D. Easley, M. M. L. de Prado, and M. O'Hara, "The volume clock: insights into the high frequency paradigm," *The Journal of Portfolio Management*, vol. 39, no. 1, pp. 19–29, 2012.

[8] K. Nyholm, "Estimating the probability of informed trading," *Journal of Financial Research*, vol. 25, no. 4, pp. 485–505, 2002.

[9] K. Nyholm, "Inferring the private information content of trades: a regime-switching approach," *Journal of Applied Econometrics*, vol. 18, no. 4, pp. 457–470, 2003.

[10] D. Easley, M. M. L. de Prado, and M. O'Hara, "The microstructure of the flash crash: flow toxicity, liquidity crashes and the probability of informed trading," *The Journal of Portfolio Management*, vol. 37, no. 2, pp. 118–128, 2011.

[11] C. Huang, X. Gong, X. Chen, and F. Wen, "Measuring and forecasting volatility in Chinese stock market using HAR-CJ-M model," *Abstract and Applied Analysis*, vol. 2013, Article ID 143194, 13 pages, 2013.

[12] H. Levy, M. Levy, and S. Solomon, *Microscopic Simulation of Financial Markets: From Investor Behavior to Market Phenomena*, Academic Press, San Diego, Calif, USA, 2000.

[13] B. LeBaron, "Agent-based financial markets: matching stylized facts with style," in *Post Walrasian Macroeconomics: Beyond the DSGE Model*, D. Colander, Ed., pp. 221–235, Cambridge University Press, 2006.

[14] L. Tesfatsion and K. L. Judd, "Agent-based computational finance," in *Handbook of Computational Economics*, vol. 2, chapter 16, pp. 831–880, North-Holland, Amsterdam, The Netherlands, 2006.

[15] T. Lux and M. Marchesi, "Scaling and criticality in a stochastic multi-agent model of a financial market," *Nature*, vol. 397, no. 6719, pp. 498–500, 1999.

[16] S. Mike and J. D. Farmar, "An empirical behavioral model of liquidity and volatility," *Journal of Economic Dynamics and Control*, vol. 32, no. 1, pp. 200–234, 2008.

[17] G. F. Gu and W. X. Zhou, "Emergence of long memory in stock volatility from a modified Mike-Farmer model," *Europhysics Letters*, vol. 86, no. 4, article 48002, 6 pages, 2009.

[18] Y. J. Zhang, W. Zhang, and X. Xiong, "Investment strategies and yield: based on the calculation of financial research experiments," *Journal of Management Sciences in China*, vol. 13, no. 009, pp. 107–118, 2010.

[19] X. Xiong, M. Wen, W. Zhang, and Y. J. Zhang, "Cross-market financial risk analysis: an agent-based computational finance," *International Journal of Information Technology and Decision Making*, vol. 10, no. 3, pp. 563–584, 2011.

[20] W. Zhang, X. Xiong, and L. J. Wei, "Analysis of market-based trading mechanisms computational experiment finance stock index futures," China Financial Futures Exchange Research Report, 2011.

[21] D. Easley, R. F. Engle, and M. O'Hara, "Time-varying arrival rates of informed and uninformed traders," *Journal of Financial Econometrics*, vol. 6, no. 2, pp. 171–207, 2008.

[22] C. Chiarella, G. Iori, and J. Perelló, "The impact of heterogeneous trading rules on the limit order book and order flows," *Journal of Economic Dynamics and Control*, vol. 33, no. 3, pp. 525–537, 2009.

[23] J. Gil-Bazo, D. Moreno, and M. Tapia, "Price dynamics, informational efficiency, and wealth distribution in continuous double-auction markets," *Computational Intelligence*, vol. 23, no. 2, pp. 176–196, 2007.

Hindawi Publishing Corporation
Discrete Dynamics in Nature and Society
Volume 2014, Article ID 597814, 9 pages
http://dx.doi.org/10.1155/2014/597814

Research Article

Risk Measurement for Portfolio Credit Risk Based on a Mixed Poisson Model

Rongda Chen[1,2,3] and Huanhuan Yu[1]

[1] *School of Finance, Zhejiang University of Finance and Economics, Hangzhou 310018, China*
[2] *Coordinated Innovation Center of Wealth Management and Quantitative Investment, Zhejiang University of Finance and Economics, Hangzhou 310018, China*
[3] *Center for Research of Regulation and Policy of Zhejiang Province, Hangzhou 310018, China*

Correspondence should be addressed to Rongda Chen; rongdachen@163.com

Received 19 February 2014; Accepted 28 April 2014; Published 22 May 2014

Academic Editor: Fenghua Wen

Experiences manifest the importance of comovement and communicable characters among the risks of financial assets. Therefore, the portfolio view considering dependence relationship among credit entities is at the heart of risk measurement. This paper introduces a mixed Poisson model assuming default probabilities of obligors depending on a set of common economic factors to construct the dependence structure of obligors. Further, we apply mixed Poisson model into an empirical study with data of four industry portfolios in the financial market of China. In the process of model construction, the classical structural approach and option pricing formula contribute to estimate dynamic default probabilities of single obligor, which helps to obtain the dynamic Poisson intensities under the model assumption. Finally, given the values of coefficients in this model calculated by a nonlinear estimation, Monte Carlo technique simulates the progress of loss occurrence. Relationship between default probability and loss level reflected through the MC simulation has practical features. This study illustrates the practical value and effectiveness of mixed Poisson model in risk measurement for credit portfolio.

1. Introduction

Financial system is the core of modern economy and the risk in it has a huge impact on economic development. Two main components of financial risk are market risk and credit risk. Whereas market risk is the risk of losses in positions arising from movements in market prices, credit risk refers to the risk that a borrower will default on any type of debt by failing to make contractual payments.

Giesecke [1] proposes that there are two main quantitative approaches to analyze how to measure portfolio credit risk. In the structural approach, a firm defaults if its assets are insufficient according to some measure and then the probability of default can be deduced by tracing the dynamics of a firm's intrinsic value. The basic application of structural approach goes back to Black and Scholes [2] and Merton [3]. In recent years, structural approach is still in widespread use; see Chan et al. [4] and Schäfer and Koivusalo [5]. The other one, reduced-form approach, is silent about why a firm defaults because the dynamics of default are exogenously given through a default probability. Thus this paper applies the structural approach to measure default risk of a single firm.

The financial crisis we experienced these years tells that the financial health of a firm varies with randomly fluctuating macroeconomic factors. Therefore, different firms are affected by common macroeconomic factors; there is dependence between defaults. The portfolio view considering dependence relationship among credit entities first introduced by CreditMetrics [6] is the most important feature of modern credit risk management. In the consideration of the integrated risk of a portfolio, we can classify credit risk models into two categories: bottom-up and top-down; see Gordy [7]. In a bottom-up model, the portfolio default intensity is an aggregate of the constituents. The approach proposed by Barnhill and Maxwell [8] relates financial market volatility to firm specific credit risk and integrates interest rate, interest rate spread, and foreign exchange rate risk into one overall fixed income portfolio risk assessment. References [9, 10] study the motion features of risk factors. In a top-down model, the portfolio intensity is specified without reference to the constituents. Instead, dependence is introduced through a set of "risk factors" and defaults become independent conditional on the risk factors. Here, copula functions originally associated with J.P. Morgan's CreditMetrics system [6] are now widely employed for linking the marginal distributions of losses resulting from different risk factors to obtain the distribution of aggregate loss; see Wen and Liu [11], Dimakos and Aas [12], and Rosenberg and Schuermann [13]. And Liang et al. [14] present a factor copula model for the integration of Chinese commercial bank's credit risk and market risk.

However, it is quite difficult to choose a correct copula function, especially because the relative scarcity of data on credit losses. Frey and McNeil [15] showed that the aggregate portfolio loss distribution is often very sensitive to the choice of copula and the estimation of parameters. For large portfolios of tens of thousands of obligors there remains considerable model risk. Therefore, Glasserman and Li [16] propose another top-down model, a mixed Poisson mechanism, originally associated with CreditRisk$^+$ [17], to capture the dependence between risk factors. This paper introduces this model and applies it into empirical study with data in financial market of China for the reason that the mixed Poisson model has less model risk, because the loss distribution in mixed Poisson is the aggregate of all units whose model risk can be offset by each other. Further, it is more convenient for statistical fitting and simulation purposes in empirical study.

The paper is organized as follows. We review the structural approach and get the formula of individual default probability in Section 2. In Section 3 we introduce the mixed Poisson model. Section 4 brings the empirical study of our model. Summary and conclusion are given in Section 5.

2. Structural Approach

Since the 1990s of the last century, quantitative analysis has been blended into models of credit risk measurement. The structural model is based on the option pricing theory of Merton who indicated that equity is a kind of call option with the strike price of corporate liability. This structural model first estimates the market value of corporate equity and also its volatility and then it obtains the default distance and the default probability under the relevant corporate liability.

We will be confronted with two fundamental questions when measuring the credit risk of portfolio. One is how to describe the relationship among the default probabilities of obligors and the other one is how to link credit risks of obligors with the economic environment they face. These two questions can be solved by mixed Poisson model in this paper, but structural approach must be used first to quantize the default probability of a single obligor.

2.1. Classical Approach. Consider a firm with intrinsic value V, which represents the expected future cash flows of the firm. The firm is financed by equity and a zero coupon bond with face value K and maturity date T. The firm has to repay the amount K to the bond investors at time T or its bond holders have the right to take over this firm. Hence the default time τ is a discrete random variable given by

$$\tau = \begin{cases} T & \text{if } V_T < K \\ \infty & \text{otherwise.} \end{cases} \quad (1)$$

Meanwhile, we make assumptions that the evolution of asset prices over time follows geometric Brownian motion:

$$\frac{dV_t}{V_t} = \mu dt + \sigma dW_t, \quad (2)$$

where $\mu \in R$ is a drift parameter, $\sigma > 0$ is a volatility parameter, and W is a standard Brownian motion. Setting $m = \mu - (1/2)\sigma^2$, Ito's lemma implies that

$$V_t = V_0 e^{mt + \sigma W_t}. \quad (3)$$

Since W_T is normally distributed with mean zero and variance T, default probabilities $p(T)$ are given by

$$\begin{aligned} p(T) &= P(V_T < K) \\ &= P(\sigma W_T < \log L - mT) = \Phi\left(\frac{\log L - mT}{\sigma T}\right), \end{aligned} \quad (4)$$

where $L = (K/V_0)$ is the initial leverage ratio and Φ is the standard normal distribution function.

2.2. Theoretical Solution of Model. Given the equity value E_t and its volatility σ^E, Jones et al. [18] suggested that a firm's intrinsic value V_t and its volatility σ can be obtained through the option pricing formula. Generally, intrinsic value as well as its volatility of a public corporation can be estimated through the market value of its shares, the volatility of its stock price, and the book value of its debt. Because the market value of a company's shares reflects investors' expectations about the future value of the company, the equity of corporation can be viewed as a European call option on the assets of the firm with strike price D and maturity T. The value of the equity at time 0 is given by

$$E_0 = e^{-rT} \widehat{E}\left[\max\left(V_T - D, 0\right)\right] \quad (5)$$

which is equivalent to the payoff of a European call. r is the risk free rate and V_T is hold-to-maturity price of the underlying assets.

Pricing equity can be transformed to pricing European options. Equity value applied with the classical Black-Scholes formula is given by

$$E_0 = e^{-rT}\left[V_0 N(d_1) e^{rT} - DN(d_2)\right], \quad (6)$$

where

$$d_1 = \frac{\ln(V_0/D) + (r + \sigma^2/2)T}{\sigma\sqrt{T}}, \quad d_2 = d_1 - \sigma\sqrt{T}. \quad (7)$$

Since $E_t = f(V_t, t)$, Ito's lemma implies that

$$df(V_t,t) = \left(f_x(V_t,t)\,uV_t\right) + \frac{1}{2} f_{xx}(V_t,t)\,\sigma^2 V_t^2 + f_t(V_t,t)\,dt + \sigma f_x(V_t,t)\,V_t dW_t. \quad (8)$$

Meanwhile, we have $dE_t = u^E E_t dt + \sigma^E E_t dW_t$ so we can obtain

$$E_t = \frac{\sigma}{\sigma^E} f_x(V_t,t)\,V_t. \quad (9)$$

The combination of (6) and (9) gives the value of V_T. Further, because the firm's value V_T follows geometric Brownian motion of (2), we can get parameters of μ and σ through (10). Consider the following:

$$\mu = \frac{\left(\overline{\Delta V} + S_{\Delta V}^2/2\right)}{\Delta t}, \qquad \sigma = \frac{S_{\Delta V}}{\sqrt{\Delta t}}, \quad (10)$$

where $\overline{\Delta V} = (\sum_{t=1}^{n} \Delta V_t/n)$, $S_{\Delta V}^2 = (\sum_{t=1}^{n} (\Delta V_t - \overline{\Delta V})^2/(n-1))$, $\Delta V_t = \ln(V_{t+1}) - \ln(V_t)$, and $t = 1, \ldots, n$.

Eventually, we put parameters of μ, σ, and L into (4) to obtain default probability of every single obligor at time T.

3. Portfolio Credit Risk

Practical experience manifests the importance of comovement and communicable characters among the risks of financial assets. It is not sufficient to study the credit risk of some assets independently. Therefore, portfolio view is at the heart of the field about credit risk measurement. Generally speaking, the credit portfolio can be classified into two species: one is homogeneous portfolio and the other one is the heterogeneous. The latter is what we study in this paper. Next we carry out two methods which can be applied to describe the dependence structure of heterogeneous portfolio. The following notations are needed:

m: number of obligors in the portfolio that have the probability to default,

c_i: default risk exposure of ith obligor,

s_i: loss given default of ith obligor,

L: gross loss of a credit portfolio.

3.1. Portfolio Credit Risk in the Normal Copula Model. Here, we introduce the widely used normal copula model to describe the dependence among lots of obligors. To specify the distribution of losses from default of this heterogeneous portfolio over a fixed horizon, the following notations are additionally needed:

Y_i: default indicator for ith obligor; if ith obligor defaults, $Y_i = 1$, otherwise 0;

p_i: marginal probability that ith obligor defaults.

If there are m obligors in a portfolio, the gross loss is

$$L = \sum_{i=1}^{m} L_i = \sum_{i=1}^{m} c_i * s_i * Y_i. \quad (11)$$

The goal is to estimate tail probabilities $P(L > x)$ to measure credit risk of the whole portfolio. To model the dependence structure among obligors, we need to introduce dependence among the default indicator Y_i. In the normal copula model, dependence is introduced through a multivariate normal vector $W = (W_1, \ldots, W_m)$. Consider the following:

$$W_i^T = \frac{\log\left(V_T^i/V_0^i\right) - m_i T}{\sigma_i} \text{ is the standardized return,}$$
$$B_i = \frac{\log(L_i) - m_i T}{\sigma_i} \text{ is the standardized book value.} \quad (12)$$

Each default indicator is represented as

$$Y_i = 1\{W_i < B_i\}, \quad i = 1, \ldots, m. \quad (13)$$

There is

$$P(Y_i = 1) = P(W_i < B_i) = p_i. \quad (14)$$

That is to say, obligor i defaults if $W_i \le \Phi^{-1}(p_i)$. Through this construction, the correlations among W_i determine the dependence among Y_i. The underlying correlations are specified through a factor model of the form

$$W_i = \sum_{k=1}^{n} a_{ik} Z_k + b_i \varepsilon_i \quad (15)$$

for some $n < m$, a n-dimensional random vector $Z \sim N_n(0, \Omega)$, and independent standard normally distributed random variables $\varepsilon_1, \ldots, \varepsilon_m$, which are also independent of Z. In practice $Z_1, \ldots, Z_n$ are systematic risk factors representing macroeconomic effects such as country and industry factors and ε_i is the specific factor associated with the ith obligor. $a_{i1}, \ldots, a_{in}$ are the factor loadings for the ith obligor and $b_i = \sqrt{1 - (a_{i1}^2 + \cdots + a_{in}^2)}$.

Denote by $F_i(x) = P(W_i < B_i)$ the marginal distribution functions of W and default probability of company i is given by $p_i = F_i(B_i)$. To determine the multivariate distribution of W most of the researchers use normal copula C^N for W, so that

$$P(W_1 < B_1, \ldots, W_m < B_m) = C^N(F_1(B_1), \ldots, F_m(B_m)). \quad (16)$$

While most credit portfolio models prevailing in this field are based on the normal copula, there is no reason why we have to assume a normal copula. Alternative copulas can lead to very different credit loss distributions and it is obvious from (16) that the copula crucially determines joint default probabilities of groups of obligors and thus the tendency of the model to produce many joint defaults.

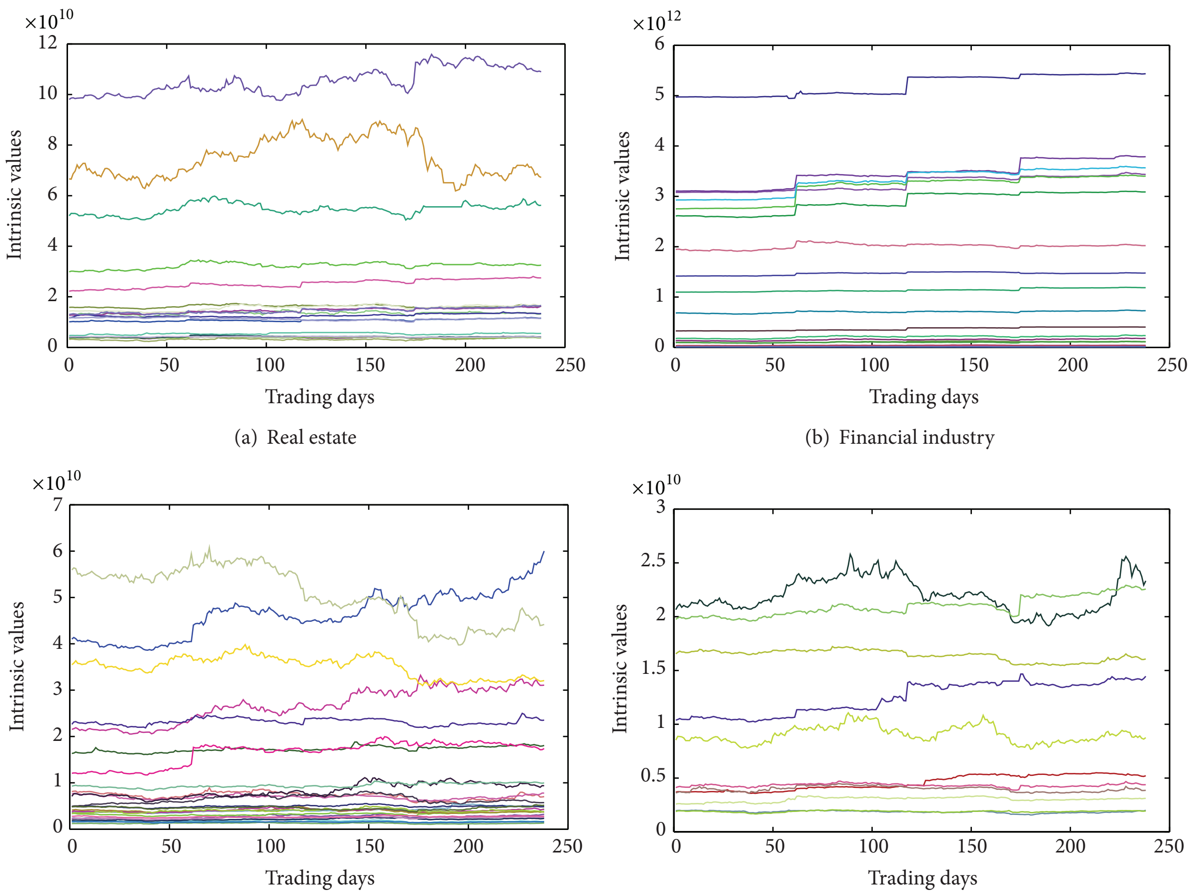

(a) Real estate

(b) Financial industry

(c) Machinery manufacturing

(d) Transportation

FIGURE 1: Paths for intrinsic values of industries.

3.2. Portfolio Credit Risk in the Mixed Poisson Model. As mentioned above, the aggregate portfolio loss distribution is often very sensitive to the choice of copula and the estimation of parameters. This paper introduces the mixed Poisson model to describe the dynamics of default occurrence for its less model risk. For large portfolios of tens of thousands of obligors, the change of several individuals will not affect the whole loss distribution, because the loss distribution in mixed Poisson is the aggregate of all units whose model risk can be offset by each other. And the other advantages of this method are as follows:

(i) mixed Poisson models are easy to simulate in Monte Carlo risk analyses;

(ii) mixed models are more convenient for statistical fitting purposes.

This model makes no assumptions about the causes of default-credit defaults which occur as a sequence of events in such a way that it is not possible to forecast neither the exact time of occurrence of any default nor the exact total number of defaults. There is an exposure to default losses from a large number of obligors and the probability of default by any particular obligor is small. This situation is well represented by the Poisson distribution.

In the mixed Poisson model, the portfolio loss over the horizon is still

$$L = \sum_{i=1}^{m} c_i * s_i * Y_i \tag{17}$$

but the default indicator Y_i is generated from a Poisson distribution instead of being generated by a variable W_i falling below some threshold. Consider the following:

$$Y_i \sim \text{Poisson}\left(R_i\right). \tag{18}$$

A Poisson random variable with a very small intensity has a very small probability of taking a value which is larger than 1. Although this assumption makes it possible to default more than once, a realistic model calibration generally ensures that the probability of this happening is little.

Mixed Poisson is also a top-down model whose default probability of an obligor is virtually assumed to depend on a set of common economic factors X_j, $j = 1, 2, \ldots, k$. This mechanism is realized through the intensity of Poisson distribution. Conditional on these factors, each Y_i has a Poisson distribution with intensity R_i,

$$R_i = a_{i0} + a_{i1} X_1 + \cdots + a_{ik} X_k \tag{19}$$

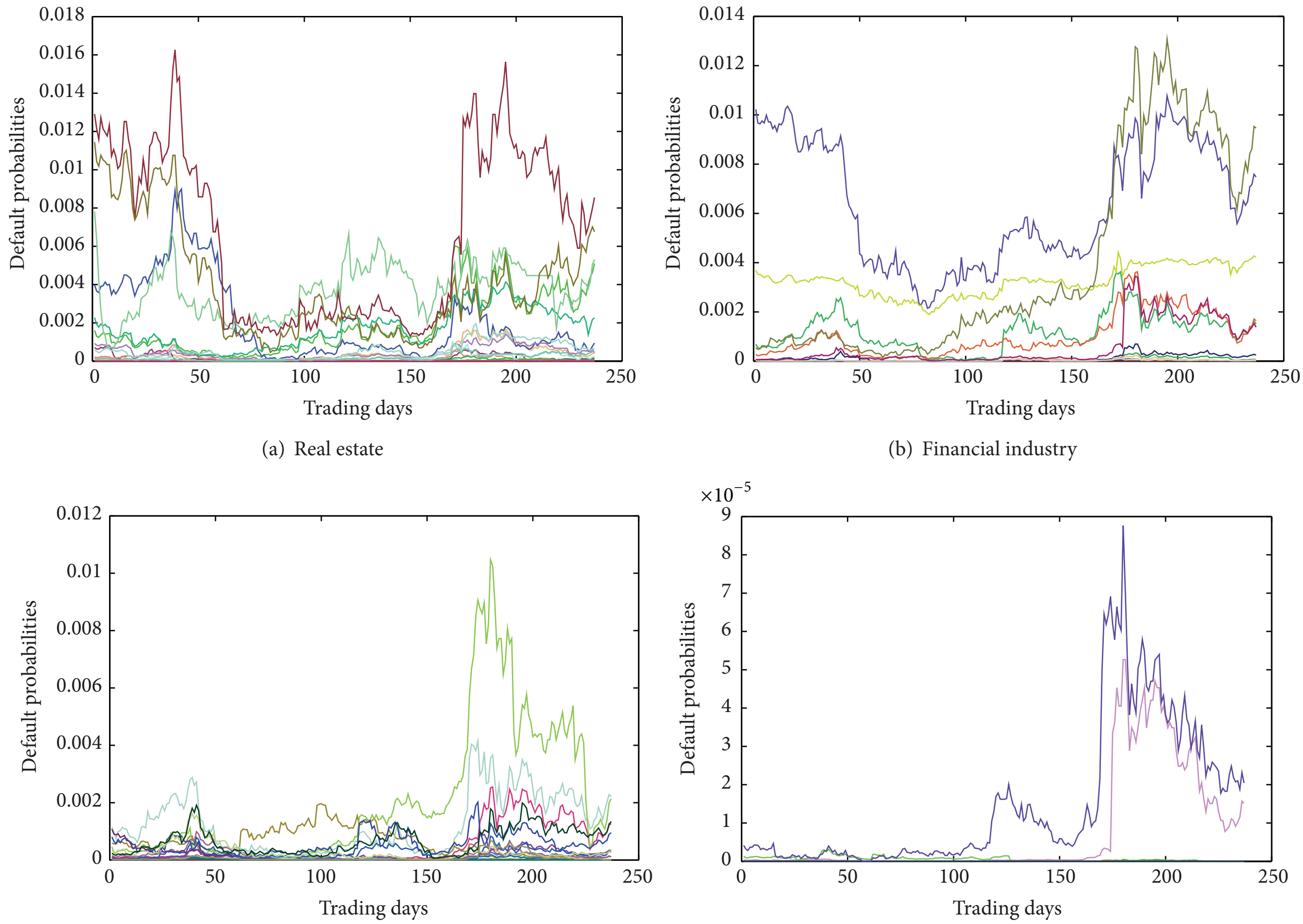

(a) Real estate (b) Financial industry (c) Machinery manufacturing (d) Transportation

Figure 2: Dynamic default probabilities of four industries.

for some positive coefficients $a_{i0}, \ldots, a_{id}$. Thus each Y_i may be viewed as a Poisson dynamic variable with a dynamic intensity—a mixed Poisson dynamic variable.

In the mixed Poisson model, Y_i, we talked about what follows the Poisson distribution. Because a Poisson random variable with a very small intensity has a trifling probability of taking a value which is larger than 1, Y_i can be applied as the default indicator in (17). We can achieve the results of default probabilities for each company at each trading day as illustrated in Section 2.1, which can help to bring out the Poisson intensity of Y_i.

Poisson distribution usually shows approximates with binominal distribution when $n \geq 10, p \leq 0.1$, so an obligor default is equal to $Y_i = 1$.

Given $P(X = k) = (e^{-\lambda}\lambda^k/k!)$ in Poisson, the intensity R_i can be estimated by

$$P_{\text{default}} = e^{-R_i} \cdot R_i. \tag{20}$$

4. Empirical Study

This paper uses mixed Poisson model to study the portfolio credit risk. Mixed Poisson is the structure describing dependence relationship among obligors and those macroeconomic factors essentially lead to the source of portfolio credit risk. It remains to find suitable factor loadings to construct a complete model. These factor loadings need to be derived from a historical default probability of single obligor.

4.1. Default Probability of Single Obligor. As mentioned in Section 2.2, public companies are the study objects of this paper. To obtain the historical default probability of single obligor, we need to know the market value of its shares, the volatility of its stock price, and the book value of its debt. Because the mixed Poisson model assumes that portfolio credit risk depends on a set of common economic factors, obviously the weight on each common factor varies with the industry characteristics. We select data of market value E_t, debt D_t, and closing price P_t for stocks in four industries of Shanghai Stock Exchange. The time horizon is from 2012.10.01 to 2013.09.30 which contains 238 trading days. Finally, we choose 20 companies from real estate, 25 from machinery manufacturing, 20 from financial industry, and 12 from transportation.

The history volatility σ^E in this study is the standard deviation of logarithmic change of closing prices.

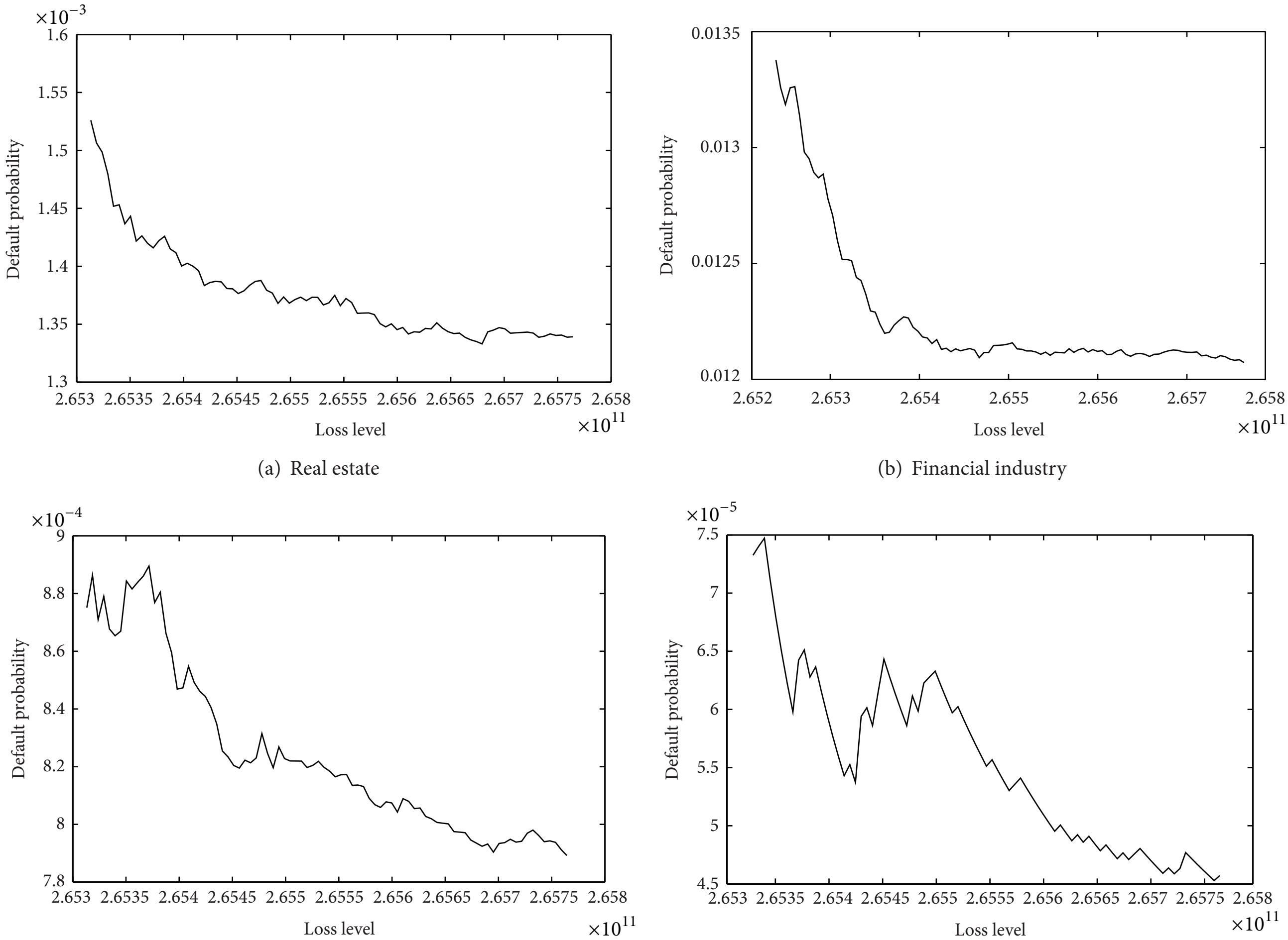

(a) Real estate

(b) Financial industry

(c) Machinery manufacturing

(d) Transportation

Figure 3: Loss distributions of each sample portfolio under Monte Carlo simulation.

We use formulas of (5) and (9) to obtain the intrinsic values of these companies at every present moment. Further, the trajectories of V_t are shown in Figure 1.

So far, V_t is already known and we put parameters of μ, σ produced by (10), and L into (4) to get historical default probability of every single company. Part of the result can be seen in Table 1. Here, an overview of dynamic default probabilities on each industry is given in Figure 2.

From Figure 2, we can find that the dynamic patterns of default curve in (a) and (b) are similar and the patterns in (c) and (d) are also similar. As a matter of fact, real estate in (a) and financial industry in (b) do have relatively strong relationship these years. And by this analogy, in the other two industries this phenomenon also exists, where it has been assumed in the mixed Poisson model that dynamic changes of default probabilities are driven by a series of common macroeconomic factors.

4.2. Mixed Poisson Model. We use default probabilities obtained before to estimate the value of Poisson intensity of each company as illustrated in (20), and the result is shown in Table 1 (as space is limited, we list part of the result for simplicity).

This model assumes that the intensity of Poisson variable is driven dynamically by several common factors. This paper chooses index prices of real estate index, infrastructure index, transportation index, and finance index to be the macroeconomic factors in this model. We need to obtain the factor loadings $a_{i0}, a_{i1}, \ldots, a_{ik}$ for each company. Since these indexes are negatively correlated with the intensity of default, letting e^{-X_j} be factors in (19) is suitable, where X_j, $j = 1, 2, 3, 4$ are the macroeconomic factors after standardization. Consider the following:

$$R_i = a_{i0} + a_{i1} \cdot e^{-X_1} + a_{i2} \cdot e^{-X_2} + a_{i3} \cdot e^{-X_3} + a_{i4} \cdot e^{-X_4}. \tag{21}$$

With the application of nonlinear estimation on this modified Poisson intensity equation, coefficients of the factors are shown in Table 2 (part of the result for simplicity).

With the combination of coefficients and common macroeconomic factors, the intensity of each Poisson variable Y_i in our model can be generated. Then we turn to formula (17) to get the loss distribution of sample credit portfolio.

Table 1: Dynamic default probabilities and Poisson intensity.

Stock code		Ordinal number of each trading day						
		1	2	3	···	236	237	238
Real Estate								
600048.SH	P^*	$1.604E-03$	$1.297E-03$	$1.243E-03$	···	$1.604E-03$	$1.297E-03$	$1.243E-03$
	R^*	$1.607E-03$	$1.299E-03$	$1.244E-03$		$4.411E-03$	$4.656E-03$	$5.134E-03$
600077.SH	P	$6.251E-03$	$5.358E-03$	$4.638E-03$		$9.777E-03$	$1.230E-02$	$1.241E-02$
	R	$6.290E-03$	$5.387E-03$	$4.660E-03$		$9.874E-03$	$1.245E-02$	$1.256E-02$
600162.SH	P	$3.985E-03$	$3.655E-03$	$3.585E-03$		$5.782E-04$	$7.794E-04$	$9.436E-04$
	R	$4.001E-03$	$3.668E-03$	$3.598E-03$		$5.785E-04$	$7.800E-04$	$9.445E-04$
Machinery								
600150.SH	P	$2.326E-02$	$2.148E-02$	$2.213E-02$	···	$2.326E-02$	$2.148E-02$	$2.213E-02$
	R	$2.382E-02$	$2.196E-02$	$2.264E-02$		$3.336E-03$	$5.137E-03$	$5.000E-03$
600166.SH	P	$1.156E-03$	$9.690E-04$	$7.421E-04$		$2.018E-03$	$2.283E-03$	$2.214E-03$
	R	$1.158E-03$	$9.700E-04$	$7.427E-04$		$2.023E-03$	$2.289E-03$	$2.219E-03$
600169.SH	P	$4.647E-04$	$2.570E-04$	$2.359E-04$		$1.387E-03$	$1.991E-03$	$2.138E-03$
	R	$4.649E-04$	$2.570E-04$	$2.360E-04$		$1.389E-03$	$1.995E-03$	$2.143E-03$
Financial Industry								
600000.SH	P	$3.869E-02$	$3.784E-02$	$3.791E-02$	···	$2.539E-02$	$2.797E-02$	$2.766E-02$
	R	$3.722E-02$	$3.644E-02$	$3.650E-02$		$2.475E-02$	$2.720E-02$	$2.691E-02$
600015.SH	P	$2.794E-02$	$2.641E-02$	$2.650E-02$		$1.737E-02$	$1.892E-02$	$1.854E-02$
	R	$2.717E-02$	$2.572E-02$	$2.580E-02$		$1.707E-02$	$1.857E-02$	$1.820E-02$
600016.SH	P	$3.719E-02$	$3.659E-02$	$3.674E-02$		$2.705E-02$	$2.758E-02$	$2.761E-02$
	R	$3.583E-02$	$3.527E-02$	$3.541E-02$		$2.633E-02$	$2.683E-02$	$2.686E-02$

* (1) P represents the default probability of each obligor.
(2) R represents the estimation of Poisson intensity.

Table 2: Coefficients of the factors in mixed Poisson model.

Stock code	Common factors				Specific factor
	a_{i1}	a_{i2}	a_{i3}	a_{i4}	a_{i0}
Real Estate					
600048.SH	$5.024E-03$	$1.455E-02$	$6.538E-02$	$-4.537E-02$	$-1.272E-02$
600077.SH	$-4.543E-02$	$1.013E-01$	$5.354E-02$	$-2.203E-02$	$-2.747E-02$
600162.SH	$-2.875E-02$	$4.103E-02$	$-3.844E-02$	$6.869E-02$	$-1.359E-02$
Machinery					
600150.SH	$1.060E-01$	$-1.010E-01$	$-2.355E-01$	$3.381E-01$	$-2.440E-02$
600166.SH	$-1.511E-03$	$2.158E-02$	$3.428E-02$	$-1.519E-02$	$-1.318E-02$
600169.SH	$1.956E-02$	$8.639E-03$	$1.278E-01$	$-8.848E-02$	$-2.282E-02$
Financial Industry					
600000.SH	$3.760E-02$	$-1.212E-01$	$1.499E-01$	$1.111E-01$	$-3.520E-02$
600015.SH	$2.131E-02$	$-1.426E-02$	$7.727E-02$	$8.240E-02$	$-4.316E-02$
600016.SH	$-4.171E-02$	$7.909E-02$	$-3.450E-02$	$1.204E-01$	$-1.721E-02$

Since the relevant data about recovery rate of default is extremely rare, we assume $s_i = 1$, which means that the default exposure is just the loss if any defaults. We now use historical data of the four macroeconomic indexes to run the Monte Carlo simulation. This is easily implemented through the following algorithm:

(1) input the relevant macroeconomic factors X_j into this model;

(2) compute R_i, $i = 1, 2, \ldots, m$, from (21);

(3) generate $Y_i \sim \text{Poisson}(R_i)$, $i = 1, 2, \ldots, m$;

(4) calculate portfolio loss L from (17);

(5) return to step (1).

The loss distribution of each sample portfolio is shown in Figure 3. Each point in it is based on 10,000 simulations. And the specific loss percentage and default probability of several points are listed in Table 3 (transportation portfolio is not listed because of its low default probabilities) which also gives the standard deviation of them.

Table 3: Standard deviations of the default probabilities.

Portfolio		Loss level (percentage)				
		0.05%	0.09%	0.13%	0.23%	0.50%
Real Estate	P^*	0.153%	0.141%	0.133%	0.120%	1.163E-004
	Std.*	$3.5E-004$	$3.1E-004$	$2.3E-004$	$1.7E-004$	$1.05E-005$
Financial Industry	P	1.32%	1.28%	1.21%	0.71%	0.14%
	Std.	$6.81E-003$	$6.77E-003$	$5.47E-003$	$7.6E-004$	$2.21E-005$
Machinery	P	$8.73E-004$	$8.69E-004$	$8.04E-004$	$6.27E-004$	$3.245E-005$
	Std.	$2.17E-004$	$3.16E-004$	$2.81E-004$	$2.11E-004$	$6.22E-006$

*(1) P represents the default probability of each portfolio.
(2) Std. represents the standard deviation of each calculation.

From Figure 3, we can observe that the default probability of each industry portfolio decreases with the increase of loss level. And the default probability in financial industry is the largest, which also does meet the fact that financial companies such as banks are usually highly leveraged. Further, the standard deviation of each calculation in Table 3 represents the reliability of MC simulation and indicates that we can accept these results. This Monte Carlo simulation illustrates the practical value and effectiveness of mixed Poisson model in risk measurement for credit portfolio.

5. Conclusions

Mixed Poisson model is introduced in this paper to replace the widely used copula model. To apply the mixed Poisson theory to practical study, we bring the structural approach into the calculation of single obligor's default probability, which helps to estimate the parameters of mixed Poisson model. Finally, Monte Carlo simulation drives out the curve about default probabilities and loss levels, which is in accordance with the practical rules. This study illustrates the practical value and effectiveness of mixed Poisson model in risk measurement for credit portfolio.

Because good data on credit losses is extremely rare in financial market of China, we use the data in stock market for substitution based on the assumptions of structural approach. If there are enough default data in a sound financial market, estimation of model parameters can be more accurate. And the number of obligors in our sample portfolio is relatively small. We believe a Monte Carlo simulation of a larger sample will be much more stable.

Conflict of Interests

The authors declare that there is no conflict of interests regarding the publication of this paper.

Acknowledgment

This research was supported by the National Natural Science Foundation of China (Grant no. 71171176).

References

[1] K. Giesecke, "Portfolio credit risk: top down vs. bottom up approaches," in *Frontiers in Quantitative Finance: Credit Risk and Volatility Modeling*, 2008.

[2] F. Black and M. Scholes, "The pricing of options and corporrate liabilities," *Journal of Political Economy*, vol. 81, no. 3, pp. 637–654, 1973.

[3] R. C. Merton, "On the pricing of corporate debt: the risk structure of interest rates," *Journal of Finance*, vol. 29, pp. 449–470, 1974.

[4] N. H. Chan, H. Y. Wong, and J. Zhao, "Structural model of credit migration," *Computational Statistics & Data Analysis*, vol. 56, no. 11, pp. 3477–3490, 2012.

[5] R. Schäfer and A. F. R. Koivusalo, "Dependence of defaults and recoveries in structural credit risk models," *Economic Modeling*, vol. 30, pp. 1–9, 2013.

[6] G. Gupton, C. Finger, and M. Bhatia, *CreditMetrics Technical Document*, J.P. Morgan, New York, NY, USA, 1997.

[7] M. B. Gordy, "A comparative anatomy of credit risk models," *Journal of Banking and Finance*, vol. 24, no. 1-2, pp. 119–149, 2000.

[8] T. M. Barnhill Jr. and W. F. Maxwell, "Modeling correlated market and credit risk in fixed income portfolios," *Journal of Banking and Finance*, vol. 26, no. 2-3, pp. 347–374, 2002.

[9] C. Huang, C. Peng, X. Chen, and F. Wen, "Measuring and forecasting volatility in chinese stock market using HAR-CJ-M model," *Abstract and Applied Analysis*, vol. 2013, Article ID 143194, 13 pages, 2013.

[10] F. Wen, Z. Li, C. Xie, and D. Shaw, "Study on the fractal and chaotic features of the Shanghai composite index," *Fractals-Complex Geometry, Patterns, and Scaling in Nature and Society*, vol. 20, no. 02, pp. 133–140, 2012.

[11] F. Wen and Z. Liu, "A copula-based correlation measure and its application in chinese stock market," *International Journal of Information Technology and Decision Making*, vol. 8, no. 4, pp. 787–801, 2009.

[12] X. K. Dimakos and K. Aas, "Integrated risk modelling," *Statistical Modelling*, vol. 4, no. 4, pp. 265–277, 2004.

[13] J. V. Rosenberg and T. Schuermann, "A general approach to integrated risk management with skewed, fat-tailed risks," *Journal of Financial Economics*, vol. 79, no. 3, pp. 569–614, 2006.

[14] C. Liang, X. Zhu, X. Sun, J. Chen, and J. Li, "Integrating credit and market risk: a factor copula based method," *Information*

Technology and Quantitative Management, vol. 17, pp. 656–663, 2013.

[15] R. Frey and A. J. McNeil, "VaR and expected shortfall in portfolios of dependent credit risks: conceptual and practical insights," *Journal of Banking and Finance*, vol. 26, no. 7, pp. 1317–1334, 2002.

[16] P. Glasserman and J. Li, "Importance sampling for a mixed poisson model of portfolio credit risk," in *Proceedings of the Winter Simulation Conference: Driving Innovation*, pp. 267–275, December 2003.

[17] Credit Suisse Financial Products, *CreditRisk^{+}: A CreditRisk Management Framework*, London, UK, 1997.

[18] E. P. Jones, S. P. Mason, and E. Rosenfeld, "Contingent claims analysis of corporate capital structures: an empirical investigation," *The Journal of Finance*, vol. 39, no. 3, 1984.

Hindawi Publishing Corporation
Discrete Dynamics in Nature and Society
Volume 2014, Article ID 840725, 11 pages
http://dx.doi.org/10.1155/2014/840725

Research Article

A Stochastic Dynamic Programming Approach Based on Bounded Rationality and Application to Dynamic Portfolio Choice

Wenjie Bi, Liuqing Tian, Haiying Liu, and Xiaohong Chen

Business School, Central South University, Changsha, Hunan 410083, China

Correspondence should be addressed to Wenjie Bi; biwenjiecsu@gmail.com

Received 14 March 2014; Accepted 5 May 2014; Published 22 May 2014

Academic Editor: Fenghua Wen

Dynamic portfolio choice is an important problem in finance, but the optimal strategy analysis is difficult when considering multiple stochastic volatility variables such as the stock price, interest rate, and income. Besides, recent research in experimental economics indicates that the agent shows limited attention, considering only the variables with high fluctuations but ignoring those with small ones. By extending the sparse max method, we propose an approach to solve dynamic programming problem with small stochastic volatility and the agent's bounded rationality. This approach considers the agent's behavioral factors and avoids effectively the "Curse of Dimensionality" in a dynamic programming problem with more than a few state variables. We then apply it to Merton dynamic portfolio choice model with stochastic volatility and get a tractable solution. Finally, the numerical analysis shows that the bounded rational agent may pay no attention to the varying equity premium and interest rate with small variance.

1. Introduction

In reality, how to choose an asset's portfolio of consumption and investment is one of the most important decisions for many people. In modern portfolio choice field, Merton [1, 2] provides a general framework for understanding the portfolio demand of long-term investors when investment opportunities change over time. In a classical Merton model [1, 2], however, the riskless interest rate, the risky mean rate of return, and the volatility coefficient are usually assumed to be constant. These assumptions are lack of realism, particularly over long time intervals. A large volume of empirical researches in financial market which indicates the assumption that these variables are stochastic volatile and follow a certain stochastic process (e.g., Ornstein-Uhlenbeck process) is more realistic [3, 4]. But when introducing these stochastic variables into the Merton-style portfolio choice model, the problem becomes increasingly complicated and formidable to solve. Also, this will lead to the "Curse of Dimensionality." Quite a lot of approaches have been developed to deal with this kind of problems, such as martingale methods [5–8] and various approximate numerical algorithms [9–12]. However, these methods have more restrictive assumptions and are too complex to get a tractable solution of strong explanations. Based on the control of small noise, Judd and Guu [13] proposed a method to solve dynamic programming problems with stochastic disturbance. He makes the simplifying assumption that uncertainty is small and obtains the first- and high-order solutions of complicated dynamic programming model. This method provides a quite suitable solution for dynamic portfolio choice model with stochastic volatility.

On the other hand, a growing body of empirical studies indicate that the agent considers only the variables with high fluctuations but ignores those with small ones [14–16]. Bordalo et al. [17] showed that the agent rationally chooses to be inattentive to news. Kőszegi and Szeidl [18] analyzed the monetary policy and found out that when price is changed, the decision makers are usually unaware of it. There are also many literatures showing that the agent pays attention to salient factors. Sims [19] uses two empirical strategies to analyze how individuals optimize fully with respect to the incentives created by tax policies and shows that tax salience affects agents' behavioral response. Peng and Xiong [20] study the allocation of investors' attention among different information. They find out that investors with limited attention will focus on macroeconomic and industry information rather than that of a specific firm. Seasholes and Wu [21] demonstrate that attention-grabbing events will attract investors' attention. In their model, they regard them as the proxy variables and their results empirically indicate that these events have a significant impact on the allocation of investor's attention. Maćkowiak and Wiederholt [22] show that decision makers' attention is usually drawn to salient payoffs.

In recent years, Gabaix [23] provides a sparse max operator to model dynamic programming with bounded rationality. In the sparse max, the agent pays less or no attention to some features the fluctuations of which are smaller than some thresholds, and he tries to strike a good balance between the utility loss of inattention and the cognitive cost which can be regarded as the loss for taking time to think about the decisions rather than to enjoy oneself. The sparse max seems more realistic than traditional economic models since it has a very robust psychological foundation. Also, it can deal with problems of maximization with constraints easily and get a tractable solution in a parsimonious way.

However, Gabaix [23] only studies the dynamic programming in a stationary environment without the stochastic volatility terms. But the financial market is strewn with numerous stochastic dynamic programming problems, and these problems are hard to solve due to multitudinous state variables. To address this issue, we extend the sparse max operator and develop a stochastic version of Gabaix's method. The distinctive feature of this method is that it considers the agent's behavioral factors (limited attention) and can effectively preclude the "Curse of Dimensionality" for multiple variables. To verify the validity and practicability of our model, we consider the Merton dynamic portfolio choice problem with stochastic volatility variables (e.g., [24, 25]) and get a tractable solution.

The remainder of this paper is organized as follows. Section 2 presents the sparse dynamic programming method proposed by Gabaix [23]. Section 3 extends this model and gives a general principle for solving continuous-time dynamic programming with stochastic variables. In Section 4, we apply our method to Merton dynamic portfolio choice. Finally, we discuss some implications of our findings and suggest topics for future research in Section 5.

2. The Sparse Max Operator without Constraints

We mainly introduce the sparse max operator proposed by Gabaix [23] in this section. In the traditional version, the agent faces a maximization problem:

$$\begin{aligned} &\max_{a} \quad u(a, \mathbf{y}) \\ &\text{subject to} \quad b(a, \mathbf{y}) \geq 0, \end{aligned} \tag{1}$$

where $\mathbf{y} = (y_1, y_2, \ldots, y_n)$, u is a utility function and b is a constraint. Variable a and function b have arbitrary dimensions. For any optimal decision, in principle, thousands of considerations are relevant to the agent. Since it would be too burdensome to take all of these variables into account, the agent is used to discarding most of them. At the same time, his attention is allocated purposefully to important variables.

Hence, the agent might sensibly pick a "sparse" representation of the variables; namely, choose the attention vector $\mathbf{m} = (m_1, m_2, \ldots, m_n)$ to replace variable y_i with $y_i^s = m_i y_i$ $i \in (1, 2, \ldots, n)$, where the superscript s of y_i^s represents sparse. The optimal attention vector is obtained by weighing the utility losses for imperfect inattention against the cost savings without thinking too much.

The utility losses from imperfect inattention can be expressed as follows [23]:

$$E[v(\mathbf{m}) - v(\mathbf{l})] = -\frac{1}{2}\sum_{i,j}(m_i - 1)\Lambda_{ij}(m_j - 1) + o\left(\|\mathbf{y}\|^2\right), \tag{2}$$

where $v(\mathbf{m}) := u(a(\mathbf{y}^s(\mathbf{m})), \mathbf{y})$ is the utility for a sparse agent, $\mathbf{y}^s(\mathbf{m}) = (y_1^s, y_2^s, \ldots, y_n^s)$, $\mathbf{l} := (1, 1, \ldots, 1)^T$, and $v(\mathbf{l})$ is the utility when the agent is fully attentive. $o(\|\mathbf{y}\|^2)$ denotes the second-order infinitesimal of $\mathbf{y}$. $\Lambda_{ij} = -\sigma_{ij} a_{y_i}^2 u_{aa}$, where $\sigma_{ij} = \operatorname{cov}(y_i, y_j)$, $E(y_i) = 0$, σ_i is the standard deviation of y_i, and $a_{y_i} = -u_{aa}/u_{ay_i}$ which indicates by how much a change y_i should change the action for traditional agent. u_{aa} is the second derivative of u with respect to a. All derivatives above are evaluated at $\mathbf{y} = \mathbf{0}$ and the default action $a^d = \operatorname{argmax}_a u(a, \mathbf{0})$.

Gabaix [23] assumes the cognitive cost is $c(m_i) = \kappa |m_i|^\beta$, where $\beta \geq 0$ and parameter $\kappa \geq 0$ is a penalty for lack of sparsity. If $\kappa = 0$, the agent will be a traditional, rational agent.

Based on above analysis, Gabaix [23] defines the sparse max operator as follows.

Definition 1 (see [23] Sparse max operator without constraints). The sparse max defined by the following procedure.

Step 1. Choose the attention vector $\mathbf{m}^*$

$$\mathbf{m}^* = \arg\min_{\mathbf{m}} \frac{1}{2}\sum_{i\cdot j=1}^{n}(1 - m_i)\Lambda_{ij}(1 - m_j) + \kappa\sum_{i=1}^{n}|m_i|^\beta. \tag{3}$$

Define $y_i^s = m_i^* y_i$ as the sparse representation of y_i.

Step 2. Choose the action

$$a^s = \arg\max_a u(a, \mathbf{y}^s), \tag{4}$$

and set the resulting utility to be $u^s = u(a^s, \mathbf{y})$.

Suppose $\mathbf{y}$ is one-dimensional vector; formula (3) can be transformed into $m^* = \min_m (1/2)(m-1)^2\sigma^2 + \kappa|m|$. Gabaix [23] defines a function A to represent the optimal attention vector, namely, $m^* = A_\beta(\sigma^2/\kappa) = \inf[\arg\min_m (1/2)(m-1)^2(\sigma^2/\kappa) + |m|^\beta]$ and points out when $\beta = 1$, the function $A_\beta(\sigma^2/\kappa)$ satisfies the sparsity and continuity. When $\beta = 1$ and $\kappa = 1$, we have $A_1(\sigma^2) = \max(1 - 1/\sigma^2, 0)$ as shown in Figure 1 [23].

From Figure 1 we know that the agent will not consider the variable when $0 \leq \sigma^2 \leq \kappa$ $(\kappa = 1)$.

When the vector $\mathbf{y}$ includes more than one variable and these variables perceived by the agent are uncorrelated, we have $m_i^* = A_1(\sigma_i^2 a_{y_i}^2 |u_{aa}|/\kappa)$ through formula (3). To

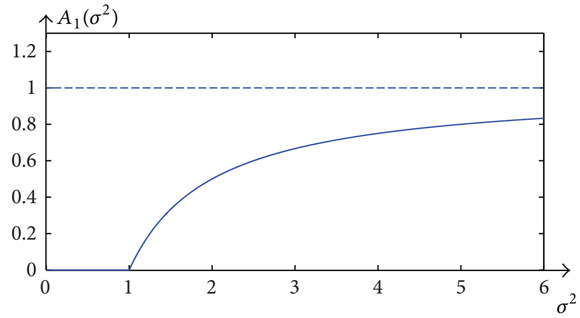

Figure 1: The attention function A_1.

analyze the agent's inattention expediently, Gabaix [23] defines the truncation function $\tau(s,p) = s\max(1 - p^2/s^2, 0)$, so we have $m_i^* = \tau(1, \kappa\sigma_a/a_{y_i}\sigma_i)$. Truncation function has more intuitive economic implications: a one-standard-deviation change of the variable y_i makes the agent change his action by $a_{y_i}(\sigma_i/\sigma_a)$. When $a_{y_i}(\sigma_i/\sigma_a)$ is small and satisfies $|a_{y_i}(\sigma_i/\sigma_a)| \le \kappa$, the agent will not consider this factor. Figure 2 shows the truncation function $\tau(s,p) = s\max(1 - p^2/s^2, 0)$ [23].

From Figure 2, we know that the agent who seeks "sparsity" should sensibly drop relatively unimportant features. In addition, if the features are larger than that cutoff, they are still dampened: in Figure 2, $\tau(s,p)$ is below the 45 degree line (for positive s, in general, $|\tau(s,p)| < |s|$).

Based on the analysis above, we can use the truncation function to represent the sparse agent's optimal action.

Remark 2 (see [23]). If rational optimal action is

$$a^r(\mathbf{y}) = a^d + \sum_i a_{y_i} y_i + o(\|\mathbf{y}\|)^2 \quad (r \text{ represents the rationality}), \tag{5}$$

which is obtained by the Taylor expansion around the default action a^d, then the sparse agent's optimal action is

$$a^s(\mathbf{y}) = a^d + \sum_i \tau\left(a_{y_i}, \frac{\kappa\sigma_a}{\sigma_i}\right) y_i + o\left(\|\mathbf{y}\|^2\right), \tag{6}$$

where σ_a is the standard deviation of a.

3. A Stochastic Dynamic Programming Approach Based on Sparse Max Operator

In order to effectively deal with stochastic dynamic programming in finance in this section, we extend Gabaix [23] sparse max operator and propose a bounded rational stochastic dynamic programming model in continuous time.

The general model of stochastic dynamic programming in continuous time is

$$\begin{gathered}\max \int_0^\infty e^{-\rho t} u(a, \mathbf{x}, \mathbf{y})\, dt \\ d\mathbf{x} = g(\mathbf{x}(t), \mathbf{y}(t), a(t))\, dt + \sigma(\mathbf{x}(t), a(t))\, dZ_{\mathbf{x}}(t), \\ d\mathbf{y} = h(\mathbf{x}(t), \mathbf{y}(t))\, dt + \sigma(\mathbf{y}(t))\, dB_{\mathbf{y}}(t),\end{gathered} \tag{7}$$

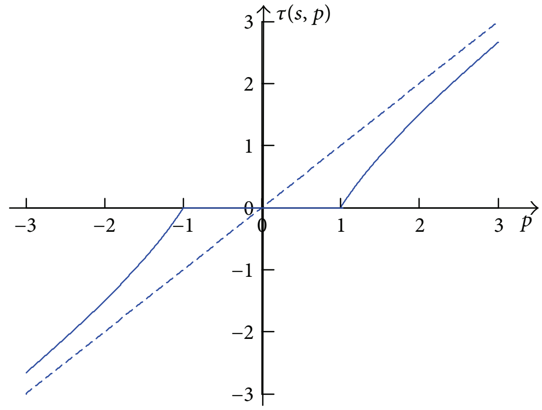

Figure 2: The truncation function $\tau(s,p)$ with $p = 1$.

where ρ denotes the discount factor, u is the utility function, a is the decision variable which has an arbitrary dimension, the vector $\mathbf{x}$ represents important factors which are always considered by the agent, and the vector $\mathbf{y}$ defined in Section 2 represents factors that that may not be considered by the sparse agent. $g(\mathbf{x},\mathbf{y},a)$, $h(\mathbf{x},\mathbf{y})$ are the state transition function of $\mathbf{x}$ and $\mathbf{y}$, respectively. And $\sigma(\mathbf{x},a)$, $\sigma(\mathbf{y})$ represent the stochastic volatility of $\mathbf{x}$ and $\mathbf{y}$, respectively. $dZ_{\mathbf{x}}$, $dB_{\mathbf{y}}$ are independent standard Brownian motions; namely $dZ_{\mathbf{x}} dB_{\mathbf{y}} = 0$. We define the value function as $V(\mathbf{x},\mathbf{y}) = \int_0^\infty e^{-\rho t} u(a,\mathbf{x},\mathbf{y}) dt$.

Assumption 3. The utility function u and value function V are n-order continuously differentiable (C^n, $n \ge 3$).

Assumption 4. All state variables are stochastic and they are independent of each other; stochastic volatility of $\mathbf{x}$ is a function of $\mathbf{x}$ and a while stochastic volatility of $\mathbf{y}$ is uncorrelated with a.

Assumption 5. $\mathbf{x}$ is one dimensional; that is, only one variable would be always considered by the agent and other variables may not be considered by the agent.

Assumption 6. According to Judd and Guu [13], we assume the variance of each component of vector $\mathbf{y}$ is small and independent of one another.

To facilitate analysis, we use x to replace $\mathbf{x}$, denote the stochastic differential equation of y_i by $dy_i = h^i(x(t), y_i(t))dt + \sigma^i(y_i(t))dB_{y_i}(t)$, $i \in (1,2,\ldots,n)$, and use the notation $D_x[f] = \partial_x[f] + a_x \partial_a[f]$ as the total derivative with respect to x (i.e., the full impact of a change in x, including the impact it has on a change in the action a).

Based on Remark 2 in Section 2, we have the following proposition.

Proposition 7. *The optimal action in bounded rationality model* (7) *is*

$$a^s(x,\mathbf{y}) = a^d(x) + \sum_i \tau\left(a_{y_i}, \frac{\kappa\sigma_a}{\sigma_i}\right) y_i + o\left(\|\mathbf{y}\|^2\right), \tag{8}$$

where σ_a is the standard deviation of a.

Proof. See the appendix. □

From Proposition 7, we know that, in order to derive the optimal action a^s, we should get the default action a^d which is related to x and a_{y_i}. The detail process of solving them is described as the following steps, which contain the main results of our method.

Step 1. Solve default action a^d.

By substituting $\mathbf{y} = 0$ into the basic model (7), we get the default model:

$$\max \int_0^\infty e^{-\rho t} u(a, x, \mathbf{0})\, dt$$
$$dx = g(x(t), \mathbf{0}, a(t))\, dt + \sigma(x(t), a(t))\, dZ_x(t). \tag{9}$$

This is a general dynamic programming model in continuous time and the state variable is one dimension, so we can get the optimal default action a^d and the value function $V(x, \mathbf{0}) = \int_0^\infty e^{-\rho t} u(a, x, \mathbf{0}) dt$ easily [26].

Step 2. Solve a_{y_i}.

The following Proposition 8 and its proof in the appendix show the result and the process of obtaining a_{y_i}.

Proposition 8. *The impact of a change in y_i on the value function is*

$$\begin{aligned} V_{xy_i} = &\Big(D_x\left[u_{ay_i} + g_{y_i}(x, \mathbf{y}, a) V_x\right] \\ &+ \sum_{i=1}^n h^i_{xy_i}(x, y_i, a) V_{y_i} + \frac{1}{2}\sigma_x^2(x, a) f(x) V_{y_i} \\ &+ \frac{1}{2}\sigma^2(x, a) f_x(x) V_{y_i}\Big) \\ &\times \left(\rho - \sum_{i=1}^n h^i_{y_i}(x, y_i, a) - \frac{1}{2}\sigma^2(x, a) f(x)\right)^{-1}, \end{aligned} \tag{10}$$

where

$$\begin{aligned} V_{y_i} = &\left(u_{ay_i} + g_{y_i}(x, \mathbf{y}, a) V_x\right) \\ &\times \left(\rho - \sum_{i=1}^n h^i_{y_i}(x, y_i, a) - \frac{1}{2}\sigma^2(x, a) f(x)\right)^{-1}, \\ f(x) = &\frac{V_{xx}}{V}. \end{aligned} \tag{11}$$

By implicit function theorem, the impact of a change in y_i on the optimal action is $a_{y_i} = -\phi_{y_i}/\phi_a$, where

$$\begin{aligned} \phi_a &= u_{aa} + g_{aa}(x, \mathbf{y}, a) V_x + \frac{1}{2}\sigma_{aa}^2(x, a) D_x[V_x], \\ \phi_{y_i} &= u_{ay_i} + g_{ay_i}(x, \mathbf{y}, a) V_x + g_a(x, \mathbf{y}, a) V_{xy_i} \\ &\quad + \frac{1}{2}\sigma_a^2(x, a) D_x\left[V_{xy_i}\right]. \end{aligned} \tag{12}$$

Proof. See the appendix. □

Now we can get the optimal action based on the two steps above. By the analysis of Proposition 7, we can see that $\tau(a_{y_i}, \kappa\sigma_a/\sigma_i)$ represents the impact of variable y_i on the action a^s. When a_{y_i} is smaller than $\kappa\sigma_a/\sigma_i$, $\tau(a_{y_i}, \kappa\sigma_a/\sigma_i) = 0$ which means the agent will discard this factor.

4. Application: Dynamic Portfolio Choice

4.1. Merton Portfolio Problem with Stochastic Volatility. In this section, we consider a Merton dynamic portfolio choice problem with stochastic volatility in continuous time [24]. In the traditional version of Merton model [1], the agent's optimal problem is

$$\begin{aligned} \max \quad & E\int_0^\infty e^{-\rho t} u(c(t))\, dt, \\ \text{s.t.} \quad & dw(t) = w(t)(r + (b - r)\theta(t))\, dt \\ & \qquad + \theta(t)\sigma w(t)\, dW(t) - c(t)\, dt, \end{aligned} \tag{13}$$

where ρ is the discount factor, u is the utility function, $w(t)$ is the wealth at time t, σ is the standard deviation of $w(t)$, and $c(t)$ is the consumption at time t. The investment control $\theta(t)$ at time t is the fraction of the wealth invested in the risky asset, so $(1-\theta(t))$ is the fraction of the wealth invested on the riskless asset. r is the riskless interest rate and b is the risky mean rate of return; dW follows standard Brownian motion. We assume the utility function $u(c) = c(t)^{1-\gamma}/(1-\gamma)$, where γ $(0 < \gamma < 1)$ is the parameter of risk preference. The goal is to choose consumption $c(t)$ and investment $\theta(t)$ control processes to maximize long-term utility.

In model (13), the riskless interest rate r and the risky mean rate of return b are assumed to be constant [1]. However, this assumption is unrealistic, particularly over long time intervals [27, 28]. Instead, now we assume that these two variables are stochastic and satisfying $r(t) = \bar{r} + \hat{r}(t)$, $b(t) = \bar{b} + \hat{b}(t)$, where $\bar{r}$, $\bar{b}$ represent the long mean of the riskless interest rate and the risky rate of return, respectively, and $\hat{r}(t)$, $\hat{b}(t)$ are their volatile part. $r(t)$ and $b(t)$ depend on some "economic factor" $\eta(t)$ [24]; namely,

$$\begin{aligned} r(t) &= R(\eta(t)), \\ b(t) &= M(\eta(t)). \end{aligned} \tag{14}$$

And $\eta(t)$ satisfies the stochastic differential formula [24]:

$$d\eta = g(\eta(t))\, dt + \tilde{\sigma}\left[\lambda dW(t) + \left(1 - \lambda^2\right)^{1/2} d\widetilde{W}(t)\right], \tag{15}$$

where $\widetilde{W}(t)$ and $W(t)$ are independent standard Brownian motions. The parameter λ with $|\lambda| < 1$ allows a correlation between the Brownian motion $W(t)$ driving the short rate and its volatility. $\tilde{\sigma}$ is the standard deviation of η.

The budget equation of model (13) now becomes

$$\begin{aligned} dw &= w(t)(r(t) + (b(t) - r(t))\theta(t))\, dt \\ &\quad + \theta(t)\sigma w(t)\, dW(t) - c(t)\, dt. \end{aligned} \tag{16}$$

We further assume that the stochastic differential equation of $r(t) = \eta(t)$ follows an Ornstein-Uhlenbeck process [25, 29]:

$$\begin{aligned} dr = & -\zeta_r (\bar{r} - r(t))\, dt \\ & + \sigma_r \left[\lambda_r dW(t) + \left(1 - \lambda_r^2\right)^{1/2} dR(t) \right], \end{aligned} \tag{17}$$

where ζ_r is the degree of mean reversion in expected excess returns, σ_r is the standard deviation of $r(t)$, $R(t)$ is a Brownian motion and independent of $W(t)$, and λ_r is the coefficient of w and r. To simplify our model, we assume $\lambda_r = 0$ [30]. By substituting $r(t) = \bar{r} + \hat{r}(t)$ into (17), we obtain $d(\bar{r} + \hat{r}(t)) = -\zeta_r \hat{r}(t)dt + \sigma_r dR(t)$. Since $d\bar{r} = 0$, it follows that $d\hat{r} = -\zeta_r \hat{r}(t)dt + \sigma_r dR(t)$.

We assume that $b(t)$ follows an Ornstein-Uhlenbeck process too, so we obtain $d\hat{b} = -\zeta_b \hat{b}(t)dt + \sigma_b dB(t)$ where ζ_b has the same meaning with ζ_r. σ_b is the standard deviation of $b(t)$, and we assume σ_r and σ_b are small [13]. $B(t)$ is a Brownian motion and independent of $R(t)$ and $W(t)$. Then we get the following model:

$$\max \quad E \int_0^\infty e^{-\rho t} \frac{c(t)^{1-\gamma}}{1-\gamma} dt \tag{18}$$

$$\begin{aligned} \text{s.t.} \quad dw = & \, w(t)\left((r(t) + \theta(t)(b(t) - r(t)))\right) dt \\ & + \theta(t)\sigma w(t)\, dW(t) - c(t)\, dt, \\ & r(t) = \bar{r} + \hat{r}(t), \\ & b(t) = \bar{b} + \hat{b}(t), \\ & d\hat{r} = -\zeta_r \hat{r}(t)\, dt + \sigma_r dR(t), \\ & d\hat{b} = -\zeta_b \hat{b}(t)\, dt + \sigma_b dB(t). \end{aligned} \tag{19}$$

From Section 3, we know that, for the bounded rational agent, the optimal consumption c^s and the optimal fraction of wealth allocated to risky market θ^s in model (18) can be expressed as

$$\begin{aligned} c^s &= c^d + \tau\left(c_{\hat{r}}, \frac{\kappa\sigma_c}{\sigma_r}\right)\hat{r} + \tau\left(c_{\hat{b}}, \frac{\kappa\sigma_c}{\sigma_b}\right)\hat{b}, \\ \theta^s &= \theta^d + \tau\left(\theta_{\hat{r}}, \frac{\kappa\sigma_\theta}{\sigma_r}\right)\hat{r} + \tau\left(\theta_{\hat{b}}, \frac{\kappa\sigma_\theta}{\sigma_b}\right)\hat{b}, \end{aligned} \tag{20}$$

where c^d and θ^d are the default actions when $\hat{r}(t) = 0, \hat{b}(t) = 0$. σ_c, σ_θ are the standard deviation of c and θ, respectively. $c_{\hat{r}}$, $c_{\hat{b}}$, $\theta_{\hat{r}}$, and $\theta_{\hat{b}}$ are the impact of $\hat{r}$ and $\hat{b}$ on c and θ, respectively. Next we will give the process of solving them using the approach described in Section 3.

Step 1. Solve the default decision c^d and θ^d.

By substituting $\hat{r}(t) = 0, \hat{b}(t) = 0$ into the basic model (18), we get the default model:

$$\begin{aligned} & \max E \int_0^\infty e^{-\rho t} \frac{c(t)^{1-\gamma}}{1-\gamma} dt \\ & dw = w(t)\left(\bar{r} + \theta(t)\left(\bar{b} - \bar{r}\right)\right) dt \\ & \quad + \theta(t)\sigma w(t)\, dW(t) - c(t)\, dt. \end{aligned} \tag{21}$$

This is the same Merton model as the model in (13); many scholars have solved this problem [1, 2]. We define the value function to be $V(w) = \int_0^\infty e^{-\rho t}(c(t)^{1-\gamma}/(1-\gamma))dt$; then we have [2]

$$\begin{aligned} c^d &= w(\Re(1-\gamma))^{-1/\gamma}, \qquad \theta^d = \frac{\bar{b} - \bar{r}}{\gamma\sigma^2}, \\ V(w) &= \Re \frac{w^{1-\gamma}}{1-\gamma}, \end{aligned} \tag{22}$$

where $\Re = [(\rho - \bar{r}(1-\gamma) - (\bar{b} - \bar{r})^2(1-\gamma)/2\sigma^2\gamma)/\gamma]^{-\gamma}/(1-\gamma)$.

Step 2. Solve $c_{\hat{r}}$, $c_{\hat{b}}$, $\theta_{\hat{r}}$, and $\theta_{\hat{b}}$.

Next we will give the results of $c_{\hat{r}}$, $c_{\hat{b}}$, $\theta_{\hat{r}}$, and $\theta_{\hat{b}}$. Proposition 9 shows their expressions, and the proof is the solution process.

Proposition 9. *Based on the results of* (22) *and implicit function theorem, we have*

$$\begin{aligned} c_{\hat{r}} &= -\frac{(1-\gamma)\left(1-\theta^d\right)c^d}{\left(\rho + \zeta_r + (1/2)\gamma(1-\gamma)\theta^{d^2}\sigma^2\right)\gamma}, \\ c_{\hat{b}} &= -\frac{(1-\gamma)c^d}{\left(\rho + \zeta_b + (1/2)\gamma(1-\gamma)\theta^{d^2}\sigma^2\right)\gamma}, \\ \theta_{\hat{r}} &= -\frac{1}{\gamma\sigma^2}, \qquad \theta_{\hat{b}} = \frac{1}{\gamma\sigma^2}. \end{aligned} \tag{23}$$

And the final results of model (18) *are*

$$\begin{aligned} c^s &= c^d + \tau\left(-\frac{1-\theta^d}{M}, \frac{\kappa\sigma_c}{\sigma_r}\right)\hat{r} + \tau\left(-\frac{1}{N}, \frac{\kappa\sigma_c}{\sigma_b}\right)\hat{b}, \\ \theta^s &= \theta^d + \tau\left(-\frac{1}{\gamma\sigma^2}, \frac{\kappa\sigma_\theta}{\sigma_r}\right)\hat{r} + \tau\left(\frac{1}{\gamma\sigma^2}, \frac{\kappa\sigma_\theta}{\sigma_b}\right)\hat{b}, \end{aligned} \tag{24}$$

where

$$\begin{aligned} M &= \frac{(1-\gamma)c^d}{\left(\rho + \zeta_r + (1/2)\gamma(1-\gamma)\theta^{d^2}\sigma^2\right)\gamma}, \\ N &= \frac{(1-\gamma)c^d}{\left(\rho + \zeta_u + (1/2)\gamma(1-\gamma)\theta^{d^2}\sigma^2\right)\gamma}, \\ c^d &= w(\Re(1-\gamma))^{-1/\gamma}, \\ \Re &= \frac{\left[\left(\rho - \bar{r}(1-\gamma) - (\bar{b} - \bar{r})^2(1-\gamma)/2\sigma^2\gamma\right)/\gamma\right]^{-\gamma}}{(1-\gamma)}, \\ \theta^d &= \frac{\bar{b} - \bar{r}}{\gamma\sigma^2}. \end{aligned} \tag{25}$$

Proof. See the appendix. □

Proposition 9 makes predictions about the sparse agent's choice. When $\kappa = 0$, the agent is the traditional, perfectly rational agent. And when $\kappa > 0$, it is a policy of a sparse agent. Larger κ indicates that the agent is less sensitive to fluctuations of both the riskless interest rate and the risky mean rate of return.

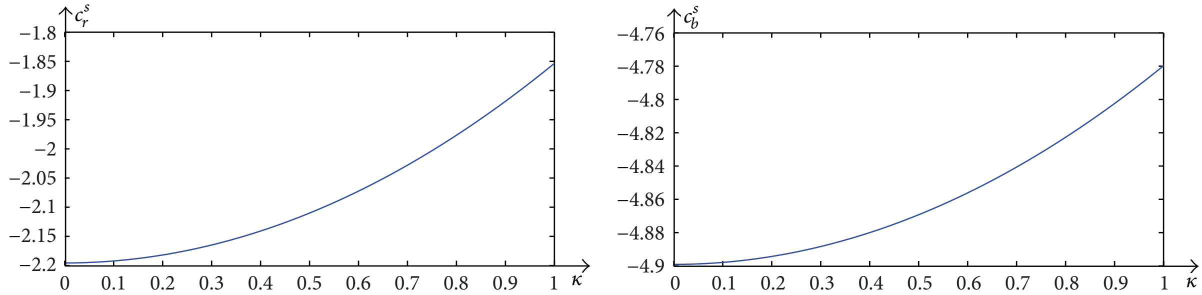

(a) (b)

Figure 3: (a) Impact of a change in $\hat{r}$ on c^s with $\sigma_r = 1.5$, $\sigma_b = 1.7$. (b) Impact of a change in $\hat{b}$ on c^s with $\sigma_r = 1.5$, $\sigma_b = 1.7$.

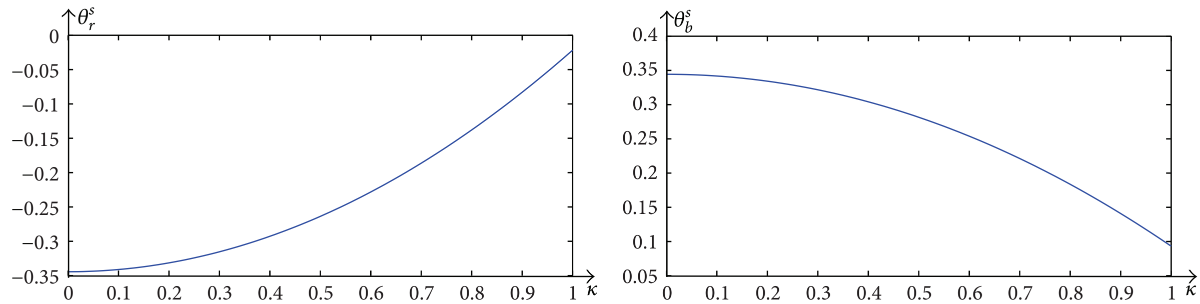

(a) (b)

Figure 4: (a) Impact of a change in $\hat{r}$ on θ^s with $\sigma_r = 1.5$, $\sigma_b = 1.7$. (b) Impact of a change in $\hat{b}$ on θ^s with $\sigma_r = 1.5$, $\sigma_b = 1.7$.

4.2. Numerical Example. The purpose of this numerical analysis is to intuitively understand how the boundedly rational agent changes its decisions with the changing of the variances of factors. Firstly, we set $c^s_{\hat{r}} = \tau(-(1-\theta^d)/M, \kappa\sigma_c/\sigma_r)$, $c^s_{\hat{b}} = \tau(-1/N, \kappa\sigma_c/\sigma_b)$, $\theta^s_{\hat{r}} = \tau(-1/\gamma\sigma^2, \kappa\sigma_\theta/\sigma_r)$, and $\theta^s_{\hat{b}} = \tau(1/\gamma\sigma^2, \kappa\sigma_\theta/\sigma_b)$. Let $\gamma = 0.6, \sigma = 2.2, \sigma_r = 1.5, \sigma_b = 1.7, \sigma_\theta = 0.5, \sigma_c = 1.3, \bar{b} = 3.2, \bar{r} = 18, \rho = 0.95, \zeta_r = 0.2, \zeta_b = 0.4$, and $w = 5$; then we have $c^s_{\hat{r}}, c^s_{\hat{b}}$ as shown in Figures 3 and 4. In these figures, the horizontal axis κ is an index of bounded rationality and $\kappa \in [0,1]$ which is also applied to Figures 5 and 6.

From Figure 3, we know that whatever κ is, $|c^s_{\hat{r}}| > 0$ and $|c^s_{\hat{b}}| > 0$, which means when the variances of $\hat{r}$ and $\hat{b}$ are big, the agent will consider them in the process of making a decision.

Figure 3(a) shows that if $\kappa = 0$, then the agent reacts like the rational agent: when $\hat{r}$ goes up by 1%, $c^s_{\hat{r}}$ will fall by −2.19% (the agent saves more). For $\kappa = 1$, if $\hat{r}$ goes up by 1%, $c^s_{\hat{r}}$ falls by −1.85%. This result indicates that the greater the cognitive cost about the factor is, the less attention will be paid to this factor by the boundedly rational agent. From Figure 3(b), we can reach a similar conclusion.

Figure 4 also shows the agent will always consider $\hat{r}$ and $\hat{b}$, that is, $|\theta^s_{\hat{r}}| > 0$ and $|\theta^s_{\hat{b}}| > 0$, whatever κ is. It addition, we can obtain that if $\kappa = 0$, $\theta^s_{\hat{r}} = -0.34\%$ and $\theta^s_{\hat{b}} = 0.34\%$, which means the rational agent has the same sensitivity about the $\hat{r}$ and $\hat{b}$ when deciding θ^s. With the increasing of κ, the absolute values of $\theta^s_{\hat{r}}$ and $\theta^s_{\hat{b}}$ both will decrease, which means that the agent will pay less attention to them. In other words, the impact of $\hat{r}$ and $\hat{b}$ on θ^s will decrease for the increasing cognitive cost.

Next, we assume that the standard deviation of riskless interest rate and the risky mean rate of return is smaller, $\sigma_r = 0.15$, $\sigma_b = 0.25$. By keeping other parameters fixed, we get results shown in Figures 5 and 6.

Figure 5(a) shows that when $\kappa \geq 0.26$, $c^s_{\hat{r}} = 0$ which means that if the fluctuation is small the agent may discard $\hat{r}$ when he decides the optimal consumption. We can get a similar conclusion from Figure 5(b): when $\kappa \geq 0.95$, $c^s_{\hat{r}} = 0$ with $\sigma_b = 0.25$.

From Figure 5(a), we know that if $\kappa = 0$, $c^s_{\hat{r}} = -2.19\%$ while Figure 3(a) also shows if $\kappa = 0$, $c^s_{\hat{r}} = -2.19\%$ which means, for the rational agent, the sensitivity of c^s to $\hat{r}$ has nothing to do with $\hat{r}$'s variance. However, the boundedly rational agents have different reactions to $\hat{r}$ as κ increases, such as when $\kappa = 0.26$, $c^s_{\hat{r}} = 0$ with $\sigma_r = 0.15$ in Figure 5(a) while $c^s_{\hat{r}} = -2.1\%$ with $\sigma_r = 1.5$ in Figure 3(a). This disparity indicates that when the cognitive costs are the same and $\kappa > 0$, that is, the agents have the same boundedly rational degree, more volatile factors will be considered while the factor with smaller variance may be neglected.

Additionally, we can know that when $0.26 \leq \kappa < 0.95$, the agent does not react to $\hat{r}$, namely, $c^s_{\hat{r}} = 0$ (in Figure 5(a)), but will react to a change in $\hat{b}$ (in Figure 5(b)), which is more important: the sensitivity of c^s to $\hat{b}$ remains high even for a high cognitive friction κ. Note that this "feature by feature"

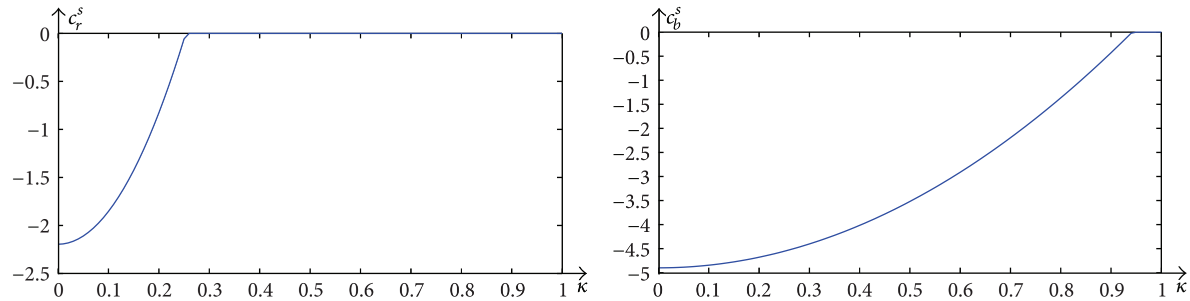

(a) (b)

FIGURE 5: (a) Impact of a change in $\hat{r}$ on c^s with $\sigma_r = 0.15$, $\sigma_b = 0.25$. (b) Impact of a change in $\hat{b}$ on c^s with $\sigma_r = 0.15$, $\sigma_b = 0.25$.

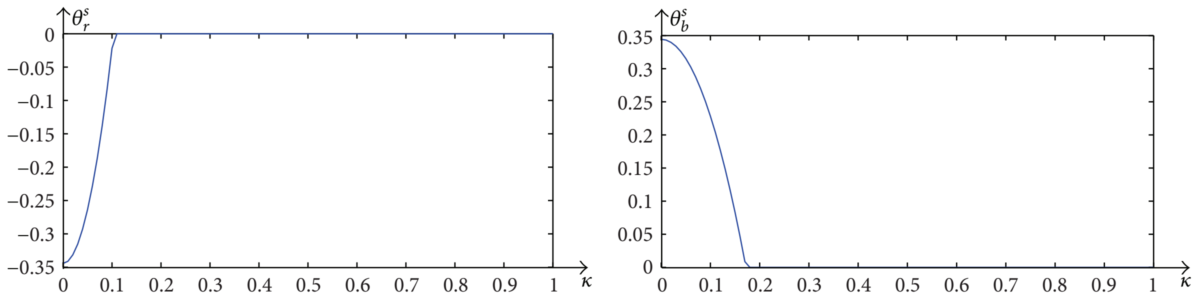

(a) (b)

FIGURE 6: (a) Impact of a change in $\hat{r}$ on θ^s with $\sigma_r = 0.15$, $\sigma_b = 0.25$. (b) Impact of a change in $\hat{b}$ on θ^s with $\sigma_r = 0.15$, $\sigma_b = 0.25$.

selective attention could not be rationalized by just a fixed cost to consumption, which is not feature dependent. But when $\kappa \geq 0.95$, $c_{\hat{r}}^s = c_{\hat{b}}^s = 0$, which indicates that the agent will pay no attention to both $\hat{r}$ and $\hat{b}$ once their thinking costs are beyond some thresholds.

Considering Figure 6(a), we can see that when $\kappa \geq 0.11$, $\theta_{\hat{r}}^s = 0$, while Figure 4(a) shows whatever κ is, $\theta_{\hat{r}}^s > 0$ with $\sigma_r = 1.5$ which means the smaller the variance of a factor is, the more likely the agent will ignore it. From Figure 6(b), we can also obtain the same conclusion.

5. Conclusion

Dynamic portfolio choice is an important but complex problem in modern financial field, but extant methods always generate complicated numerical calculations due to numerous state variables. Hence, to address this problem, this paper extends the sparse max operator proposed by Gabaix [23] and proposes a new approach to deal with dynamic programming under stochastic terms under the assumption of the agent's limited attention. We apply this method to Merton dynamic portfolio choice problem and find that it effectively simplifies the model's solution process and avoids the "Curse of Dimensionality." Finally, numerical example shows that this method has significant economic implications and clearly interprets the agent's economic behavior when he makes a portfolio choice.

Our study can be extended in several directions. Future research should consider the condition when the stochastic factors are correlated with each other for it is more realistic. Besides, information faced by the agent is always imprecise and incomplete, and the fuzzy set theory is an important approach to deal with this kind of problem [31–33]. Hence, using fuzzy set theory to handle imprecise values in dynamic programming may be another direction for further research.

Appendix

Proof of Proposition 7. Based on model (7), we define value function

$$
\begin{aligned}
U^*(a,x,\mathbf{y}) &= u(a,x,\mathbf{y}) + g(x,\mathbf{y},a)V_x \\
&\quad + \sum_{i=1}^{n} h^i(x,y_i)V_{y_i} + \frac{1}{2}\sigma^2(x,a)V_{xx} \\
&\quad + \sum_{i=1}^{n} \frac{1}{2}\left(\sigma^i(y_i(t))\right)^2 V_{y_i y_i} \\
&\quad + \sum_{i=1}^{n} \sigma(x,a)\sigma^i(y_i(t))\rho_{xy_i}V_{xy_i} \\
&\quad + \sum_{i,j=1(i\neq j)}^{n} \sigma^i(y_i(t))\sigma^j(y_j(t))\rho_{ij}V_{y_i y_j}.
\end{aligned} \tag{A.1}
$$

For $dZ_x dB_{\mathbf{y}} = 0$, we have $\rho_{xy_i} = 0$, $\rho_{y_i y_j} = 0$ where ρ_{xy_i}, $\rho_{y_i y_j}$ represent coefficient between x and y_i, y_i, and y_j, respectively.

Besides, the volatility of a variable that may not be considered by the agent is assumed to be small in Assumption 6; that is, $\sigma^i(y_i(t)) = 0$; so we have

$$U^*(a,x,\mathbf{y}) = u(a,x,\mathbf{y}) + g(x,\mathbf{y},a)V_x + \sum_{i=1}^n h^i(x,y_i)V_{y_i} + \frac{1}{2}\sigma^2(x,a)V_{xx}. \quad \text{(A.2)}$$

Similarly, we define

$$\begin{aligned} U^{**}(a,x,\mathbf{y}) &= u(a,x,\mathbf{y}) + g(x,\mathbf{y},a)V_x^s \\ &+ \sum_{i=1}^n h^i(x,y_i)V_{y_i}^s + \frac{1}{2}\sigma^2(x,a)V_{xx}^s \\ &+ \sum_{i=1}^n \frac{1}{2}\left(\sigma^i(y_i(t))\right)^2 V_{y_iy_i}^s \\ &+ \sum_{i=1}^n \sigma(x,a)\sigma^i(y_i(t))\rho_{xy_i}V_{xy_i}^s \\ &+ \sum_{i,j=1(i\neq j)}^n \sigma^i(y_i(t))\sigma^j(y_j(t))\rho_{ij}V_{y_iy_j}^s. \end{aligned} \quad \text{(A.3)}$$

From the analysis above, we have

$$U^{**}(a,x,\mathbf{y}) = u(a,x,\mathbf{y}) + g(x,\mathbf{y},a)V_x^s + \sum_{i=1}^n h^i(x,y_i)V_{y_i}^s + \frac{1}{2}\sigma^2(x,a)V_{xx}^s. \quad \text{(A.4)}$$

Then the associated optimal actions can expressed as

$$\begin{aligned} a^*(x,\mathbf{y}) &= \arg\max_a U^*(a,x,\mathbf{y}), \\ a^{**}(x,\mathbf{y}) &= \arg\max_a U^{**}(a,x,\mathbf{y}). \end{aligned} \quad \text{(A.5)}$$

First, we will prove $\partial a^*(x,\mathbf{y})/\partial y_i = \partial a^{**}(x,\mathbf{y})/\partial y_i$ at $\mathbf{y} = 0$.

From the proof of lemma 1 in Gabaix [23], we know that $V^s(x,\mathbf{y}) = V(x,\mathbf{y}) + x\pi(x,\mathbf{y})x$ where $\pi(x,\mathbf{y})$ is continuous in $(x,\mathbf{y})$ and twice differentiable at $\mathbf{y} = 0$, with $\pi(x,\mathbf{0})$ negative semidefinite. In other word, the $V^s(x,\mathbf{y})$ and $V^s(x,\mathbf{y}) = x\pi(x,\mathbf{y})x$ differ only by second-order terms in x. This basically generalizes the envelope theorem. It implies that at

$$\begin{aligned} \mathbf{y} = 0,\ \text{we have } V_x(x,0) &= V_x^s(x,0), \\ V_{xx}(x,0) &= V_{xx}^s(x,0), \\ V_{y_i}(x,\mathbf{y})\big|_{y_i=0} &= V_{y_i}^s(x,\mathbf{y})\big|_{y_i=0}, \\ V_{xy_i}(x,\mathbf{y})\big|_{y_i=0} &= V_{xy_i}^s(x,\mathbf{y})\big|_{y_i=0}. \end{aligned} \quad \text{(A.6)}$$

Differentiating formula (A.2) with respect to a gives

$$U_a^* = u_a + g_a(x,\mathbf{y},a)V_x + \frac{1}{2}\sigma_a^2(x,a)V_{xx}. \quad \text{(A.7)}$$

Differentiating formula (A.7) with respect to y_i and a, respectively, we get

$$\begin{aligned} U_{ay_i}^* &= u_{ay_i} + g_{ay_i}(x,\mathbf{y},a)V_x + g_a(x,\mathbf{y},a)V_{xy_i} \\ &+ \frac{1}{2}\sigma_a^2(x,a)D_x\left[V_{xy_i}\right], \\ U_{aa}^* &= u_{aa} + g_{aa}(x,\mathbf{y},a)V_x + \frac{1}{2}\sigma_{aa}^2(x,a)V_{xx}. \end{aligned} \quad \text{(A.8)}$$

Similarly, differentiating formula (A.4) with respect to a gives

$$U_a^{**} = u_a + g_a(x,\mathbf{y},a)V_x^s + \frac{1}{2}\sigma_a^2(x,a)V_{xx}^s. \quad \text{(A.9)}$$

Differentiating formula (A.9) with respect to y_i and a, respectively, gives

$$\begin{aligned} U_{ay_i}^{**} &= u_{ay_i} + g_{ay_i}(x,\mathbf{y},a)V_s^x + g_a(x,\mathbf{y},a)V_{xy_i}^s \\ &+ \frac{1}{2}\sigma_a^2(x,a)D_x\left[V_{xy_i}^s\right], \\ U_{aa}^* &= u_{aa} + g_{aa}(x,\mathbf{y},a)V_x^s + \frac{1}{2}\sigma_{aa}^2(x,a)V_{xx}^s. \end{aligned} \quad \text{(A.10)}$$

Hence, we have $U_{ay_i}^* = U_{ay_i}^{**}$ at $y_i = 0$ and $U_{aa}^* = U_{aa}^{**}$ at $y_i = 0$. So

$$\begin{aligned} \left.\frac{\partial a^{**}(x,\mathbf{y})}{\partial y_i}\right|_{y_i=0} &= -\frac{U_{ay_i}^{**}\big|_{y_i=0}}{U_{aa}^{**}} \\ &= -\frac{U_{ay_i}^{*}\big|_{y_i=0}}{U_{aa}^{*}} = \left.\frac{\partial a^{*}(x,\mathbf{y})}{\partial y_i}\right|_{y_i=0}. \end{aligned} \quad \text{(A.11)}$$

Given $a^r(x,\mathbf{y}) = a^d(x) + \sum_i a_{y_i}y_i + o(\|\mathbf{y}\|^2)$, we have $\partial a^r(x,\mathbf{y})/\partial y_i = a_{y_i}$. According to (A.11), we obtain $\partial a^{**}(x,\mathbf{y})/\partial y_i = a_{y_i}$, so $a^{**}(x,\mathbf{y}) = a^d(x) + \sum_i a_{y_i}y_i + o(\|\mathbf{y}\|^2)$. Finally

$$\begin{aligned} a^s(x,\mathbf{y}) &= a\left(x,\mathbf{m}^{*T}\mathbf{y}\right) = a^d(x) \\ &+ \sum_i a_{y_i}m_i^* y_i + o\left(\|\mathbf{y}\|^2\right) \\ &= a^d(x) + \sum_i a_{y_i}A_1\left(\frac{\Lambda_{ii}}{\kappa}\right)y_i + o\left(\|\mathbf{y}\|^2\right) \\ &= a^d(x) + \sum_i \tau\left(a_{y_i},\frac{\kappa\sigma_a}{\sigma_i}\right)y_i + o\left(\|\mathbf{y}\|^2\right), \end{aligned} \quad \text{(A.12)}$$

where σ_a is the standard deviation of a. □

Proof of Proposition 8. The laws of motion of model (7) are

$$\begin{aligned} dx &= g(x(t),\mathbf{y}(t),a(t))\,dt + \sigma(x(t),a(t))\,dZ_x(t) \\ dy_i &= h^i(x(t),y_i(t))\,dt + \sigma^i(y_i(t))\,dB_{y_i}(t), \end{aligned} \quad \text{(A.13)}$$

where $\mathbf{y} = (y_1, y_2, \ldots, y_n)$. Using Ito formula, Bellman's equation of model (7) can be expressed as follows:

$$\begin{aligned}\rho V &= \max_a u(a, x, \mathbf{y}) + g(x, \mathbf{y}, a) V_x \\ &\quad + \sum_{i=1}^{n} h^i(x, y_i) V_{y_i} + \frac{1}{2}\sigma^2(x, a) V_{xx} \\ &\quad + \sum_{i=1}^{n} \frac{1}{2}\left(\sigma^i(y_i(t))\right)^2 V_{y_i y_i} \\ &\quad + \sum_{i=1}^{n} \sigma(x, a)\sigma^i(y_i(t))\rho_{xy_i} V_{xy_i} \\ &\quad + \sum_{i,j=1 (i\neq j)}^{n} \sigma^i(y_i(t))\sigma^j(y_j(t))\rho_{y_i y_j} V_{y_i y_j}.\end{aligned} \tag{A.14}$$

From the proof of Proposition 7 above, we have $\rho_{xy_i} = 0$, $\rho_{y_i y_j} = 0$, and $\sigma^i(y_i(t)) = 0$. So we obtain

$$\begin{aligned}\rho V &= \max_a u(a, x, \mathbf{y}) + g(x, \mathbf{y}, a) V_x \\ &\quad + \sum_{i=1}^{n} h^i(x, y_i) V_{y_i} + \frac{1}{2}\sigma^2(x, a) V_{xx}.\end{aligned} \tag{A.15}$$

We define function $\phi(x, \mathbf{y}, a)$ as the derivative of the right side in formula (A.15) with respect to a, so a satisfies $\phi = 0$ with

$$\phi(x, \mathbf{y}, a) = u_a + g_a(x, \mathbf{y}, a) V_x + \frac{1}{2}\sigma_a^2(x, a) V_{xx}, \tag{A.16}$$

and we define $f(x) = V_{xx}/V$, where $f(x)$ can be derived from the expression of $V(x, \mathbf{0}) = \int_0^\infty e^{-\rho t} u(a, x, \mathbf{0}) dt$ in Step 1 of Section 3. Hence, differentiating formula (A.15) with respect to y_i gives

$$\begin{aligned}\rho V_{y_i} &= u_{ay_i} + g_{y_i}(x, \mathbf{y}, a) V_x \\ &\quad + \sum_{i=1}^{n} h_{y_i}^i(x, y_i, a) V_{y_i} + \frac{1}{2}\sigma^2(x, a) f(x) V_{y_i}.\end{aligned} \tag{A.17}$$

Now we differentiate at $\mathbf{y} = 0$ and evaluate at $(a, x, \mathbf{y}) = (a^d, x, 0)$:

$$\begin{aligned}\rho V_{xy_i} &= D_x\left[u_{ay_i} + g_{y_i}(x, \mathbf{y}, a) V_x\right] \\ &\quad + \sum_{i=1}^{n} h_{xy_i}^i(x, y_i, a) V_{y_i} + \sum_{i=1}^{n} h_{y_i}^i(x, y_i, a) V_{xy_i} \\ &\quad + \frac{1}{2}\sigma_x^2(x, a) f(x) V_{y_i} \\ &\quad + \frac{1}{2}\sigma^2(x, a)\left(f_x(x) V_{y_i} + f(x) V_{xy_i}\right).\end{aligned} \tag{A.18}$$

From (A.17) we get $V_{y_i} = (u_{ay_i} + g_{y_i}(x, \mathbf{y}, a)V_x)/(\rho - \sum_{i=1}^{n} h_{y_i}^i(x, y_i, a) - (1/2)\sigma^2(x, a) f(x))$.

And from (A.18) we obtain

$$\begin{aligned}V_{xy_i} &= \Big(D_x\left[u_{ay_i} + g_{y_i}(x, \mathbf{y}, a) V_x\right] \\ &\quad + \sum_{i=1}^{n} h_{xy_i}^i(x, y_i, a) V_{y_i} + \frac{1}{2}\sigma_x^2(x, a) f(x) V_{y_i} \\ &\quad + \frac{1}{2}\sigma^2(x, a) f_x(x) V_{y_i}\Big) \\ &\quad \times \left(\rho - \sum_{i=1}^{n} h_{y_i}^i(x, y_i, a) - \frac{1}{2}\sigma^2(x, a) f(x)\right)^{-1}.\end{aligned} \tag{A.19}$$

According to formula (A.16), we know that the impact of y_i on the optimal action can be expressed as $a_{y_i} = -\phi_{y_i}/\phi_a$, where

$$\begin{aligned}\phi_a &= u_{aa} + g_{aa}(x, \mathbf{y}, a) V_x + \frac{1}{2}\sigma_{aa}^2(x, a) D_x\left[V_x\right], \\ \phi_{y_i} &= u_{ay_i} + g_{ay_i}(x, \mathbf{y}, a) V_x + g_a(x, \mathbf{y}, a) V_{xy_i} \\ &\quad + \frac{1}{2}\sigma_a^2(x, a) D_x\left[V_{xy_i}\right].\end{aligned} \tag{A.20}$$

□

Proof of Proposition 9. Using Ito formula, Bellman's formula of model (18) is

$$\begin{aligned}\rho V &= \max_c u(c) \\ &\quad + \left[w(1-\theta)(\bar{r} + \hat{r}) + w\theta\left(\bar{b} + \hat{b}\right) - c\right] V_w \\ &\quad + (-\zeta_r \hat{r}) V_{\hat{r}} + \left(-\zeta_b \hat{b}\right) V_{\hat{b}} \\ &\quad + \frac{1}{2}(\theta\sigma w)^2 V_{ww} + \frac{1}{2}\sigma_r^2 V_{\hat{r}\hat{r}} + \frac{1}{2}\sigma_b^2 V_{\hat{b}\hat{b}} \\ &\quad + \sigma\sigma_r \rho_{wr} V_{wr} + \sigma\sigma_b \rho_{wb} V_{wb} + \sigma_r \sigma_b \rho_{rb} V_{rb},\end{aligned} \tag{A.21}$$

where ρ_{wr}, ρ_{wb}, and ρ_{br} represent the coefficient between w and r, w and b, and b and r, respectively. For $dWdR = 0$, $dWdB = 0$, and $dRdB = 0$, we have $\rho_{wr} = 0$, $\rho_{wb} = 0$, and $\rho_{br} = 0$. According to Assumption 6, the variances of r and b are so small that we let $\sigma_r = \sigma_b = 0$. Then formula (A.21) becomes as follows:

$$\begin{aligned}\rho V &= \max_c u(c) + \left[w(1-\theta)(\bar{r} + \hat{r}) + w\theta\left(\bar{b} + \hat{b}\right) - c\right] V_w \\ &\quad + (-\zeta_r \hat{r}) V_{\hat{r}} + \left(-\zeta_b \hat{b}\right) V_{\hat{b}} + \frac{1}{2}(\theta\sigma w)^2 V_{ww}.\end{aligned} \tag{A.22}$$

Differentiating formula (A.22) with respect to $\hat{r}$ and evaluating at $(\hat{r}, \hat{b}) = (0, 0)$, we obtain $\rho V_{\hat{r}} = w(1-\theta)V_w + (-\zeta_r)V_{\hat{r}} + (1/2)(\theta\sigma w)^2(\partial V_{ww}/\partial \hat{r})$ where $V_{ww} = ((1-\gamma)(-\gamma)/w^2)V$ which can be obtained from (22); then

$$\rho V_{\hat{r}} = w(1-\theta) V_w + (-\zeta_r) V_{\hat{r}} + \frac{1}{2}(1-\gamma)(-\gamma)\theta^2\sigma^2 V_{\hat{r}}. \tag{A.23}$$

Now differentiating (using the total derivative) formula (A.23) with respect to w and evaluating at $(\hat{r},\hat{b}) = (0,0)$, we obtain

$$\begin{aligned}\rho V_{w\hat{r}} = {} & (1-\theta) V_w + w(1-\theta) V_{ww} \\ & + (-\zeta_r) V_{w\hat{r}} + \frac{1}{2}(1-\gamma)(-\gamma)\theta^2\sigma^2 V_{w\hat{r}}.\end{aligned} \tag{A.24}$$

From formula (A.23) we have

$$V_{\hat{r}} = \frac{w(1-\theta) V_w}{\rho + \zeta_r + (1/2)\gamma(1-\gamma)\theta^2\sigma^2}. \tag{A.25}$$

According to formula (A.24) and the term $V_{ww} = (-\gamma/w)V_w$ which can be obtained from (22) we have

$$V_{w\hat{r}} = \frac{(1-\gamma)(1-\theta) V_w}{\rho + \zeta_r + (1/2)\gamma(1-\gamma)\theta^2\sigma^2}. \tag{A.26}$$

Let $\phi(c,\theta,w,\hat{r},\hat{b})$ denote the result of derivation of the right side in formula (A.22) with respect to c; then c satisfies $\phi = 0$ with $\phi(c,\theta,w,\hat{r},\hat{b}) = u_c - V_w$.

Hence, the impact of $\hat{r}$ on c is

$$c_{\hat{r}} = -\frac{\phi_{\hat{r}}}{\phi_c}, \tag{A.27}$$

where

$$\begin{aligned}\phi_c &= u_{cc}, \\ \phi_{\hat{r}} &= u_{cc}\frac{\partial c}{\partial \hat{r}} - V_{w\hat{r}}.\end{aligned} \tag{A.28}$$

Since all derivatives are evaluated at $(\hat{r},\hat{b}) = (0,0)$, we have $c = c^d$, $\theta = \theta^d$. By substituting (A.28) into (A.27) and using the results of (22), (A.25), (A.26), now we can get

$$c_{\hat{r}} = -\frac{(1-\gamma)(1-\theta^d) c^d}{\left(\rho + \zeta_r + (1/2)\gamma(1-\gamma){\theta^d}^2\sigma^2\right)\gamma}. \tag{A.29}$$

Similarly, we have

$$c_{\hat{b}} = -\frac{(1-\gamma) c^d}{\left(\rho + \zeta_b + (1/2)\gamma(1-\gamma){\theta^d}^2\sigma^2\right)\gamma}, \tag{A.30}$$

where the concrete expressions of c^d, θ^d are referred to formula (22). $\theta_{\hat{r}}$, $\theta_{\hat{b}}$ can be solved in an analogous way as $\theta_{\hat{r}} = -1/\gamma\sigma^2$, $\theta_{\hat{b}} = 1/\gamma\sigma^2$.

According to Proposition 7, c^s and θ^s can expressed as

$$\begin{aligned}c^s &= c^d + \tau\left(-\frac{1-\theta^d}{M}, \frac{\kappa\sigma_c}{\sigma_r}\right)\hat{r} + \tau\left(-\frac{1}{N}, \frac{\kappa\sigma_c}{\sigma_b}\right)\hat{b}, \\ \theta^s &= \theta^d + \tau\left(-\frac{1}{\gamma\sigma^2}, \frac{\kappa\sigma_\theta}{\sigma_r}\right)\hat{r} + \tau\left(\frac{1}{\gamma\sigma^2}, \frac{\kappa\sigma_\theta}{\sigma_b}\right)\hat{b},\end{aligned} \tag{A.31}$$

where

$$\begin{aligned}M &= \frac{(1-\gamma) c^d}{\left(\rho + \zeta_r + (1/2)\gamma(1-\gamma){\theta^d}^2\sigma^2\right)\gamma}, \\ N &= \frac{(1-\gamma) c^d}{\left(\rho + \zeta_u + (1/2)\gamma(1-\gamma){\theta^d}^2\sigma^2\right)\gamma} \\ c^d &= w(\Re(1-\gamma))^{-1/\gamma} \\ \Re &= \frac{\left[\left(\rho - \bar{r}(1-\gamma) - (\bar{b}-\bar{r})^2(1-\gamma)/2\sigma^2\gamma\right)/\gamma\right]^{-\gamma}}{(1-\gamma)}, \\ \theta^d &= \frac{\bar{b}-\bar{r}}{\gamma\sigma^2}.\end{aligned} \tag{A.32}$$

□

Conflict of Interests

The authors declare that there is no conflict of interests regarding the publication of this paper.

Acknowledgments

This research is supported by National Natural Science Foundation of China (Grant nos. 71371191, 71210003, and 712221061).

References

[1] R. C. Merton, "Lifetime portfolio selection under uncertainty: the continuous-time case," *Review of Economics and Statistics*, vol. 51, no. 3, pp. 247–257, 1969.

[2] R. C. Merton, "Optimum consumption and portfolio rules in a continuous-time model," *Journal of Economic Theory*, vol. 3, no. 4, pp. 373–413, 1971.

[3] F. Wen and X. Yang, "Skewness of return distribution and coefficient of risk premium," *Journal of Systems Science & Complexity*, vol. 22, no. 3, pp. 360–371, 2009.

[4] F. Wen, "Measuring and forecasting volatility in Chinese stock market using HAR-CJ-M model," *Abstract and Applied Analysis*, vol. 2013, Article ID 143194, 13 pages, 2013.

[5] J. C. Cox and C.-F. Huang, "Optimal consumption and portfolio policies when asset prices follow a diffusion process," *Journal of Economic Theory*, vol. 49, no. 1, pp. 33–83, 1989.

[6] I. Karatzas, J. P. Lehoczky, S. P. Sethi, and S. E. Shreve, "Explicit solution of a general consumption/investment problem," *Mathematics of Operations Research*, vol. 11, no. 2, pp. 261–294, 1986.

[7] I. Karatzas, J. P. Lehoczky, and S. E. Shreve, "Optimal portfolio and consumption decisions for a "small investor" on a finite horizon," *SIAM Journal on Control and Optimization*, vol. 25, no. 6, pp. 1557–1586, 1987.

[8] I. Karatzas, J. P. Lehoczky, and S. E. Shreve, "Existence and uniqueness of multi-agent equilibrium in a stochastic, dynamic consumption/investment model," *Mathematics of Operations Research*, vol. 15, no. 1, pp. 80–128, 1990.

[9] R. E. Hall, "The dynamic effects of fiscal policy in an economy with foresight," *The Review of Economic Studies*, vol. 38, no. 114, pp. 229–244, 1971.

[10] M. J. Magill, "A local analysis of N-sector capital accumulation under uncertainty," *Journal of Economic Theory*, vol. 15, no. 1, pp. 211–219, 1977.

[11] F. E. Kydland and E. C. Prescott, "Time to build and aggregate fluctuations," *Econometrica*, vol. 50, no. 6, pp. 1345–1370, 1982.

[12] L. J. Christiano, "Linear-quadratic approximation and value-function iteration: a comparison," *Journal of Business & Economic Statistics*, vol. 8, no. 1, pp. 99–113, 1990.

[13] K. L. Judd and S.-M. Guu, "Asymptotic methods for asset market equilibrium analysis," *Economic Theory*, vol. 18, no. 1, pp. 127–157, 2001.

[14] G. A. Miller, "The magical number seven, plus or minus two: some limits on our capacity for processing information," *Psychological Review*, vol. 63, no. 2, pp. 81–97, 1956.

[15] D. Kahneman, *Thinking, Fast and Slow*, Macmillan, New York, NY, USA, 2011.

[16] W. Bi, Y. Sun, H. Liu, and X. Chen, "Dynamic nonlinear pricing model based on adaptive and sophisticated learning," *Mathematical Problems in Engineering*, vol. 2014, Article ID 791656, 11 pages, 2014.

[17] P. Bordalo, N. Gennaioli, and A. Shleifer, "Salience theory of choice under risk," *The Quarterly Journal of Economics*, vol. 127, no. 3, pp. 1243–1285, 2012.

[18] B. Kőszegi and A. Szeidl, "A model of focusing in economic choice," *The Quarterly Journal of Economics*, vol. 128, no. 1, pp. 53–104, 2013.

[19] C. A. Sims, "Implications of rational inattention," *Journal of Monetary Economics*, vol. 50, no. 3, pp. 665–690, 2003.

[20] L. Peng and W. Xiong, "Investor attention, overconfidence and category learning," *Journal of Financial Economics*, vol. 80, no. 3, pp. 563–602, 2006.

[21] M. S. Seasholes and G. Wu, "Predictable behavior, profits, and attention," *Journal of Empirical Finance*, vol. 14, no. 5, pp. 590–610, 2007.

[22] B. Maćkowiak and M. Wiederholt, "Optimal sticky prices under rational inattention," *American Economic Review*, vol. 99, no. 3, pp. 769–803, 2009.

[23] X. Gabaix, "A sparsity-based model of bounded rationality, applied to basic consumer and equilibrium theory," Working Paper, National Bureau of Economic Research, YUN, New York, NY, USA, 2013.

[24] W. H. Fleming and H. M. Soner, *Controlled Markov Processes and Viscosity Solutions*, vol. 25, Cambridge University Press, Cambridge, UK, 2006.

[25] J.-P. Fouque, G. Papanicolaou, and K. R. Sircar, *Derivatives in Financial Markets with Stochastic Volatility*, Cambridge University Press, Cambridge, UK, 2000.

[26] M. I. Kamien and N. L. Schwartz, *Dynamic Optimization: The Calculus of Variations and Optimal Control in Economics and Management*, Courier Dover Publications, Mineola, NY, USA, 1991.

[27] F. Wen, Z. He, and X. Chen, "Investors' risk preference characteristics and conditional skewness," *Mathematical Problems in Engineering*, vol. 2014, Article ID 814965, 14 pages, 2014.

[28] F. Wen, X. Gong, Y. Chao, and X. Chen, "The effects of prior outcomes on risky choice: evidence from the stock market," *Mathematical Problems in Engineering*, vol. 2014, Article ID 272518, 8 pages, 2014.

[29] W. H. Fleming and T. Pang, "An application of stochastic control theory to financial economics," *SIAM Journal on Control and Optimization*, vol. 43, no. 2, pp. 502–531, 2004.

[30] W. H. Fleming and D. Hernández-Hernández, "An optimal consumption model with stochastic volatility," *Finance and Stochastics*, vol. 7, no. 2, pp. 245–262, 2003.

[31] L. Wang, C. X. Dun, W. J. Bi, and Y. R. Zeng, "An effective and efficient differential evolution algorithm for the integrated stochastic joint replenishment and delivery model," *Knowledge-Based Systems*, vol. 36, pp. 104–114, 2012.

[32] L. Wang, C. X. Dun, C. G. Lee, Q. L. Fu, and Y. R. Zeng, "Model and algorithm for fuzzy joint replenishment and delivery scheduling without explicit membership function," *The International Journal of Advanced Manufacturing Technology*, vol. 66, no. 9–12, pp. 1907–1920, 2013.

[33] L. Wang, H. Qu, Y. Li, and J. He, "Modeling and optimization of stochastic joint replenishment and delivery scheduling problem with uncertain costs," *Discrete Dynamics in Nature and Society*, vol. 2013, Article ID 657465, 12 pages, 2013.

Hindawi Publishing Corporation
Discrete Dynamics in Nature and Society
Volume 2014, Article ID 135818, 7 pages
http://dx.doi.org/10.1155/2014/135818

Research Article

Carbon Market Regulation Mechanism Research Based on Carbon Accumulation Model with Jump Diffusion

Dongmei Guo,[1] Yi Hu,[2] and Bingjie Zhang[3]

[1] *School of Economics, Central University of Finance and Economics, Beijing 100081, China*
[2] *School of Management, University of Chinese Academy of Sciences, Beijing 100190, China*
[3] *School of Economics and Management, Beihang University, Beijing 100083, China*

Correspondence should be addressed to Yi Hu; huyi@ucas.ac.cn

Received 13 March 2014; Accepted 6 May 2014; Published 22 May 2014

Academic Editor: Chuangxia Huang

In order to explore carbon market regulation mechanism more effectively, based on carbon accumulation model with jump diffusion, this paper studies the carbon price from two perspectives of quantity instrument and price instrument and quantitatively simulates carbon price regulation mechanisms in the light of actual operation of EU carbon market. The results show that quantity instrument and price instrument both have certain effects on carbon market; according to the comparison of the elasticity change of the expected carbon price, comparative advantages of both instruments rely on the price of carbon finance market. Where the carbon price is excessively high, price instrument is superior to quantity instrument; where carbon price is excessively low, quantity instrument is better than price instrument. Therefore, in the case of carbon market regulation based on expected carbon price, if the carbon price is too high, price instrument should prevail; if the carbon price is excessively low, quantity instrument should prevail.

1. Introduction

Given the market practice in EU ETS and RGGI, the highest risk for carbon market is drastic fluctuation in carbon price. European Union Allowance (EUA) price tumbled from 30 Euros in 2005 to near zero in 2007 at the first stage and from maximum 30 Euros in 2008 to less than 5 Euros in 2013 at the second stage. While, as an artificially designed market, carbon market greatly differs from traditional financial market in terms of price formation mechanism, the price in carbon market is highly vulnerable to the market design and policy mechanism. Therefore, in order to ensure the effective and sustainable development of the carbon market, this paper explores regulation mechanism for guaranteeing carbon price within reasonable fluctuation range and simulates quantitative mechanism of price regulation so as to provide method basis and policy guidance for stable development of carbon market.

The main objective of regulation based on carbon market mechanism is to stabilize carbon market price in the short term and reduce greenhouse gas emission in the long term. Regulation can be divided into two tools, quantity instrument and price instrument, by the mode of economic operation. Price instruments include floor price and safety valve, while quantity instruments may be similar to open market operation of monetary policy, in which allowance is increased or decreased to adjust allowance supply quantity. Debate about comparative advantages between quantity regulation and price regulation always exists. In [1], it is explicitly stated for the first time that the ratio of marginal cost of external control to marginal income of external control was the key determinant factor for the effectiveness of regulation instrument. Pizer [2] proposed composite tool for obtaining price and quantity based on stochastic computable general equilibrium model was more effective than single control. Kelly [3] estimated the effect from quantity regulation and price supervision under the condition that the regulator cannot observe productivity shocks and obtained the result indicating that quantity regulation means always generated more profits, regardless of how to express profit function. Wirl [4] analyzed the issue concerning selection of optimal regulation and control strategy for the government which served as representative for consumers and enterprises which produced fossil fuels under the differential game framework, which showed that price tool was the optimal strategy choice for both game players.

According to international market practice, for the purpose of preventing drastic fluctuation in market price, regulatory agency generally adopts the following major flexible mechanisms for regulation: safety valve, price collar, allowance reserve, allowance borrowing, carbon credit offsets, European option or American option provided to enterprises by regulator, and so forth. Price safety valve was firstly proposed in market scheme designed by USA for Kyoto Protocol. This scheme pointed out that the objective of Kyoto Protocol was too strict; thus, safety valve plan was put forward (see [5]). Jacoby and Ellerman [6] explored safety valve mechanism and stated that this mechanism designed absolute price ceiling, and when carbon price was higher than such ceiling, allowance can be purchased at such ceiling without limit so as to effectively control cap-and-trade price in carbon market. However, application of price ceiling also exerted negative impact, such as easy reduction in carbon price expectation and subsequent decrease in motive of technical progress in pollution control (see [7, 8]). Price ceiling mechanism cannot make marginal emission reduction cost lower than expected and possibly fails to provide effective incentive for emission reduction. Some scholars proposed to introduce price floor on the basis of price ceiling design, which resulted in price collar mechanism with double-price control. Simulation technique in [9] was separately used to show that price collar mechanism can effectively avoid the defects in price ceiling design. Pizer and Marika [10] further discussed the mode for selling limited quantity of reserve allowance according to safety valve price so as to translate absolute price ceiling into flexible price ceiling and ensure the effect of emission reduction while controlling costs. In addition, the mechanism for providing European option or American option to enterprises can enhance self-regulating subject to information shock, which was firstly proposed by Requate and Unold [11], under which regulator provided enterprises with European option or American option at fixed price at the beginning of compliance period, while they demonstrated that option provision mechanism can drive execution fee to become zero and thus provided the rationality and effectiveness of this mechanism design.

For the research on quantity and price regulation mechanisms, Guo et al. [12] analyzed regulation mechanism in Chinese carbon market on the basis of classical risk neutral framework in the light of pilot operation of Shenzhen carbon market. However, given practical experience in EU, external impact was easier to cause jump during carbon accumulation. And Borovkov et al. [13] adopted Poisson process to describe carbon accumulation equation in order to more tally with uncertainties in carbon market. For the sake of more accordance with carbon market price process, based on [13], this paper introduces Poisson process for depicting jump-diffusion process of carbon accumulation and setting upper and lower threshold values in line with actual operation of EU ETS carbon emission market and then separately simulates carbon market price in terms of two aspects including quantity instrument and price instrument (in carbon emission regulation mechanism in this paper, quantity instrument specifically refers to regulation of total allowance and price instrument means regulation of penalty value) and analyzes comparative advantages of two regulation modes. With comparative analysis, we find that comparative advantages of quantity regulation and price regulation rely on price level in carbon market: with elasticity of expected carbon price changes, when carbon price is too high and needs to be downwardly adjusted, price instrument is superior to quantity instrument; conversely, when carbon price is excessively low and needs to be upwardly adjusted, quantity regulation is superior to price regulation. Thus where carbon market is regulated according to expected carbon price, if carbon price is low, price regulation will prevail; if carbon price is excessively high, quantity regulation will prevail.

This paper is arranged as follows. Section 2 provides theoretical framework for carbon price simulation. Section 3 starts with upper and lower threshold values and adopts Monte Carlo method to simulate changes in carbon emission price in the case of quantity instrument and price instrument separately and makes comparison between two regulation modes. Section 4 draws conclusions and offers future research direction.

2. Modeling

EU emissions trading system (EU ETS) is the largest carbon emission trading market in the world and has demonstration effect in the world's carbon trading market. Thus quantitative simulation in this paper is conducted on the basis of practical data on EU ETS which appears as cap-and-trade scheme. This scheme specifies emission allowance (N) for member states that the sum of emission allowance for all countries will not exceed the emission committed in the protocol. Allocation of emission allowance gives comprehensive considerations to past emission, expected emission and emission standard, and so forth. If actual emission from enterprises in member states (Q_T) exceeds emission allowance within one given compliance period (T), penalty (P) will be paid for each CO_2 unit.

If carbon emission from enterprise exceeds allowance, emission allowance will be purchased from other enterprises or auctions by the government. Thus, allowance can be traded in the market and its trading price is affected by allowance cap, penalty, and supply-demand relationship. In order to explore the impact of allowance cap and penalty price on carbon emission price, this paper excludes the impact of supply-demand relationship on price and only takes into account carbon price under risk-neutral valuation method, given that, in practice, cumulative carbon emission does not necessarily change in a smooth way but presents discontinuous "jump" process. According to literatures [13, 14], cumulative carbon emission Q_T at terminal moment T consists of two parts: continuous part composed of geometrical Brownian motion and "jump" part which is described as Poisson process. Assuming that $(\Omega, \mathscr{F}, P)$ is one probability space, P is risk-neutral measure; Q_0 is expected carbon accumulation at initial moment, namely, BAU (Business-As-Usual) emission, Q_T is total cumulative carbon emission at the moment T, and $(Q_t)_{0\le t\le T}$ is one exogenous given process which is given by the following formula:

$$\frac{dQ_t}{Q_t} = (\mu - \lambda k)\, dt + \sigma dW(t) + X dN(t), \quad 0 \le t \le T, \quad (1)$$

where $W(t)$ is standard Wiener process, μ denotes the drift during carbon accumulation, suggesting carbon accumulation speed in the carbon market, and σ is volatility. $N(t)$ complies with Poisson process with parameter as λ. $W(t)$ and $N(t)$ are assumed to be independent. X is the percent of the jump size of cumulative carbon emission.

Assuming there is no arbitrage in the market, we use risk neutral method to calculate carbon emission price y_t at the moment $t \in [0, T]$ in the case of not using any mechanism:

$$y_t = E\left[PI_{\{Q_T>N\}}\mathscr{F}_t\right]. \quad (2)$$

According to formula (2), carbon emission price at time t is mainly determined by allowance N and penalty price P; thus, in the following part, the factors affecting carbon emission price are explored mainly by changing allowance N and penalty price P, and regulation effects of allowance and penalty on carbon emission price are separately simulated and compared.

3. Carbon Emission Price Regulation Mechanism

Practical implementation of cap-and-trade scheme is always entrapped in the dilemma in which it is difficult to place equal emphasis on both economic development and emission reduction. On the one hand, strict cap control is beneficial for low-carbon transformation, but high carbon price cost will add burden on economic development at the initial stage of transformation; on the other hand, slack cap constraint is easy to form relatively low carbon price so that the scarcity of carbon emission right disappears, resulting in cap objective losing its constraint. Currently, the EU ETS and RGGI markets in the world are severely questioned because of low carbon price resulting from excessive allowance. Because both excessively high carbon price and excessively low carbon price can affect carbon emission market, in order to ensure steady market operation, we preset upper and lower threshold values of carbon price to the effect that when carbon price reaches upper and lower threshold values, the government will make adjustment.

This section unfolds from regulations of upper threshold and regulations of lower threshold and simulates carbon price separately by changing allowance and penalty. According to practical experience in EU ETS, penalty is set as $P = 40$, assuming that acceptable price is 20, the upper limit which we can tolerate is set as 150% of it, and the lower limit is set as 75% of it; namely, $P_{\text{high}} = 30$, $P_{\text{low}} = 15$. Initial expected carbon accumulation is set as $Q_0 = 200$ (million tons), cumulative rate and volatility of expected carbon emission are separately set as (setting of this parameter is based on the literature [15]) $\mu = 0.15$, $\sigma = 0.15$, and one compliance period T is 3 (years) according to the first stage of EU ETS (2005–2007).

3.1. Regulations of Upper Threshold. In this part, we will proceed from the following two aspects: quantity instrument and price instrument. There is relevant practical experience concerning quantity instrument in both RGGI and EU ETS; for example, in 2013, allowance reserve mechanism was introduced in RGGI carbon trading market; namely, limited quantity of reserve allowance was sold at safety valve price. Carbon credit offset is also one kind of quantity instruments and the substitute for allowance; allowance demand decreases with increasing credit offset; carbon credit offset in EU ETS amounted to 555 million tons during 2008–2011, accounting for 7% of emission.

3.1.1. Quantity Instrument. According to formula (2), carbon emission price is jointly determined by allowance cap, actual carbon emission, and penalty price. If the government anticipates that emission reduction is excessive, too little issuance of free-of-charge allowance will cause relatively high carbon emission price and short supply in carbon emission market, which can lead to relatively large economic burden on market bubble. Based on practical experience in EU ETS and RGGI, we set specific quantity regulation as follows: if carbon price is higher than upper threshold value for n consecutive months in one compliance period T, allowance would increase by α times so as to lower the carbon price. Assuming that Q_T is actual total carbon emission of all enterprises, its process satisfies jump-diffusion process; such mechanism can be expressed as follows:

$$y_t = E\left[P \cdot I_{\{Q_T>N\}} \cdot I_{\{\tau\ge T\}} + P \cdot I_{\{Q_T>(1+\alpha)N\}} \cdot I_{\{\tau<T\}}\mathscr{F}_t\right], \quad (3)$$

where $\tau = \inf\{n \le s < t, \int_{s-n}^{s} I_{\{y_s>P_{\text{High}}\}} du = n\}$.

We use Monte Carlo method to validate the effectiveness of such mechanism; if emission reduction is expected to be excessively 50%, namely, $N = 100$ (million tons), generating $M = 1{,}00000$ different routes, simulation (parameters are set as $Q_0 = 200$, $N = 100$, $P = 40$, $P_{\text{High}} = 25$, $\mu = 0.15, \sigma = 0.15$, $\alpha = 0.15$, $\lambda = 0.5$, $T = 3$, $n = 6$) is conducted to obtain y_t frequency distribution diagram of carbon emission prices in M routes at each time point t.

As shown in Figure 1, axis x and axis y represent time t and the carbon emission price distribution, respectively, and most prices are distributed at about 30, axis z; namely, height of curved surface in diagram represents the frequency of carbon emission price. According to simulated price, carbon emission price at $t = 0$, namely, the initial stage of market, is 33.13 higher than the upper limit 30. If it is higher than 30 for six consecutive months, allowance cap will increase to be α times the previous one in the 7th month. As indicated in Figure 1, when $t > 6$, compared with diagram in the case of not using quantity instrument, diagram in the case of using this instrument shows decreased probability of distribution in relatively high price range [30, 40] and increased probability of distribution in relatively low price range [0, 10].

Furthermore, in order to show the effect from using quantity instrument more markedly, we can also obtain

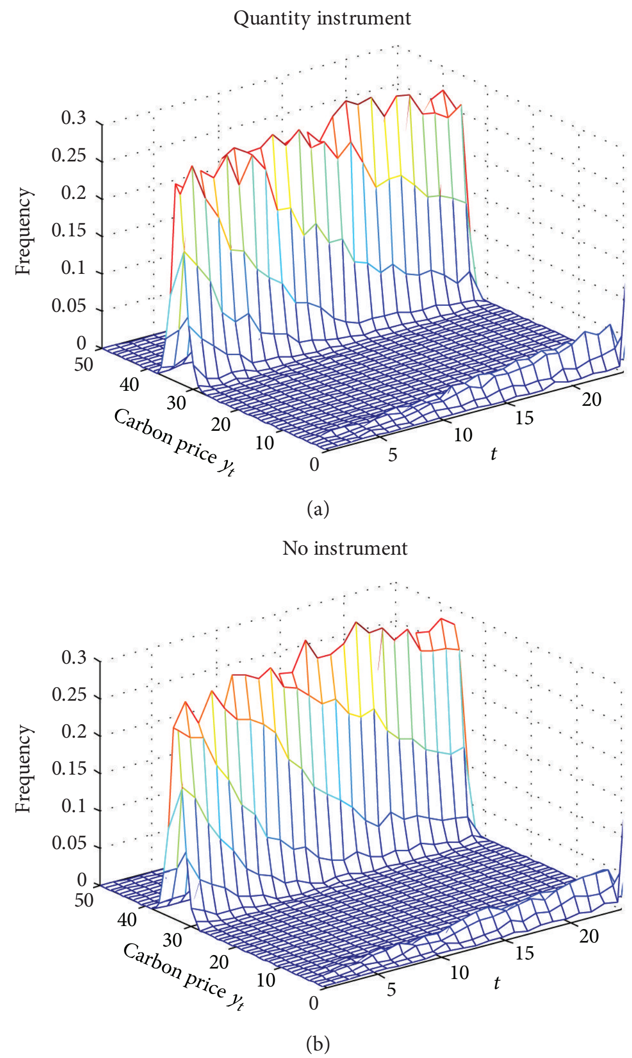

Figure 1: Carbon price frequency distribution diagram of upper threshold regulation using quantity instrument.

expected values of carbon prices at all routes and compare them with those in the case of not using this instrument, and we can find that, after this instrument is used, carbon emission price is 29.92 at $t = 7$ (when carbon price has been higher than price ceiling for six consecutive months), down 5.62% compared with price 31.2 in the case of not using this mechanism.

3.1.2. Price Instrument. If carbon emission price is extremely high, we can reduce the expectation of market participants about carbon price by decreasing penalty so as to lessen the demand for carbon emission right for cutting down carbon price. Thus, we design the following price regulation: if carbon price is higher than the upper threshold value for n consecutive months in one compliance period T, penalty P is decreased by α percentage points so as to lower the carbon price; this mechanism can be expressed as follows:

$$y_t = E\left[P \cdot I_{\{Q_T>N\}} \cdot I_{\{\tau \geq T\}} + (1-\alpha) \cdot P \cdot I_{\{Q_T>N\}} \cdot I_{\{\tau<T\}} \mathscr{F}_t\right], \quad (4)$$

where $\tau = \inf\{n \leq s < t, \int_{s-n}^{s} I_{\{y_s > P_{\text{High}}\}} du = n\}$.

Parameters are the same as those in Figure 1; we simulate this mechanism to obtain frequency distribution diagram in the case of using price instrument. According to Figure 2, initial price of carbon emission is still about 33, namely, 33.2 (Monte Carlo method simulation can cause slight difference in each result under the same parameters). After price instrument is used, frequency distribution of carbon emission price at $t = 7$ generally presents relatively obvious shift towards low price range $[20, 30]$ from high price range $[30, 40]$ and compared with the case where this mechanism is not used. And the frequency distribution at low price range $[0, 10]$ also obviously increases. As shown in Figure 2, after price instrument is used, decreasing in carbon price distribution is more obvious than that in the case of using quantity instrument, which suggests that price instrument has significant effect on controlling carbon price.

Expected values of carbon price at all routes are also calculated. Carbon emission price at $t = 7$ is found to be 26.77, down 15.26% compared with 31.59 in the case of not using this mechanism, which indicates that carbon emission price very evidently decreases after using price instrument.

Overall, in the upper threshold regulation, there is relatively vigorous control over carbon emission, less allowance cap, and relatively high carbon emission price, in which case the effect of price instrument is obviously better than that of quantity instrument (see Table 1). This result is attributable to the following two aspects: because this original price and allowance trading volume are relatively high, regulating the price has relatively large impact on expected income for enterprise; thus, price instrument produces better effect than quantity instrument; another reason is that, at this time, the allowance cap is relatively low and base number is relatively small, and only α time increase in allowance causes less obvious change in allowance; thus, the effect is not distinct.

3.2. Regulations of Lower Threshold. In practice, compared with excessively high carbon price, low carbon price emerges more frequently. Currently, excessively low carbon price resulting from the loose allowance cap occurs in both EU ETS and RGGI; thus, there is no corresponding restraint effect on carbon emission.

Allowance cap (6.47 billion tons) issued in EU ETS at the first stage (2005–2007) was 4.3% higher than emission (6.2 billion tons). At the second stage (2008–2012), allowance cap was lower than emission in the first year, while allowance in subsequent three years was 10.9%, 7.7%, and 9.9% higher than emission, respectively. The problem that RGGI allowance cap was too loose became more severe, annual allowance cap set for the first stage (2009–2011) was 188 million short tons, emission in the first year was 34% lower than allowance cap, and emission in the first three years was only 124, 136, and 119

Table 1: Upper and lower threshold regulations comparative.

	Using quantity instrument ($t = 7$)			Using price instrument ($t = 7$)		
	y_t (no instrument)	y_t (using instrument)	Variation	y_t (no instrument)	y_t (using instrument)	Variation
Upper threshold	31.7	29.92	5.62%	31.59	26.77	15.26%
Lower threshold	14.88	16.98	14.11%	14.91	15.59	4.56%

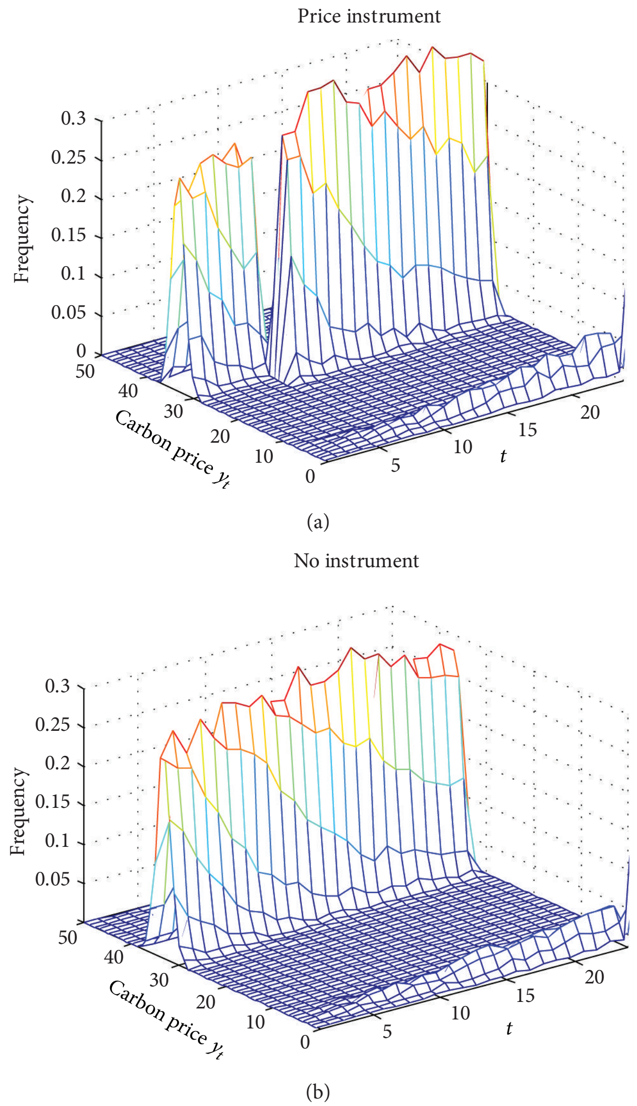

Figure 2: Carbon price frequency distribution diagram of upper threshold regulation using price instrument.

million short tons, respectively. Though subsequently emission started growing steadily, annual emission is expected to be continuously lower than annual allowance cap by a large margin until 2018. Therefore, how to increase carbon price and change the situation of low carbon price should be our great concern.

3.2.1. Quantity Instrument. Excessively high allowance cap is the major cause for low carbon price. In response to excessively low carbon price, we design the following mechanism: if carbon emission price is lower than lower threshold for n consecutive months within one compliance period T, allowance is decreased by α times so as to increase carbon price. Its specific expression is shown below:

$$y_t = E\left[P \cdot I_{\{Q_T>N\}} \cdot I_{\{\tau\geq T\}} + P \cdot I_{\{Q_T>(1-\alpha)N\}} \cdot I_{\{\tau<T\}}\mathcal{F}_t\right], \quad (5)$$

where $\tau = \inf\{n \leq s < t, \int_{s-n}^{s} I_{\{y_s<P_{\text{Low}}\}}du = n\}$.

If allowance is excessively issued by 50%, namely, $N = 300$, low carbon price is predictable, and cap control mechanism does not have its due effect. Similarly, we simulate expected carbon price changes and obtain frequency distribution diagram (parameters are set as $Q_0 = 200, N = 300$, $P = 40$, $P_{\text{Low}} = 15$, $\mu = 0.15$, $\sigma = 0.15$, $\alpha = 0.15$, $\lambda = 0.1, T = 3, n = 6$) of carbon emission prices at different time t. As shown in Figure 3, initial carbon price at $t = 0$ is 13.18, below the lower threshold value 15. According to the diagram, after quantity instrument is used, where $t > 6$, with increasing time t, the frequency of carbon emission price distribution in relatively high price range $[20, 30]$ is higher than that in the case of not using this mechanism, and the probability at low price range $[0, 20]$ is lower than that in the case of not using this mechanism.

According to calculation at $t = 7$, when allowance is lowered, expected carbon emission price is 16.98, and the price in the case of not using this mechanism is 14.88. If allowance cap decreases by 15%, expected carbon emission price increases by 14.11%, and the effect is very obvious.

3.2.2. Price Instrument. When carbon emission price is too low, increasing penalty is also one effective way for increasing carbon emission price and improving carbon trading market downturn. We design specific mechanism as follows: if carbon price is lower than lower threshold for n consecutive months within one compliance period T, penalty P is increased by α percentage points so as to increase carbon price:

$$y_t = E\left[P \cdot I_{\{Q_T>N\}} \cdot I_{\{\tau\geq T\}} + (1+\alpha) \cdot P \cdot I_{\{Q_T>N\}} \cdot I_{\{\tau<T\}}\mathcal{F}_t\right], \quad (6)$$

where $\tau = \inf\{n \leq s < t, \int_{s-n}^{s} I_{\{y_s<P_{\text{Low}}\}}du = n\}$.

We simulate this mechanism with parameters the same as above; specific frequency distribution of carbon emission

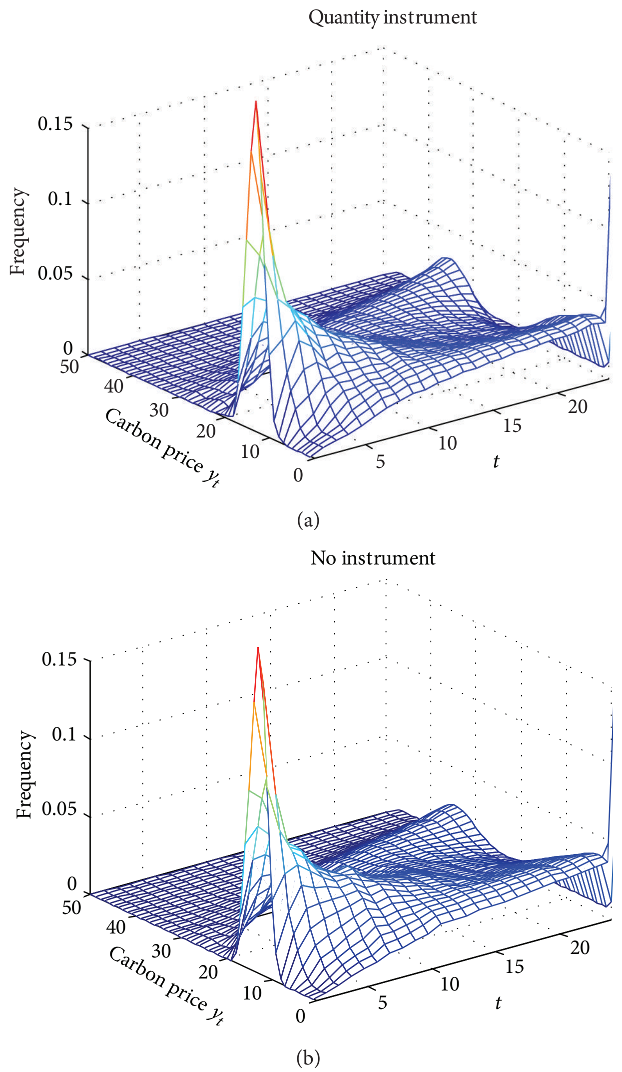

Figure 3: Carbon price frequency distribution diagram of lower threshold regulation using quantity instrument.

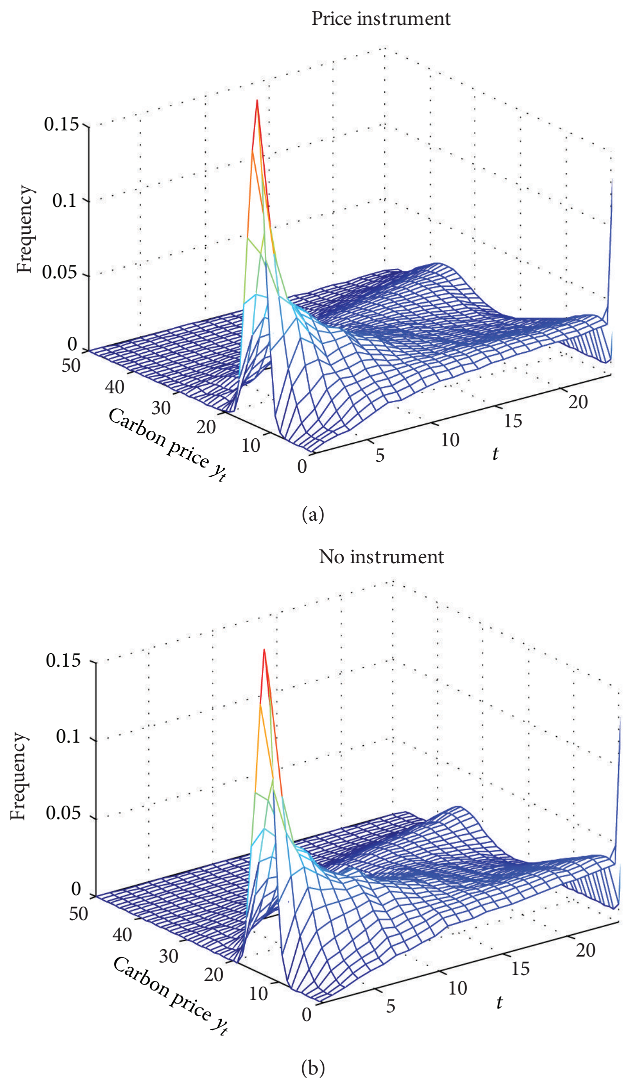

Figure 4: Carbon price frequency distribution diagram of lower threshold regulation using price instrument.

prices is shown in Figure 4. Compared with quantity instrument, price regulation mechanism produces effect which is not particularly obvious in the case of excessively low carbon price; according to this diagram, where $t > 6$, with increasing time, the frequency of carbon prices distributed in low price range $[0, 20]$ in the case of using price instrument is lower than that in the case of not using this mechanism. Thus, when price is low, price regulation has less effect than quantity regulation. According to calculation of expected values of carbon emission prices at various routes, where penalty is upwardly adjusted by 15% at time $t = 7$, expected carbon emission price is 15.59, up 4.56% compared with price 14.91 in the case of not using this mechanism.

Therefore, with respect to lower threshold regulation, quantity instrument is superior to price instrument since original price is relatively low; namely, allowance cap is excessively issued, the demand for allowance is relatively low, trading volume is small, and certain change in penalty price has little impact on expected return for enterprises.

Overall, based on carbon accumulation model with jump diffusion, we explore carbon price change routes from two perspectives of quantity instrument and price instrument in the light of actual operation of EU carbon market. We conclude that where carbon price is too high, price instrument should be adopted; if the carbon price is excessively low, quantity instrument should be mainly considered.

4. Conclusions and Suggestions

Neither EU ETS nor RGGI has perfect regulatory operation in international carbon market, for which one of the major causes lies in the case where allowance is oversupplied, leading to low carbon emission price; thus, it is difficult for cap-and-trade scheme to play the guiding role in emission reduction and low-carbon investment. Based on analysis of influencing factors, it is believed that rigid cap setting mechanism will result in lack of flexibility in allowance supply and excessive credit offset may further aggravate excessive allowance. Therefore, this paper is designed to provide effective regulation method for currently unstable carbon market and attempt to carry out basic work on this aspect. We introduce Poisson process for depicting jump diffusion process in carbon accumulation and setting upper and lower threshold in line with actual operation of EU ETS carbon emission market, separately simulate carbon market price in terms of two aspects including quantity instrument and price instrument using Monte Carlo simulation, and analyze comparative advantages of two different instruments. With comparative analysis, we find that comparative advantages of quantity regulation and price regulation depend on price level in carbon market: with regard to elasticity of expected carbon price changes, when carbon price is excessively high and needs to be downwardly adjusted, price instrument is superior to quantity instrument; conversely, when carbon price is excessively low and needs to be upwardly adjusted, quantity instrument is superior to price instrument.

In subsequent research, in order to further tally with carbon market, we will further switch pricing framework to hybrid model and, based on detailed description about endogenous mechanism for carbon price formation, explore rational regulation mechanism to guide development of carbon market and other relevant markets. Furthermore, we estimate parameters of the diffusion process more accurately based on the method in [16, 17].

Conflict of Interests

The authors declare that there is no conflict of interests regarding the publication of this paper.

Acknowledgments

This work was partially supported by the National Natural Science Foundation of China (Grant nos. 71301173 and 71301160), China Postdoctoral Science Foundation Funded Project (Grant nos. 2012M520419, 2012M520420, and 2013T60186), Beijing Planning Office of Philosophy and Social Science (13JGB018), Program for Innovation Research in Central University of Finance and Economics, and Collaborative Innovation Project of Economics School of Central University of Finance and Economics.

References

[1] M. Weitzman, "Prices versus quantities," *Review of Economic Studies*, vol. 41, pp. 477–491, 1974.

[2] W. A. Pizer, "Combining price and quantity controls to mitigate global climate change," *Journal of Public Economics*, vol. 85, no. 3, pp. 409–434, 2002.

[3] D. L. Kelly, "Price and quantity regulation in general equilibrium," *Journal of Economic Theory*, vol. 125, no. 1, pp. 36–60, 2005.

[4] F. Wirl, "Global warming: prices versus quantities from a strategic point of view," *Journal of Environmental Economics and Management*, vol. 64, pp. 217–229, 2012.

[5] W. A. Pizer, "The optimal choice of climate change policy in the presence of uncertainty," *Resource and Energy Economics*, vol. 21, no. 4, pp. 255–287, 1999.

[6] H. D. Jacoby and A. D. Ellerman, "The safety valve and climate policy," *Energy Policy*, vol. 32, no. 4, pp. 481–491, 2004.

[7] D. Burtraw, K. Palmer, and D. Kahn, "A symmetric safety valve," *Energy Policy*, vol. 38, no. 9, pp. 4921–4932, 2010.

[8] G. F. Nemet, "Robust incentives and the design of a climate change governance regime," *Energy Policy*, vol. 38, no. 11, pp. 7216–7225, 2010.

[9] C. Philibert, "Assessing the value of price caps and floors," *Climate Policy*, vol. 9, no. 6, pp. 612–633, 2009.

[10] T. Pizer and W. A. Marika, Managing Costs in a U.S. Greenhouse Gas Trading Program: A Workshop Summary, 2008.

[11] T. Requate and W. Unold, "On the incentives created by policy instruments to adopt advanced abatement technology if firms are asymmetric," *Journal of Institutional and Theoretical Economics*, vol. 157, no. 4, pp. 536–554, 2001.

[12] D. M. Guo, S. Y. Wang, and B. J. Zhang, "Research on regulatory mechanism in Chinese carbon finance market: quantity instruments or price instruments?" Working Paper.

[13] K. Borovkov, G. Decrouez, and J. Hinz, "Jump-diffusion modeling in emission markets," *Stochastic Models*, vol. 27, no. 1, pp. 50–76, 2011.

[14] R. C. Merton, "Option pricing when underlying stock returns are discontinuous," *Journal of Financial Economics*, vol. 3, no. 1-2, pp. 125–144, 1976.

[15] M. Chesney and L. Taschini, "The endogenous price dynamics of emission allowances and an application to CO_2 option pricing," *Applied Mathematical Finance*, vol. 19, no. 5, pp. 447–475, 2012.

[16] C. X. Huang, X. Gong, X. H. Chen, and F. H. Wen, "Measuring and forecasting volatility in Chinese stock market using HAR-CJ-M model," *Abstract and Applied Analysis*, vol. 2013, Article ID 143194, 13 pages, 2013.

[17] C. X. Huang, C. L. Peng, X. H. Chen, and F. H. Wen, "Dynamics analysis of a class of delayed economic model," *Abstract and Applied Analysis*, vol. 2013, Article ID 962738, 12 pages, 2013.

Hindawi Publishing Corporation
Discrete Dynamics in Nature and Society
Volume 2014, Article ID 798576, 9 pages
http://dx.doi.org/10.1155/2014/798576

Research Article

The Changes of Carbon Emission in China's Industrial Sectors from 2002 to 2010: A Structural Decomposition Analysis and Input-Output Subsystem

Guoxing Zhang[1,2] and Mingxing Liu[1]

[1] *School of Management, Lanzhou University, Lanzhou 730000, China*
[2] *School of Management, Xi'an Jiaotong University, Xi'an 710049, China*

Correspondence should be addressed to Guoxing Zhang; guoxingzh@lzu.edu.cn

Received 1 March 2014; Accepted 30 April 2014; Published 13 May 2014

Academic Editor: Chuangxia Huang

Based on 2002–2010 comparable price input-output tables, this paper first calculates the carbon emissions of China's industrial sectors with three components by input-output subsystems; next, we decompose the three components into effect of carbon emission intensity, effect of social technology, and effect of final demand separately by structure decomposition analysis; at last, we analyze the contribution of every effect to the total emissions by sectors, thus finding the key sectors and key factors which induce the changes of carbon emissions in China's industrial sectors. Our results show that in the latest 8 years five departments have gotten the greatest increase in the changes of carbon emissions compare with other departments and the effect of final demand is the key factor leading to the increase of industrial total carbon emissions. The decomposed effects show a decrease in carbon emission due to the changes of carbon emission intensity between 2002 and 2010 compensated by an increase in carbon emissions caused by the rise in final demand of industrial sectors. And social technological changes on the reduction of carbon emissions did not play a very good effect and need further improvement.

1. Introduction

Since China is the largest CO_2 emitter in the word, there is a huge pressure when facing the problems of global warming. In the year of 2009 the Chinese government promised to reduce carbon dioxide emissions per unit of GDP by 40–45% in 2020 to be less than 2005 levels. In addition, China has set a target of reducing CO_2 intensity per unit GDP by 17% in 2015 to be less than 2010 levels in the twelfth five-year plan [1]. Since reform and opening, China's industry become the main sector of carbon emissions, it's production accounting GDP 40.1% but it consumed 67.9% of the country's energy and released 83.1% of the country's carbon dioxide [2]. Moreover, the data of Chinese Energy Statistical Yearbook (2012) shows that China's total carbon emissions in the industrial sectors indicated a continuous upward trend [3]. Obviously, investigating the underlying reasons of the carbon emission changes in China's industrial sectors and studying different factors contributed to the total carbon emissions are essential for developing rational reduction policies and achieving emission reduction targets.

Much of the existing literature focuses on analyzing the influence factors leading to the changes of carbon emissions in the industrial sectors by different methods. For example, Ren et al. [4] and Lin and Moubarak [5] adopt the Log Mean Divisia Index method to explore the impact factors of the total carbon emissions in China's manufacturing industry and textile industry, respectively, during different years. The same method is used by Zhao et al. [6] and Shao et al. [7] to analyze the main factors responsible for the industrial carbon emissions in Shanghai and Tianjin, respectively. A decomposition analysis based on an additive Log Mean Divisia Index is developed by Sheinbaum-Pardo et al. [8] to explain the changes in CO_2 emissions related to energy consumption of the manufacturing industries in Mexico. Akbostanci et al. [9] use the same method to decompose the changes in the CO_2 emissions of manufacturing industry in Turkey. Hammond and Norman [10] use decomposition analysis to separate the contributions of changes in output, industrial structure, energy intensity, fuel mix, and electricity emission factor to the reduction in carbon emissions in UK's manufacturing. Priambodo and Kumar [11] use the energy use survey and detailed energy audits in Indonesia's industries to analyze the reasons leading to the increase of carbon emission. Huang and Wu [12] use two-tier KLEM input-output structural decomposition analysis to analyze the factors that lead to changes in CO_2 emissions in Taiwan's industrial sectors between 1996 and 2006. González and Martínez [13] identify the factors that have influenced the changes in the carbon dioxide emissions in the Mexican industrial sectors by the use of the Refined Laspeyres Index method. Caiman and Brian [14] combine physical and economic output data to analyze energy and CO_2 emissions trend in the Ireland industry.

Structure decomposition techniques have been applied to numerous economic and environmental subjects and often used to analyze energy intensities and emission coefficients. For example, Yuan and Cheng [15] use structural decomposition method to analyze the growth reasons of carbon emissions in China during 1992–2005. Zhao et al. [16] apply the structure decomposition techniques to study the energy consumption of urban residents in China during 1998 to 2007. Liang and Zhang [1] and Tian et al. [17], based on environment input-output structure decomposition techniques, analyze the driving force of carbon emissions in China's Jiangsu province and Beijing municipality, respectively. By combining structural decomposition and input-output analysis Guan et al. [18] assess the driving forces of China's CO_2 emissions from 1980 to 2030. Brizga et al. [19] use structural decomposition analysis to identify the drivers of change for CO_2 emissions in the Baltic states between 1995 and 2009. Cellura et al. [20] apply an energy and environmental extended input-output model, combined with SDA, to assess the indirect energy consumption and air emission changes related to Italian households' consumption. Wood [21] studies the factors of greenhouse gas emissions in Australia by applying a structure decomposition technique method. The scholars above mainly use the input-output structural decomposition method to analyze the whole economy's carbon emissions or energy consumption of some place. When a particular industry or particular sectors need to be researched, we can apply the input-output subsystems. Alcántara and Padilla [22] use a subsystem model to study the CO_2 emissions of the Spanish service sector. Cardenete and Fuentes [23] analyze the CO_2 emissions of Spanish energy activities using a subsystem representation within a social accounting matrix model. Butnar and Liop [24] study the influence factors of carbon emissions in Spain during 2000 to 2005 by applying input-output subsystem and structure decomposition analysis.

In summary, all these contributions above focus on explaining the changes in total emissions of the economy. It would be interesting, however, to analyze the changes in those emissions caused by a specific sector. And, as far as I know, no contributions in the literature have studied the changes in industrial sectors by applying structural decomposition within a subsystem approach in China. And there are a sum of literature studied the changes of carbon emissions in China's industrial sectors by applying Index method, while this approach has a disadvantage in analyzing the indirect carbon emissions caused by the industrial sectors. In this paper, we analyze the influence factors behind the changes of carbon emission in China's industry sectors during 2002 to 2010 by applying structural decomposition analysis and input-output subsystems. Because this method can comprehensively analyze various direct and indirect influential factors relied on input-output model.

2. Method and Data

2.1. Construction of Industrial Input-Output Subsystem Model. First, we decompose the N accounts of an input-output system into I sectors belonging to the industrial subsystem and S sectors not belonging to the industrial subsystem.

$A = \begin{pmatrix} A_{ii} & A_{is} \\ A_{si} & A_{ss} \end{pmatrix}$ is the matrix of direct consumption coefficient of input-output tables, in which, A_{ii} is the matrix of direct consumption coefficient of industrial sectors, A_{ss} is the matrix of direct consumption coefficient of nonindustrial sectors, A_{is} is the matrix of direct consumption coefficient of nonindustrial sectors to the industrial sectors, and A_{si} is the matrix of direct consumption coefficient of industrial sectors to the nonindustrial sectors.

$B = (I-A)^{-1} = \begin{pmatrix} B_{ii} & B_{is} \\ B_{si} & B_{ss} \end{pmatrix}$ is Leontief inverse matrix; the definition of B_{ii}, B_{is}, B_{si}, and B_{ss} is the same as direct consumption coefficient.

$X = \begin{pmatrix} X^i \\ X^S \end{pmatrix}$ denotes the vector of total output, in which X^i is the total output of industrial sectors; X^S is the total output of nonindustrial sectors.

$Y = \begin{pmatrix} Y^i \\ Y^S \end{pmatrix}$ denotes the vector of final demand, Y^i is the final demand of industrial sectors and Y^S is the final demand of nonindustrial sectors.

C^i is the column vector of carbon emissions per unit of production in the industrial sectors.

C^s is the column vector of carbon emissions per unit of production in the nonindustrial sectors.

Λ denotes diagonalization of the corresponding vector.

$'$ denotes transposition of the corresponding matrix or vector.

The input-output representation can be written as follows:

$$\begin{pmatrix} A_{ii} & A_{is} \\ A_{si} & A_{ss} \end{pmatrix}\begin{pmatrix} X^i \\ X^S \end{pmatrix} + \begin{pmatrix} Y^i \\ Y^S \end{pmatrix} = \begin{pmatrix} X^i \\ X^S \end{pmatrix}. \quad (1)$$

And the solution of total output is

$$\begin{aligned}\begin{pmatrix} X^i \\ X^S \end{pmatrix} &= \left[\begin{pmatrix} I & 0 \\ 0 & I \end{pmatrix} - \begin{pmatrix} A_{ii} & A_{is} \\ A_{si} & A_{ss} \end{pmatrix}\right]^{-1}\begin{pmatrix} Y^i \\ Y^S \end{pmatrix} \\ &= \begin{pmatrix} B_{ii} & B_{is} \\ B_{si} & B_{ss} \end{pmatrix}\begin{pmatrix} Y^i \\ Y^S \end{pmatrix}.\end{aligned} \quad (2)$$

By taking this solution into the left of (1) and assuming that the nonindustrial sectors only produce for the intermediate demand (i.e., $Y^s = 0$), then

$$\begin{pmatrix} A_{ii} & A_{is} \\ A_{si} & A_{ss} \end{pmatrix}\begin{pmatrix} B_{ii} & B_{is} \\ B_{si} & B_{ss} \end{pmatrix}\begin{pmatrix} Y^i \\ 0 \end{pmatrix} + \begin{pmatrix} Y^i \\ 0 \end{pmatrix} = \begin{pmatrix} X_i^i \\ X_i^s \end{pmatrix}. \quad (3)$$

Let X_i^i be the production of industrial sectors needed to cover the final demand of themselves, and let X_i^s be the production of nonindustrial sectors needed to cover the final demand of industrial sectors. Equation (3) can be written as

$$A_{ii}B_{ii}Y^i + A_{is}B_{si}Y^i + Y^i = X_i^i, \quad (4)$$

$$A_{si}B_{ii}Y^i + A_{ss}B_{si}Y^i = X_i^s. \quad (5)$$

Equation (4) denotes the production of industrial sectors needed to cover the final demand of themselves. On the left hand side, $A_{ii}B_{ii}Y^i$ contains the production needed by the industrial sectors from the other industrial sectors or themselves to obtain the own production. $A_{is}B_{si}Y^i$ shows the inputs of the industrial sectors subsystem required by the nonindustrial sectors to obtain the production that industrial sectors demand to them. These two components together show the internal components that affect the production of industrial sectors. Y^i is the final demand for the industrial sectors subsystem which can be considered as a demand level component. Equation (5) shows the production of the nonindustrial sectors needed to cover the final demand of the industrial sectors; therefore, we can consider it as an external component.

According to (4) and (5), first we calculate the total production of industrial sectors with three components, then multiply the carbon emissions per unit of production in the industrial sectors and nonindustrial sectors, and, finally, diagonalize Y^i, thus obtaining the carbon emissions of every industrial sector composed of three parts, calculated as follows:

$$\mathrm{DLC} = C^{i'} \overset{\wedge}{Y^i}, \quad (6)$$

$$\mathrm{IC} = C^{i'} \left(A_{ii}B_{ii} + A_{is}B_{si}\right) \overset{\wedge}{Y^i}, \quad (7)$$

$$\mathrm{EC} = C^{s'} \left(A_{si}B_{ii} + A_{ss}B_{si}\right) \overset{\wedge}{Y^i}. \quad (8)$$

The above three equations denote the demand level component, internal component, and external component that contribute to the total carbon emissions of industrial sectors, respectively. So the total carbon emissions can be written as

$$\begin{aligned} E &= \mathrm{DLC} + \mathrm{IC} + \mathrm{EC} \\ &= C^{i'} \overset{\wedge}{Y^i} + C^{i'} \left(A_{ii}B_{ii} + A_{is}B_{si}\right) \overset{\wedge}{Y^i} \\ &\quad + C^{s'} \left(A_{si}B_{ii} + A_{ss}B_{si}\right) \overset{\wedge}{Y^i}. \end{aligned} \quad (9)$$

2.2. Structural Decomposition of the Input-Output Subsystem Model. Input-output structural decomposition analysis technique is a method of analyzing the reasons of economic changes through the comparative static analysis of key parameters. There are many decomposition forms, but the polar decomposition method is used in this paper. From a mathematical point of view, such method looks not only good but also comparable between the weights of different factors, furthermore, there are no interaction terms difficult to explain, so the method get widely recognized by the international academic community [25].

Some matrix and symbols will be illustrated as follows:

$$\begin{aligned} \overline{A} &= A_{ii}B_{ii} + A_{is}B_{si}, \\ \overline{B} &= A_{si}B_{ii} + A_{ss}B_{si}. \end{aligned} \quad (10)$$

The symbol Δ denotes the changes of two different periods, that is, final value minus initial value. Subscripts 0, 1 denote initial value and final value of the corresponding matrix or vector, respectively. In order to calculate the changes of carbon emissions in two different periods,

$$\Delta E = \Delta\mathrm{DLC} + \Delta\mathrm{IC} + \Delta\mathrm{EC}. \quad (11)$$

The first term in expression (11) can be decomposed as follows:

$$\begin{aligned} \Delta\mathrm{DLC} &= C_1^{i'} \overset{\wedge}{Y_1^i} - C_0^{i'} \overset{\wedge}{Y_0^i} \\ &= \frac{1}{2}\left(\Delta C^{i'}\right)\left(\overset{\wedge}{Y_0^i} + \overset{\wedge}{Y_1^i}\right) + \frac{1}{2}\left(C_0^{i'} + C_1^{i'}\right)\Delta \overset{\wedge}{Y^i}. \end{aligned} \quad (12)$$

The first element in expression (12), $\Delta\mathrm{CEE}_{\mathrm{DLC}} = (1/2)(\Delta C^{i'})(\overset{\wedge}{Y_0^i} + \overset{\wedge}{Y_1^i})$, denotes carbon emission intensity effect and shows the contribution of changes in the carbon emission intensities of the industrial sectors to the changes in the demand level component. $\Delta\mathrm{DE}_{\mathrm{DLC}} = (1/2)(C_0^{i'} + C_1^{i'})\Delta \overset{\wedge}{Y^i}$ denotes demand effect and shows how the changes in the demand for industrial sectors contribute to the changes in the demand level component.

The second component in expression (11) can be decomposed as

$$\begin{aligned} \Delta\mathrm{IC} &= C_1^{i'}\overline{A}_1 \overset{\wedge}{Y_1^i} - C_0^{i'}\overline{A}_0 \overset{\wedge}{Y_0^i} \\ &= \frac{1}{2}\Delta C^{i'}\left(\overline{A}_0 \overset{\wedge}{Y_0^i} + \overline{A}_1 \overset{\wedge}{Y_1^i}\right) \\ &\quad + \frac{1}{2}\left[C_0^{i'}\left(\Delta\overline{A}\right)\overset{\wedge}{Y_1^i} + C_1^{i'}\left(\Delta\overline{A}\right)\overset{\wedge}{Y_0^i}\right] \\ &\quad + \frac{1}{2}\left(C_0^{i'}\overline{A}_0 + C_1^{i'}\overline{A}_1\right)\Delta \overset{\wedge}{Y^i}. \end{aligned} \quad (13)$$

In which, $\Delta\mathrm{CEE}_{\mathrm{IC}} = (1/2)\Delta C^{i'}(\overline{A}_0 \overset{\wedge}{Y_0^i} + \overline{A}_1 \overset{\wedge}{Y_1^i})$ represents carbon emission intensity effect and shows the contribution of changes in the carbon emission intensities of the industrial sectors to the changes in the internal component. $\Delta TE_{IC} = (1/2)[C_0^{i'}(\Delta\overline{A})\hat{Y}_1^i + C_1^{i'}(\Delta\overline{A})\hat{Y}_0^i]$ denotes effect of economic and technological changes and shows how the changes in the economy and technology contribute to the changes in the internal component. $\Delta DE_{IC} = (1/2)(C_0^{i'}\overline{A}_0 + C_1^{i'}\overline{A}_1)\Delta\hat{Y}^i$ represents demand effect and shows how the changes in the demand for industrial sectors contribute to the changes in the internal component.

The third component in expression (11) can be decomposed as

$$\begin{aligned}\Delta EC &= C_1^{S'}\overline{B}_1\hat{Y}_1^i - C_0^{S'}\overline{B}_0\hat{Y}_0^i \\ &= \frac{1}{2}\Delta C^{S'}\left(\overline{B}_0\hat{Y}_0^i + \overline{B}_1\hat{Y}_1^i\right) \\ &\quad + \frac{1}{2}\left[C_0^{S'}\left(\Delta\overline{B}\right)\hat{Y}_1^i + C_1^{S'}\left(\Delta\overline{B}\right)\hat{Y}_0^i\right] \\ &\quad + \frac{1}{2}\left(C_0^{S'}\overline{B}_0 + C_1^{S'}\overline{B}_1\right)\Delta\hat{Y}^i.\end{aligned} \tag{14}$$

The first element in expression (14), $\Delta CEE_{EC} = (1/2)\Delta C^{S'}(\overline{B}_0\hat{Y}_0^i + \overline{B}_1\hat{Y}_1^i)$, represents carbon emission intensity effect and shows the contribution of changes in the carbon emission intensities of the nonindustrial sectors to the changes in the external component. $\Delta TE_{EC} = (1/2)[C_0^{S'}(\Delta\overline{B})\hat{Y}_1^i + C_1^{S'}(\Delta\overline{B})\hat{Y}_0^i]$ denotes effects of economic and technological change and shows the contribution of changes in the economy and technology of the nonindustrial sectors to the changes in the external component. $\Delta DE_{EC} = (1/2)(C_0^{S'}\overline{B}_0 + C_1^{S'}\overline{B}_1)\Delta\hat{Y}^i$ represents demand effect and shows how the changes in the demand for industrial sectors contribute to the changes in the external component.

According to the above analysis, the changes of total carbon emissions also can be written as follows:

$$\begin{aligned}\Delta E &= \Delta CEE + \Delta TE + \Delta DE \\ &= \Delta CEE_{DLC} + \Delta CEE_{IC} + \Delta CEE_{EC} + \Delta TE_{IC} \\ &\quad + \Delta TE_{EC} + \Delta DE_{DLC} + \Delta DE_{IC} + \Delta DE_{EC}.\end{aligned} \tag{15}$$

In which, ΔCEE represents the contribution of total carbon emission intensity effect to the changes of total carbon emissions. ΔTE denotes the changes of economy and technology contribute to the changes of total carbon emissions. ΔDE shows the changes of final demand in the industrial sectors that contribute to the changes of total carbon emissions.

2.3. Date Preparation. Since Chinese input-output tables are compiled every five years, at the year with the last number being 2 or 7, and the extended input-output tables are compiled at the year with the last number being 0 or 5, the annual data used in this paper are those of the years 2002, 2007, and 2010 and data derived from the National Bureau of Statistics website [26]. According to National Industry Classification in China and taking the existing input-output tables sector classification into account, we set up 33 sectors (Table 1), including 24 industrial sectors and 9 nonindustrial sectors, according to need we unified the sectors in the input-output table and adjusted the positions of them (industrial sectors from 1 to 24). Since current price input-output table cannot reflect the real economic change after deducting price factors, the current price input-output tables need to be converted into comparable price input-output table. In this paper, we transferred the 2007 and 2010 current price input-output tables into 2002 comparable price input-output tables with index reduction method. The specific compilation method refers to "China 1992–2005 comparable price input-output series tables and analysis" edited by Liu and Peng [27]. In the process of compiling the comparable price input-output tables, the price indexes we needed come from China Statistical Yearbook.

Though there are no direct statistical data of carbon emissions of various industries in China, there are statistical data of energy consumption by sectors and carbon emissions are mainly derived from the consumption of a variety of energy. So, this paper calculated the direct carbon emissions of various industries according to the annual data of energy consumption by sectors and the carbon emission factors of different energy sources. And the carbon emission factors are announced by the Intergovernmental Panel on Climate, the annual data of energy consumption by sectors derived from China Energy Statistical Yearbook, the sectors also consolidated according to our need. Considering the energy statistics caliber of China Energy Statistical Yearbook and the availability of energy carbon emission factors, we selected coal, crude oil, gasoline, kerosene, diesel oil, fuel oil, and natural gas; these seven kinds of energy are calculated as follows:

$$c_i = \sum^{j} c_{ij} = \sum^{j} m_{ij} \times k_j, \tag{16}$$

where c_i represents the direct total carbon emissions of sector I, c_{ij} shows the carbon emissions of sector I consuming the jth kind of fuel, m_{ij} represents the consumption of sector I to the jth kind of fuel, and k_j shows the carbon emission factors of the jth kind fuel. After getting the carbon emissions by sectors, we divided them by the total output of the corresponding sectors, so we got the carbon emissions per unit of output by sectors.

3. Result and Discussion

3.1. Analyzing the Contribution of DLC, IC, and EC to the Changes of Total Carbon Emissions. Table 2 shows the changes of total carbon emissions mainly consisting of three components, namely, the demand level component, the internal component, and the external component. In the past eight years, the total carbon emissions of Chinese industrial

Table 1: Sectoral classification of the input-output tables.

1	Mining and washing of coal
2	Extraction of petroleum and natural gas
3	Mining and processing of metal ores
4	Mining and processing of nonmetal ores
5	Manufacture of foods and tobacco
6	Manufacture of textile
7	Manufacture of wearing apparel, leather, feather, and related products
8	Processing of timber, manufacture of furniture
9	Printing and manufacture of articles for culture and education
10	Processing of petroleum, coking, and processing of nuclear fuel
11	Manufacture of chemical products
12	Manufacture of nonmetallic mineral products
13	Smelting and pressing of metals
14	Manufacture of metal products
15	Manufacture of general and special purpose machinery
16	Manufacture of transport equipment
17	Manufacture of electrical machinery and equipment
18	Communication equipment, computers, and other electronic equipment
19	Manufacture of measuring instruments and machinery for cultural activity and office work
20	Other manufacturing
21	Recycling and disposal of waste
22	Production and distribution of electric power and heat power
23	Production and distribution of gas
24	Production and distribution of water
25	Construction
26	Transport and storage
27	Post
28	Wholesale and retail trade
29	Hotel and restaurants
30	Finance and insurance
31	Real estate
32	Other services
33	Farming, forestry, animal husbandry, fishery, and water conservancy

sectors increased to 5.34×10^8 tons. Viewing from these three different components (DLC, IC and EC), though the changes of industrial demand level decreased the total carbon emissions 1.00×10^7 tons, it is far less than the increase in total carbon emissions caused by the changes of industrial internal component and external component; they are 4.55×10^8 tons and 8.83×10^7 tons, respectively. So we can know that industrial internal component and external component are the main reasons leading to an overall increase in total carbon emissions. From Table 2 we also can learn that in the latest 8 years the following five departments increased the most in the changes of carbon emissions: transportation equipment, manufacture of general and special purpose machinery, manufacture of electrical machinery and equipment, manufacture of communication equipment computers and other electronic equipment, and manufacture of foods and tobacco; their total carbon emissions increased to 1.47×10^8 tons, 1.31×10^8 tons, 1.28×10^8 tons, 7.51×10^7 tons, and 5.97×10^7 tons.

When divided 2002–2010 into two periods; Table 2 shows that the first five years due to the changes of demand level in industrial sectors make the total carbon emissions increase to 5.38×10^6 tons, while the next three years make the carbon emissions decreased to 1.54×10^7 tons. During 2002–2007, the total carbon emissions increased to 1.24×10^8 tons caused by the changes of internal component of industrial sectors, and during 2007–2010, due to the changes of internal component of industrial sectors, it makes the total carbon emissions increase to 1.24×10^8 tons. During 2002–2007, the total carbon emissions increased to 5.77×10^7 tons caused by the changes of external component of industrial sectors, and during 2007–2010, due to the changes of external component of industrial sectors, the total carbon emissions increased to 3.06×10^7 tons. Though the two periods are asymmetric, the above data also can illustrate the level of demand structure of the industrial sectors gradually improved; it is conducive to the reduction of the total carbon emissions. And the changes of internal and external components slowing the increase of total carbon emissions also indicate the internal and external components of the industrial sectors conducive to the reduction of the total carbon emissions. It can be seen that some good results have been achieved due to the carbon reduction policy implemented by the government in recent years. However, in order to achieve a further improvement in carbon emissions, some appropriate management policies and measures should be implemented regarding the carbon-intensive enterprises. In the following we will analyze the two main components (IC and EC) of the five industrial sectors whose carbon emissions increased the most, so as to understand the underlying factors leading to the increase of carbon emissions in these sectors.

3.2. Structure Decomposition Analysis of the Main Components of the Carbon Emissions in the Key Sectors. From Table 2 we already know the five sectors whose carbon emissions increased the most, following structure decomposition analysis of the main component of the carbon emissions in the five sectors. The results are shown in Table 3; we first decompose the internal and external component of the industrial sectors into carbon emission intensity effect, effect of social technology, and effect of final demand. During 2002–2007, the first quadrant of Table 3 shows the five industrial sectors because the internal component leading to the increase of total carbon emissions is mainly caused by the effects of social technology and effect of final demand, while carbon emission intensity effect promoted the reduction of carbon emissions. The third quadrant of Table 3 shows the five industrial sectors due to the external component leading to the increase of total carbon emissions mainly caused by the effect of final

Table 2: The changes of carbon emissions in the three components in different periods.

Sectors	ΔDLC		ΔIC		ΔEC		Total
	2002–2007	2007–2010	2002–2007	2007–2010	2002–2007	2007–2010	2002–2010
1	−53.74	−61.1	−34.13	−59.67	−7.62	−11.77	−228.04
2	−72.96	−61.15	−172.18	−55.97	−26.12	−6.92	−395.31
3	−77.17	−12.58	−178.95	−93.69	−31.27	−15.86	−409.52
4	−5.01	−1.59	−10.44	−5.77	−2.27	−1.05	−26.14
5	33.64	3.1	238.89	130.34	117.22	73.96	597.15
6	68.69	−17.57	220.98	−59.97	43.35	−5.56	249.93
7	19.18	−1.02	275.42	−7.17	60.11	9.4	355.92
8	16.58	0.94	115.13	5.92	26.25	1.53	166.35
9	4.35	−3.35	27.08	−7.11	3.55	0.11	24.64
10	−30.18	−12.78	−39.18	−14.82	−5.27	−1.06	−103.29
11	−15.14	4.34	−15.44	10.35	−2.45	2.07	−16.27
12	−8.96	−26.47	16.37	−17.27	1.02	−2.37	−37.67
13	44.67	−101.66	39.07	−113.45	4.77	−12.7	−139.3
14	24.96	−8.88	227.13	−101.32	21.45	−9.21	154.13
15	54.57	23.28	664.81	419.01	81.33	65.25	1308.26
16	34.25	47.93	680.44	517.39	100.93	90.94	1471.88
17	24.54	21.74	652.46	441.18	76.14	66.58	1282.64
18	23.55	17.07	420.87	158.12	88.17	43.3	751.08
19	0.55	−0.82	17.63	−16.4	3.2	−2.48	1.68
20	7.49	17.14	139.67	80.74	23.25	17.72	286.02
21	−0.94	−1.82	−8.16	−5.85	−1.52	−1.44	−19.72
22	−42.79	−4.47	28	−9.54	1.23	−1.31	−28.88
23	−3.24	4.53	4.19	21.2	0.35	3.37	30.4
24	6.86	20.99	6.2	20.29	1.31	3.87	59.52
Total	53.76	−154.19	3315.86	1236.55	577.11	306.36	5335.45

Note: unit is 10^5 tons.

demand. However, during 2007–2010, the second quadrant of Table 3 shows the internal component of the five industrial sectors leading to the increase of total carbon emissions mainly caused by the effect of final demand. From the four quadrants we can know that the external component of the five industrial sectors leading to the increase of total carbon emissions is mainly caused by the effect of social technology and effect of final demand.

From the above analysis of the five key sectors we can learn that the social economic technologies of industrial sectors are improving, conducive to the reduction of total carbon emissions, while the social economic technologies of nonindustrial sectors are cutting down, leading to the increase of total carbon emissions. Carbon emission intensity effect is not only conducive to the reduction of carbon emissions caused by internal component but also conducive to the carbon emissions reduction caused by external component in this five sectors. However, the effect of final demand just played a opposite role, it contributed to the increase of carbon emissions both in the internal component and external component. Analyzing from the whole time 2002–2010, the contribution of carbon emission intensity effect on the reduction of carbon emissions is improving, while the increase in carbon emissions caused by the effect of final demand is also serious. Therefore, in order to control the increase of total carbon emissions in China's industrial sectors, we should pay more attention to the final demand. And at the same time we should also pay attention to the improvement of social and economical technology, because they still have much room for improvement.

3.3. Analyzing the Contribution of CEE, TE, and DE to the Changes of Total Carbon Emissions. Table 4 shows the carbon emission intensity effect, the effect of social technology, and the effect of final demand contributing to the total carbon emissions. We also can know that the total carbon emissions increased to 5.34×10^8 tons of China's industrial sectors during 2002–2010, though the carbon emissions reduced to 3.39×10^8 tons because of the carbon emission intensity effect; it is far less than the increase in carbon emissions caused by the effect of final demand; the value is 7.77×10^8 tons, and the effect of social technology has not contribute to the reduction of carbon emissions. When considering these three factors (CEE, TE and DE), the main factor leading to the increase of total carbon emissions in China's industrial sectors is the expanding final demand, which is related to the increasing population and gradually expanded consumption. Therefore, the reduction of carbon emissions in China's industrial sectors should be started from controlling the final demand

Table 3: Structure decomposition analysis of the key sectors.

Sectors	2002–2007				2007–2010			
	ΔCEE	ΔTE	ΔDE	ΔIC	ΔCEE	ΔTE	ΔDE	ΔIC
16	−226.36	114.8	792	680.44	−238.64	−45.55	801.57	517.39
15	−234.74	213.38	686.17	664.81	−240.06	31.75	627.31	419.01
17	−169.93	147.92	674.47	652.46	−206.71	−31.31	679.19	441.18
18	−171.36	6.23	586.01	420.87	−147.74	−54.99	360.85	158.12
5	−156.86	129.92	265.83	238.89	−125.96	37.61	218.7	130.34
	ΔCEE	ΔTE	ΔDE	ΔEC	ΔCEE	ΔTE	ΔDE	ΔEC
16	−9.3	−0.93	111.15	100.93	−55.85	26.8	119.99	90.94
15	−9.86	0.55	90.65	81.33	−50.12	33.05	82.33	65.25
17	−6.53	−0.38	83.05	76.14	−40.58	23	84.15	66.58
18	−7.97	−9.47	105.6	88.17	−45.42	15.92	72.8	43.3
5	−29.09	14.79	131.52	117.22	−62.13	26.62	109.48	73.96

Note: unit is 10^5 tons.

(such as recommending low carbon living). At the same time, technological innovations also should be strengthened; only in this way can we contribute to the reduction of total carbon emissions in China's industrial sectors.

Through splitting the study period into two time intervals, we can find that, in the first five years, the effect of carbon emission intensity has made the total carbon emissions of China's industrial sectors decreased 1.67×10^8 tons, while in the next three years, it has made the total carbon emissions of Chinese industrial sectors decreased 1.71×10^8 tons. It shows that the carbon emission intensity is gradually decreasing and promoting the reduction of carbon emissions. We also can know that the effect of social technology is gradually improved and conducive to the reduction of total carbon emissions in China's industrial sectors. While the contribution of the final demand to the carbon emissions is still increasing, we should pay more attention to controling it.

4. Conclusions

This paper has applied structural decomposition within an input-output subsystem model to show the reasons of the change of carbon emissions in China's industrial sectors between 2002 and 2010. The main conclusions are as follows. (1) Viewing from the three subsystem components (DLC, IC, and EC), we know that in the latest eight years the internal component of the industrial sectors is the main component leading to the increase of total carbon emissions in China; viewing from the department, we find that the department whose carbon emissions increased the most is the department whose direct and indirect carbon emissions increased the most, it is not only direct carbon emissions increased the most instead of direct carbon emissions increased the most. (2) When considering the following three factors: carbon intensity effect, social technological effect, and the effect of final demand, we find that the main reason leading to the increase of total carbon emissions is the expansion of final demand. (3) From the whole time (2002–2010) we know that the final demand effect contributed positively to carbon emission changes, with these effects being higher than the reduction caused by the carbon emission intensity effect, leading to an overall increase in carbon emissions. (4) From the analysis of the five key sectors we know that the social technology of industrial sectors is improving while the social technology of nonindustrial sectors is cutting down.

According to the results of this paper, in order to achieve our carbon reduction targets, on the one hand, we should focus on the five key sectors whose carbon emissions changed the most, controlling the exports of those products produced by these sectors strictly, encourage consumption of alternative products with low carbon emissions, and then achieve the purpose of reducing carbon emissions from the control of requirements. On the other hand, we should strengthen technological innovations. Material and spiritual rewards are given to the companies that achieved very good results on innovations, for example, reducing taxes on its products so they will have more funds for their technological innovations. We also can seek the support of advanced technology and capital from the developed countries to achieve the goal of emission reduction. Finally, we should pay attention to the control of the final demand of the products produced by the industrial sectors appropriately; we can also adjust the demand structure to reduce the carbon emissions or encourage people to use clean energy.

Our study has the following limitations. First, carbon emissions referred to in this paper only generated by energy consumption, failed to consider the production process which also generate carbon emissions. Second, our approach consists of a unique-region emission model; it cannot analyze the indirect emissions released in the supply chain outside the country. Thus, future work should pay special attention to the study of the carbon emissions by using a multiregional model which can consider the carbon emissions from import and export products, respectively, so we can understand the composition of carbon emissions in China's industrial sectors more clearly. In addition, carbon emissions from industrial sectors in China's different provinces should be studied, so we can develop appropriate low carbon policies and measures in accordance with the specific circumstances of different provinces. Finally, studies on other industries also should

Table 4: The contribution of CEE, TE, and DE to the changes of total carbon emissions in China's industrial sectors.

Sectors	ΔCEE		ΔTE		ΔDE		Total
	2002–2007	2007–2010	2002–2007	2007–2010	2002–2007	2007–2010	2002–2010
1	−4.48	22.84	10.92	−4.46	−101.94	−150.92	−228.04
2	151.08	27.47	−116.48	−57.3	−305.87	−94.22	−395.31
3	55.23	103.79	−87.01	−6.9	−255.61	−219.02	−409.52
4	2.27	3.73	−1.82	−2.25	−18.17	−9.89	−26.14
5	−269.97	−253.24	144.71	64.22	515.01	396.42	597.15
6	−113.65	−121.38	83.76	−15.01	362.91	53.29	249.93
7	−156.03	−161.52	122.5	17.58	388.25	145.15	355.92
8	−42.83	−45.32	31.08	23.74	169.7	29.97	166.35
9	−33.09	−27.75	28.49	5.93	39.59	11.48	24.64
10	24.51	11.79	−7.49	2.64	−91.66	−43.09	−103.29
11	−21.1	−14.37	12.71	0.29	−24.63	30.84	−16.27
12	−52.26	−27.54	18.66	7.63	42.04	−26.19	−37.67
13	28.29	38.29	−17.53	4.51	77.75	−270.61	−139.3
14	−85.85	−62.02	36.35	9.14	323.04	−66.54	154.13
15	−267.66	−325.21	213.93	64.8	854.45	767.95	1308.26
16	−288.11	−309.39	113.88	−18.74	989.85	984.39	1471.88
17	−191.56	−256.64	147.54	−8.31	797.15	794.45	1282.64
18	−191.9	−198.79	−3.24	−39.08	727.73	456.35	751.08
19	−10.87	−6.66	6.3	−3.41	25.95	−9.63	1.68
20	−109.56	−68.22	53.13	54.17	226.84	129.66	286.02
21	2.62	2.68	−6.62	2.27	−6.62	−14.06	−19.72
22	−70.12	−19.94	55.67	5.36	0.89	−0.75	−28.88
23	−20.68	−18.03	2.84	−1.55	19.14	48.68	30.4
24	−6.15	−9.26	2.55	2.2	17.96	52.2	59.52
Total	−1671.87	−1714.69	844.83	107.48	4773.78	2995.92	5335.45

Note: unit is 10^5 tons.

be conducted to illustrate the characteristics of main contributors to carbon emissions. At the same time, we should do more researches on the development and evaluation of low carbon policies. Because most of the current studies are just staying in the phase of phenomenon analysis, they lack specific policy implementation and evaluation system.

Conflict of Interests

The authors declare that there is no conflict of interests regarding the publication of this paper.

Acknowledgments

This paper is financially supported by the National Natural Science Foundation of China (71103077), Science Foundation of Ministry of Education of China (10YJC630377), and China Postdoctoral Science Foundation (2012M512015).

References

[1] S. Liang and T. Zhang, "What is driving CO_2 emissions in a typical manufacturing center of South China? The case of Jiangsu Province," *Energy Policy*, vol. 39, no. 11, pp. 7078–7083, 2011.

[2] S. Y. Chen, "Green industrial revolution in China: a perspective from the change of environmental total factor productivity," *Economic Research*, vol. 45, no. 11, pp. 21–34, 2010.

[3] J. W. Wen, *China Energy Statistic Year Book 2012*, China Statistics Press, 2012.

[4] S. G. Ren, H. Y. Yin, and X. H. Chen, "Using LMDI to analyze the decoupling of carbon dioxide emissions by China's manufacturing industry," *Environmental Development*, vol. 9, pp. 61–75, 2014.

[5] B. Lin and M. Moubarak, "Decomposition analysis: change of carbon dioxide emissions in the Chinese textile industry," *Renewable and Sustainable Energy Reviews*, vol. 26, pp. 389–396, 2013.

[6] M. Zhao, L. Tan, W. Zhang, M. Ji, Y. Liu, and L. Yu, "Decomposing the influencing factors of industrial carbon emissions in Shanghai using the LMDI method," *Energy*, vol. 35, no. 6, pp. 2505–2510, 2010.

[7] C. Shao, Y. Guan, Z. Wan, C. Guo, C. Chu, and M. Ju, "Performance and decomposition analyses of carbon emissions from industrial energy consumption in Tianjin, China," *Journal of Cleaner Production*, vol. 64, pp. 590–601, 2014.

[8] C. Sheinbaum-Pardo, S. Mora-Pérez, and G. Robles-Morales, "Decomposition of energy consumption and CO_2 emissions in Mexican manufacturing industries: trends between 1990 and 2008," *Energy for Sustainable Development*, vol. 16, no. 1, pp. 57–67, 2012.

[9] E. Akbostanci, G. I. Tunç, and S. Türüt-Aşik, "CO_2 emissions of Turkish manufacturing industry: a decomposition analysis," *Applied Energy*, vol. 88, no. 6, pp. 2273–2278, 2011.

[10] G. P. Hammond and J. B. Norman, "Decomposition analysis of energy-related carbon emissions from UK manufacturing," *Energy*, vol. 41, no. 1, pp. 220–227, 2012.

[11] A. Priambodo and S. Kumar, "Energy use and carbon dioxide emission of Indonesian small and medium scale industries," *Energy Conversion and Management*, vol. 42, no. 11, pp. 1335–1348, 2001.

[12] Y. H. Huang and J. H. Wu, "Analyzing the driving forces behind CO_2 emissions and reduction strategies for energy-intensive sectors in Taiwan: 1996–2006," *Energy*, vol. 57, pp. 402–411, 2013.

[13] D. González and M. Martínez, "Decomposition analysis of CO_2 emissions in the Mexican industrial sector," *Energy for Sustainable Development*, vol. 16, no. 2, pp. 204–215, 2012.

[14] J. Caiman and p. Brian, "Combining physical and economic output data to analyze energy and CO_2 emissions trends in industry," *Energy Policy*, vol. 49, pp. 422–429, 2012.

[15] P. Yuan and S. Cheng, "Determinants of Carbon Emissions Growth in China: A structural decomposition analysis," *Energy Procedia*, vol. 5, pp. 169–175, 2011.

[16] X. Zhao, N. Li, and C. Ma, "Residential energy consumption in urban China: a decomposition analysis," *Energy Policy*, vol. 41, pp. 644–653, 2012.

[17] X. Tian, M. Chang, H. Tanikawa, F. Shi, and H. Imura, "Structural decomposition analysis of the carbonization process in Beijing: a regional explanation of rapid increasing carbon dioxide emission in China," *Energy Policy*, vol. 53, pp. 279–286, 2013.

[18] D. Guan, K. Hubacek, C. L. Weber, G. P. Peters, and D. M. Reiner, "The drivers of Chinese CO_2 emissions from 1980 to 2030," *Global Environmental Change*, vol. 18, no. 4, pp. 626–634, 2008.

[19] J. Brizga, K. Feng, and K. Hubacek, "Drivers of greenhouse gas emissions in the Baltic States: a structural decomposition analysis," *Ecological Economics*, vol. 98, pp. 22–28, 2014.

[20] M. Cellura, S. Longo, and M. Mistretta, "Application of the structural decomposition analysis to assess the indirect energy consumption and air emission changes related to Italian households consumption," *Renewable and Sustainable Energy Reviews*, vol. 16, no. 2, pp. 1135–1145, 2012.

[21] R. Wood, "Structural decomposition analysis of Australia's greenhouse gas emissions," *Energy Policy*, vol. 37, no. 11, pp. 4943–4948, 2009.

[22] V. Alcántara and E. Padilla, "Input-output subsystems and pollution: an application to the service sector and CO_2 emissions in Spain," *Ecological Economics*, vol. 68, no. 3, pp. 905–914, 2009.

[23] M. A. Cardenete and P. Fuentes, "Energy consumption and CO_2 emissions in the Spanish economy," in *Air Pollution: Measurements and Control Policies*, M. Llop, Ed., Bentham E-Books, 2011.

[24] I. Butnar and M. Liop, "Structural decomposition analysis and input-output subsystems: changes in CO_2 emissions of Spanish service sectors (2000–2005)," *Ecological Economics*, vol. 70, no. 11, pp. 2012–2019, 2011.

[25] X. K. Chen and C. H. Yang, *Input-Output Technology*, Science Press of China, 2011.

[26] National Bureau of Statistics of the People's Republic of China, http://www.stats.gov.cn/.

[27] Q. Liu and Z. Peng, *China 1992–2005 Comparable Price Input-Output Series Tables and Analysis*, China Statistics Press, 2010.

Hindawi Publishing Corporation
Discrete Dynamics in Nature and Society
Volume 2014, Article ID 897278, 12 pages
http://dx.doi.org/10.1155/2014/897278

Research Article

An Empirical Study on Listed Company's Value of Cash Holdings: An Information Asymmetry Perspective

Chuangxia Huang,[1,2] Xin Ma,[3] and Qiujun Lan[4]

[1] *School of Mathematics and Computing Science, Changsha University of Science and Technology, Changsha 410004, China*
[2] *Academy of Mathematics and Systems Science, Chinese Academy of Science, Beijing 10090, China*
[3] *School of Economics and Management, Changsha University of Science and Technology, Changsha 410114, China*
[4] *School of Business, Hunan University, Changsha 410082, China*

Correspondence should be addressed to Qiujun Lan; lanqiujun@hnu.edu.cn

Received 22 January 2014; Accepted 8 April 2014; Published 13 May 2014

Academic Editor: Fenghua Wen

The value of a company's cash holdings is currently a hot issue in corporate finance research. Current studies have not reached a unified conclusion. Moreover, no one has ever studied that from the perspective of information asymmetry. However, there still exist disputes about the measurement of the degree of information asymmetry. Previous studies mostly adopt single index to analysis this issue, and the economic meaning it represents only reflects some information of asymmetric information, so it was one-sided and the conclusion also differ. Drawing on the market microstructure and the index of information asymmetry of managers and investors, this paper constructs a new proxy for information asymmetry based on the principal component analysis. We find that a company's value of cash holdings decreases increasingly with its level of information asymmetry, and the relationship between information asymmetry and the value of cash holdings is nonlinear.

1. Introduction

As early as 1970, Fama [1] proposed an efficient market hypothesis in his research on resource allocation, which implied that investors, without involving additional cost, can easily get the equal amount of information of equal quality as the management of the company. But in the real market environment, the information is asymmetric, and the company management has a better understanding of the company's development and risk and other information than external investors. Jensen and Meckling [2] proposed an agency theory, insisting that, because of information asymmetry and bounded rationality, the agency problem arises between shareholders and the company management, and the information asymmetry may have an effect on corporate cash holdings. Due to the fact that its managers have more information than external investor, so Myers and Majluf [3] proposed investment information asymmetry theory that when the capital market is not perfect enough, where information asymmetry exists between the company's external investors and insiders, investors would require the company to pay a premium for external funds, which makes external financing more expensive than internal financing. Jensen [4] proposed free cash flow theory to explain the management's motivation to hold cash from the perspective of the agency costs and maintained that the management may possibly make some low-value investments out of self-interest motivation, leading to a decrease in the value of cash holdings. Later, many scholars began to engage in research in this field, which makes the study of cash holdings values gradually become one of the mainstreams of current corporate finance research.

Researchers have not reached consensus on the relationship between the information asymmetry and the value of cash holdings. On one hand, Jensen and Meckling [2] put forward the principal-agent theory based on the information asymmetry between shareholders and the management and their bounded rationality. Because of the information asymmetry and lack of adequate supervision, managers may not always act in accordance with the clients' goal which is the maximizing interest. And that is where the agency costs come from. Jensen [4] believes that problems caused by the agent moral hazard will become very serious cash flow problems because the company's cash assets are most likely to be abused by the management, and they may use it for their own self-serving through some wasteful investment or the so-called empire building. By doing so, the value of cash held by the company will be reduced. Harford [5] suggests that cash-rich companies are more inclined to engage in acquisitions, but these irrational acquisitions tend to decrease the value of the company, which supports Jensen [4]. By directly calculating the value of cash held by a company, Faulkender and Wang [6] and Pinkowitz et al. [7] proved that the marginal value of each \$1 increase in a company is less than \$1, and this loss can partly be attributed to agency costs. Thereafter, increasingly more scholars [8–10] involve themselves in this discussion. On the other hand, Myers' information asymmetry theory, which is based on the pecking order model of corporate financing, believes the large cash assets a company holds can help avoid the increase of external financing costs due to the information asymmetry, which in turn increase the company's value as a result. Later, a large number of scholars have drawn a similar conclusion [10–12]. Mikkelson and Partch [13] find that a large sum of cash can lead to better performance due to lower external financing costs and that a company that constantly holds a large amount of cash does not necessarily cause the conflict of interests between the management and shareholders. Dennis and Sibilkov [10] find that cash holdings allow the company to carry out meaningfully value-adding investment and those companies facing financing constraints will forfeit such investment opportunities due to information asymmetry. Despite that the academic debate of the theory of information asymmetry and the principal-agent theory sparked scholars' enthusiasm about studying cash holdings value, the conclusions of empirical studies of the cash holding value varied, and no consensus has been reached.

The size of cash holdings is an important financial decision. Different motives for cash holdings will generate disparate efficiency of utilizing the cash. Various scholars put forward different theories for the value of cash holdings from different theoretical perspectives, among which some draw on the agency theory, while some others derived from the information asymmetry theory. It is still not conclusive as to whether cash holdings can enhance or impair the cash value. Previous studies mostly studied and analyzed corporate governance [12], diversification [14, 15], capital market [16], market competition [17], and so forth. For example, Pinkowitz and Willamson [16] showed that there were negative correlations between the financing leverage, the size of cash holdings, and the value of cash holdings. Up to now, few studies about the value of cash holdings are made from the perspective of information asymmetry, and there is no consensus regarding a measure for information asymmetry. It is not applicable to directly borrow foreign indicators for the Chinese market. It is believed that the information asymmetry causes higher financing costs and high agency costs, but they used the scale of a company as the proxy for information asymmetry, which is not a typical practice, and obviously not a direct measure of information asymmetry [18, 19]. Korajczyk et al. [20] built a time-varying information asymmetry model and proposed that the adverse selection caused by information asymmetry has an important effect on corporate financing. This conclusion has been supported by many scholars [21–24]. However, Fama and French [25] and Leary and Roberts [26] found that the pecking order theory cannot find a clue to the company's financing decision problems in the case of a high level of information asymmetry. Chung [27] showed that for a company with high level of information asymmetry cash holdings cannot lift the company's value. Obviously, adverse selection and moral hazard caused by the information asymmetry make the company experience higher financing costs and constraints in the capital markets, and different financing constraints lead to different values of cash holdings. Therefore, information asymmetry becomes an important factor in studying the value of cash holdings.

However, it is rather difficult to quantify information asymmetry. Researchers have made much exploratory research and testing on proxy variables of information asymmetry. Different indexes for measuring information asymmetry generated disparate study results; meanwhile, they also left space and opportunity for further studies. Previous studies mostly adopt single index to analysis, so the problem is whether we can measure the level of information asymmetry and the agency costs of the company from multiple angles and then analyze the value of cash holdings. In order to solve this problem, we take listed companies in China as samples and try to explore the effect of information asymmetry on the value of cash holdings with a couple of theories. The basic approach is to explain the effect of information asymmetry on the value of cash holdings from the perspective of the marginal value of cash holdings: on the one hand, a relatively high level of information asymmetry implies a relatively high degree of financing constraints. When the company is faced with a high degree of financing constraints, the management may have held a large amount of cash in the previous period for self-serving purposes, which contributes to decreasing in the value of cash holdings. On the other hand, the higher the level of information asymmetry a company keeps, the higher financing cost the company encounters with or faces, and the smaller available cash flow is, so it is reasonable to consider that the cash held in firm has a positive effect on the company.

In order to reflect the degree of information asymmetry comprehensively and systematically, we take a number of influencing factors into account. We know that every factor reflects some information of the asymmetric information in different extent and have a certain correlation between these variables, so the data information can overlap to a certain extent. In order to avoid the increase of calculation and complexity of analysis due to the variable increase, we use the principal component analysis to achieve the purpose of dimension reduction. Specifically, this paper selects proxy variables for information asymmetry from the perspectives of market microstructure, earnings management, and financial characteristics and then adopts the principal component analysis to form a composite index to explore the relationship between information asymmetry, agency costs, and the value of cash holdings. Our study shows that (1) the value of a company's cash holdings rises with the increase of cash held in firm, but the marginal value of cash will diminish due to the increase in the cash holdings; (2) information asymmetry has a negative impact on the company's cash value, and the higher the level of information asymmetry a company stays at, the lower the value of its cash holdings is. With the increase in terms of the level of information asymmetry, the marginal value of cash discounts further, and (3) the relationship between the agency costs caused by information asymmetry and the value of cash holdings is not a simple monotonous one.

This study contributes the following to the body of the existing literature: (1) this paper, from the perspective of information asymmetry, employs data of Chinese listed companies to probe into the relationship between information asymmetry and the value of cash holdings which presents meaningful conclusions. Information asymmetry and the value of cash holdings are significantly negatively correlated—the higher the level of information asymmetry the lower the value of the cash holdings; moreover, this paper has a full discussion of information asymmetry and the value of cash holdings in the context of Chinese characteristics, pointing out the deep-seated reasons for this phenomenon, which makes a marginal contribution to understanding the problem of the relationship between China's agency problem and value of cash holdings; (2) according to the particularities of China's capital market, a new and more comprehensive index for information asymmetry is proposed. Some scholars quantitatively analyzed factors which take effects on the value of cash holdings, and some others qualitatively studied the economic effects of financial characteristics and corporate governance on cash holdings, yet no one has conducted comprehensive study on the value of cash holdings based on various perspectives. However, this paper selects liquidity, earnings quality, and financial characteristics as proxy variables for information asymmetry and then chooses the first principal component as the proxy based on the principal component analysis. In comparison to previous research [28, 29], the information asymmetry proxy in this paper is more comprehensive and also closer to the essence of information asymmetry, which is capable of revealing the mechanism of the effect of information asymmetry on the value of cash holdings. This measure is an important supplement of the existing measure of information asymmetry in China, and (3) this paper enriches the cross-disciplinary research on the microstructure of market and corporate finance. O'Hara [30], Madhavan [31], and Lipson [32] point out that the market microstructure needs to be combined more with researches in other financial fields to highlight its economic significance. At present, China's scholars mainly study this problem from perspectives of corporate governance, diversification, capital market, and market competition; this paper tries from the market microstructure and corporate finance to rediscover the interactive relationship between information asymmetry and the value of cash holdings. This study will help promote the interdisciplinary research from the market microstructure and corporate governance, making up for the deficiency in the area of agency theory in developing countries.

This paper is organized as follows: the second part consists of the theoretical analysis and research hypotheses; the third part concerns the study design; the fourth part presents the empirical results and analyses; the fifth part shows the result of robustness test and finally concludes the study.

2. Theoretical Analysis and Research Hypotheses

Recently, scholars domestic or abroad mainly view the effect on corporate value creation which is caused by cash holding from two different angles: on the basis of the principal-agent theory, some researchers believe that corporate executives or controlling shareholders have the motivation to hold a large amount of cash for self-interest, which is detrimental to corporate value; others see it differently in terms of information asymmetry. They argue that a large amount of cash enables the company to avoid external financing costs induced by information asymmetry between the management and potential shareholders, which in turn promotes the company's value.

Jensen and Meckling [2] proposed the principal-agent theory. On the premise of information asymmetry, the corporate management, compared with external investors, has inside information. Due to information asymmetry and bounded rationality, agents may not always act for the goal of maximizing principal's interest. Agency theory holds that the decrease in format of the value of cash holdings is caused by the agency problem. The corporate management or controlling shareholders hold a large amount of free cash flow to seek their own benefits, which is detrimental to the corporate value [33]. From the perspective of agency costs which exists between shareholders and the management, Jensen [4] put forward free cash flow theory to explain the motivation of the management to hold cash. The theory proposes that holding a large amount of cash is consistent with the management's interest rather than shareholders'. That is to say, due to information asymmetry, the management is motivated to avail them of the corporate control for self-interest. When the company performs poorly, the management can still whitewash earnings through managing the surplus held in company.

Myers and Majluf [3] propose the classic pecking order theory, arguing that companies prefer internal financing rather than external financing. As the company management has inside information, external investors would believe that the equity asset tends to be overpriced due to information asymmetry and thus ask for certain premium compensation. As a result, external financing cost would increase. The company either accepts the costly external financing or just gives up a value-enhancing investment project. Corporate cash holdings can effectively avoid external financing transaction costs as well as the cost of information asymmetry and enable a company to seize good investment opportunities or repay mandatory debts. The information asymmetry theory of cash holdings was developed on the basis of Myers's [34] pecking order theory. It holds that the information asymmetry in the capital market makes it hard to launch external financing as it requires higher indirect financing costs. Therefore companies need more liquid assets to meet investment needs. In addition, when companies face financing constraints, cash reserve can be a buffer so as not to lose promising investment opportunities. Taking internal funds helps to reduce financing costs, which enables cash holdings to enhance corporate cash value.

Clearly, external financing costs affect companies' capital investment and cause underinvestment, where cash holdings will have positive effect on. Therefore, when having more cash flow at a certain period, companies will reserve more cash to save financing costs. Generally speaking, companies with large cash holdings would undertake positive NPV projects instead of missing investment opportunities because of the lack of funds. However, in the presence of agency conflicts, high level of cash holdings becomes the easiest way for the management to gain personal benefits, leading to reduction of the value of cash holdings, which has been proved empirically. Harford [5] shows that companies with sufficient cash tend to engage in merger and acquisition, which in turn results in reduction of value of their cash holdings. Faulkender and Wang [6] and Pinkowitz et al. [7] ascribe the value reduction of an extra dollar of cash holdings to agency costs. Wang Ligang, a Chinese scholar, proposes in his doctoral thesis [35] that, due to agency costs, any increase in cash holdings has a negative impact on a company performance. Yang Xingquan and Zhang Zhaonan [36] argue that China's listed companies cash holdings were worth less than book value, indicating that serious agency problem exists in China's listed companies and legal protection for investors is weak. Accordingly, this paper makes the following hypotheses.

Hypothesis 1. The value of cash holdings is negatively correlated with information asymmetry. The higher the level of information asymmetry is, the lower the value of a company's cash holdings will be.

Different from Jensen [4], Myers and Majluf [3] find that corporate financing constraints are positively correlated with the value of cash holdings. Given that Myers and Jensen and others obtained diametrically opposite conclusions on information asymmetry, we have reasons to speculate that information asymmetry is not simply linear with the value of cash holdings. In fact, when companies face serious financing constraints, they need to pay for high cost to launch external financing. In order to not miss promising projects or not to get their positions threatened, the management is inclined to hold more cash in early period as a result of reverse selection. That is to say, the management holds spare cash for self-interest because of the existence of agency costs, but the spare cash produces no economic benefits. Hence, the marginal value of these cash holdings will be declined because of high level of information asymmetry; when companies face low financing constraints and easily get funded, the management does not have to hold too much cash to cope with agency costs. In this case, cash holdings are what companies need for normal business activities; therefore, the value of cash holdings will not be reduced.

Hypothesis 2. The level of information asymmetry has a nonlinear relation with the value of cash holdings. When a company is faced with severe financing constraints, the value of cash holdings is reduced due to the agency cost. While, when they are in less financing constraints times, holding cash will have a positive impact the value of company's cash holdings.

3. Research Design

3.1. Sample Selection and Data Sources. The sampling window for this paper ranges from 2007 to 2011, with the data in 2006 as those at one period lag. The following are the concrete screening principles and processes: (1) the nonfinancial and noninsurance companies listed in Shanghai securities regulatory commission and Shenzhen securities regulatory commission are selected; (2) the companies which issue A share, B share, or H share simultaneously are eliminated; (3) companies which are listed in or after 2007 are removed; (4) the companies which have undergone special treatment (ST), special treatment with * (*ST), or have been suspended and delisted and whose net asset value or primary business revenue is negative are eliminated; (5) the companies which ration shares, increase issues in stocks or issue convertible bonds are eliminated; (6) companies with data missing and abnormal changes are dismissed.

The final samples from 2007 to 2011 used in the paper are 588 companies, with a total of 2940 samples. The data are mainly taken from CSMAR data base (http://www.gtarsc.com/), and Excel, Eviews, and Stata software are used in the analysis procedure:

information asymmetry index and its structure,

measurement of information asymmetry.

The paper selects illiquidity ratio, liquidity ratio, discretionary accruals, and earnings before interest and tax in market microstructure theory and corporate finance theory to measure the information asymmetry level.

Information asymmetry and liquidity are important components in market microstructure, and adverse selection costs (namely, information asymmetry cost) are key factors influencing the market liquidity (namely, transaction cost). Two indicators are selected in the paper which is comparatively better to measure liquidity-illiquidity ratio [37] and liquidity ratio [38] to study the effect of liquidity on information asymmetry. Illiquidity ratio is a comparatively perfect indicator to measure liquidity in two-dimension width and depth. The calculation method is $\mathrm{ILL}_{t,d}^{i} = (1/N_t^i)\sum_{d=1}^{N_t^i}|r_{t,d}^i|/v_{t,d}^i$, where ILL_t^i, $r_{t,d}^i$, and $v_{t,d}^i$ denote the illiquidity, the return rate, and the trading volume of stock i in trading day d in year t, respectively, and N_t^i is the number of market days in t year. This shows when the liquidity of the stock is at the high level (adverse selection cost in the low level), huge trading volume can only produce a small change in the stock price. So the larger the adverse selection level is, the larger the ILL is. The liquidity ratio can be used to measure the turnover rate, and the calculation method: $\mathrm{TURN}_{t,d}^{i} = (1/N_t^i)\sum_{d=1}^{N_t^i} v_{t,d}^{i}/cv_{t,d}^{i}$, where $\mathrm{TURN}_{t,d}^{i}$, $cv_{t,d}^{i}$ denotes the liquidity and the number of shares of stock i traded on day d in year t, and other variables denotes the same as the former formula. Turnover rate measures the liquidity from the aspect of depth, which is widely used in empirical studies at home and abroad and thus suitable for all markets. Besides, since not all shares of a stock can be circulated in the Chinese stock market, the turnover rate of a stock is in fact that for the circulating shares in this paper and anticipates that there is a negative correlation between the adverse selection cost of the stock and the turnover rate.

Information asymmetry level can be measured in a number of ways, among which the quality of the accounting information reflects it directly. Not only does accounting information level reflect the level of information asymmetry of a company, but it reacts upon it as well. The quality of earnings has been the most studied subject in empirical studies on the accounting information quality. Earnings quality is a kind of nondiversifiable information risk, and investors will price systematically its influence on the capital market [39]. Drobertz et al. [40] find that the earnings deviation from analysts will devalue the company's cash holdings. Xiang Kai [41] holds that the earnings quality comprehensively reflects the transparency of the accounting information, which can have vital effect on agency conflicts and financing constraints. They regard the earnings quality as the breakthrough point to investigate the value of cash holdings and then find the company with better earnings quality has higher value of cash holdings. Quality accounting information can lower the level of information asymmetry among the management, shareholders, and investors and reduce the risk of adverse selection cost and liquidity risk. This will in turn lower the nondiversifiable information cost and pricing cost for investors and increase the liquidity of the stock, thus reducing the company's financing cost [42]. Companies with high accounting information quality can have easy access to external funds with low cost, and therefore there is no need to retain a large amount of cash to support its investment programs. So the amount of cash held in company will be reduced. Because discretional accruals can be adopted to measure the earnings quality of an individual company, it has been widely used due to its reasonability and conciseness. Based on previous studies [43, 44], the paper selects the quality of discretional accruals as the proxy variable for the accounting information quality [45]. Defond [46] finds that the Jones model with time series correction performs poorer than the Jones model with industry cross-section correction, and therefore this paper adopts the industry cross-section corrected Jones model to calculate accruals. Besides, Bank and Lawrenz [47] utilize a company's EBIT-value instead of the asset value as the state variable to investigate the effect of information asymmetry between the management and investors on the optimal capital structure decision. Guoqi and Shizhuan [48] believe EBIT can be used to evaluate the profitability of a company and examine the achievements of the management. As a result, profit before interest and tax is chosen as the proxy variable for information asymmetry between the management and investors, and its calculation is the indirect method which is extensively adopted in China: net profit + income tax + interest expenditure.

Table 1: Raw information asymmetry correlation coefficient.

	ASY	ILL	TURN	DAC	EBIT
ASY	1.0000				
ILL	0.6575^{***}	1.0000			
TURN	-0.8542^{***}	-0.2219^{***}	1.0000		
DAC	0.0032	0.0220	0.0236	1.0000	
EBIT	0.2557^{***}	-0.1572^{***}	-0.1889^{***}	0.0253	1.0000

Note: ∗∗∗, ∗∗, and ∗ denote the 1%, 5%, and 10% significance level, respectively.

3.2. Construction of Information Asymmetry Index. Four indexes have been obtained to measure the information asymmetry by the methods mentioned above. The four raw information asymmetry indexes have been treated by the principal component analysis filtering out the idiosyncratic noise in raw the information asymmetry indexes but retain the common element, namely, information asymmetry.

Table 1 shows the correlation coefficient of all raw information asymmetry. As can be seen from it, there are positive and negative correlations between all information asymmetry indexes and the resultant information asymmetry proxy variables, which present comparatively complex relationships. For instance, there is a positive correlation between ILL and ASY and a significant negative correlation between TURN and ASY. The above correlation results, on the one hand, verify the reasonability of the raw information asymmetry and, on the other hand, the complicated interaction among all raw information asymmetry indexes in Chinese Capital Markets.

3.3. Models and Research Variables. The economic effect of cash holdings can be qualitatively investigated from the role cash holdings play in achieving company performance. Quantitatively, it can be estimated with the marginal value of cash holdings-the value created for shareholders by increase every 1 Yuan RMB in a company's cash holdings, and the conclusion of the two kinds of research methods should be consistent. Chinese researchers Gu and Sun [49] modify the classical value regression model from Fama-French [50], to investigate the marginal value of cash holdings. However, Faulkender and Wang [6] argue that the classical value regression model of Fama-French [50] does not include factors such as risk and lagged variables. Therefore, this paper uses the model employed by Faulkender and Wang [6] to research the effect of a company's financial characteristics on cash holdings' marginal value. Dittmar and Smith [12] also adopt the model in studying the effect of corporate governance on the value of cash holdings. Table 2 shows all the definitions of the research variables. Owing to the unavailability of R&D

Table 2: Definitions of research variables.

Variable	Definition	Calculation method
$r_{i,t} - R^B_{i,t}$	$r_{i,t}$ is the actual rate of return in an accounting year, and $R^B_{i,t}$ is benchmark rate of return	$r_{i,t}$ is the actual annual rate of return on the stock with dividend included in the return, and $R^B_{i,t}$ is the circulation-market-value-weighted actual annual rate of return on the industry
$E_{i,t}$	Earnings	
$\mathrm{NA}_{i,t}$	Net asset	Difference between total assets and cash assets
$I_{i,t}$	Interest expense	Measured by financial expenses
$D_{i,t}$	Common stock dividends	Measured by cash dividends
$C_{i,t-1}$	Cash at previous year end	
$L_{i,t}$	Market value financial leverage	Total liabilities/total asset
$\mathrm{NF}_{i,t}$	Net financing	Net cash inflow from financing
High	High financial constraints	Takes 1 for the top 20% ASY values, 0 for others
Low	Low financial constraints	Takes 1 for the bottom 20% ASY values, 0 for others

expenditure index, the model is adjusted slightly in the paper as follows:

$$r_{i,t} - R^B_{i,t} = \beta_0 + \beta_1 \frac{\Delta C_{i,t}}{M_{i,t-1}} + \beta_2 \frac{\Delta E_{i,t}}{M_{i,t-1}} + \beta_3 \frac{\Delta NA_{i,t}}{M_{i,t-1}} + \beta_4 \frac{\Delta I_{i,t}}{M_{i,t-1}} + \beta_5 \frac{\Delta D_{i,t}}{M_{i,t-1}} + \beta_6 \frac{C_{i,t-1}}{M_{i,t-1}} + \beta_7 L_{i,t} + \beta_8 \frac{NF_{i,t}}{M_{i,t-1}} + \beta_9 \frac{C_{i,t-1}}{M_{i,t-1}} \times \frac{\Delta C_{i,t}}{M_{i,t-1}} + \beta_{10} L_{i,t} \times \frac{\Delta C_{i,t}}{M_{i,t-1}} + \varepsilon_{i,t}. \quad \text{(Model 1)}$$

Based on (Model 1), the calculation formula for cash holdings' marginal value is

$$\beta_1 + \beta_9 \left(\frac{C_{i,t-1}}{M_{i,t-1}} \right) + \beta_{10} L_{i,t}. \quad (1)$$

To measure the effect of information asymmetry on the value of cash holdings, the index $\mathrm{ASY}_{i,t}$ which is to indicate the information asymmetry level is added in the right side of (Model 1), and the (Model 2) is obtained as follows:

$$r_{i,t} - R^B_{i,t} = \beta_0 + \beta_1 \frac{\Delta C_{i,t}}{M_{i,t-1}} + \beta_2 \frac{\Delta E_{i,t}}{M_{i,t-1}} + \beta_3 \frac{\Delta NA_{i,t}}{M_{i,t-1}} + \beta_4 \frac{\Delta I_{i,t}}{M_{i,t-1}} + \beta_5 \frac{\Delta D_{i,t}}{M_{i,t-1}} + \beta_6 \frac{C_{i,t-1}}{M_{i,t-1}} + \beta_7 L_{i,t} + \beta_8 \frac{NF_{i,t}}{M_{i,t-1}} + \beta_9 \frac{C_{i,t-1}}{M_{i,t-1}} \times \frac{\Delta C_{i,t}}{M_{i,t-1}} + \beta_{10} L_{i,t} \times \frac{\Delta C_{i,t}}{M_{i,t-1}} + \beta_{11} \mathrm{ASY}_{i,t} + \beta_{12} \mathrm{ASY}_{i,t} \times \frac{\Delta C_{i,t}}{M_{i,t-1}} + \varepsilon_{i,t}. \quad \text{(Model 2)}$$

These two models are basically the same, which can be calculated with the following formula:

$$\beta_1 + \beta_9 \left(\frac{C_{i,t-1}}{M_{i,t-1}} \right) + \beta_{10} L_{i,t} + \beta_{12} \mathrm{ASY}_{i,t}. \quad (2)$$

In order to test (Model 2), the paper takes Qu Wenzhou [51] for reference and divides samples into three groups according to the distribution of the ASY values. Companies with the ASY values ranking among the top 20% are regarded as the high agency cost group (high), and companies with the ASY values ranking among the bottom 20% belong to the low agency cost group (low). Assign value 1 to $\mathrm{High}_{i,t}$ of the companies in high agency cost group and 0 to other companies. Assign value 1 to the $\mathrm{Low}_{i,t}$ of the companies in low agency cost group and 0 to other companies. In (Model 3), β_{11} is the change in terms of the cash holdings marginal value of the companies with high agency cost. β_{12} is the change in the cash holdings marginal value of the companies with low agency cost. According to Hypothesis 2, the cash holdings marginal value decreases in companies with high agency cost and decreases in companies with low agency cost. So this paper anticipates $\beta_{11} < 0$ and $\beta_{12} > 0$:

$$r_{i,t} - R^B_{i,t} = \beta_0 + \beta_1 \frac{\Delta C_{i,t}}{M_{i,t-1}} + \beta_2 \frac{\Delta E_{i,t}}{M_{i,t-1}} + \beta_3 \frac{\Delta NA_{i,t}}{M_{i,t-1}} + \beta_4 \frac{\Delta I_{i,t}}{M_{i,t-1}} + \beta_5 \frac{\Delta D_{i,t}}{M_{i,t-1}} + \beta_6 \frac{C_{i,t-1}}{M_{i,t-1}} + \beta_7 L_{i,t} + \beta_8 \frac{NF_{i,t}}{M_{i,t-1}} + \beta_9 \frac{C_{i,t-1}}{M_{i,t-1}} \times \frac{\Delta C_{i,t}}{M_{i,t-1}} + \beta_{10} L_{i,t} \times \frac{\Delta C_{i,t}}{M_{i,t-1}} + \beta_{11} \frac{\Delta C_{i,t}}{M_{i,t-1}} \times \mathrm{High}_{i,t} + \beta_{12} \frac{\Delta C_{i,t}}{M_{i,t-1}} \times \mathrm{Low}_{i,t} + \varepsilon_{i,t}. \quad \text{(Model 3)}$$

Δx equals $x_t - x_{t-1}$ in models in the paper, which is the increment of X from period $t-1$ to period t. All the variables

Table 3: Statistics of the population distribution of ASY values.

Samples	Mean	Median	Min.	Max.	Std.
2007	−0.6395	−0.8345	−3.0800	4.8144	1.0288
2008	0.8006	0.7493	−3.3797	4.7013	1.1144
2009	−0.6905	−0.6934	−4.5196	3.1067	0.8605
2010	−0.0206	0.0145	−3.5360	5.0002	0.8119
2011	0.5500	0.5820	−3.0445	4.3691	0.7837

are standardized with the equity value of the company in the previous year, and this treatment enables the regression coefficient for the model variables to directly denote the effect of the unit cash change in holdings on shareholder value, namely, the marginal value of cash holdings.

4. Empirical Results and Analysis

4.1. Descriptive Statistics. From Table 3, we can see that the level of information asymmetry of listed companies is still very high from 2007 to 2011. But the difference in information asymmetry between companies is narrowing down, which may be due to improvements in the capital market and the completion of the reform of nontradable shares.

Table 4 shows the descriptive statistics of major variables. From the table we can see that the mean, the median, the minimum, the maximum, and the standard deviation of the excess return $r_{i,t} - R^B_{i,t}$ are 0.1426, 0.0066, −1.7996, 7.2598, and 0.6992, respectively, which shows there is a big excess return difference among these sample companies, depending on industries and business scopes. The mean and the standard deviation of the incremental cash $(\Delta C_{i,t}/M_{i,t-1})$ are 6.82% and 153.76%, respectively, while the mean and the median of the cash holdings $(C_{i,t-1}/M_{i,t-1})$ are 31.05% and 25.72%, respectively, indicating that the incremental cash and the cash held in company of some of these listed companies are higher than that of the sample average. Besides, there are big difference in the cash held in company, the profitability, the level of incremental investment, and financing capability; the median of the level of the added dividend is 0, lower than the mean, indicating that over half of listed companies in our country do not pay dividends, and medium and small investors' power to require listed companies to return surplus cash are quite weak; the median of net financing is −0.0207; that is to say, more than half of the listed companies' net cash inflow from financing are negative, implying that few companies have financing opportunity to access cash inflow. The mean and the median of the financing leverage are 50.17% and 49.97%, respectively, showing that the distribution of the population is fairly symmetrical, while the standard deviation of 0.2905 means sample companies utilize financing leverage differently. According to comparison, American listed companies' mean and median of financing leverage are 27.78% and 22.65%, respectively, lower than those of China, which may be the result of relatively higher financing leverage $L_{i,t}$ calculated with the equity market value, while the equity market value was reduced by the sluggish stock market before 2005.

Based on studies on the value of cash holdings, researchers at home and abroad have used different indexes as the criteria to grade the degree of financing constraints, such as company scale, dividend payout ratio, ownership concentration, and asset-liability ratio. Next, this paper will use some frequently applied criteria in traditional studies to examine the differences in ASY values grouped with those indexes mentioned in the preceding sentence. As is shown in Table 5, ASY values vary significantly with different company scale, dividend payout ratio, ownership concentration, and asset-liability ratio. For large scale companies, dividend paying companies, companies with higher ownership concentration, and companies with low asset-liability ratio, the level of information asymmetry is higher than that of small scale companies, nondividend paying companies, companies with lower ownership concentration, and companies with high asset-liability ratio; that is, the former types of companies are subject to higher financing constraints. Thus it can be seen that the information asymmetry index ASY in this paper can more comprehensively reflect the financing constraint of a company, which ultimately reflects its severity of the principal-agency problem in a company.

4.2. Analysis of Multiple Regression Results. In this paper we use least square method to carry out multiple regression analysis of cross-sectional data. The analysis results are shown in Table 6.

In (Model 1), the regression coefficient for cash increment $(\Delta C_{i,t}/M_{i,t-1})$ is 0.5970 and is significant at the confidence level of 1%, which indicates that a 1 Yuan increase in cash holding of a listed company can only add 0.5970 Yuan for shareholder. There is a cash discount of about 40%. The coefficient for $(C_{i,t-1}/M_{i,t-1}) \times (\Delta C_{i,t}/M_{i,t-1})$ is 0.0112, but not significant, meaning that, in general, the level of cash held in company cannot increase a company's value of cash holdings. This differs from the research results of Faulkender and Wang [6]. The coefficient for $L_{i,t} \times (\Delta C_{i,t}/M_{i,t-1})$ is −0.8692 and is significantly negative, meaning the value of cash holdings decreases with an increase in the leverage level. To listed companies in China, the actual leverage level has direct impacts on the value of cash. So companies with a high leverage level will use the cash increment to pay debts and interests, while companies with a low leverage level will invest them into projects with a negative net present value. From the sample regression results, we can estimate the average value of cash holdings of listed companies in China between 2007 and 2011 is $0.5970+0.0112\times0.3105-0.8692\times0.5017 = 0.1644$. This indicates that there is a discount in the value of cash holdings of these companies. Specifically, the value of 1 Yuan increase in cash holding actually is 0.1644 Yuan with a big discount.

Comparing (Model 1) and (Model 2), we can see that the model's overall significance and goodness of fit are improved dramatically and significant at the 1% confidence level, after the information asymmetry variable is introduced into the model. This indicates that information asymmetry is an important factor affecting the value of cash holding. The regression coefficient for ASY is −0.1049, significantly negatively correlated with the value of cash holdings at the

Table 4: Descriptive statistics of major variables.

Variable	Mean	Median	Min.	Max.	Std.
$r_{i,t} - R_{i,t}^B$	0.1426	0.0066	−1.7996	7.2598	0.6992
$\Delta C_{i,t}/M_{i,t-1}$	0.0682	0.0174	−10.261	80.339	1.5376
$\Delta E_{i,t}/M_{i,t-1}$	0.0630	0.0119	−4.4618	80.165	1.5281
$\Delta \mathrm{NA}_{i,t}/M_{i,t-1}$	0.4402	0.1099	−8.6546	613.83	11.439
$\Delta I_{i,t}/M_{i,t-1}$	0.0045	0.0006	−0.6003	4.0695	0.0883
$\Delta D_{i,t}/M_{i,t-1}$	$1.31E-11$	0.0000	$-7.55E-10$	$3.70E-08$	$6.89E-10$
$C_{i,t-1}/M_{i,t-1}$	0.3105	0.2572	−14.544	4.6753	0.4100
$L_{i,t}$	0.5017	0.4997	0.0071	7.1440	0.2905
$\mathrm{NF}_{i,t}/M_{i,t-1}$	−0.0347	−0.0207	−107.39	15.639	2.0522
$(C_{i,t-1}/M_{i,t-1}) \times (\Delta C_{i,t}/M_{i,t-1})$	0.0110	0.0019	−121.21	90.433	2.8233
$L_{i,t} \times (\Delta C_{i,t}/M_{i,t-1})$	0.0442	0.0059	−6.5944	53.080	1.0288
$\mathrm{ASY}_{i,t}$	−0.0004	0.0250	−4.5196	5.0002	1.1080
$\mathrm{ASY}_{i,t} \times (\Delta C_{i,t}/M_{i,t-1})$	0.0410	−0.0005	−7.3845	130.01	2.4178
$(\Delta C_{i,t}/M_{i,t-1}) \times \mathrm{High}_{i,t}$	2.2131	0.0000	0.0000	6454.4	119.06
$(\Delta C_{i,t}/M_{i,t-1}) \times \mathrm{Low}_{i,t}$	0.0065	0.0000	0.0000	1.1438	0.0442

Note: statistics in the table are of relevant variables, including the mean, median, minimum, maximum, and standard deviation.

Table 5: ASY based on different criteria.

Criteria	Sample①	Observations	Mean (ASY)	Std.	t-test
Scale	Large	588	0.22131	1.0004	−17.903***
	Small	588	0.10639	1.2406	
Dividend payout ratio	Dividend	1485	0.19240	1.09633	−35.853***
	Nondividend	1455	−0.19637	1.08525	
Ownership concentration	High	588	0.4536	1.1573	−12.552***
	Low	588	−0.4540	0.9090	
Asset-liability ratio	High	588	−0.0195	1.1493	−53.561***
	Low	588	0.1598	1.1214	

Note: *** denotes significance at the 1% significance level.
①Companies are ordered in company scale, with the top 20% as the group of large scale companies and the bottom 20% as the group of small scale companies; dividend paying ratio is decided by whether companies paid dividend in the previous year or not, and they are classified as the dividend paying group and the nondividend paying group; ordered in the ratio of total shares held by the top 5 shareholders, top 20% companies are classified as the group of high ownership concentration, and the bottom 20% as the group of low ownership concentration. Arranged in descending order of the asset-liability ratio, the top 20% of the companies are defined as the group with high liabilities and the bottom 20% as the group with low liabilities.

1% confidence level, confirming Hypothesis 1 that the value of cash holdings will decrease with an increase in the information asymmetry level. This differs from the conclusion by Myers and Majluf [3] that large amounts of cash held by companies to avoid external financing cost induced by information asymmetry do not go to valuable investments, thus not promoting company values. The higher the level of information asymmetry is, the harder for external investors to supervise the actions of the management, which will cause serious free cash flow problems. Out of self-serving motives, the management may make some low value, rather than high-value investments, causing reduction in the value of cash holdings. This agrees with the conclusion by Jensen [4] that the value of cash holdings will decrease with an increase in the information asymmetry level, and high information asymmetry level will cause impairment to the cash value of a company. Moreover, in (Model 2), the coefficient for $\mathrm{ASY}_{i,t} \times (\Delta C_{i,t}/M_{i,t-1})$ is −0.2165 and is significant at the 1% confidence level, indicating that the value of cash holdings suffers a further discount with the increase in information asymmetry. Now, we can estimate the marginal value of cash brought to shareholders through 1 Yuan cash increases from an information asymmetry perspective: $0.6525 + 0.0078 \times 0.3105 - 0.8661 \times 0.5017 - 0.2165 \times (-0.0004) = 0.2205$.

Regression results show that in China 1 Yuan in cash of listed companies creates value less than 1 (a big discount). Chinese listed companies' agency costs for cash holdings exceed the advantages that cash holdings bring in overcoming the costly expenditure for external financing; that is, Chinese companies' cash holding is an act of value destruction rather than of value creation. This reveals serious agency problems on the part of China's listed companies. The management and the controlling shareholders of a company are very likely to accumulate a large amount of cash in the company for their own interest and waste them for "in-service consumption," "empire building," or engage in "affiliate transactions" to transfer the company's cash assets, thereby reducing the role of cash holdings in creating value, which impairs the interests

Table 6: Multiple regression results.

Variable	(Model 1)	(Model 2)	(Model 3)
Constant	0.0702** (2.4376)	0.0578** (2.0491)	0.0735** (2.5586)
$\Delta C_{i,t}/M_{i,t-1}$	0.5970*** (4.2802)	0.6525*** (4.7643)	0.5061*** (3.6025)
$E_{i,t}/M_{i,t-1}$	0.2862*** (5.4522)	0.2557*** (4.9545)	0.2902***(5.5509)
$\mathrm{NA}_{i,t}/M_{i,t-1}$	−0.0355*** (−3.5361)	−0.0192* (−1.8939)	−0.0218** (−2.1271)
$I_{i,t}/M_{i,t-1}$	−0.0538 (−0.1570)	0.5377 (1.5486)	0.4179 (1.1508)
$D_{i,t}/M_{i,t-1}$	7.30E + 07 (0.6066)	2.17E + 08* (1.7662)	3.26E + 08** (2.4663)
$C_{i,t-1}/M_{i,t-1}$	−0.0746* (−1.8078)	−0.0395 (−0.9708)	−0.0872** (−2.0903)
$L_{i,t}$	0.1836*** (4.0795)	0.1713*** (3.8846)	0.1705*** (3.8057)
$\mathrm{NF}_{i,t}/M_{i,t-1}$	0.0599*** (2.6960)	−0.0193 (−0.7423)	0.0139 (0.5652)
$(C_{i,t-1}/M_{i,t-1}) \times (\Delta C_{i,t}/M_{i,t-1})$	0.0112 (1.0119)	0.0078 (0.7187)	0.0267** (2.2380)
$L_{i,t} \times (\Delta C_{i,t}/M_{i,t-1})$	−0.8692*** (−4.3652)	−0.8661*** (−4.4402)	−0.6723*** (−3.3519)
$\mathrm{ASY}_{i,t}$		−0.1049*** (−9.1320)	
$\mathrm{ASY}_{i,t} \times (\Delta C_{i,t}/M_{i,t-1})$		−0.2165*** (−5.3150)	
$(\Delta C_{i,t}/M_{i,t-1}) \times \mathrm{High}_{i,t}$			−0.3688*** (−4.1401)
$(\Delta C_{i,t}/M_{i,t-1}) \times \mathrm{Low}_{i,t}$			0.6514*** (3.9512)
F	7.5288***	17.0805***	9.4311***
Adj. R^2	0.0217	0.0616	0.0333

Note: the numerical value in parentheses is the t statistic for the coefficient; ∗∗∗, ∗∗, and ∗ denote significance at the 1%, 5%, and 10% significance level.

of medium and small shareholders. Therefore, compared with the information asymmetry theory, we believe that the agency theory is more suitable to explain the behavior of cash holdings of Chinese listed companies.

The regression results of (Model 3) present that the coefficient for $(\Delta C_{i,t}/M_{i,t-1}) \times \mathrm{High}_{i,t}$ is significantly negative, while that for $(\Delta C_{i,t}/M_{i,t-1}) \times \mathrm{Low}_{i,t}$ is significantly positive. This fact shows that the relationship between the value of cash holdings and information asymmetry is not a monotonic one. When the information asymmetry level is very high, the value of cash holdings will be reduced and vice versa. When companies are faced with high financing constraints, due to the high external financing costs, the management, out of their motive of self-serving (agency costs), tends to reserve much cash at an earlier stage; on the other hand, investors are rendered unable to oversee the behavior of the management, and thus the management will be more likely to manipulate the company's free cash flow for self-interest with ease due to the high level of information asymmetry. So the value of cash holding will be still much lower, which is consistent with Jensen [4]. But at the same time, we find that companies with low agency costs have a higher value of cash holding. This is similar to the empirical results of Myers and Majluf [3].

When there exist external financial frictions, the higher the cost of external financing is, the greater the value of cash holdings is. Particularly when companies face more valuable growth opportunities, this positive relationship will become more apparent. Generally, a high level of cash holdings will enable companies to seize opportunities to undertake projects with positive NPVs instead of losing investment opportunities because of a lack of capital. However, in the presence of agency conflicts, a high level of cash holdings is the handy tool for the management to seek personal gains, which results in the reduction in the value of cash holdings. Fama [1] proposes the efficient market hypothesis, believing that, due to inconsistent utility functions for the management and external investors of a company, the management may act, out of selfishness and self-interest of homo economicus, in deviation from the goal for interests of investors, concealing or exaggerating some information to aggravate information asymmetry and exploit their operation rights and controlling power to infringe on investors' interests [2, 33]. Meanwhile, Jensen [4] proposes the free cash flow hypothesis to explain the management's motive to hold cash. He believed that holding a large amount of cash was consistent with the interests of the company management but inconsistent with that of shareholders. The management has incentives to use their controlling right for their own personal interests thanks to information asymmetry. When a company is not doing well, the management can also whitewash earnings by managing earnings through the cash held. As a result, it is difficult for external investors to supervise the management's behavior, and managers will seek to maximize their own interests and make investment decisions deviating from the objective of maximizing the interests of enterprises by investing the company's free cash into projects that will bring in nonmonetary benefits, such as enlarging the scale of the enterprise, or managers may be keen on building their own corporate empire or diversifying investments to obtain personal prestige, power, status, remuneration, and other additional personal incomes, which will cause reduction in the value of corporate cash.

To sum up, based on empirical studies of the market microstructure theory and empirical evidence of the finance theory, the information asymmetry between the management and investors impairs the value of cash holdings of listed companies in China. The management of listed companies in China has more insider information than external investors,

Table 7: Test result of robustness.

Variables	regression (4)	regression (5)	regression (6)
Constant	0.1124^{***} (2.9497)	0.0755^{***} (2.62645)	0.0651^{**} (2.2665)
$\Delta C_{i,t}/M_{i,t-1}$	0.8683^{***} (5.5521)	0.62785^{***} (4.51225)	0.5006^{***} (3.5540)
$E_{i,t}/M_{i,t-1}$	0.2820^{***} (5.3858)	0.2607^{***} (4.8651)	0.2799^{***} (5.3469)
$\mathrm{NA}_{i,t}/M_{i,t-1}$	-0.0189^{*} (−1.7451)	−0.0064 (−0.5447)	-0.03079^{***} (−3.0505)
$I_{i,t}/M_{i,t-1}$	0.2321 (0.6659)	0.3492 (0.9529)	−0.1075 (−0.3149)
$D_{i,t}/M_{i,t-1}$	$2.36E+08^{*}$ (1.8275)	$5.25E+08^{***}$ (3.6124)	$9.30E+07$ (0.775008)
$C_{i,t-1}/M_{i,t-1}$	-0.0994^{**} (−2.3696)	-0.1046^{**} (−2.5190)	−0.0649 (−1.5677)
$L_{i,t}$	0.1817^{***} (4.0469)	0.1750^{***} (3.9046)	0.1738^{***} (3.8708)
$\mathrm{NF}_{i,t}/M_{i,t-1}$	−0.0034 (−0.1231)	−0.0330 (−1.1746)	0.0588^{***} (2.6517)
$(C_{i,t-1}/M_{i,t-1}) \times (\Delta C_{i,t}/M_{i,t-1})$	0.0240^{**} (2.0711)	0.0249^{**} (2.0590)	0.0088^{***} (0.7899)
$L_{i,t} \times (\Delta C_{i,t}/M_{i,t-1})$	-0.7798^{***} (−3.9004)	-0.7918^{***} (−3.9506)	-0.7773^{***} (−3.8939)
$\mathrm{ILL}_{i,t}$	−0.5230 (−1.4546)		
$\mathrm{ILL}_{i,t} \times (\Delta C_{i,t}/M_{i,t-1})$	-4.5138^{***} (−3.8139)		
$\mathrm{High}_{i,t}$		−0.1598 (−1.3530)	
$(\Delta C_{i,t}/M_{i,t-1}) \times \mathrm{High}_{i,t}$		-0.0061^{***} (−3.1947)	
$\mathrm{Low}_{i,t}$			0.5702^{***} (2.9534)
$(\Delta C_{i,t}/M_{i,t-1}) \times \mathrm{Low}_{i,t}$			0.5338 (1.5681)
F	7.7745^{***}	8.9657^{***}	8.1677^{***}
Adj. R^2	0.0270	0.0315	0.0284

Note: the numerical value in parentheses is the t statistic for coefficients; $***$, $**$, and $*$ denote significance at the 1%, 5%, and 10% significance level, respectively.

which makes external financing more expensive than internal financing. Investors will require the company to pay a premium for utilizing external capital, causing external financing more costly and forcing the management to hold a large amount of cash [52].

5. Robustness Test

(Model 2) is constructed based on the first principal component from the four indexes, utilizing it as the proxy variable of information asymmetry. In order to further prove the validity of the conclusion, the noncurrent ratio ILL is used as the proxy variable of information asymmetry to test the robustness of (Model 2). To make the three conclusions more general and more convincing, $\mathrm{ASY}_{i,t}$ in (Model 2) will be replaced by $\mathrm{High}_{i,t}$ and $\mathrm{Low}_{i,t}$ to test the robustness of (Model 3).

In general, the regression results of all models are basically robust. The results of regression (4) show that the value of cash holdings will decrease with the rise in the level of information asymmetry, which is consistent with the regression results of (Model 2). Regression (5) shows that when using the top 20% of the highest level of information asymmetry as the proxy variable, it has a significantly negative correlation with the value of cash holdings, and this is consistent with the coefficients of $(\Delta C_{i,t}/M_{i,t-1}) \times \mathrm{High}_{i,t}$ in (Model 3). It suggests that a higher degree of information asymmetry will lead to a lower value of cash holdings. The coefficient of $\mathrm{Low}_{i,t}$ in regression (6) is significantly positive, which is also consistent with the coefficients of $(\Delta C_{i,t}/M_{i,t-1}) \times \mathrm{Low}_{i,t}$ in (Model 3). It shows that a lower degree of information asymmetry will lead to a higher value of cash holdings. It also confirms the nonlinear relationship between the cash value and information asymmetry, which provides a strong evidence for Hypothesis 2 (Table 7).

6. Conclusion

Drawing on the research findings of the market microstructure theory and corporate finance, this paper selects illiquidity ratio, liquidity ratio, discretionary accruals, and earnings before interest and tax (EBIT) as the proxy variables of information asymmetry. Then a new composite index for information asymmetry is formed based on the first component and used to test the effect of information asymmetry on the value of cash holdings. Finally, the relationship between the agency costs rooted in information asymmetry and the value of cash holdings is further analyzed; the main conclusions are as follows.

(1) The cash increment has a significant effect on the value of cash in a company, while the effect of cash held at company has minimum effect or less significant effect on the value of cash. The former conclusion is the same as previous research results, while the latter is different from the findings of most scholars.

(2) A company with a higher level of information asymmetry has a lower value of cash holdings. With the increase in the level of information asymmetry, the value of cash further discounts. This empirical evidence is consistent with Jensen's free cash flow hypothesis [4]. That is to say, the empirical results

in this paper provide support to the free cash flow hypothesis. Our research shows that a high level of information asymmetry can lead to high external financing costs. When a company faces cost difference between internal and external financing, the management, for the purpose of saving financing costs, tends to retain more cash for future use at an earlier time when the company owns relatively abundant cash. Harford [5] shows that the management tends to hold more cash due to the existence of entrenchment effect.

(3) There is no purely monotonic relationship between the agent cost and the value of cash holdings. The empirical research, based on the market microstructure theory and the corporate finance theory, shows that when a company faces a high degree of financing constraints, the value of cash holdings will be very low; while the financing constraints are very low, the value of cash holdings would rise. This implies that the relationship between agency costs caused by information asymmetry and the value of cash holdings is not linear. The financing constraints hypothesis based on the information asymmetry cannot fully explain the value of cash holdings of listed companies in China. The value of cash holdings of listed companies in China may have something to do with the shareholder rights hypothesis induced by financing constraints and the cash expenditure hypothesis due to the agency costs. When the level of information asymmetry is low, which means low financing costs, the company can obtain abundant funds and the company management does not have to hold more cash. So, under this condition, the value of cash holdings is relatively high. When the level of information asymmetry is high, which implies high financing costs, the management tends to hold excess cash for the agent rather than the principal's interests. Thus, the puzzle of the value of cash holdings is mainly due to the agency costs.

In addition, the policy implication of this study is very obvious: at presence, the research on the value of cash holdings in companies mainly concentrates on the western countries whose financial markets are fairly developed but pays little attention to the less developed capital markets in developing countries. A large body of literature documents that the information asymmetry on the part of companies in developing countries is more serious than that in developed countries due to the imperfection of financial markets. Information asymmetry has a huge impact on companies' financial behavior in developing countries and that impact is even more significant in China. Therefore, on the one hand, this research tries to explore and solve this puzzle in corporate finance in China from the perspective of the market microstructure theory and corporate finance. This paper represents a new research perspective, new methods, and new ideas, which will contribute to the most wanted development of China's market microstructure research and corporate finance research. Meanwhile, this paper tries to reveal the mechanism of the effects of information asymmetry on the value of cash holdings, which will help deepen the study in this area in China. On the other hand, it provides theoretical support to our enterprises' efficient management of cash flows, decision making in cash holdings, and substantial reduction in the agency costs. It can also provide relevant policy recommendations for building capital markets with matched demands, a reasonable system and perfect functions, and provides a reference to investors' investment decisions.

Conflict of Interests

The authors declare that there is no conflict of interests regarding the publication of this paper.

Acknowledgments

This work was jointly supported by the National Science Foundation of China under Grant nos. 11101053, 70921001, and 71171024, the Key Project of Chinese Ministry of Education under Grant no. 211118, the China Postdoctoral Science Foundation under Grant no. 20140550097, the Hunan Provincial NSF under Grant no. 11JJ1001, and the Scientific Research Funds of Hunan Provincial Science and Technology Department of China under Grant no. 2013SK3143.

References

[1] E. F. Fama, "Efficient capital markets: a review of theory and empirical work," *The Journal of Finance*, vol. 25, no. 2, pp. 383–417, 1970.

[2] M. C. Jensen and W. H. Meckling, "Theory of the firm: managerial behavior, agency costs and ownership structure," *Journal of Financial Economics*, vol. 3, no. 4, pp. 305–360, 1976.

[3] S. C. Myers and N. S. Majluf, "Corporate financing and investment decisions when firms have information that investors do not have," *Journal of Financial Economics*, vol. 13, no. 2, pp. 187–221, 1984.

[4] M. C. Jensen, "Agency costs of free cash flow, corporate finance and takeovers," *The American Economic Review*, vol. 76, no. 2, pp. 323–329, 1986.

[5] J. Harford, "Corporate cash reserves and acquisitions," *The Journal of Finance*, vol. 54, no. 6, pp. 1969–1997, 1999.

[6] M. Faulkender and R. Wang, "Corporate financial policy and the value of cash," *The Journal of Finance*, vol. 61, no. 4, pp. 1957–1990, 2006.

[7] L. Pinkowitz, R. Stulz, and R. Williamson, "Does the contribution of corporate cash holdings and dividends to firm value depend on governance? A cross-country analysis," *The Journal of Finance*, vol. 61, no. 6, pp. 2725–2751, 2006.

[8] H. Almeida, M. Campello, and M. S. Weisbach, "The cash flow sensitivity of cash," *The Journal of Finance*, vol. 59, no. 4, pp. 1777–1804, 2004.

[9] V. V. Acharya and L. H. Pedersen, "Asset pricing with liquidity risk," *Journal of Financial Economics*, vol. 77, no. 2, pp. 375–410, 2005.

[10] D. J. Denis and V. Sibilkov, "Financial constraints, investment, and the value of cash holdings," *Review of Financial Studies*, vol. 23, no. 1, pp. 247–269, 2010.

[11] L. Pinkowitz and R. Williamson, "What is the market value of dollar of corporate cash," *Joumal of Applied Corporate Finanee*, no. 19, pp. 74–81, 2007.

[12] A. Dittmar and J. Mahrt-Smith, "Corporate governance and the value of cash holdings," *Journal of Financial Economics*, vol. 83, no. 3, pp. 599–634, 2007.

[13] W. H. Mikkelson and M. M. Partch, "Do persistent large cash reserves hinder performance?" *Journal of Financial and Quantitative Analysis*, vol. 38, no. 2, pp. 275–294, 2003.

[14] Z. Tong, "Firm diversification and the value of corporate cash holdings," *Journal of Corporate Finance*, vol. 17, no. 3, pp. 741–758, 2011.

[15] V. Subramaniam, T. T. Tang, H. Yue, and X. Zhou, "Firm structure and corporate cash holdings," *Journal of Corporate Finance*, vol. 17, no. 3, pp. 759–773, 2011.

[16] L. Pinkowitz and R. Williamson, "What is a dollar worth, the market value of cash holdings," Working Paper, Georgetown University, 2004.

[17] L. Fresard, "Financial strength and product market behavior: the real effects of corporate cash holdings," *The Journal of Finance*, vol. 65, no. 3, pp. 1097–1122, 2010.

[18] F. Wen and X. Yang, "Skewness of return distribution and coefficient of risk premium," *Journal of Systems Science and Complexity*, vol. 22, no. 3, pp. 360–371, 2009.

[19] F. Wen and Z. Liu, "A copula-based correlation measure and its application in chinese stock market," *International Journal of Information Technology and Decision Making*, vol. 8, no. 4, pp. 787–801, 2009.

[20] R. A. Korajczyk and D. J. Lucas, "Equity issues with time-varying asymmetric information," *Journal of Financial and Quantitative Analysis*, no. 7, pp. 397–417, 1992.

[21] H. Choe, R. W. Masulis, and V. Nanda, "Common stock offerings across the business cycle. Theory and evidence," *Journal of Empirical Finance*, vol. 1, no. 1, pp. 3–31, 1993.

[22] P. V. Viswanath, "Strategic considerations the pecking order hypothesis, and market react ions to equity financing," *Journal of Financial and Quantitative Analysis*, no. 28, pp. 213–234, 1993.

[23] S. T. Bharath, P. Pasquariello, and G. Wu, "Does asymmetric information drive capital structure decisions," *Review of Financial Studies*, vol. 22, no. 8, pp. 3211–3243, 2009.

[24] D. M. Autore and T. Kovacs, "Equity issues and temporal variation in information asymmetry," *Journal of Banking and Finance*, vol. 34, no. 1, pp. 12–23, 2010.

[25] E. F. Fama and K. R. French, "Financing decisions: who issues stock?" *Journal of Financial Economics*, vol. 76, no. 3, pp. 549–582, 2005.

[26] M. T. Leary and M. R. Roberts, "The pecking order, debt capacity, and information asymmetry," Working Paper, Duke University, 2007.

[27] K. H. Chung, J. Kim, Y. S. Kim, and H. Zhang, "Information asymmetry and corporate cash holdings," SSRN Working Paper, University of New York, 2012.

[28] T. Opler, L. Pinkowitz, R. Stulz, and R. Williamson, "The determinants and implications of corporate cash holdings," *Journal of Financial Economics*, vol. 52, no. 1, pp. 3–46, 1999.

[29] A. Dittmar, J. Mahrt-Smith, and H. Servaes, "International corporate governance and corporate cash holdings," *Journal of Financial and Quantitative Analysis*, vol. 38, no. 1, pp. 111–113, 2003.

[30] M. O'Hara, "Making market microstructure matter," *Financial Management*, vol. 28, no. 2, pp. 83–91, 1999.

[31] A. Madhavan, "Market microstructure: a survey," *Journal of Financial Markets*, vol. 3, no. 3, pp. 205–258, 2000.

[32] M. L. Lipson, "Market microstructure and corporate finance," *Journal of Corporate Finance*, vol. 9, no. 4, pp. 377–384, 2003.

[33] R. La Porta, F. Lopez-De-Silanes, A. Shleifer, and R. W. Vishny, "Agency problems and dividend policies around the world," *The Journal of Finance*, vol. 55, no. 1, pp. 1–33, 2000.

[34] S. C. Myers, "The capital structure puzzle," *The Journal of Finance*, vol. 39, no. 3, pp. 574–592, 1984.

[35] W. Ligang, *Analysis on the Determinants and Value Effect of the Corporate Cash Holdings in China*, Zhejiang University, Hangzhou, China, 2007.

[36] Y. Xingquan and Z. Zhaonan, "Institution background, ownership property and the value of corporate cash holdings," *Economic Research Journal*, no. 12, pp. 111–123, 2008.

[37] Y. Amihud, "Illiquidity and stock returns: cross-section and time-series effects," *Journal of Financial Markets*, vol. 5, no. 1, pp. 31–56, 2002.

[38] T. Xijin and G. Gongning, "The liquidity of Chinese level and the conduction mechanism study: an empirical analysis based on data from 2005 to 2009," *Journal of Anhui University (Humanities and Social Sciences)*, no. 3, pp. 137–143, 2010.

[39] J. Francisa, R. LaFondb, P. Olssona, and K. Schippe, "The market pricing of accruals quality," *Journal of Accounting and Economics*, vol. 39, no. 2, pp. 295–327, 2005.

[40] W. Drobetz, M. C. Grüninger, and S. Hirschvogl, "Information asymmetry and the value of cash," *Journal of Banking and Finance*, vol. 34, no. 9, pp. 2168–2184, 2010.

[41] X. Kai, "Earning quality and corporate cash holdings: empirical evidence from the Chinese stock market," *Journal of Central University of Finance and Economics*, no. 7, pp. 79–85, 2009.

[42] D. Easley and M. O'Hara, "Information and the cost of capital," *The Journal of Finance*, vol. 59, no. 4, pp. 1553–1583, 2004.

[43] K. Schipper and L. Vincent, "Earnings quality," *Accounting Horizons*, vol. 17, pp. 97–110, 2003.

[44] C. Leuz, D. Nanda, and P. D. Wysocki, "Earnings management and investor protection: an international comparison," *Journal of Financial Economics*, vol. 69, no. 3, pp. 505–527, 2003.

[45] L. Zhirui, *Information Asymmetry and Cash Holding*, Shantou University, Shantou, China, 2009.

[46] M. L. Defond and K. R. Subramanyam, "Auditor changes and discretionary accruals," *Journal of Accounting and Economics*, vol. 25, no. 1, pp. 35–67, 1998.

[47] M. Bank and J. Lawrenz, "Information asymmetry between management and investors in the optimal capital structure decision," http://www.researchgate.net/publication.

[48] F. Guoqi and H. Shizhuan, "Application and comparison of EBIT and EAT in financial management," *Cai Kuai Yue Kan*, no. 11, pp. 85–87, 2010.

[49] N. Gu and J. Sun, "The market value of cash: evidence from Chinese listed companies," *Journal of Management Sciences*, vol. 21, no. 4, pp. 96–104, 2008.

[50] E. F. Fama and K. R. French, "Taxes, financing decisions, and firm value," *The Journal of Finance*, vol. 53, no. 3, pp. 819–843, 1998.

[51] Q. Wenzhou, X. Yalu, and Y. Yumei, "Information asymmetry, financing constraints and investment: cash flow sensitivity," *Economic Research Journal*, no. 6, pp. 105–117, 2011.

[52] L. L. Lundstrum, "Firm value, information problems and the internal capital market," *Review of Quantitative Finance and Accounting*, vol. 21, no. 2, pp. 141–156, 2003.

Hindawi Publishing Corporation
Discrete Dynamics in Nature and Society
Volume 2014, Article ID 369795, 16 pages
http://dx.doi.org/10.1155/2014/369795

Research Article

Pricing American Options Using a Nonparametric Entropy Approach

Xisheng Yu[1] and Li Yang[2]

[1] *School of Economic Mathematics, Southwestern University of Finance and Economics, Chengdu 611130, China*
[2] *Australian School of Business, University of New South Wales, NSW 2052, Australia*

Correspondence should be addressed to Xisheng Yu; yuxisheng@swufe.edu.cn

Received 4 February 2014; Accepted 7 March 2014; Published 8 May 2014

Academic Editor: Fenghua Wen

This paper studies the pricing problem of American options using a nonparametric entropy approach. First, we derive a general expression for recovering the risk-neutral moments of underlying asset return and then incorporate them into the maximum entropy framework as constraints. Second, by solving this constrained entropy problem, we obtain a discrete risk-neutral (martingale) distribution as the unique pricing measure. Third, the optimal exercise strategies are achieved via the least-squares Monte Carlo algorithm and consequently the pricing algorithm of American options is obtained. Finally, we conduct the comparative analysis based on simulations and IBM option contracts. The results demonstrate that this nonparametric entropy approach yields reasonably accurate prices for American options and produces smaller pricing errors compared to other competing methods.

1. Introduction

According to modern asset pricing theory, the value of any asset can be calculated as the expectation under the risk-neutral measure of discounted future cash flows. One of the challenging tasks in applying modern asset pricing theory to value options is to find an appropriate risk-neutral pricing measure. The maximum entropy principle is regarded as a reasonable criterion for determining an appropriate risk-neutral pricing measure (see, e.g., Frittelli [1] and Stutzer [2]) because it maximizes the use of prior knowledge in obtaining the posterior distribution, while being maximally uninformative about missing or unknown information (Jaynes [3]).

Stutzer [2] is the first to propose a nonparametric entropy valuation method, named the canonical valuation method, for valuing European options. This method does not need to make any preassumption for the underlying asset and relies only upon historical underlying price data. In this nonparametric pricing method, the physical distribution is transformed to a posterior distribution under the principle of the maximum entropy framework by imposing the martingale constraint. Because of the martingale constraint, this posterior distribution can be considered as a risk-neutral distribution (RND) of the underlying asset return and is then used to price the European options. The entropy valuation approach relies more on the information contained in market prices and less on normative assumptions. Due to this appealing feature, the entropy pricing method has been extended to price American options. Liu [4] proposed a so-called canonical least-squares Monte Carlo (CLM) method for pricing American options which uses Stutzer's framework to get the canonical distribution as pricing measure and determines the optimal exercise strategy via least-squares Monte Carlo algorithm (Longstaff and Schwartz [5]). Due to the sole martingale constraint used in CLM method, however, a problem arises if the martingale constraint does not sufficiently restrict the feasible set of measures to enable the entropy pricing measure to be close enough to the correct martingale measure.

Stutzer suggests that adding additional constraints forcing a subset of options to be priced correctly which would shrink the feasible set more tightly around the correct martingale measure. Following this, Alcock and Auerswald [6] incorporate the option price constraint, that is, choosing an option following certain criteria and forcing it to be priced correctly, into the entropy framework, in empirically pricing American options. This extended method utilizes the information individually and only the information contained in that specific option is extracted and incorporated into the entropy framework. Thus, it could only be accurate to price the option with the same characteristics such as the same strike price and the same time to expiration. Therefore, more option price constraints have to be put into the framework in order to incorporate more information for obtaining a better estimate of RND. But it may be computationally impossible due to the well-known problem that Jacobian matrix required in the estimation of the RND (see (12) and (13)) is singular or perhaps ill-conditioned (Agmon et al. [7] and Buchen and Kelly [8]), as the number of option price constraints increase.

It is well known that option prices contain information about market participants' perceptions of the distribution of the underlying asset[1]. Hence, information from the option market that characterizes the asset return distribution such as volatility, skewness, and kurtosis could also be considered as additional constraints and incorporated into the entropy framework. Indeed the moments can accurately characterize the shape of the underlying distribution, for instance, a normal distribution can be identified using the first- and second-order moments. The mentioned entropy-based valuation approaches above ignore the significance of inferring the RND by using more useful information from option data and do not create any informative constraint about the moments of the underlying asset returns.

Due to those described above, this paper introduces an ideally extended entropy method, named the risk-neutral moments-constrained entropic least-squares method (RMEL), by incorporating the risk-neutral moments (RNMs) as constraints for pricing American options. It is simple, general, and suitable for pricing most type of options such as path-dependent options. The key component that differentiates the RMEL method to the methods discussed above is the way that the information contained in option markets is exploited and utilized for recovering the risk-neutral pricing measure. As a result, our approach allows us to learn much more about the shape of RND. This proposed RMEL method does not need to impose preassumptions on either the market structure (e.g., completeness) or the process of underlying asset price, further, extracting moments are model-free and forward-looking. In addition, our approach can flexibly deal with the issues of dividends and time-varying interest rates.

Our valuation method proceeds in three stages. First, we estimate the noncentral RNMs of the underlying asset return from a set of American options based on the formulas we derive using a characteristic function. These RNMs not only guarantee the discounted price process of the underlying asset to be a martingale but also take the effects of the volatility smile, as well as the skewness and kurtosis of the asset returns, into account when generating a risk-neutral distribution. Second, we transform the physical distribution to the RND by maximizing the entropy value subject to RNM constraints estimated in the first stage. As there is no closed-form solution, we use the Nelder-Mead simplex numerical method to estimate the RND. We then generate the risk-neutral underlying price paths drawn directly from the estimated RND. Third, the value of American option is calculated by incorporating the least-squares Monte Carlo (LSM) algorithm to determine an optimal exercise strategy and then averaging the discounted expected payoffs along every path. As the generated paths are under the risk-neutral measure, the discount rate is the same as the risk-free rate.

We evaluate the usefulness of our method and compare its performance in a number of ways with that of Liu [4] in the same simulation setting, and with that of Liu [4] and Alcock and Auerswald [6] as well as other benchmarks using IBM option contracts. The simulation results suggest that, with simulated returns from geometric Brownian motion (GBM), RMEL approach produces very similar prices for calls and puts as those of Black-Scholes and finite difference and outperforms the method of Liu [4] under the simulated environment. The empirical investigation also demonstrates that our valuation approach generates smaller pricing errors than those of Liu [4], Alcock and Auerswald [6], and other benchmark methods for pricing IBM options.

The remainder of this paper is organized as follows. Section 2 presents our entropy valuation framework with detailed procedures. Sections 3 and 4 compare our valuation technique with other approaches in a simulated environment and using IBM options, respectively. Section 5 presents our conclusions and remarks.

2. RNMs-Constrained Entropy Valuation Method

We present the risk-neutral moments-constrained entropic least-squares valuation approach by employing the RNMs constraints under the entropy pricing framework to price American options. First, the RNMs are estimated using a set of call options based on the formulas we derive via a characteristic function. We then replace the single martingale constraint in the entropic pricing framework with the estimated RNMs to generate a better estimate of the RND that takes into account not only the mean of the distribution but also its entire shape. Note that our first and second RNM constraints ensure the martingale property and consider the volatility smile effect. Given the RND, an independent random sample of future underlying returns is drawn to generate risk neutral price paths. Potential exercise points for American options are then determined along every sample path via the LSM algorithm proposed by Longstaff and Schwartz [5]. Finally, option prices are computed as the expectation of the discounted payoffs along the risk-neutral underlying paths. Further details of our approach are discussed in the following sections.

2.1. Recovering RNMs from the Option Market. To estimate a RND of underlying asset returns more accurately, we incorporate RNMs as constraints into an entropic pricing framework. We recover RNMs from the option market, since it is well established in the literature that the option market contains useful information about the future return distributions of underlying assets[2]. In this way, volatility smile, which is commonly observed from the option market and skewness and excess kurtosis, can be effectively reflected in the estimation of the RND.

We first introduce some notations. Denote the price of the underlying asset at time t by S_t. Let the τ-period asset gross return at time t be given by the price relative, $R_{t,\tau} = S_{t+\tau}/S_t$, and let the τ-period jth-order RNM at time t, $m_{t,\tau}(j)$, be defined as $m_{t,\tau}(j) = E_{\pi^*}([\log(R_{t,\tau})]^j)$, where the symbol E_{π^*} represents the expectation operator under the risk-neutral probability measure π^*. Here, τ can be any appropriate time period such as a day or an hour. A special case is where τ is the period from time t to the option expiration time T. In this case of $\tau = (T-t)$, the jth-order RNM at time t can be expressed as $m_{t,T-t}(j) = E_{\pi^*}([\log(R_{t,T-t})]^j)$. The relation between $m_{t,\tau}(j)$ and $m_{t,T-t}(j)$ is given in Theorem 3.

According to Bakshi et al. [9], $m_{t,T-t}(j)$ $(j = 1,2,3,4)$ can be recovered from a set of cross-sectional out-of-the-money (OTM) European options. The following lemma holds.

Lemma 1. *Under the martingale pricing measures π^*, $m_{t,T-t}(j)$ can be recovered from the market prices of OTM European calls and put as follows.*

The $(T-t)$-period first-order RNM $m_{t,T-t}(1)$ is given by

$$m_{t,T-t}(1) = e^{(r-q)(T-t)} - e^{r(T-t)}\left[\int_{S_t}^{\infty}\frac{1}{K^2}C_t^E(T;K)\,dK + \int_0^{S_t}\frac{1}{K^2}P_t^E(T;K)\,dK\right] - 1. \tag{1}$$

The $(T-t)$-period jth-order RNM $m_{t,T-1}(j)$ $(j \geq 2)$ is given by

$$\begin{aligned} m_{t,T-t}(j) = {} & je^{r(T-t)}\left[\int_{S_t}^{\infty}\frac{(j-1)-\ln(K/S_t)}{K^2}\times\left[\ln\left(\frac{K}{S_t}\right)\right]^{(j-2)}C_t^E(T;K)\,dK\right] \\ & + je^{r(T-t)}\left[\int_0^{S_t}\frac{(j-1)-\ln(K/S_t)}{K^2}\times\left[\ln\left(\frac{K}{S_t}\right)\right]^{(j-2)}P_t^E(T;K)\,dK\right], \end{aligned} \tag{2}$$

where $C_t^E(T;K)$ and $P_t^E(T;K)$ are the prices of European call and put options at time t with expiration time T and strike price K, r is the continuously compounded risk-free interest rate matching time to the option expiration, and q is the continuously compounded dividend yield. Both r and q are annualized and assumed to be constant over time.

Proof. Provided in Appendix A [3]. □

Lemma 1 provides formulas to extract the first four moments, which are related to the mean, volatility, skewness, and kurtosis of the risk-neutral return density from a set of OTM European calls and puts. We intend to recover the RNMs using American calls supposed not to be exercised prior to expiration[4] and denote the price of American call option with expiration T and strike price K by $C_t^A(T;K)$; then we have the following.

Corollary 2. *When the call options are not being exercised prior to expiration, $m_{t,T-t}(j)$ can be recovered from American calls.*

The $(T-t)$-period first-order RNM $m_{t,T-t}(1)$ is

$$\begin{aligned} m_{t,T-t}(1) = {} & e^{(r-q)(T-t)} - e^{r(T-t)}\left[\int_{S_t}^{\infty}\frac{1}{K^2}C_t^A(T;K)\,dK\right] \\ & - e^{r(T-t)}\left[\int_0^{S_t}\frac{1}{K^2}\left[C_t^A(T;K) + Ke^{-r(T-t)} - S_te^{-q(T-t)}\right]dK\right] - 1. \end{aligned} \tag{3}$$

The $(T-t)$-period jth-order RNM $m_{t,T-t}(j)$ $(j \geq 2)$ is given by

$$\begin{aligned} m_{t,T-t}(j) = {} & je^{r(T-t)}\times\left[\int_{S_t}^{\infty}\frac{(j-1)-\ln(K/S_t)}{K^2}\times\left[\ln\left(\frac{K}{S_t}\right)\right]^{(j-2)}C_t^A(T;K)\,dK\right] \\ & + je^{r(T-t)}\times\left[\int_0^{S_t}\frac{(j-1)-\ln(K/S_t)}{K^2}\left[\ln\left(\frac{K}{S_t}\right)\right]^{(j-2)}\times\left[C_t^A(T;K) + Ke^{-r(T-t)} - S_te^{-q(T-t)}\right]dK\right]. \end{aligned} \tag{4}$$

As a special case, when the American option is written on nondividend-paying asset, *The* $(T-t)$*-period first-order RNM* $m_{t,T-t}(1)$ *is then*

$$m_{t,T-t}(1) = e^{r(T-t)}\left[1-\int_{S_t}^{\infty}\frac{1}{K^2}C_t^A(T;K)\,dK\right] - e^{r(T-t)}\left[\int_0^{S_t}\frac{1}{K^2}\left[C_t^A(T;K)+Ke^{-r(T-t)} - S_t\right]dK\right]-1. \quad (5)$$

The $(T-t)$*-period* j*th-order RNM* $m_{t,T-t}(j)$ $(j \geq 2)$ *is then*

$$\begin{aligned} m_{t,T-t}(j) &= je^{r(T-t)}\left[\int_{S_t}^{\infty}\frac{(j-1)-\ln(K/S_t)}{K^2}\times\left[\ln\left(\frac{K}{S_t}\right)\right]^{(j-2)}C_t^A(T;K)\,dK\right] \\ &+ je^{r(T-t)}\left[\int_0^{S_t}\frac{(j-1)-\ln(K/S_t)}{K^2}\left[\ln\left(\frac{K}{S_t}\right)\right]^{(j-2)}\times\left[C_t^A(T;K)+Ke^{-r(T-t)}-S_t\right]dK\right]. \end{aligned} \quad (6)$$

The condition of not exercising the calls early in Corollary 2 is moderate and easy to satisfy, especially for OTM or at-the-money (ATM) American calls, since the strike price is greater than (or equal to) the stock price and the dividend rate is not greater than the interest rate in most cases[5]. Practically, one can choose deeply OTM American calls because they are unlikely to be exercised before expiration[6].

For the relation between $m_{t,\tau}(j)$ and $m_{t,T-t}(j)$, the following theorem holds.

Theorem 3. *Under the martingale pricing measures* π^* *and the assumption that the* τ*-period returns are independently and identically distributed, the first four RNMs of* $\log(R_{t,\tau})$, $m_{t,\tau}(j) = E_{\pi^*}([\log(R_{t,\tau})]^j)$ $(j = 1, 2, 3, 4)$ *are given by*

$$m_{t,\tau}(1) = \frac{1}{N}m_{t,T-t}(1), \quad (7)$$

$$m_{t,\tau}(2) = \frac{1}{N}\left[\left(\frac{1}{N}-1\right)\left[m_{t,T-t}(1)\right]^2 + m_{t,T-t}(2)\right], \quad (8)$$

$$m_{t,\tau}(3) = \frac{1}{N}\left[\left(\frac{1}{N}-1\right)\left(\frac{1}{N}-2\right)m_{t,T-t}(1) + 3\left(\frac{1}{N}-1\right)m_{t,T-t}(1)\,m_{t,T-t}(2) + m_{t,T-t}(3)\right], \quad (9)$$

$$\begin{aligned} m_{t,\tau}(4) = \frac{1}{N}\Bigg[&\left(\frac{1}{N}-1\right)\left(\frac{1}{N}-2\right)\left(\frac{1}{N}-3\right)\left[m_{t,T-t}(1)\right]^4 \\ &+ 6\left(\frac{1}{N}-1\right)\left(\frac{1}{N}-2\right)\times\left[m_{t,T-t}(1)\right]^2 m_{t,T-t}(2) \\ &+ 3\left(\frac{1}{N}-1\right)\left[m_{t,T-t}(2)\right]^2 \\ &+ 4\left(\frac{1}{N}-1\right)m_{t,T-t}(1)\,m_{t,T-t}(3) \\ &+ m_{t,T-t}(4)\Bigg], \end{aligned} \quad (10)$$

where N *is the number of the* τ*-period intervals from* t *to* T*; that is,* $N = (T-t)/\tau$.

Proof. The proof is given in Appendix B. □

The right-hand sides of (5)-(6) show that the RNMs are the integrals of option prices over a range of strike prices $[0, S_t)$ and $[S_t, \infty)$ with two singular points 0 and ∞. Given a continuum of strike prices over the intervals, calculating the integrals using a numerical method is straightforward. However, only a finite number of traded options with discrete strike prices are available in a real market. Hence, we employ a more practical and effective curve-fitting method[7] to handle the issue of option availability (see Appendix C.2 for details) and use the trapezoidal numerical method[8] to numerically evaluate the integral (see Appendix C.1).

2.2. Recovering the RND within the Entropic Pricing Framework. To estimate an RND for option valuation, we use the maximum entropy framework with risk-neutral moment constraints. We initially assign equal probabilities to each possible future price (or gross return) of the underlying asset; that is, we assume the prior empirical asset returns are uniformly distributed. In the discrete case, we denote the empirical probability $\pi_i = 1/I$, $i = 1, 2, \ldots, I$, where I is the number of return realizations. We then incorporate the constraints of RNMs recovered from options into the entropic pricing framework. The issue of estimating the risk-neutral (equivalent martingale) measure π^* reduces to a constrained optimization problem following the Kullback-Leibler information criterion[9]:

$$\hat{\pi}^* = \underset{\pi_i^*>0}{\arg\min}\sum_{i=1}^{I}\pi_i^*\log\left(\frac{\pi_i^*}{\pi_i}\right),$$
$$\text{s.t.}\begin{cases}\displaystyle\sum_{i=1}^{I}\pi_i^*\left[\log\left(R_{t-(I-i+1)\tau,\tau}\right)\right]^j = m_{t,\tau}(j), \quad j = 0, 1, 2, \ldots, J \\ m_{t,\tau}(0) = 1,\end{cases} \quad (11)$$

where π_i^* denotes the risk-neutral (martingale) probability of the underlying asset's gross return from time $t-(I-i+1)\tau$ to $t-(I-i)\tau$ and $R_{t-(I-i+1)\tau,\tau}$ and $m_{t,\tau}(j)$ are the RNMs serving as constraints[10]. This valuation framework with RNM constraints subsumes the typical canonical valuation approach (e.g., Stutzer [2] and Liu [4]). The optimal solution $\widehat{\pi}_i^*$ is given as

$$\widehat{\pi}_i^* = \frac{\exp\left(\sum_{j=1}^{J} \lambda_j^* [\log(R_{t-(I-i+1)\tau,\tau})]^j\right)}{\sum_{i=1}^{I} \exp\left(\sum_{j=1}^{J} \lambda_j^* [\log(R_{t-(I-i+1)\tau,\tau})]^j\right)}, \quad (12)$$

where the Lagrange multiplier vector $\lambda^* = (\lambda_1^*, \lambda_2^*, \ldots, \lambda_J^*)$ is obtained by solving the following convex optimization problem[11]:

$$\lambda^* = \underset{\lambda_1,\lambda 2,\ldots,\lambda_J}{\arg} \min \sum_{i=1}^{I} \exp\left(\sum_{j=1}^{J} \lambda_j \left[(\log R_{t-(I-i+1)\tau,\tau})^j - m_{t,\tau}(j)\right]\right). \quad (13)$$

2.3. Risk-Neutral Price Paths and Optimal Exercise Strategy. With the risk-neutral distribution $\widehat{\pi}^* = (\widehat{\pi}_1^*, \widehat{\pi}_2^*, \ldots, \widehat{\pi}_I^*)$ given in (12), the independent random sample of future gross returns can be drawn from the set of historical gross returns. Risk-neutral price paths for the underlying asset are then generated. Specifically, starting with time t, each historical return $R_{t-(I-i+1)\tau,\tau}$ is associated with a risk-neutral probability $\widehat{\pi}_i^*$ $(i = 1, 2, \ldots, I)$. Then a sample of N returns $(\widetilde{R}_{t,\tau}, \widetilde{R}_{t+\tau,\tau}, \ldots, \widetilde{R}_{t+(N-1)\tau,\tau})$, where $N = (T - t)/\tau$, as previously defined, is randomly drawn from the above risk-neutral distribution employing the inverse transform method (Brandmiarte [10, pp. 230–232]). A risk-neutral price path is then generated. We repeat this procedure M times and obtain M risk-neutral price paths as

$$\begin{aligned} S_{t+\tau}^{(k)} &= S_t \widetilde{R}_{t,\tau}^{(k)}, S_{t+2\tau}^{(k)} = S_t \widetilde{R}_{t,\tau}^{(k)} \widetilde{R}_{t+\tau,\tau}^{(k)}, \ldots, S_N^{(k)} \\ &= S_t \prod_{n=1}^{N} \widetilde{R}_{t+(n-1)\tau,\tau}^{(k)}, \quad (k = 1, 2, \ldots, M), \end{aligned} \quad (14)$$

where $\widetilde{R}_{t+(n-1)\tau,\tau}^{(k)}$ is the nth random sample of the gross return along the kth underlying path.

Next, we determine the optimal exercise strategy for each of the risk-neutral paths. This study utilizes the LSM algorithm of Longstaff and Schwartz [5] to determine the optimal strategy for an American option over M underlying price paths. Since the LSM algorithm directly uses sample paths simulated under a risk-neutral measure, averaging the payoffs of all paths yields the final payoff of the option.

The LSM algorithm consists of three steps: approximating the holding value, comparing the holding value with the immediate exercise value, and averaging the resulting payoffs of all paths (for full details of the LSM algorithm, see [5]). The crucial feature of the LSM algorithm lies in estimating the continuously holding value by a linear combination of simple basis functions at each early exercise point along each path. As recommended by Longstaff and Schwartz [5] and Stentoft [11][12], the set of Legendre polynomial basis functions $\{1, 2(S_{t_n}/K) - 1, 6(S_{t_n}/K)^2 - 6(S_{t_n}/K) + 1\}$ is adopted to implement the LSM algorithm in this paper, where S_{t_n} is the underlying asset price at potential exercise time t_n, where $t_n = t + n\tau$ for $n = 1, 2, \ldots, N$.

2.4. Option Pricing Algorithm. With the optimal exercise strategy for each of the M underlying paths, an American call or put option expiring at time T with a strike price K can be valued as

$$\begin{aligned} &\text{For a Call, } C_t^A(T; K) \\ &= \frac{1}{M} \sum_{k=1}^{M} e^{-r(t_n^{(k)} - t)} \max\left(0, S_t \prod_{n=1}^{n^{(k)}} \widetilde{R}_{t+(n-1)\tau,\tau}^{(k)} - K\right), \\ &\text{For a Put, } P_t^A(T; K) \\ &= \frac{1}{M} \sum_{k=1}^{M} e^{-r(t_n^{(k)} - t)} \max\left(0, K - S_t \prod_{n=1}^{n^{(k)}} \widetilde{R}_{t+(n-1)\tau,\tau}^{(k)}\right), \end{aligned} \quad (15)$$

where $t_n^{(k)} = t + n^{(k)}\tau$ is the optimal exercise time of sample path k based on the LSM algorithm. Note that, as described above, the option price is given as the average of the discounted payoff because the set of drawn samples is already risk-neutral.

3. Simulation Testing

In this section, we test the pricing accuracy of our RMEL method based on simulated data by benchmarking against the methods of Black-Scholes for pricing American calls[13] and Crank-Nicolson finite difference (FD) for pricing American puts. We also investigate the pricing errors of our method and that of Liu [4] (Liu10)[14]. We simulate a sample of daily asset returns from a geometric Brownian motion (GBM) as well as a sample of American call and put options on this asset. With these two samples, we analyze the pricing accuracy with more details specified in the following subsections.

As a proof of concept, for the American calls, the RMEL approach should give the correct results as the Black-Scholes formula does when the underlying price process is modeled by GBM. For the American puts, the prices from RMEL should also be quite close to those from the method of FD. In addition, the RMEL method should work independently of the underlying growth rate in the GBM model.

3.1. Initial Setting. For ease of comparison, the parameters from Liu [4] are used in this simulation as follows.

(i) Valuation date t: January 1, 2007

(ii) Expiration date T: January 1, 2008

(iii) Strike price K: 40

(iv) Risk-free interest rate r: 6%

(v) Volatility σ: 40%

(vi) Dividend yield q: 0%.

3.2. Samples of Returns and Options. We simulate a sample of gross returns in which the underlying asset price S_t is assumed to follow a GBM:

$$dS_t = (\mu - q) S_t dt + \sigma S_t d\omega_t, \tag{16}$$

where μ is the drift term and ω_t is the standard Wiener process. Under this assumption, the continuously compounded τ-year gross return is log-normally distributed and given by

$$R_{t,\tau} = \exp\left(\left(\mu - q - \frac{\sigma^2}{2}\right)\tau + \sigma\sqrt{\tau}\epsilon\right), \tag{17}$$

where ϵ is standard normal.

According to (17) and with the parameter values above, we generate 365 daily gross returns[15] for both the risk-neutral case ($\mu = r = 6\%$) and the unrealistic case of a growth of $\mu = 100\%$ and treat them as historical returns of $R_{t-(I-i+1)\tau,\tau}$ ($i = 1, 2, \ldots, I$; $I = 365$; $\tau = 1$ day), as previously defined in Section 2.2.

For the purpose of option valuation, we need a sample of American call and put options for this simulation experiment. To enable comparison, the same options as those in Liu10 with different underlying prices are used here. The value of underlying price S_t varies from 36 to 44 with a 2-point increment (i.e., 36, 38, 40, 42, and 44) and other values of K, r, σ, t, T, and q are fixed as those given above. Given that $q = 0$, it is never optimal to exercise an American call early on a nondividend-paying underlying asset. Hence, the value of the above American call options can be calculated using the Black-Scholes formula. For the American puts, we calculate their values using the widely-used Crank-Nicolson FD method using an 800×800 grid. The sample of call and put options is treated as the traded options and their values are considered to be the "true" market prices.

In addition to the above options to be priced, we also need to generate a sample of call options in order to estimate the RNMs. Apparently this sample is different from the sample of calls used above for the valuation purpose. In the simulation experiment, we need to estimate a set of RNMs for each of the options to be valued. Even though the theoretical values of $m_{t,T-t}(j)$ are independent of S_t (see, (19)), their estimates using option data are a function of S_t (see (5)–(8)). Recall that for the valuation purpose, we take five calls and five puts with different asset prices in the experiment. When the asset prices are different, the estimates of the RNMs may not be exactly the same. Accordingly, we generate eight samples of call options to estimate the RNMs and then the RND for each of the given asset prices. Hence, the options with the given asset price are valued based on their corresponding RND. In each of eight samples for a given asset price, there are four call options being in the money (ITM), that is, their strike prices being lower than the asset price, and four being out of the money (OTM), that is, their strike prices higher. More specifically, the strike prices for asset price 36, 38, 40, 42, and 44 are (16, 22, 28, 34, 40, 46, 52, 58), (18, 24, 30, 36, 42, 48, 54, 60), (20, 26, 32, 38, 44, 50, 56, 62), (22, 28, 34, 40, 46, 52, 58, 64), and (24, 30, 36, 42, 48, 54, 60, 66), respectively.

3.3. Estimation of RNMs and RNDs. The mathematical form of the risk-neutral probability distribution $\widehat{\pi}_i^*$ in (12) depends on the number J of the RNM constraints $m_{t,\tau}(j)$ ($j = 0, 1, 2, \ldots, J$). For example, if J is zero, no constraint is imposed and the distribution $\widehat{\pi}_i^*$ is uniform. Under the assumption of GBM, $\widehat{\pi}_i^*$ is normally distributed and can be exactly characterized by its first and second moments. Hence, we use the first two moments as constraints for deriving the RND and only estimate $m_{t,\tau}(1)$ and $m_{t,\tau}(2)$.

We first use the generated 8 call options specified in Section 3.2 to calculate $m_{t,T-t}(1)$ and $m_{t,T-t}(2)$ based on Corollary 2 and then convert them to $m_{t,\tau}(1)$ and $m_{t,\tau}(2)$ according to Theorem 3 as discussed in Section 2.1. Two issues involved in the integrals in Corollary 2 need to be addressed. For any traded option with a specified maturity in the real market, the number of available strike prices (or option prices) is finite. The first issue therefore concerns the limited availability of strike prices (or option prices). To solve this problem, we use a curve-fitting method to generate "implied" options with a range of strike prices. We first calculate implied volatilities using the Black-Scholes formula based on the simulated (or market-available) call options. These implied volatilities are then used to form a fitted function of the volatility surface via the cubic splines method. Given the fitted function of the volatility surface, we can find the required volatilities and plug them into the Black-Scholes formula to obtain the "implied" call option prices. The details are in Appendix C.2. The second issue is the calculation of the integrals on the right hand side of (5) and (6). A numerical integration is carried out using the trapezoidal method, with the integration intervals split into $m = 80$ equal subintervals. The technical details of calculating the RNMs are given in Appendix C.1 and also outlined in footnotes 7 and 8.

Through the procedure specified above, we use only 8 options that are usually available in a real market[16] to obtain the RNMs ($m_{t,\tau}(1)$ and $m_{t,\tau}(2)$). We can calculate the true (theoretical) values for the first two moments in a risk-neutral world based on the above GBM. As is well-known, the solution for the above GBM in a risk-neutral world is

$$\log(R_{t,\tau}) = \left(r - q - \frac{\sigma^2}{2}\right)\tau + \sigma\sqrt{\tau}\epsilon, \tag{18}$$

where ϵ is a standard normal random variable. Then the theoretical values, denoted as $m_{t,T-t}(j)^{\text{true}} = E([\log(R_{t,T-t})]^j)$ for the $(T-t)$-period return and $m_{t,\tau}(j)^{\text{true}} = E([\log(R_{t,\tau})]^j)$

for the τ-period return ($j = 1, 2$), can be easily calculated as follows:

$$\begin{aligned} m_{t,T-t}(1)^{\text{true}} &= \left(r - q - \frac{\sigma^2}{2}\right)(T-t), \\ m_{t,\tau}(1)^{\text{true}} &= \left(r - q - \frac{\sigma^2}{2}\right)\tau, \\ m_{t,T-t}(2)^{\text{true}} &= \left[\left(r - q - \frac{\sigma^2}{2}\right)(T-t)\right]^2 + \sigma^2(T-t), \\ m_{t,\tau}(2)^{\text{true}} &= \left[\left(r - q - \frac{\sigma^2}{2}\right)\tau\right]^2 + \sigma^2\tau. \end{aligned} \tag{19}$$

Since there are multiple underlying asset prices in the experiment, we extract the RNMs for each underlying price. Table 1 reports the estimates of RNMs and their theoretical values.

Table 1 shows that the RNM estimates are nearly the same as their theoretical values. This demonstrates that eight options can effectively capture the shape of distribution of the underlying asset returns. Furthermore, the estimated RNMs are almost indistinguishable for both moments, even though the underlying prices are different. This indicates that the two moments obtained are exactly "risk-neutral" and are not related to the current asset price. It can be seen again from (19) that the RNMs are only determined by interest rate and volatility and not by the underlying asset price.

In addition to the estimated RNMs, we also need to simulate return series following (17) for recovering the RND according to (12) and (13). In this experiment, we simulate two series of 365 returns; that is, $R_{t-(365-i+1)\tau,\tau}$ ($i = 1, 2, \ldots, 365$) for growth rates of $\mu = 6\%$ and 100%, respectively, and other parameters at values of $\sigma = 40\%$, $T - t = 1$, and $\tau = 1/365$. Thus, two corresponding RNDs of $\widehat{\pi}^{*(1)} = (\widehat{\pi}_1^{*(1)}, \widehat{\pi}_2^{*(1)}, \ldots, \widehat{\pi}_{365}^{*(1)})$ and $\widehat{\pi}^{*(2)} = (\widehat{\pi}_1^{*(2)}, \widehat{\pi}_2^{*(2)}, \ldots, \widehat{\pi}_{365}^{*(2)})$ are recovered.

3.4. Pricing Results and Comparison Analysis. This section first presents the pricing results and then compares them with the "true" values. Tables 2 and 3 report the estimated prices of American calls and puts using the RMEL method and the method of Liu10.

Tables 2 and 3 report that the estimated prices of the RMEL method are fairly close to the "true" prices for both growth rates across a range of asset prices, especially for put options. The absolute differences between the RMEL and the Black-Scholes formula are all below 1%; see columns four and six in Table 2. Even below 0.32% for put options, see columns four and six in Table 3. It appears that the RMEL method is comparable to the Black-Scholes formula for American calls and to the FD method for American puts. Furthermore, for each price estimate in both growth rates of 6% and 100%, two pricing errors are so small that the difference between two estimates is slight. This finding again illustrates that the RMEL method is actually independent of the growth rate.

Taking the absolute difference between the estimated value from a method and the "true" value as a measure for judging price deviation, the absolute difference from our method is a little bit higher than that from Liu10 for both call and put options when the asset price is 42, as well as for call options with the 6% growth rate when the asset price is 38, but the difference is still slight since the absolute differences are so small. Fortunately and importantly, all the other absolute differences from RMEL are lower and even much smaller than those from Liu10. This suggests that the magnitudes of the pricing error resulting from RMEL method are, overall, smaller than those from Liu10.

In brief, these results indicate that both American calls and puts can be priced rather accurately by our RMEL approach in the simulated market, and this method provides better precision than the method of Liu10. It should also be noted that, there is no discernible relation between the accuracy of pricing and moneyness[17].

4. Comparison Based on IBM Option Data

4.1. Data Descriptions. We collected daily data of IBM call and put options from the website http://finance.yahoo.com/. The data cover July 31, 2008 through January 30, 2009 for a total of 127 trading days. After filtering[18], 4430 calls and 4430 put options remain with the time to maturity being 16 to 357 days. The closing price of IBM stock is treated as the underlying price and here the discrete dividends (paid quarterly) are taken into consideration. Depending on the valuation date, the dividend payment dates are assumed to be on August 6, 2008 and November 6, 2008, and the corresponding quarterly dividends are actually \$0.5 according to the downloaded data. Table 4 briefly describes the filtered data of IBM calls and puts.

The daily US Treasury yield curve rate from one month to 30 years for each valuation date is used or interpolated linearly for any particular time to maturity as the corresponding continuous, constant risk-free interest rate. The yield curve is obtained directly from the website of the US Department of the Treasury, http://www.treasury.gov/resource-center/data-chart-center/interest-rates/Pages/default.aspx.

4.2. Valuation Methods. The empirical results for our method indicate that the third and fourth moments are highly linearly dependent of the first two moments. This implies that the third and fourth moments can be expressed as a linear combination of the first two moments. The linear dependence could result in an ill-conditioned problem when solving the optimization problem, that is, (11). Mathematically, if the matrix $[(\log(R_{t-(I-i+1)\tau,\tau})^j)]_{J\times I}$ is not a full rank, the Lagrange multipliers cannot be uniquely determined (Agmon et al. [7]). Consequently, many risk-neutral probabilities equal zero. This problem actually appears many times while pricing IBM options. Here is an example of options with trading date of July 31, 2008, stock price of \$127.98, and time to maturity of 78 days. In the case of three moment constraints, 176 out of 260 calculated risk-neutral probabilities are nonzero; in the case of four moment constraints, only 74 among 260 are nonzero, whereas all the probabilities are positive when using the first two moment constraints. Hence, in our

Table 1: Recovered moments and their theoretical values for a range of initial underlying prices ($S_t = 36, 38, 40, 42, 44$) in the simulation.

Underlying price	36	38	40	42	44
1st order moment	−0.0200	−0.0200	−0.0200	−0.0200	−0.0200
$(m_{t,T-t}(1))$	−0.0200	−0.0200	−0.0200	−0.0200	−0.0200
2nd order moment	0.1605	0.1605	0.1605	0.1604	0.1604
$(m_{t,T-t}(2))$	0.1604	0.1604	0.1604	0.1604	0.1604

Note: the first two moment estimates for $\log(R_{t,T-t})$ with each of the underlying prices (S_t) are compared to their corresponding theoretical values under the GBM, calculated by (19) with the parameters $r = 0.06$, $\sigma = 40\%$, $q = 0$, $T - t = 1$.
These moments are recovered using only 8 call options discussed in Section 3.2. For both moments, the top row reports the estimated values, and the bottom row reports the theoretical (true) values.

Table 2: Averaged prices of American call options for a range of asset prices ($S_t = 36, 38, 40, 42, 44; K = 40$).

Method↓	Asset price S_t	Black-Scholes formula C_t	Growth rate $\mu = 6\%$	Difference (%) $\frac{Estimated\ value - C_t}{C_t}$	Growth rate $\mu = 100\%$	Difference (%) $\frac{Estimated\ value - C_t}{C_t}$
RMEL	36	5.041	5.013	−0.555	5.029	−0.238
	38	6.164	6.123	−0.665	6.151	−0.211
	40	7.389	7.357	−0.433	7.376	−0.176
	42	8.708	8.653	−0.632	8.679	−0.333
	44	10.112	10.065	−0.465	10.092	−0.198
Liu10	36	5.041	5.076	0.694	5.074	0.655
	38	6.164	6.186	0.357	6.201	0.600
	40	7.389	7.426	0.501	7.458	0.934
	42	8.708	8.730	0.253	8.723	0.172
	44	10.112	10.169	0.564	10.158	0.455

Note: the numbers in the first two columns represent, respectively, asset prices and the corresponding true Black-Scholes prices (as the underlying asset pays no dividend). Columns 3 and 5 report the price estimates with the growth rates of 6% and 100% for the two methods, and each reported value represents an estimate for a particular combination of growth rate and asset price. The values reported in columns 4 and 6 are the corresponding difference between the estimated and the "true" Black-Scholes prices, respectively. The difference is calculated by dividing the estimated price minus the Black-Scholes price by the Black-Scholes price. For both RMEL and Liu10, each reported price estimate is the average of the prices over three independent simulations. In each simulation, 100,000 risk-neutral price paths are generated and each path is divided into $P = 73$ exercise opportunities.

Table 3: Averaged prices of American puts for a range of asset prices ($S_t = 36, 38, 40, 42, 44; K = 40$).

Method↓	Asset price S_t	Crank-Nicolson FD Formula P_t	Growth rate $\mu = 6\%$	Difference (%) $\frac{Estimatedvalue - P_t}{P_t}$	Growth rate $\mu = 100\%$	Difference (%) $\frac{Estimatedvalue - P_t}{P_t}$
RMEL	36	7.109	7.094	−0.211	7.091	−0.253
	38	6.154	6.139	−0.244	6.145	−0.146
	40	5.318	5.305	−0.244	5.301	−0.320
	42	4.588	4.575	−0.283	4.575	−0.283
	44	3.953	3.941	−0.304	3.945	−0.202
Liu10	36	7.109	7.145	0.506	7.138	0.407
	38	6.154	6.195	0.666	6.167	0.211
	40	5.318	5.364	0.865	5.360	0.789
	42	4.588	4.596	0.174	4.598	0.217
	44	3.953	3.992	0.987	3.980	0.683

Note: the reported numbers in the first two columns represent, respectively, the asset prices and the corresponding "true" prices calculated using the Crank-Nicolson finite difference (800 × 800 Grid) ($r = 0.06$). Columns 3 and 5 report the price estimates with the growth rates of 6% and 100% for the two methods. Each reported value represents an estimate of option price for a particular combination of growth rate and asset price. The values reported in Columns 4 and 6 are the corresponding difference between the estimated price and the Crank-Nicolson finite difference prices, respectively. The difference is calculated by dividing the estimated price minus the "true" price of the Crank-Nicolson finite difference by the Crank-Nicolson finite difference price. For both RMEL and Liu10, each price estimate is the average of the values over three independent simulations. Each of the simulations generates 100,000 sample price paths and each path is divided into 73 potential exercise opportunities.

Table 4: Data description of IBM calls and puts.

		Mean	Standard deviation	Minimum	Maximum
Call	Number of options	4430			
	Market prices	13.653	14.245	0.075	69.550
	Moneyness S_t/K	1.077	0.329	0.514	2.292
	Expiration	119.008	71.886	16	357
Put	Number of options	4430			
	Market prices	13.614	15.188	0.075	75.200
	Moneyness K/S_t	1.010	0.283	0.436	1.946
	Expiration	119.008	71.886	16	357

Note: the call and put prices here are the midvalues of the bid-ask quotations. Moneyness is defined as the IBM stock closing price divided by the strike price, S_t/K, for call options and the strike price divided by the closing price, K/S_t, for put options. The time to expiration is measured in days.

empirical investigation, only the first two moment constraints are incorporated into our pricing framework to price IBM options.

The empirical investigation involves four pricing methods. For IBM call options, our RMEL method with two moment constraints, the method of Liu10 without moment constraint, and Alcock and Auerswald [6] (AA10) with option-constraint, and, for IBM puts, the Crank-Nicolson FD (FD). It should be pointed out here that due to the fact that the IBM stock pays discrete dividends, the factor $e^{-q(T-t)}$ in (3)-(4) would be replaced with $(1 - D/S_t)$ when calculating the RNMs, that is, (7)-(8), where D is the present value of dividend payments at time t.

For each reported price, three independent Monte Carlo runs are carried out and the resultant prices are averaged as option prices. Each simulation generates 10,000 risk-neutral price paths, with each path made up of one-day gross returns sampled from the risk-neutral measure. The simulated risk-neutral stock price for every path on the exdividend date is reduced exactly by the dividend amount, and the previous 260 daily closing prices are used to calculate the historical gross returns. Each path is further divided into a number of potential exercise steps according to the following rule. If the number of days to expiration is less than 50, the size of the step is set to one day; otherwise, the number of days in one step is an integer part of the number of days to expiration divided by 50, while the last step can cover fewer days than the remaining ones. The least-squares algorithm uses the first two terms of the Legendre polynomial plus a constant term, $\{1, 2(S_t/K) - 1, 6(S_t/K)^2 - 6(S_t/K) + 1\}$, as basis functions. For integral calculations, each of the integration intervals $[S_t, K_{\max}]$, $[K_{\max}, K_{\infty}]$, $[K, K_{\min}]$, and $[K_{\min}, S_t]$ is split into $m = 80$ nonoverlapping intervals of equal length.

With regard to the AA10 method, we use the same criteria as those in AA10 to choose an option as the constraint. For pricing a call option, a prior day observed call option with the same strike price and the same expiration is taken, when pricing a put, the preferred constraint is a prior day observed call option with the same expiration date and moneyness closest to 1.0, and if no adequate option can be found on the day prior, the ith call option with trading date of t_i and maturity of T_i traded in the previous five days with time to maturity equal to $\max_{T_j - t_j \le T-t}(T_i - t_i)$ and moneyness closest to 1.0 is chosen as the constraint.

Finally, for the FD method, since the stock grid is fixed in the backward induction of finite difference, the option value on the exdividend date is adjusted downward by using quadratic interpolation to reflect the effect of dividend payments and thus corresponds to the option value for the dividend-adjusted stock price. If the dividend-adjusted stock price is less than the second lowest stock price on the grid, however, the corresponding option value is set to the option value for the lowest stock price in the grid and no interpolation is carried out. In addition, volatility is calculated as the standard deviations of the daily returns multiplied by square root of 252, based on the previous 260 daily IBM stock closing prices. A default grid of one-day time step and a grid of stock price spacing of $\Delta(\ln S) = \sigma\sqrt{3\tau}$ as suggested in Hull [12, pp.443] are used.

4.3. Empirical Results. The valuation results are summarized and compared using 12 categories of moneyness and time to expiration. Four levels of moneyness are given as: less than 0.85 (i.e, DOTM), from 0.85 to 1.00 (i.e., OTM), from 1.00 to 1.15 (i.e., in-the-money, ITM), and greater than 1.15 (i.e., DITM). There are three groups of time to expiration: from 16 to 60 days (short term), from 61 to 160 days (medium term), and from 161 to 357 days (long term). In addition, the following frequently-used loss measures are used to analyze the pricing errors: the mean percentage error (MPE), the mean square error (MSE), and the mean absolute percentage error (MAPE)[19].

Tables 5 and 6 summarize the pricing results from different valuation methods corresponding to either call or put options, and the number of options is also shown for each category.

Several observations of pricing errors between IBM calls and puts using RMEL method can be made. First, the RMEL pricing error is distributed more evenly for calls; for example, the MAPE is around 15% to 20% over 12 categories for calls, while the MAPE of puts generally decreases dramatically with moneyness. Table 6 shows that the MAPE of RMEL is much less than 10% for the ITM and DITM cases but basically

Table 5: MPE, MSE, and MAPE of IBM call price estimates compared to IBM market prices for a range of moneyness and time to expiration.

Moneyness (S_t/K)	Expiration	16–60 (short)			61–160 (medium)			161–357 (long)		
	Method	RMEL	Liu10	AA10	RMEL	Liu10	AA10	RMEL	Liu10	AA10
$S_t/K < 0.85$ (DOTM)	Count		199			480			529	
	MPE (%)	−5.352	−14.208	6.214	−3.508	−3.931	−7.035	−6.035	−7.932	−12.136
	MSE	1.823	5.636	1.402	1.489	4.785	2.902	1.806	4.757	6.238
	MAPE (%)	14.735	26.291	21.035	15.225	35.138	20.186	15.132	32.248	17.301
$S_t/K \in [0.85, 1.00)$ (OTM)	Count		371			304			290	
	MPE (%)	−5.130	2.620	5.326	−4.919	−4.634	−18.325	−5.726	−4.482	−20.648
	MSE	1.290	4.064	1.824	1.164	4.060	3.028	1.357	4.814	4.039
	MAPE (%)	19.868	44.545	23.894	16.825	35.937	27.682	19.781	42.443	26.026
$S_t/K \in [1.00, 1.15)$ (ITM)	Count		289			248			202	
	MPE (%)	−3.044	−2.307	−6.563	−4.688	−2.794	−19.542	−0.831	1.652	−23.249
	MSE	1.314	3.906	3.358	0.873	3.046	8.065	1.106	3.495	16.548
	MAPE (%)	17.060	34.599	18.175	18.988	38.985	25.338	20.091	41.227	28.065
$S_t/K \geq 1.15$ (DITM)	Count		434			670			414	
	MPE (%)	−2.181	−3.637	−4.212	−2.846	−7.860	−9.542	−5.096	−8.887	−11.254
	MSE	1.386	4.290	2.921	1.189	3.915	8.621	0.725	3.085	15.245
	MAPE (%)	15.663	37.031	13.984	15.690	31.904	15.938	18.616	38.707	19.351

Note: each cell represents a particular combination of moneyness and time to expiration. Three independent simulations are carried out, while 10,000 underlying price paths are generated in each simulation. The first row reports the number of call options with the corresponding combination of moneyness and time to expiration. The remaining rows show the statistic results of the MPE, RMSE, and MAPE for each combination. The total number of options analysed is 4430, the lowest moneyness is $79.66/155 = 0.514$, the highest moneyness is $91.66/40 = 2.292$, and the time to expiration is in between 16 and 357 days.

Table 6: MPE, MSE, and MAPE of IBM put price estimates compared to IBM market prices for a range of moneyness and time to expiration.

Moneyness (K/S_t)	Expiration	16–60 (short)				61–160 (medium)				161–357 (long)			
	Method	RMEL	Liu10	AA10	FD	RMEL	Liu10	AA10	FD	RMEL	Liu10	AA10	FD
$K/S_t < 0.85$ (DOTM)	Count		372				618				374		
	MPE (%)	−46.223	−78.924	−82.536	−88.694	−30.291	−53.189	−51.623	−89.083	−4.054	0.899	−40.284	−75.498
	MSE	0.057	0.439	1.206	0.634	0.115	0.754	2.064	1.945	0.826	2.397	2.203	3.219
	MAPE (%)	49.451	79.437	82.735	96.226	36.683	60.518	59.137	89.083	24.695	47.858	45.735	75.498
$K/S_t \in [0.85, 1.00)$ (OTM)	Count		351				299				241		
	MPE (%)	−2.021	−15.641	−21.253	−28.855	−0.688	4.292	−5.382	−28.834	−0.183	9.063	−8.15	−24.484
	MSE	0.127	1.150	1.851	2.526	0.521	2.712	2.685	4.631	5.193	11.681	5.346	5.218
	MAPE (%)	10.390	37.253	37.564	48.761	11.254	33.690	30.258	31.554	24.518	46.614	25.458	24.711
$K/S_t \in [1.00, 1.15)$ (ITM)	Count		331				262				254		
	MPE (%)	0.389	0.817	−3.358	9.457	−0.960	−4.337	−1.861	−1.856	−7.996	−9.825	−7.658	−4.303
	MSE	0.202	0.405	1.513	3.625	0.328	1.928	2.358	3.182	2.748	7.835	5.865	3.856
	MAPE (%)	3.336	5.780	5.632	17.023	3.470	9.756	5.861	12.354	9.309	18.275	10.843	10.473
$K/S_t \geq 1.15$ (DITM)	Count		239				523				566		
	MPE (%)	−0.566	−0.571	−0.865	5.747	−0.662	−1.706	−0.952	2.997	−2.372	−3.535	−2.536	2.041
	MSE	0.226	0.172	1.263	2.547	0.489	0.727	1.213	1.924	1.118	2.098	2.253	2.040
	MAPE (%)	1.589	1.822	1.832	5.899	1.845	2.250	1.925	3.928	2.623	3.811	3.531	3.624

Note: each reported value is for a particular combination of moneyness and time to expiration. Three independent simulations are carried out, while 10,000 underlying price paths are generated in each simulation. The first row reports the number of put options with the corresponding combination of moneyness and time to expiration. The remaining rows show the statistic results of the MPE, RMSE, and MAPE for each combination. The total number of options analyzed is 4430, the lowest moneyness is $40/91.66 = 0.436$, the highest moneyness is $155/79.66 = 1.946$, and the time to expiration is in between 16 and 357 days.

increases with time to expiration. Second, from Tables 5 and 6, based on the MPE, IBM calls are overall underpriced by the RMEL method as are IBM puts, with the exception of the case of ITM and short term to expiration. Third, the RMEL method overall outperforms methods of AA10.

Table 5 compares IBM calls priced by our methods RMEL, Liu10, and AA10. The method of RMEL shows a negative pricing bias in all combinations of moneyness and time to expiration, whereas Liu10 produces a positive bias when the option is OTM-short or ITM-long and AA10 also has two positive bias in the cases of DITM-short and ITM-short. Second, for each category, the RMEL method performs better than other methods by the important error measure MAPE although the MAPE for the RMEL method is a little bit large (over 10%), for example, the MAPE from the RMEL method is nearly a half that from Liu10 in each category. Third, compared to the method AA10, using the measure MAPE, the errors from RMEL are overall smaller especially when option is OTM or DOTM. Finally, the methods of RMEL and AA10 apparently perform much better than Liu10 because the method of Liu10 has not used any other constraint except the necessary martingale constraint.

For IBM puts, in addition to two methods above, the benchmark valuation method FD here is also compared with RMEL. First, as reported in Table 6, RMEL method produces a negative bias in 12 categories, with the exception of ITM-short; AA10 exhibit all negative bias; Liu10 has 4 positive bias in the cases of DOTM-long, OTM-long, OTM-medium, and ITM-short; and FD has 4 positive bias for all DITM options and ITM-short options. It is understandable for the methods of RMEL, Liu10, and AA10 to produce negative bias in most of 12 categories since the least-squares algorithm provides lower bounds for American puts. Second, the magnitude of pricing error decreases with moneyness for all methods. Third, FD is fairly accurate and outperforms Liu10 for the ITM-long and DITM-long cases. These results are consistent with market behaviour, since the market seems to have placed a premium on OTM puts ever since the 1987 market crash. Fortunately, RMEL performs much better than FD, even in the cases of ITM-long and DITM-long. In addition, RMEL absolutely dominates Liu10 since Liu10 has no other constraint. Compared to AA10, from the measure MAPE, RMEL outperforms AA10 in all categories. Furthermore, all the MAPE errors from RMEL are below 10% for both the ITM and DITM cases, even reaching 1.589% for DITM-short. For other cases over 10%, it is understandable and acceptable if considering the reasons below, in the IBM option data, the price for DOTM puts is very low and the bid-ask spread is relatively quite large especially for DOTM-short options.

In summary, the empirical results again illustrate that the RMEL method produces much smaller pricing errors than Liu10 and overall outperforms method of AA10 for IBM call options. The RMEL method is more stable for IBM call options from the measure MPE and can effectively estimate call prices with a reasonable pricing error. For IBM puts, the magnitudes of the pricing bias from RMEL and AA10 are much lower than those from both Liu10 and FD methods and RMEL is better than AA10. The RMEL method also produces more accurate values for IBM puts, especially when the put option is ITM or DITM. Empirical analysis suggests that on the whole, RMEL outperforms Liu10, AA10, and FD. Meanwhile, it should be pointed out that the RNM constraints used in RMEL method and the option constraint in AA10 actually contain some more useful information so that both methods greatly outperform the method of Liu10.

5. Conclusion

This paper introduces an ideally extended RNMs-constrained entropic least-squares valuation method which improves the nonparametric valuation technique to price American options. Our RMEL approach uses the RNMs recovered from a much smaller set of option data as constraints to generate a better estimate of RND as the pricing measure and then incorporates it into tractable Monte Carlo techniques to price American options.

The RNMs in our valuation approach can be estimated using several call options, and we derive the general expression for extracting the RNMs. These RNMs play a significant role in deriving a better RND, owing to their ability for capturing market information without imposing any underlying structural assumption. Compared with other existing entropic valuation methods, this is an outstanding feature for the RMEL method.

With the extracted RNMs as constraints, we establish the RNMs-constrained entropy valuation framework and by solving this RNMs-constrained entropy problem, we obtain a discrete risk-neutral distribution as the unique pricing measure. Finally, the optimal exercise strategies are also achieved via the least-squares Monte Carlo algorithm and consequently the pricing algorithm of American options are obtained.

We evaluate the usefulness of our method and compare its performance in simulation environments in a number of ways with the method of Liu [4], who extends the canonical valuation to price American options. First, the results of extracting RNMs suggest that our moment estimates match rather well with the theoretical values in simulation experiments. Second, the estimated prices using the RMEL method are fairly close to the "true" prices for American call and put options in the cases of both growth rates. Consistent with the finding of Gray and Newman [13], all price estimates are less than the "true" prices for both call and put options. But the method of Liu10 method persistently exhibits a positive bias. Furthermore, the price bias of the RMEL method is more stable for two growth rates. By comparing the absolute difference between the estimated and "true" prices, the overall accuracy of our approach is higher than that of Liu10 and particularly dominant in pricing American puts. Finally, it is not unreasonable to imagine that the RMEL method nests the method of Liu10 as special cases. We also empirically test our valuation approach and compare its performance with the methods of Liu10, AA10, and FD using the IBM options data. The results show that the pricing bias by our RMEL approach is lower than that by the method of AA10 for almost all the levels of moneyness and time to maturity, and the methods of RMEL and AA10 largely outperform the Liu10 and FD methods, whether for call options or put options. For IBM calls, the pricing errors of the RMEL method equal nearly half of that of Liu10 and the RMEL method outperforms AA10. With regard to IBM put option valuation, Liu10 performs much better than the FD when the time to maturity is short, whereas the FD outperforms Liu10 across moneyness with long maturity, but their results including those from AA10 are worse than that of RMEL method. Meanwhile, our method significantly dominates Liu10 and FD methods, especially for ITM and DITM; the RMEL method can price put options very well with a rather high accuracy. In brief, all the results suggest again that our approach performs well and much better than some benchmark approaches.

In summary, to generate a better estimate of the risk-neutral distribution of the underlying assets for pricing American options, an entropy valuation with moment constraints that can be easily constructed using a small number of options is developed and tested in simulations and with IBM option data. We demonstrate that our method prices American options quite well and outperforms several benchmarks and nonparametric approaches. In principle, the RMEL method can be applied in any other artificial circumstances and real markets due to its ability to effectively capture information in the option market to generate a better estimate of the risk-neutral measure. Also the RMEL approach is applicable to other path-dependent options. Further work is required to investigate the relation between the number of the RNM constraints and pricing accuracy, and another direction is to address the numerical solution problem when more moment constraints are incorporated into the valuation framework.

Appendices

A. Proof of Lemma 1

Let (Ω, F_t, π^*) be the probability space over time interval $[t, T]$ with filtration F_t and let $\Phi_{R_{t,T-t}}(x) = E_{\pi^*}(e^{ix\log(R_{t,T-t})})$ be the characteristic function of the underlying asset return $\log(R_{t,T-t})$, where $\log(R_{t,T-t}) \equiv \log(S_T/S_t)$ and S_t is known at time t; i is the imaginary unit under the martingale measure π^*. We begin with deriving the analytic form of $\Phi_{R_{t,T-t}}(x)$.

Defining a twice-continuously differentiable function with respect to S_T,

$$f(S_T) = e^{ix\log(S_T/S_t)}. \tag{A.1}$$

By the second-order version of Taylor's Theorem with integral remainder (e.g., Dudley [14, pp.522]), we have

$$\begin{aligned} f(S_T) &= f(S_t) + f'(S_t)(S_T - S_t) + \int_{S_t}^{S_T} f''(K)(S_T - K)\,dK \\ &= f(S_t) + f'(S_t)(S_T - S_t) + \int_{S_t}^{S_T} f''(K)(S_T - K)^+ dK + \int_{S_T}^{S_t} f''(K)(K - S_T)^+ dK. \end{aligned} \tag{A.2}$$

By definition, $\Phi_{R_{t,T-t}}(x) = E_{\pi^*}(f(S_T))$. Given (A.2), the characteristic function $\Phi_{R_{t,T-t}}(x)$ can then be expressed as

$$\begin{aligned} \Phi_{R_{t,T-t}}(x) = {} & 1 + ix\left(\frac{E_{\pi^*}(S_T)}{S_t} - 1\right) \\ & - \left[\int_{S_t}^{\infty} \frac{x(x+i)}{K^2}\left(\frac{K}{S_t}\right)^{ix} E_{\pi^*}\left((S_T - K)^+\right) dK \right. \\ & + \int_0^{S_t} \frac{x(x+i)}{K^2}\left(\frac{K}{S_t}\right)^{ix} \\ & \left. \times E_{\pi^*}\left((K - S_T)^+\right) dK \right]. \end{aligned} \tag{A.3}$$

Under no arbitrage condition, $\Phi_{R_{t,T-t}}(x)$ can be further given by

$$\begin{aligned} \Phi_{R_{t,T-t}}(x) = {} & 1 + ix\left[e^{(r-q)(T-t)} - 1\right] \\ & - \left[\int_{S_t}^{\infty} \frac{x(x+i)}{K^2}\left(\frac{K}{S_t}\right)^{ix} e^{r(T-t)} C_t^E(T;K)\,dK \right. \\ & + \int_0^{S_t} \frac{x(x+i)}{K^2}\left(\frac{K}{S_t}\right)^{ix} \\ & \left. \times e^{r(T-t)} P_t^E(T;K)\,dK \right]. \end{aligned} \tag{A.4}$$

Given (A.4), the jth order RNM, $m_{t,T-t}(j)$, defined as $E_{\pi^*}([\log(R_{T-t})]^j)$, can then be calculated by $(1/i^j)(d^j[\Phi_{R_{t,T-t}}(x)]/dx^j)|_{x=0}$ $(j = 1, 2, 3, 4, \dots, J)$.

B. Proof of Theorem 3

Denote the characteristic functions of the $(T-t)$-period return, $\log(R_{t,T-t}) = \log(S_T/S_t)$ and the τ-period return, $\log(R_{t,\tau}) = \log(S_{t+\tau}/S_t)$, as $\Phi_{R_{t,T-t}}(x) = E_{\pi^*}(e^{ix\log(R_{t,T-t})})$ and $\Phi_{R_{t,\tau}}(x) = E_{\pi^*}(e^{ix\log(R_{t,\tau})})$, respectively. Then, by the assumption that the τ-period returns are independent under the risk-neutral measure $\hat{\pi}^*$,

$$\begin{aligned}
\Phi_{R_{t,T-t}}(x) &= E_{\pi^*}\left(e^{ix\log(R_{T-t})}\right) = E_{\pi^*}\left[\left(\frac{S_T}{S_t}\right)^{ix}\right] \\
&= E_{\pi^*}\left[\left(\frac{S_T}{S_{T-\tau}}\right)^{ix}\left(\frac{S_{T-\tau}}{S_{T-2\tau}}\right)^{ix}\left(\frac{S_{T-2\tau}}{S_{T-3\tau}}\right)^{ix}\cdots\left(\frac{S_\tau}{S_t}\right)^{ix}\right] \\
&= \left[E_{\pi^*}\left(R_{t,\tau}^{ix}\right)\right]^N,
\end{aligned} \tag{B.1}$$

or, equivalently, $\Phi_{R_{t,\tau}}(x) = [\Phi_{R_{t,T-t}}(x)]^{1/N}$.

As $m_{t,\tau}(1) = (1/i)(d[\Phi_{R_{t,\tau}}(x)]/dx)|_{x=0}$, we then have

$$\begin{aligned}
m_{t,\tau}(1) &= \frac{1}{i}\frac{d[\Phi_{R_{t,\tau}}(x)]}{dx}\bigg|_{x=0} \\
&= \frac{1}{i}\frac{1}{N}\left\{\left[\Phi_{R_{t,T-t}}(x)\right]^{(1/N)-1}\right\}\bigg|_{x=0}\frac{d[\Phi_{R_{t,T-t}}(x)]}{dx}\bigg|_{x=0} \\
&= \frac{m_{t,T-t}(1)}{N}.
\end{aligned} \tag{B.2}$$

Repeating the above differentiation procedures, the remaining formulas for $m_{t,\tau}(1)$, $m_{t,\tau}(2)$, $m_{t,\tau}(3)$, and $m_{t,\tau}(4)$ are immediately obtained.

C. Calculation of Integrals for Moments

Consider

$$\begin{aligned}
m_{t,T-t}(1) &= e^{(r-q)(T-t)} \\
&\quad - e^{r(T-t)}\left[\int_{S_t}^{\infty}\frac{1}{K^2}C_t^A(T;K)\,dK\right. \\
&\quad \left. + \int_0^{S_t}\frac{1}{K^2}P_t(T;K)\,dK\right] - 1, \\
m_{t,T-t}(2) &= 2e^{r(T-t)}\left[\int_{S_t}^{\infty}\frac{1-\ln(K/S_t)}{K^2}C_t^A(T;K)\,dK\right. \\
&\quad \left. + \int_0^{S_t}\frac{1-\ln(K/S_t)}{K^2}P_t(T;K)\,dK\right],
\end{aligned} \tag{C.1}$$

where $P_t(T;K) = C_t^A(T;K) + Ke^{-r(T-t)} - S_t e^{-q(T-t)}$.

We only discuss the calculation of the integrals in the first-order moment: $\int_{S_t}^{\infty}(1/K^2)C_t^A(T;K)dK$ and $\int_0^{S_t}(1/K^2)P_t(T;K)dK$. The remaining integrals appearing in other moment equations can be solved analogously.

C.1. Calculation of Integrals

C.1.1. $\int_{S_t}^{\infty}(1/K^2)C_t^A(T;K)dK$. First, the interval of this integration $[S_t,\infty)$ is divided into three subintervals: $[S_t, K_{\max}]$, $[K_{\max}, K_\infty)$, and $[K_\infty,\infty)$, where $K_{\max}$ is the maximum available strike price in the given data, whereas K_∞ is a much larger number so that a call option with strike prices in $[K_\infty,\infty)$ is valueless. This study sets K_∞ equal to $5K_{\max}$.

Second, a numerical integration method, the trapezoidal rule, is employed to compute the integrals with the first two intervals:

$$\begin{aligned}
&\int_{S_t}^{K_{\max}}\frac{1}{K^2}C_t^A(T;K)\,dK \\
&\quad \approx \frac{1}{2}\left[\sum_{i=1}^{m}\left(\frac{1}{K_{i-1}^2}C_t^A(T;K_{i-1}) + \frac{1}{K_i^2}C_t^A(T;K_i)\right)\Delta K\right],
\end{aligned} \tag{C.2}$$

where $\Delta K = (K_{\max} - S_t)/m$, $K_i = S_t + i\Delta K$, for $i \in [0,m]$. m denotes the number of nonoverlapped subintervals of equal length and $m = 80$ in this study[20].

In a similar spirit, the integral with the second subinterval is given as

$$\begin{aligned}
&\int_{K_{\max}}^{K_\infty}\frac{1}{K^2}C_t^A(T;K)\,dK \\
&\quad \approx \frac{1}{2}\left[\sum_{i=1}^{m}\left(\frac{1}{K_{i-1}'^2}C_t^A\left(T;K_{i-1}'\right) + \frac{1}{K_i'^2}C_t^A\left(T;K_i'\right)\right)\Delta K'\right],
\end{aligned} \tag{C.3}$$

where $\Delta K' = (K_\infty - K_{\max})/m$, $K_i' = K_{\max} + i\Delta K'$ for $i \in [0,m]$.

Given the negligible integrand in interval $[K_\infty,\infty)$, we obtain

$$\begin{aligned}
&\int_{S_t}^{\infty}\frac{1}{K^2}C_t^A(T;K)\,dK \\
&\quad \approx \frac{1}{2}\left[\sum_{i=1}^{m}\left(\frac{1}{K_{i-1}^2}C_t^A(T;K_{i-1}) + \frac{1}{K_i^2}C_t^A(T;K_i)\right)\Delta K\right] \\
&\quad + \frac{1}{2}\left[\sum_{i=1}^{m}\left(\frac{1}{K_{i-1}'^2}C_t^A\left(T;K_{i-1}'\right) + \frac{1}{K_i'^2}C_t^A\left(T;K_i'\right)\right)\Delta K'\right].
\end{aligned} \tag{C.4}$$

C.1.2. $\int_0^{S_t}(1/K^2)P_t(T;K)dK$. This integral can be computed by repeating the above steps. Note that the three subintervals are $[0, K_0]$, $[K_0, K_{\min}]$, and $[K_{\min}, S_t]$, where $K_{\min}$ is the minimum available strike price in the given data, whereas K_0 is a very smaller number so that a put option with strike prices in $[0, K_0]$ is valueless. In this study, K_0 is set to the value of $0.2K_{\min}$. We then have

$$\begin{aligned}\int_0^{S_t} \left(\frac{1}{K^2}\right) P_t(T;K)\,dK &\approx \frac{1}{2}\left[\sum_{i=1}^{m}\left(\frac{1}{K_{i-1}^2} P_t(T;K_{i-1}) + \frac{1}{K_i^2} P_t(T;K_i)\right)\Delta K\right] \\ &\quad + \frac{1}{2}\left[\sum_{i=1}^{m}\left(\frac{1}{K_{i-1}'^2} P_t\left(T;K_{i-1}'\right) + \frac{1}{K_i'^2} P_t\left(T;K_i'\right)\right)\Delta K'\right],\end{aligned} \tag{C.5}$$

where $\Delta K = (K_{\min} - K_0)/m$, $\Delta K' = (S_t - K_{\min})/m$, $K_i = K_0 + i\Delta K$, and $K_i' = K_{\min} + i\Delta K'$ for $i \in [0, m]$.

C.2. Curving-Fitting for Unavailable Option Prices. As shown from the above integrals, the required strike prices are beyond the range of the available data. The option prices corresponding to such strike prices need to be inferred from the given option prices. A curve-fitting method is adapted to handle this restriction by first constructing a set of implied volatilities and then inferring the required set of option prices. The operational steps are as follows.

(1) Calculate implied volatilities using the Black-Scholes formula based on the given set of option (either simulated or observed from the market) with trading date t and expiry date T [21].

(2) Use a cubic spline function to interpolate the implied volatilities and infer implied volatilities at K_i and K_i' located in $[S_t, K_{\max}]$ or $[K_{\min}, S_t]$ from the fitted function.

(3) Inversely map the inferred volatilities, again using the Black-Scholes formula, to obtain the required option prices $C_t^A(T;K)$, $C_t^A(T;K')$, $P_t(T;K)$, and $P_t(T;K')$ over the intervals of $[S_0, K_{\max}]$ and $[K_{\min}, S_t]$.

(4) Apply two implied volatilities at the truncated endpoints K_0 and K_∞ to the intervals $[K_{\max}, K_\infty]$ and $[K_0, K_{\min}]$ to extrapolate the option prices.

Recall that in the simulation experiment, we generate a sample of 8 call options to estimate the RNMs. The other options required by calculating the integrals are referred to by the method discussed above.

Conflict of Interests

The authors declare that there is no conflict of interests regarding the publication of this paper.

Acknowledgments

The authors thank Wolfgang Buehler, David Feldman, Robert Kohn, Donald Lien, Jun Liu, and Qiang Liu for their valuable discussions and comments as well as seminar participants at the 2011 FMA annual meeting, the 24th AFB conference, and 2013 CFR conference. Xiaoke Xie is thanked for proofreading this paper. The authors are truly grateful to the anonymous reviewers for their helpful comments. The editorial support from Editor Fenghua Wen is sincerely appreciated without any reservation. This work is supported by the National Natural Science Foundation of China (no. 71301132), by the Fundamental Research Funds for the Central Universities, by the Sichuan Provincial Department of Education Research Project (14ZB0448), and by the ARC Discovery Grant (DP120104014).

Endnotes

1. See, for example, Jarrow and Rudd [15], Bahra [16], Aït-Sahalia and Lo [17], and Jackwerth [18] for a comprehensive review. See, for example, Bates [19], Grundy [20], Jackwerth and Rubinstein [21], Melick and Thomas [22], Bakshi and Madan [23], Britten-Jones and Neuberger [24], Bakshi et al. [9], Jiang and Tian [25], Kang and Kim [26], Chang et al. [27], and Diavatopoulos et al. [28] for methodologies and application issues.

2. For example, Kang and Kim [26] report that option prices exactly reflect market expectations of abnormal or rare future asset market events and return distributions. Jiang and Tian [25] show that the implied volatility simply from OTM European call options subsumes all information contained in Black-Scholes implied volatility and past realized volatility (Chiras and Manaster [29] and Day and Lewis [30]).

3. Bakshi et al. [9] use a Taylor expansion to obtain the expressions for the first four moments, which can be proved and extended by using the characteristic function instead.

4. In this study, the underlying asset is set to pay no dividend in the simulation experiments and in the empirical section, any IBM call options violating the principle of not exercising early (see footnote 18) are removed. So the call options in both cases cannot be exercised early.

5. In the simulations, $q = 0$. In the empirical investigation, we find that almost all the IBM options satisfy the condition of discrete dividends.

6. Many empirical investigations (e.g., Zivney [31] and Poteshman and Serbin [32]) show that call options with such low moneyness (S_t/K) are not being exercised before expiration in most cases. Broadie et al. [33] show empirically that for American calls of OEX 100 index options, most of the early exercises occur during the last few days prior to the expiration month only when the moneyness is close to 1.

7. Note that the idea of fitting option prices is suggested, in particular, by Jiang and Tian [25], who provide the theoretical bounds on truncation errors. In our study, the interval of integration $[0, S_t]$ is split into two subintervals, $[0, K_{\min}]$ and $[K_{\min}, S_t]$, and the other interval $[S_t, +\infty)$ is split into $[S_t, K_{\max}]$ and $[K_{\max}, +\infty)$, where $K_{\min}$ is the minimum value of strike price and

$K_{\max}$ is the maximum value. For the integrals over the intervals $[K_{\min}, S_t]$ and $[S_t, K_{\max}]$, we use a cubic spline function to interpolate the implied volatilities to obtain the fitted option prices. In addition, we use two constants (endpoint implied volatilities) to extrapolate the option prices for the other two intervals beyond the available range. The extrapolation is truncated at the strike points, denoted as K_0 and K_∞. The first (second) truncation point is very small (large), say, close to zero (an arbitrary large number), so that the corresponding options $C^A(T;K)$ $(P(T;K))$ with strike prices in the interval $[0, K_0]$ $((K_\infty, +\infty))$ are valueless. The integrals over the corresponding intervals therefore tend to be zero. For further details, see Appendix C.2.

8. When approximating the integrals using a numerical integration method, two types of Riemann integral sum are utilized. Specifically, Riemann sums of the left endpoints as well as the right endpoints are first calculated, and their average is then used as an approximation of the required integral. In this study, each of the intervals involved in integration is divided into a number m (e.g., $m = 80$) of equidistant subintervals (see Appendix C.1 for details).

9. When the empirical distribution is uniform, the Kullback-Leibler information criterion (Kullback and Leibler [34]) is equivalent to the principle of maximum entropy.

10. Note that $R_{t-(I-i+1)\tau,\tau}$ are the historical returns. We recover the RNMs using option data at time t and estimate the RND using the τ-period historical returns starting at time $t - I\tau$ up to time t.

11. In our article, λ^* is calculated via the Nelder-Mead simplex search method by setting the initial value λ_0 equal to the optimal value λ_0^* obtained using quasi-Newton method. That is, λ_0^* is first computed via quasi-Newton method, by setting initial value to be zero vector and then used as an initial value when calculating λ^*. Theoretically, Nelder-Mead simplex search method is more stable, while the frequently used quasi-Newton method is faster. For discussion about the solution, see Agmon et al. [7] and Mead and Papanicolaou [35].

12. Note that the asset prices in the basis functions should be normalized by the strike price to avoid numerical scaling issues. Moreover, to balance computational time and precision, Stentoft [11] suggests that the Legendre polynomial family with two or three simple polynomial basis functions seems to work better and is computationally less demanding than other orthogonal polynomial families, such as the Laguerre family proposed by Longstaff and Schwartz [5].

13. The dividend is not considered here for the impartiality of comparison.

14. In this simulation experiment, we just compare RMEL method with that of Liu [4] which has no other constraint, since the results not reported here show that RMEL method performs similarly to the methods of Alcock and Auerswald [6]. The reason for this might be due to that the simulation setting is based on the GBM process so that theoretically the constraints used in those two methods can determine the same risk-neutral distribution for the underlying asset's return.

15. Here $I = 365$ is used as did in Liu [4]; we can also choose I more than 365. The idea is to use the information as recent as possible. If I is too large, for example, over 70,000 historical time series data are required for obtaining the RND in Alcock and Auerswald [6], practically the data from the real market may be outdated or they may be infeasible to be collected.

16. In our empirical investigation discussed in Section 4, the minimum number of options with different strike prices is 8 (with trading date August 21, 2008 and expiration date September 19, 2008) and the maximum number is 22 (e.g., options with trading date December 16, 2008 and expiration date April 17, 2009). Further, Buchen and Kelly [8] suggest that it is sufficient even if the number is 3 in their study.

17. Moneyness is defined to be S_t/K for call options and K/S_t for put options.

18. Several filters are applied to the sample of data prior to conducting our empirical analysis. First, data with market prices less than \$0.05 are excluded. Second, the prices of put (call) options should theoretically increase (decrease) with strike prices. Data violating this rule are discarded. Third, any call options violating the principle of not exercising early ($D_i \le K[1 - e^{-r(t_{i+1}-t_i)}]$), where D_i is the dividend payment at time t_i, see Hull [12, pp.299-300], are omitted. Fourth, call options with negative implied Black-Scholes volatility are removed from the sample.

19. In this paper, the MPE is calculated by dividing the estimated price minus the "true" price by the "true" price and multiplying by 100. It is then averaged over $n = 800$ independent simulations and is given as $(1/n)\sum_{i=1}^{n}[(c_i^{\text{estimated}} - c^{\text{true}})/c^{\text{true}}]\times 100$. The MSE is calculated by the mean-squared difference between the estimated price and the "true" price over all the simulations: $(1/n)\sum_{i=1}^{n}(c_i^{\text{estimated}} - c^{\text{true}})^2$. The MAPE is calculated by dividing the absolute difference between the estimated price and the "true" price by the "true" price and multiplying by 100. It is then averaged over all the simulations and is given as $(1/n)\sum_{i=1}^{n}(|c_i^{\text{estimated}} - c^{\text{true}}|/c^{\text{true}}) \times 100$.

20. A value of $m = 80$ here is sufficiently large to obtain an accurate approximation of the required integrals (also see Jiang and Tian [25], for another example). We facilitate a comparison by setting that $m = 50$ and find no significant difference.

21. Note that the Black-Scholes formula here is merely used as a tool to build a smooth nonlinear relation between volatility and option prices.

References

[1] M. Frittelli, "The minimal entropy martingale measure and the valuation problem in incomplete markets," *Mathematical Finance*, vol. 10, no. 1, pp. 39–52, 2000.

[2] M. Stutzer, "A simple nonparametric approach to derivative security valuation," *The Journal of Finance*, vol. 51, no. 5, pp. 1633–1652, 1996.

[3] E. T. Jaynes, "On the rationale of maximum-entropy methods," *Proceedings of the IEEE*, vol. 70, no. 9, pp. 939–952, 1982.

[4] Q. Liu, "Pricing American options by canonical least-squares Monte Carlo," *The Journal of Futures Markets*, vol. 30, no. 2, pp. 175–187, 2010.

[5] F. A. Longstaff and E. S. Schwartz, "Valuing American options by simulation: a simple least-squares approach," *The Review of Financial Studies*, vol. 14, no. 1, pp. 113–147, 2001.

[6] J. Alcock and D. Auerswald, "Empirical tests of canonical nonparametric American option-pricing methods," *The Journal of Futures Markets*, vol. 30, no. 6, pp. 509–532, 2010.

[7] N. Agmon, Y. Alhassid, and R. D. Levine, "An algorithm for finding the distribution of maximal entropy," *Journal of Computational Physics*, vol. 30, no. 2, pp. 250–258, 1979.

[8] P. W. Buchen and M. Kelly, "The maximum entropy distribution of an asset inferred from option prices," *Journal of Financial and Quantitative Analysis*, vol. 31, no. 1, pp. 143–159, 1996.

[9] G. Bakshi, N. Kapadia, and D. Madan, "Stock return characteristics, skew laws, and the differential pricing of individual equity options," *The Review of Financial Studies*, vol. 16, no. 1, pp. 101–143, 2003.

[10] P. Brandimarte, *Numerical Methods in Finance and Economics: A MATLAB Based Introduction*, Statistics in Practice, John Wiley & Sons, Hoboken, NJ, USA, 2nd edition, 2006.

[11] L. Stentoft, "Assessing the least squares Monte-Carlo approach to American option valuation," *Review of Derivatives Research*, vol. 7, no. 2, pp. 129–168, 2004.

[12] J. C. Hull, *Options, Futures, and Other Derivatives*, Pearson Prentice Hall, Upper Saddle River, NJ, USA, 7th edition, 2009.

[13] P. Gray and S. Newman, "Canonical valuation of options in the presence of stochastic volatility," *The Journal of Futures Markets*, vol. 25, no. 1, pp. 1–19, 2005.

[14] R. M. Dudley, *Real Analysis and Probability*, vol. 74 of *Cambridge Studies in Advanced Mathematics*, Cambridge University Press, Cambridge, Mass, USA, 2002.

[15] R. Jarrow and A. Rudd, "Approximate option valuation for arbitrary stochastic processes," *Journal of Financial Economics*, vol. 10, no. 3, pp. 347–369, 1982.

[16] B. Bahra, "Implied risk-neutral probability density functions from option prices: theory and application," Working Paper 66, Bank of England, 1997, http://ssrn.com/abstract=77429.

[17] Y. Aït-Sahalia and A. W. Lo, "Nonparametric estimation of state-price densities implicit in financial asset prices," *The Journal of Finance*, vol. 53, no. 2, pp. 499–547, 1998.

[18] J. C. Jackwerth, "Option-implied risk-neutral distributions and implied binomial trees: a literature review," *The Journal of Derivatives*, vol. 7, no. 2, pp. 66–82, 1999.

[19] D. Bates, "The crash of '87: was it expected? The evidence from options markets," *The Journal of Finance*, vol. 46, no. 3, pp. 1009–1044, 1991.

[20] B. D. Grundy, "Option prices and the underlying asset's return distribution," *The Journal of Finance*, vol. 46, pp. 1045–1069, 1991.

[21] J. C. Jackwerth and M. Rubinstein, "Recovering probability distributions from option prices," *The Journal of Finance*, vol. 51, no. 5, pp. 1611–1631, 1996.

[22] W. R. Melick and C. P. Thomas, "Recovering an asset's implied PDF from option prices: an application to crude oil during the Gulf crisis," *Journal of Financial and Quantitative Analysis*, vol. 32, no. 1, pp. 91–115, 1997.

[23] G. Bakshi and D. Madan, "Spanning and derivative-security valuation," *Journal of Financial Economics*, vol. 55, no. 2, pp. 205–238, 2000.

[24] M. Britten-Jones and A. Neuberger, "Option prices, implied price processes, and stochastic volatility," *The Journal of Finance*, vol. 55, no. 2, pp. 839–866, 2000.

[25] G. J. Jiang and Y. S. Tian, "The model-free implied volatility and its information content," *The Review of Financial Studies*, vol. 18, no. 4, pp. 1305–1342, 2005.

[26] B. J. Kang and T. S. Kim, "Option-implied risk preferences: an extension to wider classes of utility functions," *Journal of Financial Markets*, vol. 9, no. 2, pp. 180–198, 2006.

[27] C.-C. Chang, P.-F. Hsieh, and Y.-H. Wang, "Information content of options trading volume for future volatility: evidence from the Taiwan options market," *Journal of Banking and Finance*, vol. 34, no. 1, pp. 174–183, 2010.

[28] D. Diavatopoulos, J. S. Doran, A. Fodor, and D. R. Peterson, "The information content of implied skewness and kurtosis changes prior to earnings announcements for stock and option returns," *Journal of Banking and Finance*, vol. 36, no. 3, pp. 786–802, 2012.

[29] D. P. Chiras and S. Manaster, "The information content of option prices and a test of market efficiency," *Journal of Financial Economics*, vol. 6, no. 2-3, pp. 213–234, 1978.

[30] T. E. Day and C. M. Lewis, "Stock market volatility and the information content of stock index options," *Journal of Econometrics*, vol. 52, no. 1-2, pp. 267–287, 1992.

[31] T. L. Zivney, "The value of early exercise in option prices: an empirical investigation," *Journal of Financial and Quantitative Analysis*, vol. 26, pp. 129–138, 1991.

[32] A. M. Poteshman and V. Serbin, "Clearly irrational financial market behavior: evidence from the early exercise of exchange traded stock options," *The Journal of Finance*, vol. 58, no. 1, pp. 37–70, 2003.

[33] M. Broadie, J. Detemple, E. Ghysels, and O. Torrès, "Nonparametric estimation of American options' exercise boundaries and call prices," *The Journal of Economic Dynamics and Control*, vol. 24, no. 11-12, pp. 1829–1857, 2000.

[34] S. Kullback and R. A. Leibler, "On information and sufficiency," *Annals of Mathematical Statistics*, vol. 22, pp. 79–86, 1951.

[35] L. R. Mead and N. Papanicolaou, "Maximum entropy in the problem of moments," *Journal of Mathematical Physics*, vol. 25, no. 8, pp. 2404–2417, 1984.

Hindawi Publishing Corporation
Discrete Dynamics in Nature and Society
Volume 2014, Article ID 170921, 11 pages
http://dx.doi.org/10.1155/2014/170921

Research Article

Dynamics of Foreign Exchange Networks: A Time-Varying Copula Approach

Gang-Jin Wang,[1,2] Chi Xie,[1,2] Peng Zhang,[1] Feng Han,[3] and Shou Chen[1,2]

[1] *College of Business Administration, Hunan University, Changsha 410082, China*
[2] *Center of Finance and Investment Management, Hunan University, Changsha 410082, China*
[3] *China Merchants Bank, Shenzhen 518067, China*

Correspondence should be addressed to Chi Xie; xiechi@hnu.edu.cn

Received 11 March 2014; Accepted 16 April 2014; Published 6 May 2014

Academic Editor: Fenghua Wen

Based on a time-varying copula approach and the minimum spanning tree (MST) method, we propose a time-varying correlation network-based approach to investigate dynamics of foreign exchange (FX) networks. In piratical terms, we choose the daily FX rates of 42 major currencies in the international FX market during the period of 2005–2012 as the empirical data. The empirical results show that (i) the distributions of cross-correlation coefficients (distances) in the international FX market (network) are fat-tailed and negatively skewed; (ii) financial crises during the analyzed period have a great effect on the FX network's topology structure and lead to the US dollar becoming more centered in the MST; (iii) the topological measures of the FX network show a large fluctuation and display long-range correlations; (iv) the FX network has a long-term memory effect and presents a scale-free behavior in the most of time; and (v) a great majority of links between currencies in the international FX market survive from one time to the next, and multistep survive rates of FX networks drop sharply as the time increases.

1. Introduction

Financial markets are accounted as complex dynamical systems with large quantities of interacting unties [1, 2]. Financial agents usually interact with each other and their interbehaviors change over time, which means that the interbehaviors are dynamics and widely found in economics and finance [3, 4]. To capture the interactive behaviors or cross-correlations among heterogeneous entries in financial markets, many scholars generally resort to a powerful analytical tool, namely, correlation network-based methods, which include the minimum spanning tree (MST) approach proposed by Mantegna [5], the correlation threshold methods developed by Boginski et al. [6] and Onnela et al. [7], and the approach of planar maximally filtered graph (PMFG) designed by Tumminello et al. [8]. The network analysis idea has been widely applied in financial markets, such as stock markets [9–14] and foreign exchange (FX) market [15–20]. Among correlation network-based approaches, the MST method is often preferred because of its robustness and simplicity [10]. However, the MST method and its improvements ignore the volatiles and nonlinearities of financial time series. That is to say, they cannot really detect the dynamic interbehaviors among different financial agents in financial markets. Therefore, the purpose of this paper is to propose a dynamic correlation network-based approach by combining a time-varying copula method and the MST approach for studying the dynamic topology and market natures of financial networks. In practical terms, we focus our study on networks' dynamics of the international FX market because it is the biggest and most liquid financial market where foreign currencies are traded [21].

The motivations that led us to combine the two aforementioned methods to investigate dynamics of FX networks can be summed up as follows. On the one hand, the MST and its improvements are usually used to identify the clustering behavior and dominant currencies in the FX network. To examine the dynamic behavior of the network, pervious works often employ a rolling window analysis, such as [10, 22]. However, some drawbacks are found in the dynamic

MSTs using a rolling window analysis as follows. (i) The choice of parameters of the rolling window is dependent on the scholars' preference; that is, the window width and step length are selected arbitrarily [23]. For example, Onnela et al. [10] set the size of window as four calendar years (approximately 1000 trading days), while Song et al. [22] fix the length of window as 1250 trading days. (ii) In the MST method, the cross-correlation coefficient between two financial units is usually measured by the Pearson's correlation coefficient (PCC) that is a linear correlation method. Nevertheless, the PCC cannot quantify the nonlinear relationship between two heterogeneous entries [21] and ignores financial variables' volatile and nonnormality features [24]. It should be noted that some works attempt to apply other dynamic approaches in the MST. For example, Lyócsa et al. [23] employ the dynamic conditional correlations (DCC) multivariate generalized autoregressive conditional heteroscedasticity (MV-GARCH) approach to construct the MST for the US stock market. Trancoso [25] uses the Baba-Engle-Kraft-Kroner (BEKK) model to develop the conditional correlation matrix and apply it in the dynamic network analysis. However, Lyócsa et al. [23] and Trancoso [25] assume that the financial variables obey the normal distribution and neglect their nonnormality characteristics.

On the other hand, copula methods proposed by Sklar [26, 27] are a widely useful tool for deriving joint distributions given the marginal distributions, especially when the variables follow nonnormal distributions [28]. Besides, copulas can be employed to investigate the dependence beyond the linear cross-correlation by the PCC and allow for a time-varying nonlinear analysis. Moreover, copulas can be supplied as a powerful analytical instrument to measure dynamic dependence structures between financial variables. In a word, copulas have better properties and more advantages (see [29, 30]) than the traditional linear correlation methods and attract many scholars to use them in various finance applications [31–37]. For instance, Patton [35] constructs time-varying copula models to examine the dependence between two FX rates, that is, Deutsche Mark/US Dollar (DM/USD) and Japanese Yen/US Dollar (JPY/USD). He also makes a comparison between copulas and GARCH models and finds that the former can better describe the dependence or cross-correlation of FX rates than the latter. Diks et al. [36] use several copula models to analyze the dependence among five currencies (i.e., Canadian Dollar (CAD), Swiss Franc (CHF), European Euro (EUR), British Pound (GBP), and JPY) against USD and show that the Student's t-copula model is evidently superior to the Gaussian, Gumbel, and Clayton copula models. Dias and Embrechts [37] investigate the dependence between EUR/USD and JPY/USD from October 1, 2000, to October 1, 2008, by employing the time-varying copula-GARCH models. Their empirical results suggest that the dependence between the two currencies is dynamic and a time-varying copula approach with given correlation specifications has better outcomes than some conventional dynamic methods (e.g., BEKK).

In consideration of the above-mentioned motives, based on a time-varying copula approach and the MST method, we aim to construct time-varying FX networks and analyze their topological dynamics and market properties. We choose 42 major currencies' daily FX rate series in the international FX market during the years 2005–2012 as the empirical data. In empirical process, we first use a time-varying copula to calculate the dynamic cross-correlation coefficients ρ_t among different currencies. More specifically, we adopt an AR(p)-GARCH(1,1)-t model to characterize the marginal distribution of returns for FX rates and then estimate the dependence parameters of the time-varying Student's t-copula model and obtain time-varying cross-correlation coefficients. Next, on the basis of time-varying cross-correlation coefficients, we construct time-varying cross-correlation matrices (CMs) $\mathbf{C}_t$ for 42 major currencies in the international FX market. Then, we transform the time-varying CMs into time-varying FX networks by the MST approach. Finally, we examine topological dynamics and statistic features for time-varying FX networks.

The remainder of the paper is organized as follows. Section 2 represents the empirical data. A time-varying correlation network-based approach by combining a time-varying copula model with the MST method is described in Section 3. In Section 4, the time-varying FX networks are constructed and main empirical results are showed. Some conclusions are drawn in Section 5.

2. Data Set

As for the empirical data set, we choose the daily FX rates of 42 major currencies in the international FX market from January 4, 2005, to December 31, 2012. Following Jang et al. [18] and Wang et al. [21], we select the special drawing right (SDR) as the numeraire. The 42 currencies are from 7 different continents or regions. Their detailed information is showed as follows: (1) Africa: Egyptian Pound (EGP) and South African Rand (ZAR); (2) Asia: Chinese Renminbi (CNY), Indian Rupee (INR), Indonesian Rupiah (IDR), Japanese Yen (JPY), Malaysian Ringgit (MYR), Pakistani Rupee (PKR), Philippines Peso (PHP), Singapore Dollar (SGD), South Korean Won (KRW), Taiwanese Dollar (TWD), Thai Baht (THB), and Vietnamese Dong (VND); (3) Europe: British Pound (GBP), Czech Koruna (CZK), European Euro (EUR), Hungarian Forint (HUF), Icelandic Krona (ISK), Norwegian Krone (NOK), Polish Zloty (PLN), Romanian New Leo (RON), Russian Rubles (RUB), Swedish Krona (SEK), Swiss Franc (CHF), and Turkish New Lira (TRY); (4) Latin America: Argentine Peso (ARS), Brazilian Real (BRL), Chilean Peso (CLP), Colombian Peso (COP), Peruvian New Sole (PEN), and Mexican Peso (MXN); (5) Middle East: Bahrain Dinar (BHD), Israeli New Shekel (ILS), Jordanian Dinar (JOD), Kuwaiti Dinar (KWD), Saudi Arabian Riyal (SAR), and United Arab Emirates Dirham (AED); (6) North America: Canadian Dollar (CAD) and US Dollar (USD); (7) Pacific Ocean: Australian Dollar (AUD) and New Zealand Dollar (NZD). All the FX rates are obtained from the website of the Pacific Exchange Rate Service (http://fx.sauder.ubc.ca/data.html). We define the return of currency i on day t as $r_{i,t} = 100(\ln P_{i,t} - \ln P_{i,t-1})$, where $P_{i,t}$ is the daily FX rate of currency i on day t. During the analyzed period, each currency's returns have 2003 observations.

3. Methodology

In this section, we first introduce the time-varying copula model including the model for marginal distributions, the dynamic Student's t-copula model, and the estimation of parameters. After that, we propose the time-varying correlation network-based approach by the MST method.

3.1. Model for Marginal Distributions. Following Patton [35] and Dias and Embrechts [37], we use an AR(p)-GARCH(1,1)-t model, which considers the influences of asymmetric information, to characterize the returns' marginal distributions of currency i. The proposed model is defined as follows:

$$\begin{aligned} r_{i,t} &= \mu + \sum_{j=1}^{p} \phi_j r_{i,t-j} + \varepsilon_{i,t}, \\ \varepsilon_{i,t} &= \sigma_{i,t} z_{i,t}, \quad z_{i,t} \sim t(\nu), \\ \sigma_{i,t}^2 &= \omega_i + \alpha_i \varepsilon_{i,t-1}^2 + \beta_i \sigma_{i,t-1}^2, \end{aligned} \tag{1}$$

where ϕ_j are autoregressive (AR) coefficients, $z_{i,t}$ obeys a Student's t-distribution, ν is the degree of freedom, and $\sigma_{i,t}^2$ is the conditional variance of $\varepsilon_{i,t}$ with the following parameter restrictions: $\omega_i > 0$, $\alpha_i > 0$, $\beta_i > 0$, and $\alpha_i + \beta_i < 1$. To be simple and effective enough, we use an AR(1) process.

3.2. The Dynamic t-Copula Model. According to Diks et al. [36] and Dias and Embrechts [37], the dynamic t-copula model has a better capability for quantifying dynamic correlations in the FX rates data compared with Gaussian, Gumbel, and Clayton copula models. Therefore, in this paper, we employ the dynamic Student's t-copula model to capture time-varying cross-correlations in the international FX market. Let us briefly show the dynamic Student's t-copula model as follows.

For all $u_t, v_t \in [0,1]$, the density of dynamic Student's t-copula is defined by

$$\begin{aligned} & c_t(u_t, v_t \mid \theta_t, n) \\ &= \frac{1}{\sqrt{1-\theta_t^2}} \frac{\Gamma((n+2)/2)\Gamma(n/2)}{[\Gamma((n+1)/2)]^2} \\ &\times \Big[1 + \left(T_n^{-1}(u_t)^2 + T_n^{-1}(v_t)^2 - 2\theta_t T_n^{-1}(u_t) T_n^{-1}(v_t)\right) \\ &\quad \times \left(n\left(1-\theta_t^2\right)\right)^{-1}\Big]^{-(n+2)/2} \\ &\times \left[\left(1 + \frac{T_n^{-1}(u_t)^2}{n}\right)\left(1 + \frac{T_n^{-1}(v_t)^2}{n}\right)\right]^{(n+1)/2}, \end{aligned} \tag{2}$$

where $T_n^{-1}(\cdot)$ represents the inverse of the cumulative distribution function (CDF) of the Student's t-distribution with n degrees of freedom [39], $\theta_t \in (0,1)$ denotes the linear correlation coefficient, and $\Gamma(\cdot)$ is the Gamma function.

As proposed in [31], the time-varying dependence coefficients of the Student's t-copula is defined as

$$\rho_t = \widetilde{\Lambda}\left(\gamma_0 + \gamma_1 \rho_{t-1} + \gamma_2 \frac{1}{10} \sum_{j=1}^{10} T_n^{-1}(u_{t-j}) T_n^{-1}(v_{t-j})\right), \tag{3}$$

where $\widetilde{\Lambda}(x) = (1-e^{-x})/(1+e^{x})$ is the modified logistic function, which can guarantee that cross-correlation coefficients retain in the interval $(-1,1)$ at all times; γ_k $(k = 0,1,2)$ are unknown parameters.

3.3. Estimation of Copula Parameters. Following Wang et al. [34] and Lai et al. [40], we adopt the inference-function-for-margins (IFM) method rather than the exact maximum likelihood method to estimate the copula parameters, because the former needs less computation than the latter. The IFM approach proposed by Joe and Xu [41] is a two-step estimation, which can be used to estimate the parameters of marginal distributions and the copula functions separately. For more detailed advantages, see [34, 41]. The procedure of IFM is showed as follows.

Step 1. The marginal parameters are estimated by the maximum likelihood (ML) as

$$\widehat{\xi}_i = \arg\max \sum_{t=1}^{T} \ln f_{i,t}(z_{i,t} \mid \Omega_{t-1}; \xi_i), \tag{4}$$

where $f_{i,t}(\cdot \mid \cdot)$ denotes the conditional marginal density of currency i at time t, ξ_i is the marginal parameter of returns of currency i, and Ω_{t-1} is the past information set.

Step 2. Given ξ_i, suppose we have ξ_u and ξ_v; the copula parameters can be estimated as

$$\begin{aligned} \widehat{\xi}_c = \arg\max \sum_{t=1}^{T} \ln c_t\Big(F_{u,t}\left(z_{u,t} \mid \Omega_{t-1}; \widehat{\xi}_u\right), \\ F_{v,t}\left(z_{v,t} \mid \Omega_{t-1}; \widehat{\xi}_v\right); \xi_c\Big). \end{aligned} \tag{5}$$

3.4. The Time-Varying Correlation Network-Based Approach. After obtaining the time-varying cross-correlation coefficients between any two currencies by a time-varying copula approach, we can build $N \times N$ time-varying cross-correlation matrices (CMs) $\mathbf{C}_t$ with elements $\rho_t(i,j)$ for currencies i and j, where $1 \le i$ and $j \le N$ (in our case, $N = 42$). According to the idea of MST proposed by Mantegna [5], we transform time-varying CMs into the corresponding distance matrices $\mathbf{D}_t$ by a distance measure $d_t(i,j) = \sqrt{2(1-\rho_t(i,j))}$ that falls in the interval $[0,2]$ and meets the three axioms of the Euclidean distance. On the basis of time-varying distance matrices $\mathbf{D}_t$, we can obtain time-varying networks for studying the international FX market by using the Kruskal's algorithm [42], that is, time-varying MSTs link N currencies with $N-1$ edges. At each time t, the MST network extracts the most important information (e.g., the strongest cross-correlations among currencies) in the international FX market. The proposed time-varying correlation network-based approach can be used to examine dynamics of the international FX market over time.

To investigate dynamics of FX networks, we introduce some topological measures as follows. We use a quantity of *average path length* (APL) to quantify the MST network's density [43], which is defined by

$$\mathrm{APL}_t = \frac{2}{N(N-1)} \sum_{i=1,j>i}^{N} l_{ij}^t, \tag{6}$$

where l_{ij}^t is the length of the shortest path between two vertexes (currencies) i and j at time t [21].

The measure of *mean occupation layer* (MOL) proposed by Onnela et al. [9, 10], which can be employed to analyze the spread of nodes on the MST and characterize the density changes of the network, is defined as

$$\mathrm{MOL}_t(v_c) = \frac{1}{N}\sum_{i=1}^{N} \mathrm{lev}\left(v_i^t\right), \tag{7}$$

where v_c is the central vertex of the MST at time t and $\mathrm{lev}(v_i^t)$ defines the level of vertex v_i with reference to v_c, whose level is set as zero.

We introduce a concept of *maximum degree* $k_{\max}$, which is defined as the number of linkages of the central vertex in the MST [21, 43].

The scale-free behavior is widely found in different networks [10, 15, 21, 44, 45]. The scale-free network is such that the degree distribution of the network has a power-law tail; that is,

$$P(k) \sim k^{-\alpha}, \tag{8}$$

where $P(k)$ is the distribution function of vertex degrees k, and α is the exponent. We adopt a powerful tool developed by Clauset et al. [38] to estimate the power-law exponent and the corresponding P value. This tool combines ML fitting methods with goodness-of-fit tests using the Kolmogorov-Smirnov statistic and likelihood ratios.

4. Empirical Results

4.1. Statistics of Cross-Correlation Coefficients and Distances of MST. Before studying dynamics of FX networks, we first analyze statistical properties of cross-correlation coefficients and distances of MST for 42 currencies in the international FX market. The cross-correlation coefficient series contains $N(N-1)/2$ observations, at each time, while the distance set of MST only contains the $N-1$ most important links. In Figures 1 and 2, we present the time evolution graphs for four descriptive statistics (mean, standard deviation, skewness, and kurtosis) of cross-correlation coefficients and distances of MST, respectively. From each figure, it can be found that the four descriptive statistics vary over time and have a high volatile during the US subprime crisis and the 2008 world financial crisis. Especially in the period of June 2007 to July 2009, the international FX market (network) has stronger cross-correlations or smaller distances among

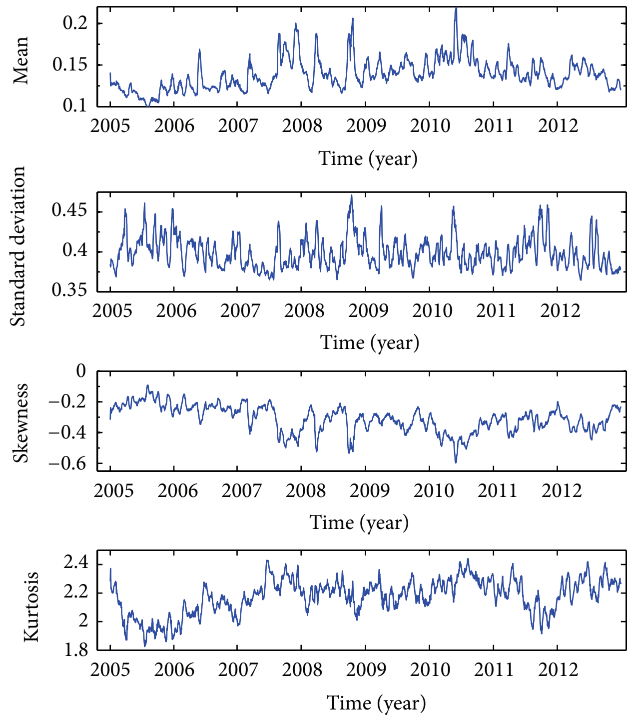

Figure 1: The mean, standard deviation, skewness, and kurtosis of cross-correlation coefficients of 42 currencies in the international FX market as functions of time.

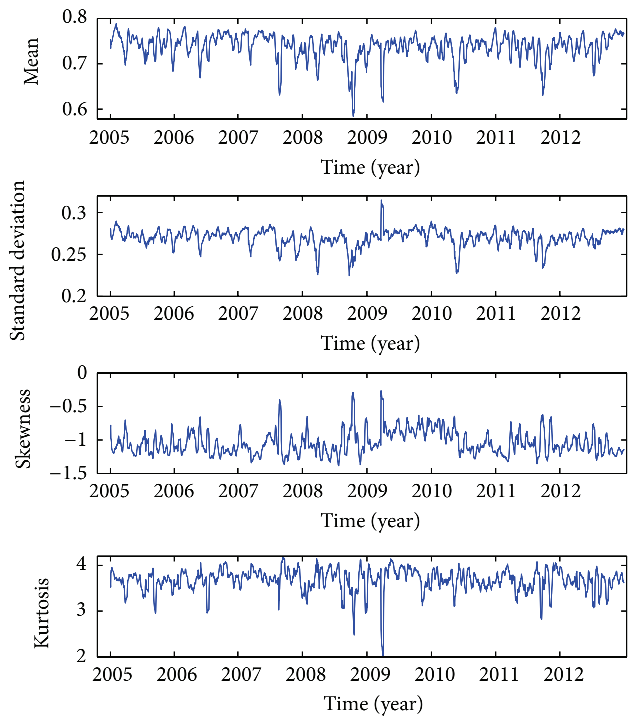

Figure 2: The mean, standard deviation, skewness, and kurtosis of distances of MST of 42 currencies in the international FX market as functions of time.

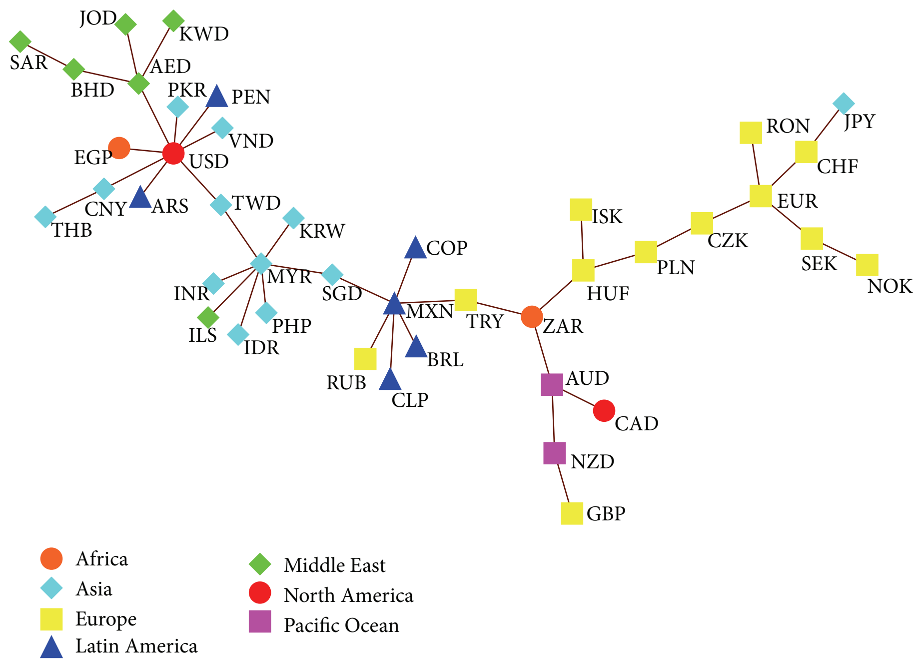

FIGURE 3: MST of 42 currencies in the international FX market on January 5, 2005, as a representative of the period of before financial crises.

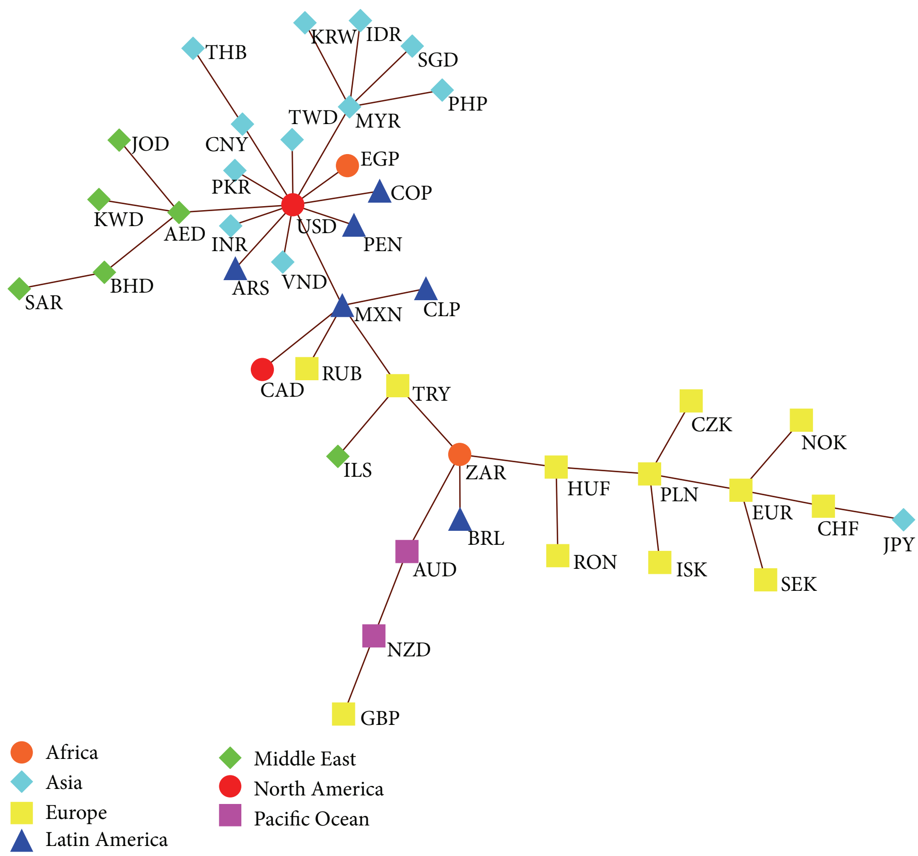

FIGURE 4: MST of 42 currencies in the international FX market on January 2, 2008, as a representative of the period of during financial crises.

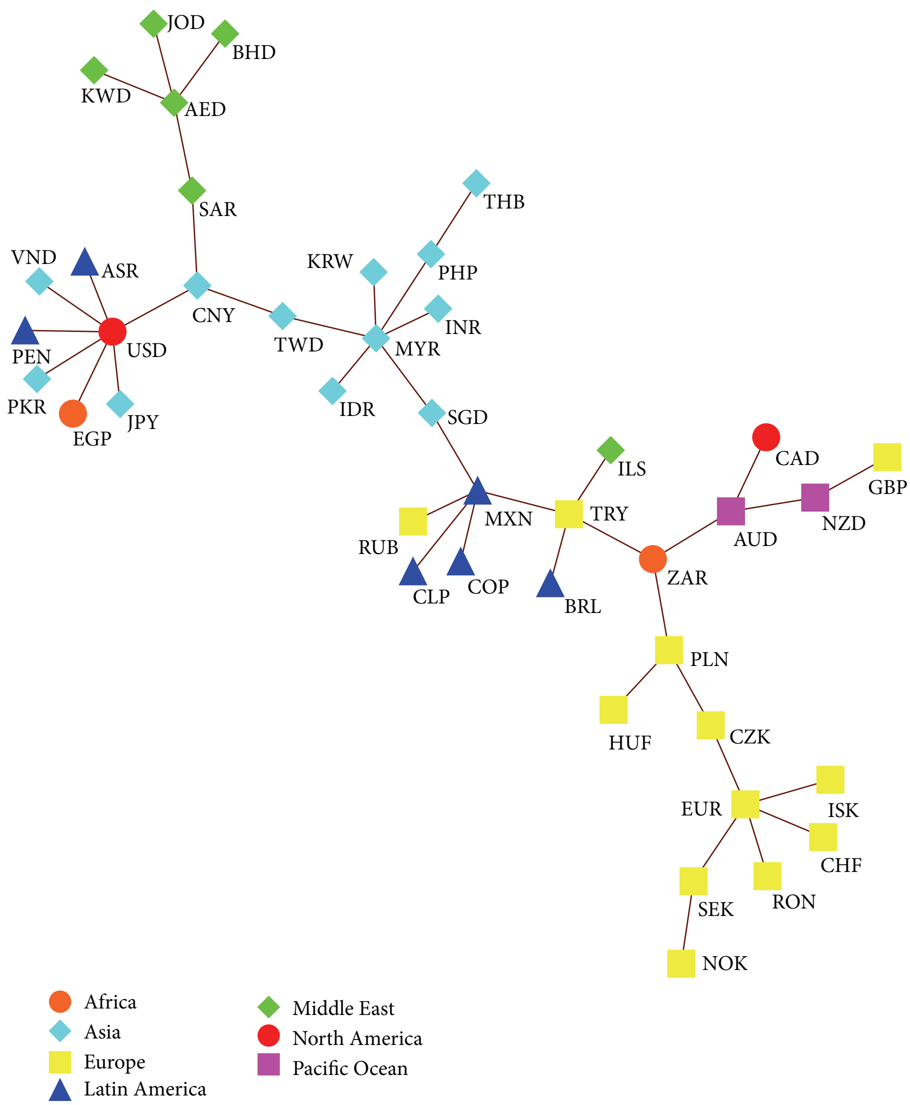

Figure 5: MST of 42 currencies in the international FX market on January 3, 2012, as a representative of the period of after financial crises.

currencies than other periods. This phenomenon confirms the proposal in [46] that the financial crisis often causes an increase of the market's cross-correlations. As shown in Figures 1 and 2, it can be found that the values of skewness of cross-correlation coefficients and distances at any time are less than 0, while values of kurtosis for most of time are not equal to 3. This finding implies that the distributions of cross-correlation coefficients (distances) in the international FX market (network) are fat-tailed and negatively skewed.

4.2. MST Results. Considering that financial crises have a strong influence on the international FX market, we choose three days (i.e., January 5, 2005; January 2, 2008; and January 3, 2012) as representatives of three periods of before, during, and after financial crises. We present the three MSTs of 42 currencies in the international FX market in Figures 3, 4, and 5, respectively. In each MST figure, currencies from the same continent (region) are marked with the same color and shape.

From Figure 3, which demonstrates the situation before financial crises, one can find that most of currencies are gathered together according to geographical distributions, such as the European cluster, Asian cluster, Middle Eastern cluster, and Latin American cluster with EUR, MYR, AED, and MXN at their centers, respectively. In the FX network, the most important cluster is the international cluster with USD at its hub, which is directly or indirectly connected with currencies from Asia, Middle East, Latin America, and Africa. This outcome shows that USD is the predominant world currency. An interesting cluster is composed of GBP from Europe, NZD and AUD from Pacific Ocean, CAD from North America, and ZAR from Africa. We denote this cluster as the Commonwealth cluster because countries of the five currencies are members of the Commonwealth of Nations. In the MST network, we find that three major currencies in the international FX market, namely, EUR, CHF, and JPY are linked together.

As illustrated in Figure 4, during the global financial crisis, it can be observed that a lot has changed in the FX network. Notable changes are that USD becomes more centered in the MST, and the Latin American cluster and Asian cluster almost broke and their currencies directly or indirectly shift to USD. That is to say, during the financial crisis, most currencies from Asia, Middle East, and Latin America are tightly linked to USD, which indicates that the financial crisis can lead to a huge comovement effect among currencies in the international FX market. Although the European cluster and the Commonwealth cluster still remain in the network, their structure and currencies' position changed as a result of the influence by the financial crisis.

Compared with the MSTs in Figures 3 and 4, as drawn in Figure 5, the FX network recovered to the precrisis state but its structure and currencies' position have a lot of changes. For instance, the Asian cluster and Latin American cluster are formed again. At this point, the Commonwealth cluster has reappeared in the network with the same structure and position of their currencies as they appeared in Figure 3. One can see a remarkable change that JPY deviates from the European cluster and connects to the international cluster with USD at its centre. It is interesting to note that CNY links with USD, TWD, and SAR. One possible interpretation of the linkages is that US, Taiwan, and Saudi Arabia are China's important and top trading partners.

From Figures 3, 4, and 5, we can obtain some conclusions as follows: (i) USD is the predominant world currency and has a powerful influence in the monetary system. (ii) The European cluster has a relatively stable structure and this may be ascribed to the influence of EUR. (iii) Currencies from the Middle East except for ILS always form a cluster and link to USD. Possible explanations are that Saudi Arabia, the United Arab Emirates, Kuwait, Jordanian, and Bahrain are oil-producing countries (the former three countries are members of the Organization of the Petroleum Exporting Countries) and have a mass of USD holdings, and most of their currencies peg to USD. (iv) The Commonwealth cluster is formed in the FX network, suggesting that the Commonwealth nations maybe have the same currency mechanism.

4.3. Dynamics of Topological Features. In this subsection, we aim to investigate the dynamical evolution of time-varying FX networks' topological features. To begin with it, we show the calculation results of the average path length (APL), mean occupation layer (MOL), and maximum degree k_{max} in Figure 6. As for the density measures of APL and MOL, both of their patterns do not show any tendency but with a fluctuation above and below. The values of maximum degree k_{max} also have a large volatility, especially during the period of financial crises. Then, we estimate the power-law exponent and the corresponding P value for each MST and present their outcomes in Figure 7. The estimated power-law exponent also changes over time and varies from 2.09 to 3.5. Although a handful of (about 309) P values are less than 0.1, the power-law hypothesis can be accepted for most MSTs. This finding suggests the FX network is a scale-free network in most of the time. That is, a small number of vertexes (currencies, such as USD) always have the vast majority of connections, while most of vertexes have a very few links.

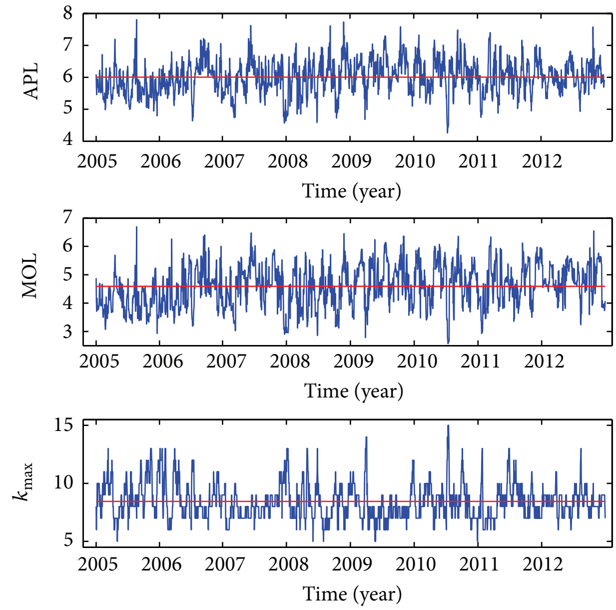

FIGURE 6: The average path length (APL), mean occupation layer (MOL), and maximum degree kmax of MST of 42 currencies in the international FX market as functions of time. In each panel, the red solid line stands for the corresponding statistical average value over the time investigated.

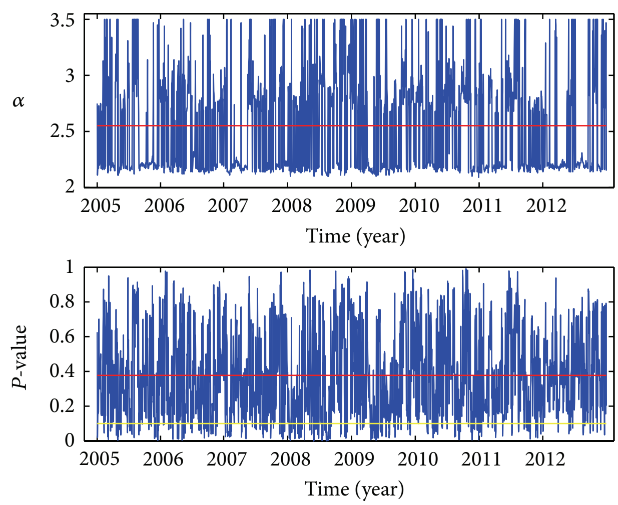

FIGURE 7: The estimated power-law exponent α and the corresponding P value of degree distribution of MST of 42 currencies in the international FX market as functions of time. In each panel, the red solid line stands for the corresponding statistical average value over the time investigated. In the bottom panel, the yellow solid line represents the value of 0.1. As proposed in [38], if the P value is greater than 0.1, the power-law hypothesis is accepted for the investigated data; otherwise it is rejected.

Similar to Qiu et al. [47], we further examine dynamics of topological features of FX networks by analyzing the time correlations. In practical terms, we employ the detrended

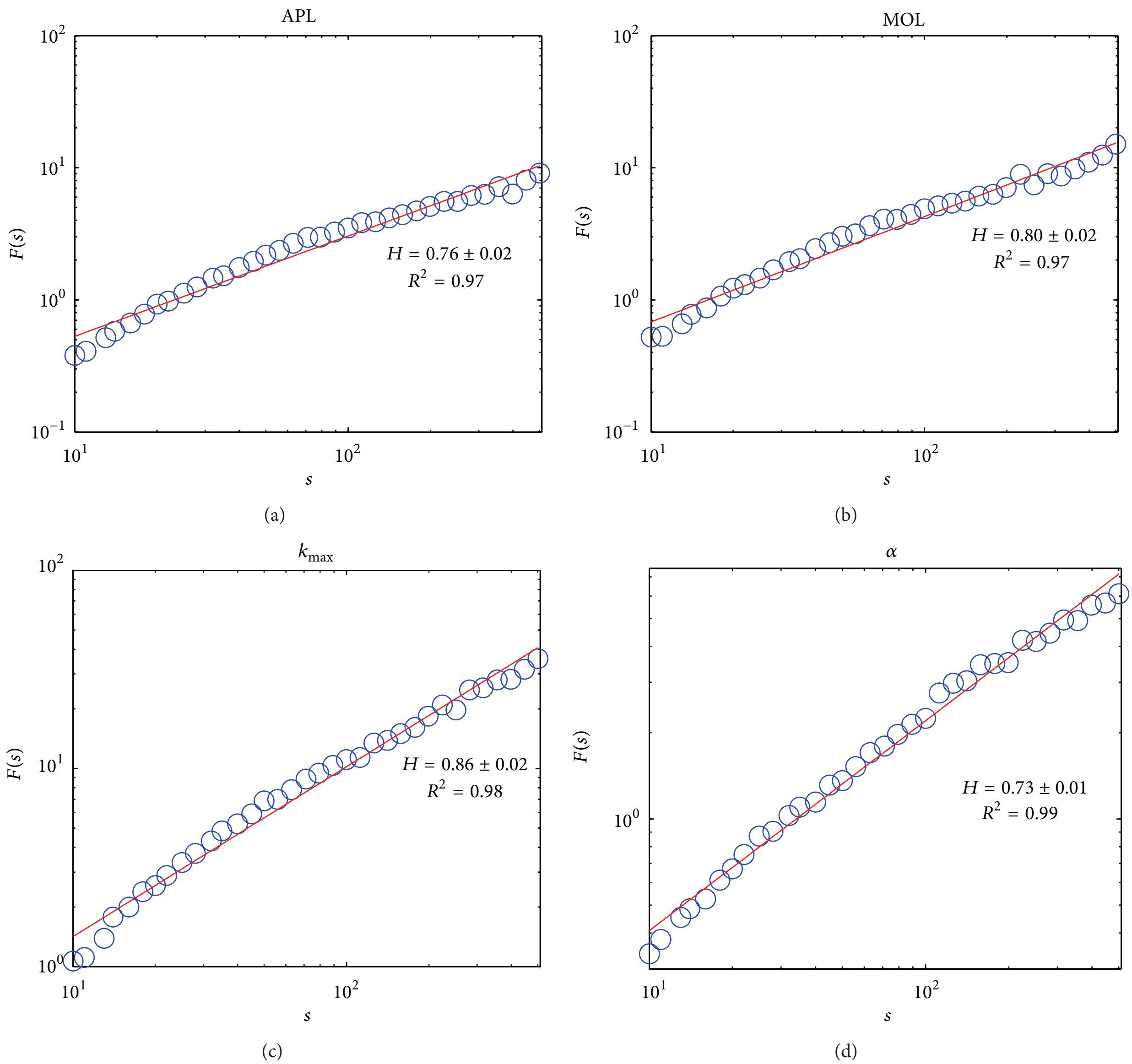

Figure 8: The DFA functions of the average path length (APL), mean occupation layer (MOL), and maximum degree $k_{\max}$ and the estimated power-law exponent α on log-log plots. In each panel, the red solid line stands for the corresponding linear fitting curve, and the estimated Hurst exponent H and its corresponding coefficient of determination R^2 are presented. The Hurst exponent $0.5 < H < 1.0$ implies that the time series is long-range correlated or has a long-term memory.

fluctuation analysis (DFA) method proposed by Peng et al. [48], which can be used to quantify long-range correlations of a nonstationary time series. The DFA approach provides a relationship between the DFA function $F(s)$ and the time scale s, characterized by a power-law $F(s) \sim s^{-H}$, where H is the well-known Hurst exponent. The Hurst exponent $H = 0.5, 0 < H < 0.5$, and $0.5 < H < 1.0$ means uncorrelated, long-term correlated, and anticorrelated time series, respectively. The DFA functions of the APL, MOL, maximum degree $k_{\max}$, and the estimated power-law exponent are drawn in Figure 8. We calculate the Hurst exponents for APL, MOL, $k_{\max}$, and the power-law exponent as 0.76 ± 0.02, 0.80 ± 0.02, 0.86 ± 0.02, and 0.73 ± 0.01, respectively, which are all larger than 0.5. These results mean that the four topological measures are long-range correlated and thus suggest that the FX network has a long-term memory effect.

4.4. Single- and Multistep Survival Rates. In order to study the robustness of links over time and the long-term evolution of FX networks, respectively, we use two measures, that is, the *single-step survival rate* (SSR) and the *multistep survival ratio* (MSR) proposed by Onnela et al. [9, 10]. The measure of SSR is defined as the fraction of links found in two consecutive MST at times t and $t+1$; that is,

$$\mathrm{SSR}(t) = \frac{1}{N-1} \left| E(t) \cap E(t+1) \right|, \quad (9)$$

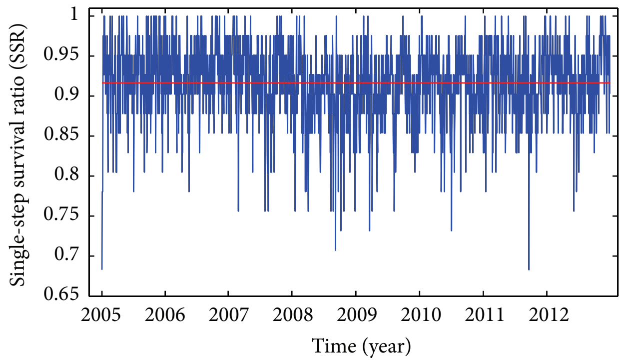

Figure 9: The single-step survival ratio (SSR) of MST of 42 currencies in the international FX market as a function of time. The red solid line stands for the corresponding statistical average value over the time investigated.

where $E(t)$ represents the set of edges of the MST at time t, $\cap$ is the intersection operator, and $|\cdots|$ gives the number of elements in the set [10]. The MSR measure is defined by

$$\mathrm{MSR}(t_0,\delta) = \frac{1}{N-1}\left|E(t_0)\cap E(t_0+1)\cdots E(t_0+\delta-1) \cap E(t_0+\delta)\right|, \quad (10)$$

where t_0 stands for the initial time and δ is the step length.

In Figure 9, we plot the time-varying SSRs for the MST. The mean value of SSR is close to 0.92, which shows that a great majority of links between currencies in the international FX market survive from one time to the next. Moreover, we find that about 80 SSRs are equal to 1, indicating that the two consecutive networks at times t and $t+1$ are identical. We also investigate the time correlations of the SSR series by the DFA method and present the results in Figure 10. One can find that the Hurst exponent for the SSR series is 0.68 ± 0.01, once again suggesting that the long-range memory effect exists in the FX network. In Figure 11, we show the MSR of MST of 42 currencies in the international FX market as a function of time for different initial time t_0. In Figure 11, the initial time t_0 is the first trading date of the year, and 8 curves of MSR are presented. For each curve of MSR, it drops rapidly as the time increases, which implies that the long-term stability of the FX network is falling as the time is increasing. However, we also find that each MSR is usually unchanged and moves toward a constant in the last or middle period of time, meaning that some structures or clusters (e.g., the Middle Eastern cluster) of the FX network are always preserved and stabilized.

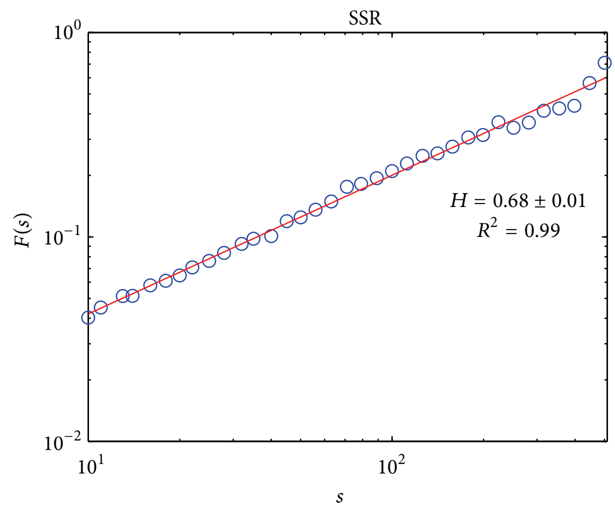

Figure 10: The DFA function of the single-step survival ratio (SSR) on a log-log plot. The red solid line stands for the associated linear fitting curve, and the estimated Hurst exponent H and its corresponding coefficient of determination R^2 are presented.

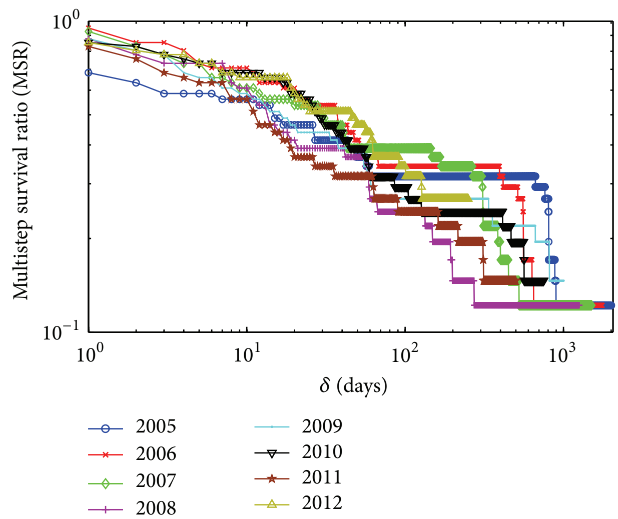

Figure 11: The multistep survival ratio (MSR) of MST of 42 currencies in the international FX market as a function of time for different initial time t_0. For each curve, the initial time t_0 is the first trading date of the year; for example, 2005 stands for January 5, 2005.

5. Conclusions

In this paper, we investigate the daily FX rates of 42 major currencies in the international FX market during the period of 2005–2012 and construct time-varying FX networks by a time-varying copula approach and the MST method. In detail, we first use the AR(p)-GARCH(1,1)-t model to characterize the returns' marginal distributions of FX rates. Then we employ the time-varying Student's t-copula to calculate the dynamic cross-correlation coefficients between each pair of rates. Finally we adopt the MST to build time-varying FX networks and analyze the networks properties including the dynamics and time correlations of topological features and survival rates of the MST.

Some basic finding for examining FX networks in this research can be summarized as follows. (i) By analyzing the descriptive statistics of cross-correlation coefficients and distances of MST, we find that distributions of cross-correlation coefficients (distances) in the international FX market (network) are fat-tailed and negatively skewed. (ii) On basis of MSTs for three different periods, we observe that some currencies gather together and form into several clusters, such as the international cluster with USD at its center, the Middle Eastern cluster, and the European cluster. The financial crises have a great influence on the FX network's topology structure and lead to USD becoming more centered in the MST because lots of currencies from Asia, Latin America, Middle East, and Africa are directly or indirectly linked to USD. (iii) The topological measures of the FX network present a large fluctuation and have a long-term memory effect. By estimating the degree distribution of MST, we find that the FX network is a scale-free network in most of the time. (iv) A great majority of links between currencies in the international FX market survive from one time to the next, and multistep survive rates descend sharply as the time increases.

Conflict of Interests

The authors declare that there is no conflict of interests regarding the publication of this paper.

Acknowledgments

The authors thank C. Yu who works in the Guosen Securities Co., Ltd., for helpful discussions. This work was supported by the Fundamental Research Funds for the Central Universities of Hunan University, the Hunan Provincial Innovation Foundation for Postgraduate (Grant no. CX2013A006), the Scholarship Award for Excellent Doctoral Student granted by the Ministry of Education of China, the National Natural Science Foundation of China (Grant no. 71373072), the Specialized Research Fund for the Doctoral Program of Higher Education (Grant no. 20130161110031), the China Postdoctoral Science Foundation (Grant no. 2013M530376), and the Foundation for Innovative Research Groups of the National Natural Science Foundation of China (Grant no. 71221001).

References

[1] R. N. Mantegna and H. E. Stanley, *Introduction to Econophysics: Correlations and Complexity in Finance*, Cambridge University Press, Cambridge, UK, 1999.

[2] J. Kwapień and S. Drożdż, "Physical approach to complex systems," *Physics Reports*, vol. 515, no. 3-4, pp. 115–226, 2012.

[3] C. Huang, C. Peng, X. Chen, and F. Wen, "Dynamics analysis of a class of delayed economic model," *Abstract and Applied Analysis*, vol. 2013, Article ID 962738, 12 pages, 2013.

[4] C. Huang, H. Kuang, X. Chen, and F. Wen, "An LMI approach for dynamics of switched cellular neural networks with mixed delays," *Abstract and Applied Analysis*, vol. 2013, Article ID 870486, 8 pages, 2013.

[5] R. N. Mantegna, "Hierarchical structure in financial markets," *European Physical Journal B*, vol. 11, no. 1, pp. 193–197, 1999.

[6] V. Boginski, S. Butenko, and P. M. Pardalos, "Statistical analysis of financial networks," *Computational Statistics and Data Analysis*, vol. 48, no. 2, pp. 431–443, 2005.

[7] J.-P. Onnela, K. Kaski, and J. Kertész, "Clustering and information in correlation based financial networks," *European Physical Journal B*, vol. 38, no. 2, pp. 353–362, 2004.

[8] M. Tumminello, T. Aste, T. Di Matteo, and R. N. Mantegna, "A tool for filtering information in complex systems," *Proceedings of the National Academy of Sciences of the United States of America*, vol. 102, no. 30, pp. 10421–10426, 2005.

[9] J.-P. Onnela, A. Chakraborti, K. Kaski, and J. Kertész, "Dynamic asset trees and portfolio analysis," *European Physical Journal B*, vol. 30, no. 3, pp. 285–288, 2002.

[10] J.-P. Onnela, A. Chakraborti, K. Kaski, J. Kertész, and A. Kanto, "Dynamics of market correlations: taxonomy and portfolio analysis," *Physical Review E—Statistical, Nonlinear, and Soft Matter Physics*, vol. 68, no. 5, Article ID 056110, 12 pages, 2003.

[11] J. G. Brida and W. A. Risso, "Dynamics and structure of the 30 largest North American companies," *Computational Economics*, vol. 35, no. 1, pp. 85–99, 2010.

[12] W.-Q. Huang, X.-T. Zhuang, and S. Yao, "A network analysis of the Chinese stock market," *Physica A: Statistical Mechanics and Its Applications*, vol. 388, no. 14, pp. 2956–2964, 2009.

[13] C. K. Tse, J. Liu, and F. C. M. Lau, "A network perspective of the stock market," *Journal of Empirical Finance*, vol. 17, no. 4, pp. 659–667, 2010.

[14] D. Y. Kenett, M. Tumminello, A. Madi, G. Gur-Gershgoren, R. N. Mantegna, and E. Ben-Jacob, "Dominating clasp of the financial sector revealed by partial correlation analysis of the stock market," *PLoS ONE*, vol. 5, no. 12, Article ID e15032, 2010.

[15] A. Z. Górski, S. Drożdż, and J. Kwapień, "Scale free effects in world currency exchange network," *The European Physical Journal B*, vol. 66, no. 1, pp. 91–96, 2008.

[16] J. Kwapień, S. Gworek, S. Drożdż, and A. Górski, "Analysis of a network structure of the foreign currency exchange market," *Journal of Economic Interaction and Coordination*, vol. 4, no. 1, pp. 55–72, 2009.

[17] J. Kwapień, A. Górski, and S. Drożdż, "Structure and evolution of the foreign exchange networks," *Acta Physica Polonica B*, vol. 40, no. 1, pp. 175–194, 2009.

[18] W. Jang, J. Lee, and W. Chang, "Currency crises and the evolution of foreign exchange market: evidence from minimum spanning tree," *Physica A: Statistical Mechanics and Its Applications*, vol. 390, no. 4, pp. 707–718, 2011.

[19] G.-J. Wang, C. Xie, F. Han, and B. Sun, "Similarity measure and topology evolution of foreign exchange markets using dynamic time warping method: evidence from minimal spanning tree," *Physica A: Statistical Mechanics and Its Applications*, vol. 391, no. 16, pp. 4136–4146, 2012.

[20] D. Matesanz and G. J. Ortega, "Network analysis of exchange data: Interdependence drives crisis contagion," *Quality & Quantity*, 2013.

[21] G.-J. Wang, C. Xie, Y.-J. Chen, and S. Chen, "Statistical properties of the foreign exchange network at different time scales: evidence from detrended cross-correlation coefficient and minimum spanning tree," *Entropy*, vol. 15, no. 5, pp. 1643–1662, 2013.

[22] D.-M. Song, M. Tumminello, W.-X. Zhou, and R. N. Mantegna, "Evolution of worldwide stock markets, correlation structure, and correlation-based graphs," *Physical Review E—Statistical, Nonlinear, and Soft Matter Physics*, vol. 84, no. 2, Article ID 026108, 9 pages, 2011.

[23] Š. Lyócsa, T. Výrost, and E. Baumöhl, "Stock market networks: the dynamic conditional correlation approach," *Physica A:*

Statistical Mechanics and Its Applications, vol. 391, no. 16, pp. 4147–4158, 2012.

[24] C. Huang, X. Gong, X. Chen, and F. Wen, "Measuring and forecasting volatility in Chinese stock market using HAR-CJ-M model," *Abstract and Applied Analysis*, vol. 2013, Article ID 143194, 13 pages, 2013.

[25] T. Trancoso, "Emerging markets in the global economic network: real(ly) decoupling?" *Physica A: Statistical Mechanics and Its Applications*, vol. 395, pp. 499–510, 2014.

[26] M. Sklar, "Fonctions de répartition à *n* dimensions et leurs marges," *Publications de l'Institut de Statistique de l'Université de Paris*, vol. 8, pp. 229–231, 1959.

[27] A. Sklar, "Random variables, joint distribution functions, and copulas," *Kybernetika*, vol. 9, pp. 449–460, 1973.

[28] A. C. Cameron, T. Li, P. K. Trivedi, and D. M. Zimmer, "Modelling the differences in counted outcomes using bivariate copula models with application to mismeasured counts," *The Econometrics Journal*, vol. 7, no. 2, pp. 566–584, 2004.

[29] F. Wen and Z. Liu, "A copula-based correlation measure and its application in chinese stock market," *International Journal of Information Technology & Decision Making*, vol. 8, no. 4, pp. 787–801, 2009.

[30] J. Hu, "Dependence structures in Chinese and US financial markets: a time-varying conditional copula approach," *Applied Financial Economics*, vol. 20, no. 7, pp. 561–583, 2010.

[31] A. J. Patton, "Estimation of multivariate models for time series of possibly different lengths," *Journal of Applied Econometrics*, vol. 21, no. 2, pp. 147–173, 2006.

[32] R. Aloui, M. S. Ben Aïssa, and D. K. Nguyen, "Conditional dependence structure between oil prices and exchange rates: a copula-GARCH approach," *Journal of International Money and Finance*, vol. 32, pp. 719–738, 2013.

[33] R. Aloui, S. Hammoudeh, and D. K. Nguyen, "A time-varying copula approach to oil and stock market dependence: the case of transition economies," *Energy Economics*, vol. 39, pp. 208–221, 2013.

[34] K. Wang, Y.-H. Chen, and S.-W. Huang, "The dynamic dependence between the Chinese market and other international stock markets: a time-varying copula approach," *International Review of Economics and Finance*, vol. 20, no. 4, pp. 654–664, 2011.

[35] A. J. Patton, "Modelling asymmetric exchange rate dependence," *International Economic Review*, vol. 47, no. 2, pp. 527–556, 2006.

[36] C. Diks, V. Panchenko, and D. van Dijk, "Out-of-sample comparison of copula specifications in multivariate density forecasts," *Journal of Economic Dynamics and Control*, vol. 34, no. 9, pp. 1596–1609, 2010.

[37] A. Dias and P. Embrechts, "Modeling exchange rate dependence dynamics at different time horizons," *Journal of International Money and Finance*, vol. 29, no. 8, pp. 1687–1705, 2010.

[38] A. Clauset, C. R. Shalizi, and M. E. J. Newman, "Power-law distributions in empirical data," *SIAM Review*, vol. 51, no. 4, pp. 661–703, 2009.

[39] Y. Wei, Y. Wang, and D. Huang, "A copula-multifractal volatility hedging model for CSI 300 index futures," *Physica A: Statistical Mechanics and Its Applications*, vol. 390, no. 23-24, pp. 4260–4272, 2011.

[40] Y. Lai, C. W. S. Chen, and R. Gerlach, "Optimal dynamic hedging via copula-threshold-GARCH models," *Mathematics and Computers in Simulation*, vol. 79, no. 8, pp. 2609–2624, 2009.

[41] H. Joe and J. J. Xu, "The estimation method of inference functions for margins for multivariate models," Tech. Rep. 166, Department of Statistics, University of British Columbia, Vancouver, Canada, 1996.

[42] J. B. Kruskal Jr., "On the shortest spanning subtree of a graph and the traveling salesman problem," *Proceedings of the American Mathematical Society*, vol. 7, pp. 48–50, 1956.

[43] C. Yang, Y. Shen, and B. Xia, "Evolution of Shanghai stock market based on maximal spanning trees," *Modern Physics Letters B*, vol. 27, no. 3, Article ID 135002, 19 pages, 2013.

[44] N. Vandewalle, F. Brisbois, and X. Tordoir, "Non-random topology of stock markets," *Quantitative Finance*, vol. 1, no. 3, pp. 372–374, 2001.

[45] R. Albert and A.-L. Barabási, "Statistical mechanics of complex networks," *Reviews of Modern Physics*, vol. 74, no. 1, pp. 47–97, 2002.

[46] T. Aste, W. Shaw, and T. Di Matteo, "Correlation structure and dynamics in volatile markets," *New Journal of Physics*, vol. 12, no. 8, Article ID 085009, 21 pages, 2010.

[47] T. Qiu, B. Zheng, and G. Chen, "Financial networks with static and dynamic thresholds," *New Journal of Physics*, vol. 12, no. 4, Article ID 043057, 16 pages, 2010.

[48] C.-K. Peng, S. V. Buldyrev, S. Havlin, M. Simons, H. E. Stanley, and A. L. Goldberger, "Mosaic organization of DNA nucleotides," *Physical Review E*, vol. 49, no. 2, pp. 1685–1689, 1994.

Hindawi Publishing Corporation
Discrete Dynamics in Nature and Society
Volume 2014, Article ID 165259, 6 pages
http://dx.doi.org/10.1155/2014/165259

Research Article

Lattice Methods for Pricing American Strangles with Two-Dimensional Stochastic Volatility Models

Xuemei Gao,[1] Dongya Deng,[2] and Yue Shan[2]

[1] *School of Economic Mathematics and School of Finance, Southwestern University of Finance and Economics, Chengdu 611130, China*
[2] *School of Finance, Southwestern University of Finance and Economics, Chengdu 611130, China*

Correspondence should be addressed to Dongya Deng; 112020204015@2012.swufe.edu.cn

Received 22 January 2014; Accepted 5 April 2014; Published 28 April 2014

Academic Editor: Chuangxia Huang

The aim of this paper is to extend the lattice method proposed by Ritchken and Trevor (1999) for pricing American options with one-dimensional stochastic volatility models to the two-dimensional cases with strangle payoff. This proposed method is compared with the least square Monte-Carlo method via numerical examples.

1. Introduction

Calculating American style options under geometric Brownian motion is far from the realistic financial market. It is more valuable to price American style options under stochastic models. In general the valuation of American options with stochastic volatility models has no closed-form solution except very few cases (see, e.g., Heston [1]). Therefore numerical methods or simulation methods are developed to price financial derivatives with stochastic volatility, among which the lattice methods receive much more attention. Ritchken and Trevor [2] proposed an efficient lattice method for pricing American options under GARCH models. Later the idea was further developed and applied by several papers, for example, Cakici and Topyan [3] and Wu [4], and recently the convergence of the method was proved by Akyildirim et al. [5].

All the abovementioned references focused on the development of lattice methods for pricing American options with one underlying asset and single stochastic volatility model. To the best of our knowledge, there are no papers studying the lattice methods for options with many underlying assets and multidimensional stochastic volatility models. Indeed there are many papers in developing lattice methods for pricing options with many underlying assets, for example, Boyle [6], Boyle et al. [7], Chen et al. [8], Gamba and Trigeorgis [9], and Moon et al. [10]. However it is not seen for lattice methods for multidimensional stochastic volatility models.

In this paper we give an attempt to this challenging topic by studying an American style option with strangle payoff, which was previously investigated by Chiarella and Ziogas [11] and Moraux [12] for single asset and constant volatility. We develop the lattice methods of Ritchken and Trevor [2] to the American strangle options with many underlying assets and multidimensional stochastic volatility GARCH models. We compare the lattice methods with the least square Monte-Carlo methods via several numerical examples.

2. Two-Dimensional Stochastic Volatility Models of American Strangles

Assume that the prices of two-dimensional assets $\mathbf{S_t} = (S_t^1, S_t^2)^T$ follow a two-dimensional GARCH model (see, e.g., Duan [13] for more explanation of the one-dimensional GARCH model). Consider

$$\begin{gathered} \ln\left(\frac{S_{t+1}^i}{S_t^i}\right) = r_f - q^i + \lambda_i\sqrt{h_t^i} - \frac{1}{2}h_t^i + \sqrt{h_t^i}\nu_{t+1}^i, \\ h_{t+1}^i = \beta_0^i + \beta_1^i h_t^i + \beta_2^i h_t^i\left(\nu_{t+1}^i - c^i\right)^2, \end{gathered} \tag{1}$$

with $i = 1, 2$, where S_t^i is the price of the ith asset corresponding to the standard Brown motion, q^i is the dividend rate for the ith asset, h_t^i is the volatility of the ith asset price, ν_{t+1}^i, conditional on information at time t, is a standard normal random variable, r_f is the riskless rate of return over the period, and λ_i is the unit risk premium for the ith asset. Under the local risk-neutralized measure, the processes (1) are written as

$$\ln\left(\frac{S_{t+1}^i}{S_t^i}\right) = r_f - q^i - \frac{1}{2}h_t^i + \sqrt{h_t^i}\mathbb{v}_{t+1}^i,$$
$$h_{t+1}^i = \beta_0^i + \beta_1^i h_t^i + \beta_2^i h_t^i\left(\mathbb{v}_{t+1}^i - c^{*,i}\right)^2, \quad (2)$$

with $i = 1, 2$, where $\mathbb{v}_{t+1}^i$, conditional on time t information, is a standard normal random variable with respect to the risk-neutralized measure, the parameters β_0^i, β_1^i, β_2^i, $c^{*,i}$ in the model can be obtained by regression on the financial market, and h_0^i is the initial variance of asset i. Let $f(\mathbf{S_t}) = \max(S_t^1, S_t^2)$ be a single-valued function of $\mathbf{S_t}$. In this paper, we consider a two-dimensional assets American strangle option whose payoff at maturity T is defined by

$$\max\left(\left[K_1 - f\left(\mathbf{S_T}\right)\right]^+, \left[f\left(\mathbf{S_T}\right) - K_2\right]^+\right), \quad (3)$$

in which K_1 and K_2, the strikes for American strangle's call and put parts, satisfy $K_1 < K_2$.

3. Lattice Algorithms

Ritchken and Trevor [2] investigated the stochastic lattice methods for one-dimensional GARCH model. This paper intends to extend the methods to two-dimensional GARCH model. The aim of this paper is to design an algorithm that avoids an exponentially exploding number of states. Toward this goal, we begin by approximating the sequence of single period log normal random variables in (2) by a sequence of discrete random variables. In particular, assume the information set at date t is (S_t^i, h_t^i), $i = 1, 2$, and let $y_t^i = \ln(S_t^i)$, $i = 1, 2$. Then, viewed from date t, y_{t+1}^i, $i = 1, 2$, are normal random variables with conditional moments. Consider

$$E_t\left[y_{t+1}^i\right] = y_t^i + r_f - q^i - \frac{1}{2}h_t^i,$$
$$\mathrm{Var}_t\left[y_{t+1}^i\right] = h_t^i. \quad (4)$$

We establish two discrete state Markov chains' approximation, $(y_{a,t}^i, h_{a,t}^i)$, $i = 1, 2$, for the dynamics of the discrete time state variables that converge to the continuous state (y_t^i, h_t^i), $i = 1, 2$. In particular, we approximate the sequence of conditional normal random variables by a sequence of discrete random variables. Given this period's logarithmic price and conditional variance, the conditional normal distribution of the next period's logarithmic price is approximated by a discrete random variable that takes on $2n + 1$ values for each asset. The lattice we construct has the property that the conditional means and variances of one period returns match the true means and variances given in (4), and the approximating sequence of discrete random variables converges to the true sequence of normal random variables. For each asset, the gap between adjacent logarithmic prices is determined by a spacing parameter γ_n^i for the logarithmic returns in such a way that all the approximating logarithmic prices are separated by

$$\gamma_n^i = \frac{\gamma^i}{\sqrt{n}}. \quad (5)$$

The size of these $2n+1$ jumps is restricted to integer multiples of γ_n^i. Another important issue is to ensure valid probability values over the grid of $2n + 1$ prices; the size of these jumps needs to be adjusted accordingly. This is efficiently handled with the inclusion of a jump parameter η^i, which is an integer that depends on the level of the variance as follows:

$$\eta^i - 1 < \frac{\sqrt{h_{a,t}^i}}{\gamma^i} \le \eta^i. \quad (6)$$

Consequently, the resulting two-asset GARCH model is

$$y_{a,t+1}^i = y_{a,t}^i + j\eta^i\gamma_n^i,$$
$$h_{a,t+1}^i = \beta_0^i + \beta_1^i h_{a,t}^i + \beta_2^i h_{a,t}^i\left(\varepsilon_{a,t+1}^i - c^{*,i}\right)^2, \quad (7)$$

for $i = 1, 2$, where

$$\varepsilon_{a,t+1}^i = \frac{j\eta^i\gamma_n^i - \left(r_f - q^i - (1/2)\,h_{a,t}^i\right)}{\sqrt{h_{a,t}^i}} \quad (8)$$

and $j = 0, \pm1, \pm2, \ldots, \pm n$, $\gamma^i = \sqrt{h_0^i}$, $i = 1, 2$. The probability distribution for $y_{a,t+1}^i$, conditional on $y_{a,t}^i$ and $h_{a,t}^i$, is then given by

$$\mathrm{Prob}\left(y_{a,t+1}^i = y_{a,t}^i + j\eta^i\gamma_n^i\right) = P^i(j), \quad j = 0, \pm1, \pm2, \ldots, \pm n, \quad (9)$$

where

$$P^i(j) = \sum_{j_u, j_m, j_d}\binom{n}{j_u j_m j_d}\left(p_u^i\right)^{j_u}\left(p_m^i\right)^{j_m}\left(p_d^i\right)^{j_d} \quad (10)$$

with $j_u, j_m, j_d \ge 0$ such that $n = j_u + j_m + j_d$ and $j = j_u - j_d$. Use the same lattice tree for assets S_1 and S_2 independently and assume each asset node has three possible paths to the next node: up, middle, and down. Then there are 9 possible combinations. The order of calculation is $(S_1^{\mathrm{up}}, S_2^{\mathrm{up}})$, $(S_1^{\mathrm{up}}, S_2^{\mathrm{middle}})$, $(S_1^{\mathrm{up}}, S_2^{\mathrm{down}})$, $(S_1^{\mathrm{middle}}, S_2^{\mathrm{up}})$, $(S_1^{\mathrm{middle}}, S_2^{\mathrm{middle}})$, $(S_1^{\mathrm{middle}}, S_2^{\mathrm{down}})$, $(S_1^{\mathrm{down}}, S_2^{\mathrm{up}})$, $(S_1^{\mathrm{down}}, S_2^{\mathrm{middle}})$, and $(S_1^{\mathrm{down}}, S_2^{\mathrm{down}})$, which is illustrated by Figure 1.

The possibilities for the nine combinations are $P^1(1)P^2(1)$, $P^1(1)P^2(0)$, $P^1(1)P^2(-1)$, $P^1(0)P^2(1)$, $P^1(0)P^2(0)$, $P^1(0)P^2(-1)$, $P^1(-1)P^2(1)$, $P^1(-1)P^2(0)$, and $P^1(-1)P^2(-1)$. Then, the volatility pattern by restricting the storage of conditional variance to the minimum and maximum values at each node under the forward-building process needs to be constructed. At each node for each asset, the option prices over a grid of K points are evaluated, covering the state space of the variances from the minimum to the maximum for each asset. Let $h_{a,t}^{i,\max}(m)$ and $h_{a,t}^{i,\min}(m)$

TABLE 1: Full volatility information at node (t, m).

$h^1_{a,t}(3,m), h^2_{a,t}(3,m)$
$h^1_{a,t}(3,m), h^2_{a,t}(2,m)$
$h^1_{a,t}(3,m), h^2_{a,t}(1,m)$
$h^1_{a,t}(2,m), h^2_{a,t}(3,m)$
$h^1_{a,t}(2,m), h^2_{a,t}(2,m)$
$h^1_{a,t}(2,m), h^2_{a,t}(1,m)$
$h^1_{a,t}(1,m), h^2_{a,t}(3,m)$
$h^1_{a,t}(1,m), h^2_{a,t}(2,m)$
$h^1_{a,t}(1,m), h^2_{a,t}(1,m)$

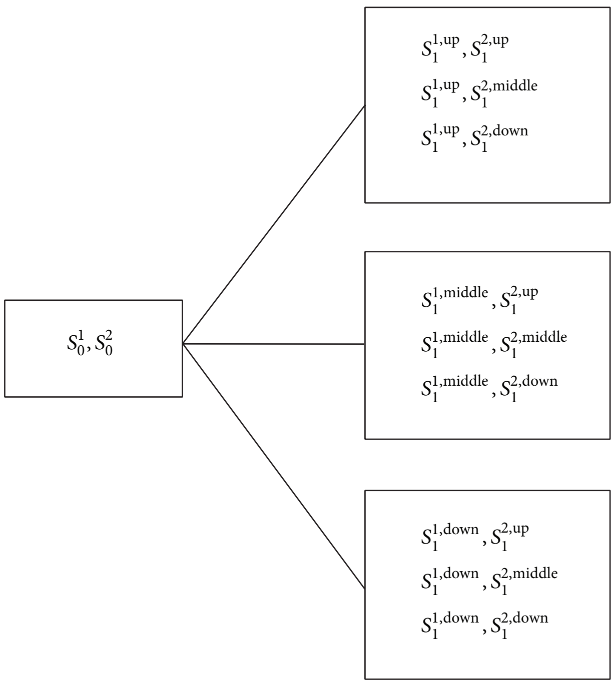

FIGURE 1: Two-asset GARCH tree.

represent the maximum and minimum variances that can be attained at node m for asset i. Option prices at this node are computed for K levels of variance ranging from the lowest to the highest at equidistant intervals. In particular, $h^i_{a,t}(k,m)$ representing the kth level of the variance at node (t,m) with $k = 1, \ldots, K$ is defined by an interpolation as follows:

$$h^i_{a,t}(k,m) = h^{i,\min}_{a,t}(m) + l^i_t(m)(k-1), \quad k = 1, \ldots, K, \tag{11}$$

where

$$l^i_t(m) = \frac{h^{i,\max}_{a,t}(m) - h^{i,\min}_{a,t}(m)}{K-1}. \tag{12}$$

For $K = 3$, the full volatility information at node (t,m) is described by Table 1.

According to Wu [4], we have

$$\begin{aligned}
p^i_u &= \frac{h^i_{a,t}}{2n(\eta^i\gamma^i_n)^2} + \frac{r_f - q^i - (1/2)\,h^i_{a,t}}{2n\eta^i\gamma^i_n} + \frac{\left(r_f - q^i - (1/2)\,h^i_{a,t}\right)^2}{2(n\eta^i\gamma^i_n)^2}, \\
p^i_m &= 1 - \frac{h^i_{a,t}}{n(\eta^i\gamma^i_n)^2} - \frac{\left(r_f - q^i - (1/2)\,h^i_{a,t}\right)^2}{(n\eta^i\gamma^i_n)^2}, \\
p^i_d &= \frac{h^i_{a,t}}{2n(\eta^i\gamma^i_n)^2} - \frac{r_f - q^i - (1/2)\,h^i_{a,t}}{2n\eta^i\gamma^i_n} + \frac{\left(r_f - q^i - (1/2)\,h^i_{a,t}\right)^2}{2(n\eta^i\gamma^i_n)^2},
\end{aligned} \tag{13}$$

where $i = 1, 2$ represent the i asset, and $h^i_{a,t}$ is the approximation volatility of asset i at time t, and η^i is the jump parameter of asset i. Cakici and Topyan [3] modified the forward-building process and used interpolated variances only during the backward recursion to make the algorithm more efficient. They adopted only real node maximum and minimum variances, not the interpolated ones that fell between the maximum and minimum variances. It is intuitive to use interpolation for K points in the backward procedure. At the terminal time T, the two-asset American strangle option's cash flow is

$$\max\left\{\left[K_1 - \max\left(S^1_t, S^2_t\right)\right]^+, \left[\max\left(S^1_t, S^2_t\right) - K_2\right]^+\right\}. \tag{14}$$

Let $C_{a,t}(m,k)$ be the kth option price at the node (m,k), for $k = 1, 2, \ldots, K$, and the variance is $h^i_{a,t}(m,k)$, $i = 1, 2$. Note that the boundary condition for a two-asset American strangle option with strike X which expires in period T is

$$\begin{aligned}
C_{a,T}(m,1) &= C_{a,T}(m,2) = \cdots = C_{a,T}(m,K) \\
&= \max\left\{\left[K_1 - \max\left(S^1_T, S^2_T\right)\right]^+, \right. \\
&\qquad \left. \left[\max\left(S^1_T, S^2_T\right) - K_2\right]^+\right\}.
\end{aligned} \tag{15}$$

We apply backward recursion to establish the option price at date 0. Consider a node (m,k) at time t. Then we compute the option price $C_{a,t}(m,k)$ corresponding to variance $h^i_{a,t}(m,k)$ at the node. Given the variance $h^i_{a,t}(m,k)$, we compute the appropriate jump parameter, η^i for each asset, by (6). The successive nodes for this variance combination are $((t+1, m + j^1\eta^1), (t+1, m + j^2\eta^2))$, where $j^1 = 0, \pm 1, \pm 2, \ldots, \pm n$ and $j^2 = 0, \pm 1, \pm 2, \ldots, \pm n$. Equation (11) is used to compute the period $(t+1)$ variance for each of these nodes. Specifically, for the transition from the kth variance element of node (t,m) to node $((t+1, m+j^1\eta^1), (t+1, m+j^2\eta^2))$, the period $(t+1)$ variance for each asset is given by

$$h_{a,t+1}^{i,\text{next}}\left(j^{1,2}\right) = \beta_0^i + \beta_1^i h_{a,t}^i(m,k) + \beta_2^i h_{a,t}^i(m,k)\left[\frac{\left(j\eta^i\gamma_n^i - r_f + h_{a,t}^i(m,k)\right)}{\sqrt{h_{a,t}^i(m,k)} - c^{i,*}}\right]^2, \quad (16)$$

where $j^{1,2}$ represents the combination of j^1 and j^2. Linear interpolation of the two stored option prices corresponding to the two stored variance entries closest to $h_{a,t+1}^{2,\text{next}}(j^2)$ is used to obtain the option price corresponding to a variance of $h_{a,t+1}^{2,\text{next}}(j^2)$ when $h_{a,t+1}^{1,\text{next}}(j^1)$ is already chosen. Let L be an integer smaller than K defined via

$$h_{a,t+1}^2\left(m+j^2\eta^2, L\right) < h_{a,t+1}^{2,\text{next}}\left(j^2\right) < h_{a,t+1}^2\left(m+j^2\eta^2, L+1\right). \quad (17)$$

The interpolated option price is

$$C^{\text{interp}}(m) = q(j)\, C_{a,t+1}\left(m + j^{1,2}\eta^{1,2}, L\right) + (1-q(j))\, C_{a,t+1}\left(m + j^{1,2}\eta^{1,2}, L+1\right), \quad (18)$$

where

$$q(j) = \frac{h_{a,t+1}^2\left(m+j^2\eta^2, L+1\right) - h_{a,t+1}^{2,\text{next}}\left(j^2\right)}{h_{a,t+1}^2\left(m+j^2\eta^2, L+1\right) - h_{a,t+1}^2\left(m+j^2\eta^2, L\right)}. \quad (19)$$

In this way an option price is identified for each of the $(2n+1)(2n+1)$ jumps from node (t,m) with variance combination $(h_{a,t+1}^{1,\text{next}}(j^1), h_{a,t+1}^{2,\text{next}}(j^2))$. In each case, either node $(t+1, m+j^{1,2}\eta^{1,2})$ contains a variance entry (and hence option value) that matches $(h_{a,t+1}^{1,\text{next}}(j^1), h_{a,t+1}^{2,\text{next}}(j^1))$, or the relevant information is interpolated from the closest two entries. We use the following formula to compute the unexercised option value $C_{a,t}^{\text{go}}(m,k)$:

$$C_{a,t}^{\text{go}}(m,k) = e^{-r_f}\sum_{j^1=-n}^{n} P^1\left(j^1\right)\sum_{j^2=-n}^{n} P^2\left(j^2\right) C^{\text{interp}}(m). \quad (20)$$

Denote the exercised value of the claim by $C_t^{a,\text{stop}}(m,k)$. For a two-asset American strangle option with strikes K_1 and K_2, $K_1 < K_2$,

$$C_{a,t}^{\text{stop}}(m,k) = \max\left\{\left[K_1 - \max\left(S_t^1, S_t^2\right)\right]^+, \left[\max\left(S_t^1, S_t^2\right) - K_2\right]^+\right\}. \quad (21)$$

The value of the claim at the kth entry of node (t,m) is then

$$C_{a,t}(m,k) = \max\left\{C_{a,t}^{\text{go}}(m,k), C_{a,t}^{\text{stop}}(m,k)\right\}. \quad (22)$$

The final option price, obtained by backward recursion of this procedure, is given by $C_{a,0}(0,1)$.

Table 2: Numerical results for Example 1.

T	n	Option prices with lattice	Option prices and intervals with LSM
5	1	0.014987254820724	0.029606167588959 [0.02804 0.03117]
	2	0.030190542190626	
	4	0.030393224336490	
	7	0.030981333835160	
	10	0.031863879158063	
7	1	0.068487810335143	0.081499912354419 [0.07999 0.08500]
	2	0.081254039347033	
	4	0.083605936631716	
	7	0.081680163494625	
	10	0.080301350887482	
10	1	0.178948896057298	0.193857807991106 [0.18842 0.19929]
	2	0.192329465764766	
	4	0.195314383716280	
	7	0.199868029599249	
	10	0.193058780881166	

4. Numerical Examples

In this section, several examples are implemented using the lattice method in this paper and least square Monte-Carlo method (LSM) developed by Longstaff and Schwartz [14].

In Examples 1, 2, and 3, we focus on the single asset American strangle options under GARCH model where the convergence with respect to n and K are studied, respectively, in the first two examples, and the optimal exercise boundaries are drawn for the third example. In Examples 4 and 5, we compute the two-dimensional assets American strangle options.

In Tables 2 and 3, the prices of the options using LSM with 5,000 paths are calculated and the intervals that the true prices fall into are provided. From the comparisons we confirm that the lattice methods developed in this paper are correct and reliable. Furthermore from Table 2 we observe that the lattice method converges as n goes larger and from Table 3 the lattice method converges as K goes larger. Figure 2 shows exercise and holding regions: the middle part is the holding region and the top and bottom parts are the exercise regions.

Example 1. Consider single asset GARCH model with parameters $r_f = 5\%$, $q = 10\%$, $\beta_0 = 6.575 \times 10^{-6}$, $\beta_1 = 0.9$, $\beta_2 = 0.04$, $S_0 = 100$, $h_0 = 0.0001096$, $K_1 = 105$, $K_2 = 95$, $\gamma = h_0$, and $c^* = 0$. Fixing $K = 20$, we investigate the convergence behavior as n increases.

Example 2. Consider single asset GARCH model with the same parameters as Example 1. In this example, $n = 5$ and the sensitivity to the volatility space parameter, K, is explored.

Example 3. Consider single asset GARCH model with the same parameters as Example 1. Draw the figure of the optimal exercise boundaries for American strangle.

Table 3: Numerical results for Example 2.

T	K	Option prices with lattice	Option prices and intervals with LSM
	2	0.028187456298155	
	4	0.029090524706680	
5	6	0.029930565933099	0.029606167588959
	10	0.030190542190626	[0.02804 0.03117]
	20	0.029391074539888	
	40	0.029489977773055	
	2	0.197070210662258	
	4	0.195700639175277	
10	6	0.196465071653130	0.193857807991106
	10	0.192329465764766	[0.18842 0.19929]
	20	0.193696054251151	
	40	0.194423204241922	
	2	1.182560819901510	
	4	1.197816540629624	
30	6	1.200350772727828	1.205198709585444
	10	1.202714267674711	[1.19372 1.22670]
	20	1.203407511987706	
	40	1.203545193979154	

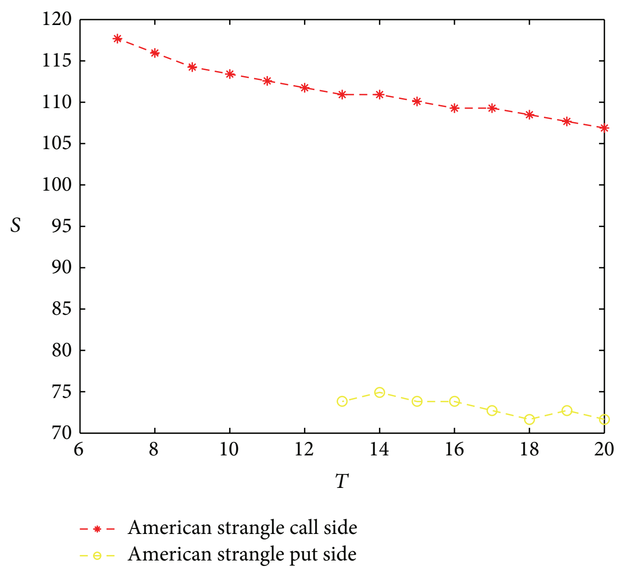

Figure 2: Optimal exercise boundaries for Example 3.

In Examples 4 and 5, we examine the stochastic lattice methods for pricing American strangle options under multi-asset under stochastic volatility model where the convergence with n and K are studied. From the numerics in Tables 4 and 5, we confirm that the lattice methods for two-dimensional models are correct and reliable and the convergence of the lattice methods with respect to n and K is observed.

Example 4. Consider two-asset American strangles with param- eters $r_f = 5\%$, $q^1 = q^2 = 10\%$, $\beta_0^1 = \beta_0^2 = 6.575\times 10^{-6}$, $\beta_1^1 = \beta_1^2 = 0.9$, $\beta_2^1 = \beta_2^1 = 0.04$, $S_0^1 = S_0^2 = 100$, $h_0^1 = h_0^2 = 0.0001096$, $K_1 = 105$, $K_2 = 95$, $\gamma^1 = \gamma^2 = h_0^1$, and $c^{*,1} = c^{*,2} = 0$. Fixing $K = 4$, we investigate the convergence behavior as n increases.

Example 5. Consider the two-dimensional GARCH model with the same parameters as Example 4. Fixing $n = 1$, we study the sensitivity to the volatility space parameter K.

Table 4: Numerical results for Example 4.

T	n	Option prices with lattice	Option prices and interval with LSM
	1	0.005974297	
	2	0.004223692	
3	3	0.004502351	0.005065587636226
	4	0.005530355	[0.00261 0.006316]
	5	0.005040507	
	1	0.014427788	
	2	0.014590056	
4	3	0.013984718	0.015018277749022
	4	0.017223364	[0.01111 0.01892]
	5	0.015988485	
	1	0.022129134	
	2	0.030507636	
5	3	0.030853276	0.034841312405081
	4	0.035594538	[0.02844 0.041235]
	5	0.034694665	

Table 5: Numerical results for Example 5.

T	K	Option prices with lattice	Option prices and intervals with LSM
	2	0.005974297	
	4	0.005974297	
3	6	0.005974297	0.005065587636226
	8	0.005974297	[0.00261 0.006316]
	10	0.005974297	
	2	0.014427788	
	4	0.014427788	
4	6	0.014427788	0.015018277749022
	8	0.014427788	[0.01111 0.01892]
	10	0.014427788	
	2	0.02194509	
	4	0.022129134	
5	6	0.022164226	0.034841312405081
	8	0.024355984	[0.02844 0.041235]
	10	0.024276964	

5. Conclusions

In this paper we studied pricing methods for stochastic volatility models of the American strangles with single asset and multiassets. Both lattice methods and LSM methods are developed and implemented. To the best of our knowledge, there are no results on the lattice methods for multidimensional stochastic volatility models. We first extended the stochastic lattice methods invented by Ritchken and Trevor [2] which are for one-dimensional GARCH models of American call to the multidimensional GARCH models of American strangles. Numerical examples confirm the correctness and reliability of the lattice methods. Future challenging works include the development of the lattice methods for multidimensional volatility models with correlations and recently developed models (e.g., [15]). One possible solution to the case of correlation is to adopt the idea (using moment-generating function) in [7]. However it needs to develop new techniques when the stochastic volatility models are involved. Furthermore, a dimensional-reduction technique should be developed to reduce the computational cost.

Conflict of Interests

The authors declare that there is no conflict of interests regarding the publication of this paper.

Acknowledgment

The work was supported by the Fundamental Research Funds for the Central Universities (Grant no. JBK130401).

References

[1] S. L. Heston, "A closed-form solution for options with stochastic volatility with applications to bond and currency options," *Review of Financial Studies*, vol. 6, pp. 327–343, 1993.

[2] P. Ritchken and R. Trevor, "Pricing options under generalized GARCH and stochastic volatility processes," *Journal of Finance*, vol. 54, no. 1, pp. 377–402, 1999.

[3] N. Cakici and K. Topyan, "The GARCH option pricing model: a lattice approach," *Quantitative Finance*, vol. 2, pp. 432–442, 2000.

[4] C.-C. Wu, "The GARCH option pricing model: a modification of lattice approach," *Review of Quantitative Finance and Accounting*, vol. 26, no. 1, pp. 55–66, 2006.

[5] E. Akyildirim, Y. Dolinsky, and H. Soner, "Approximating stochastic volatility by recombinant trees," http://arxiv.org/abs/1205.3555v1.

[6] P. Boyle, "A lattice framework for option pricing with two state variables," *Journal of Financial and Quantitative Analysis*, vol. 23, pp. 1–2, 1988.

[7] P. Boyle, J. Evnine, and S. Gibbs, "Numerical evaluation of multivariate contingent claims," *Review of Financial Studied*, vol. 2, pp. 241–250, 1989.

[8] R.-R. Chen, S.-L. Chung, and T. T. Yang, "Option pricing in a multi-asset, complete market economy," *Journal of Financial and Quantitative Analysis*, vol. 37, no. 4, pp. 649–666, 2002.

[9] A. Gamba and L. Trigeorgis, "An improved binomial lattice method for multi-dimensional options," *Applied Mathematical Finance*, vol. 14, no. 5, pp. 453–475, 2007.

[10] K.-S. Moon, W.-J. Kim, and H. Kim, "Adaptive lattice methods for multi-asset models," *Computers & Mathematics with Applications*, vol. 56, no. 2, pp. 352–366, 2008.

[11] C. Chiarella and A. Ziogas, "Evaluation of American strangles," *Journal of Economic Dynamics & Control*, vol. 29, no. 1-2, pp. 31–62, 2005.

[12] F. Moraux, "On perpetual American strangles," *Journal of Derivatives*, vol. 16, no. 4, pp. 82–97, 2009.

[13] J.-C. Duan, "The GARCH option pricing model," *Mathematical Finance*, vol. 5, no. 1, pp. 13–32, 1995.

[14] F. A. Longstaff and E. S. Schwartz, "Valuing American options by simulation: a simple least-squares approach," *Review of Financial Studies*, vol. 14, no. 1, pp. 113–147, 2001.

[15] C. X. Huang, X. Gong, X. Chen, and F. H. Wen, "Measuring and forecasting volatility in Chinese stock market using HAR-CJ-M model," *Abstract and Applied Analysis*, vol. 2013, Article ID 143194, 13 pages, 2013.

Hindawi Publishing Corporation
Discrete Dynamics in Nature and Society
Volume 2014, Article ID 324904, 8 pages
http://dx.doi.org/10.1155/2014/324904

Research Article

Higher Order Mean Squared Error of Generalized Method of Moments Estimators for Nonlinear Models

Yi Hu,[1] Xiaohua Xia,[2] Ying Deng,[3] and Dongmei Guo[4]

[1] *School of Management, University of Chinese Academy of Sciences, Beijing 100190, China*
[2] *Institute of China's Economic Reform and Development, Renmin University of China, Beijing 100892, China*
[3] *School of International Trade and Economics, University of International Business and Economics, Beijing 100029, China*
[4] *School of Economics, Central University of Finance and Economics, Beijing 100081, China*

Correspondence should be addressed to Dongmei Guo; guodongmeicufe@163.com

Received 14 February 2014; Accepted 12 April 2014; Published 28 April 2014

Academic Editor: Chuangxia Huang

Generalized method of moments (GMM) has been widely applied for estimation of nonlinear models in economics and finance. Although generalized method of moments has good asymptotic properties under fairly moderate regularity conditions, its finite sample performance is not very well. In order to improve the finite sample performance of generalized method of moments estimators, this paper studies higher-order mean squared error of two-step efficient generalized method of moments estimators for nonlinear models. Specially, we consider a general nonlinear regression model with endogeneity and derive the higher-order asymptotic mean square error for two-step efficient generalized method of moments estimator for this model using iterative techniques and higher-order asymptotic theories. Our theoretical results allow the number of moments to grow with sample size, and are suitable for general moment restriction models, which contains conditional moment restriction models as special cases. The higher-order mean square error can be used to compare different estimators and to construct the selection criteria for improving estimator's finite sample performance.

1. Introduction

It is a stylized fact that plenty of relationships are dynamic and nonlinear in nature and society, especially in economic and financial systems [1–8]. These relationships are usually depicted by nonlinear models. Generalized method of moments (GMM) has been widely applied for analysis for these nonlinear models since it was first introduced by Hansen [9] and gradually became a fundamental estimation method in econometrics [10]. Nevertheless, although GMM has good asymptotic properties under fairly moderate regularity conditions, its finite sample performance is not very well [11–13]. Similar to the maximum likelihood estimation (MLE), GMM does not have an exact finite sample distribution. In practice, we generally use the asymptotic distribution to approximate this finite sample distribution, but many applications of GMM reveal that this approximation has low precision [14].

When traditional asymptotic theory cannot precisely approximate the finite sample distributions of estimators or tests, we need higher-order asymptotic expansion for these estimators or tests to get more accurate approximation [15]. Nagar [16] studied the small sample properties of the general k-class estimators of simultaneous equations and gave the higher-order asymptotic expansion of the first- and second-order moments for two-stage least squares (2SLS) estimator. Donald and Newey [17] gave a theoretical derivation of the higher-order MSE for 2SLS based on Nagar [16]; however, their MSE formula applied to the case where the number of instruments grows with but at a smaller rate than the sample size, while Nagar [16] considered the cases where the number of instruments is fixed. Kuersteiner [18] derived the higher-order asymptotic properties of GMM estimators for linear time series models using many lags as instruments.

Besides the linear models, Rilstone et al. [19] derived and examined the second-order bias and MSE of a fairly wide class of nonlinear estimators, which included nonlinear least squares, maximum likelihood, and GMM estimators as special cases. Bao and Ullah [20] extended the second-order bias and MSE results of Rilstone et al. [19] for time series dependent observations. In addition, Bao and Ullah [21] derived the higher-order bias and mean squared error of a large class of nonlinear estimators to order $O(n^{-5/2})$ and $O(n^{-3})$, respectively. However, although these papers gave the high-order bias and MSE for nonlinear estimators, they were not suitable for two-step efficient GMM estimators.

Newey and Smith [22] studied the higher-order bias for two-step GMM estimators, empirical likelihood (EL) and generalized empirical likelihood (GEL) estimators through higher-order asymptotic expansions. But this paper needs to be improved in the following aspects. First, the data generating process considered in this paper was independently identically distributed. Second, the number of moments is fixed. Third, the MSE of GMM was not given. Anatolyev [23] extended Newey and Smith [22] to stationary time series models with serial correlation. Again, the number of moments in this paper was fixed, and this paper only gave the higher-order bias for the estimators, but not the MSE.

Donald et al. [24] examined higher-order asymptotic MSE for conditional moment restriction models. Based on this MSE, they developed moment selection criteria for two-step GMM estimator, a bias corrected version, and GEL estimators. Donald et al. [24] allowed the number of instruments to grow with sample size. However, this paper constructed moment conditions through instrumental variables, which was not suitable for general moment restriction models. Thus, our paper tends to fill an important lacuna in the literature about higher-order asymptotic expansion of nonlinear estimators. Specially, we consider a general nonlinear regression model with endogeneity, and our theoretical results are suitable for general moment restriction models, which contain conditional moment restriction models as a special case.

The remainder of the paper proceeds as follows: Section 2 introduces the model and notations. Section 3 discusses the estimation for the threshold and slope coefficients. Section 4 concludes.

2. Model

Many economic and financial models can be written as nonlinear functions of data and parameters. Consider the following nonlinear regression model with endogeneity:

$$y_i = f(X_i, \beta_0) + \varepsilon_i, \quad i = 1, \dots, n, \tag{1}$$

where y_i is dependent variable, X_i is a $p \times 1$ vector of explanatory variables, which contains endogenous variables, $\beta_0 \in \mathscr{B}$ is a $p \times 1$ vector of parameters, $\mathscr{B}$ is a compact subset of R^p, and $E(\varepsilon_i^2 \mid X_i) = \sigma_i^2$.

For model (1), the usual way to estimate β_0 is nonlinear least squares (NLS). However, X_i contains endogenous variables, which means that $E(\varepsilon_i \mid X_i) \neq 0$. In this case, NLS estimator of β_0 is not consistent. We have to look for another consistent estimator, such as GMM estimator. Let Z_i be $L \times 1$ ($L \geq p$) instrumental variables of X_i, and Z_i ($i = 1, \dots, n$) are independent random vectors. The orthogonality conditions can be written as

$$E(Z_i \varepsilon_i) = 0. \tag{2}$$

And the sample moments are

$$\begin{aligned} \overline{g}(\beta) &= \frac{1}{n}\sum_{i=1}^{n} g_i(\beta) = \frac{1}{n}\sum_{i=1}^{n} Z_i \varepsilon_i \\ &= \frac{1}{n}\sum_{i=1}^{n} Z_i (y_i - f(X_i, \beta)) = 0. \end{aligned} \tag{3}$$

Then, the two-step efficient GMM estimator of β_0 is given by

$$\widehat{\beta}_0 = \arg\min_{\beta \in \mathscr{B}} \overline{g}(\beta)' \widetilde{\Phi}(\widetilde{\beta})^{-1} \overline{g}(\beta), \tag{4}$$

where $\widetilde{\Phi}(\beta) = n^{-1}\sum_{i=1}^{n} g_i(\beta) g_i(\beta)'$, $\widetilde{\beta} = \arg\min_{\beta \in B} \overline{g}(\beta)' \widehat{W}^{-1} \overline{g}(\beta)$, and $\widehat{W}$ is a random weighting matrix that almost surely converges to a nonstochastic symmetric positive definite matrix W.

Our goal is to obtain the MSE of $\widehat{\beta}_0$. However, formula (4) does not have an analytical solution. We have to obtain it through higher-order asymptotic theory.

3. Higher-Order MSE of GMM Estimators

This part uses the iterative idea [19] to derive the higher-order MSE of the GMM estimator, which can be seen as a generalization of Donald et al. [24] to the unconditional moment restriction models. For the convenience of discussion, we use the following notations:

$$\begin{gathered} \Gamma_j = \frac{1}{n}\sum_{i=1}^{n} \Gamma_{ji}, \qquad \overline{\Gamma}_j = \frac{1}{n}\sum_{i=1}^{n} \Gamma_{ji}(\beta_0), \qquad \widehat{\Gamma}_j = \frac{1}{n}\sum_{i=1}^{n} \Gamma_{ji}(\widehat{\beta}_0), \\ j = 0, 1, 2, \\ \underset{(L \times p^{j+1})}{\Gamma_{ji}} = E(\nabla^{j+1} g_i(\beta_0)), \qquad \Gamma_{ji}(\beta) = \nabla^{j+1} g_i(\beta), \\ \eta_{ji} = \nabla^{j+1} g_i(\beta_0) - E[\nabla^{j+1} g_i(\beta_0)] = \Gamma_{ji}(\beta_0) - \Gamma_{ji}, \\ \Phi = E\left(n^{-1}\sum_{i=1}^{n} g_i(\beta) g_i(\beta)'\right) = \frac{1}{n}\sum_{i=1}^{n} E(g_i(\beta) g_i(\beta)'), \end{gathered} \tag{5}$$

where ∇ is a derivation operator defined by the following recursive method:

$$\nabla^{r+1} g(\beta) = \left(\frac{\partial[\nabla^r g(\beta)]_{ij}}{\partial \beta'}\right)_{\substack{i=1,\dots,L \\ j=1,\dots,p^r}}. \tag{6}$$

That is, $\nabla^{r+1} g(\beta)$ can be seen as a block matrix whose entry in the ith row and jth column is a $1 \times p$ vector $\partial[\nabla^r g(\beta)]_{ij}/\partial\beta'$, in which $[\nabla^r g(\beta)]_{ij}$ is the ith row and jth column element of matrix $\nabla^r g(\beta)$.

To derive the higher-order expansion of the GMM estimator $\widehat{\beta}_0$, the following assumptions for the moment function are required.

Assumption 1. For some neighborhood of β_0, f_i is, at least, three times continuously differentiable and $E(\|\nabla^r f_{i,j}\|^2) < \infty$, $r = 0, 1, 2, 3$, $i = 1, 2, \ldots$, and $j = 1, \ldots, L$.

Assumption 2. For some neighborhood of β_0, $\|\nabla^r g_{i,j}(\beta) - \nabla^r g_{i,j}(\beta_0)\| \le \|\beta - \beta_0\| M_{i,j}$, in which $E(M_{i,j}) < \infty$, $r = 0, 1, 2, 3$, and $j = 1, \ldots, L$, $i = 1, 2, \ldots$.

Assumption 3. $E(\eta_{0i,jk}^{\tau_1} g_{i,r}^{\tau_2}) = 0$, in which $\tau_1 + \tau_2 = 3$, τ_1 and τ_2 are nonnegative integers, $j = 1, \ldots, L$, $k = 1, \ldots, p$, $r = 1, \ldots, L$, and $i = 1, 2, \ldots$.

Assumption 4. The smallest eigenvalues of $E[g_i(\widetilde{\beta}_0) g_i'(\widetilde{\beta}_0)]$ and $\widetilde{\Phi}(\widetilde{\beta}_0)$ are bounded away from zero, in which $\widetilde{\beta}_0$ belongs to the neighborhood of β_0.

Assumption 5. There is $\zeta(L)$ and $\sqrt{L} \le \zeta(L) \le CL$ for some finite constant C, such that $\|g_i\| < C\zeta(L)$.

Assumption 1 is a necessary condition for a higher-order Taylor expansion. Assumption 2 is a common condition for the moments of remainder terms to bound (see also [19, 20, 23–25]). Assumption 3 requires that the third moments are zero, which can simplify the MSE calculations (see also [24, 26, 27]). Assumption 4 is a further identification condition. The purpose of Assumption 5 is to control the remainder terms of higher-order expansions (see [25] for details).

The first order condition for the optimization problem in (4) is given by

$$\left(\frac{\partial \overline{g}(\beta)}{\partial \beta'}\right)' \widetilde{\Phi}(\widetilde{\beta}_0)^{-1} \overline{g}(\beta)\bigg|_{\beta=\widehat{\beta}_0} = 0. \tag{7}$$

Define an auxiliary vector $\widehat{\lambda} = -\widetilde{\Phi}(\widetilde{\beta}_0)^{-1} \overline{g}(\widehat{\beta}_0)$; the above first order condition can be rewritten as

$$\begin{aligned} \widehat{\Gamma}_0' \widehat{\lambda} &= 0, \\ \overline{g}(\widehat{\beta}_0) + \widetilde{\Phi}(\widetilde{\beta}_0) \widehat{\lambda} &= 0. \end{aligned} \tag{8}$$

Let $K = p + L$, $\widehat{\theta}_{(K\times 1)} = (\widehat{\beta}_0', \widehat{\lambda}')'$, and $m_i(\widehat{\theta}) = \left(\begin{smallmatrix} \widehat{\Gamma}_{0i}' \widehat{\lambda} \\ g_i(\widehat{\beta}_0) + g_i(\widetilde{\beta}_0) g_i(\widetilde{\beta}_0)' \widehat{\lambda} \end{smallmatrix}\right)$. Equation (8) can be written as

$$m(\widehat{\theta}) = \frac{1}{n} \sum_{i=1}^{n} m_i(\widehat{\theta}). \tag{9}$$

For (9), the number of parameters is equal to the number of equations. A second-order Taylor expansion of (9) at $\theta_0 = (\widehat{\beta}_0', , 0')'$ yields

$$\begin{aligned} m(\widehat{\theta}) = {} & m + \widehat{M}(\widehat{\theta} - \theta_0) + \frac{1}{2} \sum_{j=1}^{K} (\widehat{\theta}_j - \theta_j) \widehat{A}_j (\widehat{\theta} - \theta_0) \\ & + \frac{1}{6} \sum_{j=1}^{K} \sum_{k=1}^{K} (\widehat{\theta}_j - \theta_j)(\widehat{\theta}_k - \theta_k) \widehat{B}_{jk}^* (\widehat{\theta} - \theta_0), \end{aligned} \tag{10}$$

where $m = m(\theta_0)$, $\widehat{M} = (1/n) \sum_{i=1}^{n} (\partial m_i(\theta_0)/\partial \theta') = (1/n) \sum_{i=1}^{n} M_i(\theta_0)$, $\widehat{A}_j = (1/n) \sum_{i=1}^{n} (\partial M_i(\theta_0)/\partial \theta_j)$, $\widehat{B}_{jk}^* = (1/n) \sum_{i=1}^{n} (\partial^2 M_i(\theta^*)/\partial \theta_j \partial \theta_k)$, and $\theta^* = t\widehat{\theta} + (1-t)\theta_0$, $t \in (0,1)$, in which $\widehat{\theta}_j$ and θ_j are the jth element of $\widehat{\theta}$ and θ_0, respectively.

From (10), we have

$$\begin{aligned} \widehat{\theta} - \theta_0 = {} & -M^{-1} m - M^{-1} (\widehat{M} - M)(\widehat{\theta} - \theta_0) \\ & - \frac{1}{2} \sum_{j=1}^{K} (\widehat{\theta}_j - \theta_j) M^{-1} A_j (\widehat{\theta} - \theta_0) + R, \\ R = {} & -\frac{1}{2} \sum_{j=1}^{K} (\widehat{\theta}_j - \theta_j) M^{-1} (\widehat{A}_j - A_j)(\widehat{\theta} - \theta_0) \\ & - \frac{1}{6} \sum_{j=1}^{K} \sum_{k=1}^{K} (\widehat{\theta}_j - \theta_j)(\widehat{\theta}_k - \theta_k) M^{-1} \widehat{B}_{jk}^* (\widehat{\theta} - \theta_0), \end{aligned} \tag{11}$$

where $M = E(\widehat{M})$ and $A_j = E(\widehat{A}_j)$.

Since the right-hand side of (11) contains terms $\widehat{\beta}_0 - \beta_0$ and $\widehat{\lambda}$, we use iterative techniques to remove these terms. For GMM estimator $\widehat{\beta}_0$ under Assumptions 1–5, if $L \to \infty$ and $\zeta^2(L)L/n \to 0$, then $\sqrt{n}(\widehat{\beta}_0 - \beta_0)$ can be decomposed as follows:

$$\sqrt{n}(\widehat{\beta}_0 - \beta_0) = \Omega^{-1} \left(h + \sum_{j=1}^{4} T_j^h + Z^h \right), \tag{12}$$

where

$$\begin{aligned} \Omega = \Gamma_0' \Phi^{-1} \Gamma_0, \qquad & h = -\sqrt{n} \Gamma_0' \Phi^{-1} \overline{g} = O_p(1), \\ T_1^h &= -\sqrt{n} (\overline{\Gamma}_0 - \Gamma_0)' \Sigma \overline{g} = O_p\left(\frac{L}{\sqrt{n}}\right), \\ T_2^h &= \sqrt{n} \widehat{\Gamma}_0' \Phi^{-1} \widetilde{\Phi}_1 \Sigma \overline{g} = O_p\left(\frac{\sqrt{L}}{\sqrt{n}}\right), \\ T_3^h &= T_{31}^h + T_{32}^h + T_{33}^h + T_{34}^h + T_{35}^h = O_p\left(\frac{1}{\sqrt{n}}\right), \end{aligned}$$

$$\begin{aligned} T_4^h &= -\sqrt{n}\Gamma_0'\Phi^{-1}\widetilde{\Phi}_1\Sigma\widetilde{\Phi}_1\Sigma\overline{g} + \sqrt{n}\Omega^{-1}\left(\overline{\Gamma}_0 - \Gamma_0\right)'\Sigma\widetilde{\Phi}_1\Sigma\overline{g} \\ &= O_p\left(\frac{\zeta(L)L}{n}\right), \\ Z^h &= \sqrt{n}\Omega\left(R^\beta + R_1^\beta + R_2^\beta + R_3^\beta + R_4^\beta + R_5^\beta + R_6^\beta\right) \\ &= o_p\left(\frac{L^2}{n}\right), \end{aligned} \tag{13}$$

and, for T_3^h,

$$\begin{aligned} T_{31}^h &= \sqrt{n}\Gamma_0'\Phi^{-1}\widetilde{\Phi}_{\eta g}\Sigma\overline{g}, \\ T_{32}^h &= \sqrt{n}\Gamma_0'\Phi^{-1}\left(\overline{\Gamma}_0 - \Gamma_0\right)\Omega^{-1}\Gamma_0'\Phi^{-1}\overline{g}, \\ T_{33}^h &= \frac{1}{2}\sqrt{n}\nabla\Gamma_0'\left[(\Sigma\overline{g})\otimes I_p\right]\Omega^{-1}\Gamma_0'\Phi^{-1}\overline{g}, \\ T_{34}^h &= \frac{1}{2}\sqrt{n}\left[\left(\overline{g}'\Phi^{-1}\Gamma_0\Omega^{-1}\right)\otimes I_p\right]\Gamma_1'\Sigma\overline{g}, \\ T_{35}^h &= -\frac{1}{2}\sqrt{n}\Gamma_0'\Phi^{-1}\Gamma_1\left[\left(\Omega^{-1}\Gamma_0'\Phi^{-1}\overline{g}\right)\otimes I_p\right]\Omega^{-1}\Gamma_0'\Phi^{-1}\overline{g}, \\ \Sigma &= \Phi^{-1} - \Phi^{-1}\Gamma_0\Omega^{-1}\Gamma_0'\Phi^{-1}. \end{aligned} \tag{14}$$

Before deriving the higher-order MSE of $\widehat{\beta}_0$, we need the following lemmas.

Lemma 6. *Consider*

$$\left(\sum_{j=1}^4 T_j^h\right)\left(\sum_{j=1}^4 T_j^h\right)' = T_1^h T_1^{h'} + o_p\left(\frac{L^2}{n}\right). \tag{15}$$

Proof. Consider

$$\begin{aligned} \left(\sum_{j=1}^4 T_j^h\right)\left(\sum_{j=1}^4 T_j^h\right)' &= T_1^h T_1^{h'} + T_1^h\left(\sum_{j=2}^4 T_j^h\right)' + \left(\sum_{j=2}^4 T_j^h\right)T_1^{h'} \\ &\quad + \left(\sum_{j=2}^4 T_j^h\right)\left(\sum_{j=2}^4 T_j^h\right)' \end{aligned} \tag{16}$$

in which

$$\begin{aligned} T_1^h\left(\sum_{j=2}^4 T_j^h\right)' &= O_p\left(\frac{L}{\sqrt{n}}\right)\left(O_p\left(\frac{\sqrt{L}}{\sqrt{n}}\right) + O_p\left(\frac{1}{\sqrt{n}}\right) \right. \\ &\quad \left. + O_p\left(\frac{\zeta(L)L}{n}\right)\right) \\ &= O_p\left(\frac{L}{\sqrt{n}}\right)O_p\left(\frac{\zeta(L)L}{n}\right) \\ &= O_p\left(\frac{\zeta(L)L^2}{n^{3/2}}\right) \\ &= o_p\left(\frac{L^2}{n}\right). \end{aligned} \tag{17}$$

Similarly, $(\sum_{j=2}^4 T_j^h)T_1^{h'} = o_p(L^2/n)$,

$$\begin{aligned} &\left(\sum_{j=2}^4 T_j^h\right)\left(\sum_{j=2}^4 T_j^h\right)' \\ &= \left(O_p\left(\frac{\sqrt{L}}{\sqrt{n}}\right) + O_p\left(\frac{1}{\sqrt{n}}\right) + O_p\left(\frac{\zeta(L)L}{n}\right)\right)^2 \\ &= O_p\left(\frac{\zeta^2(L)L^2}{n^2}\right) = o_p\left(\frac{L^2}{n}\right). \end{aligned} \tag{18}$$

□

Lemma 7. *Consider*

$$E\left(T_1^h h'\right) = o\left(\frac{L^2}{n}\right). \tag{19}$$

Proof. By definition, $h = -\sqrt{n}\Gamma_0'\Phi^{-1}\overline{g}$ and $T_1^h = -\sqrt{n}(\overline{\Gamma}_0 - \Gamma_0)'\Sigma\overline{g}$; then

$$\begin{aligned} T_1^h h' &= n\left(\overline{\Gamma}_0 - \Gamma_0\right)'\Sigma\overline{g}\cdot\overline{g}'\Phi^{-1}\Gamma_0, \\ \overline{\Gamma}_0 - \Gamma_0 &= \frac{1}{n}\sum_{i=1}^n\left(\overline{\Gamma}_{0i} - \Gamma_{0i}\right) = \frac{1}{n}\sum_{i=1}^n \eta_{0i}, \\ \overline{g}\cdot\overline{g}' &= \frac{1}{n}\sum_{i=1}^n g_i(\beta_0)g_i'(\beta_0) = \frac{1}{n}\sum_{i=1}^n g_i g_i', \end{aligned} \tag{20}$$

and according to the independence assumption,

$$\begin{aligned} E\left(T_1^h h'\right) &= E\left(n\left(\overline{\Gamma}_0 - \Gamma_0\right)'\Sigma\overline{g}\cdot\overline{g}'\Phi^{-1}\Gamma_0\right) \\ &= E\left(n\left(\frac{1}{n}\sum_{i=1}^n\eta_{0i}'\right)\Sigma\left(\frac{1}{n}\sum_{i=1}^n g_i g_i'\right)\Phi^{-1}\Gamma_0\right) \\ &= \frac{1}{n}\sum_{i=1}^n E\left(\eta_{0i}'\Sigma g_i g_i'\right)\Phi^{-1}\Gamma_0. \end{aligned} \tag{21}$$

Let $\eta_{0i}' = A_{(p\times L)}$, and $g_i g_i' = B_{(L\times L)}$; then $\eta_{0i}'\Sigma g_i g_i' = A\Sigma B \triangleq C$. Now, we examine the jth row and kth column element of C, C_{jk}: $C_{jk} = \sum_{r=1}^L\sum_{s=1}^L A_{jr}\Sigma_{rs}B_{sk} = \sum_{r=1}^L\sum_{s=1}^L \eta_{0i,rj}\Sigma_{rs}g_{i,s}g_{i,k}$. By Assumption 3, $E(C_{jk}) = E(\sum_{r=1}^L\sum_{s=1}^L \eta_{0i,rj}\Sigma_{rs}g_{i,s}g_{i,k}) = \sum_{r=1}^L\sum_{s=1}^L \Sigma_{rs}E(\eta_{0i,rj}g_{i,s}g_{i,k}) = 0$. Then we have $E(C) = 0$; that is, $E(\eta_{0i}'\Sigma g_i g_i') = 0$. Finally, we have $E(T_1^h h') = 0$. So, $E(T_1^h h') = o(L^2/n)$. □

Lemma 8. *Consider*

$$E\left(T_2^h h'\right) = o\left(\frac{L^2}{n}\right). \tag{22}$$

Proof. By definition of T_2^h and h, $T_2^h h' = n\Gamma_0'\Phi^{-1}\widetilde{\Phi}_1\Sigma\overline{g}\cdot\overline{g}'\Phi^{-1}\Gamma_0$. And by the definition of $\widetilde{\Phi}_1$, $T_2^h h' = n\Gamma_0'\Phi^{-1}[\widetilde{\Phi}(\beta_0)-\Phi]\Sigma\overline{g}\cdot\overline{g}'\Phi^{-1}\Gamma_0$. Take mathematical expectation for this formula,

$$\begin{aligned} &E\left(T_2^h h'\right)\\ &= E\left(n\Gamma_0'\Phi^{-1}\left[\widetilde{\Phi}\left(\beta_0\right)-\Phi\right]\Sigma\overline{g}\cdot\overline{g}'\Phi^{-1}\Gamma_0\right)\\ &= n\Gamma_0'\Phi^{-1}E\left(\left[\widetilde{\Phi}\left(\beta_0\right)-\Phi\right]\Sigma\overline{g}\cdot\overline{g}'\right)\Phi^{-1}\Gamma_0\\ &= n\Gamma_0'\Phi^{-1}E\left(\frac{1}{n}\sum_{i=1}^n\left[g_ig_i'-E\left(g_ig_i'\right)\right]\Sigma\left(\frac{1}{n}\sum_{j=1}^n g_j\right)\right.\\ &\qquad\left.\times\left(\frac{1}{n}\sum_{l=1}^n g_l'\right)\right)\Phi^{-1}\Gamma_0\\ &= n\Gamma_0'\Phi^{-1}E\left(\frac{1}{n^3}\sum_{i=1}^n\sum_{j=1}^n\sum_{l=1}^n\left[\left[g_ig_i'-E\left(g_ig_i'\right)\right]\Sigma g_jg_l'\right]\right)\Phi^{-1}\Gamma_0. \end{aligned} \tag{23}$$

According to the independence assumption,

$$\begin{aligned} &E\left(\frac{1}{n^3}\sum_{i=1}^n\sum_{j=1}^n\sum_{l=1}^n\left[\left[g_ig_i'-E\left(g_ig_i'\right)\right]\Sigma g_jg_l'\right]\right)\\ &= \frac{1}{n^3}E\left(\sum_{i=1}^n\left\{\left[g_ig_i'-E\left(g_ig_i'\right)\right]\Sigma g_ig_i'\right\}\right)\\ &= \frac{1}{n^3}\sum_{i=1}^n\left\{E\left(g_ig_i'\Sigma g_ig_i'\right)-E\left(g_ig_i'\right)\Sigma E\left(g_ig_i'\right)\right\}\\ &= \frac{1}{n^3}\sum_{i=1}^n O(1) = O\left(\frac{1}{n^2}\right). \end{aligned} \tag{24}$$

And by $\|\Gamma_0'\Phi^{-1}\| = O_p(1)$, we have $\Gamma_0'\Phi^{-1} = O_p(1)$. To sum up,

$$\begin{aligned} E\left(T_2^h h'\right) &= nO_p(1)\,O_p\left(\frac{1}{n^2}\right)O_p(1)\\ &= O_p\left(\frac{1}{n}\right) = o_p\left(\frac{L^2}{n}\right). \end{aligned} \tag{25}$$

□

Lemma 9. *Consider*

$$E\left(T_3^h h'\right) = o\left(\frac{L^2}{n}\right). \tag{26}$$

Proof. By definition of T_3^h and h, $T_3^h h' = (T_{31}^h + T_{32}^h + T_{33}^h + T_{34}^h + T_{35}^h)h'$.

For the first term, $E(T_{31}^h h') = -n\Gamma_0'\Phi^{-1}E(\widetilde{\Phi}_{\eta g}\Sigma\overline{g}\cdot\overline{g}')\Phi^{-1}\Gamma_0$.

Since $\widetilde{\Phi}_{\eta g} = \widetilde{\Phi}_{\eta g,1} + \widetilde{\Phi}_{\eta g,1}'$ and $\widetilde{\Phi}_{\eta g,1} = (1/n)\sum_{i=1}^n E(\eta_{0i}(\widetilde{\beta}_0-\beta_0)g_i')$, we have $nE(\widetilde{\Phi}_{\eta g}\Sigma\overline{g}\cdot\overline{g}') = nE(\widetilde{\Phi}_{\eta g,1}\Sigma\overline{g}\cdot\overline{g}') + nE(\widetilde{\Phi}_{\eta g,1}'\Sigma\overline{g}\cdot\overline{g}')$.

According to the independence assumption,

$$\begin{aligned} &nE\left(\widetilde{\Phi}_{\eta g,1}\Sigma\overline{g}\cdot\overline{g}'\right)\\ &= nE\left\{\left[\frac{1}{n}\sum_{i=1}^n E\left(\eta_{0i}\left(\widetilde{\beta}_0-\beta_0\right)g_i'\right)\right]\right.\\ &\qquad\left.\times\Sigma\left(\frac{1}{n}\sum_{j=1}^n g_j\right)\left(\frac{1}{n}\sum_{l=1}^n g_l'\right)\right\}\\ &= \frac{1}{n^2}\sum_{i=1}^n E\left\{\left[E\left(\eta_{0i}\left(\widetilde{\beta}_0-\beta_0\right)g_i'\right)\right]\Sigma g_ig_i'\right\}\\ &\quad+\frac{1}{n^2}\sum_{i=1}^n\sum_{\substack{j=1\\ j\neq i}}^n E\left\{\left[E\left(\eta_{0i}\left(\widetilde{\beta}_0-\beta_0\right)g_i'\right)\right]\Sigma g_jg_j'\right\}. \end{aligned} \tag{27}$$

According to the assumption for $\widetilde{\beta}$ and Assumption 1, the mathematical expectation of the first term is zero.

For the second term, $T_{32}^h h' = -n\Gamma_0'\Phi^{-1}(\overline{\Gamma}_0-\Gamma_0)\Omega^{-1}\Gamma_0'\Phi^{-1}\overline{g}\cdot\overline{g}'\Phi^{-1}\Gamma_0$. By Lemma 6, $E(T_{32}^h h') = 0$.

For the third term, $T_{33}^h h' = -(1/2)n\nabla\Gamma_0'[(\Sigma\overline{g})\otimes I_p]\Omega^{-1}\Gamma_0'\Phi^{-1}\overline{g}\cdot\overline{g}'\Phi^{-1}\Gamma_0$.

For the fourth term, $T_{34}^h h' = -(1/2)n[(\overline{g}'\Phi^{-1}\Gamma_0\Omega^{-1})\otimes I_p]\Gamma_1'\Sigma\overline{g}\cdot\overline{g}'\Phi^{-1}\Gamma_0$.

For the fifth term, $T_{35}^h h' = (1/2)n\Gamma_0'\Phi^{-1}\Gamma_1[(\Omega^{-1}\widehat{\Gamma}_0'\Phi^{-1}\overline{g})\otimes I_p]\Omega^{-1}\Gamma_0'\Phi^{-1}\overline{g}\cdot\overline{g}'\Phi^{-1}\Gamma_0$.

Similarly, according to the independence assumption and Assumption 1, the mathematical expectation of the third, fourth, and fifth terms are zero.

To sum up, $E(T_3^h h') = o(L^2/n)$. □

Lemma 10. *Consider*

$$E\left(T_4^h h'\right) = o\left(\frac{L^2}{n}\right). \tag{28}$$

Proof. By definition of T_4^h and h,

$$\begin{aligned} T_4^h h' &= n\Gamma_0'\Phi^{-1}\widetilde{\Phi}_1\Sigma\widetilde{\Phi}_1\Sigma\overline{g}\cdot\overline{g}'\Phi^{-1}\Gamma_0\\ &\quad-n\Omega^{-1}\left(\overline{\Gamma}_0-\Gamma_0\right)'\Sigma\widetilde{\Phi}_1\Sigma\overline{g}\cdot\overline{g}'\Phi^{-1}\Gamma_0. \end{aligned} \tag{29}$$

Similar to the proof of Lemma 8, we have

$$E\left(n\Gamma_0'\Phi^{-1}\widetilde{\Phi}_1\Sigma\widetilde{\Phi}_1\Sigma\overline{g}\cdot\overline{g}'\Phi^{-1}\Gamma_0\right) = o\left(\frac{L^2}{n}\right). \tag{30}$$

And according to the independence assumption and Assumption 1,

$$E\left(-n\Omega^{-1}\left(\overline{\Gamma}_0-\Gamma_0\right)'\Sigma\widetilde{\Phi}_1\Sigma\overline{g}\cdot\overline{g}'\Phi^{-1}\Gamma_0\right)=0=o\left(\frac{L^2}{n}\right). \tag{31}$$

To sum up, $E(T_4^h h')=o(L^2/n)$. □

Using these lemmas, then we can get the higher-order MSE of $\widehat{\beta}_0$ as follows.

Theorem 11. *For GMM estimator $\widehat{\beta}_0$ in (4), under Assumptions 1–5, if $L\to\infty$ and $\zeta^2(L)L/n\to 0$, then the higher-order MSE of $\sqrt{n}\widehat{\beta}_0$ is given by*

$$MSE\left(\sqrt{n}\widehat{\beta}_0\mid Z\right)=\Omega^{-1}+\Omega^{-1}\frac{\Pi\Pi'}{n}\Omega^{-1}+o\left(\frac{L^2}{n}\right) \tag{32}$$

in which

$$\begin{aligned}
\Omega^{-1}&=n\left[E(F\mid Z)'Z\left(\sum_{i=1}^n\sigma_i^2Z_iZ_i'\right)^{-1}Z'E(F\mid Z)\right]^{-1},\\
\Pi&=\sum_{i=1}^nB_{ii}\sigma_{u\varepsilon,i},\\
\Gamma_0&=\frac{1}{n}\sum_{i=1}^n\Gamma_{0i}=\frac{1}{n}\sum_{i=1}^nE\left(-Z_i\frac{\partial f_i}{\partial\beta'}\mid Z_i\right)\\
&=-\frac{1}{n}Z'E(F\mid Z),\\
F&=\left(\frac{\partial f_1}{\partial\beta},\dots,\frac{\partial f_n}{\partial\beta}\right)',\\
\Phi&=E\left(\frac{1}{n}\sum_{i=1}^ng_ig_i'\mid Z\right)\\
&=\frac{1}{n}E\left(\sum_{i=1}^nZ_i\varepsilon_i\varepsilon_iZ_i'\mid Z\right)\\
&=\frac{1}{n}\sum_{i=1}^n\sigma_i^2Z_iZ_i',\\
B_{ii}&=\frac{Z_i'\Sigma Z_i}{n},\\
\sigma_{u\varepsilon,i}&=E\left(u_i\varepsilon_i\mid Z_i\right),\\
u_i&=\frac{\partial f_i}{\partial\beta}-E\left(\frac{\partial f_i}{\partial\beta}\mid Z_i\right),\\
\Sigma&=\Phi^{-1}-\Phi^{-1}\Gamma_0\Omega^{-1}\Gamma_0'\Phi^{-1}.
\end{aligned} \tag{33}$$

Proof. By (12),

$$\begin{aligned}
&n\left(\widehat{\beta}_0-\beta_0\right)\left(\widehat{\beta}_0-\beta_0\right)'\\
&=\Omega^{-1}\left(h+\sum_{j=1}^4T_j^h+Z^h\right)\left(h+\sum_{j=1}^4T_j^h+Z^h\right)'\Omega^{-1}\\
&=\Omega^{-1}\left\{hh'+h\sum_{j=1}^4T_j^{h'}+\left(\sum_{j=1}^4T_j^h\right)h'\right.\\
&\quad\left.+\left(\sum_{j=1}^4T_j^h\right)\left(\sum_{j=1}^4T_j^h\right)'\right\}\Omega^{-1}+o_p\left(\frac{L^2}{n}\right).
\end{aligned} \tag{34}$$

By Lemma 6, $(\sum_{j=1}^4T_j^h)(\sum_{j=1}^4T_j^h)'=T_1^hT_1^{h'}+o_p(L^2/n)$, the above formula can be rewritten as

$$\begin{aligned}
&n\left(\widehat{\beta}_0-\beta_0\right)\left(\widehat{\beta}_0-\beta_0\right)'\\
&=\Omega^{-1}\left\{hh'+h\sum_{j=1}^4T_j^{h'}+\left(\sum_{j=1}^4T_j^h\right)h'+T_1^hT_1^{h'}\right\}\Omega^{-1}\\
&\quad+o_p\left(\frac{L^2}{n}\right).
\end{aligned} \tag{35}$$

By Lemmas 7–10,

$$\begin{aligned}
&E\left\{\Omega^{-1}\left[hh'+h\sum_{j=1}^4T_j^{h'}+\left(\sum_{j=1}^4T_j^h\right)h'+T_1^hT_1^{h'}\right]\Omega^{-1}\mid Z\right\}\\
&=\Omega^{-1}E\left[hh'\mid Z\right]\Omega^{-1}+o\left(\frac{L^2}{n}\right)+\Omega^{-1}E\left[T_1^hT_1^{h'}\mid Z\right]\Omega^{-1}\\
&=\Omega^{-1}+\Omega^{-1}E\left(T_1^hT_1^{h'}\mid Z\right)\Omega^{-1}+o\left(\frac{L^2}{n}\right).
\end{aligned} \tag{36}$$

In addition, by definition of T_1^h, $T_1^hT_1^{h'}=n(\overline{\Gamma}_0-\Gamma_0)'\Sigma\overline{g}\cdot\overline{g}'\Sigma(\overline{\Gamma}_0-\Gamma_0)$. Consider

$$\begin{aligned}
\overline{\Gamma}_0-\Gamma_0&=\frac{1}{n}\sum_{i=1}^n\left(\overline{\Gamma}_{0i}-\Gamma_{0i}\right)\\
&=-\frac{1}{n}\sum_{i=1}^nZ_i\left[\frac{\partial f_i}{\partial\beta'}-E\left(\frac{\partial f_i}{\partial\beta'}\mid Z_i\right)\right].
\end{aligned} \tag{37}$$

Denote $u_i=(\partial f_i/\partial\beta)-E((\partial f_i/\partial\beta)\mid Z_i)$; then $\overline{\Gamma}_0-\Gamma_0=-(1/n)Z'u$. $\overline{g}=(1/n)\sum_{i=1}^ng_i=(1/n)\sum_{i=1}^nZ_i\varepsilon_i=(1/n)Z'\varepsilon$. Then,

$$\begin{aligned}
T_1^hT_1^{h'}&=n\left(-\frac{1}{n}Z'u\right)'\Sigma\left(\frac{1}{n}Z'\varepsilon\frac{1}{n}\varepsilon'Z\right)\Sigma\left(-\frac{1}{n}Z'u\right)\\
&=\frac{1}{n}u'\frac{Z\Sigma Z'}{n}\varepsilon\varepsilon'\frac{Z\Sigma Z'}{n}u=\frac{1}{n}u'B\varepsilon\varepsilon'Bu.
\end{aligned} \tag{38}$$

According to the independence assumption,

$$\begin{aligned}
&E\left(T_1^h T_1^{h'} \mid Z\right) \\
&= \frac{1}{n} E\left(\sum_{i,j,k,l} u_i B_{ij} \varepsilon_j \varepsilon_k B_{kl} u_l' \mid Z\right) \\
&= \frac{1}{n} E \\
&\quad \times \left(\left\{\sum_{i=j=k=l} + \sum_{i=j=k\neq l} + \sum_{i=j\neq k=l} + \sum_{i=j\neq k\neq l}\right.\right. \\
&\qquad \left. + \sum_{i\neq j=k=l} + \sum_{i\neq j=k\neq l} + \sum_{i\neq j\neq k=l} + \sum_{i\neq j\neq k\neq l}\right\} \\
&\qquad \left. \times u_i B_{ij} \varepsilon_j \varepsilon_k B_{kl} u_l' \mid Z\right) \\
&= \frac{1}{n} E\left(\sum_{i=1}^{n} u_i B_{ii} \varepsilon_i \varepsilon_i B_{ii} u_i' \mid Z\right) \\
&\quad + \frac{1}{n} E\left(\sum_{i\neq k} u_i B_{ii} \varepsilon_i \varepsilon_k B_{kk} u_k' \mid Z\right) \\
&\quad + \frac{1}{n} E\left(\sum_{i\neq j} u_i B_{ij} \varepsilon_j \varepsilon_j B_{ji} u_i' \mid Z\right) \\
&\quad + \frac{1}{n} E\left(\sum_{i\neq j} u_i B_{ij} \varepsilon_j \varepsilon_i B_{ij} u_j' \mid Z\right) \\
&= \frac{1}{n} \sum_{i=1}^{n} B_{ii}^2 E\left(u_i \varepsilon_i \varepsilon_i u_i' \mid Z\right) \\
&\quad + \frac{1}{n} \sum_{i\neq k} B_{ii} B_{kk} E\left(u_i \varepsilon_i \mid z_i\right) E\left(\varepsilon_k u_k' \mid z_k\right) \\
&\quad + \frac{1}{n} \sum_{i\neq j} B_{ij}^2 E\left(u_i u_i' \mid z_i\right) E\left(\varepsilon_j^2 \mid z_j\right) \\
&\quad + \frac{1}{n} \sum_{i\neq j} B_{ij}^2 E\left(u_i \varepsilon_i \mid z_i\right) E\left(\varepsilon_j u_j' \mid z_j\right) \\
&= \frac{1}{n} \left[\sum_{i=1}^{n} B_{ii} \sigma_{u\varepsilon,i}\right] \left[\sum_{i=1}^{n} B_{ii} \sigma_{u\varepsilon,i}\right]' + o_p\left(\frac{L^2}{n}\right) \\
&= \frac{\Pi\Pi'}{n} + o_p\left(\frac{L^2}{n}\right).
\end{aligned} \tag{39}$$

□

In (32), Ω^{-1} is asymptotic variance of $\sqrt{n}\widehat{\beta}_0$, and $\Omega^{-1}(\Pi\Pi'/n)\Omega^{-1}$ can be seen as the asymptotic bias terms. In practice, Ω and Π can be substituted by their consistent estimators.

4. Conclusions

In this paper, we consider a general nonlinear regression model with endogeneity and derive the higher-order mean square error of two-step efficient generalized method of moments estimators for this nonlinear model. The theoretical results in this paper allow the number of moments to grow with but at smaller rate than the sample size. And the derivations are suitable for general moment restriction models, which contain conditional moment restriction models and linear models as special cases. The higher-order mean squared error got in this paper has many uses. For example, it can be used to compare among different estimators or to construct the selection criteria of moments for improving the finite sample performance of GMM estimators. This paper considered a restrictive condition in which the data generating process is independent. It would be valuable to extend the results to the dynamic panel data models, in which the moments are going with the time dimension. It is saved for future research.

Conflict of Interests

The authors declare that there is no conflict of interests regarding the publication of this paper.

Acknowledgments

This work was partially supported by the National Natural Science Foundation of China (Grant nos. 71301160, 71203224, and 71301173), Beijing Planning Office of Philosophy and Social Science (13JGB018), and Program for Innovation Research in Central University of Finance and Economics.

References

[1] A. Ciarreta and A. Zarraga, "Economic growth-electricity consumption causality in 12 European countries: a dynamic panel data approach," *Energy Policy*, vol. 38, no. 7, pp. 3790–3796, 2010.

[2] O. Galor and D. N. Weil, "Population, technology, and growth: from malthusian stagnation to the demographic transition and beyond," *The American Economic Review*, vol. 90, no. 4, pp. 806–828, 2000.

[3] Y. Hu, X.-H. Xia, M.-J. Wang, and Z.-M. Chen, "The effects of cross-section dimension n in panel co-integration test," *Communications in Nonlinear Science and Numerical Simulation*, vol. 15, no. 4, pp. 1019–1027, 2010.

[4] C.-X. Huang, C.-L. Peng, X.-H. Chen, and F.-H. Wen, "Dynamics analysis of a class of delayed economic model," *Abstract and Applied Analysis*, vol. 2013, Article ID 962738, 12 pages, 2013.

[5] C.-X. Huang, X. Gong, X.-H. Chen, and F.-H. Wen, "Measuring and forecasting volatility in Chinese stock market using HAR-CJ-M model," *Abstract and Applied Analysis*, vol. 2013, Article ID 143194, 13 pages, 2013.

[6] J. H. Lin, Y. Hu, M. J. Wang, and X. H. Xia, "A Monte Carlo comparison of panel unit root tests under factor structure," *Applied Economics Letters*, vol. 20, no. 3, pp. 288–291, 2013.

[7] F. Wen and Z. Liu, "A copula-based correlation measure and its application in chinese stock market," *International Journal*

of Information Technology & Decision Making, vol. 8, no. 4, pp. 787–801, 2009.

[8] F. Wen, Z. Li, C. Xie, and D. Shaw, "Study on the fractal and chaotic features of the Shanghai composite index," *Fractals*, vol. 20, no. 2, pp. 133–140, 2012.

[9] L. P. Hansen, "Large sample properties of generalized method of moments estimators," *Econometrica*, vol. 50, no. 4, pp. 1029–1054, 1982.

[10] Y. Hu, D.-M. Guo, Y. Deng, and S.-Y. Wang, "Estimation of nonlinear dynamic panel data models with individual effects," *Mathematical Problems in Engineering*, vol. 2014, Article ID 672610, 7 pages, 2014.

[11] B. Antoine and E. Renault, "Efficient GMM with nearly-weak instruments," *The Econometrics Journal*, vol. 12, supplement s1, pp. S135–S171, 2009.

[12] M. Caner, "Lasso-type GMM estimator," *Econometric Theory*, vol. 25, no. 1, pp. 270–290, 2009.

[13] I. A. Canay, "Simultaneous selection and weighting of moments in GMM using a trapezoidal kernel," *Journal of Econometrics*, vol. 156, no. 2, pp. 284–303, 2010.

[14] W. K. Newey and F. Windmeijer, "Generalized method of moments with many weak moment conditions," *Econometrica*, vol. 77, no. 3, pp. 687–719, 2009.

[15] J. F. Kiviet and G. D. A. Phillips, "Higher-order asymptotic expansions of the least-squares estimation bias in first-order dynamic regression models," *Computational Statistics & Data Analysis*, vol. 56, no. 11, pp. 3705–3729, 2012.

[16] A. L. Nagar, "The bias and moment matrix of the general k-class estimators of the parameters in simultaneous equations," *Econometrica*, vol. 27, no. 4, pp. 575–595, 1959.

[17] S. G. Donald and W. K. Newey, "Choosing the number of instruments," *Econometrica*, vol. 69, no. 5, pp. 1161–1191, 2001.

[18] G. M. Kuersteiner, "Kernel-weighted GMM estimators for linear time series models," *Journal of Econometrics*, vol. 170, no. 2, pp. 399–421, 2012.

[19] P. Rilstone, V. K. Srivastava, and A. Ullah, "The second-order bias and mean squared error of nonlinear estimators," *Journal of Econometrics*, vol. 75, no. 2, pp. 369–395, 1996.

[20] Y. Bao and A. Ullah, "The second-order bias and mean squared error of estimators in time-series models," *Journal of Econometrics*, vol. 140, no. 2, pp. 650–669, 2007.

[21] Y. Bao and A. Ullah, "Higher-order bias and MSE of nonlinear estimators," *Pakistan Journal of Statistics*, vol. 25, no. 4, pp. 587–594, 2009.

[22] W. K. Newey and R. J. Smith, "Higher order properties of GMM and generalized empirical likelihood estimators," *Econometrica*, vol. 72, no. 1, pp. 219–255, 2004.

[23] S. Anatolyev, "GMM, GEL, serial correlation, and asymptotic bias," *Econometrica*, vol. 73, no. 3, pp. 983–1002, 2005.

[24] S. G. Donald, G. W. Imbens, and W. K. Newey, "Choosing instrumental variables in conditional moment restriction models," *Journal of Econometrics*, vol. 152, no. 1, pp. 28–36, 2009.

[25] S. G. Donald, G. W. Imbens, and W. K. Newey, "Empirical likelihood estimation and consistent tests with conditional moment restrictions," *Journal of Econometrics*, vol. 117, no. 1, pp. 55–93, 2003.

[26] J. Alvarez and M. Arellano, "The time series and cross-section asymptotics of dynamic panel data estimators," *Econometrica*, vol. 71, no. 4, pp. 1121–1159, 2003.

[27] R. Okui, "The optimal choice of moments in dynamic panel data models," *Journal of Econometrics*, vol. 151, no. 1, pp. 1–16, 2009.

Hindawi Publishing Corporation
Discrete Dynamics in Nature and Society
Volume 2014, Article ID 158386, 9 pages
http://dx.doi.org/10.1155/2014/158386

Research Article

Investors' Risk Preference Characteristics Based on Different Reference Point

Fenghua Wen, Zhifang He, Xu Gong, and Aiming Liu

School of Business, Central South University, Changsha, Hunan 410083, China

Correspondence should be addressed to Aiming Liu; liuaiming@csu.edu.cn

Received 6 January 2014; Accepted 12 March 2014; Published 9 April 2014

Academic Editor: Chuangxia Huang

Taking the stock market as a whole object, we assume that prior losses and gains are two different factors that can influence risk preference separately. The two factors are introduced as separate explanatory variables into the time-varying GARCH-M (TVRA-GARCH-M) model. Then, we redefine prior losses and gains by selecting different reference point to study investors' time-varying risk preference. The empirical evidence shows that investors' risk preference is time varying and is influenced by previous outcomes; the stock market as a whole exhibits house money effect; that is, prior gains can decrease investors' risk aversion while prior losses increase their risk aversion. Besides, different reference points selected by investors will cause different valuation of prior losses and gains, thus affecting investors' risk preference.

1. Introduction

Many studies suggest that investors' risk preference changes over time. When investors make decision under uncertainty in financial markets, prior outcomes of investors' can influence their risk preference, which can cause their decision-making behaviors to change. Studies as discussed in [1–4] believed that people's risk preference or risk aversion changed over time and the prior outcomes could influence their current decision making. And a similar finding in futures market that both prior losses and gains could affect investors' risk preference was reached in [5–7].

However, there is no agreement on what effects will prior outcomes have on investors' risk preference, which attracts an increasing number of scholars to study it. Early studies mainly focused on disposition effect which reflects the tendency to sell assets that have gained value and keep assets that have lost value. In other words, investors tend to be risk seeking with losses and risk averse with gains. Some scholars [8–10] supported the conclusion with experimental research, while some authors [11–13] proved this conclusion using actual trading data. Disposition effect was originally attributed to loss aversion which means that investors loathe losses and are willing to take greater risks to avoid further losses. However, based on the Prospect Theory proposed by Kahneman and Tversky [14], studies [15–18] argued that investors were willing to take risk after prior gains, which was called "house money effect." Thaler and Johnson [15] pointed out that investors' behavior defied prediction and the editing rules were usually quite different, so it was hard to achieve agreement on this problem. Barberis and Xiong [19] studied the effect of prior losses and gains on current decision-making behaviors from a new perspective and they constructed a multiperiod model in which investors decided their risk preferences according to prior outcomes. They found that there was no disposition effect but in some cases investors' decision-making behaviors exhibit house money effect. Similarly, Hoffmann et al. [20] made a study on the evolution of risk behavior in a multiperiod decision context and showed how prior outcomes influenced subsequent choices. In recent studies, a lot of scholars adopted a more direct method to explore investor's risk-taking behavior after losses or gains. Coval and Shumway [21] found that futures traders in the Chicago Board of Trade were more willing to take risk after losses than gains. Frino et al. [6] qualitatively differentiated gains and losses with professional futures traders' actual trading data to compare their risk preference in the afternoon after gains and losses in the morning, respectively, for the purpose of testing the house money effect and the opposite behavior of loss aversion simultaneously; the empirical result showed that those investors' behavior supported the house money effect, but no proof of loss aversion was found. Mattos and Garcia [22] selected 12 traders' trading records in the agricultural futures and options market as sample to study continuous dynamic risk decision and they pointed out that, owing to investors' different reactions to prior gains of different investment portfolios, five traders exhibited the house money effect, and four traders showed loss aversion, while three traders' risk preferences were not influenced by prior gains. Using a set of transaction records from Taiwan Futures Exchange, Huang and Chan [23] examined risk-taking behavior subject to prior outcomes and showed that the degree of morning gains/losses nonlinearly influences afternoon risk taking for all trader types.

When studying what effects will the prior outcomes have on the investors' risk preference, the selection of the reference point is critical. Kahneman and Tversky [14] believed that people's risk preferences varied and they usually chose a reference point to value the gain and the loss under uncertainties and had different risk preferences in the face of gains and losses. Thaler and Johnson [15] designed a series of questionnaires for experimental research and the result showed that people are more willing to gamble with prior gains; that is to say, the selection of reference point will affect prior loss and gain assessment, so as to affect risk preference. Tversky and Kahneman [24] pointed out that the value of a risk-return opportunity relied more on the selection of reference point than on the ultimate total return. Therefore, they claimed that people could manipulate people's decision by changing the reference point. Zhang [25] described that different selection of reference point would result in different expectations; therefore, it was impossible for behaviors drived by their expectation to conform the rational expectation theory.

The above literatures' analysis shows that, on the one hand, the research of what effects prior losses and gains have on investors' risk preference has not achieved agreement. Under the background of professional trading, Coval and Shumway [21], Frino et al. [6], and Mattos and Garcia [22] used regression models to explore how prior losses and gains affect current risk preference from the perspective of average market risk or extreme market risk. Lam and Ozorio [26] made an experimental betting game and investigated the gender risk-taking behavior with respect to prior outcomes in three distinct groups. In view of the bounded rationality of investors, the real market scenes can hardly be simulated through experiment and data of investors' transaction accounts usually are nonrepresentative because of the difficulty of obtaining. Thus, we take the entire stock market as the object, constructing the TVRA-GARCH-M model to study the effect of prior losses and gains on current risk preference and considered the problem raised by Frino et al. [6], which is that if prior losses and gains are treated as a continuous explanatory variable with both positive and negative values, it is impossible to decide whether the effect of prior losses and gains on investors' risk preference is the house money effect or loss aversion. On the other hand, in previous studies about the risk preference of investors, the selection of a reference point is subjective and there is no uniform criterion as to the selection of reference point.

In view of previous studies about the effect of prior losses and gains on investors' risk preference and about the selection of reference price being insufficient and inadequate, this paper utilizes ten worldwide representative indexes and uses prior losses and gains as separate explanatory variables to explore their overall effects on current risk preference in the entire market on the basis of TVRA-GARCH-M model. Then, we choose the historical high price, the historical low price, the 5-day average price, the 20-day average price, the 30-day average price, and the memory-adjusted price as the reference point, respectively, to further test investors' risk preference. On the one hand, this paper has overcome the demerits of the psychological experiments of Frino et al. [6], being hard to simulate the real market and having inadequate samples, and constructed the TVRA-GARCH-M model. On the other hand, this paper has adopted six different reference prices, which makes up for the drawbacks that the subjective selection of reference point may result in conflicting conclusions.

This paper is organized as follows: the second part presents the model analysis; the third part provides the empirical study which includes the sample selection and the empirical result; the fourth part is the conclusion.

2. The Model Analysis

2.1. Selection of Reference Price. It should be pointed out that the reference price is a critical factor to the judgments of gains and losses. If the stock price exceeds the reference price, investors get gains or otherwise obtain losses. Reference price, as a kind of investors' psychological price, is different with personal evaluation criteria, and it is hard to determine which reference price is the most reasonable. Many researchers believe that investors usually take the average and extreme price as their reference points.

2.1.1. The Maximum Price and Minimum Price. Many researchers found that investors usually were affected by the historical highest or lowest price when measuring gains and losses. For example, studies as discussed in [27, 28] found that the historical highest price had significant influence on investors' decision in stock option market; Grinblatt and Keloharju [29] suggested that the highest and lowest price of the last month were important factors that could affect investors' trading behavior; Gneezy [30] studied disposition effect and discovered that investors tend to treat the historical highest price as the reference price when making investment decisions; Vinokur [31] adopted the 30-day highest price as the reference point to examine the disposition effect in the carbon market. In line with the circumstances of most stock markets, this paper takes 20 days as the average trading days for a month and then decides the maximum and minimum prices of every month as the reference points, which can be represented as

$$\begin{aligned} RP_t &= \text{Max}\left(P_{t-1}, P_{t-2}, \ldots, P_{t-20}\right) \\ RP_t &= \text{Min}\left(P_{t-1}, P_{t-2}, \ldots, P_{t-20}\right). \end{aligned} \tag{1}$$

2.1.2. The Average Price. Anderson [32] and Mandler and Ritchey [33] suggested that investors tend to remember the average level instead of some particular details. Grinblatt and Han [34] took the weighted average price as the reference price of the investor when studying the disposition effect and momentum effect. In the stock market, full consideration should be given to people's practical operations during the process of investment when choosing reference price. And the moving averages as important trend indicators of technical analysis for securities are usually decisive factors for investors making stock trading. They tend to make decisions by analyzing these trend lines (5-day, 10-day, and 30-day average lines). Accordingly, this paper adopts the frequently used moving average prices of 5 days (P_t^5), 10 days (P_t^{10}), and 30 days (P_t^{30}) as investors' reference prices, which are estimated as

$$\begin{aligned} P_t^5 &= \frac{1}{5}\left(P_{t-1} + P_{t-2} + \cdots P_{t-5}\right) \\ P_t^{10} &= \frac{1}{10}\left(P_{t-1} + P_{t-2} + \cdots P_{t-5}\right) \\ P_t^{30} &= \frac{1}{30}\left(P_{t-1} + P_{t-2} + \cdots P_{t-5}\right). \end{aligned} \tag{2}$$

2.1.3. Memory-Adjusted Price. Kopalle and Lindsey-Mullikin [35] and Taudes and Rudloff [36] pointed out that the reference price would be affected by prior losses and gains, and people tend to adjust the current reference point according to the prior decision outcome. They believed that people would adjust their reference point as the following equation:

$$mp_t = \alpha mp_{t-1} + (1-\alpha) p_{t-1} = \alpha\left(mp_{t-1} - p_{t-1}\right) + p_{t-1}, \tag{3}$$

where α ($0 \le \alpha < 1$) is a memory parameter and mp_t is the reference price during t period. p_{t-1} is the stock price of last period, which means that people would adjust the current reference price with reference to the memory of the prior loss or gain on the basis of the last-period price. In view of the above, this paper takes the memory-adjusted price as investors' reference price, where the memory parameter α is set to be 0.2 according to the study made by Taudes and Rudloff [36].

2.2. Model Construction

2.2.1. The Time-Varying Risk Preference. In GARCH-M model, the risk premium coefficient in the mean equation represents the required compensation for each unit of risk. The larger the risk premium coefficient, the greater the compensation required by investors and the stronger the tendency to be risk averse. So the risk premium coefficient can be used to measure investors' risk preference [37]. However, according to behavioral financial theory, investors make different decisions and have different risk preference for gains and losses and they measure the gain and loss by comparing the stock price with the reference price. In prospect theory, the reference price is a key factor to determine the gain and loss. Therefore, reference price should also be taken into consideration when estimating the gain and loss which can influence invertors' risk preference, as is pointed out in [38]. We argue that the part of the stock price that exceeds the reference price, that is, $(p_t - rp_t)$ (p_t and rp_t are the stock price and the reference price), is the gain. And the part of the stock price that is below the reference price is the loss. We adjust $p_t - rp_t$ to the relative size $(p_t - rp_t)/rp_t$ with logarithmic form $\ln(p_{t-1}) - \ln(rp_{t-1})$. Prior losses and gains will change with different reference prices adopted, and we construct the following TVRA-GARCH-M model:

$$\begin{aligned} r_t &= c + x_t \cdot \beta + \gamma_t \sqrt{h_t} + \varepsilon_t, \\ \gamma_t &= \rho_0 + \rho_1 \cdot \gamma_{t-1} + \rho_2 \cdot \frac{s_{t-1}}{\sqrt{h_{t-1}}}, \\ \varepsilon_t &= \sqrt{h_t} \cdot v_t, \\ h_t &= \alpha_0 + \alpha_1 \varepsilon_{t-1}^2 + \theta_1 h_{t-1}, \end{aligned} \tag{4}$$

where $s_{t-1} = \ln(p_{t-1}) - \ln(rp_{t-1})$, p_{t-1} and rp_{t-1} are the prior stock price and reference price, $s_{t-1}/\sqrt{h_{t-1}}$ is the risk adjusted gain or loss of last period, ρ_0 is the fixed risk compensation required by investors for each unit of risk, which can be regarded as investors' inherent risk preference for a certain period of time, ρ_1 means that the current risk tolerance would be affected by that of the last period, which represents an average level of the current behavior affected by historical behavior, and ρ_2 denotes that people's risk preferences are subjected to the prior losses or gains. If ρ_2 is obviously less than zero, the compensation for risk will decrease with prior gains ($s_{t-1} > 0$), thus decreasing their extent of risk aversion, while, with prior losses ($s_{t-1} < 0$), the amount of their risk aversion will increase, or otherwise. Therefore, the risk compensation coefficient γ_t is no longer fixed, but it changes with time and is affected by prior outcomes.

2.2.2. House Money Effect and Loss Aversion. Psychological experiments suggested that people's decisions exhibit asymmetry when facing gains and losses. Thaler and Johnson [15] have made multiperiod gambling experiments of real money to study the effect of prior losses and gains on investors' current risk preference. And they find that people were more willing to take risks after getting gains—risk-seeking, which is the so-called "house money effect." They also discovered that people are less willing to take risks with prior losses—risk aversion. According to the behavioral finance theory, loss aversion shows that people's risk preference is inconsistent; that is, people are risk averse with gains and risk seeking with losses. In recent years, more studies of loss aversion are extended from single-period gambling to multiperiod of dynamic decision to study loss aversion. Frino et al. [6] have studied the effect of gains and losses in the morning on the degree of risk seeking in the afternoon with trading data from Sydney Futures Exchange. They suggested that the house money effect and loss aversion are symmetric antithesis, which was to say house money effect meant the morning gain would boost higher afternoon risk seeking, but

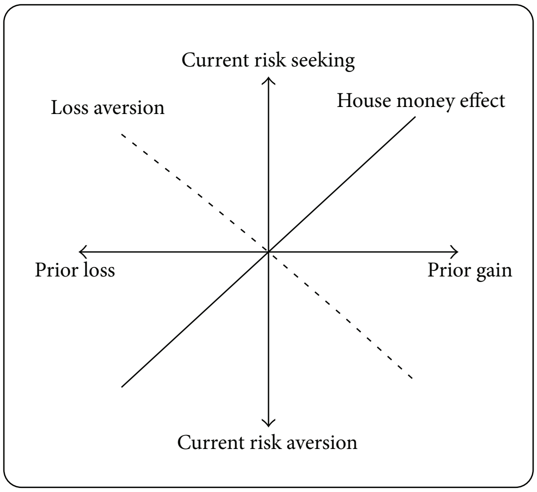

Figure 1: Hypothesized effects of prior loss and gain on current risk preference.

loss aversion meant the morning loss would enhance higher afternoon risk seeking. Mattos and Garcia [22] investigated trading behaviors in a dynamic frame and they suggested that five traders exhibited the house money effect and four investors showed risk aversion. Based on the above analysis, the house money effect and loss aversion are two separated psychological ways of motivation with regard to the effect of prior loss and gain on the current risk preference. Therefore, for the purpose of investigating the separated effect of prior losses and gains on time-varying risk preference, the key step is to examine the two psychological biases—the house money effect and loss aversion. For more visual effect, we illustrate it as in Figure 1.

Based on the TVRA-GARCH-M model, we further qualitatively distinguish the prior loss and prior gain: $s_{t-1} < 0$ means the prior loss and $s_{t-1} > 0$ shows the prior gain. In behavioral finance, there are many theoretical assumptions and empirical studies that have proved that the prior loss and the prior gain were two separated mental entities. The S-shaped value function proposed by Kahneman and Tversky [14] was based on people's different reactions to gains and losses when making risk decision. In the above TVRA-GARCH-M model, the gain and loss were treated equally as a continuous explanatory variable with both positive and negative values. However, as Figure 1 shows, to some extent, equal amount of change in a prior loss and a prior gain has the equivalent but opposite effects on current risk preference.

In essence, if we only take the prior loss and the prior gain as values with different signs, but do not estimate them as separate explanatory variables in a model, it is impossible to test the house money effect ($\rho_2 < 0$) and loss aversion ($\rho_2 > 0$) at the same time. Besides, if the two biases exist simultaneously and with almost the same level of effect, the estimated coefficient for ρ_2 will be close to zero, thus making the two effects impossible to be tested.

Consequently, the following time-varying risk compensation coefficient model is derived on the basis of the above analysis to further test the house money effect and loss aversion simultaneously. We build the model called TVRAS-GARCH-M model as follows:

$$\begin{gathered} r_t = c + x_t \cdot \beta + \gamma_t \sqrt{h_t} + \varepsilon_t, \\ \gamma_t = \rho_0 + \rho_1 \cdot \gamma_{t-1} + \lambda_{11} \cdot \frac{s'_{t-1}}{\sqrt{h_{t-1}}} + \lambda_{12} \cdot \frac{s''_{t-1}}{\sqrt{h_{t-1}}}, \\ \varepsilon_t = \sqrt{h_t} \cdot v_t, \\ h_t = \alpha_0 + \alpha_1 \varepsilon_{t-1}^2 + \theta_1 h_{t-1}, \\ s'_{t-1} = s_{t-1}, \quad s_{t-1} > 0, \\ s''_{t-1} = s_{t-1}, \quad s_{t-1} < 0, \end{gathered} \tag{5}$$

where s_{t-1} is the prior gain or loss based on reference points, variables s'_{t-1} and s''_{t-1} mean prior gains and losses, respectively, $s'_{t-1}/\sqrt{h_{t-1}}$ is the risk adjusted gain of last period, and $s''_{t-1}/\sqrt{h_{t-1}}$ is the risk adjusted loss of last period. Parameter λ_{11} reflects investors' demanding compensation for each unit of risk with prior gains and λ_{12} denotes the compensation investors demanded for each unit of risk with prior losses.

3. Empirical Study

3.1. The Sample and Descriptive Statistics. In this paper, the sample data are the composite indexes of the top 10 market values in the global stock markets in 2011, including NYSE (USA), NASDAQ (USA), N225 (Japan), the FTSE 100 (UK), SSE (China), HSI (China), TSX (Canada), BOVESPA (Brazil), AORD (Australia), and DAX (Germany). The time span is from October 15, 2002, to October 15, 2012. All data are from Yahoo finance (http://finance.yahoo.com/). The return is expressed in logarithmic return $r_t = 100 * \ln(p_t/p_{t-1})$, where r_t is the logarithmic return and p_t is the adjusted closing price in stock market. The descriptive statistics are shown in Table 1.

According to the skewness, kurtosis, and J-B statistic of each index shown in Table 1, it can be seen that the return distributions of all indexes are skewed, and the Kurtosis values exceed that of a normal distribution, which shows that all the return distributions of all indexes are not normal.

3.2. Empirical Evidence

3.2.1. Results of TVRA-GARCH-M Model with Different Reference Points. Based on previous studies, investors' different reference points will affect the judgment of prior losses and gains, thus affecting investors' risk preference. Therefore, we select six reference points on the basis of the analysis in Section 2.2.1 and use the world's ten representative indexes for the maximum likelihood estimation of model (4) to examine the risk preference of the entire stock market.

Tables 2, 3, 4, 5, 6, and 7 show the TVRA-GARCH-M' estimation results, respectively, by taking the highest price per month (MAX), the lowest price per month (MIN), 5-day moving average price (P_t^5), 10-day moving average price (P_t^{10}),

Table 1: Descriptive statistics of returns.

Statistic/index	Mean	Std.	Skewness	Kurtosis	JB statistic	Number
NYSE	−0.020146	1.379473	0.386855	12.76570	10072.59	2519
NASDAQ	−0.034578	1.456799	0.178026	8.740239	3471.719	2519
N225	0.001421	1.548458	0.547135	11.61059	7697.198	2452
FTSE	−0.013400	1.265248	0.102467	10.37660	5729.256	2525
SSE	−0.013083	1.656866	0.246740	6.634653	1412.133	2519
HSI	−0.032618	1.605285	−0.037799	12.15559	8749.820	2505
TSX	−0.025141	1.214611	0.680644	13.14799	10544.64	2414
BOV	−0.078359	1.861404	0.084820	8.040546	2623.075	2475
AORD	−0.016793	1.072880	0.553147	8.880106	3781.326	2535
DAX	−0.033998	1.539663	−0.038525	8.105775	2773.715	2553

Table 2: Results of TVRA-GARCH-M model (MAX).

Index/parameter	NYSE	NASDAQ	N225	FTSE	SSE	HSI	TSX	BOV	AORD	DAX
ρ_0	0.129	−0.055	−0.033	−0.317	0.008**	−0.061	−0.091	0.248	−0.130	−0.070
	[0.123]	[0.122]	[0.148]	[0.125]	[0.003]	[0.108]	[0.097]	[0.173]	[0.115]	[0.116]
ρ_1	−0.815***	−0.406	−0.985***	−0.707***	0.979***	−0.501	0.376	−0.979***	−0.696	−0.984***
	[0.128]	[0.957]	[0.011]	[0.203]	[0.008]	[0.719]	[0.603]	[0.021]	[0.494]	[0.009]
ρ_2	−2.503***	−1.184	−0.549	−3.251***	0.066***	−1.213*	−1.162	−0.492	−1.572	−0.759*
	[0.732]	[0.922]	[0.409]	[0.884]	[0.024]	[0.711]	[1.091]	[0.401]	[1.012]	[0.430]
Likelihood	−3574.632	−3988.067	−4083.697	−3533.477	−4436.532	−4083.826	−3298.369	−4688.108	−3153.892	−4137.287

Note: ∗ ∗ ∗, ∗∗, and ∗ in all tables denote that the parameter is significant at 1%, 5%, and 10% level, respectively.

and 30-day moving average price (P_t^{30}), and the memory-adjusted price (MP) as the reference points.

As is shown in the above tables, among the TVRA-GA0RCH-M model estimation results with MAX, MIN, P_t^5, P_t^{10}, P_t^{30}, and MP as the reference points, the time-varying processes of risk compensation coefficient estimation results show that the estimated results for ρ_1 are mostly significant at the significance level of 10% with both positive and negative values for different composite indexes and different reference points, indicating that people's prior risk tolerance would have sustained effect on the current risk tolerance, but it cannot be decided whether the influence will be strengthened or decayed from the perspective of entire stock market. Moreover, the ρ_2 in most indexes are significantly negative. For those indexes with insignificant ρ_2, most of them are also negative with the exception of China's SSE (this may be due to the immaturity of China's stock markets), which indicates that in the stock market prior gains will bring down the current risk aversion and make investors become risk seeking, which shows the house money effect, while prior losses will push up the current risk aversion. Therefore, investors' risk preferences are time varying; the factors including prior gains and losses as well as prior risk tolerance will affect investors' current required risk compensation with each unit of risk.

Further observation shows that though the ten composite indexes as a whole show the house money effect, there are still some differences. For all indexes, when selecting different reference points, the same index does not have consistent value for ρ_1 and ρ_2. Taking the NYSE index as an example, the model estimation results with MAX, MIN, P_t^5, P_t^{10}, P_t^{30}, and MP as reference points are all significant and the sizes are −0.815, −0.798, 0.668, −0.556, −0.775, and 0.777 for ρ_1 and −2.503, −3.098, −1.735, −4.623, −2.807, −3.119, and 3.119 for ρ_2. For the NASDAQ composite index, its ρ_1 results are −0.406, −0.473, −0.173, and −0.265, which are insignificant and 0.010 and 0.670, which are significant. And ρ_2 results are −1.184 and −1.302, which are insignificant, and −2.270, −2.211, 27.024, and −2.003, which are insignificant. All show that investors' risk preference is influenced by the selection of reference points. The prior loss and gains vary with different reference points, which to some extent will affect the investors' decision making.

3.2.2. Results of TVRAS-GARCH-M Model with Different Reference Points. With the empirical study described in Section 3.2.1, we get the TVRA-GARCH-M model results with different preference points. To further explore how the prior investment outcomes (gains and losses) influence the current risk preference on the basis of the analysis in Section 2.2, we further estimate the TVRAS-GARCH-M model with a variety of reference points. The results are shown in Tables 8, 9, 10, 11 ,12, and 13.

The above tables (from Table 8 to Table 13) show that the entire stock market displays house money effect. Investors will become risk seeking with prior gains and risk averse with prior losses. Specifically, with six reference points, the parameter λ_{11} or λ_{12} is mostly significant, and most are significantly negative with the exception of one or two indexes. In Table 8, parameter λ_{11} is significantly negative, with the exception of SSE being significantly positive; Table 9 shows that parameters λ_{12} are all significantly negative; Table 13 shows that λ_{11} in eight indexes is significantly negative. In

Table 3: Results of TVRA-GARCH-M model (MIX).

Index/parameter	NYSE	NASDAQ	N225	FTSE	SSE	HSI	TSX	BOV	AORD	DAX
ρ_0	0.291***	0.154	0.070	0.349***	−0.002	0.109	0.098	0.385***	0.088	0.046
	[0.101]	[0.120]	[0.114]	[0.100]	[0.001]	[0.116]	[0.098]	[0.145]	[0.09]	[0.102]
ρ_1	−0.798***	−0.473	−0.995***	−0.746***	0.982***	−0.534	0.265	0.987***	−0.758***	−0.987***
	[0.108]	[0.735]	[0.002]	[0.125]	[0.007]	[1.115]	[0.672]	[0.010]	[0.213]	[0.006]
ρ_2	−3.098***	−1.302	−0.409	−3.800***	0.056***	−0.623	−1.437	−0.601*	−2.587**	−0.614*
	[0.832]	[0.880]	[0.274]	[0.947]	[0.020]	[0.666]	[1.278]	[0.360]	[1.068]	[0.334]
Likelihood	−3572.507	−3987.908	−4083.661	−3531.389	−4434.745	−4085.042	−3298.805	−4686.645	−3152.282	−4136.812

Note: ∗ ∗ ∗, ∗∗, and ∗ in all tables denote that the parameter is significant at 1%, 5%, and 10% level, respectively.

Table 4: Results of TVRA-GARCH-M model (P_t^5).

Index/parameter	NYSE	NASDAQ	N225	FTSE	SSE	HSI	TSX	BOV	AORD	DAX
ρ_0	0.008	0.060	−0.001	0.075	0.271***	0.003	−0.004	0.051	−0.007	0.001
	[0.018]	[0.082]	[0.020]	[0.106]	[0.001]	[0.010]	[0.016]	[0.051]	[0.013]	[0.018]
ρ_1	0.668***	−0.173	0.728**	0.898**	−1.003***	0.833***	0.742***	0.577**	0.761***	0.674***
	[0.159]	[0.597]	[0.257]	[0.406]	[0.001]	[0.191]	[0.116]	[0.257]	[0.285]	[0.217]
ρ_2	−1.735***	−2.270*	−0.698	−0.164	0.229***	−0.401	−1.800***	−1.137**	−0.708	−1.062**
	[0.663]	[1.344]	[0.518]	[0.148]	[0.001]	[0.345]	[0.631]	[0.571]	[0.674]	[0.563]
Likelihood	−3598.082	−4019.787	−4145.145	−3598.893	−4518.374	−4143.122	−3344.253	−4758.705	−3197.032	−4211.978

Note: ∗ ∗ ∗, ∗∗, and ∗ in all tables denote that the parameter is significant at 1%, 5%, and 10% level, respectively.

Table 5: Results of TVRA-GARCH-M model (P_t^{10}).

Index/parameter	NYSE	NASDAQ	N225	FTSE	SSE	HSI	TSX	BOV	AORD	DAX
ρ_0	0.064	0.054	0.0279	0.105	0.002***	0.040	−0.008	0.080	−0.053	0.005
	[0.084]	[0.087]	[0.136]	[0.098]	[0.009]	[0.092]	[0.037]	[0.094]	[0.089]	[0.101]
ρ_1	−0.556**	−0.265	−0.889***	−0.736***	0.986***	−0.604 (0.31)	0.415 (0.18)	0.277 (0.6)	−0.786***	−0.984***
	[0.219]	[0.625]	[0.089]	[0.124]	[0.002]	[0.597]	[0.313]	[0.579]	[0.201]	[0.009]
ρ_2	−4.623***	−2.211*	−1.939**	−4.914***	0.112***	−1.227 (0.13)	−2.155**	−1.139 (0.18)	−2.752**	−0.768*
	[1.051]	[1.238]	[0.894]	[1.197]	[0.025]	[0.822]	[1.086]	[0.860]	[1.406]	[0.458]
Likelihood	−3587.015	−4008.689	−4102.625	−3549.934	−4447.889	−4102.110	−3309.123	−4707.524	−3165.369	−4162.044

Note: ∗ ∗ ∗, ∗∗, and ∗ in all tables denote that the parameter is significant at 1%, 5%, and 10% level, respectively.

Table 6: Results of TVRA-GARCH-M model (P_t^{30}).

Index/parameter	NYSE	NASDAQ	N225	FTSE	SSE	HSI	TSX	BOV	AORD	DAX
ρ_0	0.012	−0.990***	−0.028	0.026	0.002**	0.018	−0.072	0.297*	−0.086	−0.012
	[0.099]	[0.004]	[0.144]	[0.105]	[0.001]	[0.097]	[0.117]	[0.155]	[0.092]	[0.105]
ρ_1	−0.775***	0.010***	−0.896***	−0.791***	0.983***	−0.687 (0.2)	−0.773***	−0.983***	−0.739**	−0.984***
	[0.157]	[0.002]	[0.101]	[0.117]	[0.005]	[0.540]	[0.216]	[0.017]	[0.327]	[0.009]
ρ_2	−2.807***	27.024***	−1.448**	−3.771***	0.049***	−0.999*	−2.595***	−0.499 (0.2)	−2.089**	−0.738*
	[0.737]	[0.246]	[0.662]	[0.896]	[0.014]	[0.586]	[0.882]	[0.390]	[1.001]	[0.420]
Likelihood	−3557.889	2334.177	−4064.561	−3515.359	−4413.490	−4071.417	−3282.155	−4671.547	−3142.182	−4116.618

Note: ∗ ∗ ∗, ∗∗, and ∗ in all tables denote that the parameter is significant at 1%, 5%, and 10% level, respectively.

Table 7: Results of TVRA-GARCH-M model (MP).

Index/parameter	NYSE	NASDAQ	N225	FTSE	SSE	HSI	TSX	BOV	AORD	DAX
ρ_0	0.006	0.012	−0.001	0.105	0.118	0.001	−0.004	0.026	−0.023	0.001
	[0.013]	[0.025]	[0.013]	[0.091]	[0.124]	[0.007]	[0.009]	[0.032]	[0.072]	[0.011]
ρ_1	0.777***	0.670***	0.821***	−0.671***	−0.070	0.883***	0.857***	0.757***	−0.489	0.807***
	[0.101]	[0.245]	[0.164]	[0.191]	[0.963]	[0.141]	[0.074]	[0.178]	[0.413]	[0.144]
ρ_2	−3.119***	−2.003*	−1.236	−3.418**	−0.962	−0.693	−2.690***	−1.475**	−3.007	−1.605**
	[0.984]	[1.141]	[0.797]	[1.504]	[0.928]	[0.590]	[0.933]	[0.746]	[1.842]	[0.811]
Likelihood	−3572.617	−3986.930	−4084.460	−3535.877	−4444.961	−4084.119	−3296.610	−4686.938	−3153.422	−4140.519

Note: ∗ ∗ ∗, ∗∗, and ∗ in all tables denote that the parameter is significant at 1%, 5%, and 10% level, respectively.

Table 8: Results of TVRAS-GARCH-M model (MAX).

Index/parameter	NYSE	NASDAQ	N225	FTSE	SSE	HSI	TSX	BOV	AORD	DAX
λ_{11}	−57.180***	−32.726***	−26.952***	−55.843***	1.239**	−20.389***	−39.102***	−19.859***	−43.328***	−37.310***
	[5.467]	[4.612]	[4.533]	[5.703]	[0.602]	[3.776]	[5.432]	[3.011]	[6.125]	[3.457]
λ_{12}	−0.990**	−0.410	−0.343	−1.892***	0.030*	−0.397	−1.091***	−0.065	−0.391	−0.705**
	[0.406]	[0.390]	[0.411]	[0.661]	[0.017]	[0.349]	[0.399]	[0.293]	[0.504]	[0.372]
Likelihood	−3541.543	−3970.803	−4074.049	−3503.489	−4433.837	−4077.932	−3280.496	−4675.261	−3132.791	−4111.405

Note: ∗ ∗ ∗, ∗∗, and ∗ in all tables denote that the parameter is significant at 1%, 5%, and 10% level, respectively.

Table 9: Results of TVRAS-GARCH-M model (MIN).

Index/parameter	NYSE	NASDAQ	N225	FTSE	SSE	HSI	TSX	BOV	AORD	DAX
λ_{11}	−1.422***	−0.766	−0.048	−2.029***	0.763**	−0.166	−1.047**	−0.445	−1.446	−1.386**
	[0.555]	[0.635]	[0.129]	[0.752]	[0.332]	[0.224]	[0.467]	[0.532]	[1.024]	[0.720]
λ_{12}	−27.106***	−27.806***	−4.567**	−38.036***	−21.988***	−11.127***	−33.931***	−19.841***	−27.990***	−13.520***
	[2.665]	[2.701]	[2.166]	[2.974]	[2.514]	[2.495]	[3.541]	[2.195]	[3.758]	[2.749]
Likelihood	−3563.113	−3972.361	−4084.628	−3514.580	−4436.957	−4082.474	−3287.054	−4676.344	−3141.543	−4136.597

Note: ∗ ∗ ∗, ∗∗, and ∗ in all tables denote that the parameter is significant at 1%, 5%, and 10% level, respectively.

Table 10: Results of TVRAS-GARCH-M model (P_t^5).

Index/parameter	NYSE	NASDAQ	N225	FTSE	SSE	HSI	TSX	BOV	AORD	DAX
λ_{11}	−2.591**	−3.778**	−0.895	−0.115	0.240***	−0.409	−2.992***	−1.690*	−1.203	−2.486**
	[1.157]	[1.721]	[0.937]	[0.308]	[0.085]	[0.567]	[1.160]	[0.974]	[0.963]	[1.070]
λ_{12}	−0.734	−0.453	−0.601	−0.222	0.195***	−0.396	−0.577	−0.531	−0.072	0.127
	[0.786]	[1.447]	[0.681]	[0.295]	[0.072]	[0.551]	[0.734]	[0.671]	[0.557]	[0.709]
Likelihood	−3597.464	−4019.031	−4145.122	−3598.876	−4504.463	−4143.122	−3343.164	−4758.322	−3196.579	−4210.430

Note: ∗ ∗ ∗, ∗∗, and ∗ in all tables denote that the parameter is significant at 1%, 5%, and 10% level, respectively.

Table 11: Results of TVRAS-GARCH-M model (P_t^{10}).

Index/parameter	NYSE	NASDAQ	N225	FTSE	SSE	HSI	TSX	BOV	AORD	DAX
λ_{11}	−5.448***	−1.709	−2.752**	−7.127***	2.640***	−1.553 (0.2)	−3.250**	−0.521 (0.3)	−3.549*	−0.848 (0.2)
	[1.795]	[1.700]	[1.120]	[1.881]	[1.036]	[1.338]	[1.627]	[0.615]	[2.081]	[0.698]
λ_{12}	−3.549***	−2.769**	−0.866 (0.3)	−2.390*	−2.309***	−0.639 (0.5)	−0.844 (0.2)	−0.843 (0.14)	−2.075 (0.18)	−0.770*
	[1.268]	[1.417]	[0.855]	[1.436]	[0.923]	[0.997]	[0.781]	[0.572]	[1.567]	[0.465]
Likelihood	−3586.786	−4008.609	−4100.709	−3549.149	−4458.122	−4102.049	−3308.176	−4708.183	−3165.194	−4162.036

Note: ∗ ∗ ∗, ∗∗, and ∗ in all tables denote that the parameter is significant at 1%, 5%, and 10% level, respectively.

Table 12: Results of TVRAS-GARCH-M model (P_t^{30}).

Index/parameter	NYSE	NASDAQ	N225	FTSE	SSE	HSI	TSX	BOV	AORD	DAX
λ_{11}	−4.933***	19.093***	0.709 (0.4)	−3.365**	0.053**	0.670	−2.840*	0.178 (0.7)	−2.637 (0.12)	−1.123 (0.12)
	[1.427]	[0.079]	[0.855]	[1.710]	[0.027]	[1.068]	[1.638]	[0.529]	[1.738]	[0.734]
λ_{12}	−1.131 (0.2)	17.579***	−1.639 (0.16)	−4.008***	0.043*	−2.747***	−2.424**	−0.852*	−1.728 (0.17)	−0.633 (0.2)
	[0.920]	[0.012]	[1.190]	[1.095]	[0.026]	[0.842]	[1.117]	[0.527]	[1.281]	[0.496]
Likelihood	−3556.580	2302.776	−4063.584	−3515.318	−4413.475	−4069.571	−3282.142	−4670.078	−3142.121	−4116.474

Note: ∗ ∗ ∗, ∗∗, and ∗ in all tables denote that the parameter is significant at 1%, 5%, and 10% level, respectively.

Table 13: Results of TVRAS-GARCH-M model (MP).

Index/parameter	NYSE	NASDAQ	N225	FTSE	SSE	HSI	TSX	BOV	AORD	DAX
λ_{11}	−4.051***	−5.176***	−4.207**	−3.337**	−0.672	−3.300**	−3.888***	−1.743	−6.061**	−4.664***
	[1.378]	[1.987]	[1.773]	[1.341]	[0.509]	[1.561]	[1.471]	[1.218]	[2.578]	[1.771]
λ_{12}	−1.887	1.389	0.761	−2.176*	1.097*	1.682	−1.607	1.186	1.772	2.884
	[1.202]	[1.923]	[1.825]	[1.153]	[0.599]	[1.712]	[1.188]	[1.338]	[2.669]	[1.833]
Likelihood	−3571.901	−3984.559	−4082.694	−3532.935	−4442.370	−4083.135	−3295.887	−4687.562	−3151.470	−4138.233

Note: ∗ ∗ ∗, ∗∗, and ∗ in all tables denote that the parameter is significant at 1%, 5%, and 10% level, respectively.

Tables 10, 11, and 12, half of the indexes have significantly negative λ_{11} or λ_{12}, with the exception of the indexes SSE and NASDAQ in Table 12. Among them, parameters in SSE are significantly positive, which may be associated with the immaturity of China's stock markets. Compared with the estimation results with the other five reference points (MAX, MIN, P_t^5, P_t^{10}, P_t^{30}, and MP), the values for λ_{11} and λ_{12} of NASDAQ index in Table 13 estimated with the 30-day moving average price (P_t^{30}) as the reference point are positive, which may be related to the selection of reference points.

In addition, the values for λ_{11} and λ_{12} estimated with reference points are mostly significantly positive, but they still differ for different indexes. In all indexes, the results estimated with the highest month price, the lowest month price, and the memory-adjusted price as the reference points are generally more significant when compared with estimation results obtained with the 5-day, the 10-day, and the 30-day moving average prices as the reference points. Investors' risk aversion falls with prior gains, and the increase in investors' risk aversion is more obvious with prior losses. Specifically, the selection of reference points will affect the judgment of the prior gains and losses, thus affecting their risk preference. And we found that, for the parameters in some indexes that are not significant from Table 2 to Table 7, the parameters λ_{11} and λ_{12} from Table 8 to Table 13 are significant. This phenomenon confirms the reasonability of the TVARS-GARCH-M mode. Therefore, on the basis of TVAR-GARCH-M model, we qualitatively separate the prior gains and losses to prove that the effect that prior losses and gains have on investors' risk preference is what the solid line shows in Figure 1, which shows that the stock market overall exhibits house money effect.

4. Conclusion

This paper, based on previous studies about investors' risk preference, selects ten representative samples of the world's composite indexes and adopts six different reference points and builds the TVARS-GARCH-M model to further explore how prior losses and gains affect investors' risk preference. First of all, the data in this paper are large enough, are easy to get, and are not affected by individual investor sentiments, so the results are more convincing. Secondly, this paper takes prior losses and gains as separate explanatory variables in the TVRA-GARCH-M model, overcoming the offsetting effect that the changes in prior gains and losses have on investors' current risk preference. That is, if we do not distinguish prior losses from gains, and when equal amounts of prior losses and prior gains have opposite but equivalent effects on the current risk preference, as shown in Figure 1, these two effects may cancel each other out, resulting in a false phenomenon that the prior loss and gain in essence do not affect the continuous risk seeking or risk aversion. Or, both the prior loss and gain increase investors' risk seeking or risk aversion with one of the effects being stronger than the other, and they may also offset each other. Finally, considering the possible influence arising from the subjective selection of reference points may affect investors' judgment of the risk; we select the six commonly used reference prices to study investors' risk preference, so the result is more robust.

Through the research, the following conclusions can be made. Firstly, from the overall stock market, investor's risk preference is time varying and can be affected by the prior outcome. Secondly, the stock market as a whole shows house money effect; namely, prior gains reduce the current risk aversion while prior losses push up the current risk aversion. Thirdly, the selection of different reference points affects the judgment of prior loss and gain, causing certain influence on the investors' risk preference.

Conflict of Interests

The authors declare that there is no conflict of interests regarding the publication of this paper.

Acknowledgments

This work was supported in part by the Natural Science Foundation of China (no. 71171024, no. 71371195, and no. 71221061). The authors gratefully acknowledge the helpful work of postgraduate Mengxian Tao, who has made great contribution to this paper.

References

[1] K. Keasey and P. Moon, "Gambling with the house money in capital expenditure decisions: an experimental analysis," *Economics Letters*, vol. 50, no. 1, pp. 105–110, 1996.

[2] P. Sadorsky, "Time-varying risk premiums in petroleum futures prices," *Energy Economics*, vol. 24, no. 6, pp. 539–556, 2002.

[3] A. Y. Javid, "Time varying risk return relationship: evidence from listed Pakistani firms," *European Journal of Scientific Research*, vol. 22, no. 1, pp. 16–39, 2008.

[4] J. Kostek and L. Ashrafioun, "Tired winners: the effects of cognitive resources and prior winning on risky decision making," *Journal of Gambling Studies*, 2013.

[5] P. R. Locke and S. C. Mann, "Professional trader discipline and trade disposition," *Journal of Financial Economics*, vol. 76, no. 2, pp. 401–444, 2005.

[6] A. Frino, J. Grant, and D. Johnstone, "The house money effect and local traders on the Sydney Futures Exchange," *Pacific Basin Finance Journal*, vol. 16, no. 1-2, pp. 8–25, 2008.

[7] Y.-J. Liu, C.-L. Tsai, M.-C. Wang, and N. Zhu, "Prior consequences and subsequent risk taking: new field evidence from the Taiwan futures exchange," *Management Science*, vol. 56, no. 4, pp. 606–620, 2010.

[8] M. Weber and C. F. Camerer, "The disposition effect in securities trading: an experimental analysis," *Journal of Economic Behavior and Organization*, vol. 33, no. 2, pp. 167–184, 1998.

[9] M. S. Haigh and J. A. List, "Do professional traders exhibit myopic loss aversion? An experimental analysis," *Journal of Finance*, vol. 60, no. 1, pp. 523–534, 2005.

[10] M. Weber and H. Zuchel, "How do prior outcomes affect risk preference? Comparing escalation of commitment and the house-money effect," *Decision Analysis*, vol. 2, no. 1, pp. 30–43, 2005.

[11] H. Shefrin and M. Statman, "The disposition to sell winners too early and ride losers to long: theory and evidence," *Journal of Finance*, vol. 40, no. 3, pp. 777–790, 1985.

[12] T. Odean, "Are investors reluctant to realize their losses?" *Journal of Finance*, vol. 53, no. 5, pp. 1775–1798, 1998.

[13] D. Jordan and J. D. Diltz, "Day traders and the disposition effect," *The Journal of Behavioral Finance*, vol. 5, no. 4, pp. 192–200, 2004.

[14] D. Kahneman and A. Tversky, "Prospect theory: an analysis of decision under risk," *Econometrics*, vol. 47, no. 2, pp. 263–291, 1979.

[15] R. H. Thaler and E. J. Johnson, "Gambling with the house money and trying to break even: the effects of prior outcomes on risky choice," *Management Science*, vol. 36, no. 6, pp. 643–660, 1990.

[16] M. Massa and A. Simonov, "Behavioral biases and investment," *Review of Finance*, vol. 9, no. 4, pp. 483–507, 2005.

[17] L. F. Ackert, N. Charupat, B. K. Church, and R. Deaves, "An experimental examination of the house money effect in a multi-period setting," *Experimental Economics*, vol. 9, no. 1, pp. 5–16, 2006.

[18] Y. L. Hsu and E. H. Chow, "The house money effect on investment risk taking: evidence from Taiwan," *Pacific-Basin Finance Journal*, vol. 21, no. 1, pp. 1102–1115, 2013.

[19] N. Barberis and W. Xiong, "What drives the disposition effect? An analysis of a long-standing preference-based explanation," *Journal of Finance*, vol. 64, no. 2, pp. 751–784, 2009.

[20] A. O. I. Hoffmann, S. F. Henry, and N. Kalogeras, "Aspirations as reference points: an experimental investigation of risk behavior over time," *Theory and Decision*, vol. 75, no. 2, pp. 193–210, 2013.

[21] J. D. Coval and T. Shumway, "Do behavioral biases affect prices?" *Journal of Finance*, vol. 60, no. 1, pp. 1–34, 2005.

[22] F. Mattos and P. Garcia, "The effect of prior loss and gain on current risk-taking using quantile regression," in *Proceedings of the NCCC134 Conference on Applied Commodity Price Analysis*, Forecasting, and Market Risk Management, St. Louis, Mo, USA, 2009.

[23] Y. C. Huang and S. H. Chan, "The house money and break-even effects for different types of traders: evidence from Taiwan futures markets," *Pacific-Basin Finance Journal*, vol. 26, pp. 1–13, 2014.

[24] A. Tversky and D. Kahneman, "Advances in prospect theory: cumulative representation of uncertainty," *Journal of Risk and Uncertainty*, vol. 5, no. 4, pp. 297–323, 1992.

[25] Y. Zhang, "Prospect theory and its application," *Consume Guide*, vol. 16, pp. 225–226, 2008.

[26] D. Lam and B. Ozorio, "The effect of prior outcomes on gender risk-taking differences," *Journal of Risk Research*, vol. 16, no. 7, pp. 791–802, 2013.

[27] C. Heath, S. Huddart, and M. Lang, "Psychological factors and stock option exercise," *Quarterly Journal of Economics*, vol. 114, no. 2, pp. 601–627, 1999.

[28] A. M. Poteshman and V. Serbin, "Clearly irrational financial market behavior: evidence from the early exercise of exchange traded stock options," *Journal of Finance*, vol. 58, no. 1, pp. 37–70, 2003.

[29] M. Grinblatt and M. Keloharju, "What makes investors trade?" *Journal of Finance*, vol. 56, no. 2, pp. 589–616, 2001.

[30] U. Gneezy, *Updating the Reference Level: Experimental Evidence*, Experimental Business Research, 2005.

[31] L. Vinokur, "Dispositon in the carbon market and institutional constraints," Working Paper, 2009.

[32] J. R. Anderson, "Verbatim and propositional representation of sentences in immediate and long-term memory," *Journal of Verbal Learning and Verbal Behavior*, vol. 13, no. 2, pp. 149–162, 1974.

[33] J. M. Mandler and G. H. Ritchey, "Long-term memory for pictures," *Journal of Experimental Psychology: Human Learning and Memory*, vol. 3, no. 4, pp. 386–396, 1977.

[34] M. Grinblatt and B. Han, "Prospect theory, mental accounting, and momentum," *Journal of Financial Economics*, vol. 78, no. 2, pp. 311–339, 2005.

[35] P. K. Kopalle and J. Lindsey-Mullikin, "The effect of external reference price on consumer price expectations," *Journal of Retailing*, vol. 79, no. 4, pp. 225–237, 2003.

[36] A. Taudes and C. Rudloff, "Integrating inventory control and a price change in the presence of reference price effects: a two-period model," *Mathematical Methods of Operations Research*, vol. 75, no. 1, pp. 29–65, 2012.

[37] F. Wen and X. Yang, "Skewness of return distribution and coefficient of risk premium," *Journal of Systems Science & Complexity*, vol. 22, no. 3, pp. 360–371, 2009.

[38] F. Wen, Z. He, and X. Chen, "Investors' risk preference characteristics and conditional skewness," *Mathematical Problems in Engineering*, vol. 2014, Article ID 814965, 14 pages, 2014.

Hindawi Publishing Corporation
Discrete Dynamics in Nature and Society
Volume 2014, Article ID 839731, 8 pages
http://dx.doi.org/10.1155/2014/839731

Research Article

A Nonparametric Operational Risk Modeling Approach Based on Cornish-Fisher Expansion

Xiaoqian Zhu,[1,2] Jianping Li,[1] Jianming Chen,[1] Yingqi YangHuo,[3] Lijun Gao,[4] Jichuang Feng,[5] Dengsheng Wu,[1] and Yongjia Xie[1,2]

[1] *Institution of Policy and Management, Chinese Academy of Sciences, Beijing 100190, China*
[2] *University of Chinese Academy of Sciences, Beijing 100190, China*
[3] *Business School, University of Hull, Hull Hu6 7RX, UK*
[4] *School of Business Administration, Shandong University of Finance and Economics, Jinan, Shandong 250014, China*
[5] *Industrial Bank CO., Ltd., Fuzhou, Fujian 350003, China*

Correspondence should be addressed to Jianping Li; ljp@casipm.ac.cn

Received 7 February 2014; Accepted 11 March 2014; Published 31 March 2014

Academic Editor: Fenghua Wen

It is generally accepted that the choice of severity distribution in loss distribution approach has a significant effect on the operational risk capital estimation. However, the usually used parametric approaches with predefined distribution assumption might be not able to fit the severity distribution accurately. The objective of this paper is to propose a nonparametric operational risk modeling approach based on Cornish-Fisher expansion. In this approach, the samples of severity are generated by Cornish-Fisher expansion and then used in the Monte Carlo simulation to sketch the annual operational loss distribution. In the experiment, the proposed approach is employed to calculate the operational risk capital charge for the overall Chinese banking. The experiment dataset is the most comprehensive operational risk dataset in China as far as we know. The results show that the proposed approach is able to use the information of high order moments and might be more effective and stable than the usually used parametric approach.

1. Introduction

Operational loss is an important source of bank risk. Take the incident of Barings Bank as an example; Nick Leeson's unauthorized trading activities at Singapore office result in a total loss of US $ 1.4 billon and eventually lead to the sudden bankruptcy of Barings bank. Nowadays, researchers, practitioners, and regulatory institutions are fully aware of the importance of operational risk. Basel committee on banking supervision (BCBS for short) formally defines it as the risk of loss resulting from inadequate or failed internal processes, people, and systems from external events [1]. Besides, in Basel II accord, operational risk is covered under the Pillar I, keeping abreast of credit risk and market risk [2].

BCBS also introduces three approaches to the quantification of operational risk in a continuum of increasing sophistication and risk sensitivity, that is, basic indicator approach (BIA), standardized approach (SA), and advanced measurement approach (AMA) [3]. By allowing banks to develop their own model for assessing the regulatory capital that covers their yearly operational risk at a confidence level of 99.9%, the most sophisticated option AMA has sparked an intense discussion in financial industry [4]. Many quantitative AMAs for measuring operational risk have been proposed, such as internal measurement approach, loss distribution approach, scorecard approach, and extreme value theory based approach [1, 5].

Among the eligible variants of AMA, loss distribution approach (LDA) is the most popular methodology by far [5, 6]. It is initially developed in actuarial industry and then introduced to operational risk modeling by Frachot et al. [7]. LDA separately estimates the frequency distribution and severity distribution of operational risk loss and then combines them by convolution to derive annual operational risk distribution. The output of LDA is a full characterization of the distribution of annual operational losses, which contains all relevant information for the computation of regulatory capital charge [6]. From the statistical viewpoint, LDA is the most accurate if it utilizes the exact distributions of loss frequency and severity. In other words, choosing the right frequency and severity distribution is the key to LDA.

The choice of severity distributions is usually supposed to have a more pronounced effect on capital than the choice of frequency distributions in LDA models [4, 8]. An improper choice of severity distribution might generate a significant distortion of the results and thus leads to overestimation or underestimation of capital charge. For this reason, very few studies work on the choice of frequency distribution. Some researchers simply employ Poisson distribution for its ease of use. Some other researchers who take this a step further will discuss whether negative binomial distribution or geometric distribution better fits the frequency [6]. On the contrary, a vast majority of researchers and practitioners concentrate on the estimation of loss severity distribution.

The parametric approaches have dominated the estimation of severity distribution so far. It assumes a particular distribution for severity and then estimates the parameters by using moment estimation, maximum likelihood estimation, and so on [8]. Lognormal distribution is firstly used to model severity distribution. Afterwards, Weibull and exponential distributions are also widely used [9]. These distributions are usually able to fit "high-frequency and low-severity" loss well, that is, the middle part of the severity distribution. However, the major flaw of them is that they are badly fit for "low-frequency and high-severity" loss, that is, the tail of the severity distribution. After noticing this flaw, some heavy tail distributions are employed, for example, g-h distribution and α-stable distribution [10, 11]. Extreme value theory is also applied to this area, which uses extreme value distribution, such as Pareto distribution, to model severity [5, 12, 13]. The feature of the extreme distribution is that it only fits the tail of the distribution, and so a threshold is needed to determine where the tail starts. Improper threshold might severely affect the fitting results. However, most of the studies rely on subjective judgment to determine the threshold because there is no widely recognized objective method so far.

Unlike parametric approach, the nonparametric approach derives a loss amount at random from loss data to perform a simulation without assuming any particular severity distribution [8]. This kind of approach has received relatively limited attention so far. The most simple and classical nonparametric approach is the bootstrap resa- mpling approach. In this approach, frequency samples and severity samples are directly drawn from the raw data and then combined to attain the yearly loss. This approach is just based on the historical data and cannot extrapolate. Another approach is based on maximum entropy principle. In this approach, the most suitable distribution is regarded as the distribution which is closest to uniform distribution and simultaneously meets some known statistic requirements [14].

Under different severity distribution assumption, results from LDA are greatly different from each other [9]. Therefore improper distribution assumption will result in significant bias from the true capital charge. However, the usually used distributions either cannot fit both the body and tail well or cannot determine an objective threshold. Without so many assumptions, nonparametric approach is more robust than parametric approach. Moreover, parametric approach usually has the merit of ease of use and understanding.

The objective of this paper is to propose a nonparametric operational risk modeling approach. This approach uses Cornish-Fisher expansion to estimate the severities under the framework of LDA. Cornish-Fisher expansion is a well-known mathematical expansion which is able to approximate the quantiles of a random variable based on its first few cumulants or moments [15]. This approach does not need a predetermined distribution to fit the loss severity of operational risk. Besides, it is also able to partly solve the data sparseness problem of operational risk because, instead of the whole severity distribution, only the cumulants or moments of loss severity are required in the expansion. In this approach, samples of severity are generated by using standard normal distribution and Cornish-Fisher expansion. And then these samples are used in Monte Carlo simulation to sketch the annual operational risk loss distribution. In the experiment, based on the most comprehensive operational risk dataset in China as far as we know, the proposed approach is employed to calculate the operational risk capital charge of the overall Chinese banking.

The rest of this paper is organized as follows. Section 2 presents the proposed approach. Section 3 employs the approach to calculate the operational risk capital charge for the overall Chinese banking. Section 4 summarizes the conclusions.

2. The Proposed Cornish-Fisher Expansion Based LDA Approach

In this section, the proposed nonparametric approach using Cornish-Fisher expansion in the framework of LDA is illustrated at length. Firstly, the Cornish-Fisher expansion is introduced. Then the concept and specific steps of the proposed approach are presented.

2.1. Cornish-Fisher Expansion. The Cornish-Fisher expansion, firstly proposed by Cornish and Fisher [16], has often been applied to finance when calculating value at risk (VaR). It is a formula for approximating quantiles of a random variable based only on its first few cumulants. Assume that there is a random variable X whose mean μ is equal to 0 and standard deviation σ is equal to 1. Let κ_j $(j = 1, 2, \ldots)$ denote the jth order cumulant of X:

$$\kappa_1 = 0, \qquad \kappa_2 = 1, \qquad \kappa_j = O\left(n^{1-(j/2)}\right), \quad j = 1, 2, \ldots. \tag{1}$$

Then it can be proven that

$$F_n(x) = \exp\left\{\sum_{j=3}^{\infty}\left[\frac{\kappa_j(-D)^j}{j!}\right]\right\}\Phi(x), \tag{2}$$

where $F_n(x)$ denotes the cumulative distribution function of X, D denotes the differential operator, and $\Phi(x)$ denotes the standard normal distribution:

$$D^j \Phi(x) = \frac{\partial^j \Phi(x)}{\partial x^j} = \Phi^{(j)}(x),$$
$$\Phi^{(j)}(x) = (-1)^{j-1} H_{j-1}(x)\,\phi(x), \quad \text{for } j \geq 1, \tag{3}$$

where $\phi(x)$ denotes the probability density function of standard normal distribution and $H_j(x)$ denotes the jth order Chebyshev-Hermite polynomial:

$$H_0(x) = 1, \qquad H_1(x) = x,$$
$$H_j(x) = xH_{j-1}(x) - (j-1)\,H_{j-2}(x), \quad j \geq 2. \tag{4}$$

Next, according to (2) to (4), then we obtain

$$F_n(x) = \Phi(x) - \frac{\kappa_3}{6}\left(x^2 - 1\right)\phi(x) - \frac{\kappa_4}{24}\left(x^3 - 3x\right)\phi(x) - \frac{\kappa_3^2}{72}\left(x^5 - 10x^3 + 15x\right)\phi(x) + \cdots. \tag{5}$$

Equation (5) is the called Edgeworth expansion, from which Cornish-Fisher expansion can be deduced as follows. Assume that x_p and v_p are the p quantiles ($0 < p < 1$) of $F_n(x)$ and $\Phi(x)$, respectively. Then the Taylor expansion of $\Phi(v_p)$ at x_p is

$$\Phi\left(v_p\right) = \Phi\left(x_p\right) - \sum_{j=1}^{\infty} \frac{\left(x_p - v_p\right)^j}{j!} H_{j-1}\left(x_p\right)\phi\left(x_p\right). \tag{6}$$

According to the definition of quantile, we have

$$F_n(x) = \Phi(x) = p. \tag{7}$$

Finally, by combing (2), (5), and (7) together, x_p can be formulated by v_p as

$$\begin{aligned} x_p = {} & v_p + \frac{1}{6}\left(v_p^2 - 1\right)\kappa_3 + \frac{1}{24}\left(v_p^3 - 3v_p\right)\kappa_4 \\ & - \frac{1}{36}\left(2v_p^3 - 5v_p\right)\kappa_3^2 + \frac{1}{120}\left(v_p^4 - 6v_p^2 + 3\right)\kappa_5 \\ & - \frac{1}{24}\left(v_p^4 - 5v_p^2 + 2\right)\kappa_3\kappa_4 \\ & + \frac{1}{324}\left(12v_p^4 - 53v_p^2 + 17\right)\kappa_3^3 \cdots. \end{aligned} \tag{8}$$

Equation (8) is the Cornish-Fisher expansion of x_p by using v_p. Equation (8) is valid only if X has mean of 0 and standard deviation of 1. However, we can still use it for other variables after normalizing the variable with its mean and standard deviation.

2.2. The Framework of the Proposed Approach. LDA is a technique firstly estimating a frequency distribution for the occurrence of operational losses and a severity distribution for the economic impact of individual loss separately. Then in order to obtain the total distribution of operational losses, these two distributions are combined through n-convolution of the severity distribution with itself, where n is a random variable that follows the frequency distribution [6]. For an exhaustive introduction of LDA, please see Frachot et al. [7].

Because the multiple convolutions are usually analytically complex and do not lend themselves to implementation with closed-form formulas, Monte Carlo simulation is commonly used to derive the final annual distribution of operational risk loss. The procedure of Monte Carlo simulation based LDA is as follows: (1) determine loss frequency and loss severity distribution; (2) generate a number m from frequency distribution; (3) generate m samples from severity distribution; (4) sum the m samples to calculate the annual loss; (5) repeat (2) to (4) N times to attain N annual losses; (6) calculate VaR.

As described in (8), a random variable can be formulated by a variable from standard normal distribution in Cornish-Fisher expansion. Therefore, in this paper, we aim to use Cornish-Fisher expansion to help generate the samples of loss severity in Monte Carlo simulation. Samples are firstly generated from standard normal distribution and then transformed to the samples of loss severity by Cornish-Fisher expansion. The Cornish-Fisher expansion in the transformation process needs the cumulants of the loss severity. Compared with the original LDA approach, this approach does not need a predetermined distribution to fit loss severity. It is only the cumulants of loss severity that are required.

The framework of the proposed approach is shown in Figure 1. With respect to frequency, samples are still drawn from a fitted loss frequency distribution. With respect to severity, the samples are first generated from standard normal distribution and then transformed to severities by Cornish-Fisher expansion. After the Monte Carlo simulation, the annual loss distribution of operational risk is attained. Pioneered by J. P. Morgan, VaR has become a standard measure used in financial risk [17, 18]. So here we also use VaR to measure the magnitude of operational risk.

2.3. The Procedure of the Proposed Approach. As shown in Figure 2, the whole procedure of the proposed approach consists of 3 stages and 7 steps in total. Stage 1 prepares for simulation. In this stage, frequency distribution G is determined and the cumulants of severity are calculated. Stage 2 is the Monte Carlo simulation process. Firstly a number m is randomly generated from frequency distribution. Then m samples of loss severity are generated by using standard normal distribution and Cornish-Fisher expansion. Next these samples are summed to calculate the annual loss. Finally this process is repeated a certain number of times to generate an empirical distribution of annual loss. Stage 3 calculates the VaR from the empirical distribution.

Assume that there are n operational risk observations and the number of the Monte Carlo simulation is N. The operational risk severities are denoted as $y_1, y_2, \ldots, y_n$ and

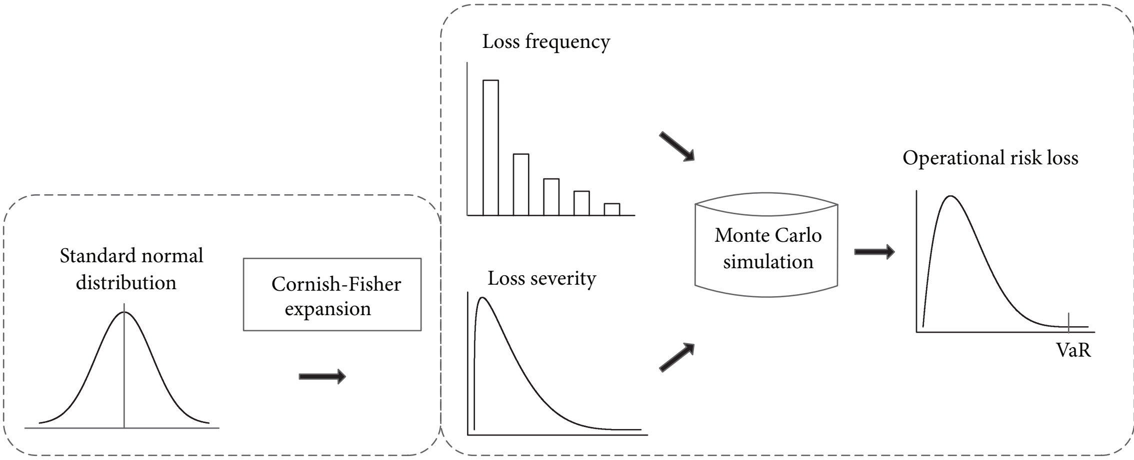

FIGURE 1: The framework of the proposed operational risk modeling approach.

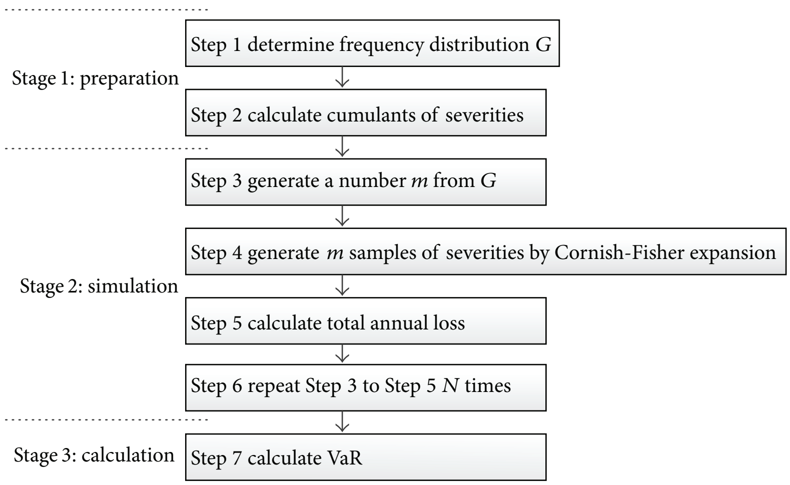

FIGURE 2: The procedure of the proposed operational risk modeling approach.

the simulated severities are denoted as $\hat{y}_1, \hat{y}_2, \ldots, \hat{y}_m$. The detailed steps of the proposed approach are presented as follows.

Stage 1 Preparation

Step 1. Determine the best-fitting distribution G for frequency.

Step 2. Calculate the cumulants of severities.

Step 2.1. Normalize the operational risk severities $y_1, y_2, \ldots, y_n$ to $x_1, x_2, \ldots, x_n$ by

$$x_i = \frac{y_i - \mu}{\sigma}, \quad i = 1, \ldots, n, \tag{9}$$

where μ denotes the mean and σ denotes the standard deviation of y_i.

Step 2.2. Calculate the cumulants κ_j $(j = 1, 2, \ldots)$ of x_i by

$$\begin{gathered}\kappa_1 = 0, \qquad \kappa_2 = 1, \\ \kappa_3 = \mu_3, \qquad \kappa_4 = \mu_4 - 3 \\ \kappa_5 = \mu_5 - 10\mu_3\mu_2 \\ \ldots,\end{gathered} \tag{10}$$

where μ_k $(k = 1, 2, \ldots)$ denotes the central moments of x_i.

Stage 2 Simulation

Step 3. Generate a number m randomly from frequency distribution G.

Step 4. Generate m samples of severities $\hat{y}_1, \hat{y}_2, \ldots, \hat{y}_m$.

Step 4.1. Generate m samples $v_1, v_2, \ldots, v_m$ from standard normal distribution.

Step 4.2. Transform $v_1, v_2, \ldots, v_m$ to samples $\hat{x}_1, \hat{x}_2, \ldots, \hat{x}_m$ by

$$\begin{aligned}\hat{x}_r = {} & v_r + \frac{1}{6}\left(v_r^2 - 1\right)\kappa_3 + \frac{1}{24}\left(v_r^3 - 3v_r\right)\kappa_4 \\ & - \frac{1}{36}\left(2v_r^3 - 5v_r\right)\kappa_3^2 + \frac{1}{120}\left(v_r^4 - 6v_r^2 + 3\right)\kappa_5 \\ & - \frac{1}{24}\left(v_r^4 - 5v_r^2 + 2\right)\kappa_3\kappa_4 \\ & + \frac{1}{324}\left(12v_r^4 - 53v_r^2 + 17\right)\kappa_3^3 \cdots, \quad r = 1, 2, \ldots, m.\end{aligned} \tag{11}$$

Step 4.3. Transform $\hat{x}_1, \hat{x}_2, \ldots, \hat{x}_m$ to samples of severities $\hat{y}_1, \hat{y}_2, \ldots, \hat{y}_m$ by

$$\hat{y}_r = \mu + \sigma\hat{x}_r, \qquad r = 1, 2, \ldots, m. \tag{12}$$

Step 5. Calculate total annual loss L by

$$L = \hat{y}_1 + \hat{y}_2 + \cdots + \hat{y}_m. \tag{13}$$

Step 6. Repeat Step 3 to Step 5 N times to derive simulated losses $L_1, L_2, \ldots, L_N$.

Stage 3. Calculation

Step 7. Calculate VaR according to losses $L_1, L_2, \ldots, L_N$ by

$$\mathrm{VaR} = \inf\{l : P(L \le l) \le 1 - \alpha\}, \tag{14}$$

where VaR is the smallest number of l such that the probability that the loss L exceeds l is not larger than $(1 - \alpha)$.

3. Experiment

In this section, the proposed approach is employed to calculate the operational risk capital charge for the overall Chinese banking based on the most comprehensive operational risk dataset as far as we know. Firstly, the dataset and its statistical characteristics are introduced. Then the experiment results on the dataset are presented.

3.1. Data Description. Today, many financial institutions have started collecting data on their own operational loss experience, but it will take some time before the size and quality of most institution's databases allow reliable estimation of the parameters in the models [19]. This problem of data sparseness is even worse in Chinese banking. Therefore, in addition to the work on the measurement approach, our laboratory also paid great attention to data collection. We have established an operational risk database of Chinese banking spanning from 1994 to 2012 with a total of 2132 collections. Each record is manually searched, labelled, and sorted out from public resources, such as the newspapers, the internet, and court documents, including the loss event description, start time, end time, exposed time, business line type, loss event type, loss amount in CNY, banks involved, location, and key person involved. As far as we know, this operational risk dataset of Chinese banking is the most comprehensive one in China. In this experiment, the end time and the loss amount are exacted from the database.

The summary statistics of operational risk loss severity are shown in Panel A of Table 1. The values of range and standard deviation are very large, which means operational risk loss severities are of great difference. The skewness is 8.51, much larger than 0, indicating that the distribution is highly right-skewed. The kurtosis is 91.63, much larger than 3, which means that the distribution has an extreme sharp peak. The statistical characteristics of this experimental data are highly in accordance with the widely-recognized "leptokurtosis and fat tail" feature of operational risk.

The closer the unknown distribution is to the standard normal distribution, the more accurate the Cornish-Fisher expansion is. Therefore, we calculate the natural logarithm of loss severity to make the distribution closer to the standard normal distribution. After taking natural logarithm, the summary statistics of new data are shown in Panel B of Table 1. The central tendency of the natural log-distribution is significantly approved. The skewness is 0.15, very close to 0, which means that the distribution is almost symmetrical with a little right-skewed. Kurtosis also significantly decreases to 2.18, which is slightly smaller than 3. In summary, the logarithmic loss severity is much closer to the normal distribution than the original data.

3.2. Experiment Results. In this section, the results of the proposed approach on the operational risk dataset are presented. Firstly, we will find a proper discrete distribution for frequency distribution. Poisson, negative binomial, and geometric distributions are three commonly used distributions in operational risk modeling [1, 6, 20]. Among the three distributions, it is beyond all disputes that Poisson distribution is the most commonly used one. In a large majority of studies, mainly for its ease of use and the viewpoint of its smaller effect on capital, Poisson distribution is directly used without any test [4, 7]. This hasty usage of Poisson distribution is questionable. In this study, goodness-of-fit test is used to decide which distribution should be used rather than simply following the majority. Kolmogorov-Smirnov goodness-of-fit test (KS test for short) has a very wide application in testing whether a theoretical distribution is fit for an empirical distribution. So in this study, KS test is used to find which one fits the frequency distribution best. The results of the KS test and estimated parameters by maximum likelihood estimation are shown in Table 2.

As for KS test, the larger the P value is, the better the theoretical distribution is fit for the empirical distribution. Generally, the threshold is set as 5%. Table 2 shows that the P values of Poisson, negative binomial, and geometric distributions are 0.00, 0.43, and 0.10, respectively. It is noteworthy that the most frequently used distribution, Poisson distribution, is strongly rejected in the test. The remaining negative binomial and geometric distribution pass the test with P values larger than 5%. Besides, the P value of negative binomial distribution is the largest, which means that negative binomial

Table 1: Summary statistics of loss severity and logarithmic loss severity.

Min.	Max.	Median	Mean	SD	Skewness	Kurtosis
Panel A: statistics of loss severity						
0.01	800000	155.03	11405.83	50083.25	8.51	91.63
Panel B: statistics of logarithmic loss severity						
−4.61	13.59	5.04	5.32	3.31	0.15	2.18

SD: standard deviation.

Table 2: Estimated parameters and goodness-of-fit test results of frequency distribution.

Distribution	Parameters	KS test	
		D value	P value
Poisson	$\lambda = 112.21$	0.45	0.00
Negative binomial	$r = 2.75$, $p = 0.98$	0.20	0.43
Geometric	$d = 0.01$	0.28	0.10

For negative binomial distribution, r denotes the specified number of failures and p denotes the probability of success in each trial. Besides, λ and d, respectively, denote the single parameters of Poisson and geometric distribution.

Table 3: Estimated parameters for Cornish-Fisher expansion.

	μ_1	μ_2	μ_3	μ_4	μ_5
Moments	0	1	0.15	2.18	0.69
	κ_1	κ_2	κ_3	κ_4	κ_5
Cumulants	0	1	0.15	−0.82	−0.83

μ_1 to μ_5 denote the first moment to the fifth moment. κ_1 to κ_5 denote the first cumulant to the fifth cumulant.

distribution is able to fit the frequency best. Therefore, in this experiment, negative binomial distribution is used to describe the distribution of frequency.

Then we normalize the logarithmic operational risk severity by its mean 5.32 and standard deviation 3.31. The moments and cumulants of operational risk severity after normalization are shown in Table 3. In Table 3, μ_1 to μ_5 denote the first moment to the fifth moment. Based on these moments, the cumulants κ_1 to κ_5 are calculated by using (10), which will be used in Cornish-Fisher expansion functions.

The larger the number of simulations is, the more accurate the results are and the longer the computational time required is. In order to balance simulation accuracy and time cost, we follow other studies and set the number of simulations as 100000 [5, 18]. Generally, the capital requirement is set to protect against losses over one year at 99.9% level because it is roughly equivalent to the default risk of an A-rated corporate bond [7]. Basel committee on banking supervision also recommends 99.9% as a proper confidence level. Therefore, the VaR value at confidence level 99.9% is calculated and shown in Table 4.

Table 4 shows that VaR at 99.9% ranges from 67 to 13290 billion CNY. The order of Cornish-Fisher expansion dramatically affects the magnitude of VaR. Besides, as the order increases, the VaR result becomes relatively stable. When the order increases to three or larger, VaR converges to about 82 billion. Generally, the larger the order of Cornish-Fisher expansion, the more accurate the results are. Larger order will use more information of cumulants. One-order Cornish-Fisher expansion actually uses κ_1 and κ_2 and VaR turns out to be 3380 billion. Two-order expansion includes κ_3 and the VaR increases to 13290 billion. When κ_4 is added in three-order expansion, VaR drastically reduces to 84 billion. Higher order expansion also leads to the VaR result of about 82 billion.

Among the parametric distributions, lognormal distribution is undoubtedly the most frequently used one for modeling operational risk severity [1]. The parameters of lognormal distribution are mean and standard deviation. In other words, lognormal distribution is only decided by the first and second moments. Nevertheless, higher order moment also contains some useful information. The results of Cornish-Fisher expansion in Table 4 show that higher order moment may have significant effects on the results. Cornish-Fisher expansion can utilize not only the mean and standard deviation, but also the information of higher order moments, so we think that the approach we propose is able to allocate the operational risk capital charge in a more effective way.

In our published book the proposed approach drew the conclusion that the capital charge for operational risk is 31 billion CNY in 2007 [14]. The dataset used in this published book only contains the operational risk records before 2006. After years of effort, the dataset is largely extended and the new dataset spans from 1994 to 2012. By using the new dataset, this study reaches the conclusion that the capital for operational risk charge is 82 billion CNY in 2013. The total assets of Chinese banking financial institutions in 2007 are 53116 billion CNY. These institutions have developed very fast in recent years. In November of 2013, their total assets have increased to 145330 billion CNY, about 2.74 times of 2007. Thus the ratio of capital charge to total assets calculated from old dataset is almost consistent with the ratio calculated from the new dataset. Besides, it is also found out that the statistical characteristics of the new dataset and the old dataset are very similar. Therefore, the dataset is supposed to be stable and authentically reveal the operational risk of Chinese banking.

4. Conclusion

In this paper, a nonparametric operational risk modeling approach based on Cornish-Fisher expansion and loss distribution approach is proposed. This approach does not need to assume a distribution for severity beforehand. Only the cumulants or moments of the severities are required in Monte Carlo simulation process. In the experiment, based

TABLE 4: VaR of operational risk by using Cornish-Fisher expansion

Orders	Cornish-Fisher expansion	VaR (99.9%)
1 order (κ_1, κ_2)	$x_p = \nu_p$	3380
2 order $(\kappa_1, \kappa_2, \kappa_3)$	$x_p = \nu_p + \frac{1}{6}(\nu_p^2 - 1)\kappa_3$	13290
3 order $(\kappa_1, \kappa_2, \kappa_3, \kappa_4)$	$x_p = \nu_p + \frac{1}{6}(\nu_p^2 - 1)\kappa_3 + \frac{1}{24}(\nu_p^3 - 3\nu_p)\kappa_4$	84
4 order $(\kappa_1, \kappa_2, \kappa_3, \kappa_4)$	$x_p = \nu_p + \frac{1}{6}(\nu_p^2 - 1)\kappa_3 + \frac{1}{24}(\nu_p^3 - 3\nu_p)\kappa_4 - \frac{1}{36}(2\nu_p^3 - 5\nu_p)\kappa_3^2$	82
5 order $(\kappa_1, \kappa_2, \kappa_3, \kappa_4, \kappa_5)$	$x_p = \nu_p + \frac{1}{6}(\nu_p^2 - 1)\kappa_3 + \frac{1}{24}(\nu_p^3 - 3\nu_p)\kappa_4 - \frac{1}{36}(2\nu_p^3 - 5\nu_p)\kappa_3^2 + \frac{1}{120}(\nu_p^4 - 6\nu_p^2 + 3)\kappa_5$	67
6 order $(\kappa_1, \kappa_2, \kappa_3, \kappa_4, \kappa_5)$	$x_p = \nu_p + \frac{1}{6}\left(\nu_p^2 - 1\right)\kappa_3 + \frac{1}{24}\left(\nu_p^3 - 3\nu_p\right)\kappa_4 - \frac{1}{36}\left(2\nu_p^3 - 5\nu_p\right)\kappa_3^2 + \frac{1}{120}(\nu_p^4 - 6\nu_p^2 + 3)\kappa_5 - \frac{1}{24}(\nu_p^4 - 5\nu_p^2 + 2)\kappa_3\kappa_4$	82
7 order $(\kappa_1, \kappa_2, \kappa_3, \kappa_4, \kappa_5)$	$x_p = \nu_p + \frac{1}{6}\left(\nu_p^2 - 1\right)\kappa_3 + \frac{1}{24}\left(\nu_p^3 - 3\nu_p\right)\kappa_4 - \frac{1}{36}\left(2\nu_p^3 - 5\nu_p\right)\kappa_3^2 + \frac{1}{120}(\nu_p^4 - 6\nu_p^2 + 3)\kappa_5 - \frac{1}{24}(\nu_p^4 - 5\nu_p^2 + 2)\kappa_3\kappa_4 + \frac{1}{324}(12\nu_p^4 - 53\nu_p^2 + 17)\kappa_3^3$	82

on the most comprehensive operational risk dataset as far as we know, the proposed approach is employed to calculate the operational risk capital charge for the overall Chinese banking.

The experiment shows that the resulting VaR values range from 67 billion CNY to 13290 billion CNY. The expansions with low order moments lead to large VaR values of 3390 and 13290 billion CNY. When higher order moments, that is, fourth and fifth moments, are added in the expansion, VaR converges to around 82 billion CNY. The widely used lognormal distribution only uses the information of the first and second moments, while the proposed approach is able to include the information of high order moments. Therefore, the proposed approach is supposed to model the operational risk in a more effective way.

Conflict of Interests

The authors declare that there is no conflict of interests regarding the publication of this paper.

Acknowledgments

This research has been supported by Grants from the National Natural Science Foundation of China (71071148 and 71301087), Key Research Program of Institute of Policy and Management and Youth Innovation Promotion Association of the Chinese Academy of Sciences.

References

[1] Basel Committee on Banking Supervision, *Working Paper on the Regulatory Treatment of Operational Risk*, Bank for International Settlements, Basel, Switzerland, 2001.

[2] J. Li, J. Feng, X. Sun, and M. Li, "Risk integration mechanisms and approaches in banking industry," *International Journal of Information Technology & Decision Making*, vol. 11, no. 6, pp. 1183–1213, 2012.

[3] Basel Committee on Banking Supervision, *International Convergence of Capital Measurement and Capital Standards: A Revised Framework*, Bank for International Settlements, Basel, Switzerland, 2006.

[4] F. Aue and M. Kalkbrener, "LDA at work: Deutsche Bank's approach to quantifying operational risk," *The Journal of Operational Risk*, vol. 1, no. 4, pp. 49–95, 2007.

[5] J. Li, J. Feng, and J. Chen, "A piecewise-defined severity distribution-based loss distribution approach to estimate operational risk: evidence from chinese national commercial banks," *International Journal of Information Technology & Decision Making*, vol. 8, no. 4, pp. 727–747, 2009.

[6] A. Chapelle, Y. Crama, G. Hübner, and J.-P. Peters, "Practical methods for measuring and managing operational risk in the financial sector: a clinical study," *Journal of Banking & Finance*, vol. 32, no. 6, pp. 1049–1061, 2008.

[7] A. Frachot, P. Georges, and T. Roncalli, "Loss distribution approach for operational risk," Working Paper, Groupe de Recherche Operationnelle, Credit Lyonnais, Paris, France, 2001.

[8] A. Mori, T. Kimata, and T. Nagafuji, "The effect of the choice of the loss severity distribution and the parameter estimation method on operational risk measurement," Working Paper, Risk Assessment Section, Financial Systems and Bank Examination Department, Bank of Japan, 2007.

[9] J. Feng, J. Li, L. Gao, and Z. Hua, "A combination model for operational risk estimation in a Chinese banking industry case," *The Journal of Operational Risk*, vol. 7, no. 2, pp. 17–39, 2012.

[10] R. Giacometti, S. Rachev, A. Chernobai, M. Bertocchi, and G. Consigli, "Heavy-tailed distributional model for operational losses," *The Journal of Operational Risk*, vol. 2, no. 1, pp. 55–90, 2007.

[11] M. Degen, P. Embrechts, and D. D. Lambrigger, "The quantitative modeling of operational risk: between g-and-h and EVT," *ASTIN Bulletin*, vol. 37, no. 2, pp. 265–291, 2007.

[12] V. Chavez-Demoulin, P. Embrechts, and J. Nešlehová, "Quantitative models for operational risk: extremes, dependence and

aggregation," *Journal of Banking & Finance*, vol. 30, no. 10, pp. 2635–2658, 2006.

[13] P. Embrechts, H. Furrer, and R. Kaufmann, "Quantifying regulatory capital for operational risk," *Derivatives Use, Trading & Regulation*, vol. 9, no. 3, pp. 217–233, 2003.

[14] J. Li, J. Feng, and L. Gao, *Modeling on Operational Risk of Commercial Bank: Theory, Method and Empirical Study*, Science Press, Beijing, China, 2013 (Chinese).

[15] S. R. Jaschke, "The Cornish-Fisher expansion in the context of Delta-Gamma-normal approximations," *The Journal of Risk*, vol. 4, no. 4, pp. 33–52, 2002.

[16] E. A. Cornish and R. A. Fisher, "Moments and cumulants in the specification of distributions," *Review of the International Statistical Institute*, vol. 5, no. 4, pp. 307–320, 1938.

[17] P. Jorion, *Value at Risk: The New Benchmark for Managing Financial Risk*, McGraw-Hill, New York, NY, USA, 3rd edition, 2007.

[18] J. Li, X. Zhu, D. Wu, C. F. Lee, J. Feng, and Y. Shi, "On the aggregation of credit, market and operational risks," *Review of Quantitative Finance and Accounting*, 2013.

[19] K. Aas, X. K. Dimakos, and A. Oksendal, "Risk capital aggregation," *Risk Management*, vol. 9, no. 2, pp. 82–107, 2007.

[20] Basel Committee on Banking Supervision, *Operational Risk-Supervisory Guidelines for the Advanced Measurement Approaches*, Bank for International Settlements, Basel, Switzerland, 2011.

Hindawi Publishing Corporation
Discrete Dynamics in Nature and Society
Volume 2014, Article ID 964275, 12 pages
http://dx.doi.org/10.1155/2014/964275

Research Article

Study on the Technical Efficiency of Creative Human Capital in China by Three-Stage Data Envelopment Analysis Model

Jian Ma,[1] Yueru Ma,[1] Yong Bai,[1,2] and Bing Xia[1]

[1] *Business School, Central South University, Changsha Hunan 410083, China*
[2] *Business School, Hunan International Economics University, Changsha Hunan 410205, China*

Correspondence should be addressed to Yong Bai; baiyong1225@163.com

Received 24 December 2013; Accepted 26 January 2014; Published 11 March 2014

Academic Editor: Taishan Yi

Previous researches have proved the positive effect of creative human capital and its development on the development of economy. Yet, the technical efficiency of creative human capital and its effects are still under research. The authors are trying to estimate the technical efficiency value in Chinese context, which is adjusted by the environmental variables and statistical noises, by establishing a three-stage data envelopment analysis model, using data from 2003 to 2010. The research results indicate that, in this period, the entirety of creative human capital in China and the technical efficiency value in different regions and different provinces is still in the low level and could be promoted. Otherwise, technical non-efficiency is mostly derived from the scale nonefficiency and rarely affected by pure technical efficiency. The research also examines environmental variables' marked effects on the technical efficiency, and it shows that different environmental variables differ in the aspect of their own effects. The expansion of the scale of education, development of healthy environment, growth of GDP, development of skill training, and population migration could reduce the input of creative human capital and promote the technical efficiency, while development of trade and institutional change, on the contrary, would block the input of creative human capital and the promotion the technical efficiency.

1. Introduction

Since American economist Schultz put forward Human Capital Theory in 1960s, the Human Capital Theory and its impact on social and economic development are one of the hot research issues for specialists and scholars at home and aboard. It is generally accepted that human capital is a reflection of the quality of labor capital, and human capital consists of economic value of knowledge, technology, ability, and healthy quality which condenses on laborers [1, 2]. Human capital usually has greater appreciation of space than material capital and other production factors, especially in the postindustry era and in the stage of rapid economic knowledge development. As a "live" capital form, human capital, with its creativity and innovation, has greater value and development potential in the aspects of optimizing allocation of resources or speeding up the economic development and promoting the social progress. Human capital, as one of those main production factors which can facilitate the economic growth, has an immediate boost to economic growth and would generate technology spillover effect by material capital and foreign direct investment (FDI) [3], spiritual morality [4], and other factors; thus it indirectly promotes economic growth. A lot of researches show that human capital is playing a more and more significant role in the development of national culture or society or economy or employment or income and so on [5–8].

Schultz claimed that the contribution to economic growth from the improvement of human capital such as human's knowledge or ability and health is more important than the increase of material force and the number of labor [9]. Generally, the formation of human capital mainly depends on the input of education, health and income, and so forth [10, 11]. The differences among education investment, health investment, and family economic income invariably tend to raise up the differences of human capital stock directly [12, 13], while the differences of human capital will lead to the differences of their effects. Studies have shown that the effects of human capital that received higher education, on individual performance, total productivity, technological progress, economic growth, and international trade, are significantly greater than the human capital which received secondary education and basic education [14–18]. According to the differences of human capital stock, human capital can be divided into general human capital, professional human capital, and creative human capital. The general human capital contains social average knowledge stock and the ability of analysis, computing ability, learning ability, and adaptability, and the corresponding social role is the division of ordinary workers. Professional human capital has a special professional knowledge and professional ability, which generally accepts special professional knowledge through formal education or on-the-job training. Creative human capital is a kind of innovative knowledge and a scarcity of innovative ability, which can realize increasing return of heterogeneity of human capital [19], and it is usually characterized by receiving higher education and is scarce in society, which means high reserve, specialization, and innovation [20]. Creative human capital would develop the ability to discover and resolve the market disequilibrium [9, 21] and then bring about more creation in strategy, institution, method, science, and technology more easily. These innovative activities tend to break through the bottlenecks in the system of technology or production constraints, make the enterprise production possibilities frontier outward or the moving-up of production function, and bring the output multiplier effect. On the one hand, creative human capital can produce its own progressive increase of marginal revenue through specialization of knowledge factors. On the other hand, through the overflow effect of knowledge, it can promote the production efficiency of the production factors like capital and labor and produce progressive increase of marginal revenue of these factors and eventually progressive increase of production scale revenue [22]. Therefore, the influence of creative human capital on the economic growth is greater than other types of human capital [23, 24].

For most developing countries, including China, the development of knowledge economy and the increase of human capital could effectively promote the economic growth rapidly [5]. In recent years, the economy in China has made rapid development, but the contribution of economic growth still mainly relies on capital investment [25]. Therefore, in order to ensure the long-term stable development of Chinese economy, it is important to increase the investment of human capital, especially the creative human capital, and to improve the efficiency of the quality of the creative human capital and technology. Continuously strengthening the role of creative human capital on economic growth is particularly important.

According to the studies of human capital, if only it limits to the single factor index of human capital investment and ignores many other factors, which tends to ignore the heterogeneity of human capital under different investment structure, so that human capital stock index is short of enough accuracy on the basis of building [26]. Therefore, the study of human capital should not only consider the number, but also need to pay attention to structure. The number and structure of the human capital investment directly restrict the amounts and the formation of human capital and thus affect the economic operation performance [27]. The investment and accumulation of human capital do not only depend on the micro main body of education or health or migration, but also depend on whether the macroeconomic system is conductive to development of the micro main body by using the potential of its investment and making it the reality of human capital or not [28]. The technical efficiency of human capital and its effect on economic growth would differ for each investment structure of human capital and each environment. Therefore, the creative human capital stock and the technical efficiency of the investment structure should both be considered when analyzing the influence of creative human capital.

Currently, some scholars studied the efficiency of human capital, such as Ferrari and Laureti who have carried an empirical research, using DEA method, on output efficiency of human capital in Italian university, based on data from the students of Florence University in 2005 [29]; Chang et al. have made an empirical analysis on the efficiency of intellectual capital and its effect on the performance in the digital industry in Taiwan by using the DEA method [30]. Ahmed and Krishnasamy have analyzed the efficiency of human capital investment and its effect on the increase of total factor productivity (TFP) in ASEAN countries [31]. Maudos et al. in 2006 [32] and Zhu et al. in 2010 [33] used SFA method to analyze the effect of human capital and its components on technical change, technical efficiency, and productivity; Ran and Zhai used DEA method to make an empirical analysis of the construction industry contribution rate of human capital in China [34]. However, few researches on the efficiency of creative human capital have been done at present.

Compared to traditional view of frontier efficiency analysis methods, such as DEA method, Fried et al. put forward the three-stage DEA method to effectively strip the influence of environment factors and the random errors on the efficiency value, overcoming the traditional shortcomings in frontier efficiency analysis model in measuring error handling [35]. This paper attempts to construct the forefront of creative human capital efficiency analysis model by using three-stage DEA method as the theoretical model, based on panel data of 31 provinces in China from 2003 to 2010. Then a quantitative research on the efficiency of creative human capital in China and the influence of its environmental factors and random errors would be made in order to support effective decision-making in promoting the development of creative human capital and improving the technology efficiency of creative human capital in China.

2. Establishing the Theoretical Model

Based on the Data Envelopment Analysis (DEA) model founded by Charnes et al. in 1978 and two-phase DEA model by Coelli in 1998, three-stage DEA model proposed by Fried et al. has been proved to be a better method to assess the efficiency of Decision-Making Units (DMU) [35]. Its contracture and application include three stages.

2.1. The First Stage: Traditional DEA Model. Charnes et al. put forward a DEA method which was called efficiency measurement model and was based on the Constant Return Scale (CRS) in 1978 [36]. According to the multiple sets of input and output data of the technical efficiency of DMU, the CCR model assumption with fixed size is not consistent with the practical situation of many industries by using the theory of mathematical programming. In 1984, Banker et al. changed the assumption of Constant Return Scale into Variable Return Scale (VRS) and built a more rigorous variable scale reward model to decompose the technical efficiency (TE) into pure technical efficiency (PTE) and scale efficiency (SE), TE = PTE × SE [37].

Generally speaking, the technical efficiency of DMU can be estimated by two ways. One is based on input technical efficiency, namely, the proportion of the minimum investment in the investment under a certain output. Another is based on the production technical efficiency, namely, the proportion of the maximum output in the practical output under the certain investment combination. The BBC model of variable returns to scale adopts the efficiency estimation when input is at the minimum level under the condition of constant output. In this paper, technical efficiency is defined as the proportion between minimum possible input and practical investment in the same deal, $0 \leq \mathrm{TE} \leq 1$. The bigger the value of TE is, the higher the efficiency level of DMU's production is. If TE = 1, the DMU has reached the minimum input under the certain constant output and realized the optimal allocation of resources. If TE < 1, it means that the DMU has not yet achieved the optimal allocation of productive resources while production technology is inefficient.

BCC model argues that the reasons of technical inefficiency are two: low efficiency of production technology and nonefficiency which is not at the optimal size. Pure technical efficiency of DMU refers to the production efficiency that is affected by management and technology factors, and it can reflect the production efficiency of input factors when production scale has reached the optimal level, namely, $0 \leq \mathrm{PTE} \leq 1$. If the PTE = 1, it means that under the current technical level, the utilization of DMU input resources is efficient, or there is lack of efficiency. Scale efficiency of DMU refers to the production efficiency that is affected by scale factor, which reflects the difference between the practical production scale and the optimal production scale. If SE = 1, DMU is in the state of optimal production scale, or it has not yet reached the optimal production scale.

The analysis result of BBC model can measure the utilization efficiency of production factors when the output is constant of each DMU. The decomposition results of the production inefficiency can accurately reflect the reason of inefficiency of production input of the DMU and thereby could support the improvement of the utilization efficiency in the production process and provide the solution and method to achieve the optimal distribution of input factors.

This article adopts the BCC model of the Variable Return Scale (VRS) and regards creative human capital investment as an independent production process, in order to measure the minimum level of investment of creative human capital to achieve a certain level. The technical efficiency (TE) of the scale-reward of creative human capital can be divided into pure technical efficiency (PTE) and scale efficiency (SE), leading to the separation of the two different causes that are the inefficiency of production technology and the inefficiency of the investment size which is less than optimal of the inefficiency of creative human capital.

Then, review the management efficiency of creative human capital in k city (PTE_k) in China; each province has m inputs and s output, and the investment-oriented BCC model is as follows:

$$\begin{aligned}
\text{Min} \quad & \mathrm{PTE}_k \\
\text{Subject to:} \quad & \sum_{j=1}^{n} \lambda_j x_{ij} + s^{+} = \mathrm{PTE}_k x_{ik} \quad i = 1, 2, \ldots, m \\
& \sum_{j=1}^{n} \lambda_j y_{rj} - s^{-} = y_{rk} \quad r = 1, 2, \ldots, s \\
& \sum_{j=1}^{n} \lambda_j = 1 \\
& \lambda_j \geq 0, \quad j = 1, 2, \ldots, n,
\end{aligned} \tag{1}$$

where x_{ij} stands for the input of creative human capital at i in j province and y_{rj} stands for the output at r in j province, λ_j is the weight in j province, s^{+} stands for the input of creative human capital, and s^{-} stands for the slack variable of output of creative human capital, $0 \leq \mathrm{PTE} \leq 1$; the bigger the number, the purer the technical efficiency of creative human capital.

We can use CCR model to get technical efficiency (TE) of creative human capital, and according to relation from TE = PTE × SE, we can get scale efficiency (SE):

$$\begin{aligned}
\text{Min} \quad & \mathrm{TE}_k \\
\text{Subject to:} \quad & \sum_{j=1}^{n} \lambda_j x_{ij} \leq \mathrm{TE}_k x_{ik} \quad i = 1, 2, \ldots, m \\
& \sum_{j=1}^{n} \lambda_j y_{rj} \geq y_{rk} \quad r = 1, 2, \ldots, s \\
& \lambda_j \geq 0, \quad j = 1, 2, \ldots, n.
\end{aligned} \tag{2}$$

2.2. The Second Stage: Establishing the SFA Model. When the output y_{rj} does not change, if the management levels of creative human capital in all provinces are at the same level, the input of creative human capital x_{ij} in good condition is less than the one in bad condition, which is affected by other provincial environment. Therefore, it cannot reflect the real level of management input of creative human capital. In order to get the real management efficiency of creative human capital in all provinces, it needs to strip the impact of environment variable and random errors and the internal management. According to the model which was put forward by Battese and Coelli in 1995, it can find regression model Stochastic Frontier Analysis (SFA) between s_{ik}^{+} and z_{ik} as follows:

$$s_{ik}^{+} = z_{ik}\beta + (v_{ik} + u_{ik}) \quad i = 1, 2, \ldots, m, \quad k = 1, 2, \ldots, n, \tag{3}$$

where z_{ik}, β stand for the environment variable and index at k in i province, if $\beta < 0$, so the environment variable is benefit for the decrease of slack variable and improves the technical efficiency, and vice versa. $v_{ik} + u_{ik}$ is composite error term, v_{ik} is random variable, and it stands for the error which cannot take into consideration, v_{ik} is single and $v_{ik} \sim N(0, \sigma_v^2)$, u_{ik} stands for management inefficiency factor, u_{ik} is normal distribution, that is, u_{ik} stands for $\sim N(\mu^i, \sigma_u^2)$, and v_{ik} and u_{ik} are independent of each other. Considering $\gamma = \sigma_u^2/(\sigma_v^2 + \sigma_u^2)$, $0 \leq \gamma \leq 1$, γ tend to be 1, so that the impact of management variable is dominant; γ tend to be 0, so that the impact of random error is dominant.

We can get efficiency value which reflects the management level when considering the environment factor and random error using SFA model, adjust the input term of creative human capital, increase the input of provinces in good condition, and make the environment factor and random error in the same level; then we can get the input of the creative human capital x_{ik}^A which, after adjusting, is

$$x_{ik}^A = x_{ik} + \left[\max_k \left\{z_{ik}\hat{\beta}^i\right\} - z_{ik}\hat{\beta}^i\right] + \left[\max_k \left\{\hat{v}_{ik}\right\} - \hat{v}_{ik}\right] \qquad i = 1, 2, \ldots, m, \quad k = 1, 2, \ldots, n, \tag{4}$$

where x_{ik} and x_{ik}^A are creative human capital which are before and after adjusting, $\hat{\beta}^i$ is the estimate of environment factor, $\hat{v}_{ik}$ is the estimate of random error, the first bracket stands for adjusting the creative human capital in all provinces to the same environment, and the second bracket stands for adjusting the random errors of creative human capital to be the same.

2.3. The Third Stage: The DEA Model after Adjusting. Replace the original value x_{ik}^A into the adjusted value, and use the BCC model to analyze the efficiency, so that we can get the efficiency value of creative human capital without the impact of environment factor and random errors.

3. Variable Selection and Data Acquisition

3.1. Output Variable. It is essential to select the reasonable input and output indicators for the final measurability of efficiency DMU when using DEA method to analyze the efficiency. A lot of researches have showed that education is the key part of human capital accumulation, and the state of education can measure the stock of human capital [10, 38]. Therefore, considering the characteristics of creative human capital, this research selected college students who receive college education or above as the research object and used the university graduates (y_1) and the university students (y_2) as output indicators.

3.2. Input Variable. Selection of input variables is reasonable to determine whether the analysis method is effective or not. In the selection of creative human capital input, the first difficulty is how to determine the origins of the input and the measurability of these variables [29]. Similar to the general process of input and output, the main factors which affect the creative human capital are the resources and factors in the production course, such as labor and capital. Combined with the measurability, the text selects college teachers (x_1), college education spending (x_2), college research spending (x_3), and fixed assets (x_4) as the input variables of creative human capital. The number of teaching staff in colleges or the education capital and fixed assets in institutions can directly affect the output level and the production scale of the creative human capital. And scientific research funds influence the output quality and efficiency of creative human capital.

3.3. Environment Variable

3.3.1. Scale Environment Variable. The enlargement of the education scale could directly increase the number of inputs of college education, improve the efficiency of education resources for the economic features of education scale, make full use of education resources, and ultimately improve the output of education. This paper selects the ordinary university number as the measure variable of scale environment.

3.3.2. Healthy Environment Variable. The good condition of health can not only improve the learning efficiency and the rate of return on education, but also affect the investment behavior on education. The better the health is, the longer the life is and the greater the benefit will be from the education [1]. And high human capital investment can resist the threat of disease or drug and optimize the quality of fertility [39]. As for the larger returns of creative human capital with high expected rate, good condition of health will get greater return from the higher education investment. Therefore, the development of healthy environment is bound to affect the investment behavior of people for higher education and to change the input and output of the creative human capital. The main measure variables of health indications are anthropometric variables, life expectancy or survival rate, mortality rate, and so forth [40]. This paper selects the population mortality (z_2) as indicator of health environment variable.

3.3.3. Economic Environment Variable. On one hand, economic growth and the improvement of people's income will continue to encourage people to pursue higher quality of life, so as to increase the investment of education. On the other hand, with the constant improvement of the level of economic development, quality requirements of the talent will be much higher, and the talent competition will be much fiercer. In order to improve the competitive ability, more human capital investment is needed and creative human capital investment is on focus. So the economy will continue to promote the input and output growth of creative human capital. This paper selects GDP (z_3) as measure variable of economic environment variable.

3.3.4. Skills Environment Variable. Training can be viewed as an extension of the education by making workers learn special skills during working, and it plays an important role in improving the level of workers' skills and working efficiency. Skill training is supposed to enhance the technical innovative ability and labor productivity of the trainees, improve their working and researching efficiency, and increase the input efficiency of human capital [41, 42]. This paper selects the number of the students (z_4) who graduate from technical college as measure indicator of skills environment variable.

3.3.5. Migration Environment Variable. Although population migration does not bring the increase of human capital stock, it can achieve the efficient allocation of human resources, so that the subjects of human capital can respond to the economic environment or system structure change effectively, find potential profit opportunities, and improve the decision-making ability to maximize the interests of using resources [27]. Migration can also increase the chances of migration employment and improve the utilization efficiency of social labor and employment [43]. This paper selects net migration rate as the migration environment variable.

3.3.6. Foreign Trade Environment Variable. Foreign trade not only can increase the total world trade, but also can accelerate the worldwide spread of advanced science, technology, and knowledge and make the participant countries benefit from the communication and trade [44]. Under different trade system, the effect of human capital on economic growth is not the same, and the effect is greater in open trade system than in the closed system [45]. This paper selects the total output (z_6) as measure indicator of foreign trade environment variable.

3.3.7. Institution Environment Variable. Changes of institutions will not add the amount of human capital, but it may fully arouse the enthusiasm of human capital investor and human capital owner by establishing good institutional environment which includes the market-oriented economic system and human capital property right arrangements [46]. Therefore, the improvement of the institutional environment is conducive to optimizing the investment environment of creative human capital and improving the utilization efficiency of elements. This paper selects the proportion of the investment of non-state-owned economy fixed assets in the investment of the fixed assets of the whole society as the measuring indicator of institution environment variable.

3.4. Sample Statements. According to the purposes and needs of research, this paper selects 31 provincial districts in mainland of China as sample investigation objects; the time is from 2003 to 2010 (this research is using data during 2003–2010, as before 2003 the data about college was not distinguished in regions); the sample data come from "Statistical Yearbook," "the Statistical Yearbook of Education in China," "the Statistical Yearbook of Education Expenditure in China," "the Statistical Yearbook of Labor in China," and "the Population Statistics of Counties and Cities in China."

According to the request of research, there must be a significant correlation between various variables; inputs and outputs should comply with the "synthetic" hypothesis that production should increase with the increase of inventory. Variable with correlation test results such as Table 1 is obtained using Pearson's correlation test.

Table 1 shows that there is a significant correlation between output variable and input variable, and they are positively related, illustrating that the selection of variables and data is in accord with the requirement of model analysis and it is rational.

4. The Empirical Analysis Results

Then, through Deap2.1 and Front4.1 analyzing software, we made an empirical analysis of creative human capital technical efficiency of 31 provincial districts in China from 2003 to 2010 by using three-stage DEA method and made a horizontal comparison on the efficiency of various provincial districts; the specific analysis results are as follows.

Firstly, the overall efficiency of creative human capital is higher.

Table 2 shows the overall level of efficiency of creative human capital and its changes before and after considering the exogenous environment variables and random factors in China in sample period. In the process of the analysis of phase 1, the comprehensive technical efficiency average of creative human capital is 0.823, average value of pure technical efficiency is 1, the scale efficiency value is 0.823, and the comprehensive technical efficiency value and scale efficiency value are on the decline, which indicates that the comprehensive technical efficiency of creative human capital has room for improvement and the scale efficiency is the main reason for technical inefficiency. In the analysis of phase 3, the influence of the environment variable and random errors on creative human capital is eliminated. Results show that the efficiency of three values is 1, indicating that the technical efficiency in frontier has no room for improvement. Compared with the results of the first stage, the third stage of technical efficiency values rises to some extent, stating that the lower technical efficiency is mainly due to adverse circumstances or bad luck, rather than the technical management level.

Secondly, efficiency levels among eastern, western, and central regions roughly have the same change trend, but certain differences among these three regions still exist.

Through the analysis of the efficiency level among eastern, western, and central regions during phase 1 and phase 2, the results in Table 3 show that, from 2003 to 2010, the average value of comprehensive technical efficiency and average of pure technical efficiency are both the highest in the eastern region, the next is in central region, and the lowest is in western region, while the highest scale efficiency value is in central region and next is in western region. And from 2003 to 2010, the average values of three regions all tend to decrease, which indicates that there is some room for improvement, and the efficiency value of pure technical efficiency is higher than the average value of scale efficiency; technical inefficiency is mainly due to scale inefficiency. Compared with the first stage, in the third phase, general average technical efficiency in these three areas and scale efficiency have obviously risen, and the pure efficiency values in eastern and western areas are slightly down, indicating that the technical efficiency value in three regions is closely related to their environment or bad luck, leading to some differences between the nominal technical management level and the actual technical management level.

We can find that the level of efficiency in central region is slightly higher than in the eastern and western regions

Table 1: The correlation coefficient of variable test table.

		Input variable			
		x_1	x_2	x_3	x_4
Output Variable	y_1	0.993^{***}	0.974^{***}	0.922^{***}	0.993^{***}
	y_2	0.998^{***}	0.959^{***}	0.912^{***}	0.991^{***}
Environment variable	z_1	0.946^{***}	0.969^{***}	0.941^{***}	0.965^{***}
	z_2	0.952^{***}	0.996^{***}	0.984^{***}	0.990^{***}
	z_3	0.995^{***}	0.960^{***}	0.905^{***}	0.988^{***}
	z_4	0.972^{***}	0.944^{***}	0.875^{***}	0.966^{***}
	z_5	-0.537	-0.758^{**}	-0.812^{**}	-0.666^{*}
	z_6	0.961^{***}	0.958^{***}	0.924^{***}	0.967^{***}
	z_7	0.884^{***}	0.721^{**}	0.617^{*}	0.799^{**}

Note: *, ** and *** indicate significance at the 10%, 5% and 1% levels, respectively.

Table 2: Nationwide efficiency values of creative human capital during 2003–2010 in China.

		2003	2004	2005	2006	2007	2008	2009	2010	Mean
First stage	TE	0.844	0.851	0.825	0.825	0.800	0.806	0.816	0.815	0.823
	PTE	1.000	1.000	1.000	1.000	1.000	1.000	1.000	1.000	1.000
	SE	0.844	0.851	0.825	0.825	0.800	0.806	0.816	0.815	0.823
Third stage	TE	1.000	1.000	1.000	1.000	1.000	1.000	1.000	1.000	1.000
	PTE	1.000	1.000	1.000	1.000	1.000	1.000	1.000	1.000	1.000
	SE	1.000	1.000	1.000	1.000	1.000	1.000	1.000	1.000	1.000

through the comprehensive comparative analysis, partly because of the fact that the education investment proportion, which means the proportion between the nongovernmental education investment and governmental education investment, in the eastern and western education in recent years is relatively low. The improvement of education input from nongovernment will have a positive impact on accumulative level of human capital, so that the level of human capital in the region with higher education investment proportion will be relatively high [47].

Thirdly, nationwide and regional efficiency values of creative human capital keep declining.

From 2003 to 2010, the change of the creative human capital in the eastern, central, and western regions in China is shown in Figure 1. As we can see, level of the comprehensive technical efficiency in three regions from 2003 to 2007 continued to decline and started to rise in 2008, but there is an obvious overall decline from 2003 to 2010. In recent years the education input in China is increasing, but the education funds investment is relatively insufficient, the use efficiency of fund and the work efficiency of administrative personnel are low, and the differences of the regional development level among these regions are still evident. The higher education spending in China accounts merely for 1.25% in GDP from 2003 to 2010 and the college education investment is insufficient, which lead to the misallocation of higher education resource, low utilization efficiency of resources, and ultimate decline of the efficiency level of creative human capital. Therefore, increasing the investment of higher education funds, expanding the scale of college education, improving the efficiency level of education resources, and realizing the balanced development of regional education in colleges and universities are important measures and approaches to improve the technical efficiency level of creative human capital.

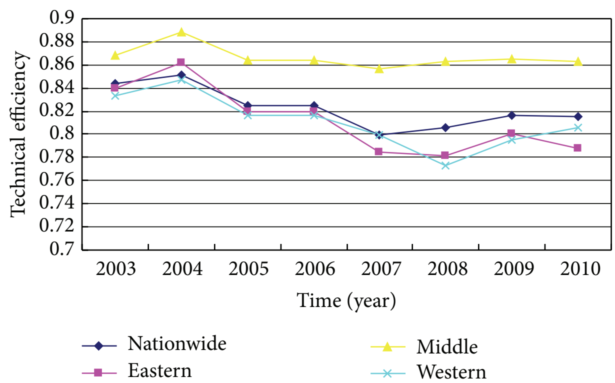

Figure 1: Description of changes of nationwide and regional efficiency values of creative human capital in China.

Fourthly, there is an obvious difference of creative human capital among various provinces and cities, significantly influenced by environment variables and random errors.

The average efficiency values of creative human capital in 31 provinces in China are shown in Table 4, by using panel data during 2003-2010. In the first phase analysis, in addition to Hebei, Shanxi, Henan, Guangxi, and Guizhou provinces that are in the frontier of technical efficiency level, the rest of provinces have a certain degree of technical inefficiency, indicating the room for improvement. The pure efficiency value in most provinces and cities is lower than the scale efficiency value, illustrating that technical nonefficiency is

Table 3: Efficiency values of creative human capital in East, Middle, West parts during 2003–2010.

			2003	2004	2005	2006	2007	2008	2009	2010	Mean
East	First stage	TE	0.840	0.862	0.820	0.820	0.785	0.782	0.801	0.788	0.812
		PTE	1.000	1.000	0.997	0.997	0.958	0.954	0.950	0.939	0.974
		SE	0.840	0.862	0.822	0.822	0.820	0.819	0.843	0.840	0.834
	Third stage	TE	0.999	1.000	0.992	0.953	0.959	0.950	0.921	0.913	0.961
		PTE	1.000	1.000	0.997	0.958	0.963	0.953	0.950	0.938	0.970
		SE	0.999	1.000	0.995	0.995	0.997	0.996	0.970	0.973	0.991
Middle	First stage	TE	0.868	0.888	0.864	0.864	0.857	0.863	0.865	0.863	0.867
		PTE	1.000	1.000	1.000	1.000	1.000	1.000	1.000	1.000	1.000
		SE	0.868	0.888	0.864	0.864	0.857	0.863	0.865	0.863	0.867
	Third stage	TE	1.000	1.000	1.000	1.000	1.000	1.000	1.000	1.000	1.000
		PTE	1.000	1.000	1.000	1.000	1.000	1.000	1.000	1.000	1.000
		SE	1.000	1.000	1.000	1.000	1.000	1.000	1.000	1.000	1.000
West	First stage	TE	0.833	0.847	0.816	0.816	0.799	0.773	0.795	0.806	0.811
		PTE	0.981	0.960	0.944	0.944	0.943	0.928	0.917	0.924	0.943
		SE	0.849	0.883	0.864	0.864	0.847	0.833	0.867	0.872	0.860
	Third stage	TE	0.943	0.932	0.931	0.901	0.909	0.916	0.916	0.915	0.920
		PTE	0.947	0.945	0.949	0.939	0.936	0.940	0.917	0.925	0.937
		SE	0.997	0.987	0.982	0.959	0.972	0.974	0.998	0.990	0.982

Note: Eastern regions include Liaoning, Hebei, Beijing, Tianjin, Shandong, Jiangsu, Zhejiang, Shanghai, Fujian, Guangdong, Guangxi and Hainan; Middlel regions include Heilongjiang, Jilin, Inner Mongolia, Shanxi, Henan, Hubei, Jiangxi, Anhui and Hunan; western regions include Shaanxi, Gansu, Qinghai, Ningxia, Xinjiang, Sichuan, Chongqing, Yunnan, Guizhou and Tibet.

mainly due to pure technical nonefficiency, and the impact of scale inefficiency is relatively mild. Comparing the analysis results of the first stage and the third stage, the efficiency values of creative human capital among various provinces have greatly changed, after eliminating the influences of environment variables and random factors.

Table 4 shows that, in the stage 1, the efficiency level among those provinces and cities in the technical efficiency frontier declined in different extent, and the comprehensive technical efficiency values of all the 31 provinces and cities still have some room for improvement. Except Beijing, Liaoning, Jiangsu, Shandong, Hubei, and Guangzhou provinces, the comprehensive technical efficiency values of the rest of provinces and cities are declining, which illustrates that these provinces and cities are affected by the favorable environment or good luck and so that the comprehensive technical values are overvalued and these values in Qinghai, Guizhou, and Tibet provinces decreased obviously by 20%. Otherwise, the scale efficiency is obviously declining compared with pure technical efficiency, indicating that the creative human capital is affected by the local environmental factors or luck, and the practical scale efficiency is lower, asking for enlarging the investment scale of creative human capital on the basis of existing condition. Besides, the pure technical efficiency values of most of the provinces and cities in third stage are increasing, indicating that the technical efficiency values are undervalued because of the environment variable or random errors, but the scale efficiency among these districts is always overvalued and the extent of overestimate is greater than the extent of underestimate, which may lead to the overestimate of comprehensive technical efficiency. After eliminating the influence of environment variable and random errors, three kinds of technical efficiency of creative human capital are all improved in some provinces like Beijing, Liaoning, Jiangsu, Shandong, Hubei, and Guangdong provinces, illustrating that the lower efficiency in these provinces and cities is due to the poor environment or bad luck, rather than their technical management level. Therefore, for these areas, it is particularly important to improve the investment environment of creative human capital.

Fifthly, environment variable can significantly affect input variables, but the direction is different.

Through the comparison of the efficiency values DEA in the first stage and the third stage, we can get that there is a significant impact of environment variable and random errors on creative human capital efficiency. The SFA model to analyze these results is shown in Table 5.

From the results of Table 5, the analysis results of SFA model are more reliable and the error is mainly due to the management inefficiency. There are seven environment variables affecting significantly the input slack variable, which means that the chosen environment variables are reasonable. We can get the result from the influence of environment variable on technical efficiency.

(1) The number of common colleges and universities obviously influences the reduction of the education expenditure, research expenditure, and fixed assets investment and the improvement of technical efficiency, which means that the expansion of education scale is conductive to forming scale economy of college education, optimizing the rational allocation of resources and improving the utilization efficiency of resources. However, its impact on the number

Table 4: Average efficiency values of creative human capital in different provinces during 2003–2010.

	First stage			Third stage		
	TE	PTE	SE	TE	PTE	SE
Beijing	0.512	0.513	0.997	0.524	0.645	0.815
Tianjin	0.798	0.808	0.987	0.792	0.932	0.851
Hebei	1.000	1.000	1.000	0.966	0.998	0.968
Shanxi	1.000	1.000	1.000	0.804	0.990	0.812
Inner Mongolia	0.885	0.897	0.986	0.738	0.958	0.771
Liaoning	0.772	0.775	0.997	0.783	0.911	0.860
Jilin	0.732	0.738	0.991	0.723	0.937	0.773
Heilongjiang	0.753	0.761	0.990	0.755	0.887	0.852
Shanghai	0.670	0.674	0.993	0.668	0.829	0.808
jiangsu	0.891	0.941	0.947	0.943	0.952	0.990
Zhejiang	0.910	0.913	0.997	0.907	0.940	0.966
Anhui	0.993	0.994	0.998	0.988	0.997	0.991
Fujian	0.869	0.875	0.993	0.860	0.961	0.896
Jiangxi	0.988	0.990	0.999	0.954	0.990	0.964
Shandong	0.960	0.991	0.968	0.993	1.000	0.993
Henan	1.000	1.000	1.000	0.998	0.999	1.000
Hubei	0.862	0.889	0.970	0.895	0.913	0.980
Hunan	0.871	0.893	0.976	0.867	0.933	0.930
Guangdong	0.891	0.899	0.991	0.953	1.000	0.953
Guangxi	1.000	1.000	1.000	0.866	1.000	0.866
Hainan	0.918	0.963	0.954	0.832	1.000	0.832
Chongqing	0.851	0.859	0.990	0.840	0.913	0.920
Sichuan	0.882	0.887	0.995	0.879	0.920	0.956
Guizhou	1.000	1.000	1.000	0.774	0.966	0.803
Yunnan	0.818	0.827	0.989	0.788	0.928	0.851
Tibet	0.866	1.000	0.866	0.650	1.000	0.650
Shaanxi	0.784	0.788	0.995	0.786	0.853	0.921
Gansu	0.881	0.902	0.977	0.849	0.931	0.912
Qinghai	0.920	1.000	0.920	0.486	0.982	0.495
Ningxia	0.718	0.924	0.782	0.605	1.000	0.605
Xinjiang	0.892	0.922	0.967	0.696	0.971	0.718

Table 5: Regression analysis results of SFA.

	College teachers slack variable	College education spending slack variable	College research spending slack variable	Fixed assets slack variable
Constant	-175.215^{***}	-12863.3^{***}	-27681.2^{***}	-608690.7^{***}
z_1	0.5843	-1704.90^{***}	-117.45^{**}	-2126.92^{***}
z_2	-0.004916	-3.0235	1.0414^{**}	2.7415
z_3	-0.000190^{***}	-2.1062^{*}	-0.5743^{***}	-3.5655^{**}
z_4	-27.616^{**}	-80226.75^{***}	-3244.31^{**}	-34122.78^{***}
z_5	51.314^{**}	-7171.76^{***}	-1864.96^{*}	-34743.21^{***}
z_6	-0.008836	332.21^{***}	24.8534^{***}	364.11^{***}
z_7	-116.891	647439.9^{***}	56196.33^{***}	106449.7^{***}
σ^2	$0.259E+07^{***}$	$0.499E+12^{***}$	$0.540E+10^{***}$	$0.729E+12^{***}$
γ	0.6831^{***}	0.7359^{***}	0.7406^{***}	0.6420^{***}
LR	117.79^{***}	131.02^{***}	136.44^{***}	85.54^{***}

Note: *, ** and *** indicate significance at the 10%, 5% and 1% levels, respectively.

of faculty is not significant, probably because the increase of college teachers depends on the education level of teachers and the number of students. The competition among higher education universities is getting more and more intense, so each university and each region tend to adopt different policies and institutions to attract outstanding teachers, which may enhance the imbalance of resources allocation among different regions and universities and affect the efficiency of resource allocation.

(2) The regression coefficient of the effect of population mortality on the input of scientific research in colleges and universities is positive and it passed the significance test that shows that good and healthy environment (i.e., low mortality) is benefit for decrease of research input and improvement of technical efficiency, but its influence on the number of faculty, education funds, and fixed assets is not obvious. The main reason may be that good health condition can improve people's cognitive ability and maintain much longer mental working; then it would improve the efficiency of study and research and guarantee the quality of higher education returns and education input. Therefore, the influence of healthy environment is mainly to optimize the quality of colleges and the impact on the education scale factor is relatively small.

(3) The regression coefficients of the effect of GDP on input variables were negative and passed the test of significance, claiming that the increase of GDP is beneficial to the decrease of input for creative human capital and to improve the technical efficiency. The increase of GDP will lead to the improvement of the income of people and help to promote the residents' consumption quality and consumption level. Besides, it could raise the investment demand on the creative human capital, which is advantageous to realize the scale economy effect of local creative human capital and to improve the utilization efficiency and outputs efficiency of inputs.

(4) The regression coefficients of the effect of the number of the students who graduate from technical college on four input variables were negative and passed the test of significance, showing that the development of skills training is beneficial to the decrease of the creative human capital investment. The development of skills training can help the trainers get higher knowledge and skills and improve their innovation ability and the efficiency of work, research, and development, which not only can create better investment environment for creative human capital, but also can optimize the resource allocation efficiency and speed up the growth of input and output efficiency.

(5) Four kinds of inputs have passed the test of significance, indicating that the population migration will affect the inputs of creative human capital. And the regression coefficient of the effect of net migration rate on expenses of education in colleges and universities, scientific research spending and fixed assets, is negative, indicating that the increase of the rate of net migration is conducive to the reduction of the three elements of the input. Besides, the regression coefficient of the effect of net migration rate on the number of teaching staff members is positive, which means the number of teaching staff members will rise with the addition of the net migration rate. From the view of Dierx in 1988 [48], the main reason for attracting domestic population migration is the income growth, and when getting higher income through migration, people would increase the investment of human capital in order to ensure their living conditions. Therefore, the increase of population migration will expand the scale of creative human capital investment, be beneficial to form scale effect, and improve investment efficiency of elements. However, on the other hand, the effect of population migration also will be affected by the rationality of the cost of migration and migration among regions. Excessive or passive population migration is likely to cause the loss of the talent and the flight of human capital and reduce the labor productivity [43]. The current migration is happening mainly from rural villages to cities and from western regions to eastern regions. This unidirectional migration is mainly due to the imbalance of regional economic development. The imbalance of population migration is bound to lead to imbalance of resource allocation, which will waste the labor resources and decrease the utilization efficiency of labor resources. The irrationality of population migration will affect the input and allocation of faculty resources, and cause some problems, like the overstaffing of teachers, the antinomy between the utilitarian concept and moral concept, and the brain drain phenomenon. And then it would reduce the labor production efficiency.

(6) The influence of total import and export on the number of staff did not pass the test of significance, but the influence of education expenses in colleges and universities, scientific research spending and fixed assets, has passed the test of significance and the regression coefficient is positive, indicating that the development of foreign trade is not conductive to the decrease of three inputs. The possible reason would be that trade liberalization is beneficial to the introduction of technology, which will increase the human capital in countries with rich technology resources and decrease the human capital in countries with poor technology resources, by increasing the reward of technical elements and decreasing the reward of labor elements in countries with rich technology resources and increasing the reward of labor elements and decreasing the reward of technical elements in countries with poor technology resources [49]. China is a typical developing country, and excessive development of foreign trade in China will

lead to more reliance on foreign technology, which is not conducive to the formation of scale effect of the creative human capital and the improvement of technical efficiency.

(7) The influence of the proportion of the investment of non-state economy fixed assets in the investment of the fixed assets of the whole society on the number of faculty did not pass the test of significance, but the influence on expenses of education in colleges and universities, the scientific research spending and fixed assets, has passed the test and the regression coefficient is positive, which means that the institutional change is bad for the improvement of technical efficiency and asks for more creative human capital investment. This is partly because the non-state-owned enterprises in China at present have not yet formed the scale economy, their technological content is low, and their consciousness of the innovative is not strong. Consequently, the economic system and education system have failed to be effectively combined, and the enthusiasm of creative human capital investors and owners is not fully aroused, wasting the human capital. So it is not conducive to the formation of scale economy creative human capital and the improvement of technical efficiency.

5. Conclusion

Based on the cognition of the continuous development of creative human capital and its increasing effect on economic growth, for the first time, this paper measures the technical efficiency value of the creative human capital in various cities from the perspective of technical efficiency and analyzes the main causes of inefficiency of human capital through the decomposition. By building the three-stage DEA model, this paper overcomes the defect of the traditional DEA and SFA method and makes the measurement of technical efficiency of creative human capital more accurate, by eliminating the influences of the exogenous environment variables and random errors and analyzing the reasons for the technical efficiency change from both the production technology level and the production scale.

Through the empirical research, we can get three conclusions. First, through the measurement and comparison of the technical efficiency level of creative human capital among different districts, the current level of comprehensive technical efficiency among different districts in China is relatively high but has not reached the optimal level and still has room to improve. According to the decomposition results of comprehensive technical efficiency, the main cause of inefficiency of creative human capital among different districts is that the production scale has not achieved the optimal production scale. In addition, through the comparison of technical efficiency between stage one and stage three, the environment factor and random error can also lead to technology inefficiency of creative human capital. From the point of time span, while the comprehensive technical efficiency level among different districts in China rose slightly after 2008, the technical efficiency level of creative human capital among different districts in China keeps declining in the long term.

Secondly, according to the measurement and comparison of the technical efficiency level of creative human capital among different provinces and cities, the comprehensive technical efficiency level of all provinces and cities has not reached the optimal level and needs to be improved. The reason of technical inefficiency of creative human capital among different provinces and cities still mainly lies in the inefficiency of the production scale and environment variables and random errors, while inefficiency of production technology has the slightest effect. The comparison results of the first stage and the third stage show that the theoretical technical efficiency level is overvalued compared with the practical technical efficiency level among most provinces and cities, except Beijing, Liaoning, Jiangsu, Shandong, Hubei, and Guangdong provinces. This is partly because the pure technical efficiency is usually underestimated and the scale efficiency is usually overvalued to some higher extent, which eventually leads to overvaluation of the comprehensive technical efficiency of creative human capital among these provinces and cities.

Thirdly, the analysis of environment variables shows that promotion of the technical efficiency of creative human capital is mostly significantly affected by the economic growth, the development of skill training, and the enlargement of the scale of universities, while the optimization of health environment and the acceleration of population migration also make a partial contribution to the improvement of the technical efficiency. However, the growth of international trade and the institutional change is not conducive to the development of the technical efficiency of creative human capital.

The research results indicate that China needs to constantly promote economic growth and increase education investment in higher education. At the same time, China needs to increase the creative human capital stock and try to achieve the optimal production scale of creative human capital. The economic growth can enable people to increase their investment in health and education especially higher education with more income and push the government to increase investment in higher education and realize the scale economy of higher education.

In recent years, although the higher education spending is increasing in China, there is still a certain gap compared with higher income countries. At present, the national higher education spending in China accounts for only 1.4% of total GDP, far below the 3% level in high-income countries. In 2008, research and development expenditure as of GDP in China is 1.07% while the average level in the world is 2.14% and 2.14% in high-income countries. Despite the increasing scale of higher education since 1999 and its positive influence on the realization of the optimal scale of creative human capital, a series of problems such as inadequate education funds, the decrease of the higher education quality, and low efficiency of school management still exist and cause the low efficiency of the production scale and management of creative human capital. Therefore, it is important for China in the future to continuously increase higher education investment, optimize the education scale and education quality, and promote the utilization efficiency of education resources, in order to achieve the optimal level of technical efficiency of creative human capital and eventually develop the role of creative human capital in economic growth.

Otherwise, as the results show, the development of skill training and moderate population migration can also improve the technology efficiency of creative human capital. Effective skill training can be the supplement of higher education. Learning more professional skills inside or outside of their profession can improve students' technical level and work efficiency in the future. In addition, a moderate amount of vocational education during their practice and work can enable their innovation ability and promote their creative human capital stock. Besides, the labor resources will be rationally allocated and the utilization efficiency of production factors will be improved, because of the rational movement of creative human capital driven by population immigration. Therefore, in the future, developing vocational education should be emphasized as with expanding the higher education scale, to improve students' skill level. Meanwhile, the adjustment of industrial structure and the optimization of college profession allocation can help to realize the rational utilization of creative human capital.

In addition, adjusting the structure of foreign trade and preferring the economic property are also conducive to promote the technical efficiency of creative human capital. Currently in China, economic development relies too much on foreign trade and high foreign trade dependence will cause excessive dependence on foreign technology and innovation, which has negative effect on the formation of the scale effect of creative human capital. Consequently, adjusting the structure of foreign trade, expanding domestic demand, and increasing the proportion of domestic trade will help to promote economic growth, adjust the industrial structure, strengthen the domestic industry's capacity for independent innovation, and promote the utilization efficiency of creative human capital. And creating a good institutional environment with economic property rights system will also help, which would inspire the investors and owners of creative human capital to improve their technical efficiency.

In short, the development of China in the future needs to constantly adjust both economic and trade structure, and institutions, in order to improve the technology efficiency of creative human capital, make full use of creative human capital, and finally promote the economic growth.

Conflict of Interests

The authors declare that there is no conflict of interests regarding the publication of this paper.

Acknowledgments

This work was supported by the National Natural Science Foundation of China (NSFC) under Grant no. 71272067. It was also supported in part by the Ministry of education of Humanities and Social Science Fund Project under Grant no. 12YAJ630090, the Philosophy and Social Science Fund Project of Hunan Province under Grant no. 12YBB153, Soft Science Project of Hunan Province no. 2011ZK3077, and Scientific Research Project of the Education Department of Hunan Province no. 12C0787.

References

[1] J. Yang, L. Gong, and Q. Zhang, "Human capital formation land its effects on economic growth," *Management World*, no. 5, pp. 10–18, 2006.

[2] P. F. Zhu and D. F. Xu, "The estimation of human capital in Chinese cities," *Economic Research Journal*, no. 9, pp. 84–95, 2007.

[3] A. Ozyigit and F. Eminer, "Bounds test approach to the relationship between human capital and foreign direct investment as regressors of economic growth in Turkey," *Applied Economics Letters*, vol. 18, no. 6, pp. 561–565, 2011.

[4] D. J. Balan and S. Knack, "The correlation between human capital and morality and its effect on economic performance: theory and evidence," *Journal of Comparative Economics*, vol. 40, no. 3, pp. 457–475, 2012.

[5] P. Plummer and M. Taylor, "Entrepreneurship and human capital: distilling models of local economic growth to inform policy," *Journal of Small Business and Enterprise Development*, vol. 11, no. 4, pp. 427–439, 2004.

[6] P. Y. Hong and S. Pandey, "Human capital as structural vulnerability of US poverty," *Equal Opportunities International*, vol. 26, no. 1, pp. 18–43, 2007.

[7] M. F. Khorasgani, "Higher education development and economic growth in Iran," *Education, Business and Society*, vol. 1, no. 3, pp. 162–174, 2008.

[8] Y. Jiang, X. Shi, S. Zhang, and J. Ji, "The threshold effect of high-level human capital investment on China's urban-rural income gap," *China Agricultural Economic Review*, vol. 3, no. 3, pp. 297–320, 2011.

[9] T. W. Schultz, "The value of the ability to deal with disequilibria," *Journal of Economic Literature*, vol. 13, no. 3, pp. 827–846, 1975.

[10] N. G. Mankiw, D. Romer, and D. N. Weil, "A contribution to the empirics of economic growth," *Quarterly Journal of Economics*, vol. 107, no. 2, pp. 407–437, 1992.

[11] R. J. Barro and J. W. Lee, "International measures of schooling years and schooling quality," *The American Economic Review*, vol. 86, no. 2, pp. 218–223, 1996.

[12] R. Somanathan, "School heterogeneity, human capital accumulation, and standards," *Journal of Public Economics*, vol. 67, no. 3, pp. 369–397, 1998.

[13] T. Ayalew, "Parental preference, heterogeneity, and human capital inequality," *Economic Development and Cultural Change*, vol. 53, no. 2, pp. 381–407, 2005.

[14] A. Garcia-Aracil, J. G. Mora, and L. E. Vila, "The rewards of human capital competences for young European higher education graduates," *Tertiary Education and Management*, vol. 10, no. 4, pp. 287–305, 2004.

[15] R. Ramcharan, "Higher or basic education? The composition of human capital and economic development," *IMF Staff Papers*, vol. 51, no. 2, pp. 309–326, 2004.

[16] M. Fincher, "Governments as human capital providers: a rationale for strong government support of broad higher education access," *Competitiveness Review*, vol. 17, no. 1-2, pp. 67–76, 2007.

[17] A. van der Merwe, "Does human capital theory explain the value of higher education? A South African case study," *The*

American Journal of Business Education, vol. 3, no. 1, pp. 107–118, 2010.

[18] T. Nakajima and H. Nakamura, "How do elementary and higher education affect human capital accumulation and inequality? A note," *Macroeconomic Dynamics*, vol. 16, no. 1, pp. 151–158, 2012.

[19] P. Romer, "Endogenous technological change," *Journal of Political*, vol. 98, no. 5, pp. 71–102, 1990.

[20] R. R. Nelson and E. S. Phelps, "Investment in humans, technological diffusion, and economic growth," *The American Economic Review*, vol. 56, no. 1-2, pp. 69–75, 1966.

[21] J. A. Schumpeter, *The Theory of Economic Development*, Oxford University Press, London, UK, 1934.

[22] R. E. Lucas Jr., "On the mechanics of economic development," *Journal of Monetary Economics*, vol. 22, no. 1, pp. 3–42, 1988.

[23] R. Florida, C. Mellander, and K. Stolarick, "Inside the black box of regional development—human capital, the creative class and tolerance," *Journal of Economic Geography*, vol. 8, no. 5, pp. 615–649, 2008.

[24] C. Zhang and L. Zhuang, "The composition of human capital and economic growth: evidence from China using dynamic panel data analysis," *China Economic Review*, vol. 22, no. 1, pp. 165–171, 2011.

[25] H. W. Wang and P. Li, "Empirical analysis of the sources of China's economic growth in 1978–2008," *Journal of Knowledge-Based Innovation in China*, vol. 3, no. 2, pp. 91–105, 2011.

[26] H. Chen, "A structural analysis of the human capital's contribution to economy growth," *The Journal of Quantitative &Technical Economics*, no. 8, pp. 9–68, 2007.

[27] J. Q. Guo, "Structural analysis of human capital investment," *China Economic Quarterly*, no. 3, pp. 689–706, 2005.

[28] C. Zhang, "Empirical research on the relation between formation of human capital and economic institutional transition," *Economic Research Journal*, no. 12, pp. 9–71, 2007.

[29] G. Ferrari and T. Laureti, "Evaluating technical efficiency of human capital formation in the Italian university: evidence from Florence," *Statistical Methods and Applications*, vol. 14, no. 2, pp. 243–270, 2005.

[30] C.-C. Chang, S.-W. Hung, and S.-Y. Huang, "Evaluating the operational performance of knowledge-based industries: the perspective of intellectual capital," *Quality and Quantity*, vol. 47, no. 3, pp. 1367–1383, 2011.

[31] M. A. Ahmed and G. Krishnasamy, "Human capital investment to achieve knowledge based economy in ASEAN5:DEA applications," *Journal of the Knowledge Economy*, vol. 4, no. 4, pp. 331–342, 2013.

[32] J. Maudos, J. M. Pastor, and L. Serrano, "Human capital in OECD countries: technical change, efficiency and productivity," *International Review of Applied Economics*, vol. 17, no. 4, pp. 419–435, 2003.

[33] C. L. Zhu, H. Z. Yue, and P. Shi, "The empirical study on the impact of human capital and its compositionon technical efficiency in China: the evidence based on the 1985–2007 provincial panel data," *Studies in Science of Science*, vol. 28, no. 11, pp. 1668–1672, 2010.

[34] L. P. Ran and F. Y. Zhai, "Empirical analysis on contribution rate of human capital in Chinese construction industry based on DEA," *Journal of Systems & Management*, vol. 19, no. 6, pp. 702–705, 2010.

[35] H. O. Fried, C. A. K. Lovell, S. S. Schmidt, and S. Yaisawarng, "Accounting for environmental effects and statistical noise in data envelopment analysis," *Journal of Productivity Analysis*, vol. 17, no. 1-2, pp. 157–174, 2002.

[36] A. Charnes, W. W. Cooper, and E. Rhodes, "Measuring the efficiency of decision making units," *European Journal of Operational Research*, vol. 2, no. 6, pp. 429–444, 1978.

[37] R. D. Banker, A. Charnes, and W. W. Cooper, "Some models for estimating technical and scale inefficiencies in data envelopment analysis," *Management Science*, vol. 30, no. 9, pp. 1078–1092, 1984.

[38] H. Li and H. Liang, "Health, education, and economic growth in East Asia," *Journal of Chinese Economic and Foreign Trade Studies*, vol. 3, no. 2, pp. 110–131, 2010.

[39] F. Y. Tatoglu, "The relationships between human capital investment and economic growth: a panel error correction model," *Journal of Economic and Social Research*, vol. 13, no. 1, pp. 75–88, 2011.

[40] D. E. Bloom, D. Canning, and J. Sevilla, "The effect of health on economic growth: a production function approach," *World Development*, vol. 32, no. 1, pp. 1–13, 2004.

[41] I. D. del Valle and M. A. S. Castillo, "Human capital and sustainable competitive advantage: an analysis of the relationship between training and performance," *International Entrepreneurship and Management Journal*, vol. 5, no. 2, pp. 139–163, 2009.

[42] S. Scicchitano, "Complementarity between heterogeneous human capital and R&D: can job-training avoid low development traps?" *Empirica*, vol. 37, no. 4, pp. 361–380, 2010.

[43] J. E. Taylor and P. L. Martin, "Human capital: migration and rural population change," in *Agricultural Production*, vol. 1 of *Handbook of Agricultural Economics*, pp. 457–511, Elsevier, London, UK, 2001.

[44] D. X. Kan and L. W. Luo, "Empirical study on influence of foreign trade over human capital: based on provincial data in China," *Research on Economics and Management*, no. 4, pp. 117–122, 2010.

[45] D. M. Gould and R. J. Ruffin, "Human capital, trade, and economic growth," *Review of World Economics*, vol. 131, no. 3, pp. 425–445, 1995.

[46] J. Y. Wang, "Impact of institutional changes on the role of human capital and physic capital in the process of economic growth," *Chinese Journal of Population Science*, no. 4, pp. 11–17, 2004.

[47] L. Y. Yu, "The ratio of education investment and differences in regional economic growth," *Economic Research Journal*, no. 10, pp. 131–143, 2008.

[48] A. H. Dierx, "Estimation of a human capital model of migration," *The Annals of Regional Science*, vol. 22, no. 3, pp. 99–110, 1988.

[49] C. W. Lai, *Essays on international trade and human capital [A Dissertation for the Degree of Doctor of Philosophy]*, University of Virginia, 2008.